Journal of Applied Mechanics

(Contributions of the ASME Applied Mechanics Division)

... 493

... Inertia in Journal-Bearing Lubrication ... J. F. Osterle, Y. T. Chow, and E. A. Saibel 494

... Existence of Irrotational Gas Flow ... Tepfel Kaye 497

... Discontinuity Surfaces and Shock Waves ... M. L. Hamza 501

... Biaxial Gyroscopes ... S. B. Goodman and A. R. Robinson 506

... Beams Under General Impact ... J. A. Betser and M. M. Frocht 509

... Forced Oscillations of Tethers ... A. Slibar and P. B. Bailey 515

... Existence as Solutions to Differential Equations ... C. R. Williams 520

... Vibrations of Stiffened Plates ... W. H. Hoppmann, II, and L. S. Magness 526

... Stress in Thin Plate ... J. L. Cutcliffe and R. S. Hoops 531

... Rectangular Plates With Two Unsupported Edges ... P. Shahinian 537

... Waves in Plates ... D. C. Gazis and R. D. Mindlin 541

... Buckling and Bending of Thin Conical Shells ... Paul Seide 547

... Under Line Load ... R. N. Clayton 553

... Beam With Initial Shear Deflection ... M. R. Lunchick and R. D. Hooft, Jr. 559

... Along Two Piles of Semicircular Nozzles ... A. Ahmadi 565

... ... Gabriel Horvay and K. L. Yinnakou 574

... Two Joined Semi-Infinite Plates ... J. T. Frasier and Leif Hougaard 582

... of a Granular Medium ... J. Duffy and R. D. Mindlin 585

... of the Theory of Consolidation ... M. A. Biot and D. G. Willis 594

... Viscoelastic Material ... P. R. Bailey 602

... Under Action of Transverse Force ... Werner Goldsmith 609

... Mounting of Equipment ... R. A. Di Taranto 617

... for a Coupling Linkage ... F. Freudenstein 621

... Velocities in Continuous Structures ... S. H. Crandall 622

... of Nonspherical Elastic Bodies ... H. Deresiewicz 623

... previously published papers by S. J. Kline and F. G. Kemler; P. M. Naghdi; E. E. G. ... I. Imanu, Jr., W. A. Nash; E. Reissner and G. Hervay; F. G. Hodge, Jr., and Nicholas ... Shabetai; J. Hirschhorn; H. G. Landau; Tokan Yokobori, R. L. Sharma; M. E. ... Gurtin; J. Kestin and H. E. Wang; H. Lee, C. B. Pittman, O. D. Sherby, and J. E. ... and R. W. Weeks 625

... 647

DECEMBER, 1957

VOL. 24, NO. 4

Transactions of The American Society of Mechanical Engineers

Applied Mechanics

Reviews

Applied Mechanics Division

Kaplan, *Technical Editor*

Published Quarterly by

The American Society of Mechanical Engineers

Publication Office, Business Press, Inc., Lancaster, Pa.

Editorial and General Offices, The American Society of Mechanical Engineers, 29 West 39th Street, New York 18, N. Y.

Subscription, Journal of Applied Mechanics, ASME, $10.00 per year; Reviews, $5.00 per year; Combined, $12.00 per year; Foreign Postage, $1.00 per year; Canada, Postage Included; Single Copies, Reviews, $1.25, Journal, $2.00

Entered as second-class matter at the Post Office, Lancaster, Pa., under the Act of March 3, 1879, with additional entry at the Post Office, Providence 12, R. I.

Acceptance for mailing at special rate of postage provided for in Section 1103, Act of October 3, 1917, authorized on June 5, 1918.

Statement required by the Act of August 24, 1912, as amended by the Act of March 3, 1933, and July 2, 1946 (Title 39, United States Code, Section 233)

Showing the ownership, management, and circulation of Applied Mechanics Reviews, published quarterly at Lancaster, Pa., for October 1, 1951.

1. The names and addresses of the publisher, editor, managing editor, and business manager are:

Publisher, The American Society of Mechanical Engineers, 29 West 39th Street, New York 18, N. Y.

Editor, Henry Kaplan, Journal of Applied Mechanics, ASME, Brown University, Providence 12, R. I.

Managing Editor, None

Business Manager, O. B. Schier, 2nd, Papers Secretary

2. The owner is: (If owned by a corporation, its name and address must be stated and also immediately thereunder the names and addresses of stockholders owning or holding 1 per cent or more of total amount of stock. If not owned by a corporation, the names and addresses of the individual owners must be given. If owned by a partnership or other unincorporated firm, its name and address, as well as that of each individual member, must be given.)

The American Society of Mechanical Engineers, 29 West 39th Street, New York 18, N. Y.

3. The known bondholders, mortgagees, and other security holders owning or holding 1 per cent or more of total amount of bonds, mortgages or other securities are: (If there are none, so state.)

None

4. Paragraphs 2 and 3 include, in cases where the stockholder or security holder appears upon the books of the company as trustee or in any other fiduciary relation, the name of the person or corporation for whom such trustee is acting, also the statements in the two paragraphs show the affiant's full knowledge and belief as to the circumstances and conditions under which stockholders and security holders who do not appear upon the books of the company as trustees, hold stock and securities in a capacity other than that of a bona fide owner.

(Signature of Editor, Publisher, Business Manager, or Owner)

Sworn to and subscribed before me this 26th day of September, 1951.

(My commission expires March 30, 1953)

(This information is required by the Act of August 24, 1912, as amended by the Act of March 3, 1933, and July 2, 1946 (Title 39, United States Code, Section 233), and this form is to be furnished in triplicate.)

Henry Kaplan, Jr., *Editor*

O. B. Schier, 2nd, *Copying Editor*

Discussion, if any, will be published in its publication (OSD, Par. 4)

Published by The American Society of Mechanical Engineers, Business Press, Inc., Lancaster, Pa. The editorial offices are located at The American Society of Mechanical Engineers, 29 West 39th Street, New York 18, N. Y. Price to members, $1.25 per copy, postpaid; to nonmembers outside the United States and Canada, $2.00 per copy, postpaid. Subscriptions to members are $5.00 per year; to nonmembers outside the United States and Canada, $10.00 per year. Subscriptions to members are for personal use only. Subscriptions to nonmembers are for the use of the subscribing library or individual. Single copies of previous issues are available at the above prices. Subscriptions are payable in advance and should be sent to the publication office. Changes of address must be received at the publication office by the 15th of the month preceding the date of issue. Please send old as well as new address. Allow one month for change to become effective.

THE TIMOSHENKO MEDAL

To honor Professor Stephen P. Timoshenko and to commemorate his contributions to Applied Mechanics, as author and teacher, The American Society of Mechanical Engineers has established the Timoshenko Medal Award.

Through his fourteen books, his inspiring lectures, his essential role in the establishment of the Society's Applied Mechanics Division and *Journal of Applied Mechanics*, Professor Timoshenko has stimulated a prodigious evolution and development of his scientific field, especially in America but also throughout the world. His books are used in every engineering school. His former students and their students have become distinguished members of the faculties of universities and institutes of technology or occupy important positions in industry. His teachings have influenced the design of every type of modern machine, instrument, and vehicle.

There has been no lack of international recognition of Professor Timoshenko's achievements. He was elected a member of the Ukrainian Academy of Sciences, Kiev, in 1918, and the American National Academy of Science in 1941; Corresponding Member of the Russian Academy of Sciences, Moscow, in 1928, the Polish Academy of Sciences, Warsaw, in 1935, and the French Academy of Sciences, Paris, in 1939; Foreign Member of the Royal Society, London, in 1944, and the National Academy of Sciences, Rome, in 1948. He holds honorary doctoral degrees from Lehigh University, 1936, the University of Michigan, 1938, the Technische Hochschule in Zürich, 1947, the Technische Hochschule in Munich, 1949, and the University of Glasgow, 1951. He was awarded the Jourawski Medal, in 1911, by the Russian Institute of Engineers of Ways of Communication for his famous paper on the stability of elastic systems; the Salow prize, in 1915, by the Russian Department of Transportation for his work on stresses in rails; the Worcester Reed Warner Medal of The American Society of Mechanical Engineers, in 1935, for his achievements in mechanics; the Lamme Medal of the American Society for Engineering Education, in 1939, for his contribution to engineering education; the Levery Medal of the Franklin Institute, in 1939, for his paper on suspension bridges; the Grande Médaille of the Association des Ingénieurs-Docteurs de France, in 1946; the James Watt International Medal of The Institution of Mechanical Engineers, in 1947; and, in 1948, the Gustave Trasenster Medal of the Association des Ingénieurs Sortis de l'École de Liège.

To this notable list of honors, the ASME Applied Mechanics Division was moved to add one other which, by its unique character, would perpetuate the esteem in which Professor Timoshenko is held by his followers. Some four hundred members of the Division joined in deeding to the Society a fund which assures the possibility of an annual award of the Timoshenko Medal, illustrated above. The striking likeness, even to the cherished twinkle in the eye, is cast in bold relief from a specially commissioned sculpture by the noted artist Elisabeth Gordon. The first award is, of course, to Professor Timoshenko himself, and is to be presented at the Banquet of the Applied Mechanics Division, on December 3, 1957, during the Annual Meeting of The American Society of Mechanical Engineers.

The Effect of Lubricant Inertia in Journal-Bearing Lubrication[1]

By J. F. OSTERLE,[2] Y. T. CHOU,[3] AND E. A. SAIBEL,[4] PITTSBURGH, PA.

The Reynolds equation of hydrodynamic theory, modified to take lubricant inertia into approximate account, is applied to the steady-state operation of journal bearings to determine the effect of lubricant inertia on the pressure developed in the lubricant. A simple relationship results, relating this "inertial" pressure to the Reynolds number of the flow. It is found that the inertia effect can be significant in the laminar regime.

Nomenclature

The following nomenclature is used in the paper:

c = radial clearance
e = eccentricity
$f = \frac{P_1}{6P_0}$, a function of n and θ
h = film thickness
$h' = \frac{dh}{dx}$
H = film thickness at which right-hand side of Equation [3] vanishes
H_0 = corresponding value of H for flow without inertia correction
H_1 = a component of H defined by Equation [11]
$n = e/c$, eccentricity ratio of bearing
p = lubricant pressure
P = nondimensional pressure defined by Equation [8]
P_0 = corresponding value of P for flow without inertia correction
P_1 = a component of P defined by Equation [10]
r = journal radius (in Appendix, r signifies radial co-ordinate)
Re = Reynolds number based on radial clearance
u = lubricant velocity along film
U = journal surface velocity
v = lubricant velocity across film
x = co-ordinate along film
y = co-ordinate across film
θ = polar angle
λ = constant defined by Equation [9]
μ = lubricant viscosity
ρ = lubricant density

[1] This work was supported in part by funds from a contract with the Office of Ordnance Research, U. S. Army.

[2] Associate Professor, Department of Mechanical Engineering, Carnegie Institute of Technology. Assoc. Mem. ASME.

[3] Research Assistant, Department of Mathematics, Carnegie Institute of Technology.

[4] Professor of Mechanics, Department of Mathematics, Carnegie Institute of Technology. Mem. ASME.

Presented at the Applied Mechanics Division Summer Conference, Berkeley, Calif., June 13–15, 1957, of THE AMERICAN SOCIETY OF MECHANICAL ENGINEERS.

Discussion of this paper should be addressed to the Secretary, ASME, 29 West 39th Street, New York, N. Y., and will be accepted until January 10, 1958, for publication at a later date. Discussion received after the closing date will be returned.

NOTE: Statements and opinions advanced in papers are to be understood as individual expressions of their authors and not those of the Society. Manuscript received by ASME Applied Mechanics Division, January 2, 1957. Paper No. 57—APM-37.

Introduction

In most hydrodynamic bearings the lubricant flow is laminar and as such is governed by a differential equation which relates the pressure and viscous forces acting on a particle of the lubricant to the lubricant inertia in accordance with Newton's second law of motion. The importance of the inertia term (relative to the viscous term) in this equation can be characterized by a Reynolds number which increases as the inertia effect increases. In the operation of most present-day bearings the Reynolds numbers are small enough so that the inertia effect can be ignored safely, reducing the governing relationship to the familiar Reynolds equation. However, with the continuing trend in machine design to higher and higher speeds, the question of how important inertia will be at high Reynolds numbers in the laminar regime is of growing interest (6).[5] Of course, if the Reynolds number becomes too high, turbulence will develop in the flow and the afore-mentioned governing equation will apply no longer even with the inertia term included.

Recent work by the authors (1) has shown that for slider bearings the inertia effect does become significant at high Reynolds numbers in the laminar regime. It is the purpose of this paper to extend our work on slider bearings to the case of journal bearings.

Theory

It is shown in the Appendix that the differential equation which governs steady-state laminar hydrodynamic lubrication without side flow is

$$\mu \frac{\partial^2 u}{\partial y^2} = \frac{dp}{dx} + \rho \left(u \frac{\partial u}{\partial x} + v \frac{\partial u}{\partial y} \right) \quad \ldots\ldots [1]$$

where

x = direction along film
y = direction across film
$p(x)$ = lubricant pressure (measured above inlet value)
μ = lubricant viscosity
ρ = lubricant density
$u(x, y)$ = lubricant velocity in x-direction
$v(x, y)$ = lubricant velocity in y-direction

In this paper the lubricant viscosity and density will be assumed constant. The first term in Equation [1] represents the viscous force, the second term the pressure force, and the third term the lubricant inertia.

In addition to Equation [1], the lubricant also must satisfy the continuity equation which, for an incompressible fluid, is

$$\frac{\partial u}{\partial x} + \frac{\partial v}{\partial y} = 0 \quad \ldots\ldots [2]$$

and the usual no-slip boundary conditions on the velocity as well as boundary conditions on the pressure.

An exact solution to Equations [1] and [2] for the lubricant pressure subject to the proper boundary conditions is extremely

[5] Numbers in parentheses refer to the Bibliography at the end of the paper.

difficult to obtain. However, owing to the relative smallness of the inertia term, an approximate solution would seem to be justifiable. Slezkin and Targ (2) suggest averaging the inertia over the film thickness $h(x)$. If this is done, Equation [1] becomes

$$\mu \frac{\partial^2 u}{\partial y^2} = \frac{dp}{dx} + \frac{\rho}{h} \int_0^h \left(u \frac{\partial u}{\partial x} + v \frac{\partial u}{\partial y} \right) dy \quad [3]$$

with the right-hand side a function of x only. Equations [2] and [3] together with the no-slip boundary conditions are then readily solvable for the pressure gradient yielding

$$\frac{dp}{dx} = \frac{6\mu U(H - h)}{h^3} + \frac{\rho U^2 h'}{30h} \left[9 \left(\frac{H}{h} \right)^2 - 4 \right] \quad [4]$$

where U is the journal surface velocity and H is the film thickness at which the right-hand side of Equation [3] vanishes. The prime indicates differentiation with respect to x. Equation [4] is derived in somewhat more detail by the authors in reference (1) where it is applied to the case of slider bearings.

For the journal-bearing problem Equation [4] becomes

$$\frac{dp}{d\theta} = \frac{6\mu Ur(H - h)}{h^3} + \frac{\rho U^2 h'}{30h} \left[9 \left(\frac{H}{h} \right)^2 - 4 \right] \quad [5]$$

with r the journal radius and the film thickness h given by

$$h = c(1 + n \cos \theta) \quad [6]$$

where c is the radial clearance and n the eccentricity ratio e/c (see Fig. 1). Equation [5] can be written in dimensionless form as

$$\frac{dP}{d\theta} = \frac{(H - h)c^2}{h^3} + \frac{\lambda}{30} \frac{h'}{h} \left[9 \left(\frac{H}{h} \right)^2 - 4 \right] \quad [7]$$

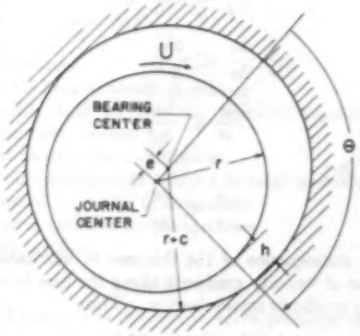

FIG. 1 JOURNAL-BEARING CONFIGURATION

where

$$P = \frac{pc^2}{6\mu Ur} \quad [8]$$

and

$$\lambda = \frac{\rho U c^2}{6\mu r} = \frac{\mathrm{Re}}{6} \left(\frac{c}{r} \right) \quad [9]$$

with Re the Reynolds number based on the radial clearance.

With the Reynolds number set equal to zero, Equation [7] reduces to the familiar Reynolds equation (which neglects inertia) as we would expect. If we let P_0 be the solution to this reduced equation and H_0 be the corresponding value of H, we can write for the solution of Equation [7]

$$P = P_0 + \lambda P_1 \quad [10]$$

with

$$H = H_0 + \lambda H_1 \quad [11]$$

where the second terms on the right of each equation are small corrections to account for inertia. Substituting Equations [10] and [11] into Equation [7] and neglecting small quantities we obtain

$$\frac{dP_0}{d\theta} = \frac{(H_0 - h)c^2}{h^3} \quad [12]$$

and

$$\frac{dP_1}{d\theta} = \frac{H_1 c^2}{h^3} + \frac{h'}{30h} \left[9 \left(\frac{H_0}{h} \right)^2 - 4 \right] \quad [13]$$

Equation [12] integrates to the classical Sommerfeld solution (3) for the full journal bearing

$$P_0 = \frac{n \sin \theta \, (2 + n \cos \theta)}{(2 + n^2)(1 + n \cos \theta)^2} \quad [14]$$

and it can be directly established that

$$H_0 = 2c \left(\frac{1 - n^2}{2 + n^2} \right) \quad [15]$$

Equation [14] expresses the pressure distribution obtained by neglecting the inertia.

Treating Equation [13] the same as Equation [12]; i. e., using the Sommerfeld substitution and boundary conditions as given in reference (3), we obtain

$$P_1 = \frac{H_1}{c(1 - n^2)^{5/2}} \left[\frac{2 + n^2}{2} \cos^{-1} \left(\frac{n + \cos \theta}{1 + n \cos \theta} \right) + \frac{n(1 - n^2)^{1/2}(n^2 - 3n \cos \theta - 4)}{2(1 + n \cos \theta)^2} \sin \theta \right] + \frac{3}{5} \left(\frac{1 - n^2}{2 + n^2} \right)^2 \left[\frac{1}{(1 + n)^2} - \frac{1}{(1 + n \cos \theta)^2} \right] + \frac{2}{15} \ln \left(\frac{1 + n}{1 + n \cos \theta} \right) \quad [16]$$

where

$$H_1 = \frac{4c(1 - n^2)^{1/2}}{5\pi(2 + n^2)} \left[\frac{6n}{(2 + n^2)^2} - \frac{1}{3} \ln \left(\frac{1 + n}{1 - n} \right) \right] \quad [17]$$

Equation (16) expresses the pressure distribution which (when multiplied by λ) must be added to P_0 in accordance with Equation [10] to correct for inertia.

DISCUSSIONS AND CONCLUSIONS

To illustrate the effect of inertia in journal-bearing lubrication we will consider a journal operating with an eccentricity ratio n of 0.20. For this case Equations [16] and [17] yield the values of P_1 for various values of θ given in Table 1. Also shown in this

TABLE 1 VALUES OF P_1

θ (deg)	P_1	P_1*
0	0	0
30	0.0041	...
60	0.0055	0.007
90	0.0030	0.004
120	−0.0035	−0.004
150	−0.0082	−0.010
180	0	0

table are the inertia corrections P_1*, computed by Kahlert (4) for the same eccentricity ratio. Kahlert also used an approximation method to calculate the inertia effect, but his was substantially different from the procedure employed in this paper and requires considerably more labor. He calculated the ve-

locities which would exist in the film if there were no inertia, substituted them into the inertia term (second on the right) of Equation [1], and proceeded to integrate along the film for the pressure correction. The agreement between the two methods is reasonably good.

The effect of inertia on the pressure can be seen more clearly by considering Equation [10] written as follows

$$\frac{P}{P_0} = 1 + \lambda \frac{P_1}{P_0}$$

By Equations [8] and [9] this can be written as

$$\frac{p}{p_0} = 1 + f \operatorname{Re} \left(\frac{c}{r}\right) \quad \ldots\ldots\ldots\ldots\ldots\ldots [18]$$

where

$$f = \frac{P_1}{6P_0} \quad \ldots\ldots\ldots\ldots\ldots\ldots [19]$$

and is a function of n and θ only. For an eccentricity ratio of 0.20, f is given in Table 2 for various values of θ.

TABLE 2 VALUES OF f

θ (deg)	f
30	0.0088
60	0.0062
90	0.0026
120	−0.0029
150	−0.0105

Now, the theory for the inertia effect given in this paper is valid throughout the laminar regime; i.e., for Reynolds numbers smaller than a certain critical value. This critical Reynolds number value was given by Taylor (5) for lightly loaded journal bearings as

$$(\mathrm{Re})_c = 41.1\ (r/c)^{1/2} \quad \ldots\ldots\ldots\ldots\ldots [20]$$

Therefore, based on this criterion the greatest pressure correction possible in the laminar regime is

$$\frac{p}{p_0} = 1 + 41.1 f\ (c/r)^{1/2} \quad \ldots\ldots\ldots\ldots\ldots [21]$$

In the example treated here, at an angle of 150 deg and for a c/r ratio of 0.01, this amounts to approximately a 4 per cent correction.

Thus it appears that for journal bearings as well as slider bearings the inertia effect can be significant in the laminar regime.

BIBLIOGRAPHY

1 "On the Effect of Lubricant Inertia in Hydrodynamic Lubrication," by F. Osterle and E. Saibel, *Journal of Applied Mathematics and Physics* (ZAMP), vol. 6, 1955, p. 334.

2 "The Generalized Equations of Reynolds," by N. A. Slezkin and S. M. Targ, *Comptes Rendus (Doklady) de l'Academie des Sciences de l'URSS*, vol. 54, no. 3, 1946, p. 205.

3 "On the Hydrodynamic Theory of Lubrication," by A. Sommerfeld, *Zeitschrift für Mathematik und Physik*, vol. 50, 1904, p. 97.

4 "Der Einfluss der Tragheitskrafte bei der Hydrodynamischen Schmiermitteltheorie," by W. Kahlert, *Ingenieur-Archiv*, vol. 16, 1947, p. 321.

5 "Stability of a Viscous Liquid Contained Between Two Rotating Cylinders," by G. I. Taylor, Transactions of the Royal Society of London, series A, vol. 223, 1923, p. 289.

6 "Inertia Forces in Lubricating Films," by R. S. Brand, JOURNAL OF APPLIED MECHANICS, Trans. ASME, vol. 77, 1955, p. 363.

Appendix

If laminar, the flow in a lubricating film is governed by the Navier-Stokes (momentum) equations and the continuity principle. These relationships, written in polar co-ordinate form since in general the film may be curved, can be expressed as follows:

Navier-Stokes equations:

(i) across the film

$$v \frac{\partial v}{\partial r} + \frac{u}{r} \frac{\partial v}{\partial \theta} - \frac{u^2}{r} = -\frac{1}{\rho} \frac{\partial p}{\partial r} + \frac{\mu}{\rho} \left(\nabla^2 v - \frac{v}{r^2} - \frac{2}{r^2} \frac{\partial u}{\partial \theta}\right)$$

(ii) along the film

$$v \frac{\partial u}{\partial r} + \frac{u}{r} \frac{\partial u}{\partial \theta} + \frac{uv}{r} = -\frac{1}{\rho} \frac{\partial p}{r \partial \theta} + \frac{\mu}{\rho} \left(\nabla^2 u - \frac{u}{r^2} + \frac{2}{r^2} \frac{\partial v}{\partial \theta}\right) \quad \ldots\ldots [1a]$$

where $\nabla^2(\ ) = \dfrac{\partial^2}{\partial r^2}(\ ) + \dfrac{1}{r} \dfrac{\partial}{\partial r}(\ ) + \dfrac{1}{r^2} \dfrac{\partial^2}{\partial \theta^2}(\ )$

Continuity equation

$$\frac{\partial v}{\partial r} + \frac{v}{r} + \frac{1}{r} \frac{\partial u}{\partial \theta} = 0 \quad \ldots\ldots\ldots\ldots [2a]$$

Since in all cases the laminar lubricating film is quite thin we may assume the pressure constant across the film and disregard the Navier-Stokes equation across the film. Furthermore, in virtually all cases the film thickness is much smaller than the radius of curvature of the film making it possible to neglect certain terms in Equations [1a] and [2a]. In detail:

Equation [1a]

$$\frac{uv}{r} \ll v \frac{\partial u}{\partial r}$$

$$\frac{1}{r} \frac{\partial u}{\partial r} \ll \frac{\partial^2 u}{\partial r^2}$$

$$\frac{u}{r^2} \ll \frac{\partial^2 u}{\partial r^2}$$

Equation [2a]

$$\frac{v}{r} \ll \frac{\partial v}{\partial r}$$

A further consequence of the thinness of lubricating films is the smallness of velocity gradients along the film in comparison with velocity gradients across the film. Thus

$$\frac{1}{r^2} \frac{\partial^2 u}{\partial \theta^2} \ll \frac{\partial^2 u}{\partial r^2}$$

We also note that

$$\frac{2}{r^2} \frac{\partial v}{\partial \theta} \ll \frac{\partial^2 u}{\partial r^2}$$

Neglecting these terms reduces Equation [1a] to the form

$$v \frac{\partial u}{\partial r} + \frac{u}{r} \frac{\partial u}{\partial \theta} = -\frac{1}{\rho} \frac{\partial p}{r \partial \theta} + \frac{\mu}{\rho} \frac{\partial^2 u}{\partial r^2}$$

and Equation [2a] to the form

$$\frac{\partial v}{\partial r} + \frac{1}{r} \frac{\partial u}{\partial \theta} = 0$$

Writing dy for dr and dx for $rd\theta$, these become Equations [1] and [2] as used in this paper. These are also the starting point of Kahlert's treatment (4).

A Method for Solving Problems of Irrotational Gas Flow by Means of High-Speed Digital Computers

By TOYOKI KOGA,[1] PASADENA, CALIF.

A numerical procedure is proposed for solution of certain problems in steady gas flow where subsonic, sonic, and supersonic regions appear simultaneously. The difficulties that occur in analytical methods for taking into account the differences of the type of the fundamental equation (elliptic, parabolic, hyperbolic) are avoided. Given a streamline and the state of the gas along that streamline, the co-ordinates of the neighboring streamline and the state of the gas along it can be computed. The procedure can be applied successively to cover a flow field. The method is described in detail for two-dimensional, steady, irrotational flow (without shocks) of a perfect gas, and an example is given.

Nomenclature

The following nomenclature is used in the paper:

- ρ = density
- p = pressure
- x, y = rectangular co-ordinates
- v_x, v_y = velocity components
- q = $(v_x^2 + v_y^2)^{1/2}$
- T = temperature
- c_v = specific heat at constant volume
- γ = (specific heat at constant pressure)/(specific heat at constant volume)
- ξ, η = local rectangular co-ordinates
- v_ξ, v_η = velocity components referred to local co-ordinates ξ, η
- r = radius of curvature of streamline
- S = distance between two streamlines
- M = Mach number

Introduction

As is well known, it is difficult to solve problems of gas flow where subsonic, sonic, and supersonic regions appear simultaneously. Where the entire flow is subsonic, there are several methods of approximation starting from the solution for incompressible flow. Where the entire flow is supersonic the method of characteristics can be used. These methods are of quite different character and are extremely difficult to apply if the flow is of mixed type. Some 10 years ago the author devised a graphical method for solution of such problems,[2] but the nature of the technique made it difficult to improve accuracy by successive approximations. Recently the author employed a high-speed digital computer to carry out numerical calculations based on the same principle. The accuracy is much better than is practical with a purely graphical procedure. In a sense, the method can be said to be quite general since programming and coding is required only once for a particular class of problems. All problems of this class differ only in initial conditions. For the present, the method is restricted to steady two-dimensional flow of a perfect gas.

The Fundamental Equations

It is assumed that the gas is thermally and calorically perfect and that the stagnation temperature is constant over the entire field.[3] The basic equations for two-dimensional steady flow are

$$\rho\left(v_x\frac{\partial v_x}{\partial x} + v_y\frac{\partial v_x}{\partial y}\right) = -\frac{\partial p}{\partial x} \quad [1]$$

$$\rho\left(v_x\frac{\partial v_y}{\partial x} + v_y\frac{\partial v_y}{\partial y}\right) = -\frac{\partial p}{\partial y} \quad [2]$$

$$\frac{\partial(\rho v_x)}{\partial x} + \frac{\partial(\rho v_y)}{\partial y} = 0 \quad [3]$$

$$\left(\rho v_x\frac{\partial}{\partial x} + \rho v_y\frac{\partial}{\partial y}\right)\left\{c_vT + \frac{1}{2}(v_x^2 + v_y^2)\right\} = -\frac{\partial(v_x p)}{\partial x} - \frac{\partial(v_y p)}{\partial y} \quad [4]$$

The flow is assumed irrotational

$$\frac{\partial v_x}{\partial y} - \frac{\partial v_y}{\partial x} = 0 \quad [5]$$

Hence[4] Equation [4] can be written as

$$p\rho^{-\gamma} = \text{const} \quad [4a]$$

With these conditions Equations [1] and [2] can be integrated to the form

$$q^2 \equiv v_x^2 + v_y^2 = \frac{2\gamma}{\gamma - 1}\frac{p_0}{\rho_0}\left\{1 - \left(\frac{p}{p_0}\right)^{(\gamma-1)/\gamma}\right\} \quad [6]$$

where the subscript 0 denotes the state where $q = 0$; i.e., at a stagnation point.

---

[1] Senior Research Fellow, Daniel and Florence Guggenheim Jet Propulsion Center, California Institute of Technology; on leave of absence from Nagoya University, Nagoya, Japan.

Presented at the Applied Mechanics Division Summer Conference, Berkeley, Calif., June 13–15, 1957, of The American Society of Mechanical Engineers.

Discussion of this paper should be addressed to the Secretary, ASME, 29 West 39th Street, New York, N. Y., and will be accepted until January 10, 1958, for publication at a later date. Discussion received after the closing date will be returned.

Note: Statements and opinions advanced in papers are to be understood as individual expressions of their authors and not those of the Society. Manuscript received by ASME Applied Mechanics Division, May 8, 1956. Paper No. 57—APM-43.

[2] "A Graphical Solution of Two-Dimensional Euler's Equation," by T. Koga, *Journal of the Society of Aeronautical Sciences of Japan*, vol. 11, no. 107, 1944, p. 175.

[3] The principle of the method is applicable where the fundamental assumptions are somewhat less restricted than considered here. For instance, a continuous distribution of vorticity might be assumed.

[4] "Elements of Aerodynamics of Supersonic Flows," by A. Ferri, The Macmillan Company, New York, N. Y., first edition, 1949, p. 5.

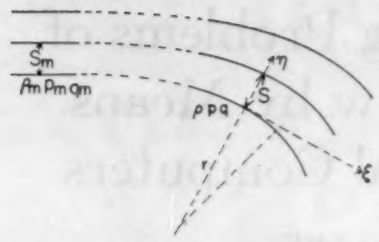

FIG. 1 $r > 0$, WHEN DIRECTION OF RADIUS FROM CENTER OF CURVATURE TO GIVEN POINT MAKES AN ACUTE ANGLE WITH y-AXIS

Consider a flow field with streamlines as shown in Fig. 1. At some reference point m on a stream tube let the velocity, pressure, and density be q_m, p_m, and ρ_m, respectively, and let the width of the stream tube be S_m. These quantities change to q, p, ρ, and S at a general point on the same streamline. Let r be the radius of curvature of the streamline at a general point and ξ, η a local co-ordinate system with origin at that point, with the axis of ξ tangent to the streamline and η normal to the streamline. In this co-ordinate system Equation [2] becomes

$$\rho\left(v_\xi \frac{\partial v_\eta}{\partial \xi} + v_\eta \frac{\partial v_\eta}{\partial \eta}\right) = -\frac{\partial p}{\partial \eta}$$

where at the origin

$$v_\xi = q, \quad v_\eta = 0, \quad \frac{\partial v_\eta}{\partial \xi} = -q/r$$

and hence

$$\frac{\rho q^2}{r} = \frac{\partial p}{\partial \eta} \qquad [7]$$

The continuity Equation [3] becomes

$$\rho q S = \rho_m q_m S_m \qquad [8]$$

and Equation [4] is rewritten as

$$p\rho^{-\gamma} = p_m \rho_m{}^{-\gamma} \qquad [9]$$

Applying Equation [5], an alternative to Equation [7] is

$$\frac{q}{r} = -\frac{\partial q}{\partial \eta} \qquad [10]$$

Given the boundary conditions along one streamline, the flow field can be calculated with Equations [6], [7], [8], and [9].

The general procedure for solution given, say, the pressure distribution along a streamline denoted by I, is as follows:

(a) The density along I is determined from Equation [9].
(b) The velocity q along I is determined from Equation [6].
(c) The radius of curvature along I is estimated.
(d) The value of $\partial p/\partial \eta$ along I is determined from Equation [7].
(e) The value of S along I is determined from Equation [8]; the streamline II can then be drawn.
(f) The pressure distribution along II is obtained from the original pressure along I plus the values of $(\partial p/\partial \eta)S$ at corresponding points.

The procedure is then repeated to work outward to streamlines III, IV, and so on

The major difficulty with the procedure as outlined is the determination of the radius of curvature r of a streamline with sufficient accuracy. This difficulty results, of course, from that fact that curvature involves a second derivative. The advantage of the computer is that accuracy can be obtained in a routine manner.

Let $K - 1$, K, and $K + 1$ denote three points along a streamline as shown in Fig. 2; the co-ordinates of these points are

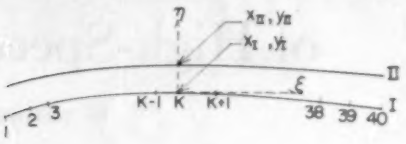

FIG. 2

$$x_{K-1}, y_{K-1};\ x_K, y_K;\ x_{K+1}, y_{K+1}$$

An approximate value of the curvature at K may be obtained from a curve of the second degree drawn through the three points.[6] The equation of the curve may be taken in the form

$$\frac{y}{S_m} = a_0 + a_1 \frac{x}{S_m} + a_2 \left(\frac{x}{S_m}\right)^2 \qquad [11]$$

where a_0, a_1, a_2 are determined by the conditions

$$\frac{y_\alpha}{S_m} = a_0 + a_1 \frac{x_\alpha}{S_m} + a_2 \left(\frac{x_\alpha}{S_m}\right)^2, \quad \alpha = K - 1, K, K + 1. \qquad [12]$$

and S_m is the reference stream-tube width as in Fig. 1. The radius of curvature at the point K is given by

$$-\frac{r_K}{S_m} = \frac{[1 + (dy/dx)_K{}^2]^{3/2}}{(d^2y/dx^2)_K S_m} = \frac{[1 + (a_1 + 2a_2 x_K/S_m)^2]^{3/2}}{2a_2} \qquad [13]$$

The closer the spacing of the three points $K - 1$, K, and $K + 1$, the better the approximation to the true streamline curvature.

Given streamline I and the values of one of the state variables, say p, along its length, the neighboring streamline II and the values of p along it can be found in terms of the notation of the previous paragraph. The equation of the straight line normal to the streamline at K is

$$\frac{x - x_1}{y - y_1} = -\left(\frac{dy}{dx}\right)_1 = -\left[a_1 + 2a_2 \left(\frac{x}{S_m}\right)_1\right] \qquad [14]$$

where x_1, y_1 are co-ordinates of the point K on streamline I. If S is the distance along the normal to streamline II

$$\left(\frac{S}{S_m}\right)^2 = \frac{(x_{II} - x_1)^2}{S_m{}^2} + \frac{(y_{II} - y_1)^2}{S_m{}^2} \qquad [15]$$

Since x_{II}, y_{II} lie on the line given by Equation [14], then

$$\frac{x_{II}}{S_m} = \frac{x_1}{S_m} - \frac{S}{S_m} \frac{a_1 + 2a_2 x_1/S_m}{\sqrt{[1 + (a_1 + 2a_2 x_1/S_m)^2]}} \qquad [16]$$

$$\frac{y_{II}}{S_m} = \frac{y_1}{S_m} + \frac{S}{S_m} \frac{1}{\sqrt{[1 + (a_1 + 2a_2 x_1/S_m)^2]}}$$

These equations give the position of streamline II when a_0, a_1, a_2, and S are known at each point of streamline I.

From Equations [6], [8], and [9] one obtains S in terms of the reference value S_m and the pressure along I; i.e.

[6] If the line has an inflection, more than three points and an approximate curve of third degree or higher may be required.

$$\frac{S}{S_m} = \frac{[(\gamma-1)M_m^2/2+1]^{1/(1-\gamma)}[1-\{(\gamma-1)M_m^2/2+1\}^{-1}]^{1/2}}{(p/p_0)^{1/\gamma}[1-(p/p_0)^{(\gamma-1)/\gamma}]^{1/2}} \quad \ldots\ldots [17]$$

where M_m is the local Mach number at the reference position corresponding to S_m. The pressure differential from I to II is, according to Equation [7]

$$\Delta(p/p_0) = \frac{\partial p}{\partial \eta}\frac{S}{p_0} = \frac{\rho q^2}{\gamma}\frac{S}{p_0} \quad \ldots\ldots [18]$$

From this expression and Equations [6], [9], and [17] one obtains

$$\Delta(p/p_0) = \frac{2\gamma}{\gamma-1}\frac{[1-(p/p_0)^{(\gamma-1)/\gamma}]^{1/2}[1-\{(\gamma-1)M_m^2/2+1\}^{-1}]^{1/2}[(\gamma-1)M_m^2/2+1]^{1/(1-\gamma)}}{r/S_m} \quad \ldots\ldots [19]$$

Since r/S_m is given by Equation [13], the pressure along II can be calculated from

$$(p/p_0)_{II} = (p/p_0)_I + \Delta(p/p_0) \quad \ldots\ldots [20]$$

where $\Delta(p/p_0)$ is given by Equation [19].

Example

To illustrate the procedure for a specific problem, consider the flow of air where the initial streamline I is a straight line with the pressure prescribed along its length. The prescribed pressure distribution is that shown in Fig. 3(*b*). The reference point for streamline I is the point at which $M_m = 1$, the sonic point. For air, $p_m/p_0 = 0.527$ and $\gamma = 1.405$. Forty equally spaced points for computation are chosen, the points numbered from 1 to 40. The radius of curvature of streamline I is infinite along its length. The maximum digital number that could be produced by the computer (a Datatron) was 10^{38}. Hence[6] the values of y/S_m (all zero) were replaced by arbitrarily chosen small numbers that give finite, although very large, values of the radius of curvature r. The streamline at point K is approximated by a quadratic in terms of a_0, a_1, and a_2 determined by the points $K-1$, K, and $K+1$; the streamline approximation at points 1 and 40, however, are determined from the quadratic through 1, 2, 3 and 38, 39, 40, respectively.

The computing sequence is as follows: The numerical values of x/S_m, y/S_m, and p/p_0 on line I were stored in the memory as well as the constants $1/(1-\gamma)$, $\gamma-1$, $2\gamma/(\gamma-1)$, and so on. The calculation began with evaluation of a_0, a_1, and a_2 from Equations [11] and [12]. From Equations [16], [17], [18], and [20] the second streamline and state variables along its length were obtained. The entire procedure requires about 500,000 commands and takes about 15 min. The programming called for printing the results for each streamline as well as storing them in the memory preparatory to calculation of the next streamline. In practice it is of course necessary to check the correctness of the programming by calculating a simple example.

The final results are plotted in Fig. 3 and compared with those calculated by the method of characteristics for the supersonic region. The agreement is quite satisfactory.

Boundary Conditions and Applications

The analysis and example of the preceding sections concerned problems where a streamline and state variables were prescribed. The method is readily modified to accommodate a problem where an equipotential line and, say, the variation of $\partial p/\partial y$ along it are prescribed. The radius of curvature at any point can be determined from Equation [7] and the distance between streamlines from Equation [8]. A second equipotential line is determined and the process repeated.

[6] A similar difficulty might occur in routine calculation. A series of branching commands combined with commands to replace an infinitely large r by an arbitrarily large finite value can be employed.

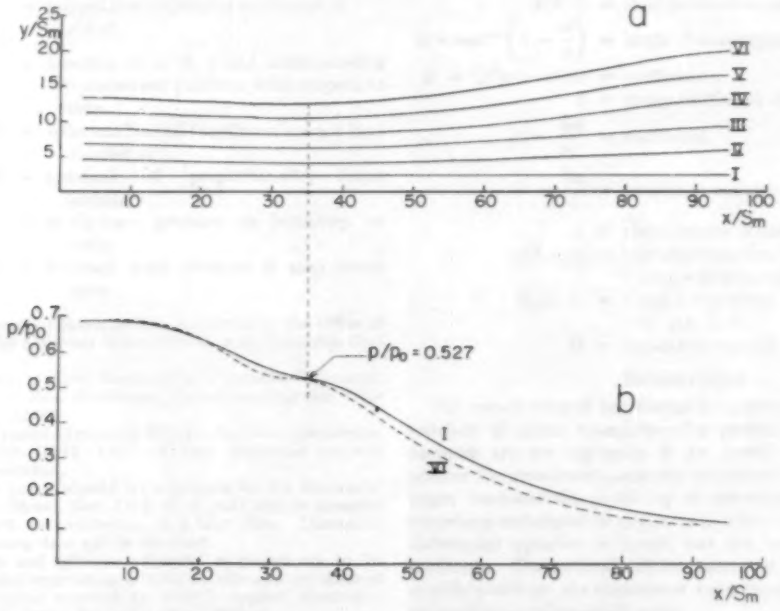

Fig. 3 (*a*) Streamlines; (*b*) Pressure Distributions on the Lines I and VI

Fields of fluid flow may be determined by conventional methods of analysis where a streamline of the flow and the state at infinity are given. As an example, we may calculate the flow field about an airfoil of known shape if we also are given the stream velocity at infinity. Boundary conditions of this kind may be referred to as A. In contrast to conventional analysis, however, the present method requires the specification of the boundary conditions in another fashion; the pressure distribution, instead of the condition at infinity, must be given along either a specified streamline or a specified equipotential line. The boundary conditions may be referred to as B. Either type A or type B constitutes a set of necessary and sufficient boundary conditions for the determination of the field of flow and they are mathematically equivalent. The relative utility of the two methods of approach can be determined only by a consideration of what is most conveniently specified and what is the objective of the calculation. For the usual wing theory it is convenient and appropriate to use the A-conditions, while in the design of nozzles or diffusers where the shapes of walls must be determined from a specification of the desired pressure distribution along an arbitrary line, the use of the B-conditions is clearly indicated.

The greatest strength of the method developed here lies in its application to problems of mixed flow which otherwise would remain intractable. The method, however, is weak in that it would seem to be applicable only to problems with boundary conditions of type B. Even this objection may disappear if we are permitted to employ iteration procedures and high-speed computing techniques. Thus the application of the present method to problems with type A boundary conditions might proceed along the following lines:

An arbitrary pressure distribution is assumed on a given streamline. On the basis of this assumption we calculate the state of the field including the condition at infinity. This then is compared with the desired condition at infinity. A change is now made in the initial pressure distribution and again the condition at infinity is compared. After a number of trials, easily accomplished by high-speed computers, we may obtain a suitable approximation to the desired boundary condition. However, it is essential for systematic progress to know in some measure the response of the flow field to modification of the initial values. It would be desirable to have a systematic procedure for evaluating the feedback to assure rapid convergence. How this may be known in a particular case or in general is a question beyond the scope of the present paper.

Conclusions

Certain classes of boundary-value problems of gas flow with mixed subsonic and supersonic regions can be solved readily by numerical techniques. Adequate accuracy is obtainable with a high-speed digital computer. The problems discussed are two-dimensional but, on extension to problems where there is an axis of rotational symmetry, are quite straightforward. One simply replaces Equation [8], the continuity relation, by

$$2\pi R\rho qS = \text{const}$$

where R is the distance of a point from the axis.

The method of calculation involves determination of the radii of curvature of the streamlines. If the radius of curvature becomes so large as to exceed the capacity of the machine, precautions must be taken in programming to avoid "overflow." Stagnation points in the flow field also will cause difficulty. The author does not feel that he has a satisfactory method for treating the region of a stagnation point at the present time.

Acknowledgments

The author, on leave of absence from his country, completed this work aided by the friendship of many people in the United States. He mentions especially the friendly encouragement of Prof. H. Lurie, the kind arrangement of Prof. G. D. McCann, the valuable criticism of Prof. W. D. Rannie and Prof. D. E. Coles, and the kind help of Messrs. R. Nathan, J. Dowling, J. Vine, and B. Fischer.

Response of Nonlinearly Supported Spherical Boundaries to Shock Waves[1]

By M. L. BARON,[2] NEW YORK, N. Y.

An integral transform technique is used to solve a boundary-value problem in which the partial differential equation is linear but the associated boundary condition is nonlinear. A spherical cavity in an infinite acoustic medium has an elastically supported boundary such that the pressure-displacement relation on the boundary is nonlinear. The response of the boundary to a plane shock wave which progresses across the cavity and envelops it is obtained by solving two auxiliary boundary-value problems with linear boundary conditions. Using influence coefficients obtained from these solutions, a nonlinear integral equation for the response of the actual boundary is obtained. The integral equation is solved numerically for a set of parameters, and curves for the pressure-time and displacement-time responses of the boundary are presented.

Nomenclature

The following nomenclature is used in the paper:

r, θ, η = spherical co-ordinates, see Fig. 1
w = radial displacement of boundary of spherical cavity, positive inward
a = radius of cavity
c = velocity of sound in medium
C_m = coefficient
$F_m(t)$ = t dependent expansion coefficient of $p(\theta, t)$
$f(r, \theta, t)$, $\bar{f}(r, \theta, \Omega)$ = function of r, θ, t and corresponding transformed function with respect to time
$H_{m+1/2}^{(2)}$ = spherical Hankel function of second kind of order m
K = constant of proportionality—linear boundary
$p(\theta, t)$ = shock-wave pressure on boundary of cavity
p = constant peak pressure of step shock wave
p_t = constant peak pressure of decaying shock wave
$P_B = f(u)$ = nonlinear pressure-displacement relation on boundary of cavity
$\bar{P}_B = f(u) - Ku_0$ = pressure for determination of corrective response, $u_c(t)$
$P_m(\cos\theta)$ = zonal harmonic of order m
$q_m(t)$ = generalized co-ordinates
$\phi_0(t)$ = influence coefficient
$Q_m(t)$ = t-dependent expansion coefficient of $Z(\theta, t)$
t = time
$u(t)$ = response of spherical cavity with a nonlinear pressure-displacement boundary relation to a decaying shock wave
$u_0(t)$ = response of spherical cavity with a linear pressure-displacement boundary relation to a decaying shock wave
$u_1(t)$ = influence coefficient of auxiliary problem
$u_c(t)$ = corrective response
$U(t)$ = unit step function
$v(\theta, t)$ = radial component of particle velocity of step shock wave
$V_m(t)$ = t-dependent expansion coefficient of $v(\theta, t)$
$Z(\theta, t)$ = fluid pressure on surface of cavity
$\alpha = \cos^{-1}\left(1 - \frac{ct}{a}\right)$ = angle of envelopment
$\beta = \sqrt{(\epsilon - \epsilon^2/4)}$ = coefficient
δ = decay coefficient of shock wave
$\epsilon = \frac{Ka}{\rho c^2}$ = coefficient
$\lambda = \frac{\Omega a}{c}$ = transform variable
ρ = mass density of medium
$\varphi(\theta, r, t)$ = potential function of reflected and radiated waves in medium
$\Psi_m(r, t)$ = r and t dependent expansion coefficient of $\varphi(r, \theta, t)$
Ω = transform variable

Introduction

The use of integral transforms is a powerful technique for the solution of linear boundary-value problems. However, these methods are not applicable if the partial differential equation and/or the associated boundary conditions are nonlinear. This paper considers the possibility of extending the application of transform techniques to problems in which the governing partial differential equation is linear, but the boundary condition is nonlinear. The method will be illustrated by the solution of a specific problem: the response of a nonlinearly supported spherical cavity to a plane shock wave.

[1] This paper is a result of investigations sponsored by the Office of Naval Research, under Contract Nonr-266(08), with Columbia University.

[2] Assistant Professor of Civil Engineering, Columbia University, and Chief Engineer at Paul Weidlinger, Consulting Engineer, New York. Assoc. Mem. ASME.

Presented at the Applied Mechanics Division Summer Conference, Berkeley, Calif., June 13–15, 1957, of The American Society of Mechanical Engineers.

Discussion of this paper should be addressed to the Secretary, ASME, 29 West 39th Street, New York, N. Y., and will be accepted until January 10, 1958, for publication at a later date. Discussion received after the closing date will be returned.

Note: Statements and opinions advanced in papers are to be understood as individual expressions of their authors and not those of the Society. Manuscript received by ASME Applied Mechanics Division, February 13, 1957. Paper No. 57—APM-12.

A spherical cavity in an infinite acoustic fluid, i.e., one whose motions conform to the linear theory of waves of expansion, has an elastically supported boundary with a nonlinear pressure-displacement relation, $P_B = f(u)$. A linearly decaying plane shock wave progresses across the boundary and envelops it. The problem of the determination of the response of the boundary to the shock wave is solved in two steps. First, the response to the shock wave of a cavity with a linear pressure-displacement boundary condition $P_B = Ku$ is obtained. The next step is a modification which introduces the effect of the actual nonlinear boundary condition. Using influence coefficients obtained by solving an auxiliary problem, a nonlinear integral equation for the response of the actual boundary is obtained. The integral equation can only be solved numerically. This is done for a particular set of parameters, and curves for the pressure and displacement responses of the boundary are presented.

Response of Boundary of Spherical Cavity

Response of Boundary of a Spherical Cavity With a Linear Pressure-Displacement Relation to a Decaying Shock Wave. Consider, first, the response of the boundary of a cavity with a linear pressure-displacement relation to a step shock wave, Fig. 1. Let

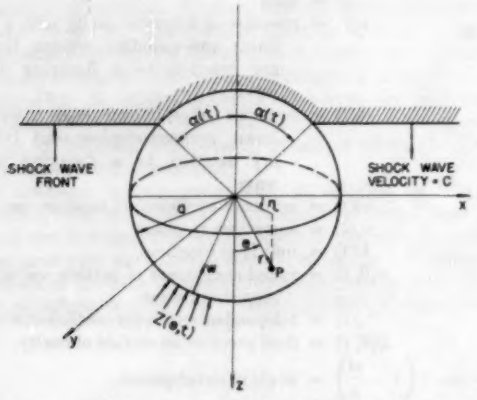

Fig. 1 Geometry of Problem—Spherical Cavity

w be the radial displacement of the boundary and Z the pressure on it, both positive inward. The pressure-displacement relation is

$$w(\theta, t) = \frac{Z(\theta, t)}{K} \quad [1]$$

where K is a constant of proportionality. Let

$$w(\theta, t) = \sum_{m=0}^{\infty} q_m(t) P_m(\cos\theta) \quad [2]$$

$$Z(\theta, t) = \sum_{m=0}^{\infty} Q_m(t) P_m(\cos\theta) \quad [3]$$

The pressure on the boundary is due to the shock wave and to waves reflected and radiated by the boundary

$$Z = p(\theta, t) + \rho\dot{\varphi}(a, \theta, t) \quad [4]$$

where $\varphi(\theta, r, t)$, the velocity potential of the acoustic medium, is given by

$$\varphi(\theta, r, t) = \sum_{m=0}^{\infty} \psi_m(r, t) P_m(\cos\theta) \quad [5]$$

For a step shock wave

$$p(\theta, t) = \begin{cases} p & \pi \geq \theta \geq \pi - \alpha \\ 0 & \pi - \alpha \geq \theta \geq 0 \end{cases} \quad [6]$$

$$p(\theta, t) = p \quad t > \frac{2a}{c} \text{ (after full envelopment)}$$

$$\alpha(t) = \cos^{-1}(1 - ct/a) \quad [7]$$

and the particle velocity at $r = a$ is

$$v(\theta, t) = \frac{-p(\theta, t)\cos\theta}{\rho c} \quad [8]$$

The radial velocity of a point on the boundary of the cavity must equal the radial components of the particle velocities of the step wave and the diffracted waves

$$\dot{w}(\theta, t) = v(\theta, t) + \left.\frac{\partial\varphi(\theta, t, r)}{\partial r}\right]_{r=a} \quad [9]$$

Letting

$$\rho c\dot{w}(\theta, t) = \sum_{m=0}^{\infty} V_m(t) P_m(\cos\theta) \quad [10]$$

$$p(\theta, t) = \sum_{m=0}^{\infty} F_m(t) P_m(\cos\theta) \quad [11]$$

substitution into Equations [1], [4], and [9] yields

$$q_m(t) = \frac{1}{K}\left[F_m(t) + \rho\dot{\psi}_m(a, t)\right] \quad [12]$$

$$q_m(t) = \frac{1}{\rho c} V_m(t) + \left[\frac{\partial}{\partial r}\psi_m(r, t)\right]_{r=a} \quad [13]$$

$$Q_m(t) = F_m(t) + \rho\dot{\psi}_m(a, t) \quad [14]$$

The velocity potential φ is governed by the wave equation

$$\nabla^2\varphi = \frac{\partial^2\varphi}{\partial r^2} + \frac{2}{r}\frac{\partial\varphi}{\partial r} + \frac{1}{r^2\sin\theta}\frac{\partial}{\partial\theta}\left(\sin\theta\frac{\partial\varphi}{\partial\theta}\right) = \frac{1}{c^2}\frac{\partial^2\varphi}{\partial t^2} \quad [15]$$

or, substituting Equation [5]

$$\frac{\partial^2\psi_m}{\partial r^2} + \frac{2}{r}\frac{\partial\psi_m}{\partial r} - \frac{m(m+1)}{r^2}\psi_m = \frac{1}{c^2}\frac{\partial^2\psi_m}{\partial t^2} \quad [16]$$

A transform with respect to time is applied.

$$\bar{f}(r, \theta, \Omega) = \frac{1}{2\pi}\int_0^{\infty} f(r, \theta, t) e^{-i\Omega t} dt \quad [17]$$

$$f(r, \theta, t) = \int_{-\infty - i\gamma}^{\infty - i\gamma} \bar{f}(r, \theta, \Omega) e^{i\Omega t} d\Omega \quad [18]$$

This is essentially the usual Laplace transform except that the variable s is replaced by $i\Omega$.

Equation [16] becomes

$$\frac{\partial^2\bar{\psi}_m}{\partial r^2} + \frac{2}{r}\frac{\partial\bar{\psi}_m}{\partial r} + \left(\frac{\Omega^2}{c^2} - \frac{m(m+1)}{r^2}\right)\bar{\psi}_m = 0 \quad [19]$$

and the solution for divergent waves is

$$\bar{\psi}_m(r, \Omega) = C_m \frac{H^{(2)}_{m+1/2}\left(\frac{\Omega r}{c}\right)}{\sqrt{\left(\frac{\Omega r}{c}\right)}} \quad [20]$$

The constant C is determined by transforming Equations [12] and [13] and substituting Equation [20]

$$C_m = \frac{\frac{i\Omega}{K}\bar{F}_m - \frac{1}{\rho c}\bar{V}_m}{H' + \frac{\rho\Omega^2}{K}\frac{H_{m+1/2}^{(2)}\left(\frac{\Omega a}{c}\right)}{\sqrt{\left(\frac{\Omega a}{c}\right)}}} \quad \ldots\ldots [21]$$

where

$$H' = \frac{d}{dr}\left(\frac{H_{m+1/2}^{(2)}\left(\frac{\Omega r}{c}\right)}{\sqrt{\left(\frac{\Omega r}{c}\right)}}\right)\Bigg]_{r=a}$$

From Equation [12], the response of the boundary is

$$\bar{q}_m = \frac{1}{K}\left[\bar{F}_m + \rho i\Omega\bar{\psi}_m\right]_{r=a}$$

which upon substitution of Equations [20] and [21] becomes

$$\bar{q}_m = \frac{1}{K}\left[\frac{\bar{F}_m H' - \frac{i\Omega}{c}\frac{H_{m+1/2}^{(2)}\left(\frac{\Omega a}{c}\right)}{\sqrt{\left(\frac{\Omega a}{c}\right)}}\bar{V}_m}{H' + \frac{\rho\Omega^2}{K}\frac{H_{m+1/2}^{(2)}\left(\frac{\Omega a}{c}\right)}{\sqrt{\left(\frac{\Omega a}{c}\right)}}}\right] \quad \ldots\ldots [22]$$

In another paper,[1] it is shown that the major effect for a wave of moderately long duration is given by the zero mode of motion. Since the present paper is concerned with a generalization of the problem considered there, it was concluded that the major effect is given by the $m = 0$ term of the series for the response of the cavity. Therefore, only the radially symmetric zero mode is considered in this paper.

For the mode $m = 0$

$$H_{1/2}^{(2)}(\lambda) = \left(\frac{2}{\pi\lambda}\right)^{1/2} ie^{-\lambda} \quad \ldots\ldots [23]$$

and

$$\bar{q}_0 = \frac{1}{K}\left[\frac{\bar{F}_0(1 - i/\lambda) + \bar{V}_0}{(1 - i/\lambda) + \frac{\rho c^2}{Ka}\lambda i}\right] \quad \ldots\ldots [24]$$

where $\lambda = \Omega a/c$. The transforms of the pressure and velocity coefficients $\bar{F}_0$ and $\bar{V}_0$ are evaluated from Equations [6]–[8] and [17]

$$\bar{F}_0 = \frac{pa}{4\pi c}\left[\frac{e^{-2i\lambda} - 1}{\lambda^2}\right] \quad \ldots\ldots [25]$$

$$\bar{V}_0 = \frac{pa}{4\pi c\lambda^2}\left[i(e^{-2i\lambda} - 1) - \lambda(e^{-2i\lambda} + 1)\right] \quad \ldots\ldots [26]$$

Substituting Equations [25] and [26] into [24]

$$\bar{q}_0(\lambda) = \frac{pa\epsilon}{2\pi iKc\lambda}\left[\frac{-1}{\lambda^2 - \epsilon i\lambda - \epsilon}\right] \quad \ldots\ldots [27]$$

where $\epsilon = (Ka)/(\rho c^2)$. The response $q_0(t)$ is obtained by inverting Equation [27]

$$q_0(t) = \frac{p\epsilon}{2\pi iK}\int_{-\infty - i\gamma}^{\infty - i\gamma}\frac{1}{\lambda}\left(\frac{-1}{\lambda^2 - \epsilon i\lambda - \epsilon}\right)e^{\Omega ct/a}d\lambda \quad \ldots [28]$$

The integrand contains three poles

$$\lambda_1 = 0$$

$$\lambda_{2,3} = \frac{\epsilon i}{2} \pm \sqrt{\left(\epsilon - \frac{\epsilon^2}{4}\right)} \quad \ldots\ldots [29]$$

and the inversion integral is evaluated by the residue theorem. The result becomes

$$q_0(t) = \frac{p}{K}\left[1 - e^{-\frac{\epsilon c}{2a}t}\left(\cos\frac{\beta ct}{a} + \frac{2\beta}{4 - \epsilon}\sin\frac{\beta ct}{a}\right)\right] \quad \ldots [30]$$

where

$$\beta = \sqrt{\left(\epsilon - \frac{\epsilon^2}{4}\right)}$$

The response of the boundary of the cavity to a linearly decaying shock wave of the form

$$p(t) = p_0 - \delta t \quad \ldots\ldots [31]$$

can be determined by the use of Duhamel's theorem. This response is given by

$$u_0(t) = p(0)\phi_1(t) + \int_0^t \phi_1(t - \theta)p'(\theta)d\theta \quad \ldots\ldots [32]$$

where $\phi_1(t)$ is the response of the boundary to a step shock wave of unit pressure and is given by Equation [30] with $p = 1$. For the linearly decaying pressure wave of Equations [31], Equation [32] takes the form

$$u_0(t) = p_0\phi_1(t) - \delta\int_0^t \phi_1(t - \theta)d\theta \quad \ldots\ldots [33]$$

and upon integration becomes

$$u_0(t) = \frac{1}{K}\left\{p_0 + \frac{\delta a}{c}\left(1 - \frac{ct}{a}\right) - \left(p_0 + \frac{\delta a}{c}\right)e^{-\frac{\epsilon c}{2a}}\cos\frac{\beta ct}{a} - \frac{2\beta}{4 - \epsilon}\left[p_0 - \frac{\delta a}{\epsilon c}(2 - \epsilon)\right]e^{-\frac{\epsilon c}{2a}t}\sin\frac{\beta ct}{a}\right\} \quad \ldots\ldots [34]$$

Auxiliary Problem

Response of Boundary of a Spherical Cavity With a Linear Pressure-Displacement Relation to a Suddenly Applied Radially Symmetric Unit Step Pressure. The second step in the determination of the response of the spherical cavity with the nonlinear pressure-displacement boundary relationship is a modification which introduces the effect of the nonlinearity of the boundary condition. This requires the use of influence coefficients $u_1(t)$, which are obtained by solving the auxiliary problem of this section.

The procedure for obtaining the response of the linear boundary to a suddenly applied radially symmetrical unit step pressure follows that of the preceding section. The pressure on the boundary is independent of θ and is given by

$$Q(t) = -U(t) + \rho\dot{\psi}_0(a, t) \quad \ldots\ldots [35]$$

The response of the boundary is

[1] "Response of an Elastic Cylindrical Shell to a Transverse Step Shock Wave," by R. D. Mindlin and H. H. Bleich, Journal of Applied Mechanics, Trans. ASME, vol. 75, 1953, p. 189.

$$u_1(t) = \frac{1}{K}\,[\rho\dot{\psi}_d(a, t) - U(t)] \quad [36]$$

and the boundary condition corresponding to Equation [9] becomes

$$\dot{u}_1(t) = \frac{\partial}{\partial a}\,\dot{\psi}_d(a, t) \quad [37]$$

Proceeding as in the preceding section, the transform $\dot{u}_1(\lambda)$ is given by

$$\dot{u}_1(\lambda) = \frac{a\epsilon}{Kc}\,\frac{1}{2\pi i}\left[\frac{i\lambda + 1}{\lambda(\lambda^2 - \epsilon i\lambda - \epsilon)}\right] \quad [38]$$

and $u_1(t)$ is obtained from the inversion integral

$$u_1(t) = \frac{\epsilon}{K}\,\frac{1}{2\pi i}\int_{-\infty - i\gamma}^{\infty - i\gamma} \frac{(1 + i\lambda)e^{\Omega ct/a}d\lambda}{\lambda(\lambda^2 - \epsilon i\lambda - \epsilon)} \quad [39]$$

The integrand contains the three poles given by Equation [29] and the integral is evaluated by the residue theorem. The influence coefficient $u_1(t)$ becomes

$$u_1(t) = -\frac{1}{K}\left[1 - e^{-\frac{\epsilon c}{2a}t}\left(\cos\frac{\beta c}{a}t - \frac{2\beta}{4 - \epsilon}\sin\frac{\beta c}{a}t\right)\right] \quad [40]$$

where β and ϵ are defined in the preceding section.

Response of a Spherical Cavity

Response of a Spherical Cavity With a Nonlinear Pressure-Displacement Boundary Relation to a Decaying Shock Wave. Let the nonlinear pressure-displacement relation at the boundary of the cavity be

$$P_B = f(u) \quad [41]$$

The displacement-time response $u(t)$ of the cavity to the decaying shock wave can be evaluated by means of the previously determined functions $u_0(t)$ and $u_1(t)$. Let $u_0(t)$ and the corresponding pressure Ku_0 be the response of a linearly supported boundary to the shock wave, where the coefficient K is the initial tangent of the pressure-displacement equation, Equation [41]

$$K = \left.\frac{dP_B}{du}\right]_{u=0} = \left.\frac{df(u)}{du}\right]_{u=0} \quad [42]$$

The difference between the actual pressure P_B and the pressure Ku_0 is at any time t

$$\bar{P}_B = P_B - Ku_0 = f(u) - Ku_0 \quad [43]$$

where u_0 and u are the corresponding values of the responses of the linear and nonlinear cavities, respectively, at the time t. The effect of the pressure $\bar{P}_B$ can be considered as a corrective response, $u_c(t)$, which is subtracted from $u_0(t)$ in order to obtain the response of the actual cavity, $u(t)$

$$u(t) = u_0(t) - u_c(t) \quad [44]$$

To determine u_c, consider the pressure $\bar{P}_B = \bar{P}_B(\xi)$ and advance along the time axis in steps of $\Delta\xi$, Fig. 3. The action of the pressure $\bar{P}_B$ is taken as an application of steps $\Delta\bar{P}_B$ at small intervals of $\Delta\xi$. Thus

$$u_c(t) = \sum_{\xi=\Delta t}^{t} \Delta\bar{P}(\xi)u_1(t - \xi) = \sum_{\xi=\Delta t}^{t} \frac{\Delta\bar{P}(\xi)}{\Delta\xi}\,u_1(t - \xi)\Delta\xi \quad [45]$$

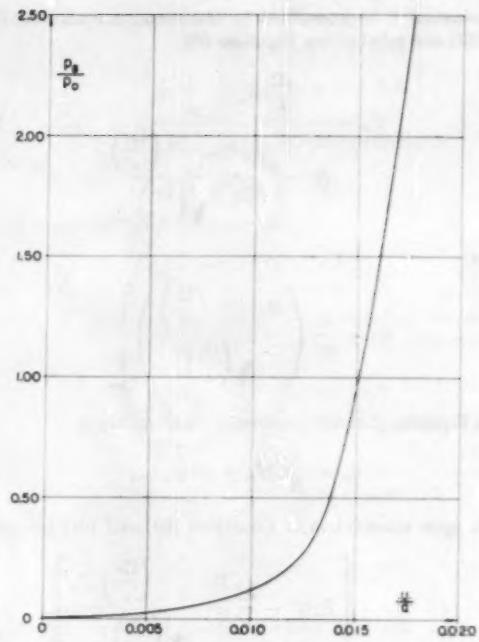

Fig. 2 Pressure-Displacement Relation on Boundary of Cavity

where the influence coefficient $u_1(t)$ is given by Equation [40] with

$$K = \left.\frac{df(u)}{du}\right]_{u=0}$$

Taking the limits as $\Delta\xi \to 0$, the response $u_c(t)$ becomes

$$u_c(t) = \int_0^t \frac{d\bar{P}_B(\xi)}{d\xi}\,u_1(t - \xi)d\xi \quad [46]$$

or, as $\bar{P}_B$ is given as a function of u

$$u_c(t) = \int_0^t \frac{d\bar{P}_B[u(\xi)]}{d\xi}\,u_1(t - \xi)d\xi \quad [47]$$

Substitution of Equations [47] into [44] gives the response of the cavity

$$u(t) = u_0(t) - \int_0^t \frac{d\bar{P}_B[u(\xi)]}{d\xi}\,u_1(t - \xi)d\xi \quad [48]$$

Equation [48] is a nonlinear integral equation for the response $u(t)$. It may be solved numerically once $u_0(t)$ and $u_1(t)$ have been evaluated. This requires the specification of the geometry of the cavity, the nonlinear pressure-displacement boundary relation, and the shock loading.

Solution of Integral Equation for a Particular Case

The integral equation, Equation [48], was solved numerically for a spherical cavity in an acoustic fluid with the pressure-displacement boundary relation[4] shown in Fig. 2.

The response of the cavity $u(t)$ to a linearly decaying plane

[4] This relation is of the form

$$P_B = f(u) = [C_1u - C_3] + [(C_1u - C_2)^2 + C_4u]^{1/2}$$

where all the constants C_i are positive.

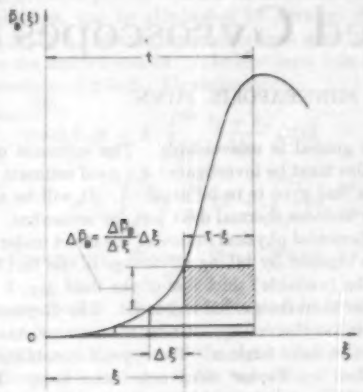

FIG. 3 DETERMINATION OF u_0

shock wave, Fig. 4, was obtained by a forward integration of Equation [48] in steps of time. The derivative $(dP_B)/(d\xi)$ was approximated by a four-point backward difference formula with an error of order (h^4), and the numerical integration for each step was performed by the use of Simpson's rule with an error of order (h^4), where h is the spacing of the time steps.[4]

The strong nonlinearity of the pressure-displacement relation of Fig. 2 required the use of small time steps in the forward integration of Equation [48]. For the major portion of the range considered, time steps of magnitude $ct/a = 0.05$ were used. As each nth step required the determination of the corrective response $u_c(t)$ by a separate integration involving $n - 1$ terms, the numerical work became exceedingly long and cumbersome. In the very steeply rising portion of the response curve shown in Fig. 4, $4.20 \leq ct/a \leq 4.50$, time steps of a magnitude smaller than $ct/a = 0.05$ would have been required for numerical accuracy. For this range, an inverse procedure in which pressure steps were taken as the variable was used. This procedure is very complex and was only used for this range of the curve.

The resulting pressure-time history at the boundary of the spherical cavity is shown in Fig. 4, along with the input pressure of the linearly decaying shock wave. It is convenient to discuss this curve in terms of the transit time of the shock wave across the cavity, $t_a = \frac{2a}{c}$. The points of interest here are the peak value of the pressure on the boundary and the extremely rapid rise to this peak. After a delay of nearly $2t_a$, the pressure rises in less than one transit time to more than twice the maximum pressure of the incoming shock wave. A less rapid decay brings the pressure down to the incoming wave pressure in the range

[4] "Numerical Methods in Engineering Problems," by M. G. Salvadori and M. L. Baron, Prentice-Hall, Inc., New York, N. Y., first edition, second printing, 1955, Chapters II–IV.

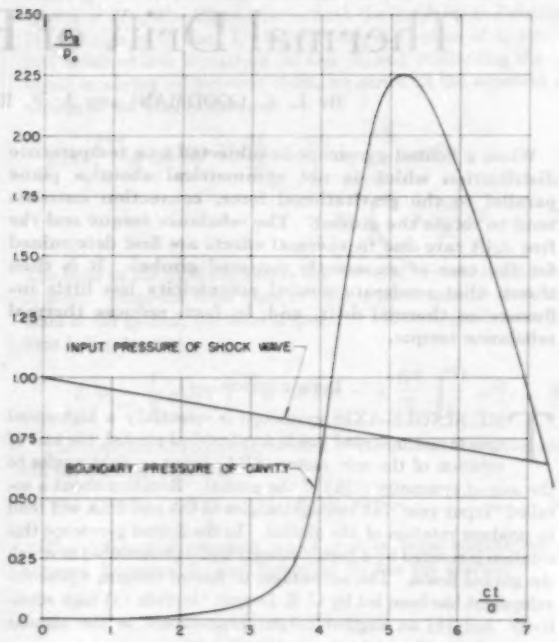

FIG. 4 PRESSURE-TIME RESPONSE OF SPHERICAL CAVITY

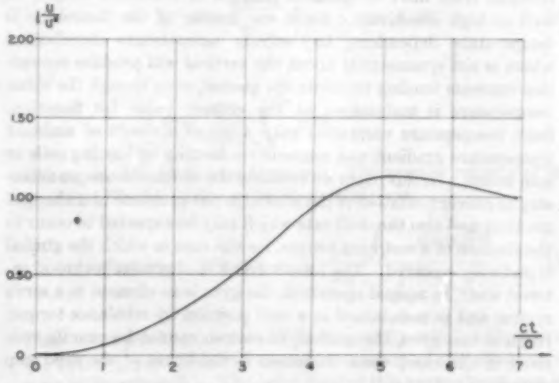

FIG. 5 DISPLACEMENT-TIME RESPONSE OF SPHERICAL CAVITY

shown in the figure. Fig. 5 shows the displacement-time response of the boundary of the cavity. The ratio u/u^* is given where u^* is the static response of the nonlinearly supported cavity to the peak shock pressure p_0.

Thermal Drift of Floated Gyroscopes[1]

By L. E. GOODMAN[2] and A. R. ROBINSON,[3] MINNEAPOLIS, MINN.

When a floated gyroscope is subjected to a temperature distribution which is not symmetrical about a plane parallel to the gravitational force, convection currents tend to rotate the gimbal. The rebalance torque and the free drift rate due to thermal effects are first determined for the case of an exactly centered gimbal. It is then shown that moderate gimbal eccentricity has little influence on thermal drift, and, in fact, reduces thermal rebalance torque.

Introduction

THE SINGLE-AXIS gyroscope is essentially a high-speed spin motor mounted inside a cylindrical gimbal, the axis of rotation of the spin motor (SRA) being at right angles to the axis of symmetry (OA) of the gimbal. Rotation about a so-called "input axis" (IA) at right angles to OA and SRA will tend to produce rotation of the gimbal. In the floated gyroscope this rotation is resisted by a highly viscous liquid (fluorolube) in which the gimbal floats. The advantages of floated designs, whose development has been led by C. S. Draper,[4] include (*a*) high sensitivity and (*b*) an angular output proportional to the angular input, whence the name "integrating" gyro.

The requirements of modern inertial guidance systems include freedom from drift or spurious changes in rebalance torque, as well as high sensitivity. Since the density of the fluorolube is temperature dependent, any steady temperature distribution which is not symmetrical about the vertical will produce convection currents tending to rotate the gimbal, even though the mean temperature is maintained at the correct value for flotation. Such temperature variations may arise as a result of ambient temperature gradient and nonuniform heating by heating coils or spin motor. In this paper we evaluate the rebalance torque necessary to prevent rotation of the gimbal in the presence of a thermal gradient and also the drift rate which may be expected to occur in the absence of a restoring torque, for the case in which the gimbal is perfectly centered. The former result is of greater technical interest since, in normal operation, the gyro is an element in a servo system and is maintained in a null position by rebalance torque. In an actual gyro, the gimbal, of course, cannot be exactly centered in the case; some variation in thickness of the fluid gap around the gimbal is unavoidable. The influence of such eccentricity also must be investigated if a good estimate of thermal effects on a real gyro is to be attained. It will be shown that eccentricity reduces thermal drift torques somewhat.

The fundamental physical nature of the effect under consideration can be exposed by taking advantage of the fact that, in application, the (variable) thickness of the fluid gap, $h = h(\theta)$, is much smaller than the gimbal radius R. The Reynolds number of the flow is less than unity. Under these circumstances flow in the gap is essentially laminar. The type of instability of viscous flow described by Taylor[5] does not occur here. Taking OA horizontal, the most unfavorable orientation, and neglecting axial flow, we have a two-dimensional problem. Conservation of mass requires that at any time t

$$\bar{u}\rho h = \text{const, say} = C(t) \quad \ldots\ldots\ldots\ldots\ldots [1]$$

Here $\bar{u} = \bar{u}(\theta, t)$ is the mean circumferential component of velocity at any radial section. The circumstance that the temperature $T = T(\theta)$ and that the velocity is small permits taking the fluid density ρ as a function of θ only. The shear stresses acting on the surfaces $r = R$ and $r = R + h$ are: $\mu[\partial u(R, \theta, t)/\partial r]$; $\mu[\partial u(R + h, \theta, t)/\partial r]$, respectively. The symbol μ denotes the absolute coefficient of viscosity and $u(r, \theta, t)$ is the circumferential component of fluid velocity. For convenience of notation we write

$$\partial u(R, \theta, t)/\partial r = k_i\bar{u}/h;\ \partial u(R + h, \theta, t)/\partial r = -k_o\bar{u}/h \ldots [2]$$

The dimensionless quantities k_i and k_o defined by Equation [2] will be independent of θ if the velocity distribution is similar at all cross sections. They will be independent of time when the flow is steady. The equation of motion, in a circumferential direction, for the fluid included between two nearby radii and of unit thickness along OA (see Fig. 1) takes the form

$$-h\frac{\partial p}{\partial \theta} - gRh\rho\cos\theta - R(k_i + k_o)\mu\frac{\bar{u}}{h} = Rh\rho\frac{D\bar{u}}{Dt}$$

$$= Rh\rho\left(\frac{\partial \bar{u}}{\partial t} + \frac{\bar{u}}{R}\frac{\partial \bar{u}}{\partial \theta}\right) \ldots\ldots [3]$$

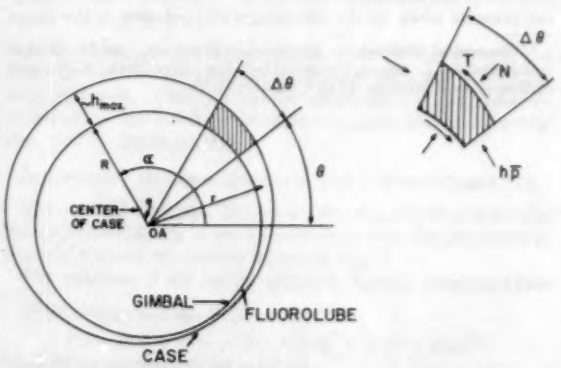

Fig. 1 Cross Section of Floated Gimbal (Not to Scale)

[1] These results are part of an investigation of the sources of gyroscope drift undertaken by the Gyro Section, Design and Development Department, Aeronautical Division, Minneapolis-Honeywell Regulator Co., under supervision of J. W. Lower, Section Chief.

[2] Professor of Mechanics, Department of Mechanics and Materials, University of Minnesota. Mem. ASME.

[3] Research Associate, Department of Mechanics and Materials, University of Minnesota. Assoc. Mem. ASME.

[4] "The Floating Integrating Gyro and Its Application to Geometrical Stabilization Problems on Moving Bases," by C. S. Draper, W. Wrigley, and L. R. Grohe, *Aeronautical Engineering Review*, vol. 15, June, 1956, pp. 46–62.

[5] "Modern Developments in Fluid Dynamics," edited by S. Goldstein, Oxford University Press, London, England, 1938, pp. 196–197, 322, 385–390.

Presented at the Applied Mechanics Division Summer Conference, Berkeley, Calif., June 13–15, 1957, of The American Society of Mechanical Engineers.

Discussion of this paper should be addressed to the Secretary, ASME, 29 West 39th Street, New York, N. Y., and will be accepted until January 10, 1958, for publication at a later date. Discussion received after the closing date will be returned.

Note: Statements and opinions advanced in papers are to be understood as individual expressions of their authors and not those of the Society. Manuscript received by ASME Applied Mechanics Division, August 27, 1956. Paper No. 57—APM-31.

The mean pressure $p(\theta, t)$, which is of little engineering interest in this problem, can be eliminated by dividing each term of Equation [3] by h and then integratin; each term with respect to θ between the limits 0 and 2π. The first term falls out by virtue of the periodicity of p in θ. Consequently

$$-gR\int_0^{2\pi}\rho\cos\theta\,d\theta - R\int_0^{2\pi}\frac{k_i+k_o}{h^2}\mu\bar{u}d\theta = R\int_0^{2\pi}\rho\frac{\partial\bar{u}}{\partial t}d\theta + \int_0^{2\pi}p\bar{u}\frac{\partial\bar{u}}{\partial\theta}d\theta \quad [4]$$

Case I—Concentric Gimbal Held Fixed by Rebalance Torque

In this case the flow is steady so that the first term on the right-hand side of Equation [4] vanishes. If h is constant (concentric gimbal) the remaining term on the right-hand side of Equation [4] also disappears in view of the equation of conservation of mass, Equation [1], and the periodicity of $\bar{u}$. The torque L exerted on the gimbal by the fluid is given by the expression

$$L = lR^2\int_0^{2\pi}\frac{k_i}{h}\mu\bar{u}_i l\theta \quad [5]$$

where l is the length of the gimbal. If the flow pattern is similar at all cross sections, k_i and k_o are numerical constants. Since both boundaries are at rest and $(h/R)\ll 1$, $k_i = k_o$. Substituting Equation [5] in [4] and remembering that the right-hand side of Equation [4] is zero for this case, we have at once the desired result

$$L_o = -\frac{1}{2}g\rho hR^2\int_0^{2\pi}\rho(\theta)\cos\theta d\theta \quad [6]$$

It should be noted that the torque is independent of the viscosity and, moreover, of any temperature-induced variations in the viscosity. This implies that a fluid of low viscosity circulates more rapidly than a highly viscous one, but both give the same total drag. As one would expect, uniform temperature distribution, or, indeed, any temperature distribution which results in a density symmetrical about the vertical axis, produces no torque.

Some feeling for the magnitudes of the quantities involved may be obtained by considering a temperature variation of 1 deg C across the gimbal. Taking $T = T_0 + (0.5)\cos\theta$ and $\rho = \rho_0 + 1.5(10^{-3})(T_0 - T)$ it follows that

$$-\int_0^{2\pi}\rho(\theta)\cos\theta d\theta = 2.4(10^{-3}) \text{ gm per cc}$$

For $l = 6.0$ cm, $R = 3.0$ cm, and $h = 0.015$ cm, the rebalance torque predicted by Equation [6] is 0.95 dyne-cm. In practice, some of the fluid will be short-circuited around the ends of the gimbal. Such axial flow will result in a torque slightly smaller than the calculated value. The fact that 1 dyne-cm is by no means a negligible torque in the applications contemplated provides an indication of the extent to which temperature control is necessary in the design of sensitive drift-free gyros. The effect is proportional to the fourth power of the linear dimensions of the gyro.

Case II—Free Drift of Concentric Gimbal

If the rebalance torque is released the gimbal will rotate under the influence of the convection currents. Take the radial distribution of velocity to be quadratic. Then

$$u = -(6\bar{u} - 3u_i)\left(\frac{r-R}{h}\right)^2 + (6\bar{u} - 4u_i)\left(\frac{r-R}{h}\right) + u_i, \qquad R \le r \le R + h$$

where $u_i = u(R, \theta, t)$. One easily finds that $k_i = 6 - 4(u_i/\bar{u})$ and $k_o = 6 - 2(u_i/\bar{u})$. Since h is constant the last term in Equation [4] vanishes as in Case I. Substituting the values of k_i and k_o just obtained into Equations [4] and [5] and eliminating the integral involving $\mu\bar{u}$ between them, we arrive at the equation of motion of the fluid in the form

$$-g\rho h\int_0^{2\pi}\rho\cos\theta d\theta - \frac{2L}{lR} - \frac{2R}{h}u_i\int_0^{2\pi}\mu d\theta = Rh\int_0^{2\pi}\rho\frac{\partial\bar{u}}{\partial t}d\theta \quad [7]$$

The term on the right represents the inertia of the entrained mass of fluid. Since the total mass of fluid is much smaller than the mass of the gimbal, the term in question will be neglected for the time being, leaving

$$L = -\frac{1}{2}g\rho hR^2 l\int_0^{2\pi}\rho\cos\theta d\theta - u_i\frac{R^2 l}{h}\int_0^{2\pi}\mu d\theta \quad [8]$$

The equation of rotational motion of the gimbal about the axis OA through the pivots is

$$L = (I_{OA}/R)(du_i/dt) \quad [9]$$

The differential equation which results from eliminating L between Equation [8] and Equation [9] has the solution

$$u_i = \frac{A}{B}(1 - e^{-Bt})$$

where

$$A = -\frac{g\rho hR^2 l}{2I_{OA}}\int_0^{2\pi}\rho\cos\theta\,d\theta \quad [10]$$

and

$$B = \frac{R^2 l}{hI_{OA}}\int_0^{2\pi}\mu d\theta$$

if the gimbal is accelerated from rest. The angular velocity of the gimbal u_i/R approaches a limiting value; viz.

$$\text{Maximum drift rate} = -\frac{g\rho h^2}{2R}\frac{\int_0^{2\pi}\rho\cos\theta d\theta}{\int_0^{2\pi}\mu d\theta} \quad [11]$$

Flow corresponding to this drift rate exactly satisfies Equations [7] and [9], justifying the temporary neglect of the accelerative term in Equation [7]. The only effect of this approximation is an overestimate of the time constant B. For a gyro of the type under consideration, B is greater than 2×10^2 per sec, and the steady state is reached in a small fraction of a second.

For a 1 deg C temperature drop across a gyroscope of the dimensions given in Case I, and a mean fluorolube viscosity of 600 centipoises, the maximum drift rate predicted by Equation [11] is 0.48 deg per hr. As in the previous case, any axial flow that may be present will operate to reduce this drift rate.

Case III—Eccentric Gimbal Held Fixed by Rebalance Torque

If the gimbal is mounted eccentrically the thickness h may be approximated very closely by $h = h_0 + e\cos(\theta - \alpha)$, where h_0 is the mean thickness, $e(\le h)$ the eccentricity, and α gives the direction along which the center of the gimbal is displaced from the center of the case. Since the gimbal is held fixed, $\bar{u}$ is not a function of time, and Equation [4] reduces to

$$-gR\int_0^{2\pi}\rho\cos\theta d\theta - R\int_0^{2\pi}(k_i+k_o)\mu\frac{\bar{u}}{h^2}\,d\theta = \int_0^{2\pi}\rho\bar{u}\frac{d\bar{u}}{d\theta}\,d\theta \quad [12]$$

The torque L is given by Equation [5] with $h = h(\theta)$. Replacing the mean circumferential velocity $\bar{u}$ by $C/\rho h$ in accordance with Equation [1], we see from Equations [12] and [5] that

$$C^2\int_0^{2\pi}\frac{1}{\rho^3h^3}\frac{d(\rho h)}{d\theta}d\theta - CR\int_0^{2\pi}(k_i+k_o)\frac{\mu}{\rho h^2}\,d\theta - gR\int_0^{2\pi}\rho\cos\theta d\theta = 0 \quad [12a]$$

$$L = ClR^2\int_0^{2\pi}\frac{k_i\mu}{\rho h^2}\,d\theta \quad [5a]$$

Here, as in Case I, k_i and k_o will be equal constants, $k_i = k_o = k$. Equation [12a] is a quadratic equation in C, whose solution is

$$C = \frac{Rk\int_0^{2\pi}\frac{\mu}{\rho h^2}\,d\theta}{\int_0^{2\pi}\frac{1}{\rho^2h^2}\frac{d(\rho h)}{d\theta}\,d\theta}\left\{1-\left[1+gR\int_0^{2\pi}\rho\cos\theta d\theta\times\int_0^{2\pi}\frac{1}{\rho^2h^2}\frac{d(\rho h)}{d\theta}\,d\theta\left(Rk\int_0^{2\pi}\frac{\mu}{\rho h^2}\,d\theta\right)^{-2}\right]^{1/2}\right\} \quad [13]$$

The negative sign has been chosen in front of the radical in order that C be zero when ρ is constant.

Since ρ, μ, and h are positive, and $(d\rho/d\theta) < \rho$

$$\int_0^{2\pi}\frac{1}{\rho^2h^2}\frac{d(\rho h)}{d\theta}\,d\theta < \frac{3h_0}{\mu_{min}}\int_0^{2\pi}\frac{\mu}{\rho h^2}\,d\theta;$$

$$\int_0^{2\pi}\frac{\mu}{\rho h^2}\,d\theta > \frac{\mu_{min}}{\rho_{max}}\frac{2\pi}{(2h_0)^3}$$

Applying these results to the second term under the radical in Equation [13], it is easy to show that this term is smaller than 10^{-3} for a gyroscope with constants given under Cases I and II. The square root may then be approximated by the first two terms in its binomial expansion, leaving

$$C = -\frac{g}{2k}\frac{\int_0^{2\pi}\rho\cos\theta d\theta}{\int_0^{2\pi}\frac{\mu}{\rho h^3}\,d\theta} \quad [14]$$

This value of C might have been obtained by dropping the term in C^2 in Equation [12a]; i.e., the term which arose from substituting for $\bar{u}(d\bar{u}/d\theta)$. As is expected when dealing with small velocities, this nonlinear term in $\bar{u}$ is much smaller than the other two terms.

The rebalance torque, Equation [5a], becomes finally

$$L = -\frac{1}{2}glR^2\int_0^{2\pi}\rho\cos\theta d\theta\frac{\int_0^{2\pi}\frac{\mu}{\rho h^2}\,d\theta}{\int_0^{2\pi}\frac{\mu}{\rho h^3}\,d\theta} = L_0\frac{\frac{1}{h_0}\int_0^{2\pi}\frac{\mu}{\rho h^2}\,d\theta}{\int_0^{2\pi}\frac{\mu}{\rho h^3}\,d\theta} \quad [15]$$

where L_0 is the rebalance torque with a concentric gimbal, Case I. Even for an eccentric gimbal, thermal drift will occur only if there is a thermal gradient at right angles to the gravitational field. Since $\mu\rho$ does not change by more than a few per cent for moderate temperature gradients, the inequalities

$$\frac{\mu_{min}\rho_{min}}{\mu_{max}\rho_{max}}\frac{\frac{1}{h_0}\int_0^{2\pi}\frac{d\theta}{h^2}}{\int_0^{2\pi}\frac{d\theta}{h^3}} < \frac{L}{L_0} < \frac{\mu_{max}\rho_{max}}{\mu_{min}\rho_{min}}\frac{\frac{1}{h_0}\int_0^{2\pi}\frac{d\theta}{h^2}}{\int_0^{2\pi}\frac{d\theta}{h^3}}$$

lead to the approximation

$$\frac{L}{L_0} \cong \frac{\frac{1}{h_0}\int_0^{2\pi}\frac{d\theta}{h^2}}{\int_0^{2\pi}\frac{d\theta}{h^3}} \quad [16]$$

Note that the integrals involved are independent of α, for

$$\int_0^{2\pi}\frac{d\theta}{[h_0+e\cos(\theta-\alpha)]^n} = \int_0^{2\pi}\frac{d\theta}{[h_0+e\cos\theta]^n}$$

These definite integrals may easily be evaluated by complex integration around the unit circle, or by noting their relation to Jacobi's integral[6] for the Legendre functions

$$P_n(x) = \frac{1}{\pi}\int_0^{\pi}\frac{d\theta}{[x+(x^2-1)^{1/2}\cos\theta]^{n+1}}$$

We have

$$\frac{L}{L_0} \cong \frac{P_1(\beta)}{\beta P_2(\beta)} = \frac{1-\left(\frac{e}{h_0}\right)^2}{1+\frac{1}{2}\left(\frac{e}{h_0}\right)^2} \quad [17]$$

where

$$\beta = [1-(e/h_0)^2]^{-1/2}$$

The effect of eccentricity is to reduce the rebalance torque below the value which it would have were the gimbal perfectly centered. For small eccentricity ratios e/h_0 the reduction is slight. Furthermore it seems not unlikely that the temperature gradients will be more severe for an eccentric gimbal. The maximum eccentricity ratio of unity, corresponding to the gimbal rubbing on the case and cutting off the circulation altogether, results in zero torque. Of course, large eccentricities are undesirable for other reasons.

The principal conclusions to be drawn from Case III are that Equations [6] and [11] provide close upper bounds for thermal drift torque and free thermal drift rate even when the gimbal is eccentric.

[6] "Course of Modern Analysis," by E. T. Whittaker and G. N. Watson, Cambridge University Press, London, England, second edition, 1915, p. 308.

A Photoelastic Study of Maximum Tensile Stresses in Simply Supported Short Beams Under Central Transverse Impact

By A. A. BETSER[1] and M. M. FROCHT[2]

Simply supported short Castolite beams of uniform rectangular cross section were subjected to central transverse impact by a heavy mass. Photoelastic streak photographs were taken of the transverse section of symmetry for a wide range of spans, widths, and impact velocities at exposures of less than 1 microsec. The maximum tensile stresses were determined. Comparison with the elementary theory for long beams shows that while this theory is satisfactory for long beams, it does not agree with the results from short beams. An approximate theory for short beams under central impact is developed which gives satisfactory agreement. The duration of impact also was determined and the appearance of isotropic points is discussed.

Introduction

In recent years, stresses produced by impact and shock loading have been the subject of considerable research by theoreticians and experimentalists. Because of the mathematical complications, relatively few impact problems have thus far been solved theoretically. Also, the more exact solutions available are not readily usable even in such simple cases as the compression bar.

Most practical problems cannot be solved theoretically and it becomes imperative to look for a solution through an experimental method. In a recent paper, Frocht and Flynn (1)[3] have shown that the photoelastic method employing streak photography holds much promise for the solution of impact problems. By means of this method it is now possible to determine boundary stresses and maximum shears in two-dimensional problems.

A streak photograph is obtained by masking the whole model except for a narrow rectangular zone or line element through which the light is allowed to pass. The image of this line element is adjusted on a strip of moving film so that it is perpendicular to the direction of motion. The stress pattern thus obtained gives a continuous time record of the changing birefringence on the chosen line.

This paper deals with the application of streak photography to the determination of the maximum tensile stresses in simply supported short beams under central impact. An approximate theory is developed for the maximum tension in such beams which agrees satisfactorily with the experimental results. In addition, the duration of impact is discussed and some observations are made on the fluctuation of the isotropic points.

In 1935 some work on beams was done by Tuzi and Nisida (2) who also employed photoelastic streak photography. However, their time of exposure was of the order of 20 microsec as compared with less than 1 microsec for the present investigation. Tuzi and Nisida investigated the maximum fiber stresses on a transverse line close to the load. In the present study, the maximum tension was determined on the transverse section directly through the line of impact. The only beam dimension varied by Tuzi and Nisida was the span. In the present work the scope was extended to include variations in the depth of the beam. Also, our range of spans was considerably greater than that employed by Tuzi and Nisida.

The photoelastic study of the stresses in beams rests on the assumption that the dynamic stress-optic law is linear with respect to the thickness t, and the difference of the principal stresses $p - q$; i.e., that the fringe value is a constant. This has been established for Castolite for the one-dimensional case by Frocht, Flynn, and Betser (3, 4, 5).

Equipment and Scope of Investigation

The photoelastic equipment and techniques used in the present investigation are, with minor changes, the same as those employed by P. D. Flynn in his dynamic studies and described in previous papers (1, 6, 7). The beam was supported on a heavy anvil, Fig. 1, and struck by a hammer which formed the lower part of a pendulum consisting of a 48.2-in. arm of thin-walled tubing, and a steel hammer weighing 10.19 lb.

Fig. 2 shows a typical streak-type dynamic stress pattern which provides quantitative source data for the maximum ten-

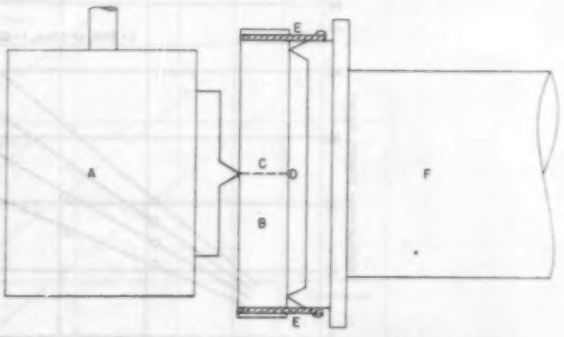

Fig. 1 Simply Supported Beam Under Central Impact
(A) Hammer (D) Point of interest
(B) Castolite beam (E) Rubber bands
(C) Line of interest (F) Anvil

[1] Research Officer, Scientific Department, Ministry of Defense, Haifa, Israel; formerly, Graduate Assistant, Illinois Institute of Technology, Chicago, Ill.

[2] Research Professor of Mechanics, Director of Experimental Stress Analysis, Illinois Institute of Technology, Chicago, Ill. Mem. ASME.

[3] Numbers in parentheses refer to the Bibliography at the end of the paper.

Presented at the Applied Mechanics Division Summer Conference, Berkeley, Calif., June 13–15, 1957, of The American Society of Mechanical Engineers.

Discussion of this paper should be addressed to the Secretary, ASME, 29 West 39th Street, New York, N. Y., and will be accepted until January 10, 1958, for publication at a later date. Discussion received after the closing date will be returned.

Note: Statements and opinions advanced in papers are to be understood as individual expressions of their authors and not those of the Society. Manuscript received by ASME Applied Mechanics Division, October 9, 1956. Paper No. 57—APM-36.

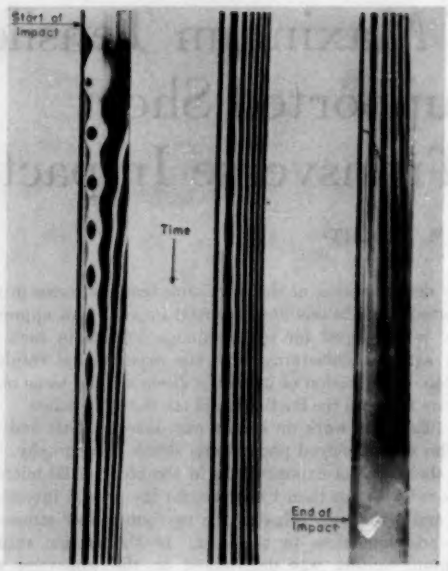

FIG. 2 DYNAMIC PHOTOELASTIC STRESS PATTERN FOR SIMPLY SUPPORTED CASTOLITE BEAM UNDER CENTRAL IMPACT

Transverse slit through point of impact
Span of beam, $L = 5.0$ in.
Depth of beam, $d = 0.94$ in.
Thickness of beam, $t = 0.213$ in.
Impact velocity, $v_0 = 14.4$ ips
Duration of impact, $T_1 = 8.42$ millisec

sile stress and the duration of impact during the entire period of impact.

Castolite beams were subjected to impact velocities v_0, ranging from 9.6 ips to 28.8 ips. The spans L were 3.4 in., 5.0 in., and 10.0 in., respectively. The beams studied were between 0.21 in. and 0.33 in. thick. The influence of overhang also was investigated.

EXPERIMENTAL RESULTS

The primary purpose of this study was to determine the maximum tensile stress in beams under impact as a function of the impact velocity, the span, and the depth of the beam. This stress occurs at point D, Fig. 1. This fact was established by analyzing the stress patterns from many transverse and longitudinal slits, and corroborated by actual fractures. Streak photographs, Fig. 2, were obtained of the transverse section through the line of impact and from these the value of the maximum fringe intensity N at point D was determined. The maximum fringe intensity is defined as

$$N = n/t \quad [1]$$

in which n is the maximum birefringence at point D during impact and t is the length of the light path; i.e., the thickness of the beam. The maximum tensile stress is proportional to the fringe intensity N.

Fig. 3 gives the relationship between the maximum fringe intensity and the impact velocity v_0 for several beams. It is seen that N is proportional to the impact velocity.

Fig. 4 shows N as a function of the span L for beams of various depths d, and a constant velocity v_0 of 19.2 ips. Inspection of the curves shows that for the ranges of d and L studied, N varies much more sharply with the depth than with the span. For example, for $L = 5$ in. the value of N more than doubles as d goes from 2 to 1 in. However the value of N varies much less when L goes from 5 to 10 in. Curves (ii) and (iii) suggest that there exists a span, L_0, for which N tends to reach a peak value.

The curves in Fig. 5 give N as a function of the depth for three different spans. It is interesting to note that any two of these curves intersect, showing that for two beams of different spans there exists one depth for which N is the same.

Experiments also were made to determine the effect of overhang on N. It was found that under the conditions of our experiments; i.e., a heavy hammer and light beams, the overhang has practically no influence on the maximum fringe intensity N. For example, two beams having the same depth of 1.5 in. and having over-all lengths of 11.3 in. and 5.6 in., respectively, give essentially the same value of N when the distance between the supports L is 5 in.

COMPARISON WITH ELEMENTARY LONG-BEAM THEORY

The approximate theory for long beams under impact is based on the following assumptions:

1 The mass of the beam is neglected.
2 The normal stresses are given by the flexure formula.

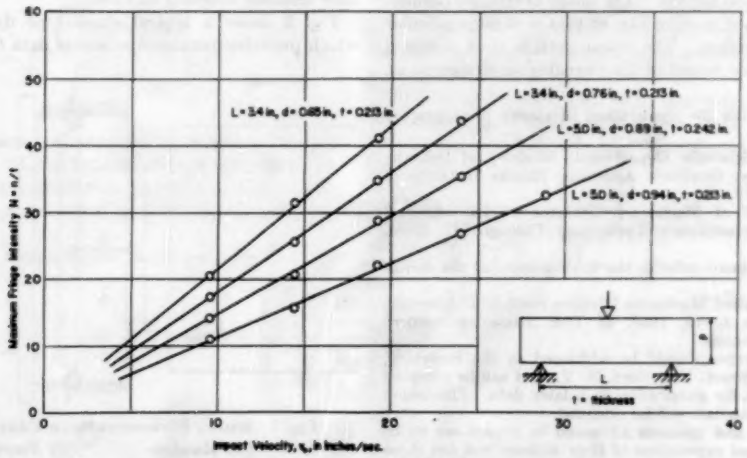
L = 3.4 in., d = 0.65 in., t = 0.213 in.
L = 3.4 in., d = 0.76 in., t = 0.213 in.
L = 5.0 in., d = 0.89 in., t = 0.242 in.
L = 5.0 in., d = 0.94 in., t = 0.213 in.
Maximum Fringe Intensity N = n/t
Impact Velocity, v0, in inches/sec.
0
10
20
30
40
50
60
L
t = thickness

FIG. 3 MAXIMUM FRINGE INTENSITY VERSUS IMPACT VELOCITY

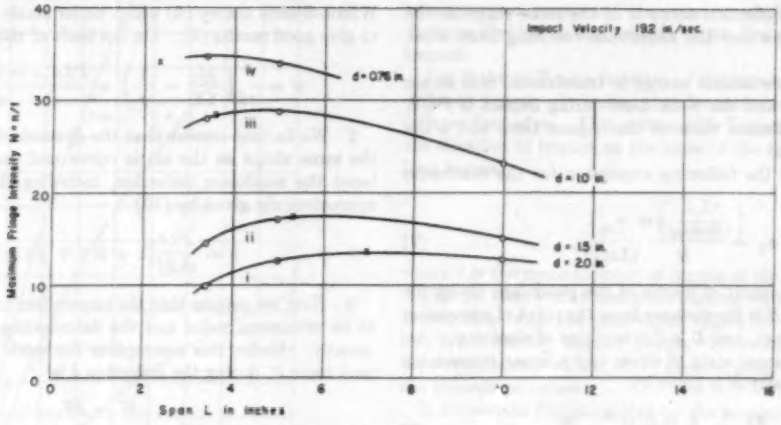

FIG. 4 MAXIMUM FRINGE INTENSITY VERSUS SPAN

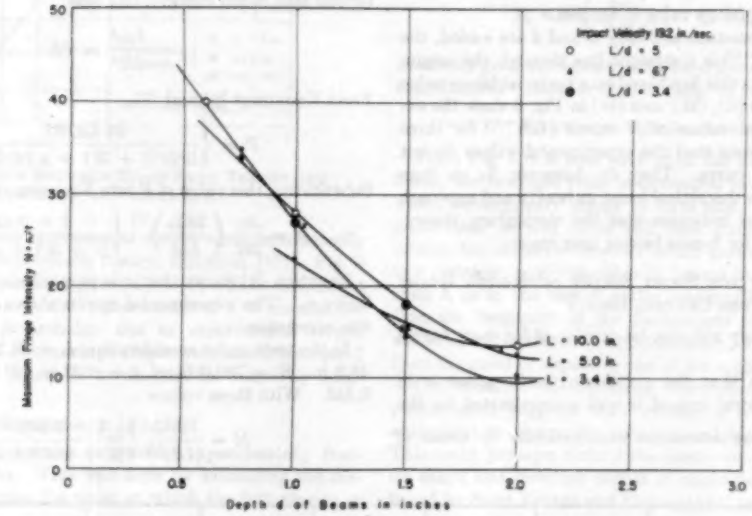

FIG. 5 MAXIMUM FRINGE INTENSITY VERSUS DEPTH

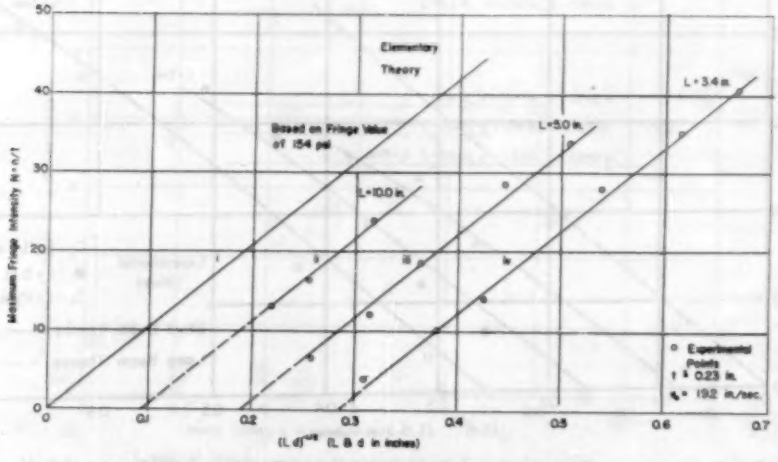

FIG. 6 COMPARISON BETWEEN LONG-BEAM THEORY AND EXPERIMENT

3 The dynamic deflection curve is of the same shape as the static deflection curve and the deflections resulting from shear are neglected.

4 All the available kinetic energy is transformed into strain energy of the beam and the work done during impact is $P\delta/2$, where P is the maximum value of the impact force and δ the maximum deflection.

This theory gives the following expression for the maximum tensile stress

$$\sigma_L = \frac{3(EI_0)^{1/3}}{R} \frac{v_0}{(Ld)^{1/3}} \quad [2]$$

in which I_0 is the moment of inertia of the pendulum about the point of suspension, R is the distance from the point of suspension to the point of contact, and E is the modulus of elasticity. Assuming a unidimensional state of stress and a linear stress-optic law, the fringe intensity N is given by

$$N = \frac{\sigma_L}{2f} = \frac{1}{2f} \frac{3(EI_0)^{1/3}}{R} \frac{v_0}{(Ld)^{1/3}} \quad [3]$$

where $2f$ is the material fringe value in tension.

If v_0 and t are kept constant and only L and d are varied, the plot of N versus $(Ld)^{-1/3}$ is a straight line through the origin. Curve (i) in Fig. 6 shows this line based on a material fringe value $2f = 154$ psi.[4] Curves (ii), (iii), and (iv) in Fig. 6 show the experimentally determined values of N versus $(Ld)^{-1/3}$ for three different spans. It is seen that the experimental values do not fall on the theoretical curve. They do, however, lie on lines which are parallel to the theoretical locus, curve (i), and approach it as L increases. This indicates that the elementary theory, Equation [2], is sound for beams having long spans.

Approximate Theory for Short Simply Supported Beams Under Central Impact

An approximate theory will now be developed for short beams under impact.

1 We shall assume that the maximum tensile stress σ in short beams under central impact is well approximated by the Wilson-Stokes theory (8) which under static conditions is known to give good results (9). On the basis of this theory

$$\sigma = \frac{P}{td}\left(\frac{3L}{2d} - \frac{2}{\pi}\right) = \frac{PLd[1 - 0.424(d/L)]}{8I} \quad [4]$$

2 We further assume that the dynamic deflection curve is of the same shape as the static curve and that for a rectangular beam the maximum deflection, including the effect of shear, is approximately given by (10)

$$\delta = \frac{PL^3}{48EI}[1 + 3(1 + \mu)(d/L)^2] \quad [5]$$

3 Next we assume that the impact force rises instantaneously to its maximum value and the deformation is developed subsequently. Under this assumption the work W, done by the impact force P, during the deflection δ is

$$W = P\delta \quad [6]$$

4 Lastly, we assume that all available kinetic energy is transformed into strain energy; i.e., that

$$\frac{I_0 v_0^2}{2R^2} = P\delta \quad [7]$$

From Equations [5] and [7]

$$P = \left\{\frac{24\, I_0 v_0^2 EI}{R^2L^3[1 + 3(1 + \mu)(d/L)^2]}\right\}^{1/3} \quad [8]$$

Substituting this value of P into Equation [4] we get

$$\sigma = \frac{3v_0}{2R}\left(\frac{2EI_0}{Ld}\right)^{1/3}\left\{\frac{1 - 0.424(d/L)}{[1 + 3(1 + \mu)(d/L)^2]^{1/3}}\right\} \quad [9]$$

Equation [9] shows that σ is proportional to the impact velocity v_0. The experimental results shown in Fig. 3 corroborate this conclusion.

In the tests under consideration, $I_0 = 56.77$, $v_0 = 19.2$ ips, $R = 48.2$ in., $E = 700{,}000$ psi, $t = 0.23$ in., $2f = 154$ psi, and $\mu = 0.355$. With these values

$$N = \frac{72.13}{(Ld)^{1/3}}\left\{\frac{1 - 0.424(d/L)}{[1 + 4.065(d/L)^2]^{1/3}}\right\} \quad [10]$$

[4] This fringe value was determined experimentally by means of SR-4 strain gages.

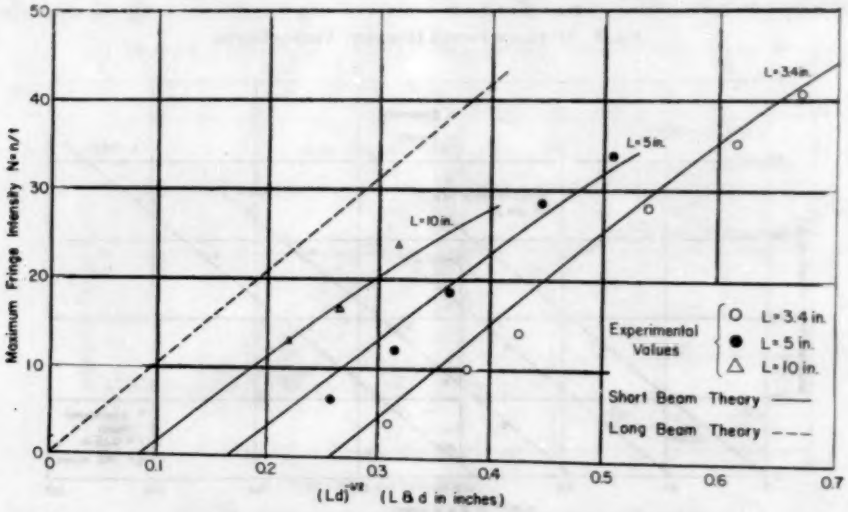

Fig. 7 Comparison Between Short-Beam Theory and Experiment—N Versus $(Ld)^{-1/3}$

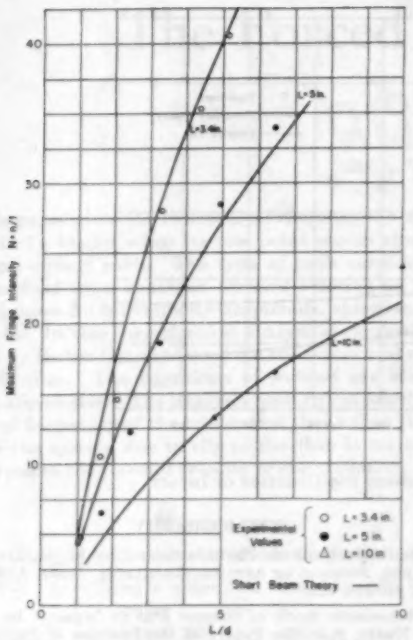

FIG. 8 COMPARISON BETWEEN SHORT BEAM THEORY AND EXPERIMENT—N VERSUS L/d

Fig. 7 shows that the experimental results agree satisfactorily with those from the short-beam theory, Equation [10]. Fig. 8 shows the same data plotted against L/d. It will be noted that the agreement is better at the higher values of L/d than at the lower values. This is probably due to experimental errors. At the lower values of N the fringe orders were small, between 2 and 3, so that small errors in n can produce relatively large errors in N.

DURATION OF IMPACT

The duration of impact was determined experimentally from the streak photographs. This was done by measuring the distance on the film between the point at which the first change in birefrigence occurred and the point at which it vanished. This distance divided by the velocity of the film gives the duration of impact.

Fig. 9 shows T_i as a function of the impact velocity v_0 for four different beams. It is seen that for each beam, T_i is essentially independent of v_0. This agrees with Equation [11] which gives the duration of impact on the basis of the elementary theory for long beams

$$T_i = \pi \left(\frac{I_0 L^3}{48 R^3 E I} \right)^{1/2} \quad \ldots\ldots\ldots\ldots\ldots [11]$$

where I is the usual moment of inertia of the beam.

Fig. 10 shows that the experimental values of T_i agree approximately with the theoretical values for L/d larger than 5; i.e., for relatively slender beams. However, as L/d decreases the experimental values of T_i become progressively larger than the theoretical values.

If we replace Equation [11] by the empirically modified equation

$$T_i = \pi \left(\frac{I_0 L^3}{48 R^3 E I} \right)^{1/2} [1 + 6.7(d/L)^2] \ldots\ldots\ldots [12]$$

relatively good agreement is obtained between the calculated and experimental values for the full range of tests covered, Fig. 10.

FLUCTUATION OF ISOTROPIC POINTS

From Fig. 2 it is seen that when the hammer first strikes the beam, one isotropic point is developed which separates into two which subsequently merge to form one. This phenomenon repeats itself several times and then stabilizes at two isotropic points, the distance between which periodically changes. The two isotropic points develop in beams in which L/d is greater than 5, as in the case of static loading (9). It has been found that the frequency of the fluctuations of the isotropic points varies linearly with $1/S$, approximately, where S is the distance from the point of impact to one of the supports.

The cause of the foregoing fluctuations is not clear. The phenomenon suggests that something is happening which is equivalent to alternately reducing and increasing the L/d ratio. This could, perhaps, occur if the elastic curve periodically changes its shape and develops points of contraflexure similar to those found by Saint Venant and Flamant (11) and photoelastically ob-

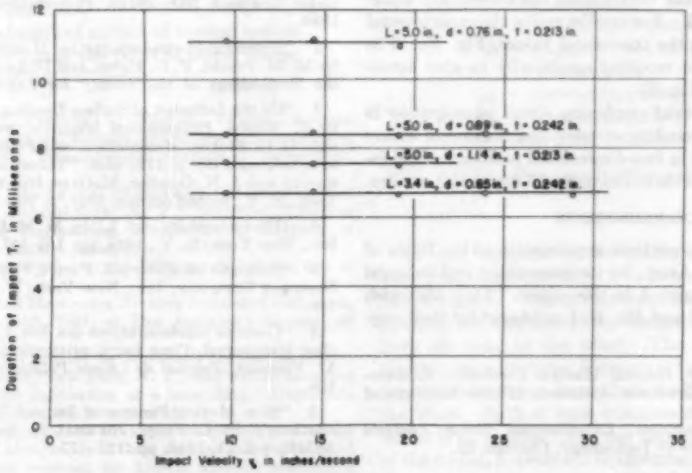
Duration of Impact T_i in Milliseconds
Impact Velocity v_0 in inches/second
L=5.0 m, d=0.76 m, t=0.213 m
L=5.0 m, d=0.89 m, t=0.242 m
L=5.0 m, d=1.14 m, t=0.213 m
L=3.4 m, d=0.65 m, t=0.242 m

FIG. 9 DURATION OF IMPACT VERSUS IMPACT VELOCITY

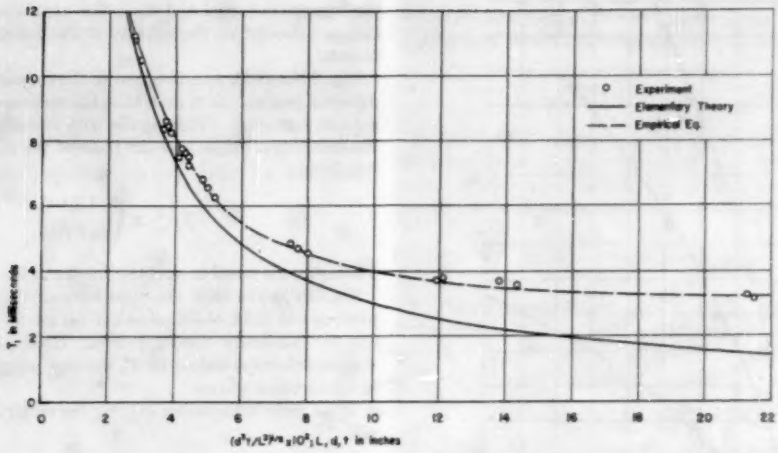

FIG. 10 COMPARISON BETWEEN THEORY AND EXPERIMENT FOR DURATION OF IMPACT

served by Föppl (12). The stress pattern in Fig. 2 shows that during the first cycle the formation of the two isotropic points is associated with a fluctuation of the contact pressure. This may be the case for all cycles, although the pattern does not have sufficient resolution in the region of contact to show this definitely.

CONCLUSIONS

1 In a simply supported beam subjected to central transverse impact the maximum tensile stress is directly proportional to the impact velocity, Fig. 3.

2 In the beams investigated, the amount of overhang has little or no effect on the maximum tensile stress.

3 The maximum tensile stress varies sharply with the depth d, and much less sharply with the span L.

4 For short beams the maximum tensile stress does not agree with the elementary long-beam theory, Equation [2].

5 The experimental results are in satisfactory agreement with the short-beam theory, Equation [9].

6 The duration of impact is independent of the impact velocity, Fig. 9.

7 The experimentally determined values for the duration of impact tend to approach the values from the elementary equation for L/d greater than 5. For smaller ratios the experimental values differ sharply from the theoretical values, Fig. 10. The theoretical formula can be modified empirically to give agreement, Equation [12] and Fig. 10.

8 The photoelastic method employing streak photography is capable of determining boundary stresses and maximum shears (in the plane of the model) in two-dimensional problems. Castolite has proved to be a suitable model material for impact studies.

ACKNOWLEDGMENTS

The authors wish to express their appreciation to the Office of Ordnance Research, U. S. Army, for its sponsorship and financial assistance of the work reported in this paper. They also wish to thank Dr. P. D. Flynn[5] and Mr. D. Landsberg[6] for their suggestions and co-operation.

[5] Engineer-Photoelasticity, General Electric Company, Schenectady, N. Y. Formerly, Graduate Assistant, Illinois Institute of Technology, Chicago, Ill.

[6] Associate Research Engineer, Experimental Stress Analysis Laboratory, Illinois Institute of Technology, Chicago, Ill.

BIBLIOGRAPHY

1 "Studies in Dynamic Photoelasticity," by M. M. Frocht and P. D. Flynn, JOURNAL OF APPLIED MECHANICS, Trans. ASME, vol. 78, 1956, pp. 116–122.

2 "Photoelastic Study of Stresses Due to Impact," by Z. Tuzi and M. Nisida, Scientific Papers of the Institute of Physical and Chemical Research, Tokyo, Japan, no. 566, 26, April, 1935, pp. 277–309; also *Philosophical Magazine*, series 7, vol. 21, 1936, pp. 448–473.

3 "On the Stress-Optic Law Under Impact Loading," by A. A. Betser, P. D. Flynn, and M. M. Frocht, presented at the Ninth International Congress for Theoretical and Applied Mechanics, Brussels, Belgium, September 5–13, 1956; also, Technical Report No. 3 to the Office of Ordnance Research, U. S. Army, under Contract DA-11-022-ORD-1609, November, 1956.

4 "Studies in Dynamic Photoelasticity," by P. D. Flynn, Ph.D. thesis, Illinois Institute of Technology, Chicago, Ill., June, 1954.

5 "Studies in Dynamic Photoelasticity; Fringe Values and Beams Under Impact," by A. A. Betser, Ph.D. thesis, Illinois Institute of Technology, Chicago, Ill., June, 1956.

6 "A Photoelastic Study of Dynamic Stresses in Structures," by M. M. Frocht, P. D. Flynn, and D. Landsberg, Final Report to U. S. Navy Bureau of Yards and Docks, U. S. Naval Civil Engineering Research and Evaluation Laboratory, Port Hueneme, Calif., under Contract NOy-28149, Project Order 10703, November 30, 1954.

7 "Dynamic Photoelasticity by Means of Streak Photography," by M. M. Frocht, P. D. Flynn, and D. Landsberg, to be published in the Proceedings of the Society for Experimental Stress Analysis.

8 "On the Influence of Surface Loading on the Flexure of Beams," by C. Wilson, *Philosophical Magazine*, vol. 32, 1891, pp. 481–503; also, G. G. Stokes, *Mathematical and Physical Papers*, vol. 5, p. 238; also, reference (9), p. 112; also, "Theory of Elasticity," by S. Timoshenko and J. N. Goodier, McGraw-Hill Book Company, Inc., New York, N. Y., second edition, 1951, p. 99.

9 "Photoelasticity, vol. 2," by M. M. Frocht, John Wiley & Sons, Inc., New York, N. Y., 1948, pp. 104–117.

10 "Strength of Materials, Part 1," by S. Timoshenko, D. Van Nostrand Company, Inc., New York, N. Y., first edition, 1930, p. 189.

11 "Courbes représentatives des lois du choc longitudinal et du choc transversal d'une barre prismatique," by Saint Venant and M. Flamant, *Journal de l'École Polytechnique*, vol. 59, 1889, pp. 97–128.

12 "Slow Motion Pictures of Impact Tests by Means of Photoelasticity," by L. Föppl, JOURNAL OF APPLIED MECHANICS, Trans. ASME, vol. 71, 1949, pp. 173–177.

The Forced Lateral Oscillations of Trailers

By A. SLIBAR[1] and P. R. PASLAY[2]

This paper gives the mechanical response of a simplified model of a trailer when its tow point moves along a certain prescribed path. The type of path considered here is described by a constant forward velocity on which is superimposed a low-velocity-amplitude, sidewise, periodic motion. In this investigation analytical expressions proposed by Huber (3)[3] were used for the forces and moments on the tires. The equations of motion are studied for small slip angles. The analysis leads to a prediction of the natural frequency of the trailer and shows that the damping of the system due to slip of the tires is inversely proportional to the forward velocity of the trailer.

Nomenclature

The following nomenclature is used in the paper:

- A = force in η-direction wheel transmits to body of trailer
- b = radius of tire
- c', $\bar{c}$ = coefficients in Equation [2] relating side force S_w to slip angle α and vertical load P of tire
- D = force in ξ-direction wheel transmits to body of trailer
- D_w = drag force acting on tire from road
- F = dimensionless parameter defined by Equation [10]
- g = acceleration of gravity
- H = force acting in y-direction transmitted by tow hitch to body of trailer
- i_B = radius of gyration of body of trailer about an axis parallel to z-axis through center of gravity body
- $i_\xi = i_\zeta$ = radius of gyration of wheel about its diametral axis
- i_η = radius of gyration of wheel about η-axis
- k = drag coefficient
- L = wave length of motion of towing vehicle
- l = distance from tow point to axle of trailer
- M = mass of body of trailer
- m = mass of wheel
- M_{ξ_1} = moment acting to body of trailer transmitted by tow hitch
- $M_{\xi_2}, M_{\eta_2}, M_{\zeta_2}$ = moments acting on wheel in ξ, η, ζ-directions transmitted from body of trailer
- N = force acting in x-direction transmitted by tow hitch to body of trailer
- P = load tire supports
- r = distance from tow point to center of gravity of trailer
- S_w = side force acting on wheel from road
- t = time
- V = force acting in x-direction transmitted by tow point
- $\bar{V}$ = resultant velocity of tow point, $\bar{V} = (V_0^2 + \dot{y}_1^2)^{1/2}$
- V_0 = x component of forward velocity of tow point
- V_1 = force acting in ζ-direction transmitted from wheel to body of trailer
- V_w = force acting in ζ-direction transmitted from road to wheel of trailer
- x_1, y_1, z_1 = absolute co-ordinates of tow point of trailer
- x_B, y_B, z_B = absolute co-ordinates of center of gravity of body of trailer
- x_w, y_w, z_w = absolute co-ordinates of center of gravity of fictitious wheel
- α = slip angle, defined as angle measured in a horizontal plane between vector of relative motion of axle of wheel with respect to road and plane of wheel
- μ = coefficient of static friction between road and tire
- ξ, η, ζ = rectangular co-ordinate system fixed to body of trailer (see Fig. 3)
- φ = angle between line connecting tow point to center of gravity of trailer and negative x-direction
- ϕ = amplitude of φ at resonance
- ψ = angle absolute velocity of tow point makes with x-direction
- ω_0 = natural frequency of linearized system
- ω_e = exciting frequency
- ω_r = angular velocity of wheel about its axle

The dot is used to denote differentiation with respect to time.

Introduction

At present there is no satisfactory theory explaining the mechanical behavior of a system consisting of a pulling vehicle and a trailer. This is partially due to the complexity of the problem and the lack of knowledge about the forces transmitted from the road to the wheel. The first attempts to solve this problem were made by Williams (1) and Ziegler (2), both making special assumptions about the forces transmitted from the road to the wheel. Both of these solutions state that the response of the trailer (i.e., snaking) does not depend upon the forward velocity of the trailer, a result not in agreement with observations. Ziegler treated the problem as a stability phenomenon while Williams did

---

[1] Dozent, Technical University of Vienna, Vienna, Austria. Formerly, Visiting Fellow of the Foreign Operations Administration, Scientists Research Project, Massachusetts Institute of Technology, Cambridge, Mass.

[2] Engineer—Vibration, Mechanical Engineering Laboratory, General Electric Company, Schenectady, N. Y.; formerly, Assistant Professor of Mechanical Engineering, Massachusetts Institute of Technology, Cambridge, Mass. Assoc. Mem. ASME.

[3] Numbers in parentheses refer to the Bibliography at the end of the paper.

Presented at the Applied Mechanics Division Summer Conference, Berkeley, Calif., June 13–15, 1957, of The American Society of Mechanical Engineers.

Discussion of this paper should be addressed to the Secretary, ASME, 29 West 39th Street, New York, N. Y., and will be accepted until January 10, 1958, for publication at a later date. Discussion received after the closing date will be returned.

Note: Statements and opinions advanced in papers are to be understood as individual expressions of their authors and not those of the Society. Manuscript received by ASME Applied Mechanics Division, December 3, 1956. Paper No. 57—APM-4.

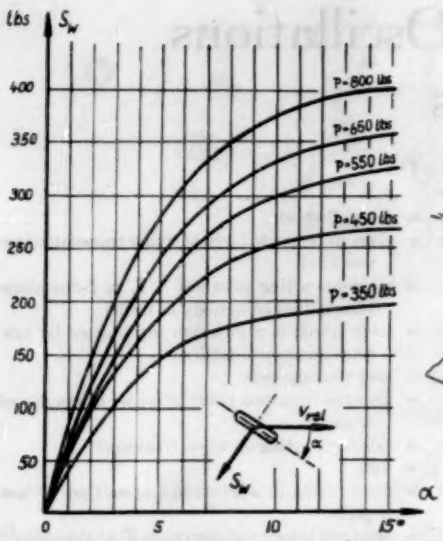

FIG. 1 THE SIDE FORCE S_w AS A FUNCTION OF SLIP ANGLE α FOR VARIOUS VALUES OF TIRE LOAD P
(Taken from Rieckert and Schunck.)

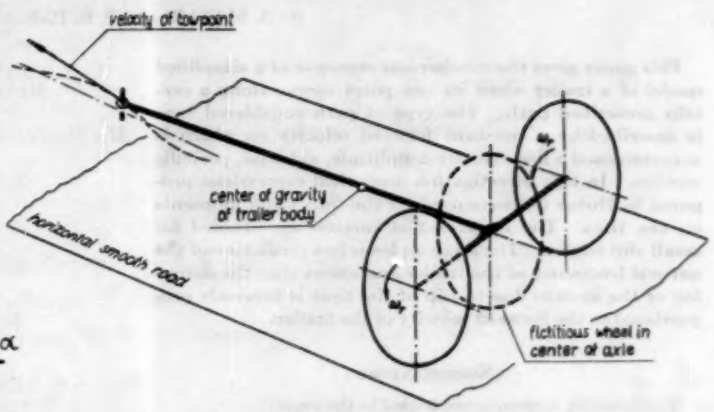

FIG. 2 SKETCH OF TRAILER

not take into account the sidewise slipping of the wheel. Huber (3) and Olley (4) demonstrated that the side force on a tire depends on the slip angle. This side force is essentially the driving force for the snaking of a trailer. Any analysis that does not take into account the relation between the slip angle and the side force cannot be expected to explain the physical phenomena.

A trailer and a towing vehicle possess many degrees of freedom, and a large number of parameters influence the response of the system. These circumstances make it necessary to idealize the given system to a simpler one accessible to analytical treatment.

The resulting motion depends on both the towing vehicle and the trailer. If snaking of the trailer occurs, both elements of the system take part in the motion. Only when the towing vehicle is many times heavier than the trailer may the motion of the pulling vehicle produced by the trailer be neglected. Even in the case of a heavy towing vehicle, corrections in the steering make the assumption of the towing vehicle running on a straight line unsatisfactory. The assumption of a straight-line motion of the tow point does not yield the forced lateral response of the trailer. For this analysis the forward component of the tow-point velocity is assumed to be constant while the lateral component varies sinusoidally with time.

Since the road is assumed to be smooth and level the influence of the springs of the trailer as well as of the towing vehicle is neglected.

General Tire Behavior

Huber (3) has shown experimentally that sidewise force on tires can be produced only if the velocity of the wheel axle is not in the plane of the wheel to which the tire is mounted. This angle of inclination is called the slip angle, Fig. 1. Using the foregoing results, Rieckert and Schunck (5) and the authors (6) developed a theory governing the motion of a single vehicle which showed good agreement with experiment.

As stated in the foregoing, the side force S_w acting from the road perpendicular to the plane of the wheel depends on the slip angle α between the plane of the wheel and the velocity of the axle of the wheel relative to the road. Furthermore, in accordance with Huber's results, the side force is assumed to act in the vertical plane which includes the axle of the wheel. The angle α is measured in a horizontal plane. The side force S_w further depends on the load P the wheel supports. Fig. 1, taken from experiments, shows that the side force increases less than proportionally with the load on the wheel [for details of experiments see, for example, Olley (4)].

The side force is a function of the coefficient of static friction μ, but to a first approximation does not depend upon the driving velocity. Huber's experimental results may be represented by the relation

$$S_w = \mu P \tanh (C_p \alpha) \quad [1]$$

making use of a "pressure coefficient" C_p. The problem considered in this paper is restricted to small slip angles, thus giving a simplification of Equation [1] in the form

$$S_w = (c - c'P)P\alpha \quad [2]$$

Equation [2] was shown by Huber to be in good agreement with experimental results for small values of α.

The most complete résumé of tire behavior in the English literature is given by Olley (4). His conclusions agree with the tire characteristics set forth in this paper. He also discusses many other factors such as forward velocity, smoothness of the road, tire pressure, and size of the rim.

Equations of Motion

The system under consideration is drawn schematically in Fig. 2. For this analysis the wheels of the trailer are replaced by a fictitious wheel located on the same axis. This assumption causes little change in the mechanical behavior of the trailer since the road is flat and level. The fictitious wheel is sketched in Fig. 2 with a dotted line.

Fig. 3 shows the major parts of the trailer with all the forces and moments acting on the wheel and body of the trailer, positive directions as shown. The co-ordinates x_B, y_B define the position of the center of gravity of the trailer body with respect to the

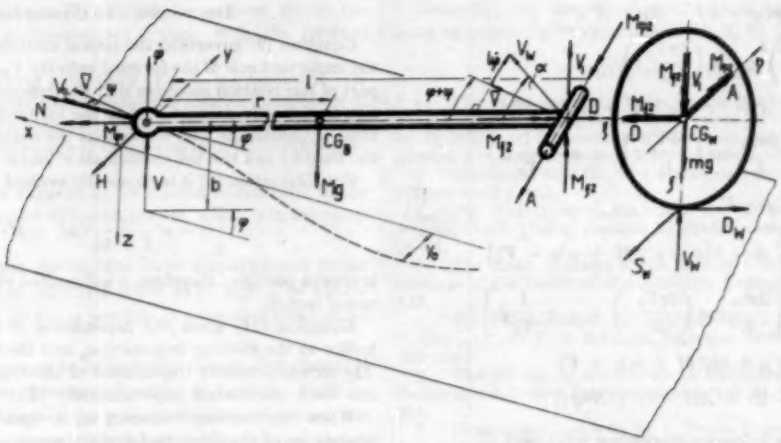

FIG. 3 GEOMETRY, FORCES, AND MOMENTS OF SYSTEM

road while x_w, y_w define the position of the wheel with respect to the road and ξ, η, ζ represent a co-ordinate system fixed to the body of the trailer.

The equations of motion for the body are

$$\left.\begin{aligned} M\ddot{x}_B &= N - A\sin\varphi - D\cos\varphi \\ M\ddot{y}_B &= -H - A\cos\varphi + D\sin\varphi \\ 0 &= -V + Mg - V_1 \\ 0 &= M_{\xi_1} - M_{\xi_2} \\ 0 &= Vr - V_1(l-r) - M_{\eta_2} \\ -Mi_B^2\ddot{\varphi} &= -Hr\cos\varphi + A(l-r) - M_{\zeta_2} + Nr\sin\varphi \end{aligned}\right\} \quad \ldots [3]$$

and for the wheel are

$$\left.\begin{aligned} m\ddot{X}_w &= D\cos\varphi - D_w\cos\varphi + A\sin\varphi - S_w\sin\varphi \\ m\ddot{y}_w &= -D\sin\varphi + D_w\sin\varphi + A\cos\varphi - S_w\cos\varphi \\ 0 &= V_1 - V_w + mg \end{aligned}\right\} \quad \ldots [4]$$

Euler's equations applied to the wheel lead to

$$\left.\begin{aligned} M_{\xi_2} + bS_w &= -mi_\eta^2\omega_r\dot{\varphi} \\ M_{\eta_2} - bD_w &= -mi_\eta^2\dot{\omega}_r \\ M_{\zeta_2} &= -mi_\zeta^2\ddot{\varphi} \end{aligned}\right\} \quad \ldots [4a]$$

The position of the tow point x_1, y_1 is given by

$$x_1 = V_0 t, \quad y_1 = y_0 \sin\frac{2\pi V_0}{L} t$$

From the geometry of the system we get the relations

$$\left.\begin{aligned} x_B &= V_0 t - r\cos\varphi \\ y_B &= y_0 \sin\frac{2\pi V_0}{L} t + r\sin\varphi \\ x_w &= V_0 t - l\cos\varphi \\ y_w &= y_0 \sin\frac{2\pi V_0}{L} t + l\sin\varphi \end{aligned}\right\} \quad \ldots [5]$$

$$\left.\begin{aligned} \psi &= \tan^{-1}\left(\frac{\dot{y}_1}{V_0}\right) = \tan^{-1}\left(\frac{2\pi y_0}{L}\cos\frac{2\pi V_0}{L} t\right) \\ \alpha &= \tan^{-1}\left[\frac{\bar{V}\sin(\varphi+\psi) + l\dot{\varphi}}{\bar{V}\cos(\varphi+\psi)}\right] \\ \omega_r &= \frac{\bar{V}\cos(\varphi+\psi)}{b}\,. \\ \bar{V} &= (V_0^2 + \dot{y}_1^2)^{1/2} \\ &= V_0\left[1 + \left(\frac{2\pi y_0}{L}\right)^2\cos^2\left(\frac{2\pi V_0}{L} t\right)\right]^{1/2} \end{aligned}\right\} \quad \ldots [5] \text{ (Cont.)}$$

The rolling resistance of the wheel is accounted for by a force on the wheel from the road D_w, Fig. 3. This force depends on the load V_w the wheel supports and, to a lesser extent, on the angular velocity ω_r of the wheel about its axle. For this investigation D_w is assumed proportional to V_w as follows

$$D_w = kV_w \quad \ldots [6]$$

Making use of measured tire behavior mentioned previously, the side force transmitted from the road to the wheel becomes

$$S_w = (e - c'V_w)V_w\alpha \quad \ldots [2a]$$

Substituting the values given by Equations [5] into Equations [3], [4], and [4a] and requiring that

$$\frac{y_0}{L} \ll 1 \quad \text{and} \quad \varphi \ll 1$$

there results

$$\left.\begin{aligned} 0 &= N - A\varphi - D \\ Mr\ddot{\varphi} &= M\left(\frac{2\pi V_0}{L}\right)^2 y_0 \sin\left(\frac{2\pi V_0}{L} t\right) - H - A + D\varphi \\ V_1 &= Mg - V \\ M_{\xi_2} &= M_{\xi_1} \\ M_{\eta_2} &= Mgr - l(Mg - V) \\ M_{\zeta_2} &= Mi_B^2\ddot{\varphi} - Hr + A(l-r) + Nr\varphi \end{aligned}\right\} \quad \ldots [7]$$

$$
\left.\begin{aligned}
D &= k[(M+m)g - V] - A\varphi \\
ml\ddot{\varphi} &= m\left(\frac{2\pi V_0}{L}\right)^2 y_0 \sin\left(\frac{2\pi V_0}{L}t\right) \\
&- D\varphi + kV_w\varphi + A - \{e - c'[(M+m)g - V]\} \\
&[(M+m)g - V]\left\{\frac{2\pi y_0}{L}\cos\left(\frac{2\pi V_0}{L}t\right) + \varphi + \frac{l}{V_0}\dot{\varphi}\right\} \\
V_w &= (M+m)g - V \\
M_{\xi_1} &= -mi_\tau^2\frac{V_0}{b}\dot{\varphi} - b\{e - c'[(M+m)g - V]\} \\
&[(M+m)g - V]\left[\frac{2\pi y_0}{L}\cos\left(\frac{2\pi V_0}{L}t\right) + \varphi + \frac{l}{V_0}\dot{\varphi}\right] \\
Mgr &= (Mg - V)l + kb[(M+m)g - V] \\
mi_\xi^2\ddot{\varphi} &= Mi_B^2\ddot{\varphi} - Hr + A(l-r) + Nr\varphi
\end{aligned}\right\} \quad \ldots [7] \text{ (Cont.)}
$$

In Equations [7] the following expressions were used

$$
\left.\begin{aligned}
\psi &= \frac{2\pi y_0}{L}\cos\left(\frac{2\pi V_0}{L}t\right), \quad \dot{\psi} = V_0 \\
\text{and} \\
\alpha &= \frac{2\pi y_0}{L}\cos\left(\frac{2\pi V_0}{L}t\right) + \varphi + \frac{l}{V_0}\dot{\varphi}
\end{aligned}\right\} \quad \ldots\ldots [8]
$$

Eliminating the forces A, D, H, N, V, V_1, V_w and the moments $M_{\xi_1}, M_{\xi_2}, M_{\pi}, M_{\xi_3}$ in Equations [7], the governing equation for the angle φ of lateral oscillations becomes

$$
\left.\begin{aligned}
&[m(i_\xi^2 + l^2) + M(i_B^2 + r^2)]\ddot{\varphi} \\
&\quad + \left[e - c'\frac{g}{l+kb}(ml + Mr)\right]\times \\
&\qquad \frac{gl(ml+Mr)}{l+kb}\left(\frac{l}{V_0}\dot{\varphi} + \varphi\right) \\
&= \frac{2\pi y_0}{L}\left\{\frac{2\pi V_0^2}{L}(ml+Mr)\sin\left(\frac{2\pi V_0}{L}t\right)\right. \\
&\left. - \frac{lg(ml+Mr)}{l+kb}\left[e - c'\frac{g(ml+Mr)}{l+kb}\right]\cos\left(\frac{2\pi V_0}{L}t\right)\right\}
\end{aligned}\right\} \quad \ldots [9]
$$

Using the abbreviations

$$
\left.\begin{aligned}
\omega_0^2 &= \frac{\left[e - c'\dfrac{g(ml+Mr)}{l+kb}\right]\dfrac{gl(ml+Mr)}{l+kb}}{m(i_\xi^2 + l^2) + M(i_B^2 + r^2)} \\
\omega_e &= \frac{2\pi V_0}{L} \\
F &= \frac{(ml+Mr)l}{m(i_\xi^2 + l^2) + M(i_B^2 + r^2)}
\end{aligned}\right\} \quad \ldots [10]
$$

the particular solution representing the steady-state lateral vibration is

$$
(\varphi)_{\text{particular}} = \frac{\dfrac{2\pi y_0}{L}}{\left[1 - \left(\dfrac{\omega_e}{\omega_0}\right)^2\right]^2 + \left(\dfrac{l}{V_0}\omega_e\right)^2}\left\{\left[\left[F\left(\frac{\omega_e}{\omega_0}\right)^2\frac{L}{2\pi l}\left[1 - \left(\frac{\omega_e}{\omega_0}\right)^2\right] - \left(\frac{l}{V_0}\omega_e\right)\right]\right]\sin\omega_e t\right.
$$
$$
\left. - \left[\left[\left[1 - \left(\frac{\omega_e}{\omega_0}\right)^2\right] + F\left(\frac{\omega_e}{\omega_0}\right)^2\right]\right]\cos\omega_e t\right\} \quad \ldots\ldots [11]
$$

Discussion and Conclusions

Equation [9] governing the lateral motion of the trailer shows the important role of the forward velocity V_0. The homogeneous part of this relation indicates that the damping of a lateral oscillation is inversely proportional to the forward velocity of the system. Equation [9] also shows that the damping is influenced by the length l and the tire coefficients c' and e.

From Equation [2] it is physically evident that

$$
\left[e - c'\frac{g}{l+kb}(ml + Mr)\right]
$$

is always positive; therefore, a self-excited vibration of the trailer never occurs.

Equation [11] gives the dependence of the response of the trailer on the exciting frequency ω_e and the forward velocity V_0. The forward-velocity dependence of the response predicted here has been established experimentally (2).

When the exciting frequency ω_e is equal to the natural frequency ω_0 of the linearized system, resonance results. For resonance the amplitude of φ, denoted by ϕ, is given by

$$
\phi = \frac{\dfrac{2\pi y_0}{L}}{\left(\dfrac{l\omega_e}{V_0}\right)^2}\left[F^2\left(\frac{\omega_e}{\omega_0}\right)^4 + \left(\frac{l}{V_0}\omega_e\right)^2\right]^{1/2}
$$
$$
= \frac{\dfrac{2\pi y_0}{L}}{\dfrac{2\pi l}{L}}\left[F^2\left(\frac{2\pi V_0}{L\omega_0}\right)^4\left(\frac{L}{2\pi l}\right)^2 + 1\right]^{1/2} \quad \ldots\ldots [12]
$$

Fig. 4 shows the amplification factor $\phi l/y_0$ at resonance as a function of the dimensionless parameter

$$
\frac{FL}{2\pi l}\left(\frac{2\pi V_0}{L\omega_0}\right)^2
$$

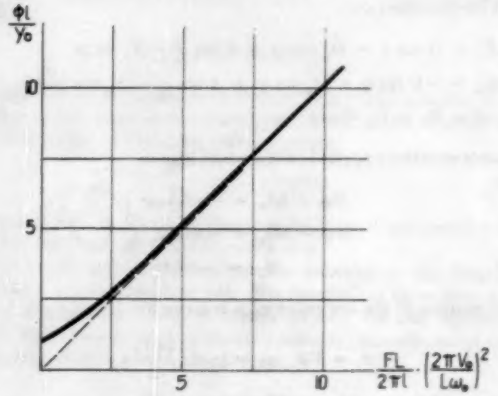

Fig. 4 Amplification Factor at Resonance, $\frac{\phi l}{y_0}$, as a Function of Dimensionless Parameter $\frac{FL}{2\pi l}\left(\frac{2\pi V_0}{L\omega_0}\right)^2$

The reader will note from Fig. 4 that for a given trailer the amplification factor at resonance increases with the forward velocity.

For anticipated driving conditions (V_0, L, y_0) Equation [12] can be used by a designer to determine the resonant amplitude of lateral oscillations for a proposed design. By adjusting variables at his disposal the amplitude will have to be kept within permissible limits.

A calculation of the value of ω_0 for a 1-ton commercial trailer showed that ω_0 is the order of 1 cycle per sec, which is in the range of practical interest.

Experiments (7) have shown that large amplitudes of trailer vibrations may occur at velocities as low as 35 mph. By appropriate steering corrections it is possible to overcome this critical driving situation.

Since the road is assumed to be perfectly smooth, Solution [11] gives no answer to the questions of rolling of trailers. Furthermore, only steady motion of the pulling vehicle and trailer was considered. This means that Solution [11] does not include behavior while the pulling vehicle is accelerated or braked.

Generally, the theoretical results given in this paper are in good agreement with experiments (1, 2, 6).

BIBLIOGRAPHY

1 "The Mathematical Theory of the Snaking of Two-Wheeled Trailers, With Practical Rules and Devices for Preventing Snaking," by D. Williams, Proceedings of The Institution of Mechanical Engineers, Automobile Division, 1951–1952, pp. 175–187.

2 "Mechanik, vol. III," by H. Ziegler, Birkhäuser, Basel, first edition, 1952, p. 132.

3 "Die Fahrtrichtungsstabilität des schnellfahrenden Kraftwagens," by L. Huber, *Deutsche Kraftfahrtforschung*, no. 44, 1940, pp. 18–64.

4 "The Road Manners of the Modern Car," by M. Olley, Proceedings of the Institute of Automobile Engineers, vol. 41, 1946, p. 147.

5 "Zur Fahrmechanik des gummibereiften Kraftfahrzeugs," by P. Rieckert and T. E. Schunck, *Ingenieur-Archiv*, vol. 11, 1940, pp. 210–224.

6 "The Motion of Automobile in Unbanked Curves," by P. R. Paslay and A. Slibar, *Ingenieur-Archiv*, vol. 24, no. 6, 1956, pp. 412–424.

7 "Communications," by M. F. Neale, Proceedings of The Institution of Mechanical Engineers, Automobile Division, 1951–1952, p. 188.

Superharmonic Oscillations as Solutions to Duffing's Equation as Solved by an Electronic Differential Analyzer

By C. P. ATKINSON,[1] BERKELEY, CALIF.

This paper presents the experimental response curves for the solutions of Duffing's equation for that frequency range where higher-order harmonics (called superharmonics as opposed to lower order or subharmonics) of the fundamental are important components of the solution. The experimental results were obtained by solving Duffing's equation on an electronic differential analyzer. The paper presents corroboration of analytical results for the third-order superharmonic component of solutions which were calculated by a two-term Ritz approximation. The results of this paper indicate that superharmonics of higher order than the third, that is, fifth and seventh order, and even-order harmonics such as second and fourth order can be found in the frequency range studied. This paper points out a definite relationship which exists between the superharmonic generated and the free-vibration curve ("backbone") of the system. For example, if we compare the maximum displacement of the solution containing an *n*th order superharmonic with the same amplitude of the free-vibration curve, it is seen that the frequency of the fundamental (the forcing frequency) is $1/n$ times this natural frequency or, conversely, the frequency of the superharmonic component is *n* times that of the fundamental and has in fact the frequency of the free vibration for that amplitude. Thus a superharmonic of order *n* can be pictured as a sustained free vibration which is generated when the frequency of the forcing function is $1/n$ of the frequency of the free-vibration response curve. The phenomenon of superharmonic oscillations is pictured here as a nonlinear resonance. Experimental evidence of the superharmonic-jump phenomenon as discovered analytically by John Burgess (1)[2] also is presented in this paper.

Nomenclature

The following nomenclature is used in the paper:

- A = arbitrary constant in multiplier circuit
- D = damping coefficient, ratio of actual damping to critical damping
- α, β = scale factors relating machine variables with problem variables
- F = forcing function $s \cos \Omega t$ in Fig. 2
- Q_n = amplitude of *n*th order superharmonic
- q_{max} = maximum displacement of $q(t)$
- $q(t)$ = solution of Equation [1]
- s = amplitude of forcing function
- t = time, independent variable
- $E(t)$ = machine solution of Equation [2] simulating $q(t)$ the solution of Equation [1]
- η = frequency ratio Ω/K
- K = circular frequency of linear system
- Ω = circular frequency of forcing function and of fundamental component of $q(t)$

Introduction

The existence of solutions to Duffing's equation containing superharmonic components has been predicted by the two-term Ritz approximation in a report by Burgess (1). He indicates that in the frequency range below $\Omega = 0.8$, Fig. 1, harmonic solutions are not valid; that is, a single sine or cosine term is not sufficient to represent the solution adequately. Burgess shows that the third superharmonic is the dominant component of the solution in the range $0.45 < \Omega < 0.55$, Fig. 3 for the particular amplitude ($s = 1$) of the sinusoidal forcing function used. The amplitude of the third superharmonic component reaches a peak in the range $0.45 < \Omega < 0.50$. Kats (8) also uses a two-term approximation to the solution of Duffing's equation and shows the presence of superharmonic components in the frequency range $\Omega < 0.5$. Kats shows how the amplitude of the superharmonic increases with increase in forcing function amplitude.

Young and Hess (2) show that in certain areas of the fre-

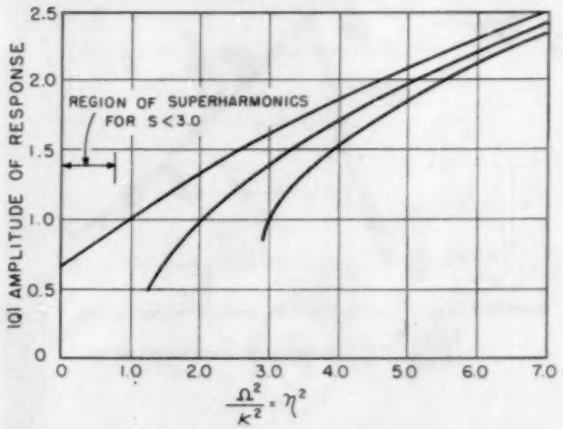

Fig. 1 Response Curves for Duffing's Equation, Equation [1], for Free and Forced Oscillations as Obtained by a Single-Term Approximation

(Since K, the circular frequency of linear system was set at unity for this work, Ω, the response frequency, has the same numerical value as η, the frequency ratio.)

---

[1] Assistant Professor of Design Engineering, University of California.

[2] Numbers in parentheses refer to the Bibliography at the end of the paper.

Presented at the Applied Mechanics Division Summer Conference, Berkeley, Calif., June 13–15, 1957, of The American Society of Mechanical Engineers.

Discussion of this paper should be addressed to the Secretary, ASME, 29 West 39th Street, New York, N. Y., and will be accepted until January 10, 1958, for publication at a later date. Discussion received after the closing date will be returned.

Note: Statements and opinions advanced in papers are to be understood as individual expressions of their authors and not those of the Society. Manuscript received by ASME Applied Mechanics Division, February 19, 1957. Paper No. 57—APM-45.

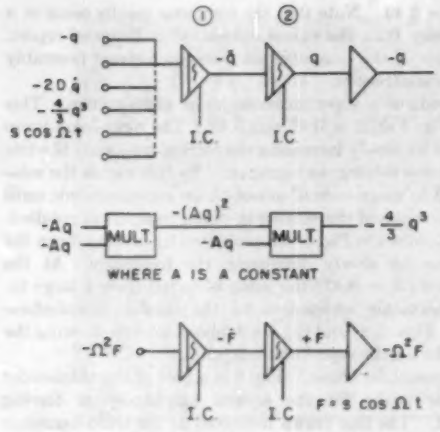

FIG. 2 COMPUTER CIRCUIT FOR SOLVING DUFFING'S EQUATION, EQUATION [1]

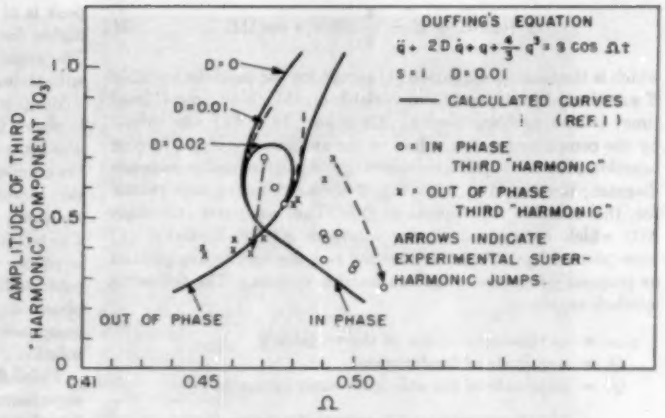

FIG. 3 CALCULATED RESPONSE CURVES FOR THIRD-ORDER SUPERHARMONICS; $s = 1.0$, $D = 0$, AND $D = 0.02$

(Dashed line marked $D = 0.01$ was extrapolated from calculated results. Computer results for $D = 0.01$ are indicated by crosses and circles.)

quency range $\Omega < 2.0$ harmonic solutions are unstable. This work of Young and Hess uses a stability technique based on Mathieu functions (3, 4). They experimentally confirmed their work by an electronic analog computer. The forcing function used by Young and Hess differs from Burgess' in being a two-term cosine function containing a fundamental and a third harmonic. In this form the forcing function resembles an elliptic function which is the natural response (free vibration) of the system.

PURPOSE OF PAPER

The purpose of this paper is to present the results of an electronic analog computer[3] study of the superharmonic region ($\Omega < 0.8$) for the response curves of Duffing's equation

$$\frac{\ddot{q}}{K^2} + \frac{2Dq}{K} + q + \frac{4}{3}q^3 = s\cos\Omega t$$

The main concern is with solutions in that region where the two-term Ritz approximation predicts the presence of the third-order superharmonics. This region corresponds with a region predicted by Young and Hess to contain unstable harmonic solutions. It is proposed further to show that the remaining areas of unstable harmonic solutions of Young and Hess are areas where higher-order harmonics are generated, such as those of fifth and seventh order. The particular superharmonic generated as a component of any solution $q(t)$ of Equation [1] seems to depend on the amplitude of that point on the free-vibration response curve to which the maximum displacement of the solution $q(t)$ corresponds. For example, if the forcing function has a frequency of $\Omega = 0.49$, the solution $q(t)$ of Equation [1] is seen to have a superharmonic component with an amplitude $Q_3 = 0.7$, Fig. 6, and a fundamental component with amplitude $Q_1 = 0.5$. The maximum displacement $q_{max} = Q_1 + Q_3 = 1.2$. An amplitude of 1.2 on the free-vibration curve requires a frequency of $\Omega = 1.56$; slightly more than three times the frequency of the forcing function. Looked at in this way, superharmonics can be pictured as nonlinear resonance phenomena owing to that feature of the driving function which is capable of sustaining an oscillation at the natural frequency of the system.

Further evidence for this assumption that superharmonics can be pictured as nonlinear resonance phenomena is supplied by the results of applying other amplitudes of the forcing function (s in Equation [1]) than the value used by Burgess or Young and Hess. As the amplitude of the forcing function is increased, the frequency at which the third-superharmonic component reaches its maximum is seen to increase also, thus maintaining the suspected relationship of the superharmonic with the free vibration backbone. A "superharmonic backbone" can be drawn, Fig. 6, the amplitude of which corresponds with the amplitude of the free-vibration backbone while its frequency is 1/3 of the natural frequency. It is along this superharmonic backbone or very close to it that values for q (max) appear to lie. Similar superharmonic backbones of higher order can be drawn; i.e., for the fourth, fifth, sixth, seventh, and so on, superharmonics. Along these higher-order superharmonic backbones of order n, the values q_{max} will lie.

DIFFERENTIAL EQUATION SOLVED BY COMPUTER

The differential equation used for the study of superharmonic oscillations as presented in this paper is Duffing's nonlinear differential equation

$$\frac{\ddot{q}}{K^2} + \frac{2Dq}{K} + q + \frac{4}{3}q^3 = s\cos\Omega t \quad \ldots\ldots [1]$$

D is the damping ratio which was set at $D = 0.01$, s is the amplitude of the forcing function $s\cos\Omega t$, and has each of the following values: 1.0, 1.5, 2.0, 2.4, and 3.0. The frequency range of the investigation was limited to the range $\Omega < 0.8$, Fig. 1; K, the natural frequency of the linear system, was set = 1. Equation [1] was transformed to a "machine" equation (7). The transformation equations used are $E = \alpha q$, $T = \beta t$, where E is the machine-dependent variable which appears as a voltage in the computer, T is machine time, α and β are scale factors.

The machine equation is

$$E'' + 2\frac{D}{\beta}E' + \frac{E}{\beta^2} + \frac{4}{3}\frac{E^3}{\beta^2\alpha^2} = \frac{\alpha}{\beta^2}s\cos\frac{\Omega}{\beta}T \quad \ldots [2]$$

The most convenient values for the scale factors α and β were $\alpha = \beta = 1$. The machine equation was then

[3] The electronic analog computer used for this study was the Beckman EASE computer located at the computer facility of Berkeley Division, Beckman Scientific Instruments, Richmond, Calif. Some additional data were taken at the EASE computer located in the Analog Laboratory, Department of Engineering, University of California, Berkeley, Calif.

$$\ddot{E} + 2D\dot{E} + E + \frac{4}{3}E^3 = s\cos\Omega T \ldots\ldots\ldots [3]$$

which is the same as Equation [1] except for the machine variable E substituted for the problem variable q. Machine time T (real time) is also problem time t. Equation [3] or [1] was solved by the computer for five values of the amplitude s of the forcing function over the superharmonic range of the frequency-response diagram; that is, $\Omega < 0.8$. Fig. 2 shows the computer circuit for the solution of Equation [1]. The computer solutions $E(t)$ which correspond to the solutions $q(t)$ of Equation [1] were plotted by a Sanborn recorder and the results are plotted as frequency-response diagrams for this system. The following symbols are used:

q_{max} = maximum excursion of the variable q
Q_1 = amplitude of fundamental
Q_n = amplitude of the nth order superharmonic

Discussion of Computer Results

Third Harmonic With $s = 1$. The analysis of the computer results for the solution of Equation [1] are given in Figs. 3 through 7. Fig. 3 is a plot of the amplitude of the third harmonic for the forcing-frequency range $0.45 < \Omega < 0.51$. The computer solutions containing the third superharmonic take two forms in this range. For Ω increasing from 0.4 the peaks of the fundamental and the third-harmonic component are referred to as "out of phase" and the corresponding displacement is $q = Q_1 - Q_3$, Fig. 4(*a*). For Ω decreasing from $\Omega = 0.51$ the harmonic peaks occur in such a way that $q_{max} = Q_1 + Q_3$. The components are considered to be "in phase" when their peaks are additive in this manner, Fig. 4(*b*). The lines drawn on Fig. 3 are taken from Burgess' work and are the response curves for the third-superharmonic component. Damping reduces the peaks as shown. The curve for $D = 0.01$ was extrapolated from the calculated data. The loop indicates the continuous change from an in-phase to out-of-phase superharmonic component. Note that the in-phase superharmonic resonates at a lower frequency than the out-of-phase superharmonic. The computer data do not outline a complete loop as indicated by Burgess' data, but they show clearly the in-phase solutions and the out-of-phase solutions. The upper portion of the loops are considered unstable. The in-phase superharmonic has its peak for $s = 1$ at $\Omega = 0.475$ for light damping ($D = 0.01$). The out-of-phase peak is at $\Omega = 0.49$. Note that the computer results occur at a higher frequency than the values calculated in Burgess' report. The amplitudes of the computer solutions correspond favorably with the calculated results.

Burgess predicts a superharmonic-jump phenomenon. This is shown in Fig. 3 at $\Omega = 0.47$ and 0.49. The right-hand jump was generated by slowly increasing the forcing frequency Ω while the computer was solving the equation. By this means the solution increased in magnitude of out-of-phase superharmonic until the jump occurred and the smaller in-phase component resulted. The left jump shown in Fig. 3 was generated by moving down the in-phase curve by slowly decreasing the frequency. At the point indicated ($\Omega = 0.47$) the jump occurred from a large in-phase superharmonic component to the smaller out-of-phase component. Figs. 5(*a*) and (*b*) are Sanborn records showing the solution $q(t)$ during the superharmonic jump.

Third-Harmonic Backbone. Fig. 6 is a plot of the third-order superharmonic peaks for the several amplitudes of forcing function used. The line drawn indicated as the third-harmonic backbone is the line along which the points have the amplitude of the free vibration but a frequency of 1/3 that of the free vibration. The purpose of such a line is to indicate the nature of these superharmonic components by relating their frequency of three times the forcing frequency (3Ω) with the frequency of free vibrations. That is to say, for a particular amplitude of forcing function there is a frequency (or better, a frequency range, since the phase relation between the harmonic components is important here) at which a third harmonic will reach its maximum value. At this frequency, the sum of the fundamental and the superharmonic produces a maximum displacement of oscillation q_{max} that is very close to the amplitude of the free vibration of the system at approximately three times the forcing frequency.

The points plotted in Fig. 6 are the third-superharmonic peaks as generated by the computer for the solution of Equation [1] for the different amplitudes s of the forcing function. Note that as the amplitude s increases so does the peak for the third harmonic as well as the frequency at which the peak occurs. This increase seems necessary in order to maintain the relationship of q_{max} of the oscillation with the amplitude of the free vibration at 3Ω.

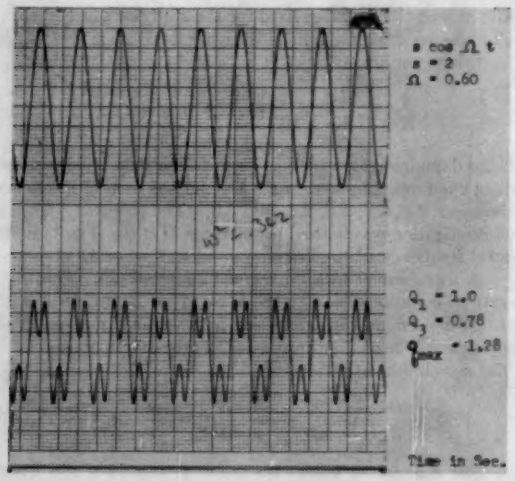

Fig. 4(*a*) Out-of-Phase Third-Order Superharmonic

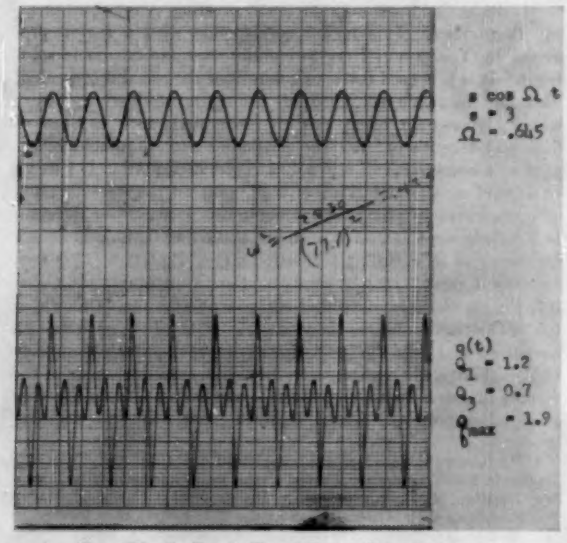

Fig. 4(*b*) In-Phase Third-Order Superharmonic

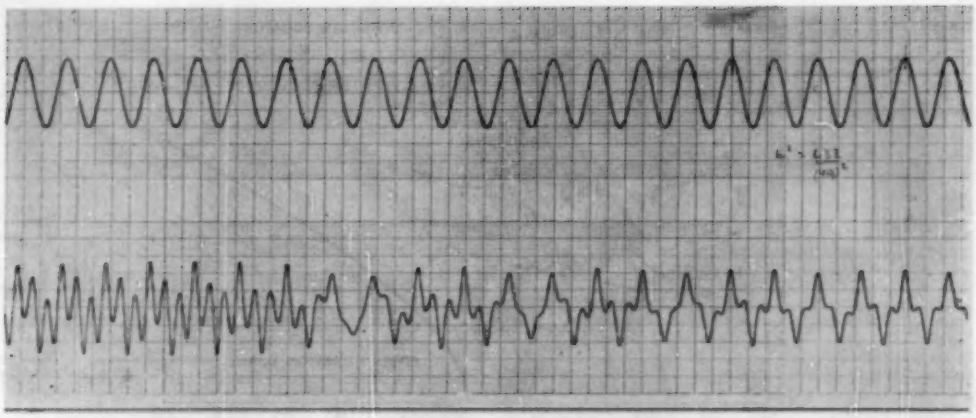

FIG. 5(a) SUPERHARMONIC JUMP FROM OUT OF PHASE TO IN PHASE AS Ω IS INCREASED FROM 0.49 TO 0.51
(Upper curve is forcing function $s \cos \Omega t$ with $s = 1.0$. Lower curve is solution $q(t)$ of Duffing's equation, Equation [1], to a scale of one volt per centimeter. Ticks along bottom represent seconds. Q_3 changes from 0.7 to 0.5.)

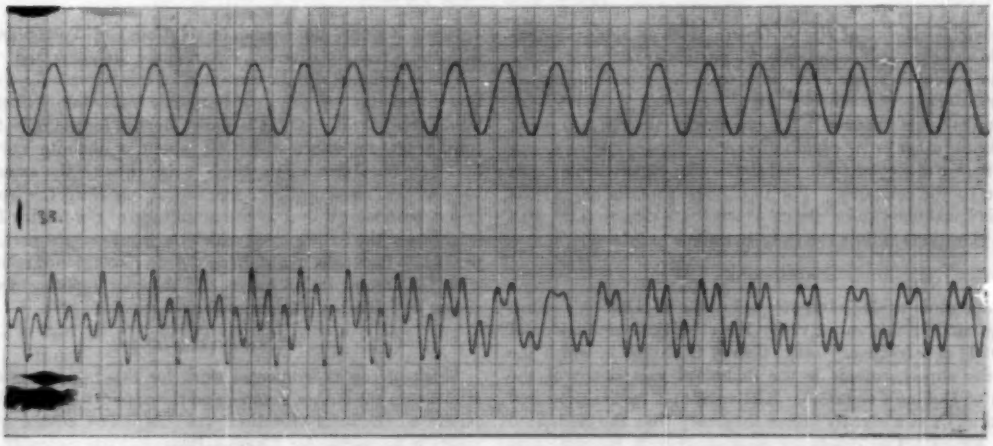

FIG. 5(b) SUPERHARMONIC JUMP FROM IN PHASE TO OUT OF PHASE AS Ω IS DECREASED FROM 0.47 TO 0.465
(Q_3 changes from 0.7 to 0.35, same legend as Fig. 5a.)

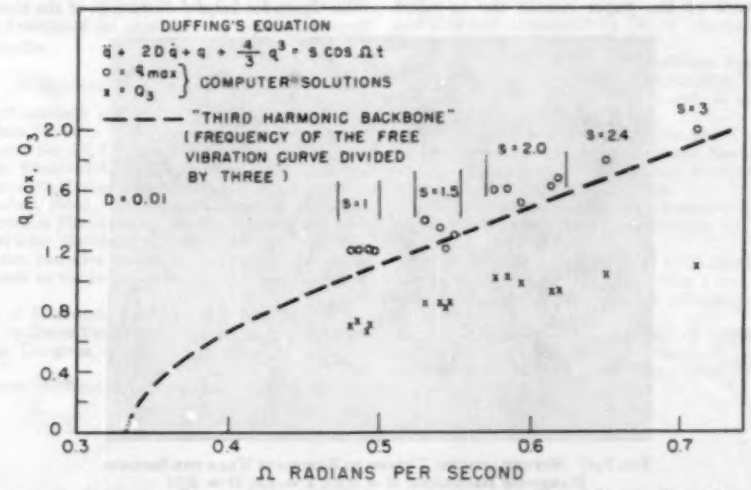

FIG. 6 MAXIMUM DISPLACEMENT q_{max}, AND AMPLITUDE OF THIRD-ORDER SUPERHARMONIC Q_3 AS OBTAINED FROM COMPUTER SOLUTIONS WITH DIFFERENT AMPLITUDES s OF FORCING FUNCTION
(Dashed line represents third-harmonic backbone.)

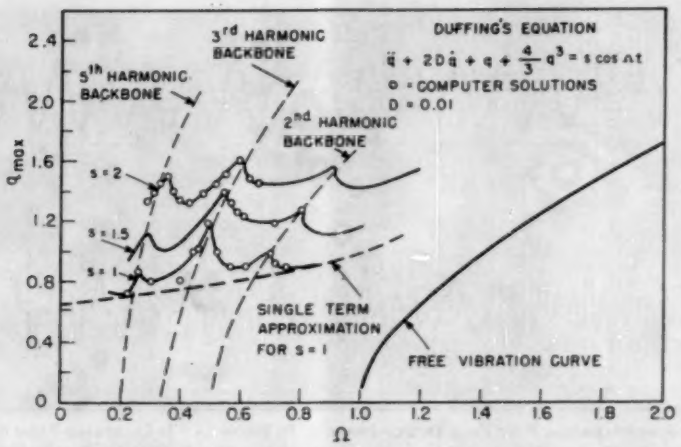

FIG. 7 SUPERHARMONIC REGION SHOWING SECOND, THIRD, AND FIFTH-HARMONIC BACKBONES WITH COMPUTER RESULTS PEAKING AT APPROPRIATE BACKBONES

Harmonic Backbones of Higher Order. Just as a third superharmonic was seen to have a peak at a particular frequency for a particular forcing-function amplitude, so a similar peaking occurs for other order superharmonics. Fig. 7 is a sketch of the response curve for Duffing's equation in the superharmonic region showing the peaks for other order superharmonics. Examples are shown in Figs. 8*a*, *b*, *c* of second, fifth, and sixth-order superharmonics as produced by the computer. For all of these superharmonics the harmonic backbone can be drawn which has a similar ratio with the free vibrations as does the third-harmonic backbone.

CONCLUSIONS

The electronic-analog-computer solutions of Duffing's equation presented in this paper verify the analytical predictions of Burgess (1) of a frequency range $0.45 < \Omega < 0.50$ in which the third-order superharmonic is the dominant component of the solution of Duffing's equation. The computer results produced a maximum Q_3 at a slightly higher frequency than the calculated results, Fig. 3. The computer solutions verify Burgess' prediction of superharmonic-jump phenomena. Fig. 5 shows the Sanborn record of these superharmonic jumps.

The experimental work of the paper relates the so-called unstable regions (nonharmonic solutions) of Young and Hess with those regions where superharmonics are generated.

The experimental data presented in this paper offer a descriptive explanation of the superharmonic oscillation as being sustained free vibrations. It is shown herein, for example, that the third-order superharmonic falls about a definite curve, the harmonic-backbone curve which is drawn with the same amplitude as the free-vibration curve but at one third the frequency. It has been shown that as the amplitude of the forcing function is increased the frequency at which the third-order superharmonic peaks also increases, maintaining the afore-mentioned relationship with the free-vibration curve. Fifth-order superharmonics are shown to fall along their respective backbone.

ACKNOWLEDGMENTS

Much of the experimental work for this paper was done by students in the author's courses on the application of analog computers to nonlinear-vibration problems. The author wishes to mention in particular Charles Bourne, Dale Schmidt, Arville Trostrud, John Rodden, and Patrick Gildea.

The author wishes to express his indebtedness to Mr. Katsuhiko Ogata for helpful discussion of the theoretical aspects of the

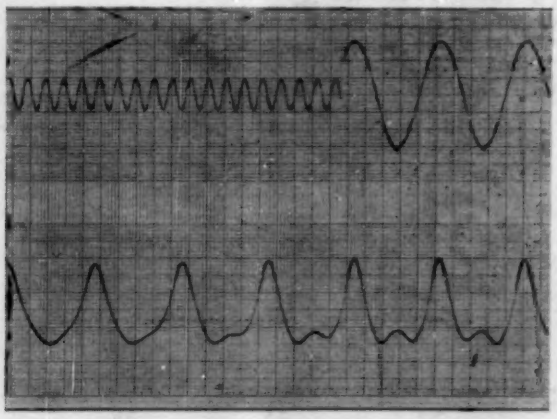

FIG. 8(*a*) SUPERHARMONIC TRYING TO RESONATE NEAR THE SECOND-HARMONIC BACKBONE; $\Omega = 0.82$, $s = 1.5$, $D = 0.01$
(Forcing function $s \cos \Omega t$ is upper right-hand curve.)

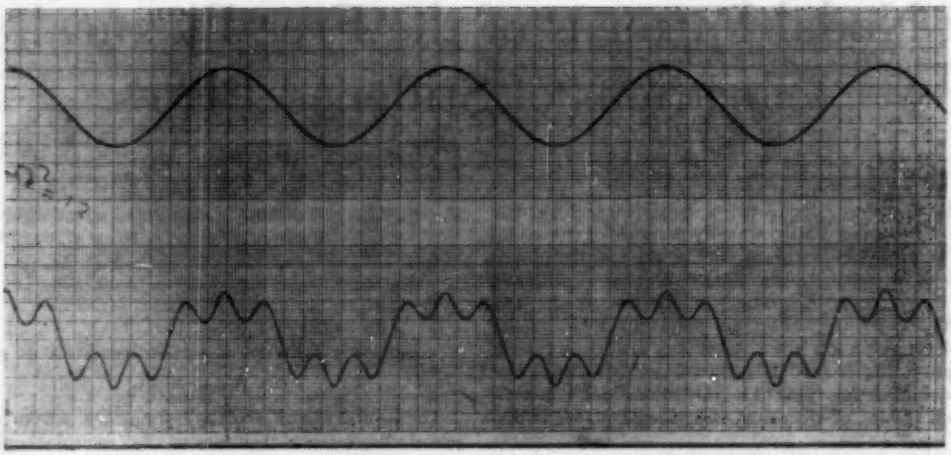

FIG. 8(b) FIFTH-ORDER SUPERHARMONIC: $\Omega = 0.348$, $s = 2.0$, $q_{max} = 1.3$, $Q_1 \approx 0.8$, $Q_3 \approx 0.5$; UPPER CURVE IS $s \cos \Omega t$; $\beta = \sqrt{10}$, $D = 0.01$

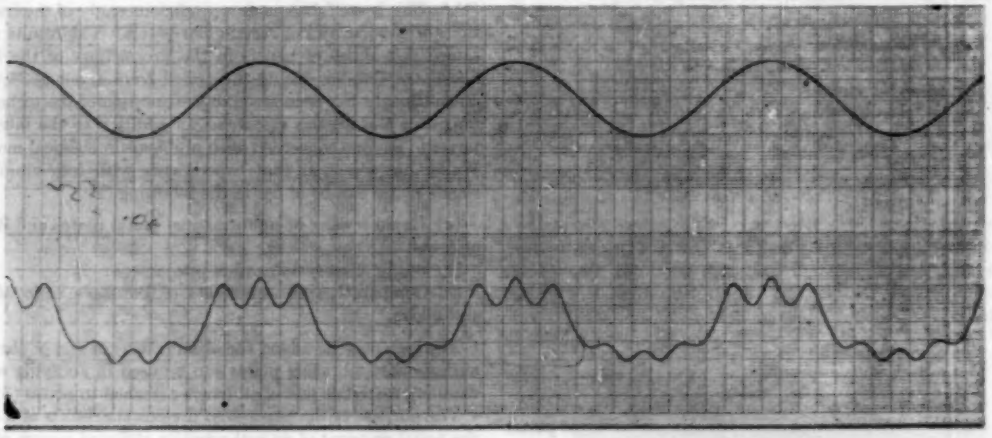

FIG. 8(c) SIXTH-ORDER SUPERHARMONIC: $s = 2$, $\Omega = 0.285$, $\beta = \sqrt{10}$, $D = 0.01$

paper as well as his assistance in maintaining the laboratory equipment in working order.

BIBLIOGRAPHY

1 "Harmonic, Superharmonic and Subharmonic Responses for Single Degree of Freedom Systems of the Duffing Type," by J. C. Burgess, Technical Report No. 27, Division of Engineering Mechanics, Stanford University, Stanford, Calif., September, 1954. (A report based on Dr. Burgess' PhD dissertation, School of Engineering, Stanford, Calif., September, 1954). See also, a discussion of "Subharmonic and Superharmonic Phenomena," by Dr. Burgess, appearing in JOURNAL OF APPLIED MECHANICS, Trans. ASME, vol. 77, 1955, pp. 280–282, which contains response curves for both sub and superharmonics as well as the jump region for third-order superharmonics.

2 "On the Stability of Harmonic Solutions of a Modified Form of Duffing's Equation," by Dana Young and P. N. Hess, Proceedings of the Second National Congress of Applied Mechanics, ASME, 1955, pp. 79–84.

3 "Ordinary Nonlinear Differential Equations in Engineering and Physical Sciences," by N. W. McLachlan, Clarendon Press, Oxford, England, 1950.

4 "Forced Oscillations in Nonlinear Systems," by C. Hayashi, Nippon Printing and Publishing Company, Osaka, Japan, 1953.

5 "Tables of Functions," by E. Jahnke and F. Emde, Dover Publications, New York, N. Y., 1945.

6 "Steady State Motion of One and Two Degrees of Freedom Vibrating Systems With a Nonlinear Restoring Force," by P. R. Sethna, Proceedings of the Second National Congress of Applied Mechanics, ASME, 1955, pp. 69–78.

7 "Instrumentation Manual, Berkeley Electronic Analog Simulating Equipment," Berkeley Division of Beckman Instruments, Inc., Richmond, Calif., 1954.

8 "Biharmonic Oscillations in a Dissipative Nonlinear Vibrating System With a Sinusoidal Disturbing Force," by A. M. Kats, *Prikladnaia Matematika I Mekhanika* (USSR), vol. 18, July, 1954, pp. 425–444.

9 "The Existence and Stability of Ultraharmonics and Subharmonics in Forced Nonlinear Oscillations," by T. K. Caughey, JOURNAL OF APPLIED MECHANICS, Trans. ASME, vol. 76, 1954, pp. 327–335.

Nodal Patterns of the Free Flexural Vibrations of Stiffened Plates

By W. H. HOPPMANN, II,[1] and L. S. MAGNESS,[2] BALTIMORE, MD.

With the aid of results from previous research on the vibration of stiffened plates, a study is made of the nodal patterns of a particular plate with orthogonally placed stiffeners. The pertinent theory of vibration of stiffened plates is introduced. Experiments are described. The normal modes of vibration are investigated. Frequencies of flexural vibration are given for theory and experiment. The compounding of modes is illustrated by a single but rather convincing example. The rôle of research concerning normal modes of vibration of stiffened plates is discussed.

Nomenclature

The following nomenclature is used in the paper:

ϵ_i = extensional strain
γ = shear strain
σ_i = extensional stress
τ = shear stress
S_{ij} = elastic constants ($S_{ij} = S_{ji}$)
$\epsilon_i = S_{ij}\sigma_j (i, j$, summed over 1, 2)
$\gamma = S_{66}\tau$
$S^* = \begin{vmatrix} S_{11} S_{12} \\ S_{21} S_{22} \end{vmatrix}$
$E_x' = \dfrac{S_{22}}{S^*}$
$E_y' = \dfrac{S_{11}}{S^*}$
$E' = \dfrac{S_{11}}{S^*}$
$G_{xy} = \dfrac{1}{S_{66}}$
h^* = thickness of plate (equivalent orthotropic plate)
ρh^* = mass per unit area of middle surface of plate
t = time
p_{mn} = circular frequency of m,n-mode of vibration of rectangular plate
a = width of plate
b = length of plate
x, y = co-ordinates of point in middle surface of plate
M_x = bending couple per unit length on edges parallel to y-axis
M_y = bending couple per unit length on edges parallel to x-axis
A_x, A_y, A_{xy} = constants in differential equation of plate and are expressions in terms of elastic constants S_{ij}
$D_x = A_x$
$D_y = A_y$
$2H = A_{xy}$
w = deflection of plate perpendicular to plane x, y

Introduction

The flexural vibrations of flat isotropic plates have been a subject of study for more than one and a half centuries beginning with the famous investigation of Chladni in the eighteenth century. Mary Waller reviews the history of the subject briefly but quite critically in one of her several voluminous papers on the subject (1).[3] She, herself, has made a prodigious study of the free vibrations of circular and of rectangular plates. The results are contained in a series of papers in the Proceedings of the Physical Society of London during the period from about 1938 to 1949. Some thought has been given to the question of the technological importance of all this research. In addition to the intrinsic interest to anyone concerned with problems in classical mechanics, Waller has observed that experiments with free vibrations of elastic plates can be of use in the following (2):

(*a*) Rapid testing of uniformity of metal plates and detection of flaws.

(*b*) Study of recrystallization phenomena.

(*c*) Comparative measurements of Poisson's ratio of metals and alloys.

To these may be added the observations of one of the present authors that vibrating plates can be used in studying effects of damping materials and of stiffeners attached to plates (3).

The purpose of the paper is to present the results of a study of the nodal patterns of an orthogonally stiffened square plate. It is believed that this is the first time such a study has been made for stiffened plates along the lines of the numerous studies that have been made in the past for freely vibrating isotropic plates (1).

Résumé of Theory

The elemental theory of flexural vibrations of orthogonally stiffened plates has been presented elsewhere (4) and will not be repeated here. However, for the present purpose the pertinent portions will be summarized. The differential equations of free vibrations of the stiffened plate, neglecting shear deformation and rotatory inertia, may be written as follows (4)

$$A_x \frac{\partial^4 w}{\partial x^4} + A_{xy} \frac{\partial^4 w}{\partial x^2 \partial y^2} + A_y \frac{\partial^4 w}{\partial y^4} + \rho h^* \frac{\partial^2 w}{\partial t^2} = 0 \ldots [1]$$

The A_x, A_y, and A_{xy} are constants which can be written explicitly in terms of elastic compliances S_{ij}. The quantities S_{ij} have been explained in detail in previous papers (4, 5, 6) and hence will not be discussed further in this paper.

In order to study in some detail the nodal patterns for vibrating

---

[1] Associate Professor, Department of Mechanical Engineering, The Johns Hopkins University. Mem. ASME.

[2] Research Assistant, The Johns Hopkins University. Assoc. Mem. ASME.

Presented at the Applied Mechanics Division Summer Conference, Berkeley, Calif., June 13–15, 1957, of The American Society of Mechanical Engineers.

Discussion of this paper should be addressed to the Secretary, ASME, 29 West 39th Street, New York, N. Y., and will be accepted until January 10, 1958, for publication at a later date. Discussion received after the closing date will be returned.

Note: Statements and opinions advanced in papers are to be understood as individual expressions of their authors and not those of the Society. Manuscript received by ASME Applied Mechanics Division, August 10, 1956. Paper No. 57—APM-38.

[3] Numbers in parentheses refer to the Bibliography at the end of the paper.

plates with given boundary conditions, the analytically simple one of hinged edges is chosen. They may be written simply as follows for a rectangular plate

$$\left.\begin{aligned} M_x &= 0 \text{ for boundary perpendicular to } x\text{-axis} \\ M_y &= 0 \text{ for boundary perpendicular to } y\text{-axis} \\ w &= 0 \text{ entire boundary} \end{aligned}\right\} \quad \ldots [2]$$

The x-axis and y-axis are chosen along the principal directions of plate stiffness. As a consequence, the boundary conditions reduce to

$$\left.\begin{aligned} \frac{\partial^2 w}{\partial x^2} &= 0 \\ \frac{\partial^2 w}{\partial y^2} &= 0 \\ w &= 0 \end{aligned}\right\} \text{ along appropriate portions of boundary} \quad \ldots [3]$$

A solution of the differential Equation [1] for a rectangular plate of sides a, b and satisfying Boundary Conditions [3] is obviously

$$w = \Sigma\Sigma \sin \frac{m\pi x}{a} \sin \frac{n\pi y}{b} F(t) \quad \ldots [4]$$

The $F(t)$ in this case is of course a harmonic function of time.

The frequency equation then is (4)

$$p_{mn} = \frac{\pi^2}{\sqrt{(\rho h^*)}} \left(D_x \frac{m^4}{a^4} + 2H \frac{m^2 n^2}{a^2 b^2} + D_y \frac{n^4}{b^4} \right)^{1/2} \quad \ldots [5]$$

where

$$D_x = \frac{E_x' h^3}{12} \qquad D_{xy} = \frac{G_{xy} h^3}{12}$$

$$D_y = \frac{E_y' h^3}{12} \qquad H = D_1 + 2D_{xy}$$

$$D_1 = \frac{E'' h^3}{12}$$

and

$$E_x' = \frac{S_{22}}{S_{11}S_{22} - S_{12}^2}$$

$$E_y' = \frac{S_{11}}{S_{11}S_{22} - S_{12}^2}$$

$$E'' = \frac{S_{12}}{S_{12}^2 - S_{11}S_{22}}$$

$$G_{xy} = \frac{1}{S_{33}}$$

For the particular stiffened plate being studied in this paper the values (5) of S_{ij} are given in Table 1.

TABLE 1 VALUES OF S_{ij}

$\frac{S_{11}}{h^3} \times 10^6$	$\frac{S_{12}}{h^3} \times 10^6$	$\frac{S_{21}}{h^3} \times 10^6$	$\frac{S_{22}}{h^3} \times 10^6$	$\frac{S_{33}}{h^3} \times 10^6$
306	1.4	−18.1	13.0	370

Units are inches and pounds. Plate material is aluminum.

The stress-strain law is assumed to be symmetrical so that

$$S_{ij} = S_{ji}$$

With actual experimental data, it may be necessary to average S_{12} and S_{21}. Also it may be noted that the appropriate sign for S_{12} and S_{21} in the tabulated figures is minus. In this case S_{12} and S_{21} then equal −8.35.

The quantity ρh^* is mass per unit area of the plate. That is, for the square plate discussed in the latter part of this paper, it is the total mass of the plate within the supports around the boundary divided by the square of the length of one side.

Experimental Plate and Boundary Conditions

In order to make an experimental study of the nodal patterns for vibrating plates with orthogonal stiffeners, the boundary condition was assumed to be simple support or hinged, as it is sometimes called, and the stiffeners were made as deep as practicable for use with the available experimental apparatus.

The boundary condition was obtained by making a sufficiently deep notch at the boundary of the plate leaving a narrow flat rim extending beyond. This rim was then mounted rigidly in a surrounding support as described more fully in previous papers (3, 6, 11).

The plate with integral stiffeners was machined by milling it out of a solid sheet of aluminum. The dimensions may be of interest and are given in Table 2.

TABLE 2 PLATE AND STIFFENER DIMENSIONS

Length of side of plate	= 11 in.
Thickness of plate	= 0.065 in.
Depth of stiffener	= 0.210 in.
Width of stiffener	= 0.125 in.
Spacing of stiffeners	= 0.75 in.
Total no. of stiffeners	= 15

NOTE: Stiffeners were on one side of plate only.

Experimental Apparatus

A massive test stand was used in mounting the plate for study. It is shown in Fig. 1. The heavy steel holding-down bars are shown with the bolts that held the edge of the plate clamped rigidly in a horizontal plane. The notched portion of the plate was adjacent to this clamping area, causing very small elastic rotational constraint.

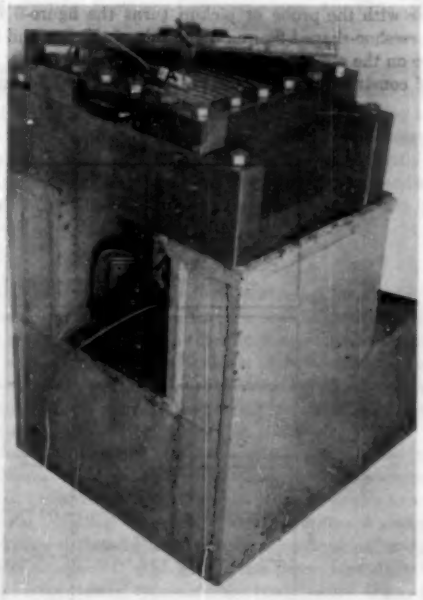

FIG. 1 TEST STAND FOR VIBRATION EXPERIMENTS ON PLATES

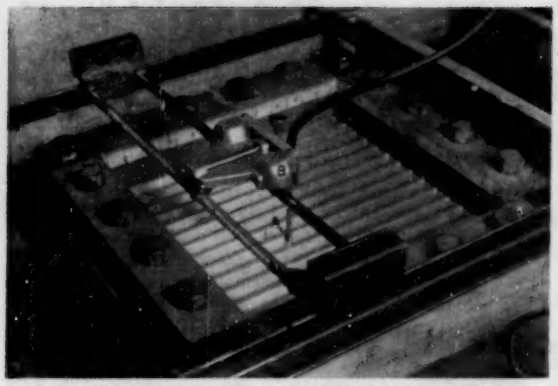

FIG. 2 APPARATUS FOR STUDY OF FREQUENCIES AND NODAL PATTERNS

The plate was driven by an electromagnet mounted beneath the plate and on the solid test stand. Because the plate was of aluminum it was necessary to cement to it a very small piece of iron in order to drive it with a magnet. The equipment is described elsewhere (6) and therefore will not be dealt with further in this paper.

Apparatus for determining the frequencies of vibration and the nodal patterns is shown in Fig. 2. The pickup marked A is of the capacity type and is fully described by S. N. Shafer and R. Plunkett in a technical paper on that subject (7). It may suffice here to note that a nodal line on the vibrating plate is detected by the change in shape of a figure on a cathode-ray oscilloscope to which the electrical output from the pickup is fed through a preamplifier. On account of the nature of the magnet the frequency from the oscillator is one half the frequency of the driving force. The output from the oscillator is connected to one set of plates of the cathode-ray oscilloscope and the magnetic drive is connected across the other set of plates. Since the frequency ratio is 2 to 1, a figure-8 lissajou is shown on the screen of the scope. Crossing a nodal line with the probe or pickup turns the figure-8 lissajou into a horseshoe-shaped figure on one side of the line and inverts the figure on the opposite side. This fact provides a very precise means of constructing the nodal pattern for the stiffened plate. Frequencies also were checked by means of a small crystal-type pickup which was placed in contact with the vibrating plate. The pickup is shown as A in Fig. 1.

The capacity-type pickup was mounted to a carriage shown in Fig. 2 at B. The pickup could be raised by a screw above the stiffeners and rolled to any position along two parallel tracks shown there. Also, these tracks were mounted solidly to two sets of rollers, one of which is shown at C. These rollers in turn could move freely over a pair of parallel tracks running orthogonally to the two just mentioned. One of these latter tracks is marked D. In this fashion the pickup could be moved readily to any point on the stiffened plate under test. It can be seen then that, with this device, nodal patterns may be traced readily.

FREQUENCIES OF FLEXURAL VIBRATION OF NORMAL MODES

With the experimental equipment it was relatively easy to determine frequencies of flexural vibration of the normal modes. Also, the frequencies can be calculated by means of Frequency Equation [5]. The results of calculation and of experiment are shown in Table 3.

The corresponding nodal patterns for the various modes are shown in Fig. 3. The theoretical nodal lines are shown as

TABLE 3 FREQUENCIES OF FLEXURAL VIBRATION

n \ m	1	2	3	4	5
1	244 / 238	340 / 336	538 / 534	800 / 831	1152 / 1220
2	794 / 880	960 / 954	1020 / 1100	1268 / 1344	1580 / 1669
3	1700 / 1950	1800 / 2080	1840 / 2150	2110 / 2349	2340 / 2636

Note: 1 Theoretical frequency is in lower half of box. Experimental frequency is in upper half of box.
2 Frequencies are in cycles per second.

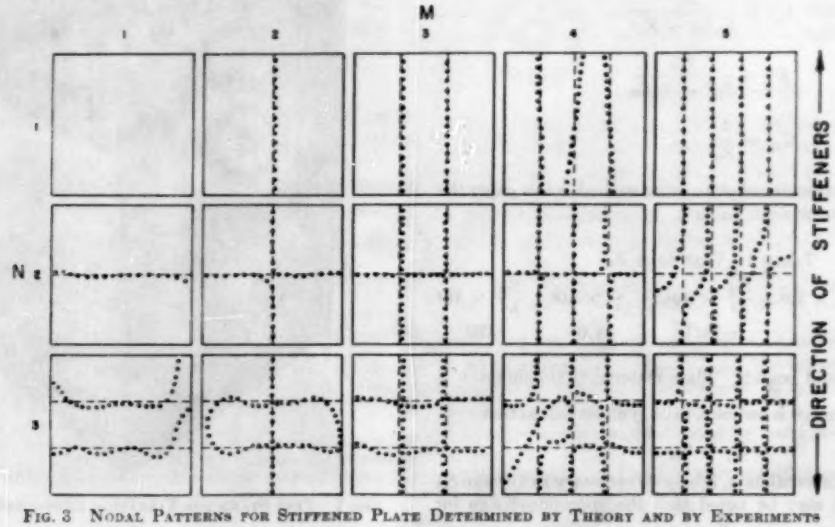

FIG. 3 NODAL PATTERNS FOR STIFFENED PLATE DETERMINED BY THEORY AND BY EXPERIMENTS

dashed lines and the experimentally determined nodal lines are shown by dots. The values of m give the number of half waves in one direction and the values of n give the number of half waves in the orthogonal direction. It can be seen that for n equals unity and all values of m tested the agreement between theory and experiment is excellent. This is true also for n equals 2 and all values of m except m equals 5. When n equals 3 a considerable amount of distortion occurs in the experimental data. It is quite difficult to decide what caused this distortion. It may be related to boundary condition or to heterogeneity in the stiffened plate, or both.

Compounded Normal Modes of Flexural Vibrations

The problem of compounding two normal modes of flexural vibration for isotropic plates has been discussed by Waller (8, 9) and by Warburton (10). Compounding of modes is an interesting phenomenon for theoretical considerations of the vibration of plates with different kinds of boundary conditions. It assumes a peculiar significance in the study of the vibration of plates with stiffeners attached in the manner described in the present paper. As a matter of fact, it can be used in an interesting manner to support arguments in favor of the theory of vibration of stiffened plates used in this paper. A brief review will now be given of the matter as it applies to the theory of stiffened plates.

Waller has noted that complicated nodal designs sometimes occur on isotropic plates with various boundary conditions which cannot be recognized as belonging to any of the normal classes. It is shown that such designs generally consist of two compounded modes of vibration, the periods of which are nearly equal. Such combinations, she says, are possible because the internal damping of the plate reduces the sharpness of resonance. In an earlier paper on circular plates she also observed the same phenomenon and there stated that the vibration frequencies corresponding to the designs are intermediate between those of the combining modes. Warburton in one of his papers (10) further indicates that the combining phenomenon does not occur in the case of freely supported (simply supported) square plates of isotropic material. Now the reason for this fact may be seen from Equation [5]. If a plate is isotropic, then in that equation we have D_x, D_y, and H all equal to each other. Furthermore, if the plate is square, that is, side a equals side b, the frequency of vibration is proportional to $(m^2 + n^2)$. Obviously, in this case there are no two distinct modes with frequencies nearly equal. For the symmetrical modes $m|n$ and $n|m$ the two frequencies become identical because $(m^2 + n^2)$ is the same in both cases. Also, there is no difference in the modal shapes for this case when the plate is square. For any other combination of two modes we would have a great difference in the frequency ratio. For example, 1|3 and 2|1 give a ratio of 2 to 1.

Now, however, if we consider an orthogonally stiffened square plate with simply supported boundary like the one in the present investigation for example, it can be seen that, although the modal shapes for the stiffened plate are identically like those for the isotropic plate, the frequency equation is much different in that the frequency is no longer proportional to $(m^2 + n^2)$. In fact, the elastic compliances may be chosen so that D_x, D_y, and H are unequal and their values may be such that for given pairs of frequency sets $m|n$ the corresponding frequencies may be close to each other. Then it would appear that the phenomenon of compounding normal modes might be observed in this case even though the boundaries are square and simply supported. It turns out that this is exactly what happens. For the experimental plate we are considering, it develops that for $m|n$ given as 4|1 for one mode and 1|2 for the other the two normal frequencies are 800 and 794 cycles per sec (cps), respectively, as may be seen from Table 3.

The frequency ratio is 1.01 so it might then appear possible to excite these two normal modes simultaneously at a driving frequency between the two resonant frequency values. Such is the case and a very beautiful check of the compounded nodal pattern is obtained. If the two different modes of vibration are compounded from Equation [4] for equal amplitudes of the separate modes we obtain the equation of a possible nodal line on the plate. The equation for this case is

$$w = \sin\frac{\pi x}{a}\sin\frac{2\pi y}{a} + \sin\frac{4\pi x}{a}\sin\frac{\pi y}{a} = 0 \ldots\ldots [6]$$

The plate was found actually to have this pattern when driven at a frequency of 800 cps. The results are plotted in Fig. 4. This fact is taken as a rather striking corroboration of the proposed theory of vibrating plates with stiffeners. While with simple support boundaries the modal shapes are no different than those for isotropic plates, the vast difference in the frequency equations makes the two cases contrast sharply. This phenomenon of compounding is clearly demonstrated in the case with stiffeners

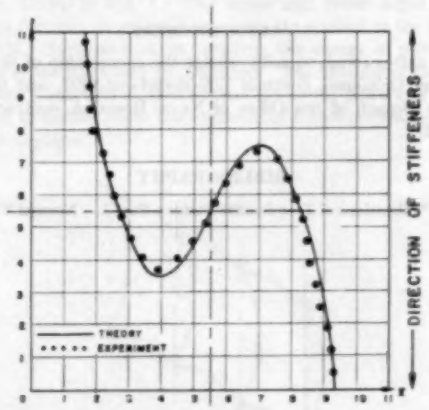

Fig. 4 Nodal Pattern Corresponding to Two Different Modes Excited Simultaneously

whereas it is theoretically and experimentally impossible for the isotropic plate with such boundary conditions. Hence a boundary condition which might be thought to be uninteresting really develops into a good argument for the validity of the theory of stiffened plates which is proposed. It may be seen by study of Fig. 4 that the nodal curve crosses over the stiffeners in directions which are not orthogonal to the stiffeners and hence not in principal directions of stiffness.

Conclusions

It would appear that the proposed theory for vibrating plates with closely spaced and moderately deep stiffeners provides useful results and certainly may be considered at least as a starting point in any serious study of the vibration of such stiffened plates.

Experimental work on nodal patterns of vibrating plates provides an effective means for studying the relation of theory and experiment for vibrating plates with stiffeners.

While good agreement was obtained between the theoretical and experimental frequencies of vibration, more importance is attached to the phenomenon of compounding of modes as a verification of the proposed vibration theory for stiffened plates.

For square stiffened plates with simply supported boundary the predicted compounding of modes has been beautifully verified. This fact is considered to be an important feature of any study of the correctness of the theory.

The authors agree with the findings of Waller in her study on isotropic plates that distorted figures arise unless the experimental conditions are perfect. Some of the reasons she enumerates as causes of the distortions are: (*a*) a want of uniformity in the length of the sides or the thickness of the plate, (*b*) a directional difference in its elastic properties which is often caused by mechanical rolling (note that she is thinking here of plates assumed to be isotropic), (*c*) a want of freedom in the method of support, (*d*) an element of forcing in the method of excitation. Notwithstanding the great care taken in the fabrication of the stiffened plates and in the method of testing in the present investigation, it is clear that the remarks of Waller apply and are even somewhat complicated here by the presence of stiffeners and the need for approximating the condition of simple support at the boundary.

However, notwithstanding the many ways of possible deviation from assumed conditions, the results demonstrate conclusively that if a precise and reliable pickup for nodal patterns, such as that described by Shafer and Plunkett (7), coupled with a carefully devised experimental setup are used, very informative results may be obtained from experiments with stiffened plates.

Acknowledgment

The authors wish to acknowledge the sponsorship of the Office of Army Ordnance, contract DA-36-034-ord-1297, and the Mechanics Branch of the Office of Naval Research, contract Nonr 248 (12).

BIBLIOGRAPHY

1 "Vibrations of Free Square Plates: Part I. Normal Vibrating Modes," by Mary D. Waller, Proceedings of the Physical Society of London, England, vol. 51, 1939, pp. 831–844.

2 "Vibrations of Free Circular Plates: Part I. Normal Modes," by Mary D. Waller, Proceedings of the Physical Society of London, vol. 50, 1938, p. 70.

3 "An Experimental Device for Obtaining Elastic Rotational Constraint on Boundary of a Plate," by W. H. Hoppmann, II, and J. Greenspon, Proceedings of the Second U. S. National Congress of Applied Mechanics, 1954, p. 187.

4 "Bending of Orthogonally Stiffened Plates," by W. H. Hoppmann II, Journal of Applied Mechanics, Trans. ASME, vol. 77, 1955, p. 267.

5 "Elastic Compliances of Orthogonally Stiffened Plates," by W. H. Hoppmann, II, Proceedings of the Society of Experimental Stress Analysis, vol. 14, no. 1, 1956, pp. 137–144.

6 "A Study of Orthogonally Stiffened Plates," by W. H. Hoppmann, II, N. J. Huffington, Jr., and L. S. Magness, Journal of Applied Mechanics, Trans. ASME, vol. 78, 1956, p. 343.

7 "A Miniature Oscilloscope and Vibration Pickup for Nodal Pattern Tracing," by S. N. Shafer and R. Plunkett, Proceedings of the Society for Experimental Stress Analysis, vol. 8, no. 1, 1955, pp. 123–128.

8 "Vibrations of Free Square Plates: Part II. Compounded Normal Modes," by Mary D. Waller, Proceedings of the Physical Society of London, vol. 52, 1940, p. 452.

9 "Vibrations of Free Circular Plates: Part II. Compounded Normal Modes," by Mary D. Waller, Proceedings of the Physical Society of London, vol. 50, 1938, p. 77.

10 "The Vibration of Rectangular Plates," by G. B. Warburton, Proceedings of The Institution of Mechanical Engineers, vol. 168, 1954, pp. 374–375.

11 "Note on the Boundary Conditions for Bending Experiments With Bars and Plates," by W. H. Hoppmann II and W. G. Soper, Journal of Applied Mechanics, Trans. ASME, vol. 78, 1956, p. 646.

12 "Vibrations of Free Rectangular Plates," by Mary D. Waller, Proceedings of the Physical Society of London, section B, vol. 62, 1949, p. 277.

Symmetrical Buckling of a Series of Uniformly Loaded Parallel Struts Supported by Spot Connections to a Long Thin Plate

By J. L. CUTCLIFFE[1] and H. S. HEAPS[2]

The deflection in buckling of a long panel consisting of parallel stiffeners across a rectangular plate is found when equal buckling loads are applied to the ends of each stiffener. The critical load for buckling is found as a function of the elastic properties of the plate and the stiffeners for various spacings of stiffeners, and the number of spot connections to the plate.

Introduction

FORMULAS for the critical loads required to produce buckling of a long thin rectangular plate subject to uniform compressive forces applied to the shorter edges were first obtained by Bryan (1).[3] The critical buckling load and deflection of a rectangular plate of general dimensions and subject to uniform compressive forces applied to a pair of opposite edges were determined by Houbolt and Stowell (2). Conway and others (3, 4, 5) have considered the deflection of a uniformly loaded rectangular plate under the action of uniform tensile or compressive forces applied to opposite edges. The buckling of rectangular plates subject to loads distributed over short portions of the edges has been treated by Zetlin (6). The deflection and buckling of rectangular sandwich plates have been investigated in the case of cylindrical buckling of Goodier (7) and in the general case by Flügge (8) and Gerard (9). Wang (10) has discussed the buckling of a transversely stiffened rectangular plate when shearing forces are applied to the edges perpendicular to the direction of the stiffeners. The similar problem when compressive loads are applied to the edges parallel to the stiffeners has been treated by Cox and Smith (11).

The buckling of compressed rectangular plates whose free edges are intermittently supported has been considered by Norris, Polychrone, and Caposzoli (12), while the buckling of laminated columns has been treated by Clark (13). It is also of some practical interest to consider the effect of stiffeners that are spot-welded or otherwise point-connected to a plate subject to compression in the direction parallel to each stiffener. In many instances it is convenient to apply the compressive loads directly to the stiffeners which then behave as struts partially restrained by the plate.

The present paper considers the buckling of a series of parallel struts equally spaced and spot-connected to a long rectangular plate as shown in Fig. 1. The upper and lower edges of the plate are free and no external moments are applied to the ends of the struts. Suppose that, at buckling, the energy of pure compression of the strut may be neglected. The bending of the strut introduces a reaction at each connection to the plate and causes the plate to deflect under the influence of forces perpendicular to its original plane.

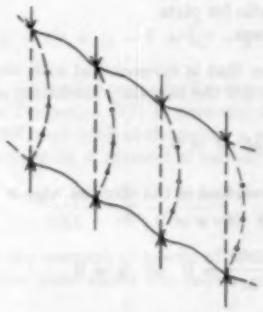

Fig. 1 Buckling of Long Rectangular Plate Spot-Connected to Loaded Parallel Struts

Each spot connection between the plate and the strut may experience either tension or compression. The possibility that part of the reaction may consist of a pressure distributed continuously along a line of contact is not considered in the present paper. However, the method of the present paper may be used to treat the case of a line reaction approximated by a series of point forces.

The usual assumptions concerning the small-deflection theory of plates are adopted. The equation for the deflection of the plate under the unknown reactions is obtained as a Fourier series, and numerical values of the deflection are listed. Subject to equal, but opposite reactions, the deflections of the strut at the spot connections are equal to those of the plate, and hence equations are obtained to determine the unknown reactions. The eigenvalues of these equations lead to the determination of the critical loads for buckling.

Deflection of Plate

Let x and y-axes be chosen along adjacent edges of one panel of the plate as shown in Fig. 2. The plate is attached to a pair of struts which form the edges $x = 0$ and $x = a$. It is supposed

[1] Structures Engineer, Robb Engineering Works, Amherst, Nova Scotia, Canada.

[2] Associate Professor of Applied Mathematics, Nova Scotia Technical College, Halifax, Canada.

[3] Numbers in parentheses refer to the Bibliography at the end of the paper.

Presented at the Applied Mechanics Division Summer Conference, Berkeley, Calif., June 13–15, 1957, of The American Society of Mechanical Engineers.

Discussion of this paper should be addressed to the Secretary, ASME, 29 West 39th Street, New York, N. Y., and will be accepted until January 10, 1958, for publication at a later date. Discussion received after the closing date will be returned.

Note: Statements and opinions advanced in papers are to be understood as individual expressions of their authors and not those of the Society. Manuscript received by ASME Applied Mechanics Division, November 21, 1956. Paper No. 57—APM-7.

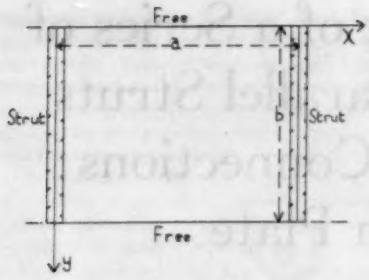

FIG. 2 SINGLE PANEL OF PLATE

that each strut may deform only in a direction perpendicular to the xy-plane and that at each strut the plate is parallel to the x-axis.

The deflection $w(x, y)$ of the plate must satisfy the equation

$$\frac{\partial^4 w}{\partial x^4} + \frac{2\partial^4 w}{\partial x^2 \partial y^2} + \frac{\partial^4 w}{\partial y^4} = \frac{q(x, y)}{D} \quad \ldots\ldots [1]$$

where

$q(x, y)$ = force per unit area perpendicular to plate

$D = \dfrac{Et^3}{12(1 - \nu^2)}$

E = Young's modulus for plate

ν = Poisson's ratio for plate

t = plate thickness

For a deflection that is symmetrical with respect to the lines $x = a/2$ and $y = b/2$ the boundary conditions are as follows

(i) $\dfrac{\partial w}{\partial x} = 0$ at $x = 0$

(ii) $q(0, y)$ = reaction of the strut on edge $x = 0$
$q(x, y) = 0$ if $x \neq 0$

(iii) $\dfrac{\partial^3 w}{\partial y^3} + \nu \dfrac{\partial^3 w}{\partial x^2} = 0$ at $y = 0$

(iv) $\dfrac{\partial^3 w}{\partial y^3} + (2 - \nu) \dfrac{\partial^3 w}{\partial x^2 \partial y} = 0$ at $y = 0$

The deflection w may be represented in the form of a Fourier series in which the coefficients are determined by the transform method described by Deverall and Thorne (14). A line reaction $R(y)$ is regarded as the limit, as d tends to zero, of a pressure of magnitude $R(y)/d$ per unit area uniformly distributed over a strip of width d. Similarly, a point reaction R is the limit of a pressure of magnitude R/d^2 distributed uniformly over an area d^2.

Equation [1] and the condition (i) are satisfied by any function of the form

$$w = \Sigma \epsilon_n a_n(y) \cos p_n x \quad \ldots\ldots [2]$$

in which p_n denotes $2\pi n/a$ and ϵ_n is equal to $1/2$ if $n = 0$ and to unity of $n \neq 0$. Substitution of Equation [2] into Equation [1], multiplication by $\cos p_n x$, and integration in x from zero to a leads to the differential equation

$$\left(\frac{d^2}{dy^2} - p_n^2\right)^2 a_n(y) = \frac{4R(y)}{aD} \quad \ldots\ldots [3]$$

where $R(y)$ is the reaction per unit length of the strut at $x = 0$ upon the plate lying to the positive side of $x = 0$. The total reaction of the plate upon the strut is a line load of magnitude $2R(y)$ per unit length.

A complementary solution of Equation [3] which is symmetrical about $y = b/2$ is the function

$$\text{C.F: } a_n(y) = A_n \cosh p_n \left(y - \frac{b}{2}\right) + B_n p_n \left(y - \frac{b}{2}\right) \sinh p_n \left(y - \frac{b}{2}\right) \quad \ldots\ldots [4]$$

A particular solution of Equation [3] may be found by means of the Laplace transform of $a_n(y)$. Multiplication of Equation [3] by $\exp(-py)$ and integration from zero to infinity with the neglect of arbitrary constants leads to

$$\int_0^\infty a_n(y) \exp(-py)dy = \frac{4}{aD(p^2 - p_n^2)^2} \int_0^\infty R(y) \exp(-py)dy \quad \ldots\ldots [5]$$

In the case that the reaction $R(y)$ is a force of magnitude R at the point $y = h$ the integral on the right-hand side of Equation [5] has the value $R \exp(-hp)$. If the right-hand side of Equation [5] is then written as a sum of four partial fractions involving $p - p_n$ and $p + p_n$ it is found[4] to be the Laplace transform of a function $a_n(y)$ defined as follows

$$\text{P.I: } a_n(y) = \left\{ \begin{array}{l} \dfrac{2R}{aDp_n^3} [p_n(y - h) \cosh p_n(y - h) \\ \qquad - \sinh p_n(y - h)] \quad \text{if} \quad y > h \\ 0 \quad \text{if} \quad y < h \end{array} \right\} \quad \ldots [6]$$

The form of Equation [6] suggests also the following particular solution which has the further property of being symmetrical about $y = h$

$$\text{P.I.: } a_n(y) = \frac{R}{aDp_n^3} [p_n|y - h| \cosh p_n|y - h| - \sinh p_n|y - h|] \quad \ldots\ldots [7]$$

In the case that the reaction $R(y)$ consists of equal point forces of magnitude R acting at $y = h$ and $y = b - h$, the function $a_n(y)$ is given by Equations [4] and [7] as

$$\frac{aDp_n^3}{R} a_n(y) = A_n \cosh p_n \left(y - \frac{b}{2}\right) + B_n p_n \left(y - \frac{b}{2}\right) \sinh p_n \left(y - \frac{b}{2}\right) + f_n(h, y) \quad \ldots\ldots [8]$$

provided $n \neq 0$. For later convenience A_n and B_n have been multiplied by a factor aDp_n^3/R. The term $f_n(h, y)$ denotes the expression

$$f_n(h, y) = p_n|y - h| \cosh p_n|y - h| - \sinh p_n|y - h| + p_n|y - b + h| \cosh p_n|y - b + h| - \sinh p_n|y - b + h| \quad \ldots\ldots [9]$$

When $n = 0$ the Formula [8] must be replaced by

$$\frac{D}{R} a_0 = A_0 + B_0 \left(y - \frac{b}{2}\right)^2 + \frac{a^2}{3} \left(\left|\frac{y - h}{a}\right|^3 + \left|\frac{y - b + h}{a}\right|^3\right) \quad \ldots\ldots [10]$$

If the reaction $R(y)$ consists of a series of point forces of different magnitude and position then for statical equilibrium the sum of such forces must be zero.

The boundary conditions (iii) and (iv) provide two equations to determine the constants A_n and B_n. When n is different from zero the resulting expressions obtained for A_n and B_n are

[4] Reference (15), p. 127.

$$A_n = Y \cosh p_n\left(h - \frac{b}{2}\right) - X\left(h - \frac{b}{2}\right) p_n \sinh p_n\left(h - \frac{b}{2}\right) \quad [11]$$

$$B_n = Zp_n\left(h - \frac{b}{2}\right) \sinh p_n\left(h - \frac{b}{2}\right) - X \cosh p_n\left(h - \frac{b}{2}\right) \quad [12]$$

where

$$X = \frac{2[(3+\nu)\cosh p_n b + 1 - \nu]}{(3+\nu)\sinh p_n b - (1-\nu)p_n b} \quad [13]$$

$$Y = \frac{2\left\{[4 - (1+\nu)^2]\cosh p_n b + 4 + (1+\nu)^2 + \frac{1}{2}(1-\nu)^2(p_n b)^2\right\}}{(1-\nu)[(3+\nu)\sinh p_n b - (1-\nu)p_n b]} \quad [14]$$

$$Z = \frac{4(1-\nu)^2}{(1-\nu)[(3+\nu)\sinh p_n b - (1-\nu)p_n b]} \quad [15]$$

The similar boundary conditions for a_0 are that $B_0 = b/a$ and that $\partial a_0^3/\partial y^3 = 0$ at $y = 0$. This last condition is not satisfied by the single Expression [10] unless $R = 0$. However, in the subsequent application a_0 is represented as a sum of terms of type [10] with different reactions R whose sum is zero. Hence the condition $\partial^3 a_0/\partial y^3$ is indeed fulfilled. In such a sum the terms involving B_0 add to zero and so it may be assumed that, apart from the constant translation A_0

$$\frac{D}{R} a_0 = \frac{a^3}{3}\left(\left|\frac{y-h}{a}\right|^3 + \left|\frac{y-b+h}{a}\right|^3\right) \quad [16]$$

The values of A_n and B_n for some commonly occurring values of $p_n b = 2\pi b/a$ are tabulated in Table 1 for $\nu = 0.3$ and $h = 0$, $b/8$, $b/4$, $3b/8$, and $b/2$. As n tends to infinity, X and Y tend to the value of 2 while Z tends to zero. The rapidity of the convergence of X and Y is apparent from Table 1 since X and Y coincide respectively with $-B_n$ and A_n when $h = b/2$. It then follows from Equation [8] that $a_n(y)$ tends to zero at the rate of $1/n^3$ for large values of n. Thus the Series [2] is convergent.

The values of $p_n b$ in Table 1 are chosen in order to facilitate calculation of the deflection of plates for which $b/a = 1/8, 1/4, 1/2$, or 1. The value of 6.4 is the magnitude of $p_1 b$ when $b/a = 1.02$, which is regarded as a sufficient approximation to unity and is referred to as such in the subsequent description of results.

With values of A_n and B_n, as listed in Table 1, the deflection given by Equations [2] and [8] has been calculated for the case in which the reaction consists of point forces of magnitude R at $y = h$ and $y = b - h$ together with equal and opposite reactions R at the ends $y = 0$ and $y = b$. Under such a set of forces the plate is in statical equilibrium. Values of $(D/Rb^2)w$ at 45 positions on the plate are listed in Tables 2 to 5 for $b/a = 1/8, 1/4, 1/2$, and 1, and $h = b/8, b/4, 3b/8$, and $b/2$. The tabulated figures represent the sum of the first four terms of the Series [2] save in the instance of $b/a = 1$ when the first three terms were considered sufficient for the accuracy listed.

As a check upon the accuracy of Tables 2 to 5 it may be noted that in each case when $x = 0$, the tabulated deflection at $y = y_1$ caused by a force at $y = y_2$ should be equal to the tabulated deflection at y_2 caused by the same force at y_1. This result follows from the reciprocal theorem based upon strain-energy considerations and is also implied by the form of Equations [4] and [7]. Examination of each table shows that the listed values are consistent to within about 1 per cent.

It may be observed that when $x = 0$ the ratio of the deflections for the different b/a-values considered differ only by a constant multiple. This is not surprising since at each strut the plate is supposed parallel to the x-axis and hence appears to buckle cylindrically in the immediate vicinity of $x = 0$.

Comparison of Tables 2 to 5 indicates that with closer spacing of the struts the deflection of the plate becomes more cylindrical in form. The first term in the Expansion [2] corresponds to the cylindrical deflection

$$w = \frac{R}{6Da}(|y-h|^3 + |y-b+h|^3 - y^3 - |y-b|^3) \quad [17]$$

As b/a increases, the further terms in Expansion [2] become less important. The Deflection [17] is precisely that produced by loads $-2R$, $2R$, $2R$, and $-2R$ at the points $y = 0$, h, $b - h$, and b, respectively, on a strut of moment of inertia

$$\frac{t^3 a}{12(1-\nu^2)} = \frac{I}{1-\nu^2}$$

where I denotes the moment of inertia of the cross section of a single panel of the plate about the neutral axis of cylindrical buckling.

Deflection of Strut

Consider a strut of length b freely supported at each end and subject to a compressive load P. Let the modulus of elasticity of the material of the strut be E_s and the moment of inertia of the cross section of the strut about the neutral axis be I_s. Denote $P/E_s I_s$ by q^2. Then buckling first occurs when $\frac{1}{2}qb = \pi/2 = 1.5708$.

Suppose that the edges $x = 0$ and $x = a$ of the plate previously considered are attached at the points $y = 0$, h, $b - h$, and b to a strut of length b which is subject to a compressive load P. If the

Table 1 Values of A_n and B_n When $\nu = 0.3$

	$h = 0$		$h = b/8$		$h = b/4$		$h = 3b/8$		$h = b/2$	
$P_n b$	A_n	B_n	A_n	B_n	A_n	B_n	A_n	B_n	A_n	B_n
0.8	10.933	−4.4694	10.864	−4.4015	10.811	−4.3527	10.780	−4.3234	10.769	−4.3136
1.6	5.0315	−3.3684	5.1389	−3.0891	5.1906	−2.8938	5.2123	−2.7783	5.2177	−2.7400
2.4	2.0892	−3.9043	2.8400	−3.1774	3.2390	−2.6940	3.4277	−2.4176	3.4822	−2.3275
3.2	−1.1570	−5.2917	1.0430	−3.7802	2.1266	−2.8383	2.6053	−2.3244	2.7382	−2.1612
4.0	−6.1447	−7.5986	−1.0494	−4.7942	1.2266	−3.1744	2.1416	−2.3388	2.3802	−2.0816
4.8	−14.564	−11.158	−3.9791	−6.2684	0.28321	−3.6707	1.8266	−2.4147	2.1986	−2.0414
6.4	−53.540	−24.592	−14.958	−11.135	−2.3462	−5.1714	1.3194	−2.6868	2.0546	−2.0105
8.0	−163.60	−54.628	−39.906	−20.144	−6.9471	−7.5305	0.75546	−3.0897	2.0148	−2.0027
9.6	−461.60	−121.52	−94.988	−36.628	−15.109	−11.115	0.00456	−3.6219	2.0039	−2.0005
12.8	−3249.9	−601.82	−461.67	−121.52	−53.798	−24.574	−2.4465	−5.1550	2.0002	−2.0000

TABLE 2 VALUES OF wD/Rb^2 WHEN $b/a = 0.125$

	$h = b/8$			$h = b/4$			$h = 3b/8$			$h = b/2$		
y/b	$x/a = 0$	0.25	0.5	0	0.25	0.5	0	0.25	0.5	0	0.25	0.5
0	0	0.056	0.074	0	0.096	0.128	0	0.121	0.160	0	0.129	0.170
0.125	0.011	0.055	0.074	0.017	0.095	0.127	0.020	0.119	0.159	0.020	0.127	0.169
0.25	0.017	0.055	0.072	0.031	0.094	0.124	0.038	0.118	0.156	0.040	0.125	0.167
0.375	0.020	0.054	0.072	0.038	0.093	0.125	0.052	0.116	0.156	0.054	0.124	0.165
0.5	0.021	0.054	0.072	0.041	0.093	0.124	0.054	0.116	0.155	0.059	0.124	0.165

TABLE 3 VALUES OF wD/Rb^2 WHEN $b/a = 0.25$

	$h = b/8$			$h = b/4$			$h = 3b/8$			$h = b/2$		
y/b	$x/a = 0$	0.25	0.5	0	0.25	0.5	0	0.25	0.5	0	0.25	0.5
0	0	0.0331	0.0432	0	0.0570	0.0742	0	0.0715	0.0938	0	0.0762	0.0998
0.125	0.0131	0.0333	0.0426	0.0218	0.0770	0.0733	0.0270	0.0731	0.0923	0.0285	0.0904	0.0986
0.25	0.0219	0.0339	0.0421	0.0398	0.0894	0.0725	0.0501	0.0741	0.0910	0.0531	0.0968	0.0973
0.375	0.0269	0.0346	0.0416	0.0499	0.0979	0.0717	0.0656	0.0750	0.0902	0.0707	0.0979	0.0963
0.5	0.0286	0.0349	0.0418	0.0530	0.1027	0.0744	0.0704	0.0757	0.0906	0.0779	0.0970	0.0962

TABLE 4 VALUES OF wD/Rb^2 WHEN $b/a = 0.5$

	$h = b/8$			$h = b/4$			$h = 3b/8$			$h = b/2$		
y/b	$x/a = 0$	0.25	0.5	0	0.25	0.5	0	0.25	0.5	0	0.25	0.5
0	0	0.0182	0.0243	0	0.0309	0.0429	0	0.0376	0.0528	0	0.0398	0.0562
0.125	0.0152	0.0223	0.0271	0.0252	0.0391	0.0468	0.0300	0.0485	0.0710	0.0314	0.0517	0.0622
0.25	0.0252	0.0265	0.0286	0.0452	0.0466	0.0498	0.0555	0.0587	0.0800	0.0587	0.0626	0.0668
0.375	0.0299	0.0292	0.0299	0.0554	0.0519	0.0524	0.0724	0.0655	0.0837	0.0779	0.0701	0.0700
0.5	0.0314	0.0302	0.0304	0.0586	0.0537	0.0532	0.0780	0.0679	0.0855	0.0860	0.0727	0.0710

TABLE 5 VALUES OF wD/Rb^2 WHEN $b/a = 1$

	$h = b/8$			$h = b/4$			$h = 3b/8$			$h = b/2$		
y/b	$x/a = 0$	0.25	0.5	0	0.25	0.5	0	0.25	0.5	0	0.25	0.5
0	0	0.0060	0.0122	0	0.0094	0.0188	0	0.0111	0.0225	0	0.0116	0.0233
0.125	0.0192	0.0175	0.0218	0.0294	0.0319	0.0356	0.0354	0.0397	0.0444	0.0373	0.0422	0.0472
0.25	0.0296	0.0283	0.0290	0.0525	0.0507	0.0509	0.0652	0.0643	0.0646	0.0691	0.0688	0.0692
0.375	0.0355	0.0346	0.0340	0.0652	0.0625	0.0609	0.0856	0.0809	0.0785	0.0922	0.0873	0.0844
0.5	0.0374	0.0367	0.0359	0.0692	0.0666	0.0648	0.0923	0.0869	0.0836	0.1020	0.0940	0.0902

reaction of the strut upon the plate at $y = h$ and $y = b - h$ is a force $2R$ in the direction of w in Series [2], then the strut is acted upon by forces $-2R$ at $y = h$ and $b - h$ and by forces $2R$ at $y = 0$ and b. Under the influence of the compressive load P let the deflection of the strut be w_1 if $0 < y < h$ and w_2 if $h < y < b/2$. Then

$$w_1 = \frac{2R}{P}\left[y - \frac{1}{q}\sec\frac{qb}{2}\cos q\left(h - \frac{b}{2}\right)\sin qy\right] \quad [18]$$

and

$$w_2 = \frac{2R}{P}\left[h - \frac{1}{q}\sec\frac{qb}{2}\cos q\left(y - \frac{b}{2}\right)\sin qh\right] \quad [19]$$

DEFLECTION OF PLATE CONNECTED TO STRUTS

In the case that the plate and struts are connected when $x = 0$ and a at $y = 0$, $b/2$, and b through reactions $-2R_1$, $4R_1$, and $-2R_1$ the deflection of the strut at $y = b/2$ is given by Equation [18] or [19] as

$$w = \frac{2R_1}{P}\left[\frac{b}{2} - \frac{1}{q}\tan\frac{qb}{2}\right] \quad [20]$$

The deflection of the plate at $x = 0$, $y = b/2$ is

$$(R_1b^2/D)c_{11}$$

where c_{11} is the value tabulated in Tables 2–5 for $h = b/2$. Equating the deflection of the plate and strut at $y = b/2$, and denoting $qb/2$ by μ leads to the following equation to determine μ

$$\frac{1}{\mu^2}\left(1 - \frac{1}{\mu}\tan\mu\right) = 48(1 - \nu^2)\left(\frac{E_s}{E}\right)\left(\frac{I_s}{bt^3}\right)c_{11} \quad [21]$$

The right-hand side of Equation [21] is always positive. The left-hand side is zero when $\mu = 0$ and increases negatively as μ increases to $\pi/2$. Between $\mu = \pi/2$ and 4.493 the left-hand side is positive and has values k as indicated in Fig. 3. As the modulus E of the plate increases from zero the value of μ for buckling increases from $\pi/2$ to 4.493, which is the first critical load for a strut held freely at each end and clamped at its mid-point. It may be recalled that the third critical load of a strut of length b unrestrained at its mid-point is given by $\mu = 3\pi/2 = 4.712$.

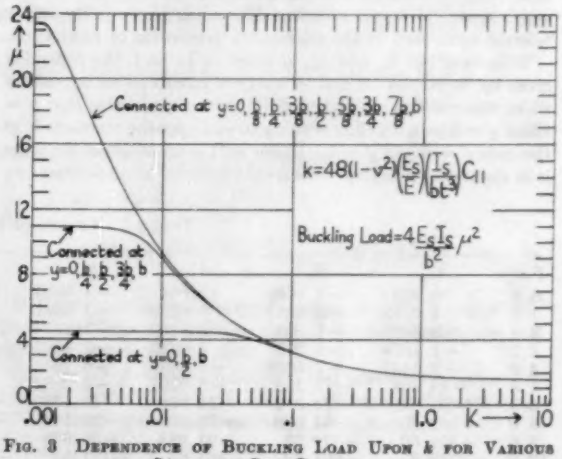

FIG. 3 DEPENDENCE OF BUCKLING LOAD UPON k FOR VARIOUS SPACING OF SPOT CONNECTIONS

In the case that the plate and strut are connected at $y = 0$, $b/4$, $b/2$, $3b/4$, and b through reactions $-2R_1 - 2R_2$, $2R_2$, $4R_1$, $2R_2$, and $-2R_1 - 2R_2$, respectively, the deflections of the strut at $y = b/2$ and $b/4$ are, respectively

$$\frac{2R_1}{P}\left[\frac{b}{2} - \frac{1}{q}\tan\frac{qb}{2}\right] + \frac{2R_2}{P}\left[\frac{b}{4} - \frac{1}{q}\sec\frac{qb}{2}\sin\frac{qb}{4}\right] \quad [22]$$

and

$$\frac{2R_1}{P}\left[\frac{b}{4} - \frac{1}{q}\sec\frac{qb}{2}\sin\frac{qb}{4}\right] + \frac{R_2}{P}\left[\frac{b}{2} - \frac{1}{q}\tan\frac{qb}{2}\right] \quad [23]$$

The deflections of the plate at $y = b/2$ and $b/4$ are, respectively

$$\frac{b^2}{D}(R_1c_{11} + R_2c_{12}) \quad [24]$$

and

$$\frac{b^2}{D}(R_1c_{21} + R_2c_{22}) \quad [25]$$

where the c_{ij} are quantities tabulated in Tables 2–5. Specifically c_{ij} is the quantity tabulated when $x = 0$ at y and h values corresponding, respectively, to the position of R_i and R_j. For example when $b/a = 1$, $c_{11} = 0.1020$, $c_{12} = c_{21} = 0.0691$, and $c_{22} = 0.0525$. Equating [22] to [24] and [23] to [25] shows that $\mu = qb/2$ must satisfy the equation

$$\left[\frac{1}{\mu^2}\left(1 - \frac{1}{\mu}\tan\mu\right) - k\right]\left[\frac{1}{2\mu^2}\left(1 - \frac{1}{\mu}\tan\mu\right) - \frac{kc_{21}}{c_{11}}\right] - \left[\frac{1}{2\mu^2}\left(1 - \frac{2}{\mu}\sec\mu\sin\frac{\mu}{2}\right) - \frac{kc_{12}}{c_{11}}\right]^2 = 0 \quad [26]$$

where

$$k = 48(1 - \nu^2)\left(\frac{E_s}{E}\right)\left(\frac{I_s}{bt^3}\right)c_{11} \quad [27]$$

Inspection of Tables 2 to 5 shows that for b/a values of $1/3$, $1/2$, $1/1$, and 1, the value of c_{22}/c_{11} is within 2 per cent of 0.515 while the value of c_{12}/c_{11} is within 1 per cent of 0.678. The dependence of μ upon k is shown in Fig. 3, which applies to all the values of b/a. As k ranges from zero to infinity, the solution μ of Equation [26] ranges from $\pi/2$ to 10.89, the former value applying to an unrestrained strut and the latter to a strut held freely at each end, and clamped at the points $y = b/4$, $b/2$, $3b/4$, and $b/2$.

Equating [22] to [24] shows that during buckling the reactions R_1 and R_2 are related by

$$\frac{R_2}{R_1} = \frac{-\left[\frac{1}{\mu^2}\left(1 - \frac{1}{\mu}\tan\mu\right) - k\right]}{\frac{1}{2\mu^2}\left[1 - \frac{2}{\mu}\sec\mu\sin\frac{\mu}{2} - \frac{kc_{12}}{c_{11}}\right]} \quad [28]$$

The variation of R_2/R_1 with μ is shown in Fig. 4. The corresponding deflection of the buckled plate may then be found from Tables 2–5.

Consider now the case in which the plate and struts are connected at $y = 0$, $b/8$, $b/4$, $3b/8$, $b/2$, etc. through respective reactions $-2R_1 - 2R_2 - 2R_3 - 2R_4$, $2R_3$, $2R_2$, $2R_4$, $4R_1$, etc. The deflection of the strut at the reaction R_i may be written as

$$w_i = \frac{\mu^2}{q}\sum_{j=1}^{4} a_{ij}(\mu)\,(2R_j/P) \quad [29]$$

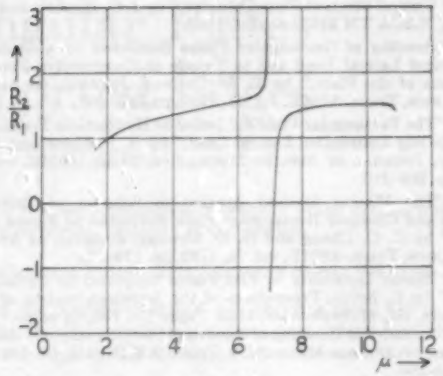

FIG. 4 DEPENDENCE OF R_2/R_1 UPON BUCKLING LOAD $4E_sI_s\mu^2/b^2$

where the $a_{ij}(\mu)$ are expressions of the form of Equation [18] or [19]. The deflection of the plate at the reaction R_i is

$$w_i = \frac{b^2}{D}\sum_{j=1}^{4} c_{ij}R_j \quad [30]$$

When Equation [29] is equated to [30] it is seen that $\mu = qb/2$ must satisfy the determinantal equation

$$\begin{vmatrix} a_{11} - k & a_{12} - \frac{kc_{12}}{c_{11}} & a_{13} - \frac{kc_{13}}{c_{11}} & a_{14} - \frac{kc_{14}}{c_{11}} \\ a_{12} - \frac{kc_{12}}{c_{11}} & a_{22} - \frac{kc_{22}}{c_{11}} & a_{23} - \frac{kc_{23}}{c_{11}} & a_{24} - \frac{kc_{24}}{c_{11}} \\ a_{13} - \frac{kc_{13}}{c_{11}} & a_{23} - \frac{kc_{23}}{c_{11}} & a_{33} - \frac{kc_{33}}{c_{11}} & a_{34} - \frac{kc_{34}}{c_{11}} \\ a_{14} - \frac{kc_{14}}{c_{11}} & a_{24} - \frac{kc_{24}}{c_{11}} & a_{34} - \frac{kc_{34}}{c_{11}} & a_{44} - \frac{kc_{44}}{c_{11}} \end{vmatrix} = 0 \quad [31]$$

For various values of μ the Equation [31] has been solved for k by trial and error to give the dependence of μ upon k as shown in Fig. 3. As k ranges from zero to infinity the value of μ ranges from $\pi/2$ to 23.5. The values of the reactions R_i are very sensitive to small variations in k and no attempt has been made to determine k sufficiently accurately over the whole range to permit the plotting of a graph corresponding to Fig. 4. However, for any particular value of μ the value of k from Fig. 3 may be improved after substitution of neighboring values into Equation [31]. Slide-rule accuracy has proved sufficient in the cases worked to date. The reactions R_i may then be found for the particular value of μ.

CONCLUSION

Inspection of Fig. 3 shows that in order to prevent buckling of the panel when

$$k = 48(1 - \nu^2)(E_s/E)(I_s/bt^3)$$

is greater than 0.06, there is little to be gained by including more than one spot connection between the plate and the strut in addition to the end connections. When k is greater than 0.01, then three spot connections are sufficient. Seven spot connections suffice when k exceeds 0.0005.

BIBLIOGRAPHY

1 "On the Stability of a Plane Plate Under Thrusts in Its Own Plane," by G. H. Bryan, Proceedings of the London Mathematical Society, vol. 22, 1891, pp. 54–67.

2 "Critical Stress of Plate Columns," by J. C. Houbolt and E. Z. Stowell, NACA TN 2163, August, 1950.

3 "Bending of Rectangular Plates Subjected to a Uniformly Distributed Lateral Load and to Tensile or Compressive Forces in the Plane of the Plate," by H. D. Conway, JOURNAL OF APPLIED MECHANICS, Trans. ASME, vol. 71, 1949, pp. 301–309.

4 "The Rectangular Plate Subjected to Hydrostatic Tension and to Uniformly Distributed Lateral Load," by R. F. Morse and H. D. Conway, JOURNAL OF APPLIED MECHANICS, Trans. ASME, vol. 73, 1951, pp. 209–210.

5 "The Marcus Method Applied to Solution of Uniformly Loaded and Clamped Rectangular Plate Subjected to Forces in Its Plane," by C. C. Chang and H. D. Conway, JOURNAL OF APPLIED MECHANICS, Trans. ASME, vol. 74, 1952, pp. 179–184.

6 "Elastic Instability of Flat Plates Subjected to Partial End Loads," by L. Zetlin, Proceedings of the American Society of Civil Engineers, vol. 81, September, 1955, Paper No. 795, 24 pages.

7 "Cylindrical Buckling of Sandwich Plates," by J. N. Goodier, JOURNAL OF APPLIED MECHANICS, Trans. ASME, vol. 68, 1946, pp. A-253–A-260.

8 "The Optimum Problem of the Sandwich Plate," by W. Flügge, JOURNAL OF APPLIED MECHANICS, Trans. ASME, vol. 74, 1952, pp. 104–108.

9 "Linear Bending Theory of Isotropic Sandwich Plates by an Order-of-Magnitude Analysis," by G. Gerard, JOURNAL OF APPLIED MECHANICS, Trans. ASME, vol. 74, 1952, pp. 13–15.

10 "Buckling of Transverse Stiffened Plates Under Shear," by T. K. Wang, JOURNAL OF APPLIED MECHANICS, Trans. ASME, vol. 69, 1947, pp. A-269–A-274.

11 "The Buckling of a Thin Sheet Transversely Stiffened," by H. L. Cox and H. E. Smith, Proceedings of the London Mathematical Society, vol. 48, 1945, pp. 27–34.

12 "Buckling of Intermittently Supported Rectangular Plates," by C. H. Norris, D. A. Polychrone, and L. J. Capozzoli, *Welding Journal*, vol. 30, 1951 (Research Supplement), pp. 546–556.

13 "Buckling of Laminated Columns," by L. G. Clark, JOURNAL OF APPLIED MECHANICS, Trans. ASME, vol. 77, 1955, pp. 553–556.

14 "Some Thin-Plate Problems by the Sine Transform," by L. I. Deverall and C. J. Thorne, JOURNAL OF APPLIED MECHANICS, Trans. ASME, vol. 73, 1951, pp. 152–156.

15 "Formulas and Theorems for the Special Functions of Mathematical Physics," by W. Magnus and F. Oberhettinger, Chelsea Publishing Company, New York, N. Y., 1949.

Buckling of Rectangular Plates With Two Unsupported Edges

By P. SHULESHKO,[1] SYDNEY, N.S.W., AUSTRALIA

In this paper the elastic stability of rectangular plates compressed in two perpendicular directions by forces uniformly distributed along the edges is considered. Edges $x = 0$, and $x = a$ are simply supported, edges $y = \pm b/2$ are unsupported (Fig. 2a). The nondimensional coefficient $k = Pa^2/\pi^2 D$ for various ratios b/a and $\nu = P_1/P_2$ $(0 \leq \nu \leq \infty)$ is tabulated and corresponding graphs are presented.

Nomenclature

The following nomenclature is used in the paper:

a, b = length and width of rectangular plate
h = thickness of plate
w = deflection of a typical point in middle surface of plate
D = flexural stiffness per unit width of plate

$$D = \frac{Eh^3}{12(1-\mu^2)}$$

E = Young's modulus of isotropic material
P_1, P_2 = resultant compressive forces per unit length of edge of plate
μ = Poisson's ratio of isotropic material
m = number of half waves of buckled plate in x-direction
P_{cr} = critical force per unit length of edge of plate
k = nondimensional coefficient (see Formulas [1] and [4])

$$\lambda = m\pi/a, \quad b_1 = \frac{P_1 a^2}{Dm^2\pi^2}, \quad k = \frac{P_2 a^2}{Dm^2\pi^2}$$

α, β (see Formulas [3])
A, B (see Formulas [5])
$p, q, c, d, \delta, \nu, \theta$, and i (see Formulas [9])

Introduction

The elastic stability of a rectangular plate which has two opposite edges $x = 0$ and $x = a$ simply supported and edges $y = \pm b/2$ unsupported is considered, Fig. 2a. The plate is compressed in its middle plane by means of uniformly distributed forces of intensity P_1 along edges $x = 0$ and $x = a$ and P_2 along the edges $y = \pm b/2$ where

$$P_1 = \nu P_2, \quad 0 \leq \nu \leq \infty$$

By gradually increasing P_2 the critical condition of the plate will be reached.[2] This condition can be determined by critical force

$$P_{cr} = k\frac{\pi^2 D}{a^2} \qquad [1]$$

where k is a nondimensional coefficient which can be obtained from an eigenvalue equation of the problem.

General Eigenvalue Equation of the Problem

Using the method described in a previous paper,[2] after satisfying the boundary conditions at the edges of plate, the following eigenvalue equation for determination values of k is obtained

$$(\beta A^2 \sinh \alpha b_1 \cosh \beta b_1 - \alpha B^2 \sinh \beta b_1 \cosh \alpha b_1) \times (\beta A^2 \sinh \beta b_1 \cosh \alpha b_1 - \alpha B^2 \sinh \alpha b_1 \cosh \beta b_1) = 0 \qquad [2]$$

where

$$\left.\begin{aligned} \alpha &= \lambda\sqrt{\left\{\left(1-\frac{k}{2}\right) + \sqrt{\left[\left(1-\frac{k}{2}\right)^2 - (1-\nu k)\right]}\right\}} \\ \beta &= \lambda\sqrt{\left\{\left(1-\frac{k}{2}\right) - \sqrt{\left[\left(1-\frac{k}{2}\right)^2 - (1-\nu k)\right]}\right\}} \end{aligned}\right\} \qquad [3]$$

$$\lambda = \frac{m\pi}{a}, \quad k = \frac{P_2 a^2}{m^2\pi^2 D} \qquad [4]$$

$$A = \alpha^2 - \lambda^2\mu, \quad B = \beta^2 - \lambda^2\mu, \quad b_1 = b/2 \qquad [5]$$

Equation [2] can be rewritten in the form

$$\left.\begin{aligned} &\beta A^2 \sinh \beta b_1 \cosh \alpha b_1 - \alpha B^2 \sinh \alpha b_1 \cosh \beta b_1 = 0 \\ \text{or} \\ &\beta A^2 \sinh \alpha b_1 \cosh \beta b_1 - \alpha B^2 \sinh \beta b_1 \cosh \alpha b_1 = 0 \end{aligned}\right\} \qquad [6]$$

Equations [6] can be simplified by the following substitution

$$\alpha b_1 = (\theta/2)(p + iq), \quad \beta b_1 = (\theta/2)(p - iq) \qquad [7]$$

i.e., we have

$$\left.\begin{aligned} &d \sinh \theta p - c \sin \theta q = 0 \\ \text{or} \\ &d \sinh \theta p + c \sin \theta q = 0 \end{aligned}\right\} \qquad [8]$$

where

$$\left.\begin{aligned} p &= \sqrt{[2 - k + 2\sqrt{(1-\nu k)}]} \\ q &= \sqrt{[-2 + k + 2\sqrt{(1-\nu k)}]} \\ d &= q[\sqrt{(1-\nu k)}(k - 2\delta) - (1-\nu k) + \mu^2] \\ c &= p[\sqrt{(1-\nu k)}(k - 2\delta) + (1-\nu k) - \mu^2] \\ \delta &= 1 - \mu, \quad \nu = P_1/P_2, \quad \theta = m\pi b/2a, \quad i = \sqrt{-1} \end{aligned}\right\} \qquad [9]$$

---

[1] The New South Wales University of Technology. Formerly, Professor of Theoretical and Applied Mechanics, Ukrainian Technical University at Regensburg and Munich, Germany.

[2] "Buckling of Rectangular Plates Uniformly Compressed in Two Perpendicular Directions With One Free Edge and Opposite Edge Elastically Restrained," by P. Shuleshko, Journal of Applied Mechanics, Trans. ASME, vol. 78, 1956, pp. 359–363.

Presented at the Applied Mechanics Division Summer Conference, Berkeley, Calif., June 13–15, 1957, of The American Society of Mechanical Engineers.

Discussion of this paper should be addressed to the Secretary, ASME, 29 West 39th Street, New York, N. Y., and will be accepted until January 10, 1958, for publication at a later date. Discussion received after the closing date will be returned.

Note: Statements and opinions advanced in papers are to be understood as individual expressions of their authors and not those of the Society. Manuscript received by ASME Applied Mechanics Division, January 30, 1957. Paper No. 57—APM-46.

TABLE 1 VALUES OF NONDIMENSIONAL COEFFICIENT k FOR PLATE WITH SIMPLY SUPPORTED ENDS ($x = 0, a$), AND UNSUPPORTED SIDES ($y = \pm b/2$) UNIFORMLY COMPRESSED IN y-DIRECTION BY FORCES $P_2(\nu = 0)$

	b/a	0.00	0.10	0.20	0.40	0.60	0.80	1.00	1.20	1.316	1.40	1.60	1.80	2.00	2.30	2.632	3.29	3.95	4.606	5.264	∞
Symmetrical forms	k	∞	...	24.50	7.35	4.13	3.06	2.63	2.37	2.31	2.28	2.24	2.246	2.26	2.29	2.31	2.314	2.31	2.307	2.31	2.31
Antisymmetrical forms	k	1.40	1.402	1.428	1.516	1.657	1.84	2.04	2.23	2.31	2.36	2.397	2.39	2.366	2.33	2.31	2.306	2.31	2.313	2.31	2.31
Smallest roots	k	1.40	1.402	1.428	1.516	1.657	1.84	2.04	2.23	2.31	2.28	2.24	2.246	2.26	2.29	2.31	2.306	2.31	2.307	2.31	2.31

TABLE 3 VALUES OF NONDIMENSIONAL COEFFICIENT k FOR A PLATE WITH SIMPLY SUPPORTED ENDS ($x = 0, a$) AND UNSUPPORTED SIDES ($y = \pm b/2$), UNIFORMLY COMPRESSED IN TWO PERPENDICULAR DIRECTIONS BY FORCES P_1 AND P_2, WHEN $P_1 = P_2 = P(\nu = 1)$

	b/a	0.00	0.20	0.40	0.60	0.80	1.00	1.20	1.40	1.60	2.00	3.00	4.00	5.00	∞
Symmetrical forms	k	0.91	0.911	0.914	0.919	0.926	0.930	0.934	0.939	0.942	0.949	0.962	0.968	0.971	0.9753
Antisymmetrical forms	k	1.40	1.37	1.33	1.287	1.243	1.184	1.145	1.14	1.093	1.053	1.011	1.01	1.01	1.000

TABLE 4 VALUES OF NONDIMENSIONAL COEFFICIENT k FOR A PLATE WITH SIMPLY SUPPORTED ENDS ($x = 0, a$), AND UNSUPPORTED SIDES ($y = \pm b/2$) UNIFORMLY COMPRESSED IN x-DIRECTION BY FORCES P_1 ($\nu = \infty$)

	b/a	0.00	0.20	0.40	0.60	0.80	1.00	1.20	1.40	1.60	1.80	2.00	2.50	3.00	4.00	∞
Symmetrical forms	k	0.910	0.913	0.923	0.933	0.943	0.951	0.957	0.962	0.965	0.97	0.973	0.977	0.981	0.985	0.993
Antisymmetrical forms	k	∞	...	11.80	5.76	3.66	2.69	2.16	1.85	1.65	1.52	1.41	1.25	1.17	1.09	1.00

TABLE 5 VALUES OF NONDIMENSIONAL COEFFICIENT k FOR A PLATE WITH SIMPLY SUPPORTED ENDS ($x = 0, a$) AND UNSUPPORTED SIDES ($y = \pm b/2$), UNIFORMLY COMPRESSED IN TWO PERPENDICULAR DIRECTIONS BY FORCES P_1 AND P_2, WHEN RATIO $\nu = P_1/P_2$ HAS VARIOUS VALUES IN INTERVAL $0 \leq \nu \leq \infty$

b/a / ν	0	0.20	0.40	0.60	0.80	1.00	1.20	1.40	1.60	1.80	2.00	2.50	3.00	3.50	4.00	5.00	∞
0.00	1.40	1.425	1.516	1.657	1.84	2.04	2.23	2.28	2.24	2.246	2.26	2.306	2.306	2.307	2.31	2.31	2.31
0.05	1.40	1.42	1.505	1.64	1.80	1.99	2.15	2.23	2.198	2.19	2.20	2.24	2.246	2.245	2.247	2.247	2.247
0.10	1.40	1.418	1.50	1.623	1.76	1.93	2.08	2.17	2.146	2.134	2.14	2.176	2.180	2.178	2.181	2.182	2.182
0.15	1.40	1.416	1.49	1.593	1.714	1.85	1.98	2.095	2.102	2.08	2.075	2.112	2.116	2.116	2.116	2.116	2.116
0.20	1.40	1.414	1.48	1.57	1.67	1.773	1.883	1.995	2.048	2.024	2.02	2.04	2.05	2.05	2.05	2.051	2.051
0.25	1.40	1.413	1.47	1.55	1.64	1.73	1.83	1.91	1.966	1.97	1.966	1.967	1.98	1.98	1.98	1.98	1.98
0.30	1.40	1.411	1.46	1.53	1.61	1.687	1.77	1.835	1.875	1.91	1.90	1.90	1.908	1.91	1.91	1.91	1.912
0.35	1.40	1.409	1.45	1.51	1.576	1.643	1.703	1.756	1.802	1.832	1.84	1.833	1.84	1.843	1.843	1.843	1.843
0.40	1.40	1.407	1.44	1.49	1.54	1.596	1.65	1.694	1.726	1.75	1.766	1.77	1.768	1.772	1.774	1.774	1.774
0.45	1.40	1.405	1.432	1.47	1.51	1.55	1.59	1.627	1.653	1.673	1.685	1.690	1.695	1.697	1.697	1.697	1.697
0.50	1.40	1.404	1.426	1.453	1.48	1.51	1.54	1.562	1.582	1.597	1.607	1.616	1.625	1.625	1.625	1.625	1.625
0.55	1.40	1.402	1.417	1.433	1.453	1.475	1.495	1.51	1.522	1.53	1.537	1.548	1.549	1.55	1.55	1.55	1.55
0.60	1.40	1.40	1.407	1.415	1.425	1.436	1.448	1.456	1.462	1.467	1.47	1.471	1.472	1.473	1.473	1.473	1.473
0.65	1.40	1.40	1.40	1.40	1.40	1.40	1.40	1.40	1.40	1.40	1.40	1.40	1.40	1.40	1.40	1.40	1.40
0.70	1.30	1.30	1.301	1.304	1.308	1.31	1.312	1.313	1.315	1.318	1.32	1.32	1.32	1.32	1.321	1.321	1.323
0.75	1.213	1.214	1.217	1.22	1.222	1.227	1.23	1.234	1.238	1.24	1.245	1.25	1.251	1.252	1.253	1.254	1.26
0.80	1.14	1.141	1.142	1.147	1.15	1.155	1.16	1.163	1.167	1.17	1.173	1.18	1.183	1.187	1.19	1.192	1.194
0.85	1.07	1.072	1.075	1.079	1.084	1.09	1.096	1.10	1.102	1.104	1.107	1.114	1.12	1.123	1.126	1.128	1.133
0.90	1.01	1.012	1.017	1.021	1.027	1.033	1.038	1.042	1.046	1.05	1.053	1.06	1.062	1.063	1.067	1.068	1.075
0.95	0.96	0.961	0.964	0.97	0.974	0.98	0.987	0.992	0.995	0.998	1.000	1.005	1.01	1.012	1.014	1.017	1.024
1.00	0.91	0.911	0.914	0.919	0.926	0.93	0.934	0.94	0.942	0.945	0.949	0.955	0.962	0.965	0.968	0.971	0.9753
∞	0.91	0.913	0.923	0.933	0.943	0.957	0.961	0.962	0.967	0.97	0.973	0.977	0.981	0.983	0.985	0.987	0.993

TABLE 6 VALUES OF NONDIMENSIONAL COEFFICIENT k AND RATIO b/a DETERMINED BY POINTS OF INTERSECTION OF CURVES OF EQUATIONS [13] FOR VARIOUS VALUES $\nu = P_1/P_2$

	$n = 0$	$n = 1, 2, 3, \ldots$													
ν	$0 < \nu < 0.65$	0.00	0.05	0.10	0.15	0.20	0.25	0.30	0.35	0.40	0.45	0.50	0.55	0.60	0.65
b/a	0.00	$1.316n$	$1.37n$	$1.43n$	$1.505n$	$1.587n$	$1.69n$	$1.81n$	$1.964n$	$2.17n$	$2.45n$	$2.82n$	$3.54n$	$5.90n$	∞n
k	1.40	2.31	2.247	2.182	2.116	2.051	1.98	1.912	1.843	1.773	1.70	1.625	1.55	1.473	1.40

($n = 1, 2, 3, \ldots\ldots$)

The numerical factor k which determines the critical load P_{cr} is obtained as the least root of Equation [8].

The three cases, given by $\nu = 0$, $\nu = 1$, and $\nu = \infty$ are considered here before the general case for which ν may have any value between 0 and ∞.

Buckling of Rectangular Plates with Two Unsupported Edges and Uniformly Compressed in y-Direction ($\nu = 0$)

The eigenvalue equations for this case are obtained by substituting $\nu = 0$ into Equations [8]. Thus

$$\left.\begin{aligned} &\sqrt{k}(k - 3 + 2\mu + \mu^2)\sinh\theta\sqrt{(4-k)} - \\ &\qquad \sqrt{(4-k)}(k - 1 + 2\mu - \mu^2)\sin\theta\sqrt{k} = 0 \\ &\sqrt{k}(k - 3 + 2\mu + \mu^2)\sinh\theta\sqrt{(4-k)} \\ &\qquad + \sqrt{(4-k)}(k - 1 + 2\mu - \mu^2)\sin\theta\sqrt{k} = 0 \end{aligned}\right\} \quad \ldots [10]$$

The first line of Table 1 gives values of the least root of the first of Equations [10] for various values of the ratio b/a, and the second line of Table 1 gives the values of the least root of the second of Equations [10]. The third line of Table 1 gives the smallest values of the least root of Equations [10]. The same values also are represented by curves in Fig. 1. The distance between two curves in the intervals $2.632 < b/a < 3.950$ and $3.950 < b/a < 5.264$ was made for obviousness bigger than it should be. The value of 0.30 has been adopted for μ.

Trial calculation shows that the smallest value of P_{cr} for all values of b/a occurs when $m = 1$; i.e., the buckled plate will have only one half wave in the x-direction. Contrary, in the y-direction the buckled plate will have various numbers of half waves and various forms, depending upon the ratio b/a, Fig. 1.

The curve in Fig. 1, which initially has the higher values, represents the roots of the first of Equations [10] and the curve, which initially has lower values, represents the roots of the second of Equations [10]. The co-ordinates of the points of an intersection of the curves can be determined (see Equations [10]) from the following equations

$$k - 3 + 2\mu + \mu^2 = 0, \quad \text{and} \quad \sin\theta\sqrt{k} = 0 \ldots . [11]$$

from which

$$k = 3 - 2\mu - \mu^2, \quad b/a = 2n/\sqrt{k} = 2n/\sqrt{(3 - 2\mu - \mu^2)} \quad \ldots \ldots [12]$$

$$(n = 1, 2, 3, \ldots .)$$

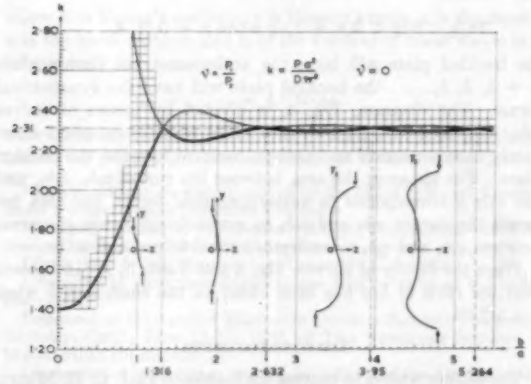

Fig. 1 Graphical Representation of Nondimensional Coefficient k for Rectangular Plates With Simply Supported Ends ($x = 0$ and $x = a$) and Unsupported Sides ($y = \pm b/2$), Uniformly Compressed in Vertical Direction; the Least Value of k Is Shown by Thickened Line

(For different intervals of b/a are shown different forms of the buckled plate.)

The values of the ratio b/a at $\mu = 0.30$ and various n, where the curves are intersected, are given in Table 2.

Table 2 Values of Ratio b/a for Points of Intersection of Curves

n	1	2	3	4	5
b/a	1.316	2.632	3.95	5.264	6.58

From the graph, Fig. 1, it is seen that the buckled plate has antisymmetrical forms for intervals

$$2n/\sqrt{k} \leq b/a \leq 2(n+1)/\sqrt{k}$$

when $n = 0, 2, 4, \ldots .$, and symmetrical forms when $n = 1, 3, 5, \ldots$

Buckling of Rectangular Plates With Two Unsupported Edges and Uniformly Compressed in Two Perpendicular Directions ($\nu = 1$)

The eigenvalue equations for this case are Equations (8) with notation [9], where the ratio $\nu = P_1/P$ should be taken equal to unity. The values of the least root of the first of Equations [8] for various values of the ratio b/a and $\mu = 0.30$ are given in the first line of Table 3, and the values of the least root of the second equation in the second line of Table 3. The values of the smallest root of Equations [8] in this case are given by the first line of Table 3. Also these values of the roots are represented by curves in Fig. 2.

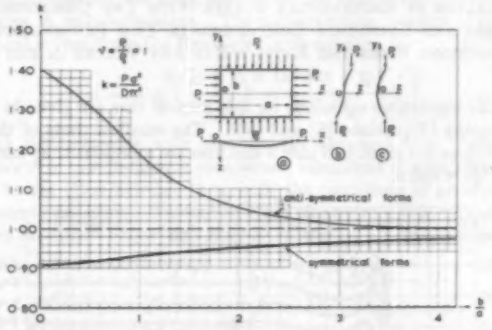

Fig. 2 Curves of Nondimensional Coefficient k for Rectangular Plates With Simply Supported Ends and Unsupported Sides, Uniformly Compressed in Two Perpendicular Directions ($P_1 = P_2$)

Buckling of Rectangular Plates With Two Unsupported Edges and Uniformly Compressed in x-Direction ($\nu = \infty$)

The eigenvalue equations for this case can be obtained from Equations [6] by substituting in expressions for α and β the value of $P_2 = 0$ (see Nomenclature) and taking $k_1 = k$ thus

$$\left.\begin{aligned} &(\sqrt{(k)} + \delta)^2\sqrt{(1-\sqrt{k})}\tanh\theta\sqrt{(1-\sqrt{k})} \\ &\quad - (\sqrt{(k)} - \delta)^2\sqrt{(1+\sqrt{k})}\tanh\theta\sqrt{(1+\sqrt{k})} = 0 \\ &(\sqrt{(k)} + \delta)^2\sqrt{(1-\sqrt{k})}\tanh\theta\sqrt{(1+\sqrt{k})} \\ &\quad - (\sqrt{(k)} - \delta)^2\sqrt{(1+\sqrt{k})}\tanh\theta\sqrt{(1-\sqrt{k})} = 0 \end{aligned}\right\} \quad \ldots [13]$$

where

$$\theta = \frac{m\pi b}{2a}, \quad \delta = 1 - \mu, \quad k = P_1 a^2/(Dm^2\pi^2)$$

The values of the least root of the first Equations [13] for various values of the ratio b/a and $\mu = 0.30$ are given in the first line of Table 4, the values of the least root of the second of Equa-

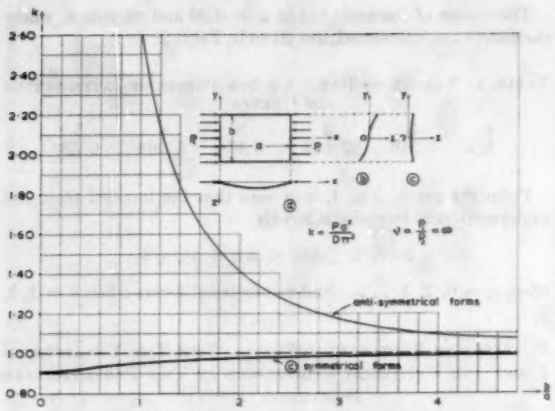

FIG. 3 CURVES OF NONDIMENSIONAL COEFFICIENT k FOR RECTANGULAR PLATES WITH SIMPLY SUPPORTED ENDS AND UNSUPPORTED SIDES, UNIFORMLY COMPRESSED IN HORIZONTAL DIRECTION ($P_1 = P$, $P_2 = 0$)

tions [13] in the second line of Table 4. The values of the smallest root of Equations [13] correspond to the symmetrical forms of the buckled plate and are given in the first line of Table 4. These values of the roots also are represented by curves in Fig. 3.

BUCKLING OF RECTANGULAR PLATES WITH TWO UNSUPPORTED EDGES AND UNIFORMLY COMPRESSED IN TWO PERPENDICULAR DIRECTIONS WHEN THE RATIO ν HAS ANY VALUES IN THE INTERVAL $0 \leq \nu \leq \infty$

The eigenvalue equations for this general case are given in the foregoing (Equations [8] and [9]). The smallest roots of these equations are given in Table 5 and also are represented by curves in Figs. 4 and 5.

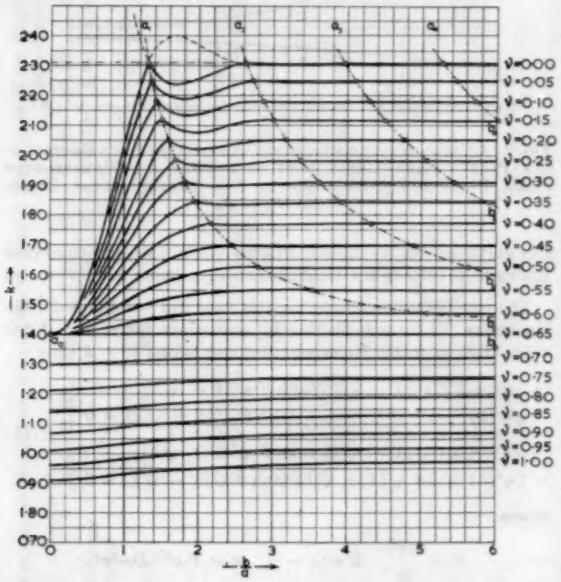

FIG. 4 CURVES OF NONDIMENSIONAL COEFFICIENT k FOR RECTANGULAR PLATES WITH SIMPLY SUPPORTED ENDS AND UNSUPPORTED SIDES, COMPRESSED IN TWO PERPENDICULAR DIRECTIONS WITH DIFFERENT INTENSITIES OF LOADING ($0 \leq \nu \leq \infty$ WHERE $\nu = P_1/P_2$)

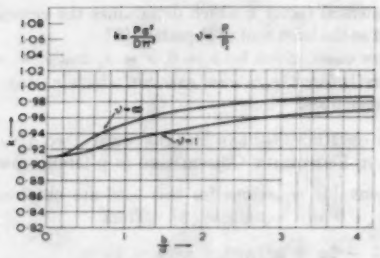

FIG. 5 CURVES OF NONDIMENSIONAL COEFFICIENT k FOR RECTANGULAR PLATES WITH SIMPLY SUPPORTED ENDS AND UNSUPPORTED SIDES FOR TWO CONDITIONS OF LOADING (1) $P_1 = P_2$ ($\nu = 1$) AND (2) $P_1 = P$, $P_2 = 0$ ($\nu = \infty$)

The encircled points placed on curves a_1b_1, a_2b_2, a_3b_3, ... are the intersection points of two curves which are determined by the two Equations of [8]. These points were found as common roots of Equations [8].

The common roots were determined from the following equations

$$\left.\begin{aligned} & d = 0, \quad \text{and} \quad \sin q\theta = 0 \\ \text{or} \quad & \sqrt{(1-\nu k)(k-2\delta)} - (1-\nu k) + \mu^2 = 0 \\ \text{and} \quad & q\theta = n\pi \; (n = 0, 1, 2, 3, \ldots) \end{aligned}\right\} \quad \ldots [14]$$

from which (see Equations [9])

$$\left.\begin{aligned} & k = 2\delta + \sqrt{(1-\nu k)} - \mu^2/\sqrt{(1-\nu k)} \\ \text{and} \quad & b/a = 2n/q = 2n/\sqrt{[k - 2 + 2\sqrt{(1-\nu k)}]} \end{aligned}\right\} \quad \ldots [15]$$

The values of k and b/a for various values ν and n are given in Table 6.

For $\nu = 0.65$ the nondimensional coefficient k is independent on the ratio b/a and equal to 1.40. This coefficient k is represented in Fig. 4 by straight line a_0b_0 which has the point of intersection with the curve a_1b_1 at $b/a = \infty$. When $\nu > 0.65$ the curves have no intersection points and the buckled plate, as investigation showed, has only the symmetrical forms. When $0 \leq \nu \leq 0.65$ the buckled plate can have both symmetrical and antisymmetrical forms, depending on the ratio b/a. For example, for intervals

$$2n/q < b/a < 2(n+1)/q \text{ when } n = 0, 2, 4, \ldots .$$

the buckled plate will have the antisymmetrical forms; when $n = 1, 3, 5, \ldots$ the buckled plate will have the symmetrical forms. The diagram, Fig. 4, is divided by means of curves a_0b_0, a_1b_1, a_2b_2, a_3b_3, ... into areas which correspond alternately to symmetrical and antisymmetrical forms of the buckled plate. For instance, the area between the curves a_0b_0, a_1b_1, and the axis x corresponds to antisymmetrical forms, the area between the curves a_1b_1 and a_2b_2 to symmetrical forms, the areas between a_1b_2 and a_2b_2 to antisymmetrical forms, and so on.

From the family of curves, Fig. 4 and Table 5, it can be seen that the ratio of b/a has little effect on the coefficient k when $b/a > 2.50$.

ACKNOWLEDGMENTS

The author wishes to express his thanks to Prof. C. H. Munro, Head of the School of Civil Engineering of the N. S. W. University of Technology for his encouragement during the preparation of this paper; he is also grateful to Mr. I. J. Somervaille for the reading and checking of the manuscript, and to Mr. R. A. Duncan for preparation of drawings for this manuscript.

Influence of Width on Velocities of Long Waves in Plates[1]

By D. C. GAZIS[2] and R. D. MINDLIN,[3] NEW YORK, N. Y.

This paper contains a discussion of the velocities of propagation of long flexural and extensional waves in a plate or bar in the transition region between the states of generalized plane stress and plane strain; i.e., for arbitrary width-thickness ratios (h/a) of rectangular sections. The investigations are carried out mathematically on the basis of approximate equations of motion. It is found that, for flexural waves, as h/a increases from zero, the velocity remains close to that for generalized plane stress until quite large values of h/a are reached, after which the velocity rises asymptotically toward that for plane strain. For extensional waves the velocity is slightly smaller than that for generalized plane stress for all $h/a > 0$.

Introduction

THE VELOCITIES of flexural and extensional waves in an infinite elastic plate were deduced by Rayleigh (1)[4] and Lamb (2, 3) from the equations of elasticity. In their treatment of straight-crested waves, they employed the theory of plane strain, so that the results pertain to a plate of infinite width. By a simple change of the constants of elasticity the velocities may be converted to those for generalized plane stress, applicable to a plate of small width; i.e., a beam or bar of narrow rectangular section. It is the purpose of this paper to study the velocities in the intermediate range of widths for the case of long wave lengths of the lowest flexural and extensional modes.

Consider an elastic body bounded by traction-free planes $x = \pm a$, $z = \pm h$ and infinite in the direction y, of wave propagation, Fig. 1. For the case of plane strain (corresponding to h/a infinite) the lowest flexural mode, in the Rayleigh-Lamb solution, has as its limiting phase velocity, for waves long compared with $2a$

$$c = \eta a c_2 \sqrt{\left[\frac{2}{3(1-\nu)}\right]} = \eta a \sqrt{\left[\frac{E}{3\rho(1-\nu^2)}\right]} \quad \ldots [1]$$

where E is Young's modulus, ν is Poisson's ratio, ρ is the density, η is the wave number, and c_2 is the velocity of shear waves in an infinite body, i.e.

$$c_2 = \sqrt{(G/\rho)}$$

where G is the shear modulus. As pointed out by Rayleigh and Lamb, the velocity given in Equation [1] is the same as that obtained from the classical (Lagrange) theory of low-frequency flexural vibrations of thin plates (4) for the case of straight-crested waves in an infinite plate. The corresponding velocity of extensional waves, from the Rayleigh-Lamb solution, is

$$c = c_2 \sqrt{\left(\frac{2}{1-\nu}\right)} = \sqrt{\left[\frac{E}{\rho(1-\nu^2)}\right]} \quad \ldots [2]$$

and this coincides with the velocity obtained from Poisson's theory[5] of low-frequency extensional vibrations of thin plates.

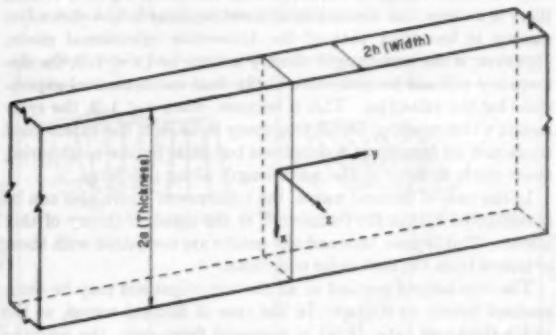

Fig. 1 Reference Co-Ordinates and Dimensions

At the other extreme ($h/a \to 0$) the conditions of generalized plane stress apply. To convert from plane strain it is only necessary to replace ν by ν' and E by E' where[6]

$$\nu' = \frac{\nu}{1+\nu}, \quad E' = \frac{(1+2\nu)E}{(1+\nu)^2}$$

Equations [1] and [2] then become

$$c = \eta a c_2 \sqrt{\left[\frac{2(1+\nu)}{3}\right]} = \eta a \sqrt{\left(\frac{E}{3\rho}\right)} \quad \ldots [3]$$

for flexural waves and

$$c = c_2 \sqrt{[2(1+\nu)]} = \sqrt{\left(\frac{E}{\rho}\right)} \quad \ldots [4]$$

for extensional waves.

At intermediate values of h/a, waves in the plane of x and y couple with waves reflecting back and forth between the boundaries $z = \pm h$ (i.e., with transverse vibrations across the width), and this alters the phase velocities.

To take into account the additional free boundaries at $z = \pm h$ within the framework of the three-dimensional theory would be a very difficult task because each of the infinity of modes in the Rayleigh-Lamb solution gives rise to an infinity of modes in the presence of the additional boundaries. If, however, attention is confined to the lowest extensional and flexural modes it is necessary to take into account only the lowest width mode inasmuch as the higher width modes will have little influence.

[1] This investigation was supported by the Office of Naval Research under a contract with Columbia University.

[2] Research Assistant, Department of Civil Engineering and Engineering Mechanics, Columbia University.

[3] Professor of Civil Engineering, Columbia University.

[4] Numbers in parentheses refer to the Bibliography at the end of the paper.

Presented at the Applied Mechanics Division Summer Conference, Berkeley, Calif., June 13–15, 1957, of The American Society of Mechanical Engineers.

Discussion of this paper should be addressed to the Secretary, ASME, 29 West 39th Street, New York, N. Y., and will be accepted until January 10, 1958, for publication at a later date. Discussion received after the closing date will be returned.

Note: Statements and opinions advanced in papers are to be understood as individual expressions of their authors and not those of the Society. Manuscript received by ASME Applied Mechanics Division, January 19, 1957. Paper No. 57—APM-29.

[5] Reference (4), p. 497.

[6] Reference (4), p. 208.

Equations of motion already are available which take into account the first symmetric extensional mode across the width (5). These equations result from retaining the zero-order and first-order terms of an expansion of the displacements in a series of powers of the width co-ordinate (z). They are referred to in the sequel as "first-order equations" and are used here in the investigation of both the flexural and extensional velocities. From a physical point of view the first-order equations are appropriate only for small values of Poisson's ratio inasmuch as, for $\nu > 1/3$, there is at least one transverse symmetric shear mode whose frequency is less than that of the transverse extensional mode. However, if the wave length along y is large and $\nu < 1/3$, the discrepancy will not be noticeable in the final mathematical expressions for the velocities. This is because, when $\nu < 1/3$, the symmetric width mode of lowest frequency is, in fact, the extensional mode and its frequency is depressed but little by the neighboring shear mode as long as the wave length along y is large.

In the case of flexural waves, the influence of width also can be investigated within the framework of the classical theory of thin plates. This is done here and the results are compared with those obtained from the first-order equations.

The conclusions reached in all the investigations may be summarized briefly as follows: In the case of flexural waves, as the width-thickness ratio (h/a) is increased from zero, the velocity remains close to that for generalized plane stress until quite large values of h/a are reached; after which the velocity rises asymptotically toward that for plane strain. In the case of extensional waves the velocity is slightly smaller than that for generalized plane stress for all $h/a > 0$.

First-Order Equations

The plate displacements, as defined in reference (5), are expressed in terms of three potentials $\Phi_i(x, y, t)$

$$\left.\begin{aligned} v_x &= \frac{\partial \Phi_1}{\partial x} + \frac{\partial \Phi_2}{\partial x} + \frac{\partial \Phi_3}{\partial y} \\ v_y &= \frac{\partial \Phi_1}{\partial y} + \frac{\partial \Phi_2}{\partial y} - \frac{\partial \Phi_3}{\partial x} \\ v_z &= \sigma_1 \Phi_1 + \sigma_2 \Phi_2 \end{aligned}\right\} \quad \ldots\ldots\ldots\ldots [5]$$

where the Φ_i satisfy the equations

$$(\nabla^2 + \delta_i^2)\Phi_i = 0, \quad i = 1, 2, 3 \ldots\ldots\ldots\ldots [6]$$

In Equations [6], ∇^2 is Laplace's operator in the plane of x and y and

$$\left.\begin{aligned} \delta_i^2 &= \frac{3\kappa^2}{2\beta h^2}\left[(\alpha+\beta)\frac{\omega^2}{\bar{\omega}^2} - 1 - (-1)^i\psi\right], \quad i = 1, 2 \\ \psi &= \left\{\left[(\alpha+\beta)\frac{\omega^2}{\bar{\omega}^2} - 1\right]^2 + 4\alpha\beta\frac{\omega^2}{\bar{\omega}^2}\left(1 - \frac{\omega^2}{\bar{\omega}^2}\right)\right\}^{1/2} \\ \delta_2^2 &= \frac{\omega^2}{c_2^2}, \quad \bar{\omega}^2 = \frac{\pi^2}{4h^2}c_1^2, \quad c_1^2 = \frac{\lambda + 2G}{\rho}, \quad c_2^2 = \frac{G}{\rho} \\ \alpha &= \frac{c_1^2}{c_2^2}, \quad \beta = \frac{c_3^2}{c_2^2}, \quad c_3^2 = \frac{4G(\lambda+G)}{\rho(\lambda+2G)} = \frac{E}{\rho(1-\nu^2)} \\ \kappa^2 &= \frac{\pi^2}{12}, \quad \sigma_i = \frac{h(\lambda+2G)}{\kappa\lambda}\left(\delta_i^2 - \frac{\omega^2}{c_1^2}\right), \quad i = 1, 2 \end{aligned}\right\} \ldots [7]$$

where λ, G are Lamé's constants.

It should be noted that the dimension $2h$ which was called the thickness of the plate in reference (5) is here called the width.

Let

$$\Phi_i = f_i(x) \exp [i(\eta y + \omega t)] \ldots\ldots\ldots\ldots [8]$$

then Equations [6] yield

$$f_i'' = \xi_i^2 f_i, \quad i = 1, 2, 3 \ldots\ldots\ldots\ldots [9]$$

where prime denotes differentiation with respect to x and

$$\xi_i^2 = \eta^2 - \delta_i^2 \ldots\ldots\ldots\ldots [10]$$

The plate displacements, expressed in terms of the f_i, are

$$\left.\begin{aligned} v_x &= [f_1' + f_3' + i\eta f_2] \exp [i(\eta y + \omega t)] \\ v_y &= [i\eta(f_1 + f_2) - f_3'] \exp [i(\eta y + \omega t)] \\ v_z &= [\sigma_1 f_1 + \sigma_2 f_2] \exp [i(\eta y + \omega t)] \end{aligned}\right\} \ldots [11]$$

and the plate stresses, after omission of the exponential factor, are

$$\left.\begin{aligned} N_x &= 2Gh[(\eta^2 + \xi_3^2)(f_1 + f_2) + 2i\eta f_3'] \\ N_{xy} &= 2Gh[i\eta(f_1' + f_3') - (\eta^2 + \xi_3^2)f_3] \\ R_x &= \frac{2Gh^3}{3}(\sigma_1 f_1' + \sigma_2 f_2') \end{aligned}\right\} \ldots [12]$$

In the problems under consideration, the boundary conditions are

$$N_x = N_{xy} = R_x = 0 \quad \text{at } x = \pm a \ldots\ldots\ldots [13]$$

Flexural Vibrations. When the motion is antisymmetric with respect to the plane $x = 0$ we take as the solutions of Equation [9]

$$f_1 = A_1 \sinh \xi_1 x, \quad f_2 = A_2 \sinh \xi_2 x, \quad f_3 = A_3 \cosh \xi_3 x \ldots [14]$$

The plate stresses on the faces $x = \pm a$ are now computed by means of Equations [12] and [14], and equated to zero. This results in a homogeneous system of linear equations in the A_i. The vanishing of the determinant of the coefficients of the A_i leads to the frequency equation

$$\sigma_2 \xi_3 F_1 = \sigma_1 \xi_1 F_2 \ldots\ldots\ldots\ldots [15]$$

where

$$F_i = \frac{\tanh \xi_i a}{\tanh \xi_3 a} - \frac{4\eta^2 \xi_i \xi_3}{(\eta^2 + \xi_3^2)^2}, \quad i = 1, 2 \ldots\ldots [16]$$

Equation [15] may be employed for the determination of $\omega/\bar{\omega}$ for a given ηa; i.e., for the evaluation of the frequencies of various modes corresponding to any given wave length. We are interested in the variation of the phase velocity c with the wave length of the lowest antisymmetric mode only, and in the region of wave lengths large in comparison with $2a$, or $\eta a \ll 1$.

It can be verified that Equation [15] has a root for vanishing $\omega/\bar{\omega}$ and ηa. It is assumed, further, that $c/c_2 \to 0$ as $\eta a \to 0$, which is seen to be verified by the results.

Expanding expressions [7] for δ_i and σ_i in series of powers of c/c_2 and ηa, and dropping terms above the second power, we obtain

$$\left.\begin{aligned} \delta_1^2 &= \frac{\eta^2 c^2}{c_1^2}, \quad \delta_2^2 = \frac{\eta^2 c^2}{c_2^2} \\ \delta_3^2 &= \frac{\eta^2 c^2}{c_2^2}\left(\frac{1}{\beta} + \frac{1}{\alpha} - 1\right) - \frac{\pi^2}{4h^2}\frac{c_2^2}{c_3^2} \\ \frac{\sigma_1}{\sigma_2} &= \frac{\eta^2(c^2/c_2^2 - c^2/c_1^2)}{\eta^2(1 - c^2/c_1^2) - \xi_3^2} \end{aligned}\right\} \ldots [17]$$

In addition we observe that $\xi_1 a$ and $\xi_3 a$ tend to zero with ηa, hence we may write

$$\tanh \xi_i a \approx \xi_i a \left(1 - \frac{1}{3}\xi_i^2 a^2\right), \quad i = 1, 3 \ldots\ldots \quad [18]$$

and finally

$$\left.\begin{aligned} \tanh \xi_1 a &\approx \eta a \sqrt{\left(1 - \frac{c^2}{c_2^2}\right)} \left[1 - \frac{1}{3}\eta^2 a^2 \left(1 - \frac{c^2}{c_2^2}\right)\right] \\ \tanh \xi_3 a &\approx \eta a \sqrt{\left(1 - \frac{c^2}{c_2^2}\right)} \left[1 - \frac{1}{3}\eta^2 a^2 \left(1 - \frac{c^2}{c_2^2}\right)\right] \end{aligned}\right\} . \quad [18a]$$

In virtue of Equations [17] and [18a], Equation [15] yields

$$\frac{c^2}{c_2^2} = \frac{4}{3}\eta^2 a^2 \left\{\frac{1+\nu}{2} + \frac{3\nu^2}{\pi^2}\left(\frac{h}{a}\right)^2 \left[1 - \frac{h}{\kappa a}\sqrt{\left(\frac{1-\nu}{6}\right)} \tanh\left(\frac{\kappa a}{h}\sqrt{\left\langle\frac{6}{1-\nu}\right\rangle}\right)\right]\right\} \ldots\ldots [19]$$

Let

$$\gamma = \kappa \sqrt{\left(\frac{6}{1-\nu}\right)}, \quad c'^2 = \frac{E}{3\rho} = \frac{2}{3}(1+\nu)c_2^2 \ldots [20]$$

Then Equation [19] becomes

$$\frac{c}{c'} = \eta a \left[1 + \frac{6\nu^2}{\pi^2(1+\nu)}\left(\frac{h}{a}\right)^2 \left(1 - \frac{\tanh(\gamma a/h)}{\gamma a/h}\right)\right]^{1/2} \ldots\ldots [21]$$

For $\gamma a/h \geqslant 1$, that is, when the width is not large in comparison with the thickness of the plate, we may write

$$\tanh(\gamma a/h) \approx 1$$

and Equation [21] yields

$$\frac{c}{c'} = \eta a \left\{1 + \frac{6\nu^2}{\pi^2(1+\nu)}\left(\frac{h}{a}\right)^2 \left[1 - \frac{2h}{\pi a}\sqrt{\left(\frac{1-\nu}{2}\right)}\right]\right\}^{1/2} \ldots\ldots [22]$$

For $\gamma a/h \ll 1$, that is for shallow plates, we have

$$\frac{\tanh(\gamma a/h)}{\gamma a/h} \approx 1 - \frac{1}{3}(\gamma a/h)^2 \left[1 - \frac{2}{5}\left(\frac{\gamma a}{h}\right)^2\right]$$

and

$$\frac{c}{c'} = \frac{\eta a}{(1-\nu^2)^{1/2}} \left[1 - \frac{\pi^2\nu^2}{10(1-\nu)}\left(\frac{a}{h}\right)^2\right] \ldots\ldots [23]$$

The second term in the bracket of Expression [22] gives the increase of the phase velocity, over the velocity for generalized plane stress, for a relatively thin slice of a plate. Similarly, the second term in the bracket of Expression [23] gives the departure from plane strain, for a shallow plate. These equations yield the same results as Equations [1] and [3], for the limiting values of h/a.

The magnitude of the phase velocity of long flexural waves, expressed as the per cent excess over the velocity for generalized plane stress, is shown in Fig. 2, for three values of Poisson's ratio. The same curves give the per cent excess, over the case of generalized plane stress, for the value of the tangent

$$\frac{d(c/c_2)}{d(\eta a)}$$

at the origin $\eta a = c/c_2 = 0$. It is seen that as the width $2h$ increases with respect to the thickness $2a$, the velocity corresponding to plane stress is not greatly exceeded until the width becomes considerably larger than the thickness.

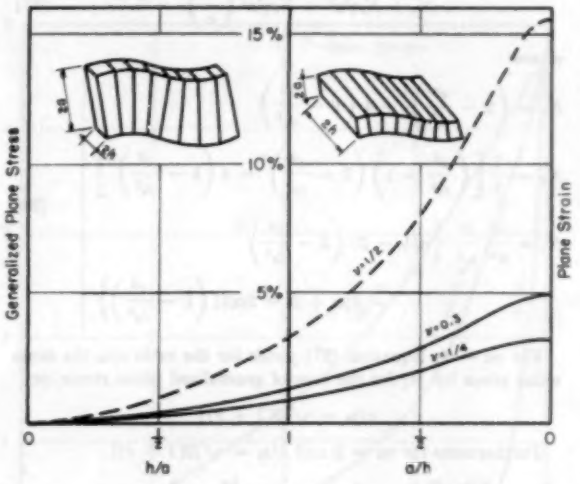

FIG. 2 VELOCITY OF LONG FLEXURAL WAVES; PER CENT EXCESS OVER GENERALIZED PLANE STRESS

Extensional Vibrations. When the motion is symmetric with respect to the plane $z = 0$ we take as the solutions of Equation [9]

$$f_1 = A_1 \cosh \xi_1 z, \quad f_2 = A_2 \cosh \xi_3 z, \quad f_3 = A_3 \sin \xi_1' z, \quad (\xi_1' = i\xi_1) \ldots\ldots [24]$$

The trigonometric, rather than the hyperbolic function is assumed for f_3, in anticipation that $\delta_3 a > \eta a$.

Proceeding as for the antisymmetric case, we derive the frequency equation

$$\sigma_2 \xi_3 G_1 \tanh \xi_3 a = \sigma_1 \xi_1 G_2 \tanh \xi_1 a \ldots\ldots [25]$$

where

$$G_i = \frac{\tanh \xi_i a}{\tan \xi_1' a} - \frac{(\eta^2 - \xi_3'^2)^2}{4\eta^2 \xi_i \xi_1'}, \quad i = 1, 2 \ldots\ldots [26]$$

For $\omega/\bar{\omega} = \eta a = 0$ Equation [25] is satisfied, thus there is a mode whose frequency approaches zero, as the wave length becomes large in comparison with the thickness. It is the behavior of this mode at long wave lengths in which we are interested.

Furthermore

$$\frac{\omega}{\bar{\omega}} = \frac{2}{\pi}\frac{c}{c_1}\eta h$$

hence, under the verifiable supposition that c/c_1 is finite and nonzero, we conclude that

$$\text{if } \frac{\omega}{\bar{\omega}} \ll 1 \quad \text{then} \quad \eta h \ll 1 \ldots\ldots\ldots\ldots [a]$$

that is, the approximations given by Equation [17] are valid for wave lengths large in comparison with both of the transverse dimensions of the plate.

We now assume $\eta a \ll 1$, expand Equation [25] and drop terms beyond the second power of ηa. It should be remarked that it follows from [a] that

$$\xi_2 a \tanh \xi_2 a \gg \eta^2 a^2$$

for all values of the ratio h/a, hence only the terms multiplied by $\xi_2 a \tanh \xi_2 a$ contribute to the final equation. We thus obtain

$$N_1 + N_2 \eta^2 a^2 + N_3 \eta^2 a^2 \left(\frac{h}{a}\right)^2 = 0 \quad \ldots\ldots [27]$$

where

$$\left.\begin{aligned} N_1 &= \left(2 - \frac{c^2}{c_2^2}\right)^2 - 4\left(1 - \frac{c^2}{c_2^2}\right) \\ N_2 &= \frac{1}{3}\left[\left(\frac{c^2}{c_2^2} - 1\right)\left(2 - \frac{c^2}{c_2^2}\right)^2 - 4\left(1 - \frac{c^2}{c_2^2}\right)^2\right] \\ N_3 &= \frac{4}{\pi^2}\frac{c^2}{c_1^2}\left\{\alpha(1-\beta)\left(2 - \frac{c^2}{c_2^2}\right)^2 \right. \\ &\qquad \left. - 4[\alpha + \beta - 2\alpha\beta]\left(1 - \frac{c^2}{c_2^2}\right)\right\} \end{aligned}\right\} \quad \ldots [28]$$

For $\eta a \to 0$, Equation [27] yields for the ratio c/c_2 the same value given by [4] for the case of generalized plane stress, or

$$c/c_2 = \sqrt{[2(1+\nu)]}$$

Furthermore for $\eta a = 0$ and $c/c_2 = \sqrt{[2(1+\nu)]}$

$$\frac{d(c^2/c_2^2)}{d(\eta^2 a^2)} = -\frac{4}{\pi^2}\nu^2(1-2\nu)\frac{h^2}{a^2} - \frac{2}{3}\nu^2(1+\nu) \quad \ldots [29]$$

Hence, near the origin

$$\frac{c^2}{c_2^2} = 2(1+\nu) - \frac{2}{3}\nu^2(1+\nu)\eta^2 a^2 - \frac{4}{\pi^2}\nu^2(1-2\nu)\eta^2 h^2 \quad \ldots\ldots [30]$$

or, approximately

$$\frac{c}{c_2} = \sqrt{[2(1+\nu)]}\left[1 - \frac{\nu^2}{6}\eta^2 a^2 - \frac{\nu^2(1-2\nu)}{\pi^2(1+\nu)}\eta^2 h^2\right] \quad \ldots\ldots [31]$$

Equation [31] describes the variation of the phase velocity with the wave length of the first extensional mode. Now, h and a are not interchangeable in this equation, inasmuch as only the first transverse extensional mode in the z-direction has been taken into account, whereas all the modes in the x-direction have been included. However Equation [31] is in agreement with the expectation that the predominant coupling effect, at long wave lengths, is associated with the larger transverse dimension; i.e., with the lower transverse frequency.

It is well known that coupling is stronger when the difference of the frequencies of the coupled modes is small. As the wave length of the extensional mode decreases from infinity, its frequency rises from zero, and approaches first the frequency of the lowest transverse mode, which corresponds to the larger transverse dimension. Hence the predominance of this dimension in Equation [31]. It should be noted that this equation is not to be used if $\nu > 1/3$, for the reason given in the "Introduction."

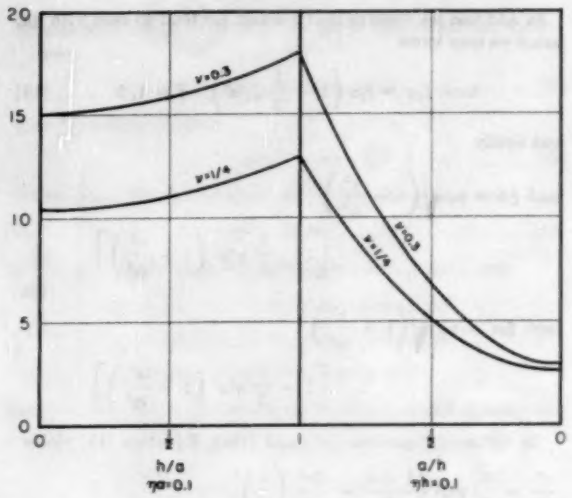

FIG. 3 VELOCITY OF LONG EXTENSIONAL WAVES; DECREASE IN 10^{-4} PER CENT FROM GENERALIZED PLANE STRESS

The per cent decrease of the phase velocity from the limiting velocity for generalized plane stress is plotted in Fig. 3 for two values of Poisson's ratio, and for $\eta a = 0.1$ or $\eta h = 0.1$, respectively, for $a/h > 1$ or $h/a > 1$. Actually Fig. 3 should be symmetrical about the line $a/h = 1$. The asymmetry is due to the first order approximation in z, which constrains the motion in this direction, thus resulting in higher frequencies.

As is well known for the case of generalized plane stress, the phase velocity of the lowest extensional mode diminishes as the wave length diminishes. It is seen from Equation [31], and the left-hand side of Fig. 3, that this drop in velocity is accentuated as the width increases from zero to the neighborhood of the thickness.

It should be remarked that if the dimension $2h$ is increased to infinity, the first extensional mode degenerates to a zero mode, and a higher one becomes the mode of plane strain, with motion only in the plane of x and y.

LAGRANGE'S EQUATION

Referring to Fig. 1, we consider a plate with the plane of y and z its middle plane and w (a function of y, z, and t) its deflection. In the classical theory of flexure, w is governed by (4)

$$D\nabla^4 w + 2\rho a \frac{\partial^2 w}{\partial t^2} = 0, \quad w = w(y, z, t) \quad \ldots\ldots [32]$$

where

$$D = 2Ea^3/3(1-\nu^2) \quad \ldots\ldots [33]$$

For free edges, the boundary conditions are

$$\left.\begin{aligned} \frac{\partial^2 w}{\partial z^2} + \nu\frac{\partial^2 w}{\partial y^2} &= 0 \\ \frac{\partial^3 w}{\partial z^3} + (2-\nu)\frac{\partial^3 w}{\partial y^2 \partial z} &= 0 \end{aligned}\right\} \quad \text{at } z = \pm h \quad \ldots [34]$$

Let

$$w = Z(z)\exp[i(\eta y + \omega t)] \quad \ldots\ldots [35]$$

Then Equation [32] yields the linear differential equation

$$Z^{IV} - 2\eta^2 Z'' + \left(\eta^4 - \frac{\omega^2}{m^2}\right)Z = 0 \quad \ldots\ldots [36]$$

where

$$m^2 = D/2\rho a \quad [37]$$

A solution of Equation [36], symmetric in z, is

$$Z = A_1 \cosh \lambda_1 z + A_2 \cosh \lambda_2 z \quad [38]$$

with

$$\lambda_i = \eta^2 - (-1)^i(\omega/m), \quad i = 1, 2 \quad [39]$$

Introducing Expression [38] into Equations [34], we derive the frequency equation[7]

$$M_1 \tanh \lambda_1 h = M_2 \tanh \lambda_2 h \quad [40]$$

where

$$M_i = \lambda_i/(\lambda_i^2 - \nu\eta^2)^2, \quad i = 1, 2 \quad [41]$$

The quantities $\lambda_i h$ are of the order of magnitude of ηh, or smaller. Hence, for $\eta h \ll 1$, we can write

$$\tanh \lambda_i h \approx \lambda_i h \left(1 - \frac{1}{3}\lambda_i^2 h^2\right) \quad [42]$$

Equation [40] then yields

$$\frac{\omega^2}{\eta^2}\left(1 - \frac{2\nu\eta^2 h^2}{3}\right) = \frac{1-\nu^2}{m^2}\eta^2 - \frac{2h^2}{3}\frac{\nu(1-\nu)}{m^2}\eta^4 \quad [43]$$

and finally

$$\frac{c}{c'} = \eta a\left[1 + \frac{\nu^2}{3(1+\nu)}\eta^2 h^2\right] \quad [44]$$

where c' is given by Equation [20].

To study the case of larger ηh, we write Equation [40] in the form

$$\sqrt{(1-r)}[(1-\nu)+r]^2 \tanh [\eta h\sqrt{(1-r)}] = \sqrt{(1+r)}[(1-\nu)-r]^2 \tanh[\eta h\sqrt{(1+r)}] \quad [45]$$

where r describes the departure of the phase velocity from the velocity of plane strain, and is given by

$$r = \frac{\omega m}{\eta^2} = \frac{c}{c'}\sqrt{(1-\nu^2)} \quad [46]$$

The value $r = 1$ corresponds to the velocity of long flexural waves in plane strain, and the value $r = (1-\nu^2)^{1/2}$ to that in generalized plane stress.

Equation [45] constitutes a relation between ηh and r; i.e., it yields the velocity corresponding to a given ratio of the wave length to the width $2h$. Alternatively, for a constant ηa, it may be regarded as a relation between h/a and r. That is, if the ratio of the wave length to the thickness $2a$ is kept constant, Equation [45] yields the velocity corresponding to a given ratio of width to thickness.

From Equation [44] it is ascertained that, if $\eta h \to 0$

$$c/c' \to 1, \quad r \to \sqrt{(1-\nu^2)}$$

However, for $\eta h \to \infty$, Equation [45] reduces to the algebraic equation

$$\sqrt{(1-r)}[(1-\nu)+r]^2 - \sqrt{(1+r)}[(1-\nu)-r]^2 = 0, \quad r \neq 1 \quad [47]$$

whose only acceptable root is

$$r^2 = (1-\nu)[(3\nu-1) + 2\sqrt{(1-2\nu+2\nu^2)}] \leqslant 1 \quad [48]$$

Hence, the phase velocities given by Equation [45] never reach the values of plane strain, however large the ratio h/a may become. This is due to the anticlastic curvature present in the classical theory even when the width of the plate is very large. Prevention of the anticlastic curvature could be obtained, within the framework of the classical theory, by couples

$$M_y = -\nu M_x$$

along the free edges, and this would raise the phase velocity to the value for plane strain. To obtain suppression of the anticlastic curvature when the edges are free would require that finite rotations be taken into account.

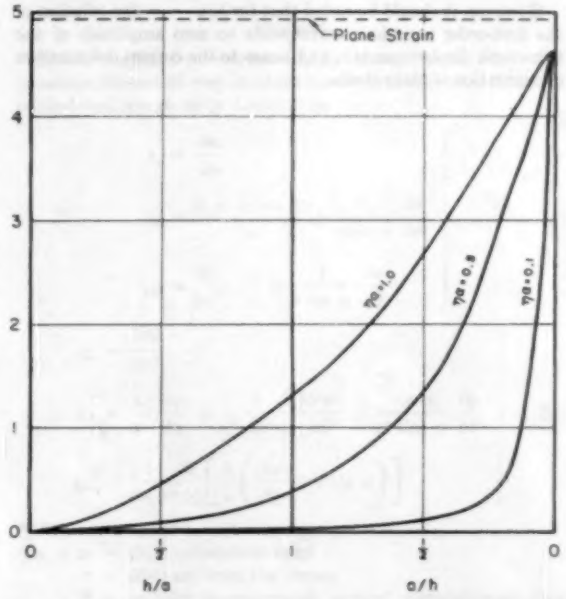

FIG. 4 VELOCITY OF LONG FLEXURAL WAVES; PER CENT EXCESS OVER GENERALIZED PLANE STRESS; SOLUTION OF LAGRANGE EQUATION FOR $\nu = 1/4$

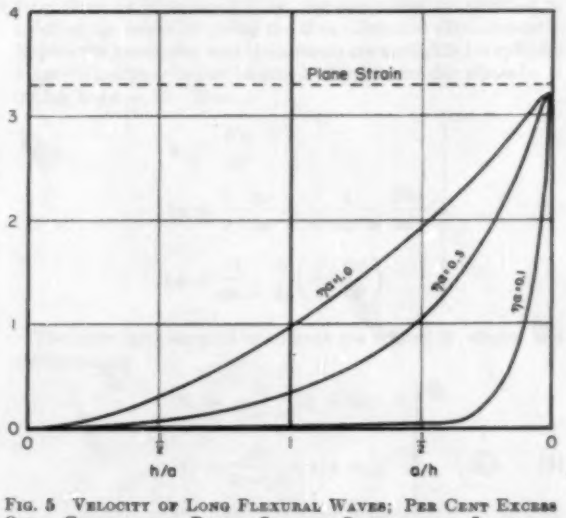

FIG. 5 VELOCITY OF LONG FLEXURAL WAVES; PER CENT EXCESS OVER GENERALIZED PLANE STRESS; SOLUTION OF LAGRANGE EQUATION FOR $\nu = 0.3$

[7] This frequency equation is given by Voigt (6).

Curves computed from the solution of Lagrange's equation are shown in Figs. 4 and 5, for $\nu = 1/4$ and $\nu = 0.3$, respectively, and for three values of ηa. These are to be compared with the results from the first-order equations shown in Fig. 2. The presence of anticlastic curvature in the Lagrange theory is the cause of the difference between the two. The first-order theory does not contain displacements which could produce anticlastic curvature and, in this respect contains an additional constraint, resulting in higher frequencies. For example, for $\nu = 0.3$ and $a = h$, Fig. 2 gives an excess of 1.3 per cent over the velocity of generalized plane stress, whereas Fig. 5 gives less than 0.05 per cent for $\eta a = 0.1$.

However, it should be noted that for $h/a \to \infty$ the solution of the first-order equations corresponds to zero amplitude of the transverse displacements v, and hence to the correct deformation configuration of plane strain.

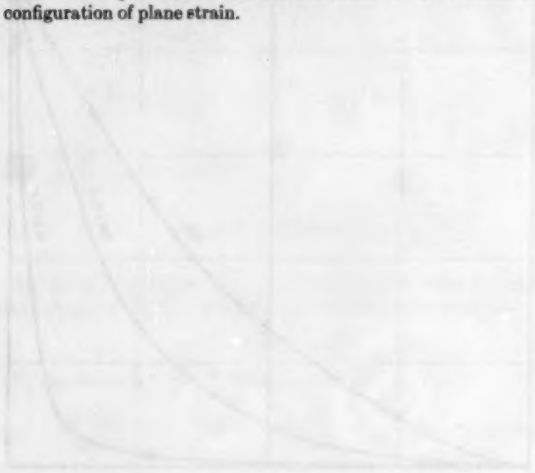

BIBLIOGRAPHY

1 "On the Free Vibrations of an Infinite Plate of Homogeneous Isotropic Elastic Matter," by Lord Rayleigh, Proceedings of the London Mathematical Society, vol. 20, 1889, pp. 225–234.

2 "On the Flexure of Elastic Plates," by H. Lamb, Proceedings of the London Mathematical Society, vol. 21, 1889, p. 85.

3 "On Waves in an Elastic Plate," by H. Lamb, Proceedings of the Royal Society of London, series A, vol. 93, 1917, pp. 114–128.

4 "A Treatise on the Mathematical Theory of Elasticity," by A. E. H. Love, Cambridge University Press, London, England, 1927, p. 496.

5 "High-Frequency Extensional Vibrations of Plates," by T. R. Kane and R. D. Mindlin, JOURNAL OF APPLIED MECHANICS, Trans. ASME, vol. 78, 1956, pp. 277–283.

6 "Bemerkung zu dem Problem der transversalen Schwingungen rechteckiger Platten," by W. Voigt, Göttingen Nachrichten, 1893, p. 225.

A Donnell Type Theory for Asymmetrical Bending and Buckling of Thin Conical Shells

By PAUL SEIDE,[1] LOS ANGELES, CALIF.

Equations, somewhat more accurate than those recently presented by N. J. Hoff, are derived for bending and buckling of thin circular conical shells under arbitrary loading. These equations reduce to Donnell's equations for thin cylindrical shells when the cone semivertex angle becomes very small and the minimum radius of curvature of the median surface approaches a constant value. At the other end of the scale the equations reduce to the well-known equations for flat circular plates when the cone semivertex angle approaches a right angle. In addition, for the entire range of cone semivertex angles the equations reduce to the known equations for axisymmetrical bending when variations of the displacements around the circumference vanish. The problem of bending is reduced to the solution of a single fourth-order partial differential equation with variable coefficients.

Introduction

A THEORY for the bending of thin circular conical shells under arbitrary loading was recently presented by N. J. Hoff (1)[2] who showed that, by neglecting certain terms in the expressions for middle surface strains and curvatures, a set of equations that reduced to Donnell's equations for cylindrical shells in the limit could be obtained. The approximations were such that it was recommended they not be used for cone semi-vertex angles α greater than 30 deg. In the present paper it is shown that, by retaining certain terms omitted by Hoff, a theory which reduces to three well-known limiting cases—Donnell's theory for cylinders, the flat circular plate, and axisymmetrical bending and buckling of cones—is obtained. The equations also can be expressed in a form that is somewhat more recognizable. Unfortunately, the equations are subject to the same difficulty as Hoff's equations, that of not being solvable in terms of known functions except for special cases. These equations, however, should yield more accurate results when solved approximately by the various methods available. It is interesting to note that the equations are related to those for a circular plate in the same manner as Donnell's equations for a cylinder are related to those for a rectangular plate.

[1] Member of the Technical Staff, The Ramo-Wooldridge Corporation.

[2] Numbers in parentheses refer to the Bibliography at the end of the paper.

Presented at the Applied Mechanics Division Summer Conference, Berkeley, Calif., June 13-15, 1957, of The American Society of Mechanical Engineers.

Discussion of this paper should be addressed to the Secretary, ASME, 29 West 39th Street, New York, N. Y., and will be accepted until January 10, 1958, for publication at a later date. Discussion received after the closing date will be returned.

Note: Statements and opinions advanced in papers are to be understood as individual expressions of their authors and not those of the Society. Manuscript received by ASME Applied Mechanics Division, November 13, 1956. Paper No. 57—APM-42.

Bending

Middle-Surface Deformations and Stresses of Conical Shell. Expressions for middle-surface strains and curvatures of a deformed conical shell are given by Love (2) as

$$\left.\begin{aligned} \epsilon_s &= \frac{\partial u}{\partial s} \\ \epsilon_\theta &= \frac{u - w\cot\alpha}{s} + \frac{1}{s\sin\alpha}\frac{\partial v}{\partial\theta} \\ \gamma_{s\theta} &= \frac{\partial v}{\partial s} - \frac{v}{s} + \frac{1}{s\sin\alpha}\frac{\partial u}{\partial\theta} \end{aligned}\right\} \quad \ldots\ldots [1]$$

$$\left.\begin{aligned} \chi_s &= \frac{\partial^2 w}{\partial s^2} \\ \chi_\theta &= \frac{1}{s}\frac{\partial w}{\partial s} + \frac{1}{s^2\sin^2\alpha}\frac{\partial^2 w}{\partial\theta^2} + \frac{\cos\alpha}{s^2\sin^2\alpha}\frac{\partial v}{\partial\theta} \\ \chi_{s\theta} &= \frac{1}{\sin\alpha}\frac{\partial}{\partial s}\left[\frac{1}{s}\left(\frac{\partial w}{\partial\theta} + v\cos\alpha\right)\right] \end{aligned}\right\} \quad \ldots [2a]$$

where

u, v, w = displacements in cone
s = distance from the vertex
θ = angular measurement around circumference (see Fig. 1)

In the present investigation, the strains are retained in the form given by Equation [1], but the curvatures are modified by deleting the terms involving the circumferential displacement v. Experience has shown that these terms are negligible for cylindrical shells and they vanish identically for flat circular plates (α = 90 deg, $\cos\alpha = 0$). Then

$$\left.\begin{aligned} \chi_s &= \frac{\partial^2 w}{\partial s^2} \\ \chi_\theta &= \frac{1}{s}\frac{\partial w}{\partial s} + \frac{1}{s^2\sin^2\alpha}\frac{\partial^2 w}{\partial\theta^2} \\ \chi_{s\theta} &= \frac{1}{\sin\alpha}\frac{\partial}{\partial s}\left(\frac{1}{s}\frac{\partial w}{\partial\theta}\right) \end{aligned}\right\} \quad \ldots\ldots [2b]$$

The force and moment resultants are related to strains and curvatures by

$$\left.\begin{aligned} N_s &= \frac{Et}{1-\nu^2}(\epsilon_s + \nu\epsilon_\theta) \\ N_\theta &= \frac{Et}{1-\nu^2}(\epsilon_\theta + \nu\epsilon_s) \\ N_{s\theta} = N_{\theta s} &= \frac{Et}{2(1+\nu)}\gamma_{s\theta} \end{aligned}\right\} \quad \ldots\ldots [3]$$

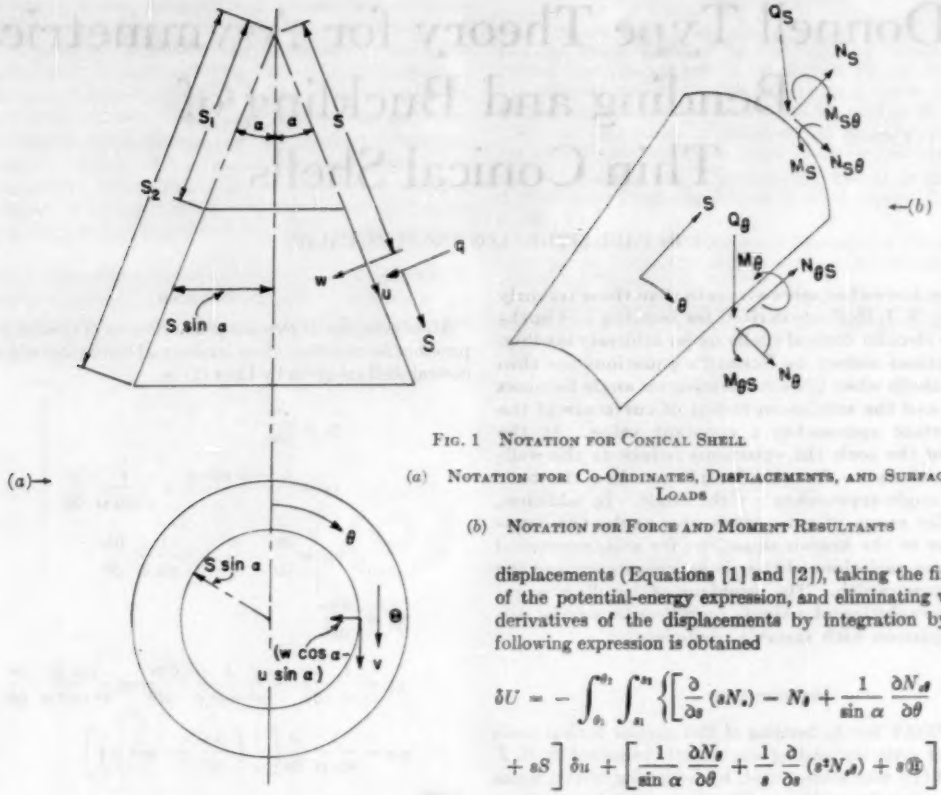

FIG. 1 NOTATION FOR CONICAL SHELL

(a) NOTATION FOR CO-ORDINATES, DISPLACEMENTS, AND SURFACE LOADS

(b) NOTATION FOR FORCE AND MOMENT RESULTANTS

$$\left.\begin{aligned} M_s &= -D(\chi_s + \nu\chi_\theta) \\ M_\theta &= -D(\chi_\theta + \nu\chi_s) \\ M_{s\theta} &= -M_{\theta s} = D(1-\nu)\chi_{s\theta} \end{aligned}\right\} \quad \ldots\ldots\ldots [4]$$

Equilibrium Equations and Boundary Conditions. The equations of equilibrium and boundary conditions may be established, as in Hoff's paper, by minimizing the potential energy of the conical shell. The potential energy is given by the strain energy of the cone minus the work done by external loads and is expressible as

$$\left.\begin{aligned} U = &\int_{\theta_1}^{\theta_2}\int_{s_1}^{s_2}\left[\frac{1}{2}(N_s\epsilon_s + N_\theta\epsilon_\theta + N_{s\theta}\gamma_{s\theta} - M_s\chi_s \right. \\ &\left. - M_\theta\chi_\theta + 2M_{s\theta}\chi_{s\theta}) - (Su + \mathfrak{V}v + qw)\right]s\sin\alpha\, ds\, d\theta \\ &- \int_{\theta_1}^{\theta_2}\left[s(\bar{N}_s u + \bar{N}_{s\theta}v - \bar{M}_s\frac{\partial w}{\partial s} + \bar{M}_{s\theta}\frac{1}{s\sin\alpha}\frac{\partial w}{\partial\theta} \right. \\ &\left. + \bar{Q}_s w)\right]_{s=s_1}^{s=s_2}\sin\alpha\, d\theta \\ &- \int_{s_1}^{s_2}\left(\bar{N}_\theta v + \bar{N}_{s\theta}u - \bar{M}_\theta\frac{1}{s\sin\alpha}\frac{\partial w}{\partial\theta} + \bar{M}_{s\theta}\frac{\partial w}{\partial s} \right. \\ &\left. + \bar{Q}_\theta w\right)_{\theta=\theta_1}^{\theta=\theta_2} ds \end{aligned}\right\} \quad \ldots [5]$$

By substituting into Equation [5] the equations for middle-surface forces and moments in terms of strains and curvatures (Equations [3] and [4]) and strains and curvatures in terms of displacements (Equations [1] and [2]), taking the first variation of the potential-energy expression, and eliminating variations of derivatives of the displacements by integration by parts, the following expression is obtained

$$\left.\begin{aligned} \delta U = &-\int_{\theta_1}^{\theta_2}\int_{s_1}^{s_2}\left\{\left[\frac{\partial}{\partial s}(sN_s) - N_\theta + \frac{1}{\sin\alpha}\frac{\partial N_{s\theta}}{\partial\theta} \right. \right. \\ &\left. + sS\right]\delta u + \left[\frac{1}{\sin\alpha}\frac{\partial N_\theta}{\partial\theta} + \frac{1}{s}\frac{\partial}{\partial s}(s^2N_{s\theta}) + s\mathfrak{V}\right]\delta v \\ &\left. - \left[sD\nabla^4 w - N_\theta\cot\alpha - qs\right]\delta w\right\}\sin\alpha\, ds\, d\theta \\ &+ \int_{\theta_1}^{\theta_2}\left\{s\left[(N_s - \bar{N}_s)\,\delta u + (N_{s\theta} - \bar{N}_{s\theta})\,\delta v \right. \right. \\ &\left. - (M_s - \bar{M}_s)\delta\frac{\partial w}{\partial s}\right] + \left[\frac{\partial}{\partial s}(sM_s) - M_\theta \right. \\ &\left. \left. - \frac{2}{\sin\alpha}\frac{\partial M_{s\theta}}{\partial\theta} - s\bar{Q}_s + \frac{1}{\sin\alpha}\frac{\partial\bar{M}_{s\theta}}{\partial\theta}\right]\delta w\right\}_{s=s_1}^{s=s_2}\sin\alpha d\theta \\ &+ \int_{s_1}^{s_2}\left\{(N_\theta - \bar{N}_\theta)\,\delta v + (N_{s\theta} - \bar{N}_{s\theta})\,\delta u \right. \\ &- \frac{1}{s\sin\alpha}(M_\theta - \bar{M}_\theta)\delta\frac{\partial w}{\partial\theta} + \left[\frac{1}{s\sin\alpha}\frac{\partial M_\theta}{\partial\theta} \right. \\ &\left. \left. - \frac{2}{s}\frac{\partial}{\partial s}(sM_{s\theta}) - \bar{Q}_\theta + \frac{\partial\bar{M}_{s\theta}}{\partial s}\right]\delta w\right\}_{\theta=\theta_1}^{\theta=\theta_2} ds \\ &+ 2(M_{s\theta} - \bar{M}_{s\theta})\delta w\Big|_{s=s_1}^{s=s_2}\Big|_{\theta=\theta_1}^{\theta=\theta_2} \end{aligned}\right\} \quad \ldots [6]$$

For minimum potential energy, the first variation of U must vanish. Since δu, δv, and δw are independent in the interior of the shell, each of their factors under the double integral sign must vanish to yield the equations of equilibrium. Similarly, the factors of each of the variations in the line integrals or the variations themselves may vanish, as well as the last corner terms. This procedure yields the following equilibrium equations and a typical set of boundary conditions:

Axial direction

$$\frac{1}{s}\frac{\partial}{\partial s}(sN_s) - \frac{N_\theta}{s} + \frac{1}{s\sin\alpha}\frac{\partial N_{s\theta}}{\partial\theta} + S = 0 \quad \ldots\ldots [7a]$$

Circumferential direction

$$\frac{1}{s\sin\alpha}\frac{\partial N_\theta}{\partial\theta} + \frac{1}{s^2}\frac{\partial}{\partial s}(s^2 N_{s\theta}) + \mathfrak{E} = 0 \quad \ldots\ldots [7b]$$

Radial direction

$$D\nabla^4 w - \frac{N_\theta}{s}\cot\alpha - q = 0 \quad \ldots\ldots [7c]$$

where

$$\nabla^4 = \nabla^2\nabla^2 \equiv \left(\frac{\partial^2}{\partial s^2} + \frac{1}{s}\frac{\partial}{\partial s} + \frac{1}{s^2\sin^2\alpha}\frac{\partial^2}{\partial\theta^2}\right)^2$$

Along $s = s_1$ and $s = s_2$

$$\left.\begin{aligned} &N_s = \bar{N}_s \quad \text{or} \quad \delta u = 0 \\ &N_{s\theta} = \bar{N}_{s\theta} \quad \text{or} \quad \delta v = 0 \\ &M_s = \bar{M}_s \quad \text{or} \quad \delta\frac{\partial w}{\partial s} = 0 \\ &\frac{\partial}{\partial s}(sM_s) - M_\theta - \frac{2}{\sin\alpha}\frac{\partial M_{s\theta}}{\partial\theta} \\ &\qquad = s\bar{Q}_s - \frac{1}{\sin\alpha}\frac{\partial\bar{M}_{s\theta}}{\partial\theta} \text{ or } \delta w = 0 \end{aligned}\right\} \ldots [8]$$

Along $\theta = \theta_1$ and $\theta = \theta_2$

$$\left.\begin{aligned} &N_\theta = \bar{N}_\theta \quad \text{or} \quad \delta v = 0 \\ &N_{s\theta} = \bar{N}_{s\theta} \quad \text{or} \quad \delta u = 0 \\ &M_\theta = \bar{M}_\theta \quad \text{or} \quad \delta\frac{\partial w}{\partial\theta} = 0 \\ &\frac{1}{s\sin\alpha}\frac{\partial M_\theta}{\partial\theta} - \frac{2}{s}\frac{\partial}{\partial s}(sM_{s\theta}) = \bar{Q}_\theta - \frac{\partial\bar{M}_{s\theta}}{\partial s} \text{ or } \delta w = 0 \end{aligned}\right\} \ldots [9]$$

It will be noted that, unlike Hoff's equation for equilibrium, in the radial direction, Equation [7c] does not contain Poisson's ratio in the operator acting on w.

Transformation of the Equations. The Equations of Equilibrium [7a] and [7b] are identical with those for plane stress or strain in polar co-ordinates, when the transformation

$$\bar{\theta} = \theta\sin\alpha \quad \ldots\ldots [10]$$

is made (3). The quantity $\bar{\theta}$ is the angle measured on the developed cone surface between the two generators corresponding to $\theta = 0$ and θ. This circumstance suggests that the introduction of a stress function F would be in order since the number of unknowns is thereby reduced from three (u, v, and w) to two (F and w). Then N_s, N_θ, and $N_{s\theta}$ can be expressed in terms of the stress function F as

$$\left.\begin{aligned} N_s &= \frac{1}{s}\frac{\partial F}{\partial s} + \frac{1}{s^2}\frac{\partial^2 F}{\partial\bar{\theta}^2} - \frac{1}{s}\int s S ds \\ N_\theta &= \frac{\partial^2 F}{\partial s^2} + \frac{\partial\mathfrak{B}_p}{\partial\bar{\theta}} \\ N_{s\theta} &= -\frac{\partial}{\partial s}\left(\frac{1}{s}\frac{\partial F}{\partial\bar{\theta}}\right) + \mathfrak{A}_p \end{aligned}\right\} \ldots\ldots [11]$$

where $\mathfrak{A}_p$ is a particular solution of

$$\frac{1}{s}\frac{\partial^2(s^2 N_{s\theta})}{\partial\bar{\theta}^2} + \frac{\partial(s^2 N_{s\theta})}{\partial s} = -s^2\mathfrak{B} \quad \ldots\ldots [12]$$

However, in order to use the stress-function approach an equation of compatibility is needed to define F. This is readily obtained from Equations [1] by observing that

$$\frac{\partial}{\partial s}\left(s\frac{\partial\gamma_{s\theta}}{\partial\bar{\theta}}\right) - \frac{\partial^2\epsilon_s}{\partial\bar{\theta}^2} - \frac{\partial}{\partial s}\left(s^2\frac{\partial\epsilon_\theta}{\partial s}\right) + s\frac{\partial\epsilon_s}{\partial s} = s\frac{\partial^2 w}{\partial s^2}\cot\alpha \quad \ldots\ldots [13]$$

Substitution of Equations [3] and [11] into Equation [13] then yields the desired compatibility condition

$$\nabla^4 F = -\frac{Et}{s}\frac{\partial^2 w}{\partial s^2}\cot\alpha + \frac{\partial}{\partial\bar{\theta}}\left[\frac{\partial^2\mathfrak{A}_p}{\partial s^2} - \frac{2}{s^2}\mathfrak{B}_p + \frac{\nu}{s}\mathfrak{A}\right] + \left[(1+\nu)\frac{1}{s}S + \nu\frac{\partial S}{\partial s} - \frac{1}{s^2}\int s\left(S + \frac{\partial^2 S}{\partial\bar{\theta}^2}\right)ds\right] \quad \ldots [14]$$

Then the two simultaneous equations that define F and w are

$$D\nabla^4 w - \cot\alpha\frac{1}{s}\frac{\partial^2 F}{\partial s^2} = \left(q - \cot\alpha\frac{1}{s}\frac{\partial\mathfrak{A}_p}{\partial\bar{\theta}}\right) \quad \ldots [15a]$$

$$\nabla^4 F + Et\cot\alpha\frac{1}{s}\frac{\partial^2 w}{\partial s^2} = \frac{\partial}{\partial\bar{\theta}}\left(\frac{\partial^2\mathfrak{A}_p}{\partial s^2} - \frac{2}{s^2}\mathfrak{B}_p + \frac{\nu}{s}\mathfrak{A}\right) + \left[(1+\nu)\frac{1}{s}S + \nu\frac{\partial S}{\partial s} - \frac{1}{s^2}\int s\left(S + \frac{\partial^2 S}{\partial\bar{\theta}^2}\right)ds\right] \quad \ldots [15b]$$

A single fourth-order equation for the solution of Equations [15] can be obtained in the following manner: Multiply Equation [15b] by $i[D/(Et)]^{1/3}$ and add the result to Equation [15a]. Then with the notation

$$\left.\begin{aligned} \bar{s} &= i\left(\frac{Et}{D}\right)^{1/3} s\cot\alpha \\ \bar{\nabla}^2 &= \frac{\partial^2}{\partial\bar{s}^2} + \frac{1}{\bar{s}}\frac{\partial}{\partial\bar{s}} + \frac{1}{\bar{s}^2}\frac{\partial^2}{\partial\bar{\theta}^2} \\ \zeta &= w + i\frac{F}{(DEt)^{1/3}} \end{aligned}\right\} \ldots\ldots [16]$$

the procedure yields the following equation

$$\bar{\nabla}^4\zeta + \frac{1}{\bar{s}}\frac{\partial^3\zeta}{\partial\bar{s}^3} = K(\bar{\theta},\bar{s}) \quad \ldots\ldots [17]$$

where

$$K(\bar{\theta},\bar{s}) = \frac{D}{E^2t^2}\tan^4\alpha\left\{q - \cot\alpha\left[\frac{\nu}{s}\frac{\partial\mathfrak{A}}{\partial\bar{\theta}} + \frac{1+\nu}{\bar{s}}S + \nu\frac{\partial S}{\partial\bar{s}} - \frac{1}{\bar{s}^2}\int\bar{s}\left(S + \frac{\partial^2 S}{\partial\bar{\theta}^2}\right)d\bar{s}\right] - i\left(\frac{Et}{D}\right)^{1/3}\cot^2\alpha\frac{\partial}{\partial\bar{\theta}}\left(\frac{\partial^2\mathfrak{A}_p}{\partial\bar{s}^2} - \frac{2}{\bar{s}^2}\mathfrak{B}p + \frac{1}{s}\mathfrak{A}_p\right)\right\} \quad \ldots [18]$$

It should be noted that the arbitrary constants of the solution of Equation [17] are complex; i.e., ζ can be written as

$$\zeta = \sum_{n=1}^{\infty}\sum_{j=1}^{4}(A_{jn} + B_{jn}i)\zeta_{jn}(\bar{s})\cos n\theta + \zeta p \quad \ldots [19]$$

The problem of the bending of a thin circular conical shell under arbitrary load has thus been reduced to the problem of finding the solutions of a single fourth-order differential equation which yields values of the deflection w perpendicular to the shell wall and the stress function F, the real and imaginary parts of ζ_i, respectively. Force components may be obtained from the stress function. With these force components and the deflection w, the displacements u and v may be obtained from Equations [1] and [3]; i.e.

$$\left.\begin{aligned}\frac{\partial u}{\partial s} &= \frac{1}{Et}\left[\frac{1}{s}\frac{\partial F}{\partial s} + \frac{1}{s^2}\frac{\partial^2 F}{\partial \bar{\theta}^2} - \frac{1}{s}\int s\,Ds - \nu\left(\frac{\partial^2 F}{\partial s^2} + \frac{\partial \textcircled{11}_p}{\partial \bar{\theta}}\right)\right] \\ s\,\frac{\partial}{\partial s}\left(\frac{v}{s}\right) &= \frac{2(1+\nu)}{Et}\left[-\frac{\partial}{\partial s}\left(\frac{1}{s}\frac{\partial F}{\partial \bar{\theta}}\right) + \textcircled{11}_p\right] - \frac{1}{s}\frac{\partial u}{\partial \bar{\theta}}\end{aligned}\right\} \quad [20]$$

Unfortunately, in general, the solutions of Equation [17] are unestablished. A discussion of Hoff's paper by Pohle (4) indicates that attempts at series expansions are apt to be useless from a numerical standpoint in view of the poor convergence of the series. An investigation of the solution of the equation should be the subject of further studies.

Buckling

Differential Equations. For the problem of buckling of circular conical shells, we proceed in much the same way as in part *I*, with some extensions. The displacements u, v, and w and the forces and moments N_s, N_θ, $N_{s\theta}$, M_s, M_θ, and $M_{s\theta}$ are now taken as the additional displacements, forces, and moments in the shell after buckling occurs. The deformed shell prior to buckling is assumed to be close enough to its original conical shape so that Equations [1] and the modified Equations [2] may still be used for strains and curvatures. The potential-energy expression must be modified by adding to it the energy stored in the plate during buckling by the middle-surface forces and moments present prior to buckling. In computing this additional energy, the nonlinear stretching of the middle surface must be taken into account. The nonlinear terms suggested by Langhaar (5) will be used in the strain expressions; i.e.

$$\left.\begin{aligned}\epsilon_s' &= \frac{1}{2}\left(\frac{\partial w}{\partial s}\right)^2 \\ \epsilon_\theta' &= \frac{1}{2}\left(\frac{1}{s\sin\alpha}\frac{\partial w}{\partial \theta}\right)^2 \\ \gamma_{s\theta}' &= \frac{\partial w}{\partial s}\left(\frac{\partial w}{\partial \theta}\frac{1}{s\sin\alpha}\right)\end{aligned}\right\} \quad [21]$$

Then to the potential energy expression (Equation [5]) must be added the term

$$U_w = \int_{\theta_1}^{\theta_2}\int_{s_1}^{s_2}\left[N_{s_0}(\epsilon_s + \epsilon_s') + N_{\theta_0}(\epsilon_\theta + \epsilon_\theta') + N_{s\theta_0}(\gamma_{s\theta} + \gamma_{s\theta}') - M_{s_0}\chi_s - M_{\theta_0}\chi_\theta + 2M_{s\theta_0}\chi_{s\theta}\right] s\sin\alpha\,ds\,d\theta \quad [22]$$

where the subscript 0 indicates the computed stress state prior to buckling.

Minimization of the potential-energy expression then yields the following differential equations and typical boundary conditions, where a stress function F has been introduced for the additional stresses after buckling occurs

$$\left.\begin{aligned}N_s &= \frac{1}{s}\frac{F}{\partial s} + \frac{1}{s^2}\frac{\partial^2 F}{\partial \bar{\theta}^2} \\ N_\theta &= \frac{\partial^2 F}{\partial s^2} \\ N_{s\theta} &= -\frac{\partial}{\partial s}\left(\frac{1}{s}\frac{\partial F}{\partial \bar{\theta}}\right)\end{aligned}\right\} \quad [23]$$

$$\nabla^4 F + Et\cot\alpha\,\frac{1}{s}\frac{\partial^2 w}{\partial s^2} = 0 \quad [24a]$$

$$D\nabla^4 w - \frac{1}{s}\frac{\partial}{\partial s}\left(N_{s_0}\,s\frac{\partial w}{\partial s}\right) - \frac{1}{s^2}\frac{\partial}{\partial \bar{\theta}}\left(N_{\theta_0}\frac{\partial w}{\partial \bar{\theta}}\right) - \frac{1}{s}\frac{\partial}{\partial \bar{\theta}}\left(N_{s\theta_0}\frac{\partial w}{\partial s}\right) - \frac{1}{s}\frac{\partial}{\partial s}\left(N_{s\theta_0}\frac{\partial w}{\partial \bar{\theta}}\right) - \cot\alpha\,\frac{1}{s}\frac{\partial^2 F}{\partial s^2} = 0 \quad [24b]$$

Along $s = s_1$ and $s = s_2$

$$\left.\begin{aligned}&N_s = 0 \text{ or } \delta u = 0 \\ &N_{s\theta} = 0 \text{ or } \delta v = 0 \\ &M_s = 0 \text{ or } \delta\frac{\partial w}{\partial s} = 0 \\ &\frac{\partial}{\partial s}(sM_s) - M_\theta - 2\frac{\partial M_{s\theta}}{\partial \bar{\theta}} + N_{s_0}\,s\frac{\partial w}{\partial s} + N_{s\theta_0}\frac{\partial w}{\partial \bar{\theta}} = 0 \\ &\text{or} \\ &\delta w = 0\end{aligned}\right\} \quad [25]$$

Along $\theta = \theta_1$ and $\theta = \theta_2$

$$\left.\begin{aligned}&N_\theta = 0 \text{ or } \delta v = 0 \\ &N_{s\theta} = 0 \text{ or } \delta u = 0 \\ &M_\theta = 0 \text{ or } \delta\frac{\partial w}{\partial \bar{\theta}} = 0 \\ &\frac{1}{s}\frac{\partial M_\theta}{\partial \bar{\theta}} - \frac{2}{s}\frac{\partial}{\partial s}(sM_{s\theta}) + \frac{1}{s}N_{\theta_0}\frac{\partial w}{\partial \bar{\theta}} + N_{s\theta_0}\frac{\partial w}{\partial s} = 0 \\ &\text{or} \\ &\delta w = 0\end{aligned}\right\} \quad [26]$$

Terms involving the initial moments M_{s_0}, M_{θ_0}, and $M_{s\theta_0}$ vanish by virtue of equilibrium Equation [7c] and the boundary conditions given by Equations [8] and [9].

Equation [24b] can be transformed to a more usual form if we proceed as follows: Consider the terms involving the middle-surface forces. These can be written as

$$\frac{1}{s}\frac{\partial}{\partial s}\left(N_{s_0}\,s\frac{\partial w}{\partial s}\right) + \frac{1}{s^2}\frac{\partial}{\partial \bar{\theta}}\left(N_{\theta_0}\frac{\partial w}{\partial \bar{\theta}}\right) + \frac{1}{s}\frac{\partial}{\partial \bar{\theta}}\left(N_{s\theta_0}\frac{\partial w}{\partial s}\right) + \frac{1}{s}\frac{\partial}{\partial s}\left(N_{s\theta_0}\frac{\partial w}{\partial \bar{\theta}}\right) \quad [27]$$

$$= \frac{1}{s}\frac{\partial}{\partial s}(N_{s_0}s)\frac{\partial w}{\partial s} + N_{s\theta}\frac{\partial^2 w}{\partial s^2} + \frac{1}{s^2}\frac{\partial N_{\theta_0}}{\partial \bar{\theta}}\frac{\partial w}{\partial \bar{\theta}} + \frac{1}{s^2}N_{\theta_0}\frac{\partial^2 w}{\partial \bar{\theta}^2} + \frac{2}{s}N_{s\theta_0}\frac{\partial^2 w}{\partial s\partial\bar{\theta}} + \frac{1}{s}\frac{\partial N_{\theta_0}}{\partial \bar{\theta}}\frac{\partial w}{\partial s} + \frac{1}{s}\frac{\partial N_{\theta_0}}{\partial s}\frac{\partial w}{\partial \bar{\theta}} = \frac{\partial w}{\partial s}\left[\frac{1}{s}\frac{\partial}{\partial s}(N_{s_0}s) - \frac{\partial N_{\theta_0}}{s} + \frac{1}{s}\frac{\partial N_{\theta_0}}{\partial \bar{\theta}}\right] + \frac{1}{s}\frac{\partial w}{\partial \bar{\theta}}\left[\frac{1}{s}\frac{\partial N_{\theta_0}}{\partial \bar{\theta}} + \frac{\partial N_{\theta_0}}{\partial s} + \frac{2}{s}N_{s\theta_0}\right] + N_{s_0}\frac{\partial^2 w}{\partial s^2} + N_{\theta_0}\left(\frac{1}{s^2}\frac{\partial^2 w}{\partial \bar{\theta}^2} + \frac{1}{s}\frac{\partial w}{\partial s}\right) + 2N_{s\theta_0}\left(\frac{1}{s}\frac{\partial^2 w}{\partial s\partial\bar{\theta}} - \frac{1}{s^2}\frac{\partial w}{\partial \bar{\theta}}\right) \quad \left.\begin{array}{l}\\ \\ \\ \\ \\ \\ \\ \\ \\ \end{array}\right\} \ldots [27] \text{ (cont.)}$$

The terms in brackets may be replaced by $-S$ and $-\textcircled{H}$, respectively, in view of Equations [7a] and [7b]. Then the expression becomes

$$N_{s_0}\frac{\partial^2 w}{\partial s^2} + N_{\theta_0}\left(\frac{1}{s^2}\frac{\partial^2 w}{\partial \bar{\theta}^2} + \frac{1}{s}\frac{\partial w}{\partial s}\right) + 2N_{s\theta_0}\frac{\partial}{\partial s}\left(\frac{1}{s}\frac{\partial w}{\partial \bar{\theta}}\right) - S\frac{\partial w}{\partial s} - \textcircled{H}\frac{1}{s}\frac{\partial w}{\partial \bar{\theta}} \ldots\ldots [28]$$

The first three terms are the usual radial components of middle-surface forces and can be shown to be of the same form as those for flat circular plates. The last two terms are the circumferential and generator-surface force components normal to the deformed surface of the cone. The surface forces do not vary in direction. Thus, the final radial equilibrium equation can be written as

$$D\nabla^4 w - N_{s_0}\frac{\partial^2 w}{\partial s^2} - N_{\theta_0}\left(\frac{1}{s^2}\frac{\partial^2 w}{\partial \bar{\theta}^2} + \frac{1}{s}\frac{\partial w}{\partial s}\right) - 2N_{s\theta_0}\frac{\partial}{\partial s}\left(\frac{1}{s}\frac{\partial w}{\partial \bar{\theta}}\right) + S\frac{\partial w}{\partial s} + \textcircled{H}\frac{1}{s}\frac{\partial w}{\partial \bar{\theta}} - \frac{\cot\alpha}{s}\frac{\partial^2 F}{\partial s^2} = 0 \ldots\ldots [29]$$

Transformation of Equations. A single eighth-order differential equation for w can be obtained in the following manner: We note that

$$\frac{1}{s^5}\frac{\partial^2}{\partial s^2}(s^4\nabla^4 F) = \left(\frac{1}{s}\nabla^4 + \frac{8}{s^2}\frac{\partial^3}{\partial s^3} + \frac{24}{s^3}\frac{\partial^2}{\partial s^2} + \frac{8}{s^4}\frac{\partial}{\partial s} + \frac{8}{s^4}\frac{\partial^3}{\partial s\partial\bar{\theta}^2}\right)\frac{\partial^2 F}{\partial s^2} = L_1\frac{\partial^2 F}{\partial s^2} \ldots\ldots [30]^3$$

Then by multiplying Equation [29] by s and performing the operation L_1, we obtain

$$L_1\left\{s\left[D\nabla^4 w - N_{s_0}\frac{\partial^2 w}{\partial s^2} - N_{\theta_0}\left(\frac{1}{s^2}\frac{\partial^2 w}{\partial \bar{\theta}^2} + \frac{1}{s}\frac{\partial w}{\partial s}\right) - 2N_{s\theta_0}\frac{\partial}{\partial s}\left(\frac{1}{s}\frac{\partial w}{\partial \bar{\theta}}\right) + S\frac{\partial w}{\partial s} + \textcircled{H}\frac{1}{s}\frac{\partial w}{\partial \bar{\theta}}\right]\right\} - \cot\alpha L_1\frac{\partial^2 F}{\partial s^2} = 0 \ldots\ldots [31]$$

But from Equations [30] and [24]

$$\cot\alpha L_1\frac{\partial^2 F}{\partial s^2} = \frac{\cot\alpha}{s^5}\frac{\partial^2}{\partial s^2}(s^4\nabla^4 F) = -\frac{Et\cot^3\alpha}{s^5}\frac{\partial^2}{\partial s^2}\left(s^3\frac{\partial^2 w}{\partial s^2}\right) \ldots\ldots [32]$$

so that the eighth-order differential equation for w is

$$\left(\frac{1}{s}\nabla^4 + \frac{8}{s^2}\frac{\partial^3}{\partial s^3} + \frac{24}{s^3}\frac{\partial^2}{\partial s^2} + \frac{8}{s^4}\frac{\partial}{\partial s} + \frac{8}{s^4}\frac{\partial^3}{\partial s\partial\bar{\theta}^2}\right)\left\{s\left[D\nabla^4 w - N_{s_0}\frac{\partial^2 w}{\partial s^2} - N_{\theta_0}\left(\frac{1}{s^2}\frac{\partial^2 w}{\partial \bar{\theta}^2} + \frac{1}{s}\frac{\partial w}{\partial s}\right) - 2N_{s\theta_0}\frac{\partial}{\partial s}\left(\frac{1}{s}\frac{\partial w}{\partial \bar{\theta}}\right) + S\frac{\partial w}{\partial s} + \textcircled{H}\frac{1}{s}\frac{\partial w}{\partial \bar{\theta}}\right]\right\} + \frac{Et\cot^3\alpha}{s^5}\frac{\partial^2}{\partial s^2}\left(s^3\frac{\partial^2 w}{\partial s^2}\right) = 0 \ldots\ldots [33]$$

For the special case of a cone under concentrated axial load, where the force resultants are assumed to be given by the membrane stress solution

$$N_{s_0} = -\frac{P}{\pi s\sin 2\alpha}, \qquad N_{\theta_0} = N_{s\theta_0} = 0 \ldots\ldots [34]$$

a much simpler set of equations can be obtained. For this case Equations [24] and [29] become

$$\nabla^4 F + Et\cot\alpha\frac{1}{s}\frac{\partial^2 w}{\partial s^2} = 0, \qquad D\nabla^4 w - \frac{1}{s}\frac{\partial^2}{\partial s^2}\left(\frac{Pw}{\pi\sin 2\alpha} - F\cot\alpha\right) = 0 \ldots [35]$$

On multiplying the first of these equations by a constant A and subtracting it from the second, we obtain

$$\nabla^4(Dw - AF) + \frac{1}{s}\frac{\partial^2}{\partial s^2}\left[\left(\frac{P}{\pi\sin 2\alpha} - AEt\cot\alpha\right)w - F\cot\alpha\right] = 0 \ldots\ldots [36]$$

We then wish to define A such that

$$\frac{A}{D} = -\left(\frac{\cot\alpha}{\dfrac{P}{\pi\sin 2\alpha} - AEt\cot\alpha}\right) \ldots\ldots [37a]$$

or

$$A_{1,2} = \left(\frac{D}{Et}\right)^{1/2}\left\{\frac{P}{P_{cyl_{cr}}\cos^2\alpha} \pm \left[\left(\frac{P}{P_{cyl_{cr}}\cos^2\alpha}\right)^2 - 1\right]^{1/2}\right\} \ldots\ldots [37b]$$

Therefore, with the notation

[3] An error in the expansion of Equation [30] was pointed out to the author by Prof. J. Kempner of the Polytechnic Institute of Brooklyn.

$$\left.\begin{aligned} w + \frac{A_{1,2}}{D} F &= \zeta_{1,2} \\ \beta_{1,2} &= \frac{s \cot \alpha}{A_{1,2}} \\ \nabla_{1,2}^2 &= \frac{\partial^2}{\partial \beta_{1,2}^2} + \frac{1}{\beta_{1,2}} \frac{\partial}{\partial \beta_{1,2}} + \frac{1}{\beta_{1,2}^2} \frac{\partial^2}{\partial \theta^2} \end{aligned}\right\} \quad \ldots\ldots [38]$$

we obtain the equations

$$\left.\begin{aligned} \nabla_1^4 \zeta_1 + \frac{1}{\beta_1} \frac{\partial^2 \zeta_1}{\partial \beta_1^2} &= 0 \\ \nabla_2^4 \zeta_2 + \frac{1}{\beta_2} \frac{\partial^2 \zeta_2}{\partial \beta_2^2} &= 0 \end{aligned}\right\} \quad \ldots\ldots [39]$$

which are distinct equations since A_1 and A_2 are distinct, unless

$$\frac{P}{P_{cyl_{cr}} \cos^2 \alpha} = 1$$

Then

$$\left.\begin{aligned} w &= \frac{A_2 \zeta_1 - A_1 \zeta_2}{A_2 - A_1} \\ F &= \frac{\zeta_2 - \zeta_1}{A_2 - A_1} D \end{aligned}\right\} \quad \ldots\ldots [40]$$

Thus, for buckling under concentrated load the problem can be reduced approximately to solving a single fourth-order homogeneous equation of the type encountered in the section on solution of bending problems. For other problems similar tricks may prove possible for special cases, but, in general, recourse to variational methods, using the potential-energy expression already established or the differential equations by means of the Galerkin method, seems called for.

Discussion

It can be shown that the equations derived in the foregoing reduce to well-known equations for special cases.

1 By letting the cone semi-vertex angle α approach zero, and the distance from the vertex s approach infinity, while the projection of this distance on a plane perpendicular to the cone axis ($s \sin \alpha$) approaches a constant value R, the Donnell equations (6) for a cylinder of radius R can be obtained. These are somewhat more general than usual since surface forces have been included in the bending equations.

2 By letting the semivertex angle approach a right angle, the equations for bending and buckling of a flat circular plate may be obtained (7).

3 By letting variations in the θ-direction vanish in the bending equations, another form of the Meissner equations for a cone (8) can be obtained. This is somewhat more general than Timoshenko's derivation since surface forces are included. The equations in their present form contain some extraneous solutions since the compatibility equation can be integrated once.

4 Finally, by letting variations in the θ-direction vanish in the approximate equation for buckling under axial load, an equation similar to that derived elsewhere by the author (9) can be obtained. Again this is of higher order than is actually necessary.

It can thus be seen that the equations as derived are of fairly general application and should be accurate for the entire range of cone semi-vertex angles. Further study should be given to the fourth-order partial differential equation whose solution is necessary for bending problems; and to approximate methods for solving the buckling equations, in particular to reasonable functions for deflection surfaces of buckled cones.

Author's Note Added in Proof: It has been called to the author's attention that Equation [17] is similar to Equation (11.S.11) of "Theoretical Elasticity" (by A. E. Green and W. Zerna, Oxford University Press, 1954, p. 401) derived for the general shallow shell. It should be pointed out that the main difference between the equations is that in Equation [17] the deflection w is normal to the shell middle surface, while in shallow shell theory the deflection is normal to some projective plane. Equations similar to Equations [24] for the stability of a general shell are given by V. S. Vlasov in his paper, "Basic Differential Equations in General Theory of Elastic Shells," 1944 (available as NACA TM 1241, Feb., 1951), which was pointed out by Prof. Kempner in his paper, "Stability Equations for Conical Shells" (General Electric Company Memo 531-56, July, 1957). Equations similar to Equations [15] for the bending of the general shell are given as well, although their derivation is not as straightforward. The author has not been able to obtain a copy of H. M. Mushtari's paper, "A Few Generalizations About the Theory of Thin Shells With Applications for Solving the Problems of the Stability of the Elastic Equilibrium" (*Prikl. Mat. Mekh.*, vol. 2, 1939), but believes that equations similar to those of Vlasov and the present paper may be found therein.

BIBLIOGRAPHY

1 "Thin Conical Shells Under Arbitrary Loads," by N. J. Hoff, Journal of Applied Mechanics, Trans. ASME, vol. 77, 1955, pp. 557–562.

2 "A Treatise on the Mathematical Theory of Elasticity," by A. E. H. Love, Dover Publications, New York, N. Y., fourth edition, 1944, pp. 515–524.

3 "Theory of Elasticity," by S. Timoshenko, McGraw-Hill Book Company, Inc., New York, N. Y., first edition, 1934, pp. 52–55.

4 "Discussion by F. W. Pohle of "Thin Conical Shells Under Arbitrary Loads," by N. J. Hoff, Journal of Applied Mechanics, Trans. ASME, vol. 78, 1956, pp. 322–323.

5 "A Strain-Energy Expression for Thin Elastic Shells," by H. L. Langhaar, Journal of Applied Mechanics, Trans. ASME, vol. 71, 1949, pp. 183–189.

6 "A Simplified Method of Elastic-Stability Analysis for Thin Cylindrical Shells. II—Modified Equilibrium Equation," by S. B. Batdorf, NACA TN 1342, June, 1947.

7 "Theory of Elastic Stability," by S. Timoshenko, McGraw-Hill Book Company, Inc., New York, N. Y., 1936, p. 305.

8 "Theory of Plates and Shells," by S. Timoshenko, McGraw-Hill Book Company, Inc., New York, N. Y., 1940, pp. 450–458, 475–480.

9 "Axisymmetrical Buckling of Circular Cones Under Axial Compression," by Paul Seide, Journal of Applied Mechanics, Trans. ASME, vol. 78, 1956, pp. 625–628.

Cylindrical Shells Under Line Load[1]

By R. M. COOPER,[2] SANTA MONICA, CALIF.

The problem of a line load along a segment of a generator of a simply supported circular cylindrical shell is treated using shallow cylindrical shell equations which include the effect of transverse-shear deformation. The line load is first treated as a sinusoidally-varying edge load over the length of the shell, with boundary conditions prescribed along the loaded generator such that the continuity of the shell is maintained. The solution for the problem of a uniform line load over a segment of a generator is obtained from the preceding solution, using the principle of superposition. By means of a numerical example it is shown that the results predicted by the Donnell equations for the stresses are in excellent agreement with those obtained from the system of equations employed here. However, the radial displacement predicted by the Donnell equations is in error by as much as 20 per cent in the range of shell geometry considered.

Introduction

THE PROBLEM of line loads applied along a generator of a thin, finite cylindrical shell having simply supported end conditions has received considerable attention in the literature. These solutions were obtained by employing different approximate theories where the effects of transverse shear deformation and normal stress have been neglected. The problem has recently been re-examined by Hoff, Kempner, and Pohle in (1),[3] where a historical account of the line-load problem is given. In reference (1) the classical Donnell equations (2) are used to obtain closed form solutions[4] for sinusoidally distributed loads and series solutions for uniformly distributed loads along a segment of a generator of the shell.

In the present paper, dealing with cylindrical shells under line loads, use is made of a system of equations which constitute a special case of the shallow shell equations given by Naghdi (5), where only the effects of transverse-shear deformation have been retained. The general solution of this system of equations is obtained for a simply supported cylindrical shell and the resulting coefficients are evaluated for the case of a sinusoidally distributed line load along a generator of the shell. As in (1), the solution for the case of a uniform line load over a segment of a generator is then obtained in series form using the sinusoidally varying load solution and the principle of superposition. A numerical example is given for a uniform line load distributed over one twentieth of the total length ($l/L = 1/20$) of a generator of a shell having a radius-to-length ratio of one to four ($a/L = 1/4$), for a broad range of shell thicknesses.

It may be mentioned that the dynamical counterpart of the approximate system of equations used here leads to results for phase velocities and amplitude ratios (in connection with the propagation of elastic waves in infinite cylindrical shells) which are in remarkable agreement with those obtained by means of a more complete system of equations (6). The character of the shallow-cylindrical-shell equations employed in this study is such that upon the neglect of the effect of transverse-shear deformation, they reduce to the Donnell equations of classical shell theory. From the numerical example given, it is found that the results predicted by the Donnell equations for the stresses, as given in (1), are in excellent agreement with those obtained by means of the shallow-cylindrical-shell equations which include the effects of transverse-shear deformation. The radial displacement predicted by the Donnell equations, however, may be in error by as much as 20 per cent, in the range of shell geometry considered.

Basic Equations of Shallow Cylindrical Shells

The co-ordinate system is taken on the shell middle surface with the origin at the mid-section; the x-axis is along a generator and s is measured along a circumferential arc. The third co-ordinate ζ, measured positively along the outward normal to the middle surface, together with x and s as lines of curvature form a right-handed orthogonal triad, Fig. 1. The radius from the shell axis to the middle surface is denoted by a.

The components of displacement along the axial, circumferential, and radial directions are approximated by

$$\left.\begin{aligned} U_x(x, s, \zeta) &= u(x, s) + \zeta\beta_x(x, s) \\ U_s(x, s, \zeta) &= v(x, s) + \zeta\beta_s(x, s) \\ W(x, s, \zeta) &= w(x, s) \end{aligned}\right\} \quad \ldots\ldots\ldots [1]$$

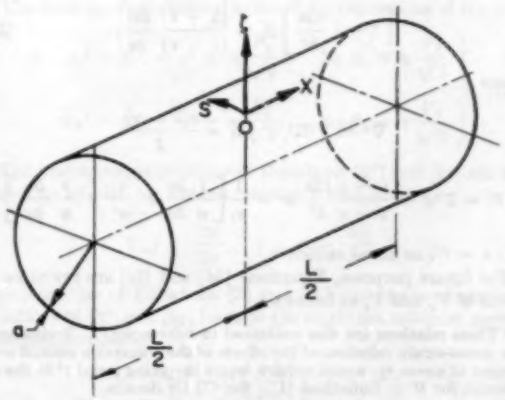

FIG. 1 CO-ORDINATE SYSTEM

[1] The results presented in this paper were obtained in the course of research sponsored by the Office of Naval Research under Contract Nonr-1224 (01), Project NR-064-408, with the University of Michigan.

[2] Design Specialist, Douglas Aircraft Co.; formerly Assistant Professor of Engineering Mechanics, University of Michigan. Assoc. Mem. ASME.

[3] Numbers in parentheses refer to the Bibliography at the end of the paper.

[4] It has been shown subsequently by Hoff (3) and Kempner (4) that within a certain range of shell geometry the higher-order terms of more complete classical shell theories do not significantly alter the results as found via the Donnell equations.

Presented at the Applied Mechanics Division Summer Conference, Berkeley, Calif., 1957, of THE AMERICAN SOCIETY OF MECHANICAL ENGINEERS.

Discussion of this paper should be addressed to the Secretary, ASME, 29 West 39th Street, New York, N. Y., and will be accepted until January 10, 1958, for publication at a later date. Discussion received after the closing date will be returned.

NOTE: Statements and opinions advanced in papers are to be understood as individual expressions of their authors and not those of the Society. Manuscript received by ASME Applied Mechanics Division, December 6, 1956. Paper No. 57—APM-28.

and the stress-strain relations which are consistent with Equations [1], as given in (5),[5] are

$$\left.\begin{aligned} N_x &= \frac{Eh}{(1-\nu^2)}\left[\frac{\partial u}{\partial x}+\nu\left(\frac{\partial v}{\partial s}+\frac{w}{a}\right)\right], \\ N_s &= \frac{Eh}{(1-\nu^2)}\left[\frac{\partial v}{\partial s}+\frac{w}{a}+\nu\frac{\partial u}{\partial x}\right] \\ M_x &= \frac{Eh^3}{12(1-\nu^2)}\left[\frac{\partial \beta_x}{\partial x}+\nu\frac{\partial \beta_s}{\partial s}\right], \\ M_s &= \frac{Eh^3}{12(1-\nu^2)}\left[\frac{\partial \beta_s}{\partial s}+\nu\frac{\partial \beta_x}{\partial x}\right] \\ N_{xs} = N_{sx} &= \frac{Eh}{2(1+\nu)}\left[\frac{\partial v}{\partial x}+\frac{\partial u}{\partial s}\right], \\ M_{xs} = M_{sx} &= \frac{Eh^3}{24(1+\nu)}\left[\frac{\partial \beta_x}{\partial s}+\frac{\partial \beta_s}{\partial x}\right] \\ V_x &= \kappa\frac{Eh}{2(1+\nu)}\left[\frac{\partial w}{\partial x}+\beta_x\right], \\ V_s &= \kappa\frac{Eh}{2(1+\nu)}\left[\frac{\partial w}{\partial s}+\beta_s\right] \end{aligned}\right\} \quad \ldots [2]$$

where E is Young's modulus, ν is Poisson's ratio; $u(x, s)$, $v(x, s)$, and $w(x, s)$ are the components of displacement at the middle surface, β_x and β_s are the changes in slope of the normal to the middle surface in the axial and circumferential directions, respectively, and the transverse-shear coefficient κ has the value 5/6.

As in (5) and (6), substitution of Equations [2] into the stress differential equations of equilibrium for shallow cylindrical shells (in the absence of body forces), and subsequent uncoupling[6] of the resulting displacement equations of equilibrium yields

$$\nabla^4 w + \frac{12(1-\nu^2)}{h^2a^2}\left[1-\frac{h^2}{12\kappa_1}\nabla^2\right]\frac{\partial^4 w}{\partial x^4} = 0 \quad \ldots [3a]$$

$$\nabla^4 u = \frac{1}{a}\frac{\partial}{\partial x}\left[\frac{\partial^2 w}{\partial s^2}-\nu\frac{\partial^2 w}{\partial x^2}\right] \quad \ldots [3b]$$

$$\nabla^4 v = -\frac{1}{a}\frac{\partial}{\partial s}\left[\frac{\partial^2 w}{\partial s^2}+(2-\nu)\frac{\partial^2 w}{\partial x^2}\right] \quad \ldots [3c]$$

$$\left[\nabla^2-\frac{12\kappa}{h^2}\right]\beta_x = \frac{(1+\nu)}{(1-\nu)}\frac{\partial P}{\partial x} \quad \ldots [3d]$$

$$\left[\nabla^2-\frac{12\kappa}{h^2}\right]\beta_s = \frac{(1+\nu)}{(1-\nu)}\frac{\partial P}{\partial s} \quad \ldots [3e]$$

where

$$\nabla^4 \equiv \nabla^2\nabla^2, \qquad \kappa_1 = \frac{\kappa(1-\nu)}{2}$$

$$P = \nabla^2 w + \frac{1-\nu}{1+\nu}\frac{12\kappa}{h^2}w - \frac{1}{\kappa_1}\left[\frac{1}{a}\frac{\partial v}{\partial s}+\frac{w}{a^2}+\frac{\nu}{a}\frac{\partial u}{\partial x}\right]$$

and $\kappa = 5/6$ as noted earlier.

For future purposes, Equations [3d] and [3e] are rewritten in terms of V_x and V_s as follows

$$\left[\nabla^2-\frac{10}{h^2}\right]V_x = \frac{10}{h^2}\frac{Eh^3}{12(1-\nu^2)}\frac{\partial(\nabla^2 w)}{\partial x} - \frac{1+\nu}{1-\nu}\frac{1}{a}\frac{\partial N_x}{\partial x} \quad \ldots [3f]$$

$$\left[\nabla^2-\frac{10}{h^2}\right]V_s = \frac{10}{h^2}\frac{Eh^3}{12(1-\nu^2)}\frac{\partial}{\partial s}(\nabla^2 w) - \frac{1+\nu}{1-\nu}\frac{1}{a}\frac{\partial N_s}{\partial s} \quad \ldots [3g]$$

It may be noted that Equations [3b] and [3c] do not yield independent homogeneous solutions, and that the homogeneous solutions of Equations [3d] and [3e], or [3f] and [3g] can be made to satisfy the same second-order partial differential equation.

Upon neglecting the effects of transverse-shear deformation the last two of Equation [2] yield

$$\beta_x = -\frac{\partial w}{\partial x}, \qquad \beta_s = -\frac{\partial w}{\partial s}$$

and the remaining Relations [2] then reduce to the stress-strain relations given by Donnell, while Equation [3a] reduces to the corresponding eighth-order differential equation of the Donnell theory. Equations [3f] and [3g] reduce to the familiar expressions of classical theory, obtained directly from the moment equations of equilibrium. Equations [3b] and [3c] are already identical with the corresponding Donnell equations since the expressions involving membrane stresses and the extensional displacements $u(x, s)$ and $v(x, s)$ have the same form as those given in (2), and the effect of transverse-shear deformation appears in the flexural terms only.

The boundary conditions appropriate to the system of Equations [2] and [3], as given in (7), are as follows

$$\left.\begin{aligned} \bar{N}_n &= N_n \text{ or } u_n \text{ prescribed} \\ \bar{N}_{nt} &= N_{nt} \text{ or } u_t \text{ prescribed} \\ \bar{M}_n &= M_n \text{ or } \beta_n \text{ prescribed} \\ \bar{M}_{nt} &= M_{nt} \text{ or } \beta_t \text{ prescribed} \\ \bar{V}_n &= V_n \text{ or } w \text{ prescribed} \end{aligned}\right\} \quad \ldots [4]$$

where the bar denotes a prescribed edge resultant and the subscripts n and t refer to the normal and tangential directions along an edge curve, respectively.

General Solution for Simply Supported Cylindrical Shells

For simply supported cylindrical shells, the boundary conditions at the ends, by Equations [4], are

$$N_x = v = M_x = \beta_s = w = 0, \qquad x = \pm\frac{L}{2} \quad \ldots [5]$$

If the displacements are assumed to have the form

$$\left.\begin{aligned} W(x, s, \zeta) &= w(x, s) = Ae^{\lambda\varphi}\cos\eta\xi \\ U_x(x, s, \zeta) &= u(x, s) + \zeta\beta_x(x, s) = (B+\zeta B_1)e^{\lambda\varphi}\sin\eta\xi \\ U_s(x, s, \zeta) &= v(x, s) + \zeta\beta_s(x, s) = (C+\zeta C_1)e^{\lambda\varphi}\cos\eta\xi \end{aligned}\right\} \quad \ldots [6]$$

where

[5] These relations are also contained in reference (7). Inclusion in the stress-strain relations of the effects of the transverse normal component of stress σ_ζ, would require terms involving ζ and ζ^2 in the expression for W in Equations [1]. See (7) for details.

[6] In a manner similar to that carried out in (6) and (8).

$$\left.\begin{aligned} &\eta = \frac{m\pi r}{L}, \qquad m = 1, 3, 5, \ldots \\ &x = r\xi, \qquad s = r\varphi, \\ &\text{and} \\ &r^4 = h^2a^2/12(1-\nu^2), \\ &\frac{r}{L} = \left(\frac{h}{a}\right)^{1/2}\left(\frac{a}{L}\right)\Big/\sqrt[4]{[12(1-\nu^2)]} \end{aligned}\right\} \ldots [7]$$

then Conditions [5] are identically satisfied. Introduction of the change of variables from [7] into [3a] yields

$$\overline{\nabla}^4 w + [1 - b^2\overline{\nabla}^2]\frac{\partial^4 w}{\partial \xi^4} = 0 \ldots\ldots\ldots\ldots\ldots [8]$$

where $\overline{\nabla}^2 \equiv \partial^2/\partial\xi^2 + \partial^2/\partial\varphi^2, \qquad b^2 = \left(\frac{h}{r}\right)^2\Big/12\kappa_1$

and substitution from Equations [6] into [8] leads to the following eighth-order characteristic equation

$$G^4 - b^2\eta G + \eta^4 = 0 \ldots\ldots\ldots\ldots\ldots [9]$$

where $G = \lambda^2 - \eta^2$. The parameter η is treated as known since it is fixed by the order of the harmonic m and the shell geometry which determines r/L. For the range of the parameters b^2 and η encountered in the present problem, the roots of Equation [9] may be written in the form

$$\left.\begin{aligned} G_{1,3} &= (\eta/\sqrt{2})(P_1 \mp iP_2) = \lambda^2_{1,3} - \eta^2 \\ G_{2,4} &= (\eta/\sqrt{2})(-P_1 \mp iP_4) = \lambda^2_{2,4} - \eta^2 \end{aligned}\right\} \ldots . [10]$$

The occurrence of P_3 in both roots of Equations [10] is a consequence of the requirement that the sum of the roots is zero, since a cubic term is not present in Equation [9]. The corresponding values of λ which satisfy Equation [9] have the form

$$\left.\begin{aligned} \lambda_1 &= -\alpha_1 + i\beta_1, & \lambda_5 &= \alpha_1 + i\beta_1 \\ \lambda_3 &= -\alpha_1 - i\beta_1, & \lambda_7 &= \alpha_1 - i\beta_1 \\ \lambda_2 &= -\alpha_2 + i\beta_2, & \lambda_6 &= \alpha_2 + i\beta_2 \\ \lambda_4 &= -\alpha_2 - i\beta_2, & \lambda_8 &= \alpha_2 - i\beta_2 \end{aligned}\right\} \ldots\ldots [11]$$

where only the roots having negative real parts will be retained, since the roots which have positive real parts imply indefinitely increasing radial displacement with increase in s, in the range $0 \leq s \leq 2\pi a$. It may be noted that the displacements assumed in Equations [6] represent the first term of an infinite series in the s-direction. An interesting geometrical interpretation for the displacements is offered in (1), where it is further remarked that most often only the first term of this series is necessary for a satisfactory approximation to the displacements.

Following introduction of the change of variables given in [7] and the displacement Equations [6] into [3b] and [3c], the coefficients B and C are obtained in terms of A for each of the four roots λ_i ($i = 1, 2, 3, 4$) retained from Equations [11]. The displacements u, v, and w are accordingly given by

$$\left.\begin{aligned} u = \Big[\Big[&\bar{A}_1 e^{-\alpha_1\varphi}\left[\frac{P_2}{\sqrt{2}}\cos\beta_1\varphi - \left\{(1+\nu)\eta + \frac{P_1}{\sqrt{2}}\right\}\sin\beta_1\varphi\right] + \bar{A}_2 e^{-\alpha_1\varphi}\left[\left\{(1+\nu)\eta + \frac{P_1}{\sqrt{2}}\right\}\cos\beta_1\varphi + \frac{P_2}{\sqrt{2}}\sin\beta_1\varphi\right] \\ &+ \bar{A}_3 e^{-\alpha_2\varphi}\left[-\frac{P_4}{\sqrt{2}}\cos\beta_2\varphi - \left\{-(1+\nu)\eta + \frac{P_1}{\sqrt{2}}\right\}\sin\beta_2\varphi\right] + \bar{A}_4 e^{-\alpha_2\varphi}\left[\left\{-(1+\nu)\eta + \frac{P_1}{\sqrt{2}}\right\}\cos\beta_2\varphi - \frac{P_4}{\sqrt{2}}\sin\beta_2\varphi\right]\Big]\frac{r}{a}\sin\eta\xi \end{aligned}\right\} \ldots [12] \text{ (Cont.)}$$

$$\left.\begin{aligned} v = -\Big[\Big[&\bar{A}_1 e^{-\alpha_1\varphi}[V_1\cos\beta_1\varphi - V_2\sin\beta_1\varphi] + \bar{A}_2 e^{-\alpha_1\varphi}[V_2\cos\beta_1\varphi + V_1\sin\beta_1\varphi] \\ &+ \bar{A}_3 e^{-\alpha_2\varphi}[V_3\cos\beta_2\varphi - V_4\sin\beta_2\varphi] + \bar{A}_4 e^{-\alpha_2\varphi}[V_4\cos\beta_2\varphi + V_3\sin\beta_2\varphi]\Big]\frac{r}{a\eta}\cos\eta\xi \end{aligned}\right\} \ldots [13]$$

where

$$V_1 = \frac{-\alpha_1 P_2}{\sqrt{2}} + \beta_1\left[(1+\nu)\eta - \frac{P_1}{\sqrt{2}}\right], \qquad V_2 = \alpha_1\left[(1+\nu)\eta - \frac{P_1}{\sqrt{2}}\right] + \frac{\beta_1 P_2}{\sqrt{2}}$$

$$V_3 = \frac{\alpha_2 P_4}{\sqrt{2}} - \beta_2\left[(1+\nu)\eta + \frac{P_1}{\sqrt{2}}\right], \qquad V_4 = -\alpha_2\left[(1+\nu)\eta + \frac{P_1}{\sqrt{2}}\right] - \frac{\beta_2 P_4}{\sqrt{2}}$$

and

$$\left.\begin{aligned} w = \Big[\Big[&\bar{A}_1 e^{-\alpha_1\varphi}[\bar{B}_1\cos\beta_1\varphi + \bar{B}_2\sin\beta_1\varphi] + \bar{A}_2 e^{-\alpha_1\varphi}[-\bar{B}_2\cos\beta_1\varphi + \bar{B}_1\sin\beta_1\varphi] \\ &+ \bar{A}_3 e^{-\alpha_2\varphi}[\bar{B}_3\cos\beta_2\varphi + \bar{B}_4\sin\beta_2\varphi] + \bar{A}_4 e^{-\alpha_2\varphi}[-\bar{B}_4\cos\beta_2\varphi + \bar{B}_3\sin\beta_2\varphi]\Big]\cos\eta\xi \end{aligned}\right\} \ldots [14]$$

where

$$\left.\begin{aligned} \bar{B}_1 &= P_1P_3, \qquad \bar{B}_3 = P_3^2 - P_1^2 = -\frac{\beta}{P_1}, \qquad \beta = \frac{b^2\eta}{\sqrt{2}} \\ \bar{B}_2 &= P_1P_4, \qquad \bar{B}_4 = P_1^2 - P_3^2 = -\frac{\beta}{P_1} \end{aligned}\right\} \ldots [15]$$

The roots α_i, β_i are related to the P_i by expressions of the type

$$\left.\begin{aligned} \alpha_1^2 - \beta_1^2 &= \eta^2 + \eta\frac{P_1}{\sqrt{2}}, \qquad 2\alpha_1\beta_1 = \eta\frac{P_2}{\sqrt{2}} \\ \alpha_2^2 - \beta_2^2 &= \eta^2 - \eta\frac{P_1}{\sqrt{2}}, \qquad 2\alpha_2\beta_2 = \eta\frac{P_4}{\sqrt{2}} \end{aligned}\right\} \ldots [16]$$

The homogeneous solutions of Equations [3f] and [3g] are obtained by introducing a stress function χ such that

$$V_{sH} = \frac{\partial\chi}{\partial s}, \qquad V_{xH} = -\frac{\partial\chi}{\partial x} \ldots\ldots\ldots\ldots [17]$$

Substitution of Equations [7] and [17] into the homogeneous equations of [3f] and [3g] leads to the single second-order partia differential equation

$$\overline{\nabla}^2\chi - 10\left(\frac{r}{h}\right)^2\chi = 0 \ldots\ldots\ldots\ldots [18]$$

whose solution leads to the homogeneous solutions of Equations [3f] and [3g].

The particular solutions of V_x and V_s are obtained following substitution of Equations [7] and [6] into [3f] and [3g]. Employing a procedure similar to that employed in the foregoing to obtain B and C in terms of A, the particular solutions are found to be

$$\left.\begin{aligned} V_{xP} = {} & \{\bar{A}_1 e^{-\alpha_1\varphi}[N_3\cos\beta_1\varphi + N_1\sin\beta_1\varphi] \\ & + \bar{A}_2 e^{-\alpha_1\varphi}[-N_1\cos\beta_1\varphi + N_3\sin\beta_1\varphi] \\ & + \bar{A}_3 e^{-\alpha_2\varphi}[N_4\cos\beta_2\varphi + N_2\sin\beta_2\varphi] \\ & + \bar{A}_4 e^{-\alpha_2\varphi}[-N_2\cos\beta_2\varphi + N_4\sin\beta_2\varphi]\}K\eta\sin\eta\xi \end{aligned}\right\} \quad [19]$$

$$\left.\begin{aligned} V_{sP} = {} & -\{\bar{A}_1 e^{-\alpha_1\varphi}[R_3\cos\beta_1\varphi + R_1\sin\beta_1\varphi] \\ & + \bar{A}_2 e^{-\alpha_1\varphi}[-R_1\cos\beta_1\varphi + R_3\sin\beta_1\varphi] \\ & + \bar{A}_3 e^{-\alpha_2\varphi}[R_4\cos\beta_2\varphi + R_2\sin\beta_2\varphi] \\ & + \bar{A}_4 e^{-\alpha_2\varphi}[-R_2\cos\beta_2\varphi + R_4\sin\beta_2\varphi]\}K\cos\eta\xi \end{aligned}\right\} \quad [20]$$

where

$$\left.\begin{aligned} K &= \frac{E}{12(1-\nu^2)}\left(\frac{h}{r}\right)^3\frac{\eta}{2\sqrt{2}}, \qquad c = \frac{1}{\beta} = 10\left(\frac{r}{h}\right)^2\frac{\sqrt{2}}{\eta} \\ d' &= 4\left(\frac{1+\nu}{1-\nu}\right)^2, \qquad c' = \frac{4\nu}{(1-\nu^2)c}\frac{\sqrt{2}}{\eta} \\ R_1 &= -\beta_1 N_3 - \alpha_1 N_1, \qquad R_3 = -\alpha_1 N_3 + \beta_1 N_1 \\ R_2 &= -\beta_2 N_4 - \alpha_2 N_2, \qquad R_4 = -\alpha_2 N_4 + \beta_2 N_2 \end{aligned}\right\} \quad [21]$$

and

$$\left.\begin{aligned} N_1 &= \frac{1}{\left(1 - \frac{2P_1}{c} + \frac{P_1^2+P_3^2}{c^2}\right)}\left\{P_1\left[3P_3^2 - P_1^2 - \frac{d'}{c^2} + c'\right] + \frac{1}{c}[P_1^4 - P_3^4 + d' - c'(P_1^2+P_3^2)]\right\} \\ N_3 &= \frac{1}{\left(1 + \frac{2P_1}{c} + \frac{P_1^2+P_3^2}{c^2}\right)}\left\{P_1\left[3P_3^2 - P_1^2 - \frac{d'}{c^2} + c'\right] + \frac{1}{c}[P_3^4 - P_1^4 - d' + c'(P_1^2+P_3^2)]\right\} \\ N_2 &= \frac{P_2}{\left(1 - \frac{2P_1}{c} + \frac{P_1^2+P_3^2}{c^2}\right)}\left\{P_1^2 + P_3^2 - \frac{2P_1}{c}(P_1^2+P_3^2) - \frac{d'}{c^2} - c'\right\} \\ N_4 &= \frac{P_4}{\left(1 + \frac{2P_1}{c} + \frac{P_1^2+P_3^2}{c^2}\right)}\left\{-(P_1^2+P_3^2) - \frac{2P_1}{c}(P_1^2+P_3^2) + \frac{d'}{c^2} + c'\right\} \end{aligned}\right\} \quad [22]$$

As in (1), the coefficients $\bar{A}_i$ are first evaluated for the problem of a sinusoidally-varying load along the generator $s = 0$. The solution for the problem of a uniform line load over a segment of the generator $s = 0$ is then obtained by using the principle of superposition. The latter solution is in the form of an infinite series whose terms are derived from the harmonics of the sinusoidally-varying load solution, in accordance with the well-known technique for representing a function by its Fourier series.

Simply Supported Cylindrical Shells Under Sinusoidally Varying Line Load

The sinusoidally-varying load is treated as an edge load, equally distributed between the edges $s = 0^+$ and $s = 0^-$. Boundary conditions from Equations [4] are written for $s = 0$ such that continuity of the shell is maintained. Thus

$$v = N_{ss} = \beta_s = M_{ss} = 0, \qquad V_s = \bar{V}\cos\eta\xi, \qquad s = 0 \quad [23]$$

where $2V = 2\bar{V}\cos\eta\xi$ is the applied load per unit length along the generator, acting radially inward.

The solution of Equation [18] is obtained by assuming

$$\chi = \Phi(\varphi)\sin\eta\xi \quad [24]$$

Discarding those solutions which imply indefinitely increasing shear resultants with increase in s, the solution for χ is given by

$$\chi = Fe^{-d\varphi}\sin\eta\xi, \qquad d^2 = \eta^2 + 10\left(\frac{r}{h}\right)^2 \quad [25]$$

From Equations [17]

$$\left.\begin{aligned} V_{xH} &= -\frac{d}{r}Fe^{-d\varphi}\sin\eta\xi \\ V_{sH} &= -\frac{\eta}{r}Fe^{-d\varphi}\cos\eta\xi \end{aligned}\right\} \quad [26]$$

From the Boundary Conditions [23]

$$V_s = V_{sP} + V_{sH} = \bar{V}\cos\eta\xi \quad [27a]$$

$$\beta_s = -\frac{1}{r}\frac{\partial w}{\partial\varphi} + \frac{6}{5}\frac{1}{Gh}V_s = 0 \quad [27b]$$

$$M_{ss} = -\frac{(1-\nu)}{r^2}\frac{\partial}{\partial\xi}\left(\frac{\partial w}{\partial\varphi}\right) + \frac{h^2}{10r}\left(\frac{\partial V_s}{\partial\xi} + \frac{\partial V_x}{\partial\varphi}\right) = 0 \quad [27c]$$

On adding and subtracting

$$\frac{h^2}{10r}\frac{\partial V_s}{\partial\xi}$$

to Equation [27c], employing [27b] and observing that

$$\frac{\partial V_{xP}}{\partial\varphi} = \frac{\partial V_{sP}}{\partial\xi}$$

by Equations [19], [20], [21], and [22], it can be shown that $F = 0$ and only particular solutions for V_x and V_s are required in this problem.

The four boundary conditions from Equations [23] not involving M_{ss} lead to solutions of the four $\bar{A}_i$ in a manner completely analogous to that given in (1). On substitution of Equations [12] and [13] into the first two of [23] and forming the sum and difference of the resulting equations, then combining the latter results with Equation [27b], $\bar{A}_1$ and $\bar{A}_3$ can be eliminated, yielding

$$\bar{A}_2 = \bar{A}_4\frac{\alpha_2 P_5 + \beta_2 P_6}{\alpha_2 P_6 - \beta_2 P_5} \quad [28]$$

where

$$\left.\begin{aligned} P_5 &= P_3(B_3^* + B_4^*) + 2P_1B_1^* \\ P_6 &= P_3B_2^* + P_4B_1^* \\ B_1^* &= \bar{B}_1 + \frac{\beta N_3}{2}, \qquad B_3^* = \bar{B}_3 + \frac{\beta N_1}{2} \\ B_2^* &= \bar{B}_2 + \frac{\beta N_4}{2}, \qquad B_4^* = \bar{B}_4 + \frac{\beta N_2}{2} \end{aligned}\right\} \quad \ldots [29]$$

By combining the equations from Equations [23], [12], and [13] in a slightly different manner and using Equation [28], $\bar{A}_3$ and $\bar{A}_3$ are obtained in terms of $\bar{A}_4$ as follows

$$\left.\begin{aligned} \bar{A}_1 &= \frac{-\bar{A}_4(\alpha_2^2 + \beta_2^2)}{B_1^*(\alpha_1^2 + \beta_1^2)} \left\{\frac{\alpha_1 B_2^* P_5 - \beta_1 B_1^* P_6 - \alpha_1 P_6(B_3^* + B_4^*)}{\alpha_2 P_6 - \beta_2 P_5}\right\} \\ \bar{A}_3 &= \frac{\bar{A}_4(\alpha_2^2 + \beta_2^2)}{B_1^*(\alpha_1^2 + \beta_1^2)} \left\{\frac{\alpha_1 B_1^* P_6 + \beta_1 B_2^* P_5 - \beta_1 P_6(B_3^* + B_4^*)}{\alpha_2 P_6 - \beta_2 P_5}\right\} \end{aligned}\right\} \quad \ldots [30]$$

$\bar{A}_4$ is finally obtained explicitly from the last of Equations [23], using [28] and [30], and is given by

$$\bar{A}_4 = -\frac{1}{K}\,\frac{(\alpha_2 P_6 - \beta_2 P_5)}{(\alpha_2^2 + \beta_2^2)}\,\frac{\bar{\nabla}}{\psi} \quad \ldots [31]$$

where

$$\psi = N_3[2P_1B_2^* - P_6(B_3^* + B_4^*)] - N_4P_5 + (N_1 + N_2)P_6$$

$$K = \frac{E}{12(1-\nu^2)}\left(\frac{h}{r}\right)^3 \frac{\eta}{2\sqrt{2}}$$

The circumferential and axial stress couples M_φ and M_x are obtained following substitution of Equations [12], [13], and [14] into the appropriate equations from [2] and using Equations [19] and [20] in the last of Equations [2] for β_x and β_φ, giving

$$\left.\begin{aligned} M_\varphi = -\Big\{ &\bar{A}_1 e^{-\alpha_1\varphi}[S_1 \cos\beta_1\varphi + S_3 \sin\beta_1\varphi] \\ &+ \bar{A}_3 e^{-\alpha_1\varphi}[-S_3 \cos\beta_1\varphi + S_1 \sin\beta_1\varphi] \\ &+ \bar{A}_2 e^{-\alpha_2\varphi}[S_2 \cos\beta_2\varphi + S_4 \sin\beta_2\varphi] \\ &+ \bar{A}_4 e^{-\alpha_2\varphi}[-S_4 \cos\beta_2\varphi + S_2 \sin\beta_2\varphi]\Big\} \frac{D\eta}{r^2} \cos\eta\xi \end{aligned}\right\} \quad \ldots [32]$$

where

$$D = \frac{Eh^3}{12(1-\nu^2)}, \qquad S_1 = \left[(1-\nu)\eta + \frac{P_1}{\sqrt{2}}\right]B_1^* - \frac{P_3}{\sqrt{2}}B_3^*$$

$$S_2 = \left[(1-\nu)\eta - \frac{P_1}{\sqrt{2}}\right]B_2^* - \frac{P_4}{\sqrt{2}}B_4^*$$

$$S_3 = \left[(1-\nu)\eta + \frac{P_1}{\sqrt{2}}\right]B_3^* + \frac{P_3}{\sqrt{2}}B_1^*$$

$$S_4 = \left[(1-\nu)\eta - \frac{P_1}{\sqrt{2}}\right]B_4^* + \frac{P_4}{\sqrt{2}}B_2^*$$

and

$$\left.\begin{aligned} M_x = -\Big\{ &\bar{A}_1 e^{-\alpha_1\varphi}[X_1 \cos\beta_1\varphi + X_3 \sin\beta_1\varphi] + \bar{A}_3 e^{-\alpha_1\varphi}[-X_3 \cos\beta_1\varphi + X_1 \sin\beta_1\varphi] \\ &+ \bar{A}_2 e^{-\alpha_2\varphi}[X_2 \cos\beta_2\varphi + X_4 \sin\beta_2\varphi] + \bar{A}_4 e^{-\alpha_2\varphi}[-X_4 \cos\beta_2\varphi + X_2 \sin\beta_2\varphi]\Big\} \frac{D\nu\eta}{r^2} \cos\eta\xi \end{aligned}\right\} \quad \ldots [33]$$

where

$$X_1 = \left[\left(1 - \frac{1}{\nu}\right)\eta + \frac{P_1}{\sqrt{2}}\right]B_1^* - \frac{P_3}{\sqrt{2}}B_3^*$$

$$X_2 = \left[\left(1 - \frac{1}{\nu}\right)\eta - \frac{P_1}{\sqrt{2}}\right]B_2^* - \frac{P_4}{\sqrt{2}}B_4^*$$

$$X_3 = \left[\left(1 - \frac{1}{\nu}\right)\eta + \frac{P_1}{\sqrt{2}}\right]B_3^* + \frac{P_3}{\sqrt{2}}B_1^*$$

$$X_4 = \left[\left(1 - \frac{1}{\nu}\right)\eta - \frac{P_1}{\sqrt{2}}\right]B_4^* + \frac{P_4}{\sqrt{2}}B_2^*$$

and the appropriate expressions for w and $V_x \equiv V_{xP}$ have been given in Equations [14] and [19], respectively.

This completes the solution for the sinusoidally-varying load problem by means of the shallow cylindrical-shell equations given in (5), where the effect of transverse-shear deformation has been retained. The corresponding results from the Donnell equations have been given in (1), and may be obtained from the results given here by putting the parameter b equal to zero. The roots α_i and β_i become the roots of Equations [9] with $b = 0$, the P_i all become equal to unity, the $\bar{B}_i$ and B_i^* reduce to unity or zero, the $\bar{A}_i$ are obtained from Equations [28], [30], and [31] following substitution of the new values noted, and Equations [14], [19], [32], and [33] accordingly reduce to the results given in (1).

Simply Supported Cylindrical Shells Under Uniform Line Load

The uniform line load over a segment of the generator $s = 0$ is first represented by its Fourier series. It is assumed that

$$\left.\begin{aligned} 2V &= \frac{P}{l}, \qquad 0 \le |x| \le \frac{l}{2} \\ &= 0, \qquad |x| \ge \frac{l}{2} \end{aligned}\right\} \quad \ldots [34]$$

where l is the length over which the line load is distributed, P is the resultant force of the load applied to the shell, and $2V$ is the radial force per unit length, directed radially inward, acting on the shell. Then, by the usual method, it is found that

$$2V = \sum_{m=1,3,5,\ldots}^{\infty} 2\bar{\nabla}_m \cos\frac{m\pi x}{L} \quad \ldots [35]$$

where

$$\bar{\nabla}_m = \frac{2P}{m\pi l} \sin\frac{m\pi l}{2L}$$

$\bar{\nabla}_m$ will be used in place of $\bar{\nabla}$ in the sinusoidally-varying load solutions, taking $m = 1, 3, 5, \ldots$, and the solution for the uniform line load given by Equations [34] is then obtained by summing as many of the weighted harmonics as are necessary for the desired accuracy of the results.

As an example, consider the case of a shell with $a/L = 1/4$, $l/L = 1/20$ and a range of values of a/h, including that for which the Donnell equations yield results which are in good agreement with a more complete classical theory.[4] Denoting the system of equations of (5), as employed in this paper, as system I and the Donnell equations as system II, the variation of w_I/w_{II} with a/h

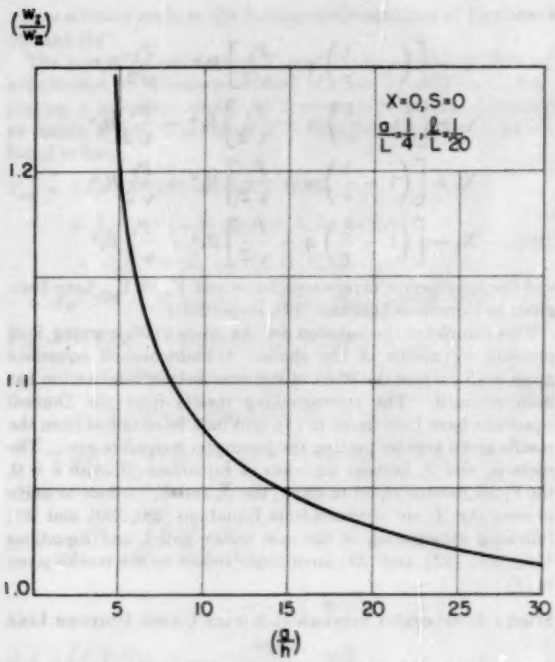

FIG. 2 VARIATION OF RATIO OF w_I/w_{II} VERSUS a/h AT $x = s = 0$ FOR $a/L = 1/4$, $l/L = 1/20$

TABLE 1 SUMMARY OF RESULTS AT $x = l/2$, $s = 0$ FOR FIXED VALUES OF (a/L) AND (l/L)

$(a/L) = 1/4$ $\quad (l/L) = 1/20$

a/h	M_{xII}/M_{xI}	V_{xII}/V_{xI}	w_I/w_{II}
5	1.022	1.009	1.136
10	1.010	1.003	1.058
30	1.002	1.000	1.009

is shown in Fig. 2, for $x = 0$, $s = 0$; i.e., at the mid-section of the shell and directly under the line load. w_I/w_{II}, M_{xII}/M_{xI}, and V_{xII}/V_{xI} at $x = l/2$, $s = 0$ are given in Table 1 for several values of a/h. The corresponding ratios were not computed for the membrane stresses N_x, N_s, and $N_{xs} = N_{sx}$ since there is no essential difference in these stresses as given by the two systems.

M_x and V_x were not computed at $x = 0$, $s = 0$. The complicated intermingling of parameters in each of the terms of the series for M_{xI} makes a general proof of the convergence of the series untractable. For the numerical example given here, the convergence of the series for M_{xI} follows from the comparison test, since the series for M_{xII} converges[7] and it was found that term by term $M_{xI} < M_{xII}$.

Between 13 and 19 terms have been included in the various series to obtain results accurate to three digits, in all cases.

CONCLUSION

From the numerical example, it is found that the results predicted in (1) by the Donnell equations for the bending couple M_x and the transverse-shear resultant V_x are in agreement with those obtained in the present analysis, which includes the effect of transverse-shear deformation. These results are especially interesting inasmuch as there is a significant difference between the expressions for V_{xI} and V_{xII} from a theoretical standpoint. The former is obtained from the solution of a second-order differential Equation, [3*f*], which plays a key role in determining the proper number of boundary conditions in the problem, whereas V_{xII} is computed directly from a moment equation of equilibrium and plays a minor role throughout. On account of the boundary conditions employed in the line-load problem, the homogeneous solution of V_{xI} vanishes and the numerical difference between V_{xI} and V_{xII} is accordingly found to be negligible here.

On the other hand, the error in the radial displacement w, as predicted by the Donnell equations undergoes a marked increase as a/h decreases from 30 to 5, in the case considered. This difference is evidently due to the neglect of the effect of transverse-shear deformation in the Donnell equations.

Although the parameter directly controlling the influence of transverse-shear deformation is b^2, in the various expressions of the foregoing analysis it appears in the form $\beta = b^2\eta/\sqrt{2}$. Since $\eta = m\pi r/L$ and (r/L) is determined by h/a and a/L from Equations [7], the terms due to transverse-shear-deformation effects become more important with increase in a/L or in the order of the harmonic, m. It is this complicated intermingling of parameters which makes a study of the convergence of the series for M_{xI} and M_{xI} untractable, and which makes the possibility of a solution in the form $w_I = w_{II}$ + correction due to shear deformation very unlikely.

From the foregoing results, it is evident that the stresses may be computed by means of the Donnell equations with good accuracy for a wide range of shell geometry. However, depending on the shell geometry and the ratio of l/L, the neglect of the effect of transverse-shear deformation may lead to a significant error for the radial displacement.

ACKNOWLEDGMENT

The author wishes to express his appreciation to Prof. P. M. Naghdi for suggesting this problem and for invaluable aid in its solution.

BIBLIOGRAPHY

1 "Line Load Applied Along Generators of Cylindrical Shells," by H. J. Hoff, J. Kempner, and F. V. Pohle, *Quarterly of Applied Mathematics*, vol. 11, 1954, pp. 411–425.

2 "Stability of Thin-Walled Tubes Under Torsion," by L. H. Donnell, U. S. NACA Technical Report 479, Washington, D. C., 1933.

3 "The Accuracy of Donnell's Equations," by N. J. Hoff, JOURNAL OF APPLIED MECHANICS, Trans. ASME, vol. 77, 1955, pp. 329–334.

4 "Remarks on Donnell's Equations," by J. Kempner, JOURNAL OF APPLIED MECHANICS, Trans. ASME, vol. 77, 1955, pp. 117–118.

5 "Note on the Equations of Shallow Elastic Shells," by P. M. Naghdi, *Quarterly of Applied Mathematics*, vol. 14, 1956, p. 331.

6 "Propagation of Elastic Waves in Cylindrical Shells," by P. M. Naghdi and R. M. Cooper, *Journal of the Acoustical Society of America*, vol. 28, 1956, pp. 56–63.

7 "On the Theory of Thin Elastic Shells," by P. M. Naghdi, *Quarterly of Applied Mathematics*, vol. 14, 1957, pp. 369–380.

8 "On the Equations of Motion of Cylindrical Shells," by P. M. Naghdi and J. G. Berry, JOURNAL OF APPLIED MECHANICS, Trans. ASME, vol. 76, 1954, pp. 160–166.

[7] See paragraph 11 of reference (1).

Behavior of Cylinders With Initial Shell Deflection

By M. E. LUNCHICK[1] and R. D. SHORT, JR.,[2] WASHINGTON, D. C.

Evidence is presented which indicates that, for stiffened cylinders fabricated by welding, initial deflections exist for the shell between frames. The initial deflections of the shell of a stiffened cylinder were measured and found to be approximated closely by a second-degree curve. Using the mathematical expression for the initial deflection curve, a theoretical analysis was made for a cylinder subjected to external hydrostatic pressure, resulting in expressions for the additional deflections and stresses caused by the initial deflection of the shell. Since the initial deflections of the shell for internally and externally framed cylinders were found to be of opposite sign, the theory is offered as a possible explanation of the observed differences in behavior between internally and externally framed cylinders.

Introduction

THE THEORETICAL analysis of closed stiffened cylinders subjected to external hydrostatic pressure has been treated by a number of investigators. Considerable progress has been achieved in that more refinements have been made to the theory. Continuous refinement is necessary and desirable in order to increase the accuracy with which stresses and collapse pressures can be predicted, thus resulting in more satisfactory designs of stiffened cylinders.

Von Sanden and Gunther (1)[3] obtained the basic solution for the deflections and stresses for a stiffened cylinder which was perfectly circular, had a shell of uniform diameter, and consisted of a material that deformed elastically at all times. Von Sanden and Gunther neglected, however, to account for the moments developed in the longitudinal direction due to the pressure on the ends of a closed cylinder. Salerno and Pulos (2) in their solution, however, accounted for the longitudinal moments due to the pressure on the ends of a closed cylinder. Bodner and Berks (3), Galletly and Bart (4), and Donnell (5) obtained expressions for the stresses developed in the shell of a stiffened cylinder resulting from out-of-roundness in the shell.

Another source of imperfection is the initial deflection of the shell between frames. Previously, measurements of this type of imperfection had been made at the Taylor Model Basin for externally framed cylinders. It was found that the shell between frames was initially convex toward the exterior of the cylinder, but no analysis had been made of the influence of these initial deflections on structural behavior.

Wu, Goodman, and Newmark (6) analyzed the problem of a cylindrical shell with a dent varying in depth along the longitudinal direction. They derived the governing displacement equations of equilibrium. However, they did not examine the type of imperfection which is axisymmetric in form, nor did they consider the influence of stiffening rings on the elastic behavior of the cylinder.

In the present paper the initial deflection of the shell is reported for an internally framed cylinder. It was found that, for this case, the shell was initially convex toward the interior of the cylinder. These initial deflections, when magnified, cause the cylinder to resemble an accordion; hence this type of imperfection will be referred to hereafter as initial accordion deflection.

It is conjectured that the initial accordion deflection is due mainly to the contraction of the welds between frame and shell. These contractions of the weld induce moments at the frames which bend the shell toward the frame. This results in convex curvature of the shell for external framing and concave curvature for internal framing, considering the curvature from the exterior of the cylinder.

An analytical solution will be derived for the additional deflections and stresses resulting from initial accordion deflection when the cylinder is subjected to external hydrostatic pressure. The resulting theoretical analysis is applicable to both internal and external framing. The theory will then be used to explain some of the differences in behavior between internally framed and externally framed cylinders.

Measurement of Initial Accordion Deflection

Initial longitudinal contours of an internally framed cylinder were measured at the David Taylor Model Basin. These measurements were taken along two generators of the cylinder 90 deg apart. The method of measurement was developed to provide not only the maximum deviation of the shell from that of a perfect cylinder but also the contours of the shell between frames.

The arrangement devised for measuring these contours is shown in Fig. 1. The cylinder was placed with its axis horizontal. A rod with an Ames dial gage (accurate to 0.001 in.) attached at one end was clamped to another horizontal rod graduated in inches. This graduated rod was placed in the radial plane containing a line scribed on the surface of the shell along one generator. As can be seen in Fig. 1, the graduated rod was supported on vertical stands. The Ames dial gage was moved horizontally along the line scribed on the cylinder, and deflection readings were taken at the frames and at five intermediate points. By this procedure measurements could be repeated to within 0.001 in. Plots of measured initial accordion deflections are shown in Fig. 2.

In Fig. 2 plots of the following equation also are shown

$$w_i = \frac{4}{L}\left(x - \frac{x^2}{L}\right)\Delta \qquad [1]$$

where w_i is the initial deflection at any point, x is the co-ordinate measured along a generator from an origin located at a frame, L is the frame spacing, and Δ is the maximum initial deflection of the shell. The terms just defined are indicated in Fig. 3. In plotting Equation [1] the maximum initial deflection Δ was set equal to

---

[1] Head, Structural Evaluation Section, David Taylor Model Basin.

[2] Structural Research Engineer, David Taylor Model Basin.

[3] Numbers in parentheses refer to the Bibliography at the end of the paper.

Presented at the Applied Mechanics Division Summer Conference, Berkeley, Calif., June 13–15, 1957, of The American Society of Mechanical Engineers.

Discussion of this paper should be addressed to the Secretary, ASME, 29 West 39th Street, New York, N. Y., and will be accepted until January 10, 1958, for publication at a later date. Discussion received after the closing date will be returned.

Note: Statements and opinions advanced in papers are to be understood as individual expressions of their authors and not those of the Society. Manuscript received by ASME Applied Mechanics Division, January 2, 1957. Paper No. 57—APM-35.

FIG. 1 ARRANGEMENT FOR MEASURING INITIAL ACCORDION DEFLECTION

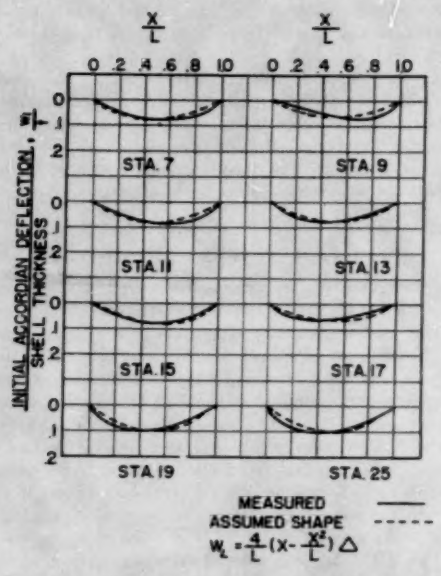

FIG. 2 COMPARISON OF MEASURED INITIAL ACCORDION DEFLECTION AND ASSUMED SECOND-DEGREE CURVE

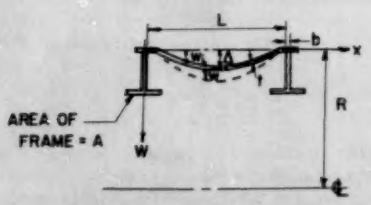

FIG. 3 NOTATION FOR ANALYSIS OF STIFFENED CYLINDERS WITH INITIAL ACCORDION DEFLECTION

the observed value at mid-bay, considered positive toward the axis of the cylinder. From Fig. 2 it can be seen that the measured deflection contours and the curves represented by Equation [1] are in fair agreement.

DERIVATION OF DIFFERENTIAL EQUATION OF EQUILIBRIUM OF A STIFFENED CYLINDER WITH INITIAL ACCORDION DEFLECTION

The moment M_E resulting from the pressure on the ends of a closed cylinder of radius R is

$$M_E = -N_x(w_i + w) \quad [2]$$

where w_i is given by Equation [1], and $N_x = -pR/2$ (the axial load per inch of circumference), and w denotes the additional radial displacements from the initial deflection surface, taken positive when inward. The deflections w are caused by the applied pressure p which is considered positive when applied externally. If it is assumed that the initial accordion deflection contour does not change about the circumference of the cylinder, the moment M_E is obtained by combining Equations [1] and [2], thus

$$M_E = -N_x\left[\frac{4}{L}\left(x - \frac{x^2}{L}\right)\Delta + w\right] \quad [3]$$

The differential shear resulting from the moment M_E can be obtained by taking the second derivative of Equation [3], thus

$$\frac{d^2M}{dx^2} = -N_x\left(\frac{d^2w}{dx^2} - \frac{8\Delta}{L^2}\right) \quad [4]$$

The differential equation of equilibrium for a cylinder of perfectly uniform diameter $2R$ is as follows (7)

$$D\frac{d^4w}{dx^4} = p + \frac{1}{R}\mu N_x - \frac{w}{R^2}Et + N_x\frac{d^2w}{dx^2} \quad [5]$$

where E is Young's modulus, μ is Poisson's ratio, t is the shell thickness, and

$$D = \frac{Et^3}{12(1-\mu^2)}$$

The last term on the right side of Equation [5] is the differential shear resulting from the moment caused by pressure on the ends of the cylinder. When Equation [4] is substituted for the last term of Equation [5], the differential equation of equilibrium governing the deformation of a cylinder with an initial accordion deflection, expressed by Equation [1], is obtained as follows

$$D\frac{d^4w}{dx^4} = p + \frac{1}{R}\mu N_x - \frac{w}{R^2}Et + N_x\left(\frac{d^2w}{dx^2} - \frac{8\Delta}{L^2}\right) \quad [6]$$

Equation [6] also can be written

$$\frac{d^4w}{dx^4} + 4\alpha^4\beta^2\frac{d^2w}{dx^2} + 4\alpha^4\left[w - \frac{pR^2}{Et}\left(1 - \frac{\mu}{2}\right) - \frac{8\beta^2}{L^2}\Delta\right] = 0 \quad [7]$$

where

$$\alpha^4 = \frac{3(1-\mu^2)}{R^2t^2} \quad [8]$$

and

$$\beta^2 = \frac{pR^2}{2Et} \quad [9]$$

If a change in variable is made in Equation [7] as follows

$$Z = \frac{pR^2}{Et}\left(1 - \frac{\mu}{2}\right) + \frac{8\beta^2}{L^2}\Delta - w \quad [10]$$

a simplified expression is obtained

$$\frac{d^4Z}{dx^4} + 4\alpha^4\beta^2\frac{d^2Z}{dx^2} + 4\alpha^4 Z = 0 \quad [11]$$

Solution of Differential Equation of Equilibrium for a Stiffened Cylinder With Initial Accordion Deflection

Equation [11] is a linear differential equation and its solution can be shown to be of the form

$$Z = C_1 \sinh K_1x \sin K_2x + C_2 \sinh K_1x \cos K_2x + C_3 \cosh K_1x \sin K_2x + C_4 \cosh K_1x \cos K_2x \quad [12]$$

where

$$K_1 = \alpha\,(1 - \alpha^2\beta^2)^{1/2} \quad [13]$$

and

$$K_2 = \alpha\,(1 + \alpha^2\beta^2)^{1/2} \quad [14]$$

For the geometries generally used in practice, values of the parameters K_1 and K_2 are real and positive.

As a result of symmetry and continuity, the following boundary conditions are assumed to exist (see Fig. 3)
At

$$x = 0, \quad w = w_0 \quad [15]$$

$$x = L, \quad w = w_0 \quad [16]$$

$$x = 0, \quad \frac{dw}{dx} = 0 \quad [17]$$

$$x = L, \quad \frac{dw}{dx} = 0 \quad [18]$$

where w_0 is the deflection occurring at a frame. When the four boundary conditions of Equations [15] to [18] are substituted into Equation [12] and its first derivative, four equations are obtained which, when solved simultaneously, yield expressions for the four coefficients of Equation [12] as follows

$$C_1 = \left[\frac{K_2 \sin K_2L - K_1 \sinh K_1L}{K_1 \sinh K_1L + K_1 \sin K_2L}\right] Z_0 \quad [19]$$

$$C_2 = \left[\frac{K_2\,(\cos K_2L - \cosh K_1L)}{K_2 \sinh K_1L + K_1 \sin K_2L}\right] Z_0 \quad [20]$$

$$C_3 = \left[\frac{K_1(\cosh K_1L - \cos K_2L)}{K_2 \sinh K_1L + K_1 \sin K_2L}\right] Z_0 \quad [21]$$

$$C_4 = Z_0 \quad [22]$$

where

$$Z_0 = \frac{pR^2}{Et}\left(1 - \frac{\mu}{2}\right) + \frac{8\beta^2}{L^2}\Delta - w_0 \quad [23]$$

When Equations [19] to [22] are substituted into Equation [12], the variable Z can be expressed in terms of its value Z_0 at a frame as

$$Z = \frac{f(x)}{G} Z_0 \quad [24]$$

where

$$f(x) = K_2 \sinh K_1x \cos K_2(L - x) + K_1 \cosh K_1x \sin K_2(L - x) + K_1 \sin K_2x \cosh K_1(L - x) + K_2 \cos K_2x \sinh K_1(L - x) \quad [25]$$

and

$$G = K_2 \sinh K_1L + K_1 \sin K_2L \quad [26]$$

The value of the parameter Z at the frame denoted as Z_0 can be obtained by considering the equilibrium of radial forces at the frame, which is assumed to deform as a thin ring. Referring to

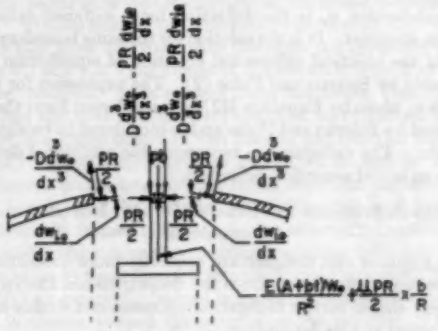

Fig. 4 Forces at a Frame

Fig. 4, the summation of radial forces at a frame is as follows

$$2D\left.\frac{d^3w}{dx^3}\right|_{x=0} + \frac{E(A + bt)}{R^2} w_0 - pb + \mu\frac{pR}{2}\frac{b}{R} + 2\frac{pR}{2}\left.\frac{dw_1}{dx}\right|_{x=0} = 0 \quad [27]$$

where the derivatives of the deflections are evaluated at the frame as indicated. In terms of the variable Z, Equation [27] can be expressed as

$$\left.\frac{d^3Z}{dx^3}\right|_{x=0} + 2\alpha^4\left(\frac{A + bt}{t}\right) Z_0 - \frac{4\alpha^4\beta^2}{Rt} A\left(1 - \frac{\mu}{2}\right) - 16\alpha^4\beta^2\frac{(A + bt)}{tL}\frac{\Delta}{L} - 16\alpha^4\beta^2\frac{\Delta}{L} = 0 \quad [28]$$

Substituting Equation [24] and its third derivative evaluated at $x = 0$ into Equation [28] and solving for Z_0 yields

$$Z_0 = \frac{2\alpha^2\beta^2 G}{H}\left[\frac{A\left(1 - \frac{\mu}{2}\right)}{Rt} + \frac{4\Delta}{L}\left(1 + \frac{A + bt}{Lt}\right)\right] \quad [29]$$

where

$$H = \frac{\alpha^2}{t}(A + bt)G + 2K_1K_2(\cosh K_1L - \cos K_2L) \quad [30]$$

When Equations [10] and [29] are substituted into Equation [24], the general expression for the deflection of a stiffened cylinder with the assumed form of initial accordion deflection results

$$w = \frac{\beta^2}{R}(2 - \mu) - \frac{2\alpha^2\beta^2}{H}\left[\frac{A\left(1 - \frac{\mu}{2}\right)}{Rt}\right] f(x) + \frac{8\beta^2\Delta}{L^2}\left[1 - \frac{\alpha^2}{H}\frac{(A + bt + tL}{t} f(x)\right] \quad [31]$$

Let

$$w_s = \frac{\beta^2}{R}(2-\mu) - \frac{2\alpha^2\beta^2}{H}\left[\frac{A\left(1-\frac{\mu}{2}\right)}{Rt}\right] f(x) \ldots [32]$$

and

$$w_\Delta = \frac{8\beta^2\Delta}{L^2}\left[1 - \frac{\alpha^2}{H}\frac{(A+bt+tL)}{t} f(x)\right] \ldots [33]$$

Then

$$w = w_s + w_\Delta \ldots [34]$$

The deflection w_s is the deflection for a stiffened cylinder of uniform diameter. It is the solution for the same boundary conditions of the identical differential equation of equilibrium solved previously by Salerno and Pulos (2). The expression for the deflection w_s given by Equation [32] is in a different form than that presented by Salerno and Pulos and is considered to be simpler to evaluate. The deflection w_Δ represents the additional deflection due to an initial accordion deflection.

Additional Stresses and Strains Due to Initial Accordion Deflection

The engineer and designer are generally more concerned with stresses than deflections. Once the deflections are known, it is a relatively simple matter to determine stresses and strains in terms of deflection and its derivatives.

The expression for the circumferential membrane strain $\sigma_{m\phi}$ is well known as (7)

$$\sigma_{m\phi} = \frac{Ew}{R} + \mu\frac{pR}{2t} \ldots [35]$$

Introducing Equation [34] into Equation [35], the total membrane stress in the circumferential direction is

$$\sigma_{m\phi} = \frac{Ew_s}{R} + \mu\frac{pR}{2t} + \frac{Ew_\Delta}{R} \ldots [36]$$

The first two terms on the right side of Equation [36] represent that portion of the stress for a cylinder of perfectly uniform diameter. On the other hand, the last term is that portion of the total stress attributed to initial accordion deflection. Thus the additional membrane stress $\sigma_{m\phi\Delta}$ in the circumferential direction due to initial accordion deflection can be expressed as

$$\sigma_{m\phi\Delta} = \frac{Ew_\Delta}{R} \ldots [37]$$

where the additional deflection w_Δ is given by Equation [33].

The total bending stress σ_{bx} in the longitudinal direction on the surface of the cylinder is given by

$$\sigma_{bx} = \pm\frac{Et}{2(1-\mu^2)}\ddot{w} \ldots [38]$$

or since

$$w = w_s + w_\Delta \ldots [34]$$

$$\sigma_{bx} = \pm\frac{Et}{2(1-\mu^2)}\ddot{w}_s \pm \frac{Et}{2(1-\mu^2)}\ddot{w}_\Delta \ldots [39]$$

The component $\sigma_{bx\Delta}$, attributable to initial accordion deflection, of the total bending stress in the longitudinal direction is as follows

$$\sigma_{bx\Delta} = \pm\frac{Et}{2(1-\mu^2)}\ddot{w}_\Delta \ldots [40]$$

where $\ddot{w}_\Delta$ is the second derivative of Equation [33] which is found to be

$$\ddot{w}_\Delta = -\frac{16\alpha^4\beta^2}{HL^2}\Delta\left(\frac{A+bt+tL}{t}\right)[K_1\cosh K_1x\sin K_2(L-x) - K_2\sinh K_1x\cos K_2(L-x) - K_2\cos K_2x\sinh K_1(L-x) + K_1\sin K_2x\cosh K_1(L-x)] \ldots [41]$$

The bending stress $\sigma_{b\phi\Delta}$ in the circumferential direction due to initial accordion deflection is then simply

$$\left.\begin{aligned}\sigma_{b\phi\Delta} &= \mu\sigma_{bx\Delta}\\ \text{or}\\ \sigma_{b\phi\Delta} &= \pm\frac{\mu}{2}\frac{Et}{(1-\mu^2)}\ddot{w}_\Delta\end{aligned}\right\} \ldots [42]$$

The circumferential stress $\sigma_{\phi\Delta}$ on the surface of the cylinder attributable to initial accordion deflection is the sum of the additional membrane and additional bending stresses. Thus, adding Equations [37] and [42]

$$\sigma_{\phi\Delta} = \frac{Ew_\Delta}{R} \pm \frac{\mu}{2}\frac{Et}{(1-\mu^2)}\ddot{w}_\Delta \ldots [43]$$

where the terms w_Δ and $\ddot{w}_\Delta$ can be expressed by Equations [33] and [41], respectively.

The stress $\sigma_{x\Delta}$ in the longitudinal direction on the surface of the cylinder due to initial accordion deflection is simply the additional bending stress given by Equation [40], as the membrane stress in this direction is not altered by any initial accordion deflection. Thus

$$\sigma_{x\Delta} = \pm\frac{Et}{2(1-\mu^2)}\ddot{w}_\Delta \ldots [44]$$

The choice of signs in Equations [42] and [43] is dependent upon the location of the point at which the stress is determined. Keeping in mind that all radially inward deflections are considered positive, for cylinders subjected to external pressure the additional stresses due to initial accordion deflection on the exterior surface of the cylinders are

$$\sigma_{\phi\Delta_e} = \frac{Ew_\Delta}{R} - \frac{\mu}{2}\frac{Et}{(1-\mu^2)}\ddot{w}_\Delta \ldots [45]$$

and

$$\sigma_{x\Delta_e} = -\frac{Et}{2(1-\mu^2)}w_\Delta \ldots [46]$$

and on the interior surface are

$$\sigma_{\phi\Delta i} = \frac{Ew_\Delta}{R} + \frac{\mu}{2}\frac{Et}{(1-\mu^2)}\ddot{w}_\Delta \ldots [47]$$

and

$$\sigma_{x\Delta i} = \frac{Et}{2(1-\mu^2)}\ddot{w}_\Delta \ldots [48]$$

If the stresses in Equations [45] to [48] are expressed in terms of strain using Hooke's law for biaxial state of strain, the strain $\epsilon_{\phi\Delta}$ in the circumferential direction and the strain $\epsilon_{x\Delta}$ in the longitudinal direction, both attributable to initial accordion deflection, can be obtained as follows

$$\epsilon_{\phi\Delta} = \frac{w_\Delta}{R} \ldots [49]$$

and for a point on the exterior surface of the cylinder

$$\epsilon_{x\Delta_e} = -\frac{t}{2}\ddot{w}_\Delta - \mu\frac{w_\Delta}{R} \ldots [50]$$

and for a point on the interior surface

$$\epsilon_{x\Delta_i} = \frac{t}{2}\,\ddot{w}_\Delta - \mu\,\frac{w_\Delta}{R} \qquad [51]$$

Discussion

In order to examine the influences of initial accordion deflection on structural behavior, calculations were conducted for a hypothetical cylinder. The geometry selected was as follows

$$L/2R = 0.1$$

$$t/2R = 0.005$$

$$A/Lt = 0.5$$

$$b/L = 0.05$$

Pressure-strain curves were computed for this geometry and are presented in Figs. 5, 6, and 7. The strains in the circumferential direction and the strains in the longitudinal direction were investigated at a mid-bay point. These strains were computed by the linear theory of von Sanden and Gunther and the nonlinear theory for no accordion deflection and several ratios of initial accordion deflection to shell thickness. Figs. 5 to 7 were determined only for positive values of Δ or for internal framing.

It can be seen from Fig. 5 that for internal framing an initial accordion deflection increases the deflection (or circumferential strain) at mid-bay. On the other hand, a theoretical analysis would indicate that the deflection at a frame would be decreased owing to initial accordion deflection. The discrepancy between strains for a perfectly uniform cylinder and one with initial accordion deflection becomes much more pronounced for strains in the longitudinal direction. This is indicated in Figs. 6 and 7; in Fig. 7 it should be noticed that the initial accordion deflection can even cause the internal longitudinal strain to change sign from compression to tension.

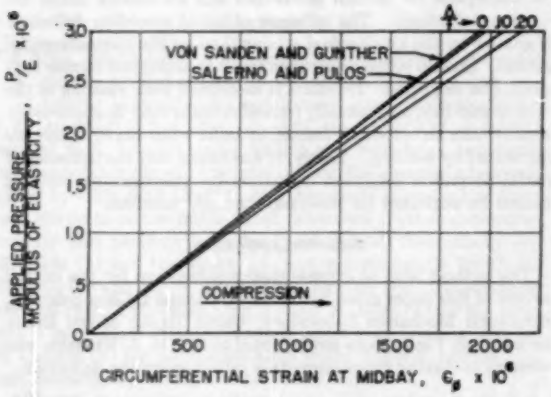
Δ→0 10 20
VON SANDEN AND GUNTHER
SALERNO AND PULOS
COMPRESSION
APPLIED PRESSURE / MODULUS OF ELASTICITY, P/E x 10⁶
CIRCUMFERENTIAL STRAIN AT MIDBAY, εφ x 10⁶
0 .5 1.0 1.5 2.0 2.5 3.0
0 500 1000 1500 2000

Fig. 5 Variation of Circumferential Strain at Mid-Bay With Pressure

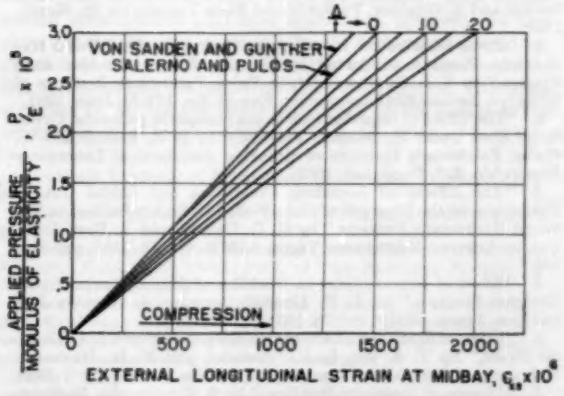
Δ→0 10 20
VON SANDEN AND GUNTHER
SALERNO AND PULOS
COMPRESSION
APPLIED PRESSURE / MODULUS OF ELASTICITY, P/E x 10⁶
EXTERNAL LONGITUDINAL STRAIN AT MIDBAY, εx x 10⁶
0 .5 1.0 1.5 2.0 2.5 3.0
0 500 1000 1500 2000

Fig. 6 Variation of External Longitudinal Strain at Mid-Bay With Pressure

Of course, the additional strains resulting from initial accordion deflection increase as the magnitude of the initial deflection increases. Measurements on stiffened cylinders at the Taylor Model Basin have indicated that the ratio Δ/t generally varies between 0.1 and 0.2. The values of Δ/t shown in Figs. 5 to 7 are, therefore, realistic. It is evident from examining Figs. 5 to 7 that, when stiffened cylinders are designed to withstand higher pressures, the linear theory of von Sanden and Gunther becomes eventually inadequate. Recourse must then be had to a nonlinear theory, taking into account initial accordion deflection.

Figs. 5 to 7 show the variation of elastic strain with pressure for an internally framed cylinder. For an externally framed cylinder the additional strains due to initial accordion deflection are of opposite sense to those for an internally framed cylinder. This is true, as for an externally framed cylinder the initial accordion deflection is convex toward the exterior of the cylinder. On the other hand, the initial deflection is concave for the case of an internally framed cylinder. The differences in sign of the additional stresses between internally and externally framed cylinders suggest the possibility of differences in strength between internally framed and externally framed cylinders.

Calculations were made to ascertain whether the difference in strength between internal and external framing was significant. In particular, the strength of cylinders against axisymmetric yielding was examined. It was reasoned that the initial accordion deflection being axisymmetric would have the greatest influence on that mode of failure involving excessive axisymmetric deformations. On the other hand, a circumferential imperfection such as shell out-of-roundness would be expected to play a predominant role in failure by shell buckling during which numerous lobes form around the circumference of the cylinder. In actuality, welded stiffened cylinders have both types of imperfections, out-of-roundness superimposed on an initial accordion deflection. However, as the pressure for failure (of perfect cylinders) by axisymmetric yielding becomes smaller in relation to that by shell

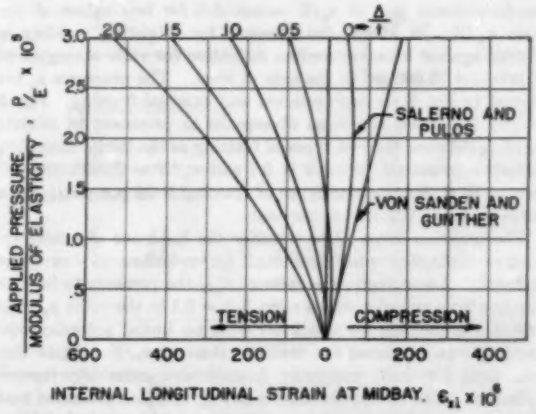
Δ
20 15 10 05 0
SALERNO AND PULOS
VON SANDEN AND GUNTHER
TENSION
COMPRESSION
APPLIED PRESSURE / MODULUS OF ELASTICITY, P/E x 10⁶
INTERNAL LONGITUDINAL STRAIN AT MIDBAY, εx1 x 10⁶
0 .5 1.0 1.5 2.0 2.5 3.0
600 400 200 0 200 400

Fig. 7 Variation of Internal Longitudinal Strain at Mid-Bay With Pressure

buckling, the initial accordion deflection would exert an increasingly greater influence on the collapse pressure. This being the case, the collapse pressures to be discussed are less than the shell-buckling pressures in order for the conclusions drawn to be valid.

In examining the strength of stiffened cylinders against axisymmetric yielding, the pressure at which yielding would occur at an exterior point at mid-bay was determined for the geometry previously selected under the assumption that the cylinder is initially stress-free. This particular point was chosen since failure by axisymmetric yielding is usually associated with a critical stress condition there. The criterion of yielding was taken as the octahedral shear stress or Hencky-von Mises criterion as follows

$$\sigma_y^2 = \sigma_x^2 + \sigma_\phi^2 - \sigma_x\sigma_\phi \quad [52]$$

where σ_y denotes the compressive yield strength of the material. The pressures p_y at which yielding would be initiated were determined for different values of yield strength. Actually, the calculations were made for various ratios of yield strength to modulus of elasticity, σ_y/E. In addition, the pressures p_y were determined for a range of values of the ratio of initial accordion deflection to shell thickness, Δ/t, and for positive values of Δ/t associated with internally framed cylinders and also negative values of Δ/t for externally framed cylinders.

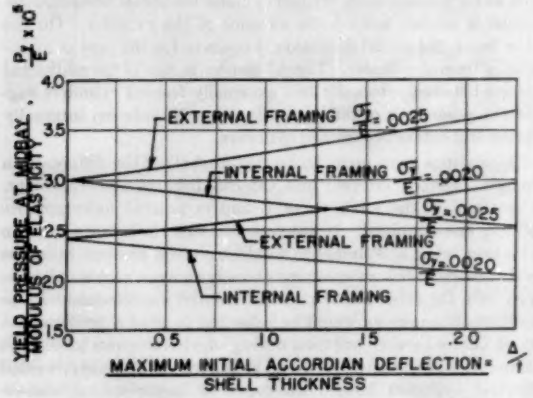

FIG. 8 INFLUENCE OF INITIAL ACCORDION DEFLECTION ON PRESSURE TO INITIATE YIELDING

Results of these calculations are shown in Fig. 8, which is a nondimensional plot of p_y/E versus Δ/t for two values of the ratio σ_y/E. In effect, the pressure for initiating yielding is plotted against initial accordion deflection for yield strengths of 60,000 and 75,000 psi in the case of steel. The pressures p_y are plotted in Fig. 8 for both internal and external framing. Fig. 8 vividly illustrates the large divergence in pressures to initiate yielding between the two types of framing as the initial accordion deflection increases. At $\Delta/t = 0.1$ and $\sigma_y/E = 0.0025$, the difference in p_y for the two types of framing is 18 per cent; for a value of $\Delta/t = 0.2$, it is 40 per cent.

The question arose as to whether the influence of initial accordion deflection was significant for cylinders of low yield strength. Accordingly, the ratio of $p_{y\Delta}$, the pressure to initiate yielding for a cylinder with a ratio $\Delta/t = 0.1$ to the value p_{y_0}, the pressure at yielding for a cylinder with no initial accordion deflection, was computed for various values of σ_y/E. Again this was done for both internally framed and externally framed cylinders. The results are shown in Fig. 9, which indicates that the influence of initial accordion deflection on the onset of yielding can be almost as severe for low yield strength as for the higher

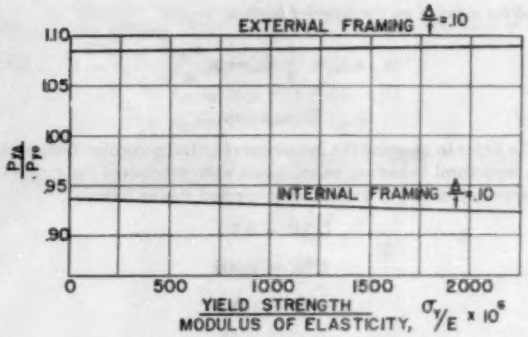

FIG. 9 COMPARISON OF PRESSURES TO INITIATE YIELDING BETWEEN CYLINDERS WITH AND WITHOUT INITIAL ACCORDION DEFLECTION

yield strengths. Fig. 9 does indicate, however, that as the yield strength increases the influence of initial accordion deflections becomes gradually more severe.

SUMMARY AND CONCLUSIONS

A theoretical analysis of a cylinder with initial accordion deflection indicates that the theory of von Sanden and Gunther may be inadequate for certain geometries and for sizable initial accordion deflections. The influence of initial accordion deflection is greater on the longitudinal strains than on the circumferential strains. Sizable initial deflections result in additional strains that cannot be neglected. If failure is associated with yielding of the shell at mid-bay, an internally framed cylinder may be appreciably weaker than an externally framed cylinder when the cylinders are fabricated by welding. Lastly, it was found that the influence of initial accordion deflection on failure by axisymmetric yielding cannot be neglected for low-yield-strength materials.

ACKNOWLEDGMENTS

The authors wish to express their appreciation for the critical review of this paper given by Dr. E. H. Kennard, Chief Scientist, Structural Mechanics Laboratory, David Taylor Model Basin. In addition, the authors are indebted to Mr. M. A. Krenzke, who assisted in making measurements of initial accordion deflection.

BIBLIOGRAPHY

1 "The Strength of Cylindrical Shells Stiffened by Frames and Bulkheads, Under Uniform External Pressure on All Sides," by K. von Sanden and K. Gunther, Taylor Model Basin Translation 38, March, 1952.

2 "Stress Distribution in a Circular Cylindrical Shell Under Hydrostatic Pressure Supported by Equally Spaced Circular Ring Frames," by V. L. Salerno and J. G. Pulos, Polytechnic Institute of Brooklyn Aeronautical Laboratory Report No. 171-A, June, 1951.

3 "The Effect of Imperfections on the Stresses in a Circular Cylindrical Shell Under Hydrostatic Pressure," by S. R. Bodner and W. Berks, Polytechnic Institute of Brooklyn Aeronautical Laboratory Report No. 210, December, 1952.

4 "The Effects of Boundary Conditions and Initial Out-Of-Roundness on the Strength of Thin-Walled Cylinders Subject to External Hydrostatic Pressure," by G. D. Galletly and R. Bart, JOURNAL OF APPLIED MECHANICS, Trans. ASME, vol. 78, 1956, pp. 351–358.

5 "Effect of Imperfections on Buckling of Thin Cylinders Under External Pressure," by L. H. Donnell, JOURNAL OF APPLIED MECHANICS, Trans. ASME, vol. 78, 1956, pp. 569–575.

6 "Effect of Small Initial Irregularities on the Stresses in Cylindrical Shells," by T. S. Wu, L. E. Goodman, and N. M. Newmark, University of Illinois Structural Research Series No. 50, April, 1953.

7 "Theory of Elasticity Stability," by S. Timoshenko, McGraw-Hill Book Company, Inc., New York and London, first edition, 1936, pp. 424–425.

Stress Concentrations in a Strip Under Tension and Containing Two Pairs of Semicircular Notches Placed on the Edges Symmetrically

By A. ATSUMI, SENDAI,[1] JAPAN

Distributions of stresses in an infinite strip of finite breadth under tension and containing two pairs of equal semicircular notches placed symmetrically on the edges are studied theoretically. The state of decreasing of stress concentration is studied and compared with those corrected by M. Isida or newly determined by the author in their calculations as the reliable results of Ling's problem of an infinite strip of finite breadth under tension and containing two semicircular notches placed symmetrically on the edges.

Introduction

THE distributions of stresses in a semi-infinite plate under tension applied parallel to its straight boundary and containing a semicircular notch were given theoretically by F. G. Maunsell (1)[2] in 1936. In 1947, the problem of an infinite strip of finite breadth under tension and containing two semicircular notches placed symmetrically on the opposite edges was solved by Chih-Bing Ling (2), but the results given by him have been shown to be unreliable. Reliable values of stress concentration for this problem have been determined theoretically by M. Isida (3) and the author (4) and experimentally by R. E. Peterson (5) and M. M. Frocht (6). In 1952 and 1953 solutions were given by Chih-Bing Ling (7) and M. Isida (8) for the strip with a pair of semi-circular notches under pure bending and by O. Tamate (9) for an infinite strip under uniform tension and pure bending containing a semicircular notch.

Although it appears important for us to know how the values of stress concentration in a strip decrease as the notches increase in number, there appears to have been no theoretical investigation which gives much information about the problem; some experimental investigations (10) have been made, however. In this paper the distributions of stresses for the problem mentioned are determined theoretically; the reduction of the stress concentration is studied and the results obtained are compared with those corrected by M. Isida or newly determined by the author as the reliable results of Ling's problem.

Method of Analysis

We consider the strip to be unnotched and calculate the radial and tangential stresses along the circumference of each notch resulting from the applied tensile force. We then apply to the edge of each notch stresses equal to the negative of the stresses resulting from the tension. Thus we wish to find a complete set of stress functions, such that the stresses at infinity and along the straight edges vanish while the radial and tangential stresses at the edge of each notch may be set equal to the negative of the radial and tangential stresses resulting from the tension. A method for constructing these stress functions was first suggested by R. C. Knight (11), and used since by many investigators of the problems of strips with notches or holes. Following this method we first obtain the individual stress functions for an unnotched strip with concentrated longitudinal and transverse forces applied at points corresponding to the center of each notch. For the present problem this would correspond to eight stress functions—four for longitudinal forces at each notch and four for transverse forces at each notch. We next arrange these stress functions so that they are symmetrical about one axis and symmetrical and antisymmetrical about the other axis. For the present problem these correspond to the loading conditions shown in Fig. 1.

We take as our final stress functions the functions obtained by differentiating χ_1 and χ_3 an odd number of times and χ_2 and χ_4 an even number of times; thus

$$\chi = \sum_{s=0}^{\infty} \left[a_s \frac{\partial^{2s+1}\chi_1}{\partial x^{2s+1}} + b_s \frac{\partial^{2s+2}\chi_2}{\partial x^{2s+2}} + c_s \frac{\partial^{2s+1}\chi_3}{\partial x^{2s+1}} + d_s \frac{\partial^{2s+2}\chi_4}{\partial x^{2s+2}} \right] \quad \ldots\ldots [1]$$

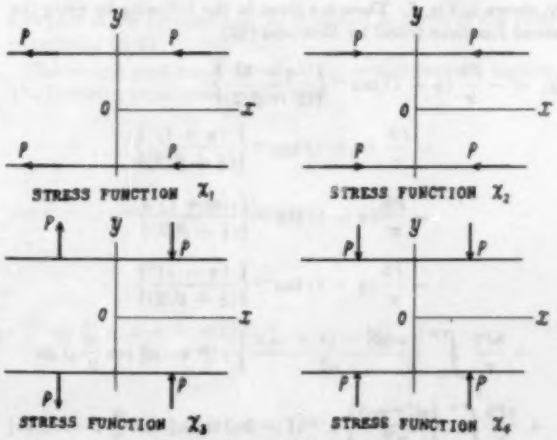

FIG. 1 LOADING CONDITIONS

[1] Assistant Professor of Mechanical Engineering, Tohoku University.

[2] Numbers in parentheses refer to the Bibliography at the end of the paper.

Presented at the Applied Mechanics Division Summer Conference, Berkeley, Calif., June 13–15, 1957, of THE AMERICAN SOCIETY OF MECHANICAL ENGINEERS.

Discussion of this paper should be addressed to the Secretary, ASME, 29 West 39th Street, New York, N. Y., and will be accepted until January 10, 1958 for publication at a later date. Discussion received after the closing date will be returned.

NOTE: Statements and opinions advanced in papers are to be understood as individual expressions of their authors and not those of the Society. Manuscript received by ASME Applied Mechanics Division, January 14, 1957. Paper No. 57—APM-41.

Since this stress function is symmetrical about the x and y-axis, it is sufficient that the stress conditions on the edge of any of the notches be satisfied. If a new system of co-ordinates r, θ is taken at the center of one of the semicircular notches and the stress function referred to that system and expanded in a Fourier series with respect to the angle θ, we must have

$$\sigma_r = \frac{1}{r}\frac{\partial\chi}{\partial r} + \frac{1}{r^2}\frac{\partial^2\chi}{\partial\theta^2} = -\frac{1}{2}T(1-\cos 2\theta) \quad \ldots[2a]$$

$$\tau_{r\theta} = -\frac{\partial^2\left(\frac{1}{r}\chi\right)}{\partial r\partial\theta} = -\frac{1}{2}T\sin 2\theta \quad \ldots\ldots[2b]$$

at $r = a$ for $\pi/2 < \theta < 3\pi/2$, where T is the uinform tensile stress at infinity. Equating coefficients of $\cos n\theta$ and $\sin n\theta$ on the left side of Equations [2a] and [2b] to the corresponding coefficients on the right side then gives us an infinite set of equations for the undetermined coefficients a_n, b_n, c_n, and d_n, which yields the solution of the problem. Stresses in the notched strip are then given by

$$\sigma_r = \frac{1}{2}T(1-\cos 2\theta) + \frac{1}{r}\frac{\partial\chi}{\partial r} + \frac{1}{r^2}\frac{\partial^2\chi}{\partial\theta^2} \quad \ldots\ldots[3a]$$

$$\sigma_\theta = \frac{1}{2}T(1+\cos 2\theta) + \frac{\partial^2\chi}{\partial r^2} \quad \ldots\ldots[3b]$$

$$\tau_{r\theta} = \frac{1}{2}T\sin 2\theta - \frac{\partial^2\left(\frac{1}{r}\chi\right)}{\partial r\partial\theta} \quad \ldots\ldots[3c]$$

Fundamental Stress Functions

Let the strip of isotropic and elastic material be bounded in the x, y-plane by the lines $y = \pm b$, and grooved by two pairs of semi-circular notches of equal radius $a(<b)$, with the centers at the points $O_1(h/2, b)$, $O_2(-h/2, -b)$, $O_3(-h/2, b)$, $O_4(h/2, -b)$.

The present problem is to determine the distributions of stresses in the notched strip, shown in Fig. 2, under a uniform tension T applied parallel to the straight edges in its plane. Here, under the usual conditions of generalized plane stress, we will find a solution of the biharmonic equation $\nabla^4\chi = 0$ satisfying the boundary conditions of two straight edges and four rims of semi-circular notches of the strip being free from stresses and the stresses at infinity being equal to the uniform tension T.

We start with the fundamental stress functions χ_1, χ_2, χ_3, and χ_4 shown in Fig. 1. These are given in the following by using the stress functions found by Howland (12)

$$\chi_1 = -\frac{Pb}{\pi}(\eta-1)\tan^{-1}\left\{\frac{(\eta-1)}{(\xi-\beta/2)}\right\} - \frac{Pb}{\pi}(\eta+1)\tan^{-1}\left\{\frac{(\eta+1)}{(\xi+\beta/2)}\right\} - \frac{Pb}{\pi}(\eta+1)\tan^{-1}\left\{\frac{(\eta+1)}{(\xi-\beta/2)}\right\} - \frac{Pb}{\pi}(\eta-1)\tan^{-1}\left\{\frac{(\eta-1)}{(\xi+\beta/2)}\right\} + \frac{8Pb}{\pi}\int_0^\infty\left\{\frac{u\eta sS-(s+uc)C}{u\Sigma}\right\}e^{-2u}\sin u\xi\cos\frac{u}{2}\beta\,du + \frac{4Pb}{\pi}\int_0^\infty\left\{\frac{sC-\eta cS}{u\Sigma}\right\}e^{-2u}(1-2u)\sin u\xi\cos\frac{u}{2}\beta\,du \quad \ldots[4a]$$

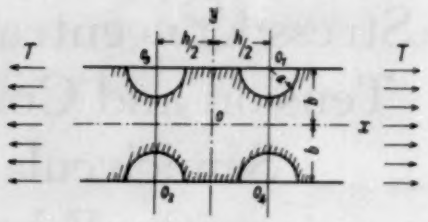

Fig. 2 Present Problem

$$\chi_2 = -\frac{Pb}{\pi}(\eta-1)\tan^{-1}\left\{\frac{(\eta-1)}{(\xi-\beta/2)}\right\} + \frac{Pb}{\pi}(\eta+1)\tan^{-1}\left\{\frac{(\eta+1)}{(\xi+\beta/2)}\right\} - \frac{Pb}{\pi}(\eta+1)\tan^{-1}\left\{\frac{(\eta+1)}{(\xi-\beta/2)}\right\} + \frac{Pb}{\pi}(\eta-1)\tan^{-1}\left\{\frac{(\eta-1)}{(\xi+\beta/2)}\right\} - \frac{8Pb}{\pi}\int_0^\infty\left\{\frac{u\eta sS-(s+uc)C}{u\Sigma}\right\}e^{-2u}\cos u\xi\sin\frac{u}{2}\beta\,du - \frac{4Pb}{\pi}\int_0^\infty\left\{\frac{sC-\eta cS}{u\Sigma}\right\}e^{-2u}(1-2u)\cos u\xi\sin\frac{u}{2}\beta\,du \quad \ldots[4b]$$

$$\chi_3 = -\frac{Pb}{\pi}(\xi-\beta/2)\tan^{-1}\left\{\frac{(\eta-1)}{(\xi-\beta/2)}\right\} - \frac{Pb}{\pi}(\xi+\beta/2)\tan^{-1}\left\{\frac{(\eta+1)}{(\xi+\beta/2)}\right\} + \frac{Pb}{\pi}(\xi-\beta/2)\tan^{-1}\left\{\frac{(\eta+1)}{(\xi-\beta/2)}\right\} + \frac{Pb}{\pi}(\xi+\beta/2)\tan^{-1}\left\{\frac{(\eta-1)}{(\xi+\beta/2)}\right\} + \frac{4Pb}{\pi}\int_0^\infty\left\{\frac{u\eta sS-(s+uc)C}{u^2\Sigma}\right\}e^{-2u}(1+2u)\sin u\xi\sin\frac{u}{2}\beta\,du + \frac{8Pb}{\pi}\int_0^\infty\left\{\frac{\eta cS-sC}{\Sigma}\right\}e^{-2u}\sin u\xi\sin\frac{u}{2}\beta\,du \quad \ldots[4c]$$

$$\chi_4 = -\frac{Pb}{\pi}(\xi-\beta/2)\tan^{-1}\left\{\frac{(\eta-1)}{(\xi-\beta/2)}\right\} + \frac{Pb}{\pi}(\xi+\beta/2)\tan^{-1}\left\{\frac{(\eta+1)}{(\xi+\beta/2)}\right\} + \frac{Pb}{\pi}(\xi-\beta/2)\tan^{-1}\left\{\frac{(\eta+1)}{(\xi-\beta/2)}\right\} - \frac{Pb}{\pi}(\xi+\beta/2)\tan^{-1}\left\{\frac{(\eta-1)}{(\xi+\beta/2)}\right\} + \frac{4Pb}{\pi}\int_0^\infty\left\{\frac{u\eta sS-(s+uc)C}{u^2\Sigma}\right\}e^{-2u}(1+2u)\cos u\xi\cos\frac{u}{2}\beta\,du + \frac{8Pb}{\pi}\int_0^\infty\left\{\frac{\eta cS-sC}{\Sigma}\right\}e^{-2u}\cos u\xi\cos\frac{u}{2}\beta\,du \quad \ldots[4d]$$

where the symbols denote

$$\left.\begin{aligned} &\xi = x/b, \quad \eta = y/b, \quad \beta = h/b, \quad s = \sinh u, \quad c = \cosh u \\ &S = \sinh u\eta, \quad C = \cosh u\eta, \quad \Sigma = \sinh 2u + 2u \end{aligned}\right\} \ldots\ldots\ldots\ldots [5]$$

As the stress system in the present problem should be symmetrical about the y-axis, we have to find the even functions in χ, which may be obtained by differentiating χ_1 and χ_3 an odd number of times and χ_2 and χ_4 an even number of times with respect to ξ. The functions representing an unbalanced force at the center of each notch also must be excluded and the functions having no residual stresses at infinity must be obtained. These are defined as follows

$$U_{2s} = \frac{\pi 2(-)^{s+1}\partial^{2s+1}\chi_3}{Pb(2s)!\partial\xi^{2s+1}} (s \geq 0) \ldots\ldots\ldots\ldots [6]$$

$$U_{2s+1} = \frac{\pi 2(-)^s\partial^{2s+2}\chi_2}{Pb(2s+1)!\partial\xi^{2s+2}} (s \geq 0) \ldots\ldots\ldots [7]$$

$$V_0 = -\frac{\pi 2\partial\chi_3}{Pb\partial\xi} \ldots\ldots\ldots\ldots [8a]$$

$$V_{2s} = \frac{\pi 2(-)^{s+1}\partial^{2s+1}\chi_3}{Pb(2s-1)!\partial\xi^{2s+1}} (s \geq 1) \ldots\ldots\ldots [8b]$$

$$V_{2s+1} = \frac{\pi 2(-)^{s+1}\partial^{2s+2}\chi_4}{Pb(2s)!\partial\xi^{2s+2}} (s \geq 0) \ldots\ldots\ldots [9]$$

To express these functions in terms of the polar co-ordinate, referring to one of the centers of the notches, say, to the point O_1 $(h/2, b)$, we define (r, θ) by

$$\xi - \beta/2 + i\eta - i = i\rho e^{-i\theta} \ldots\ldots\ldots\ldots [10]$$

so that

$$\left.\begin{aligned} \xi - \beta/2 &= \rho \sin\theta \\ \eta - 1 &= \rho \cos\theta \end{aligned}\right\} \ldots\ldots\ldots\ldots [11]$$

where ρ is dimensionless variable, $\rho = r/b$.

It appears that each function can be expressed by separating it into two parts. We will illustrate it by the function U_{2s}. It is separated in the manner

$$\frac{2(-)^{s+1}}{(2s)!}\partial^{2s+1}\left\{-(\eta-1)\tan^{-1}\frac{\eta-1}{\xi-\beta/2} - (\eta+1)\tan^{-1}\frac{\eta+1}{\xi+\beta/2} - (\eta+1)\tan^{-1}\frac{\eta+1}{\xi-\beta/2} - (\eta-1)\tan^{-1}\frac{\eta-1}{\xi+\beta/2}\right\}\Big/\partial\xi^{2s+1} \ldots\ldots [12a]$$

$$+ \frac{8}{(2s)!}\int_0^\infty \frac{\{2uc^n(\eta S - C) - \eta cS - sC\}u^{2s}e^{-2u}}{\Sigma}\cos u\xi \cos\frac{u}{2}\beta \, du \ldots\ldots [12b]$$

If new systems of co-ordinates (r', θ'), (r'', θ''), and (r''', θ''') are taken symmetrically at the points O_2, O_3, and O_4 as shown in Fig. 3, Expression [12a] can be given in the form

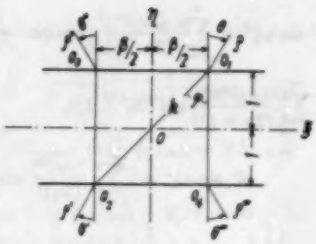

FIG. 3 RELATIONS OF CO-ORDINATES

$$\frac{2(-)^{s+1}}{(2s)!}\partial^{2s+1}\{\rho\theta\cos\theta + (\rho\cos\theta + 2)\theta' - \rho\theta''\cos\theta - (\rho\cos\theta + 2)\theta'''\}/\partial\xi^{2s+1} \ldots\ldots [13]$$

Expressions of θ', θ'', θ''' in terms of ρ and θ are first required and may be obtained as follows:

Let $$\zeta = (\xi - \beta/2) + i(\eta - 1) = i\rho e^{-i\theta} \qquad \zeta' = \beta + 2i = i\gamma e^{-i\phi} \ldots\ldots\ldots [14]$$

so that

$$\gamma = k/b = (4 + \beta^2)^{1/2}, \qquad \phi = \tan^{-1}\beta/2 \ldots\ldots [15]$$

Then since

$$\left.\begin{aligned} \log(\zeta + \zeta') &= \log\rho' + i(\pi/2 - \phi), \qquad (\rho' = r'/b) \\ &= \log\zeta' + \sum_{n=1}^{\infty}\frac{(-)^{n-1}}{n}(\zeta/\zeta')^n \end{aligned}\right\} \ldots [16]$$

We have

$$\theta' = \sum_{n=1}^{\infty}(-)^{n-1}\rho^n \sin n(\theta - \phi)/n\gamma^n \ldots\ldots [17a]$$

Similarly

$$\theta'' = \sum_{n=0}^{\infty}\frac{(-)^n}{(2n+1)\beta^{2n+1}}\rho^{2n+1}\cos(2n+1)\theta + \sum_{n=1}^{\infty}\frac{(-)^n}{2n\beta^{2n}}\rho^{2n}\sin 2n\theta \ldots\ldots [17b]$$

$$\theta''' = \sum_{n=1}^{\infty}(-)^n\rho^n \sin n\theta/n2^n \ldots\ldots [17c]$$

In Equations [13] and [17] trivial terms are omitted as they contribute nothing to the stresses. Using these equations the first part of the function may be expressed in terms of the polar co-ordinate (r, θ).

The second part can be obtained by straightforward algebra. The following expansions will be used

$$
\left.
\begin{aligned}
C' \cos u\xi' &= \sum_{n=0}^{\infty} \frac{(u\rho)^{2n}}{(2n)!} \cos 2n\theta, \\
C' \sin u\xi' &= \sum_{n=0}^{\infty} \frac{(u\rho)^{2n+1}}{(2n+1)!} \sin (2n+1)\theta \\
S' \cos u\xi' &= \sum_{n=0}^{\infty} \frac{(u\rho)^{2n+1}}{(2n+1)!} \cos (2n+1)\theta, \\
S' \sin u\xi' &= \sum_{n=1}^{\infty} \frac{(u\rho)^{2n}}{(2n)!} \sin 2n\theta \\
\eta' C' \cos u\xi' &= \frac{1}{2}\left[2\rho \cos\theta + \frac{1}{2} u^2\rho^3 \cos\theta \right. \\
&\quad \left. + \sum_{n=1}^{\infty} \left\{ \frac{u^{2n}\rho^{2n+1}}{(2n)!} + \frac{u^{2n+2}\rho^{2n+3}}{(2n+2)!} \right\} \cos (2n+1)\theta \right] \\
\eta' C' \sin u\xi' &= \frac{1}{2} \sum_{n=1}^{\infty} \left\{ \frac{u^{2n+1}\rho^{2n+2}}{(2n+1)!} + \frac{u^{2n-1}\rho^{2n}}{(2n-1)!} \right\} \sin 2n\theta \\
\eta' S' \cos u\xi' &= \frac{1}{2}\left[u\rho^2 + \sum_{n=1}^{\infty} \left\{ \frac{u^{2n-1}\rho^{2n}}{(2n-1)!} + \frac{u^{2n+1}\rho^{2n+2}}{(2n+1)!} \right\} \cos 2n\theta \right] \\
\eta' S' \sin u\xi' &= \frac{1}{2}\left[\frac{u^2\rho^3 \sin\theta}{2} + \sum_{n=1}^{\infty} \left\{ \frac{u^{2n}\rho^{2n+1}}{(2n)!} + \frac{u^{2n+2}\rho^{2n+3}}{(2n+2)!} \right\} \sin (2n+1)\theta \right]
\end{aligned}
\right\} \quad \ldots [18a]
$$

where

$$
\left.
\begin{aligned}
C' &= \cosh u\eta', \qquad S' = \sinh u\eta' \\
\eta' &= \rho \cos\theta, \qquad \xi' = \rho \sin\theta
\end{aligned}
\right\} \quad \ldots\ldots [18b]
$$

Hence, by omitting the trivial terms which produce no effect on the stresses, we obtain the following expression of U_{2s}

$$
\begin{aligned}
U_{2s} = &-\{\cos 2s\theta + \cos (2s+2)\theta\}/\rho^{2s} \\
&+ \sum_{n=0}^{\infty} ({}^{2s}A_{2n} + {}^{2s}\bar{A}_{2n}\rho^2)\rho^{2n} \cos 2n\theta \\
&+ \sum_{n=0}^{\infty} ({}^{2s}A_{2n+1} + {}^{2s}\bar{A}_{2n+1}\rho^2)\rho^{2n+1} \cos (2n+1)\theta \\
&+ \sum_{n=1}^{\infty} ({}^{2s}B_{2n} + {}^{2s}\bar{B}_{2n}\rho^2)\rho^{2n} \sin 2n\theta \\
&+ \sum_{n=0}^{\infty} ({}^{2s}B_{2n+1} + {}^{2s}\bar{B}_{2n+1}\rho^2)\rho^{2n+1} \sin (2n+1)\theta \quad \ldots [19]
\end{aligned}
$$

where, for $s \geqslant 0$

$$
\left.
\begin{aligned}
{}^{2s}\bar{A}_{2n} = &-\left\{ 2(I_{2n+2s+2} + I'_{2n+2s+2}) - \frac{1}{2}(I_{2n+2s+1} \right. \\
&+ I'_{2n+2s+1}) + 2(J_{2n+2s+2} + J'_{2n+2s+2}) \\
&- (J_{2n+2s+1} + J'_{2n+2s+1}) - \frac{1}{2}(K_{2n+2s+1} + K'_{2n+2s+1}) \\
&+ 2(2n+2s+2)!\,(I_{2n+2s+1} + I'_{2n+2s+1} \\
&\left. + \bar{I}_{2n+2s+1}) \right\} \Big/ (2n+1)!(2s)!
\end{aligned}
\right\} \quad \ldots [20a]
$$

$$
\left.
\begin{aligned}
{}^{2s}\bar{A}_{2n+1} = &-\left\{ 2(I_{2n+2s+3} + I'_{2n+2s+3}) - \frac{1}{2}(I_{2n+2s+2} \right. \\
&+ I'_{2n+2s+2}) - 2(J_{2n+2s+3} + J'_{2n+2s+3}) + \frac{1}{2}(K_{2n+2s+2} \\
&+ K'_{2n+2s+2}) + 2(2n+2s+3)!(I_{2n+2s+2} \\
&\left. + \bar{I}_{2n+2s+2}) \right\} \Big/ (2n+2)!(2s)!
\end{aligned}
\right\} \quad \ldots [20a] \ (cont.)
$$

$$
\left.
\begin{aligned}
{}^{2s}\bar{B}_{2n} = &\left\{ 2I_{2n+2s+2} - \frac{1}{2} I_{2n+2s+1} - 2J_{2n+2s+2} \right. \\
&+ \frac{1}{2} \bar{K}_{2n+2s+1} + 2(2n+2s+2)!m_{2n+2s+1} \Big\} \Big/ (2n \\
&+ 1)!(2s)! \\
{}^{2s}\bar{B}_{2n+1} = &\left\{ 2I_{2n+2s+3} - \frac{1}{2} I_{2n+2s+2} + 2J_{2n+2s+3} - J_{2n+2s+2} \right. \\
&- \frac{1}{2} \bar{K}_{2n+2s+2} + 2(2n+2s+3)!(m_{2n+2s+2} \\
&\left. + m'_{2n+2s+2}) \right\} \Big/ (2n+2)!(2s)!
\end{aligned}
\right\}
$$

The coefficients in Equation [19] are to be related by the equation as U_{2s} satisfies the conditions of straight edge being free from stresses

$$
\left.
\begin{aligned}
{}^{2s}A_{2n} &= {}^{2s}\bar{A}_{2n-2}, \qquad {}^{2s}B_{2n} = (n-1)\,{}^{2s}\bar{B}_{2n-2}/n \\
{}^{2s}A_{2n+1} &= (2n-1)\,{}^{2s}\bar{A}_{2n-1}/(2n+1), \quad {}^{2s}B_{2n+1} = {}^{2s}\bar{B}_{2n-1}
\end{aligned}
\right\} \quad \ldots [20b]
$$

In a similar manner, detailed expressions of the other functions are obtained as follows

$$
\begin{aligned}
U_{2s+1} = &-\{\sin (2s+1)\theta + \sin (2s+3)\theta\}/\rho^{2s+1} \\
&+ \sum_{n=0}^{\infty} ({}^{2s+1}C_{2n} + {}^{2s+1}\bar{C}_{2n}\rho^2)\rho^{2n} \cos 2n\theta \\
&+ \sum_{n=0}^{\infty} ({}^{2s+1}C_{2n+1} + {}^{2s+1}\bar{C}_{2n+1}\rho^2)\rho^{2n+1} \cos (2n+1)\theta \\
&+ \sum_{n=0}^{\infty} ({}^{2s+1}D_{2n} + {}^{2s+1}\bar{D}_{2n}\rho^2)\rho^{2n} \sin 2n\theta \\
&+ \sum_{n=0}^{\infty} ({}^{2s+1}D_{2n+1} + {}^{2s+1}\bar{D}_{2n+1}\rho^2)\rho^{2n+1} \sin (2n+1)\theta \quad \ldots [21]
\end{aligned}
$$

where, for $s \geqslant 0$

$$
\left.
\begin{aligned}
{}^{2s+1}\bar{C}_{2n} = &\left\{ 2I_{2n+2s+3} - \frac{1}{2} I_{2n+2s+2} + 2J_{2n+2s+3} - J_{2n+2s+2} \right. \\
&- \frac{1}{2} \bar{K}_{2n+2s+2} + 2(2n+2s+3)!\,(m_{2n+2s+2} \\
&\left. + m'_{2n+2s+2}) \right\} \Big/ (2n+1)!(2s+1)!
\end{aligned}
\right\} \quad \ldots [22a]
$$

$$
\left.\begin{aligned}
{}^{2s+1}\bar{C}_{2n+1} &= \Big\{2I_{2n+2s+4} - \frac{1}{2}I_{2n+2s+2} - 2J_{2n+2s+4} \\
&\quad + \frac{1}{2}K_{2n+2s+2} + 2(2n+2s+4)!\, m_{2n+2s+2}\Big\}\Big/(2n+2)!(2s+1)! \\
{}^{2s+1}\bar{D}_{2n} &= -\Big\{2(I_{2n+2s+2} - I'_{2n+2s+2}) - \frac{1}{2}(I_{2n+2s} \\
&\quad - I'_{2n+2s+2}) - 2(J_{2n+2s+2} - J'_{2n+2s+2}) + \frac{1}{2}(K_{2n+2s} \\
&\quad - K'_{2n+2s+2}) - 2(2n+2s+3)! \\
&\quad (l_{2n+2s+2} - \bar{l}_{2n+2s+2})\Big\}\Big/(2n+1)!(2s+1)! \\
{}^{2s+1}\bar{D}_{2n+1} &= -\Big\{2(I_{2n+2s+4} - I'_{2n+2s+4}) - \frac{1}{2}(I_{2n+2s+2} \\
&\quad - I'_{2n+2s+2}) + 2(J_{2n+2s+4} - J'_{2n+2s+4}) - (J_{2n+2s+2} \\
&\quad - J'_{2n+2s+2}) - \frac{1}{2}(K_{2n+2s+2} - K'_{2n+2s+2}) \\
&\quad - 2(2n+2s+4)!\,(l_{2n+2s+2} + l'_{2n+2s+2} - \\
&\quad \bar{l}_{2n+2s+2})\Big\}\Big/(2n+2)!(2s+1)!
\end{aligned}\right\} \text{. [22a] (cont.)}
$$

and

$$
\left.\begin{aligned}
{}^{2s+1}C_{2n} &= {}^{2s+1}\bar{C}_{2n-2}, \qquad {}^{2s+1}D_{2n} = (n-1)^{2s+1}\bar{D}_{2n-2}/n \\
{}^{2s+1}C_{2n+1} &= (2n-1)^{2s+1}\bar{C}_{2n-1}/(2n+1), \\
&\qquad {}^{2s+1}D_{2n+1} = {}^{2s+1}\bar{D}_{2n-1}
\end{aligned}\right\} \text{. [22b]}
$$

$$
\begin{aligned}
V_0 = -(2\theta + \sin 2\theta) &+ \sum_{n=0}^{\infty} ({}^0E_{2n} + {}^0\bar{E}_{2n}\rho^2)\rho^{2n}\cos 2n\theta \\
&+ \sum_{n=0}^{\infty} ({}^0E_{2n+1} + {}^0\bar{E}_{2n+1}\rho^2)\rho^{2n+1}\cos(2n+1)\theta \\
&+ \sum_{n=1}^{\infty} ({}^0F_{2n} + {}^0\bar{F}_{2n}\rho^2)\rho^{2n}\sin 2n\theta + \sum_{n=0}^{\infty} ({}^0F_{2n+1} \\
&\qquad + {}^0\bar{F}_{2n+1}\rho^2)\rho^{2n+1}\sin(2n+1)\theta \text{. . . [23a]}
\end{aligned}
$$

$$
\begin{aligned}
V_{2s} = -\{(2s+2)\sin 2s\theta + 2s\sin(2s+2)\theta\}/\rho^{2s} &\\
+ \sum_{n=0}^{\infty} ({}^{2s}E_{2n} + {}^{2s}\bar{E}_{2n}\rho^2)\rho^{2n}\cos 2n\theta &\\
+ \sum_{n=0}^{\infty} ({}^{2s}E_{2n+1} + {}^{2s}\bar{E}_{2n+1}\rho^2)\rho^{2n+1}\cos(2n+1)\theta &\\
+ \sum_{n=1}^{\infty} ({}^{2s}F_{2n} + {}^{2s}\bar{F}_{2n}\rho^2)\rho^{2n}\sin 2n\theta &\\
+ \sum_{n=0}^{\infty} ({}^{2s}F_{2n+1} + {}^{2s}\bar{F}_{2n+1}\rho^2)\rho^{2n+1}\sin(2n+1)\theta \text{. . [23b]} &
\end{aligned}
$$

where, for $s \geqslant 0$

$$
\left.\begin{aligned}
{}^{2s}E_{2n} &= -\Big\{2I_{2n+2s+2} + \frac{1}{2}I_{2n+2s+1} + 2J_{2n+2s+2} \\
&\quad - \frac{1}{2}K_{2n+2s+1} - 2(2n+2s+2)! \\
&\quad m_{2n+2s+1}\Big\}\Big/(2n+1)!(2s-1)! \\
{}^{2s}E_{2n+1} &= -\Big\{2I_{2n+2s+2} + \frac{1}{2}I_{2n+2s} - 2J_{2n+2s+2} \\
&\quad - J_{2n+2s+2} + \frac{1}{2}\bar{K}_{2n+2s+2} - 2(2n+2s+3)! \\
&\quad (m_{2n+2s+2} - m'_{2n+2s+2})\Big\}\Big/(2n+2)!(2s-1)! \\
{}^{2s}\bar{F}_{2n} &= \Big\{2(I_{2n+2s+2} - I'_{2n+2s+2}) + \frac{1}{2}(I_{2n+2s+1} - I'_{2n+2s+1}) \\
&\quad - 2(J_{2n+2s+2} - J'_{2n+2s+2}) - (J_{2n+2s+1} - J'_{2n+2s+1}) \\
&\quad + \frac{1}{2}(K_{2n+2s+1} - K'_{2n+2s+1}) \\
&\quad + 2(2n+2s+2)!\,(l_{2n+2s+1} - l'_{2n+2s+1} \\
&\quad - \bar{l}_{2n+2s+1})\Big\}\Big/(2n+1)!(2s-1)! \\
{}^{2s}\bar{F}_{2n+1} &= \Big\{2(I_{2n+2s+2} - I'_{2n+2s+2}) + \frac{1}{2}(I_{2n+2s} - I'_{2n+2s}) \\
&\quad + 2(J_{2n+2s+2} - J'_{2n+2s+2}) - \frac{1}{2}(K_{2n+2s+2} - K'_{2n+2s+2}) \\
&\quad + 2(2n+2s+3)!\,(l_{2n+2s+2} \\
&\quad - \bar{l}_{2n+2s+2})\Big\}\Big/(2n+2)!(2s-1)!
\end{aligned}\right\} \text{. [24a]}
$$

and

$$
\left.\begin{aligned}
{}^{2s}E_{2n} &= {}^{2s}\bar{E}_{2n-2}, \qquad {}^{2s}F_{2n} = (n-1)^{2s}\bar{F}_{2n-2}/n \\
{}^{2s}E_{2n+1} &= (2n-1)^{2s}\bar{E}_{2n-1}/(2s+1), \quad {}^{2s}F_{2n+1} = {}^{2s}\bar{F}_{2n-1}
\end{aligned}\right\} \text{. . [24b]}
$$

${}^0\bar{E}_{2n}$, ${}^0\bar{E}_{2n+1}$, ${}^0\bar{F}_{2n}$, and ${}^0\bar{F}_{2n+1}$ in Equation [23a] are defined by Equations [24a] in which s is taken as zero and $(2s-1)!$ is omitted.

$$
\begin{aligned}
V_{2s+1} = -\{(2s+3)\cos(2s+1)\theta + (2s+1)\cos(2s+3)\theta\}/\rho^{2s+1} &\\
+ \sum_{n=0}^{\infty} ({}^{2s+1}G_{2n} + {}^{2s+1}\bar{G}_{2n}\rho^2)\rho^{2n}\cos 2n\theta &\\
+ \sum_{n=0}^{\infty} ({}^{2s+1}G_{2n+1} + {}^{2s+1}\bar{G}_{2n+1}\rho^2)\rho^{2n+1}\cos(2n+1)\theta &\\
+ \sum_{n=1}^{\infty} ({}^{2s+1}H_{2n} + {}^{2s+1}\bar{H}_{2n}\rho^2)\rho^{2n}\sin 2n\theta &\\
+ \sum_{n=0}^{\infty} ({}^{2s+1}H_{2n+1} + {}^{2s+1}\bar{H}_{2n+1}\rho^2)\rho^{2n+1}\sin(2n+1)\theta \text{. . [25]} &
\end{aligned}
$$

where, for $s \geqslant 0$

$$
\left.
\begin{aligned}
{}^{2s+1}\bar{G}_{2n} &= \Big\{2(I_{2n+2s+2} + I'_{2n+2s+2}) + \frac{1}{2}(J_{2n+2s+2} \\
&\quad + I'_{2n+2s+2}) + 2(J_{2n+2s+2} + J'_{2n+2s+2}) - \frac{1}{2}(K_{2n+2s+2} \\
&\quad + K'_{2n+2s+2}) - 2(2n+2s+3)!(l_{2n+2s+2} \\
&\quad + \bar{l}_{2n+2s+2})\Big\}\Big/(2n+1)!(2s)! \\
{}^{2s+1}\bar{G}_{2n+1} &= \Big\{2(I_{2n+2s+4} + I'_{2n+2s+4}) + \frac{1}{2}(I_{2n+2s+2} \\
&\quad + I'_{2n+2s+2}) - 2(J_{2n+2s+4} + J'_{2n+2s+4}) - (J_{2n+2s+2} \\
&\quad + J'_{2n+2s+2}) + \frac{1}{2}(K_{2n+2s+4} + K'_{2n+2s+2}) - 2(2n+2s \\
&\quad + 4)!(l_{2n+2s+2} - l'_{2n+2s+2} + \bar{l}_{2n+2s+2})\Big\}\Big/(2n+2)!(2s)! \\
{}^{2s+1}\bar{H}_{2n} &= -\Big\{2I_{2n+2s+2} + \frac{1}{2}I_{2n+2s+2} - 2J_{2n+2s+2} \\
&\quad - J_{2n+2s+2} + \frac{1}{2}\bar{K}_{2n+2s+2} - 2(2n+2s+3)!(m_{2n+2s+2} \\
&\quad - m'_{2n+2s+2})\Big\}\Big/(2n+1)!(2s)! \\
{}^{2s+1}\bar{H}_{2n+1} &= -\Big\{2I_{2n+2s+4} + \frac{1}{2}I_{2n+2s+2} + \\
&\quad 2J_{2n+2s+4} - \frac{1}{2}\bar{K}_{2n+2s+2} \\
&\quad - 2(2n+2s+4)!\,m_{2n+2s+2}\Big\}\Big/(2n+2)!(2s)!
\end{aligned}
\right\} \quad \ldots [26a]
$$

and

$$
\left.
\begin{aligned}
{}^{2s+1}G_{2n} &= {}^{2s+1}\bar{G}_{2n-2}, \quad {}^{2s+1}H_{2n} = (n-1)^{2s+1}\bar{H}_{2n-2}/n \\
{}^{2s+1}G_{2n+1} &= (2n-1)\,{}^{2s+1}\bar{G}_{2n-1}/(2n+1), \quad {}^{2s+1}H_{2n+1} \\
&\qquad = {}^{2s+1}\bar{H}_{2n-1}
\end{aligned}
\right\} \quad \ldots [26b]
$$

The new symbols denote

$$
\left.
\begin{aligned}
I_n &= \int_0^\infty \frac{u^n}{\Sigma}\,du, \quad J_n = \int_0^\infty \frac{u^n e^{-2u}}{\Sigma}\,du, \\
&\qquad K_n = \int_0^\infty \frac{u^n e^{-4u}}{\Sigma}\,du \\
I_n' &= \int_0^\infty \frac{u^n \cos u\beta}{\Sigma}\,du, \quad J_n' = \int_0^\infty \frac{u^n e^{-2u}\cos u\beta}{\Sigma}\,du, \\
&\qquad K_n' = \int_0^\infty \frac{u^n e^{-4u}\cos u\beta}{\Sigma}\,du \\
\bar{I}_n &= \int_0^\infty \frac{u^n \sin u\beta}{\Sigma}\,du, \quad \bar{J}_n = \int_0^\infty \frac{u^n e^{-2u}\sin u\beta}{\Sigma}\,du, \\
&\qquad \bar{K}_n = \int_0^\infty \frac{u^n e^{-4u}\sin u\beta}{\Sigma}\,du
\end{aligned}
\right\} \quad .[27a]
$$

and

$$
\left.
\begin{aligned}
l_n &= (-)^n \cos(n+1)\phi/2(n+1)\gamma^{n+1} \\
l'_{2n+1} &= (-)^n/2(2n+2)\beta^{2n+2} \\
\bar{l}_n &= (-)^n/(n+1)2^{n+2} \\
m_n &= (-)^{n+1}\sin(n+1)\phi/2(n+1)\gamma^{n+1} \\
m'_{2n} &= (-)^{n+1}/2(2n+1)\beta^{2n+1}
\end{aligned}
\right\} \quad .[27b]
$$

Solution of the Problem

Now, the required stress function may be constructed in the form

$$\chi = \chi_0 + \sum_{s=0}^{\infty}(a_{2s}U_{2s} + b_{2s}V_{2s} + c_{2s+1}U_{2s+1} + d_{2s+1}V_{2s+1})T \ldots [28]$$

where a_{2s}, b_{2s}, c_{2s+1}, and d_{2s+1} are parametric coefficients to be determined from the boundary conditions at the rim of the notches, that is, at $\rho = \lambda(a/b)$ and $\pi/2 < \theta < 3\pi/2$, the stresses

$$\sigma_r = 0, \qquad \tau_{r\theta} = 0 \ldots\ldots [29]$$

χ_0 is the function which, in the absence of the notches, represents a uniform tension T along the strip. Its expression in the polar co-ordinates is

$$\chi_0 = \frac{1}{4}b^2 T\rho^2(1 + \cos 2\theta) \ldots\ldots [30]$$

It is readily seen that the stress function thus constructed gives a uniform longitudinal tension T at infinity of the strip and no stresses along the straight edges.

To satisfy the boundary conditions at the rim of the notches the stresses σ_r and $\tau_{r\theta}$ of Equation [28] are first obtained with the aid of Equations [19] to [26] and expanded at $\rho = \lambda$ into Fourier series between $\theta = \pi/2$ and $\theta = 3\pi/2$ as required by the rim. It develops that the resulting expansions contain terms of cosines and sines of even multiple of θ only. The terms of odd multiples of θ are expanded into the following series

$$
\left.
\begin{aligned}
\cos(2n+1)\theta &= \frac{4}{\pi}\Big\{\frac{(-)^{n+1}}{2(2n+1)} \\
&\qquad + \sum_{m=1}^{\infty}\frac{(-)^{n+m+1}(2n+1)}{\{(2n+1)^2 - 4m^2\}}\cos 2m\theta\Big\} \\
\sin(2n+1)\theta &= \frac{4}{\pi}\sum_{m=1}^{\infty}\frac{(-)^{n+m+1}2m}{\{(2n+1)^2 - 4m^2\}}\sin 2m\theta
\end{aligned}
\right\} \quad \ldots [31]
$$

For brevity, the equations thus given are not shown here. Then they are equated to zero and two sets of equations are constructed so that the coefficient of each term may vanish identically. The boundary conditions at the rim are thus satisfied. These sets of equations may be replaced as follows

$$b^2/2 + 2S_0 + \sum_{n=0}^{\infty}16(n+1)(2n+1)(2n+3)^n a_0 S_{2n+1}\lambda^{2n+1}/\pi + \sum_{n=0}^{\infty}(2n+1)^n a_0 d'_{2n+1}/2 = 0 \ldots [32a]$$

$$b^2/2 + 2S_0 + 12S_2\lambda^2 + 10S_4\lambda^4 + \sum_{n=0}^{\infty}32(n+1)(2n+1)\{(2n+7)^{n+1}\beta_1 + (2n+3)^n\beta_1\}S_{2n+1}\lambda^{2n+1}/\pi + \sum_{n=0}^{\infty}\{(2n+1)^n\alpha_1 + (2n-3)^n\alpha_3\}d'_{2n+1} = 0 \ldots [32b]$$

$$\{(4m-2)S_{2m-2}\lambda^{2m-2}+(8m+4)S_{2m}\lambda^{2m}$$
$$+(4m+6)S_{2m+2}\lambda^{2m+4}\}+\sum_{n=0}^{\infty}32(n+1)(2n+1)\{(2n+2m$$
$$+5)^{n+1}\beta_m+(2n+2m+1)^n\beta_m\}S_{2n+2}\lambda^{2n+4}/\pi$$
$$+\sum_{n=0}^{\infty}\{(2n-2m+3)^n\alpha_n+(2n-2m-1)^n\alpha_{m+1}\}d'_{2n+2}$$
$$=0,\quad (m>1)\ldots[32c]$$

$$b^2+4S_0+6S_2\lambda^2+\sum_{n=0}^{\infty}32(n+1)(2n+1)(2n$$
$$+5)^n\alpha_1S_{2n+2}\lambda^{2n+4}/\pi+(2n-1)^n\alpha_1d'_{2n+2}-2a_0/\lambda^2=0\ldots[32d]$$

$$\{4mS_{2m-2}\lambda^{2m-2}+(4m-2)S_{2m}\lambda^{2m}\}$$
$$+\sum_{n=0}^{\infty}32(n+1)(2n+1)(2n+2m+3)^n\alpha_mS_{2n+2}\lambda^{2n+4}/\pi$$
$$+\sum_{n=0}^{\infty}(2n-2m+1)^n\alpha_nd'_{2n+2}-2a_{2m-2}/\lambda^{2m}$$
$$=0,\quad (m>1)\ldots.[32e]$$

$$6T_2\lambda^2+\sum_{n=0}^{\infty}64(n+1)(2n+5)^n\alpha_1T_{2n+2}\lambda^{2n+4}/\pi$$
$$+\sum_{n=0}^{\infty}(2n-1)^n\alpha_1c'_{2n+2}=0\ldots.[33a]$$

$$12T_2\lambda^2+20T_4\lambda^4+\sum_{n=0}^{\infty}16(n+1)\{(2n+3)^2(2n$$
$$+7)^{n+1}\beta_1+(2n+1)^2(2n+3)^n\beta_1\}T_{2n+4}\lambda^{2n+4}/\pi$$
$$+\sum_{n=0}^{\infty}\{(2n+1)^n\alpha_1+4(2n-3)^n\alpha_2\}c'_{2n+2}=0\ldots[33b]$$

$$\{(2m-1)(2m-2)T_{2m-2}\lambda^{2m-2}+4m(2m+1)T_{2m}\lambda^{2m}$$
$$+(2m+2)(2m+3)T_{2m+2}\lambda^{2m+4}\}+\sum_{n=0}^{\infty}16(n+1)\{(2n$$
$$+3)^2(2n+7)^{n+1}\beta_1+(2n+1)^2(2n+3)^n\beta_1\}T_{2n+4}\lambda^{2n+4}/\pi$$
$$+\sum_{n=0}^{\infty}\{m^2(2n-2m+3)^n\alpha_n+(m+1)^2(2n$$
$$-2m-1)^n\alpha_{n+1}\}c'_{2n+2}=0,\quad (m>1)\ldots.[33c]$$

$$b_0=0\ldots\ldots\ldots\ldots\ldots\ldots\ldots[33d]$$

$$\{(4m-4)T_{2m-2}\lambda^{2m-2}+(4m+2)T_{2m}\lambda^{2m}\}$$
$$+\sum_{n=0}^{\infty}64(n+1)m(2n+2m+3)^n\alpha_mT_{2n+2}\lambda^{2n+4}/\pi$$
$$+\sum_{n=0}^{\infty}m(2n-2m+1)^n\alpha_mc'_{2n+2}$$
$$-(4m-4)b_{2m-2}/\lambda^{2m}=0,\ (m>1)\ldots[33e]$$

where the new symbols denote

$$\left.\begin{aligned}
S_r&=\sum_{s=0}^{\infty}(a_{2s}\lambda^{2s}\bar{A}_r+b_{2s}\lambda^{2s}\bar{E}_r+c_{2s+1}\lambda^{2s+1}\bar{C}_r+d_{2s+1}\lambda^{2s+1}\bar{G}_r)\\
T_r&=\sum_{s=0}^{\infty}(a_{2s}\lambda^{2s}\bar{B}_r+b_{2s}\lambda^{2s}\bar{F}_r+c_{2s+1}\lambda^{2s+1}\bar{D}_r+d_{2s+1}\lambda^{2s+1}\bar{H}_r)\\
{}^n\alpha_m&=(-)^{n+m+1}/\{(2n+1)^2-4m^2\}\{(2n+3)^2\\
&\qquad-4m^2\}\\
{}^n\beta_m&=(-)^{n+m}/\{(2n+1)^2-4(m+1)^2\}\{(2n+1)^2\\
&\qquad-4m^2\}\\
c'_{2n+1}&=32(2n+2)c_{2n+1}/\pi\lambda^{2n+3}\\
d'_{2n+1}&=16(2n+1)(2n+2)(2n+3)d_{2n+1}/\pi\lambda^{2n+3}
\end{aligned}\right\}\ldots[34]$$

A similar method of successive approximation as shown in Ling's paper (2) is taken to determine the unknown constants in the equations. Solving each set of the first fifteen equations given by [32a]–[32c], [33a]–[33c] after setting $S_r=0$, $T_r=0$, we determine the first approximate values of d_{2n+1} and c_{2n+1}. Substituting the values in the remaining equations with $S_r=T_r=0$, we determine those for a_{2m} and b_{2m}. Their second approximate values are determined similarly but taking the values of S_r, T_r as those calculated using the first approximate one instead of as zero. The same process is repeated until the required degree of convergence is given.

It may be noted that the method is valid in so far as the subsequent approximate values obtained are convergent. Though it is necessary to prove the convergency, we do not give it. But it may be seen later in the numerical examples that this method gives results to any required degree of approximation.

Numerical Examples

The numerical calculations have been carried out for the cases $\lambda=0.25$ and 0.10 with $\beta=1.0$. The values of σ_θ along the periphery of the notch and that across the minimum cross section of the strip and the values of σ_r on the straight edge have been given for two cases.

First, an evaluation of the integrals in Equation [27a] is to be discussed, while the integrals I_n, J_n have been calculated by Howland (13), and I_n', J_n' have been discussed by the author (14). The evaluations of the remaining integrals follow closely that of $I_n\sim J_n'$. Using these values of the integrals the coefficients in U_{2s}, V_{2s}, U_{2s+1}, V_{2s+1} were calculated and then the unknown constants a_{2s}, b_{2s}, c_{2s+1}, and d_{2s+1} were determined. Finally, using Equation [28], the values of the stresses required were calculated with negligibly small errors.

In Tables 1 to 5 and Figs. 4 and 5, these results are shown and are compared with that given by M. Isida and the author for Ling's problem mentioned in a previous section.

Discussion of Results

From a consideration of the results given in this paper the following conclusions seem to be justified:

1 The maximum stress is found at $\theta<180$ deg at the edge of each notch. For each case of $\beta=1.0$, $\lambda=0.1$, and $\lambda=0.25$ it is found at $\theta\doteq 180$ deg and $\theta=175$ deg and its value is $2.98T$ and $2.86T$, respectively. The latter is about 1 per cent greater than the value of the stress produced at $\theta=180$ deg on the periphery.

Although no experimental work has been done corresponding to this case, the closest comparison possible is to the values of the photoelastic test for the case of neighboring two notches given by A. J. Durelli, R. L. Lake, and E. Phillips for $1/(2\lambda)=2$ and 5 (10). It may be said that a very satisfactory agreement is shown, con-

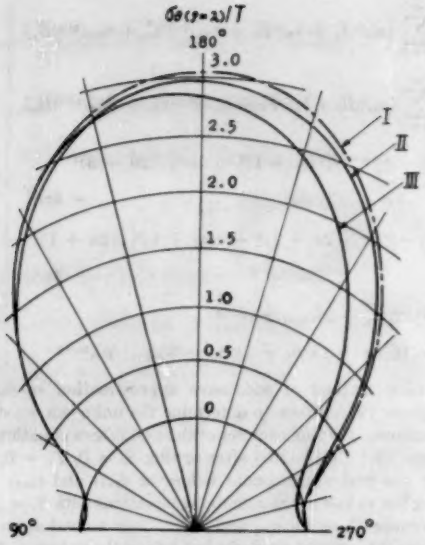

FIG. 4 VALUES OF σ_θ/T AT RIM OF EACH NOTCH FOR $\beta = 1.0$
(I, Values calculated by author for Ling's problem. II, III, Values given for cases of $\lambda = 0.1$, $\beta = 1.0$, and $\lambda = 0.25$ of present problem.)

sidering, in the case cited, the ratio between the width of plate and the radius of the notch is 18:1.

2 The values of stress-concentration factor for the case treated in this paper are smaller than the values for the case of two semicircular notches of the same geometry treated by Chih-Bing Ling. This rate of decrease becomes larger as λ increases and becomes conspicuous along the periphery near the other notch on the same straight edge. This is shown in Figs. 4 and 5 in which the results, given by M. Isida or the author for the problem treated by Ling, are adopted for comparison, since the results given by M. M. Frocht (6) seem to be slightly too small.

3 The stress on the straight edge between two notches is tension if the notches are distant. As they come close together, this tension rapidly decreases and once tends to change into compression of a very small amount.

The stress outside the notches is almost the same one given by the author for Ling's problem. This means that the effects of the other notches are not shown outside the notches.

4 The stress across the minimum section of the strip has an asymptotic value which is larger than that given by the author for Ling's problem.

ACKNOWLEDGMENT

The author wishes to express his hearty thanks to Professor Emeritus S. Higuchi of Tohoku University for his kind advice

TABLE 1A VALUES OF a_{2s}, b_{2s}, c_{2s+1}, d_{2s+1} FOR $\lambda = 0.25$, $\beta = 1.0$

s	a_{2s}/b^2	b_{2s}/b^2	c_{2s+1}/b^2	d_{2s+1}/b^2
0	4.36638×10^{-2}	0	8.20666×10^{-4}	4.62263×10^{-3}
1	8.26916×10^{-4}	6.33694×10^{-3}	1.71717×10^{-3}	2.90456×10^{-3}
2	3.8646×10^{-3}	2.5585×10^{-7}	-1.7387×10^{-7}	-7.9469×10^{-3}
3	-6.358×10^{-3}	-6.110×10^{-3}	-2.006×10^{-11}	5.125×10^{-10}
4	1.394×10^{-3}	6.555×10^{-11}	-2.762×10^{-11}	-3.970×10^{-13}
5	-3.986×10^{-11}	-2.027×10^{-12}	-8.233×10^{-14}	-3.874×10^{-14}
6	1.30×10^{-12}	2.66×10^{-14}	1.22×10^{-15}	4.98×10^{-15}
7	-4.57×10^{-14}	-1.46×10^{-15}	1.38×10^{-16}	-2.77×10^{-16}
8	1.68×10^{-15}	4.14×10^{-17}	-3.27×10^{-17}	1.37×10^{-17}
9	-5.9×10^{-17}	-1.4×10^{-18}	3.2×10^{-18}	-6.5×10^{-19}
10	2.0×10^{-18}	5.2×10^{-20}	-2.6×10^{-19}	3.0×10^{-20}

TABLE 1B VALUES OF a_{2s}, b_{2s}, c_{2s+1}, d_{2s+1} FOR $\lambda = 0.10$, $\beta = 1.0$

s	a_{2s}/b^2	b_{2s}/b^2	c_{2s+1}/b^2	d_{2s+1}/b^2
0	7.69702×10^{-2}	0	5.06098×10^{-4}	3.22080×10^{-4}
1	2.12109×10^{-4}	1.64049×10^{-7}	2.28288×10^{-8}	2.76892×10^{-7}
2	9.0208×10^{-9}	2.1781×10^{-10}	-1.2468×10^{-12}	-1.8311×10^{-10}
3	-3.239×10^{-11}	-2.893×10^{-13}	-4.110×10^{-14}	3.007×10^{-13}
4	1.457×10^{-13}	3.656×10^{-16}	3.402×10^{-17}	-6.508×10^{-16}
5	-7.420×10^{-16}	-1.838×10^{-18}	-4.605×10^{-19}	1.416×10^{-18}
6	4.09×10^{-18}	6.18×10^{-21}	2.42×10^{-21}	-1.456×10^{-21}
7	-2.38×10^{-20}	-3.05×10^{-23}	-9.04×10^{-24}	-1.67×10^{-23}
8	1.45×10^{-22}	1.53×10^{-25}		

TABLE 2 VALUES OF σ_θ/T AT RIM OF NOTCH FOR $\beta = 1.0$

λ/θ deg	90	105	120	135	150	165	180	195	210	225	240	255	270
0.10	0.00	−0.00	0.44	1.25	2.11	2.76	2.98	2.73	2.06	1.20	0.41	−0.00	0.00
0.25	0.00	−0.00	0.46	1.28	2.14	2.71	2.83	2.43	1.65	0.78	0.13	−0.08	−0.00

TABLE 3 VALUES OF σ_θ/T ACROSS MINIMUM SECTION

λ/ρ	0.10	0.15	0.20	0.25	0.30	0.40	0.50	0.60	0.70	0.80	0.90	1.00
0.10	2.98	1.53	1.22	1.11	1.06	1.03	1.02			asymptote		
0.25	...	...	...	2.83	1.99	1.42	1.25	1.20		asymptote		
0.25*	...	...	...	3.04	2.13	1.48	1.26	1.17	1.12	1.10	1.09	1.09

TABLE 4 VALUES OF σ_x/T ALONG STRAIGHT EDGE OUTSIDE NOTCHES FOR $\beta = 1.0$

λ/ρ	0.10	0.15	0.20	0.25	0.30	0.40	0.50	0.60	0.70	0.80	0.90	1.00
0.10	0.00	0.09	0.36	0.55	0.67	0.81	0.88	0.91	0.94	0.95	0.96	0.97
0.25	...	...	...	0.00	−0.04	0.16	0.38	0.55	0.67	0.76	0.83	0.86
0.25*	...	...	...	0.00	−0.04	0.15	0.37	0.54	0.66	0.75	0.83	0.86

NOTE: Values for 0.25* are as calculated by the author for Ling's problem.

and interest throughout the progress of the present investigation, and to Professor F. Numachi of Tohoku University for his interest and kind criticism in connection with this work. He also wishes to express his hearty thanks to the reviewers of The American Society of Mechanical Engineers for their valuable comments.

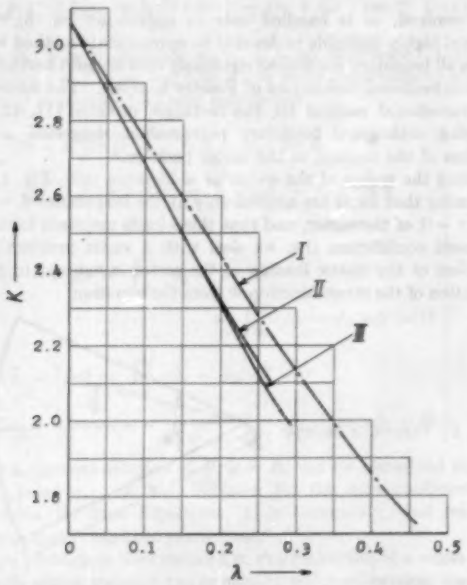

FIG. 5 STRESS CONCENTRATION FACTOR [$K = \sigma_{\theta max}(1 - \lambda)/T$] (I, Factor re-examined by M. Isida for Ling's problem. II, Factors given for present problem. III, Factor of σ_θ at crown of the notch.)

TABLE 5 VALUES OF σ_r/T ALONG THE STRAIGHT EDGE BETWEEN NOTCHES FOR $\beta = 1.0$

λ/ρ	0.10	0.15	0.20	0.25	0.30	0.40	0.50
0.10	0.00	0.08	0.34	0.52	0.63	0.73	0.76
0.25	...	...	...	0.00	−0.05	−0.04	−0.00

BIBLIOGRAPHY

1 "Stress in a Notched Plate Under Tension," by F. G. Maunsell, *Philosophical Magazine*, series 7, vol. 21, 1936, pp. 765–773.

2 "Stresses in a Notched Strip Under Tension," by Chih-Bing Ling, JOURNAL OF APPLIED MECHANICS, Trans. ASME, vol. 69, 1947, pp. A-275–280.

3 "On the Tension of the Strip With Semi-Circular Notches," by M. Isida, Transactions of the Japan Society of Mechanical Engineers, vol. 19, no. 83, 1953, pp. 5–10, in Japanese.

4 "Stress Functions for an Infinite Strip With Semi-Circular Notches," by A. Atsumi, Transactions of the Japan Society of Mechanical Engineers, vol. 20, no. 99, 1954, pp. 699–706, in Japanese.

5 Discussion by R. E. Peterson of reference (2), JOURNAL OF APPLIED MECHANICS, Trans. ASME, vol. 70, 1948, p. 176.

6 "A Photoelastic Re-Examination of Notched Tension Bars," by M. M. Frocht, R. Guernsey, Jr., and D. Landsberg, JOURNAL OF APPLIED MECHANICS, Trans. ASME, vol. 74, 1952, p. 124.

7 "On the Stresses in a Notched Strip," by Chih-Bing Ling, JOURNAL OF APPLIED MECHANICS, Trans. ASME, vol. 74, 1952, pp. 141–146.

8 "On the Bending of a Strip With Semi-Circular Notches," by M. Isida, Transactions of the Japan Society of Mechanical Engineers, vol. 19, no. 87, 1953, pp. 94–99, in Japanese.

9 "Stresses in an Infinite Strip With a Semi-Circular Notch Under Uniform Tension and Pure Bending," by O. Tamate, *The Technology Reports of the Tohoku University*, vol. 16, no. 2, 1952, pp. 34–53.

10 "Stress Concentrations Produced by Multiple Semi-Circular Notches in Infinite Plates Under Uniaxial State of Stress," by A. J. Durelli, R. L. Lake, and E. Phillips, Proceedings of the Society for Experimental Stress Analysis, vol. 10, no. 1, 1952, pp. 53–64.

11 "On the Stresses in a Perforated Strip," by R. C. Knight, *Quarterly Journal of Mathematics*, vol. 5, 1934, pp. 255–268.

12 "Stress Systems in an Infinite Strip," by R. C. J. Howland, Proceedings of the Royal Society of London, England, series A, vol. 124, 1929, pp. 89–119.

13 "On the Stresses in the Neighborhood of a Circular Hole in a Strip Under Tension," by R. C. J. Howland, Philosophical Transactions of the Royal Society of London, England, series A, vol. 229, 1930, pp. 49–86.

"Bi-Harmonic Analysis in a Perforated Strip," by R. C. J. Howland and A. C. Stevenson, Philosophical Transactions of the Royal Society of London, England, series A, vol. 232, 1933, pp. 155–222.

14 "On the Stresses in a Strip Under Tension and Containing Two Equal Circular Holes Placed Longitudinally," by A. Atsumi, JOURNAL OF APPLIED MECHANICS, Trans. ASME, vol. 78, 1956, pp. 555–562.

The Sector Problem

By G. HORVAY[1] and K. L. HANSON,[2] SCHENECTADY, N. Y.

On the basis of the variational method, approximate solutions

$$f_k(r)h_k(\theta), \quad f_k(r)g_k(\theta), \quad F_k(\theta)H_k(r), \quad F_k(\theta)G_k(r)$$

of the biharmonic equation are established for the circular sector with the following properties: The stress functions f_kh_k create shear tractions on the radial boundaries; the stress functions f_kg_k create normal tractions on the radial boundaries; the stress functions F_kH_k create both shear and normal tractions on the circular boundary, and the stress functions F_kG_k create normal tractions on the circular boundary. The enumerated tractions are the only tractions which these function sets create on the various boundaries of the sector. The factors $f_k(r)$ constitute a complete set of orthonormal polynomials in r into which (more exactly, into the derivatives of which) self-equilibrating normal or shear tractions applied to the radial boundaries of the sector may be expanded; the factors $F_k(\theta)$ constitute a complete set of orthonormal polynomials in θ into which shear tractions applied to the circular boundary of the sector may be expanded; and the functions $F_k'' + F_k$ constitute a complete set of nonorthogonal polynomials into which normal tractions applied to the circular boundary of the sector may be expanded. Function tables, to facilitate the use of the stress functions, are also presented.

Introduction

MANY ANALYSES of circular sectors are confined to investigation of the stress conditions in the neighborhood of the corner where the two radial boundaries meet. J. H. A. Brahtz (1)[3] wrote a fundamental paper on the subject 25 years ago; and then the problem lay dormant until rather recently. The renewed interest in the subject may be ascribed partly to the recurrent need for a practical solution of this important class of problems, partly to the improved mathematical techniques that have since become available. Mellin transform methods (2, 3), biharmonic eigenfunction-expansion methods (4, 5), conformal-mapping methods (6), and combinations of these and modified techniques (7) are the favored approaches in these investigations. Because of the laboriousness of these rigorous approaches, the problem along the circular arc is usually not resolved, or is handled only in approximation (8).[4,5] It seemed highly desirable to develop an approximate method which takes all boundary conditions rigorously into account and utilizes the conventional techniques of Fourier analysis. The success of the variational method for the rectangle problem (11, 12, 13), utilizing orthogonal boundary polynomials, suggested an extension of the method to the sector problem.[6]

Using the radius of the sector as a distance unit, Fig. 1, and assuming that loads are applied only at the boundaries $\theta = \pm\omega$ and $r = 1$ of the sector, and that these loads maintain force and moment equilibrium (i.e. we deal with a static problem), the problem of the elastic loading of the sector is reduced to determination of the stress function Φ from the equation

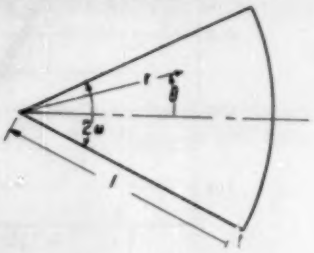

Fig. 1 Circular Sector

$$\nabla^4\Phi = 0, \quad \left(\nabla^2 \equiv \frac{\partial^2}{\partial r^2} + \frac{1}{r}\frac{\partial}{\partial r} + \frac{1}{r^2}\frac{\partial^2}{\partial\theta^2}\right) \ldots\ldots [1]$$

subject to the boundary conditions, the stresses

$$\sigma_r = \frac{\partial^2\Phi}{r^2\partial\theta^2} + \frac{\partial\Phi}{r\partial r}, \quad \tau = -\frac{\partial}{\partial r}\frac{\partial\Phi}{r\partial\theta}. \qquad \ldots\ldots [2a]$$

obey prescribed conditions at $r = 1$, the stresses

$$\sigma_\theta = \frac{\partial^2\Phi}{\partial r^2}, \quad \tau = -\frac{\partial}{\partial r}\frac{\partial\Phi}{r\partial\theta} \ldots\ldots \qquad \ldots\ldots [2b]$$

obey prescribed conditions at $\theta = \pm\omega$.

We may assume that all boundary data are decomposed into even and odd constituents in θ, so the effects of only even or odd loads in θ need to be considered. We shall use the bar above a quantity to denote boundary values at $r = 1$, the circumflex above a quantity to denote boundary values at $\theta = +\omega$, and the inverted circumflex above a quantity to denote boundary values at $\theta = -\omega$

$$\bar{\sigma}(\theta) \equiv \sigma(1, \theta)$$
$$\hat{\sigma}(r) \equiv \sigma(r, +\omega)$$
$$\check{\sigma}(r) \equiv \sigma(r, -\omega)$$

Because of the evenness or oddness of the boundary tractions, the data $\hat{\sigma}_\theta, \hat{\tau}$ also specify $\check{\sigma}_\theta, \check{\tau}$.

---

[1] Research Associate, Metallurgy and Ceramics Research Department, General Electric Research Laboratory. Mem. ASME.

[2] Advanced Engineering Program, General Electric Company, on a 4-month assignment in the Metallurgy and Ceramics Research Department, General Electric Research Laboratory.

[3] Numbers in parentheses refer to the Bibliography at the end of the paper.

Presented at the Applied Mechanics Division Summer Conference, Berkeley, Calif., June 13–15, 1957, of The American Society of Mechanical Engineers.

Discussion of this paper should be addressed to the Secretary, ASME, 29 West 39th Street, New York, N. Y., and will be accepted until January 10, 1958, for publication at a later date. Discussion received after the closing date will be returned.

Note: Statements and opinions advanced in papers are to be understood as individual expressions of their authors and not those of the Society. Manuscript received by ASME Applied Mechanics Division, January 10, 1957. Paper No. 57—APM-30.

[4] See also references in item (7) of the Bibliography.

[5] For the special case of the semicircle the use of bipolar coordinates permits rigorous solution of the problem along the arc (9, 10).

[6] Indeed, the simpler problem for the circular sector, $\nabla^2\Phi = 0$, was solved in this manner several years ago, in (14). A variational approach for the triangle stress problem was used recently by I. K. Silverman (15), but the paper stopped short of trying to satisfy all boundary conditions. For a complete bibliography on the method of orthogonal boundary polynomials, see (17).

We proceed to the method of self-equilibrating functions by splitting off from the stress function Φ the component

$$\Phi_1 = a_0 r^2 + r^{\pi/2\omega}\left[(a_1 + b_1 r^2)\cos\frac{\pi\theta}{2\omega} + (c_1 + d_1 r^2)\sin\frac{\pi\theta}{2\omega}\right] + r^{\pi/\omega}\left[(a_2 + b_2 r^2)\cos\frac{\pi\theta}{\omega} + (c_2 + d_2 r^2)\sin\frac{\pi\theta}{\omega}\right] \quad \ldots\ldots [3]$$

with the nine coefficients $a_0, \ldots, d_2$ so determined that *each boundary $r = 1$, $\theta = +\omega$, $\theta = -\omega$ is under the remaining stresses, by itself in force and moment equilibrium*

$$\left.\begin{aligned}
&\int_{-\omega}^{\omega}(\bar\tau - \bar\tau_1)d\theta = \int_{-\omega}^{\omega}[(\bar\sigma_r - \bar\sigma_{r1})\sin\theta \\
&\quad + (\bar\tau - \bar\tau_1)\cos\theta]d\theta = \int_{-\omega}^{\omega}[(\bar\sigma_r - \bar\sigma_{r1})\cos\theta \\
&\qquad - (\bar\tau - \bar\tau_1)\sin\theta]d\theta = 0 \\
&\int_0^1(\hat\tau - \hat\tau_1)dr = \int_0^1(\hat\sigma_\theta - \hat\sigma_{\theta 1})dr \\
&\qquad = \int_0^1(\hat\sigma_\theta - \hat\sigma_{\theta 1})r dr = 0 \\
&\int_0^1(\check\tau - \check\tau_1)dr = \int_0^1(\check\sigma_\theta - \check\sigma_{\theta 1})dr \\
&\qquad = \int_0^1(\check\sigma_\theta - \check\sigma_{\theta 1})r dr = 0
\end{aligned}\right\} \quad \ldots [4]$$

Φ_1 is a rigorous solution of $\nabla^4\Phi = 0$, and its associated stresses are labeled σ_{r1}, $\sigma_{\theta 1}$, τ_1. Solution for the nine coefficients of Equation [3] from Equations [4] is elementary, and we shall assume that it has been carried out.[7]

The problem is then reduced to determination of a stress function Φ_2 which matches the remaining self-equilibrating tractions along the radii $\theta = \pm\omega$ and gives zero σ_r and τ at $r = 1$, and determination of another stress function Φ_3 which matches the remaining self-equilibrating tractions along the arc $r = 1$ and gives zero σ_θ and τ on $\theta = \pm\omega$. The expressions of Φ_2, Φ_3 will be obtained in the form of series

$$\Phi_2 = \sum_2^\infty f_k(r)[A_k h_k(\theta) + B_k g_k(\theta)] \quad \ldots\ldots [5a]$$

$$\Phi_3 = \sum_2^\infty F_k(\theta)[C_k H_k(r) + D_k G_k(r)] \quad \ldots\ldots [5b]$$

where $f_k(r)$, $F_k(\theta)$ are complete sets of orthogonal polynomials in terms of whose derivatives the boundary tractions along the radii and the circular arc, respectively, may be expanded; the products $f_k(r)h_k(\theta)$, . . ., $F_k(\theta)G_k(r)$ are approximate (variational) eigensolutions of the biharmonic equation.[8]

Solution of the Radial Problem

The requirement that the products $f_k(r)h_k(\theta)$ [or $f_k(r)g_k(\theta)$] give, on using Formulas [2], zero shear and zero normal stresses at $r = 1$, finite stresses at $r = 0$, implies

$$f_k(1) = f_k'(1) = f_k(0) = f_k'(0) = 0 \quad \ldots\ldots [6]$$

This leads to the requirement that the self-equilibrating polynomials $f_k(r)$ contain $r^3(1 - r)^3$ as a factor.[9] Using $f_2(r) = 30^1/_7 r^3(1 - r)^3$ as the initial function, and orthonormalizing in accordance with

$$\langle r^{-3} f_k f_l\rangle \equiv \int_0^1 r^{-3} f_k(r) f_l(r) dr = \left\{\begin{matrix} 1, k = l \\ 0, k \neq l \end{matrix}\right\} \quad \ldots\ldots [7]$$

one is led to the recurrence relations ($k > 2$)

$$\left.\begin{aligned}
f_k(r) &= n_k[r f_{k-1} + a_k f_{k-1} + b_k f_{k-2}], \quad (f_1 \equiv 0) \\
a_k &= -\int_0^1 f_{k-1}^2 r^{-2} dr \\
b_k &= -\int_0^1 f_{k-1} f_{k-2} r^{-3} dr \\
n_k^{-2} &= \int_0^1 [r f_{k-1} + a_k f_{k-1} + b_k f_{k-2}]^2 r^{-3} dr
\end{aligned}\right\} \quad \ldots [8]$$

and hence to the complete orthonormal set of polynomials

$$f_k(r) = N_k \chi_k(r) \quad \ldots\ldots [9a]$$

$$\left.\begin{aligned}
\chi_2 &= r^3(1 - r)^3 \\
\chi_3 &= \chi_2(7r - 2) \\
\chi_4 &= \chi_2(12r^2 - 8r + 1) \\
\chi_5 &= \chi_2(165r^3 - 180r^2 + 54r - 4) \\
\chi_6 &= \chi_2(143r^4 - 220r^3 + 110r^2 - 20r + 1) \\
&\ldots\ldots\ldots
\end{aligned}\right\} \quad \ldots [9b]$$

$$\left.\begin{aligned}
N_2^2 = 30, \quad N_3^2 = 24, \quad N_4^2 = 210, \\
N_5^2 = 24, \quad N_6^2 = 630
\end{aligned}\right\} \quad \ldots\ldots [9c]$$

The r^{-3} factor in the integrand of Equation [7] follows from the requirement that h''^2 appear in Equation [13] with the coefficient, unity. The completeness of the Set [9] with respect to the Boundary Conditions [6] follows from the completeness of the powers r^n ($n = 0, 1, 2, \ldots$) in the interval 0 to 1, with respect to inhomogeneous boundary conditions (Weierstrass' theorem) as follows: From the Weierstrass set we must extract a subset which obeys the four homogeneous Conditions [6]; the lowest such polynomial, $f_2(r)$, is of 4th degree.[10] Since the orthogonalization process insures linear independence, and since all powers r^n are utilized, one is assured of the completeness of the set of polynomials $f_n(r)$ with respect to Conditions [6].

The functions $f_k(r)$ ($k = 2, \ldots, 6$) are listed, in a form somewhat different from Equation [9], in Table 1(a), the integrals

$$\int_0^1 r^{-1} f_k'^2 dr, \quad \int_0^1 r f_k'^2 dr, \quad \int_0^1 r^{n-3} f_k^2 dr \qquad (n = 1, \ldots, 8)$$

are listed in Tables 1(b, c). The functions $f_k(r)$, $r^{-3}f_k(r)$, $r^{-1}f_k'(r)$, $f_k''(r)$ are tabulated in Table 2.

The functions $h_k(\theta)$, $g_k(\theta)$ satisfy the boundary conditions (e = even function in θ, o = odd function in θ)[11]

$$\left.\begin{aligned}
h_e'(\pm\omega) = \pm 1, \quad h_e(\pm\omega) = 0 \quad &\text{for} \quad \tau(-\omega) = -\tau(\omega), \\
&\sigma_\theta(-\omega) = \sigma_\theta(\omega) = 0 \\
h_o'(\pm\omega) = 1, \quad h_o(\pm\omega) = 0 \quad &\text{for} \quad \tau(-\omega) = \tau(\omega), \\
&\sigma_\theta(-\omega) = \sigma_\theta(\omega) = 0
\end{aligned}\right\} \quad \ldots [10]$$

[7] Expression [3] holds for $2\omega < \pi$. For $2\omega > \pi$ the terms $r^{\pi/2\omega}(a_1 \cos \pi\theta/2\omega + c_1 \sin \pi\theta/2\omega)$ must be replaced by $r^{-\pi/2\omega}(B_1 r^2 \cos \pi\theta/2\omega + D_1 r^2 \sin \pi\theta/2\omega)$
The cases $2\omega = \pi$, $2\omega = 2\pi$ are exceptional and must be treated by special methods.

[8] This method of approach was first proposed in (16).

[9] The term "self-equilibrating" is used to point out that the average of $f_k'(r)$, average and moment of $f_k''(r)$ vanish over the range 01. These are immediate consequences of the Boundary Conditions [6].

[10] The subscript k of $f_k(r)$ agrees with the degree of the $f_k''(r)$ polynomial.

[11] We omit subscript k of f, g, h in Equations [10]–[14], of $\alpha + i\beta$ in Equations [15]–[17], and of Δ, L, M, P, Q in [17], for the sake of simpler notation.

TABLE 1

(a) Self-Equilibrating Polynomials, $f_k(r) = N_k \chi_k(r)$.

(b) Scalar Products

k	N_k	$\chi_k(r)$	$\int_0^1 r^{-1} f_k'^2(r)\,dr$	$\int_0^1 r f_k^2(r)\,dr$
2	$\sqrt{5\cdot6} = 5.4772256$	$r^4 - 2r^3 + r^2$	2	$2^2\cdot3$
3	$2\sqrt{6} = 4.8989795$	$7r^5 - 16r^4 + 11r^3 - 2r^2$	29/5	$2^3\cdot3\cdot31/5$
4	$\sqrt{5\cdot6\cdot7} = 14.6913767$	$12r^6 - 32r^5 + 29r^4 - 10r^3 + r^2$	2·7	$2^2\cdot3^2\cdot5^2$
5	$2\sqrt{6} = 4.8989795$	$165r^7 - 510r^6 + 579r^5 - 292r^4 + 62r^3 - 4r^2$	3·47/5	$2^3\cdot3\cdot5393/5\cdot7$
6	$3\sqrt{2\cdot5\cdot7} = 25.0998008$	$143r^8 - 506r^7 + 693r^6 - 460r^5 + 151r^4 - 22r^3 + r^2$	$2\cdot5^2$	$2^2\cdot3\cdot23\cdot43$

(c) Expansion Coefficients, $\int_0^1 r^{n-3} f_k(r)\,dr$

k	n = 1	n = 2	n = 3	n = 4	n = 5	n = 6	n = 7	n = 8
2	1.8257419	0.4564355	0.1825742	0.0912871	0.0521641	0.0326025	0.0217350	0.0152145
3	-0.4082483	0.3265986	0.2449490	0.1632993	0.1108103	0.0777616	0.0563771	0.0420619
4	0.9660918	0.2415229	0.2070197	0.1725164	0.1380131	0.1092604	0.0867810	0.0695293
5	-0.4082483	0.1866278	0.1691314	0.1516351	0.1341387	0.1166424	0.1003831	0.0860271
6	0.7171372	0.1494036	0.1394433	0.1294831	0.1195229	0.1095626	0.0996024	0.0899208

TABLE 2* NUMERICAL VALUES FOR $f_k(r)$, $r^{-2}f_k(r)$, $r^{-1}f_k'(r)$, AND $f_k''(r)$

r	$f_2(r)$	$f_3(r)$	$f_4(r)$	$f_5(r)$	$f_6(r)$	r	$r^{-1}f_2'(r)$	$r^{-1}f_3'(r)$	$r^{-1}f_4'(r)$	$r^{-1}f_5'(r)$	$r^{-1}f_6'(r)$
0	0	0	0	0	0	0	10.95445 ·	-19.59592	28.98275	-39.19184	50.19960
0.02	$0.0^2$2106131	$-0.0^2$3500505	$0.0^2$4703008	$-0.0^2$5628436	$0.0^2$6392917	0.02	10.30595	-16.48643	20.96196	-23.14536	22.68656
0.05	0.01235799	-0.01823798	0.02059859	-0.02311534	0.02406689	0.05	9.366056	-12.27581	11.16480	-6.255453	-1.320887
0.10	0.04436953	-0.05258625	0.05756245	$-0.0^2$9335208	-0.0214.8970	0.10	7.887205	-6.393168	0.184.3379	7.449143	-12.02965
0.15	0.08903915	-0.07565758	0.0746.9029	0.0683.3093	-0.0796.0894	0.15	6.517898	-1.821868	-5.703081	9.453150	-5.608668
0.20	0.1402170	-0.0726.832	-0.0465.1751	0.115.1808	-0.0853.0320	0.20	5.258137	1.561673	-7.405075	5.455516	3.829627
0.25	0.1925587	-0.0430.742	-0.1273656	0.1286278	$-0.0^2$3466705	0.25	4.107919	3.903874	-6.798833	-0.4446253	9.412650
0.30	0.2415456	0.0216.650	-0.2065023	0.0983047	0.1309644	0.30	3.067846	5.315393	-4.301063	-5.557157	9.201609
0.35	0.2834807	0.1116987	-0.2475043	-0.0191.7481	0.2143381	0.35	2.136118	5.930827	-1.007875	-8.375873	4.347607
0.40	0.3154882	0.1957.63	-0.2337149	-0.1905960	0.2613918	0.40	1.314534	5.678775	2.346993	-8.373376	-2.496326
0.45	0.3355143	0.2652071	-0.1509064	-0.3168112	0.1405187	0.45	0.6026848	5.289936	5.252600	-5.777122	-8.360071
0.50	0.3423266	0.2972793	0	-0.4270936	-0.0986735	0.50	0	4.864607	7.346688	-1.377838	-10.98116
0.55	0.3355143	0.2951724	0.2016890	-0.3895570	-0.3722300	0.55	-0.5899503	4.403687	8.097809	3.702894	-9.191296
0.60	0.3154882	0.2607987	0.4340457	-0.2116577	-0.5596009	0.60	-0.8763581	3.587673	7.697819	8.211609	-3.379939
0.65	0.2834807	0.2146595	0.6525192	0.0920.142	-0.5.05893	0.65	-1.150217	2.672452	6.121882	10.99238	4.668790
0.70	0.2415456	0.1626305	0.8180092	0.4782212	-0.2498434	0.70	-1.334534	-1.249340	3.582868	11.16894	12.10614
0.75	0.1925587	0.1097666	0.8925588	0.8369515	0.2721822	0.75	-1.369306	-0.372943	0.4528555	8.306514	15.78577
0.80	0.1402170	0.0513899	0.8458327	1.063510	0.8563801	0.80	-1.334534	-0.735972	3.009933	3.009933	13.22609
0.85	0.0890391	0.0116742	0.6760966	1.049685	1.229991	0.85	-1.150217	-0.167853	-5.297323	-3.662477	3.998398
0.90	0.0443653	0.0106315	0.4131781	0.7573332	1.126730	0.90	-0.8763581	-3.061862	-6.387799	-9.186076	-8.616762
0.95	0.0123579	0.0053813	0.1383057	0.2908524	0.5168049	0.95	-0.4899503	-1.968777	-5.007895	-9.756338	-15.62163
0.98	$0.0^2$2106131	$0.0^2$9111435	0.0260818	0.0590.331	0.1113987	0.98	-0.2103255	-0.9008143	-2.519775	-5.557092	-10.16662
1.00	0	0	0	0	0	1.00	0	0	0	0	0

r	$r^{-2}f_2(r)$	$r^{-2}f_3(r)$	$r^{-2}f_4(r)$	$r^{-2}f_5(r)$	$r^{-2}f_6(r)$	r	$f_2''(r)$	$f_3''(r)$	$f_4''(r)$	$f_5''(r)$	$f_6''(r)$
0	5.477226	-9.797959	14.69138	-19.59592	25.09980	0	10.95445	-19.59592	28.98275	-39.19184	50.19960
0.02	5.260327	-8.751263	11.75752	-14.07109	15.48229	0.02	9.466808	-13.50002	13.53694	-9.167881	0.3689155
0.05	4.943196	-7.295193	8.239135	-7.646136	5.686757	0.05	7.838413	-5.695048	-3.010584	15.64754	-27.52390
0.10	4.436953	-5.158685	3.756145	-0.9325207	-2.116970	0.10	5.039068	4.017163	-16.28831	20.94620	-10.17827
0.15	3.957295	-3.369518	2.148042	-3.538176	4.032458	0.15	2.574296	10.05515	-16.63758	4.032458	23.15030
0.20	3.505474	-1.881208	-1.112938	2.884519	-2.107580	0.20	0.4381780	12.93331	-9.062619	-16.57031	36.52230
0.25	3.080939	-0.6889190	-2.037850	2.282043	-0.0551.928	0.25	-1.369306	13.16601	2.264278	-29.69052	22.89378
0.30	2.683840	0.2408500	-2.272218	1.092227	1.456960	0.30	-2.843157	11.86765	13.85376	-30.32517	-8.170725
0.35	2.314128	0.9311285	-2.090640	-0.1565322	1.997844	0.35	-3.998375	7.752635	23.07389	-18.36898	-40.12755
0.40	1.971801	1.410906	-1.460732	-1.128725	1.633696	0.40	-4.819958	3.135347	28.05531	2.759205	-57.11987
0.45	1.656861	1.704232	-0.7632191	-1.651141	0.6939095	0.45	-5.312909	-2.069819	27.71111	27.18865	-49.26888
0.50	1.369306	1.837117	0	-1.684026	-0.3921854	0.50	-5.477226	-7.348569	21.73707	48.07124	-15.66738
0.55	1.109138	1.835280	0.6769359	-1.287800	-1.230568	0.55	-5.312909	-12.18823	10.61131	58.75366	34.67537
0.60	0.8763581	1.721411	1.205683	-0.5957159	-1.550983	0.60	-4.819958	-16.06865	-4.165379	54.06906	84.57880
0.65	0.6709601	1.530319	1.548418	0.2179609	-1.279412	0.65	-3.998375	-18.48110	-21.26972	31.41458	112.1911
0.70	0.4929503	1.278834	1.668407	0.9677934	-0.5098523	0.70	-2.843157	-19.91006	-37.15589	-6.980556	97.10109
0.75	0.3423866	0.9952052	1.584994	1.487869	0.1861752	0.75	-1.369306	-16.84021	-48.45554	-54.77843	58.57863
0.80	0.2190890	0.7054530	1.321614	1.661734	1.338070	0.80	0.4381780	-11.75755	-50.77778	-98.26177	-43.88855
0.85	0.1232376	0.4352968	0.9357807	1.452890	1.702268	0.85	2.574296	-3.147594	-38.96980	-136.0583	-197.8361
0.90	0.0547226	0.2106561	0.5100965	0.9349702	1.391032	0.90	5.039068	9.506000	-7.013826	-77.66989	-222.7582
0.95	0.0136906	0.0569504	0.1533649	0.3223528	0.5725266	0.95	7.838413	26.71169	51.76622	57.80212	-2.811178
0.98	$0.0^2$2190890	$0.0^2$9523426	0.0271668	0.0611320	0.1192265	0.98	9.666208	39.43718	103.0172	207.0284	342.6976
1.00	0	0	0	0	0	1.00	10.95445	48.98979	144.9138	342.9296	702.7946

* The f_k columns may be regarded as reliable to 6 decimals; the f_k'' columns to 4 decimals; the others to 5 decimals.

$$\left.\begin{aligned} &g_s(\pm\omega) = 1, \quad g_s'(\pm\omega) = 0 \quad \text{for} \quad \sigma_\theta(-\omega) = \sigma_\theta(\omega), \\ &\qquad\qquad \tau(-\omega) = \tau(\omega) = 0 \\ &g_s(\pm\omega) = \pm 1, \quad g_s'(\pm\omega) = 0 \quad \text{for} \\ &\qquad \sigma_\theta(-\omega) = -\sigma_\theta(\omega), \quad \tau(-\omega) = \tau(\omega) = 0 \end{aligned}\right\} \ldots [11]$$

Writing the stress function Φ_k as a product $f_k h_k$ (or $f_k g_k$), the expressions for h_k (or g_k) are determined by minimizing the strain-energy expression[13]

$$U = \frac{1}{2E}\int_{-\omega}^{\omega} d\theta \int_0^1 [\sigma_r^2 + \sigma_\theta^2 + 2\tau^2 + 2\nu(\tau^2 - \sigma_r\sigma_\theta)]rdr \ldots\ldots [12]$$

Noting Equations [2], [6], [7], and placing $\nu = 0$ in Expression [12], there results

$$2E\delta U = \delta\int_{-\omega}^{\omega} d\theta \int_0^1 [r^{-1}f^{\prime 2}h^{\prime 2} + (2r^{-2}f^{\prime 2} - 4r^{-1}f^{\prime 2})h^{\prime 2} + (f^{\prime 2} + r^{-2}f^{\prime 2})h^2]rdr = \delta\int_{-\omega}^{\omega} [h^{\prime 2} - (4 - 2\langle r^{-1}f^{\prime 2}\rangle)h^{\prime 2} + \langle rf^{\prime 2} + r^{-1}f^{\prime 2}\rangle h^2]d\theta = 0 \ldots\ldots [13]$$

Hence, $h_k(\theta)$ (or $g_k(\theta)$) obeys the differential equation

$$h^{IV} + (4 - 2\langle r^{-1}f^{\prime 2}\rangle)h'' + \langle rf^{\prime 2} + r^{-1}f^{\prime 2}\rangle h = 0 \ldots [14]$$

from which we obtain the solutions, even and odd in θ, appropriate to Conditions [10], [11]

$$\left.\begin{aligned} h_{k_e} &= L_{kk}\cosh\alpha\theta\cos\beta\theta + M_{kk}\sinh\alpha\theta\sin\beta\theta \\ h_{k_o} &= P_{kk}\sinh\alpha\theta\cos\beta\theta + Q_{kk}\cosh\alpha\theta\sin\beta\theta \\ g_{k_e} &= L_{k_g}\cosh\alpha\theta\cos\beta\theta + M_{k_g}\sinh\alpha\theta\sin\beta\theta \\ g_{k_o} &= P_{k_g}\sinh\alpha\theta\cos\beta\theta + Q_{k_g}\cosh\alpha\theta\sin\beta\theta \end{aligned}\right\} \ldots [15]$$

where

$$\left.\begin{aligned} \Delta_{k_e} &= \beta\sinh 2\alpha\omega + \alpha\sin 2\beta\omega \\ \Delta_{k_o} &= \beta\sinh 2\alpha\omega - \alpha\sin 2\beta\omega \end{aligned}\right\} \ldots\ldots [16]$$

$$\left.\begin{aligned} &\Delta_s L_k = -2\sinh\alpha\omega\sin\beta\omega, \quad \Delta_s M_k = 2\cosh\alpha\omega\cos\beta\omega \\ &\Delta_s P_k = -2\cosh\alpha\omega\sin\beta\omega, \quad \Delta_s Q_k = 2\sinh\alpha\omega\cos\beta\omega \\ &\Delta_s L_g = \Delta_s(-\alpha P_k + \beta Q_k), \quad \Delta_s M_g = \Delta_s(-\beta P_k - \alpha Q_k) \\ &\Delta_s P_g = \Delta_s(-\alpha L_k + \beta M_k), \quad \Delta_s Q_g = \Delta_s(-\beta L_k - \alpha M_k) \end{aligned}\right\} \ldots [17]$$

and

$\alpha_k + i\beta_k$ = root of

$$m^4 + (4 - 2\langle r^{-1}f_k^{\prime 2}\rangle)m^2 + \langle rf_k^{\prime\prime 2} + r^{-1}f_k^{\prime 2}\rangle = 0 \ldots [18]$$

which has positive real and imaginary parts ($\alpha_k - i\beta_k$ and $-\alpha_k + i\beta_k$, $-\alpha_k - i\beta_k$ are also roots). The first five roots are plotted in Fig. 2, and are tabulated in Table 3. The coefficients $L_{kk}, \ldots, Q_{k_g}$ are tabulated in Table 4.

The functions $f_k h_k$, $f_k g_k$ resolve the problem of the sector which is free of loads along arc $r = 1$ and which has only self-equilibrating tractions $\hat{\tau} - \hat{\tau}_1$, $\hat{\sigma}_\theta - \hat{\sigma}_{\theta 1}$ applied on the boundaries $\theta = \pm\omega$.

[13] The stress function is, as well known, independent of ν for simply connected plane figures. The value of ν in Equation [12] may therefore be chosen arbitrarily. $\nu = 0$ is the simplest choice.

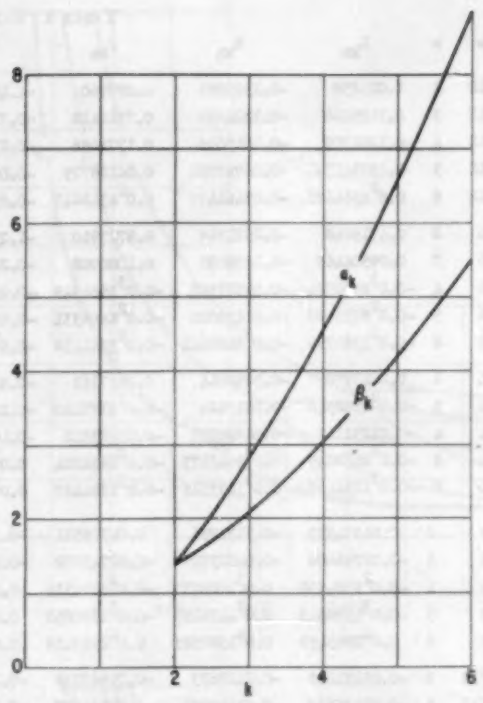

FIG. 2 ROOTS $\alpha_k + i\beta_k$ OF EIGENVALUE EQUATION [18] FOR CASE WHERE SELF-EQUILIBRATING TRACTIONS ARE PRESCRIBED ALONG $\theta = \pm\omega$, ZERO TRACTIONS ALONG $r = 1$

TABLE 3 THE ROOTS $(\alpha_k + i\beta_k)$ OF CHARACTERISTIC EQUATION [18]

k	α_k	β_k
2	1.367782	1.367782
3	2.849019	2.077718
4	4.595238	3.019307
5	6.604660	4.173912
6	8.864806	5.530352

For we may expand the integrals of the tractions into the polynomials

$$\left.\begin{aligned} &-r\int_1^r [\hat{\tau}(r) - \hat{\tau}_1(r)]dr \equiv \hat{\Phi}_{2\tau}(r) = A_2 f_2 + A_3 f_3 + \ldots \\ &\int_1^r dr\int_0^r [\hat{\sigma}_\theta(\rho) - \hat{\sigma}_{\theta 1}(\rho)]d\rho \\ &\qquad\qquad \equiv \hat{\Phi}_{2\sigma}(r) = B_2 f_2 + B_3 f_3 + \ldots \\ &\qquad A_k \equiv \langle r^{-2} f_k \hat{\Phi}_{2\tau}\rangle, \quad B_k \equiv \langle r^{-2} f_k \hat{\Phi}_{2\sigma}\rangle \end{aligned}\right\} \ldots [19]$$

and then Series [5a] is the approximate stress function for the radial problem. According to whether the given loadings $\tau(r, \pm\omega)$, $\sigma_\theta(r, \pm\omega)$ are even or odd, we insert above the even or odd expressions of the functions h_k, g_k as given in Equations [15].

One may rightfully inquire whether the same $h_k(\theta)$ are obtained when the entire series $\Sigma A_k f_k(r)h_k(\theta)$ is placed into the Dirichlet Integral [12] as when the terms $f_k(r)h_k(\theta)$ are placed there individually. The answer is: Certainly not, unless the integrals of the cross products $f_k(r)f_i(r)$, $f_k'(r)f_i'(r)$, $f_k''(r)f_i''(r)$ which would arise in [13], were the complete series inserted into [12], turned out to be negligibly small. The selection of the $f_k(r)$, $f_i(r)$ functions as precisely orthogonal eliminates the inte-

TABLE 4 VALUES OF COEFFICIENTS*

ω	k	L_{kh}	M_{kh}	P_{kh}	Q_{kh}	L_{kg}	M_{kg}	P_{kg}	Q_{kg}
$\pi/12$	2	1.015838	−0.1305895	4.089960	−4.455372	0.9972655	0.04264473	18.37803	−14.19115
$\pi/12$	3	0.3199420	−0.1224252	0.7514412	−0.7183346	0.9718661	−0.1746568	3.762541	−2.439543
$\pi/12$	4	0.1204707	−0.1015636	0.1774686	−0.2148056	0.8627836	−0.09458070	1.465837	−0.4358779
$\pi/12$	5	0.03734579	−0.06767384	0.04128779	−0.08486269	0.6223860	0.06923300	0.7098075	0.04216216
$\pi/12$	6	$0.0^2$4364683	−0.03464499	$0.0^2$4346247	−0.03585519	0.3367819	0.15737617	0.3362865	0.1552253
$\pi/6$	2	0.4715048	−0.2521768	0.8727910	−1.236067	0.9575994	0.1649580	2.981570	−0.9036318
$\pi/6$	3	0.09504469	−0.1638091	0.1080908	−0.2281409	0.6949069	0.1319474	0.8358785	0.08754935
$\pi/6$	4	$-0.0^3$6090584	−0.05927368	$-0.0^3$5986349	−0.06018519	0.2750329	0.1846531	0.2702672	0.1815824
$\pi/6$	5	$-0.0^2$8735028	−0.01235022	$-0.0^2$8666331	−0.01230178	0.04534391	0.1092287	0.04484385	0.1085966
$\pi/6$	6	$-0.0^2$3382739	$-0.0^3$8488641	$-0.0^2$3381158	$-0.0^3$8487830	−0.01117776	0.03467748	−0.01117949	0.03467242
$\pi/4$	2	0.2247978	−0.3282044	0.2657161	−0.6199447	0.8107132	0.3242526	1.130215	0.2113403
$\pi/4$	3	$-0.0^2$6362548	−0.1017624	$-0.0^2$6172140	−0.1033178	0.2836804	0.2340234	0.2746066	0.2278210
$\pi/4$	4	−0.01291142	−0.01250731	−0.01283512	−0.01246991	0.01863199	0.09706296	0.01840823	0.09666229
$\pi/4$	5	$-0.0^2$2652249	$0.0^3$3645173	$-0.0^2$2652224	$0.0^3$3645595	−0.01347722	0.01599455	−0.01347848	0.01599659
$\pi/4$	6	$-0.0^3$1234465	$0.0^3$3193515	$-0.0^3$1234467	$0.0^3$3193533	$-0.0^2$3513727	$-0.0^3$6717898	$-0.0^2$3513737	$-0.0^3$6717876
$\pi/3$	2	0.04954533	−0.3171996	0.04705511	−0.3785000	0.5467694	0.4258530	0.5340105	0.3897264
$\pi/3$	3	−0.02796606	−0.04023707	−0.02745972	−0.03991551	0.05741645	0.1632994	0.05579220	0.1611445
$\pi/3$	4	$-0.0^2$5384938	$0.0^3$1088771	$-0.0^2$5381314	$0.0^3$1088933	−0.01675702	0.02441303	−0.01675937	0.02441674
$\pi/3$	5	$-0.0^3$1590849	$0.0^3$4476193	$-0.0^3$1590852	$0.0^3$4476219	$-0.0^2$3620384	$-0.0^3$8176273	$-0.0^2$3620394	$-0.0^3$8176247
$\pi/3$	6	$0.0^4$2963459	$0.0^4$1587585	$0.0^4$2963459	$0.0^4$1587585	$0.0^4$2315183	$-0.0^3$3505069	$0.0^4$2315183	$-0.0^3$3505069
$5\pi/12$	2	−0.05174243	−0.2429633	−0.04667338	−0.2461901	0.2854435	0.4189924	0.2500510	0.3853735
$5\pi/12$	3	−0.02175330	−0.01060954	−0.02166679	−0.01059401	−0.01487544	0.08396897	−0.01492972	0.08379058
$5\pi/12$	4	$-0.0^2$1255028	$0.0^2$1201404	$-0.0^2$1255063	$0.0^2$1201471	$-0.0^2$9310077	$0.0^2$2139615	$-0.0^2$9310443	$0.0^2$2139834
$5\pi/12$	5	$0.0^4$5920106	$0.0^4$7229524	$0.0^4$5920105	$0.0^4$7229523	$-0.0^3$2303855	$-0.0^3$6927569	$-0.0^3$2303854	$-0.0^3$6927567
$5\pi/12$	6	$0.0^5$2444980	$-0.0^5$2896748	$0.0^5$2444980	$-0.0^5$2896748	$0.0^4$3920100	$-0.0^5$5654489	$0.0^4$3920100	$-0.0^5$5654489
$\pi/2$	2	−0.09685277	−0.1445800	−0.08967079	−0.1413481	0.07429454	0.3321270	0.06210746	0.3141765
$\pi/2$	3	−0.01088055	$0.0^2$1334581	−0.01087959	$0.0^2$1335157	−0.02640408	0.02821725	−0.02641350	0.02823086
$\pi/2$	4	$0.0^4$1472580	$0.0^3$4854064	$0.0^4$1472578	$0.0^3$4854068	$-0.0^2$2186099	$-0.0^2$1533261	$-0.0^2$2186096	$-0.0^2$1533259
$\pi/2$	5	$0.0^4$1440307	$-0.0^5$4035513	$0.0^4$1440307	$-0.0^5$4035513	$0.0^4$8677031	$-0.0^4$7828348	$0.0^4$8677031	$-0.0^4$7828348
$\pi/2$	6	$-0.0^6$2398704	$-0.0^6$2180229	$-0.0^6$2398704	$-0.0^6$2180229	$0.0^6$6061845	$0.0^5$3332172	$0.0^6$6061845	$0.0^5$3332172

* The last digit shown in the entries is unreliable.

grals of the cross products $f_k(r)f_i(r)$. But it is found, in addition, that the orthogonality of $f_k(r)$, $f_i(r)$ insures a near orthogonality for the $f_k'(r)$, $f_i'(r)$ and $f_k''(r)$, $f_i''(r)$ functions, and so renders the integrals of these cross products negligible in first approximation. This tremendously simplifies the variational method as it permits one to dispense with the variational determination of the series $\Sigma A_k f_k(r)h_k(\theta)$ for problem after problem, and replace it by the individual determination of the functions $h_k(\theta)$, once and for all. The power of the method of orthogonal boundary polynomials derives from this simplification.

SOLUTION OF PROBLEM ALONG ARC

Our starting point now is the definition of the orthonormal polynomials

$$F_k(\theta) = \omega^{-1/2} f_k(\theta/\omega) \equiv \omega^{-1/2} \mathbf{f}_k(y) \quad \ldots\ldots [20]$$

where

$$\left.\begin{aligned} \mathbf{f}_0(y) &= (3/16)(5\cdot7)^{1/2}(1-y^2)^3 \\ \mathbf{f}_2(y) &= (3/16)(5\cdot7\cdot11)^{1/2}(1-y^2)^2 y \\ \mathbf{f}_4(y) &= -(3/32)(7\cdot13)^{1/2}(1-y^2)^2(1-11y^2) \\ &\cdots\cdots \end{aligned}\right\} \quad \ldots [21]$$

are the well-known "self-equilibrating polynomials" for the interval $-1 \leqslant y \leqslant 1$ (reference 11),[13] which give zero shear, zero normal stress

$$f_k(\pm 1) = f_k'(\pm 1) = 0; \quad F_k(\pm\omega) = F_k'(\pm\omega) = 0 \ldots [22]$$

at the two end points, and are orthonormalized according to

$$\left.\begin{aligned} \langle f_k f_l \rangle &\equiv \int_{-1}^{1} f_k(y) f_l(y)\,dy = \begin{cases} 1, & k = l \\ 0, & k \neq l \end{cases} \\ \langle F_k F_l \rangle &\equiv \int_{-\omega}^{\omega} F_k(\theta) F_l(\theta)\,d\theta = \begin{cases} 1, & k = l \\ 0, & k \neq l \end{cases} \end{aligned}\right\} \quad \ldots [23]$$

By placing[14]

$$\left.\begin{aligned} \sigma_r &= r^{-2}HF'' + r^{-1}H'F \\ \sigma_\theta &= H''F \\ \tau &= (r^{-2}H - r^{-1}H')F' \end{aligned}\right\} \quad \ldots\ldots [24]$$

[13] In (11) the functions $\mathbf{f}_k(y)$ were denoted by $f_k(y)$. We now use bold-face print to distinguish the arc function $\mathbf{f}_k(\theta/\omega)$ from the radial function $f_k(r)$.

[14] To simplify notation, we omit the subscripts k in Equations [24]–[26], [29].

into the strain-energy integral, Expression [12], and setting the variation equal to zero we obtain

$$2E\delta U = \delta \int_0^1 rdr \int_{-\omega}^{\omega} [H'^2F^2 + r^{-2}H'^2(2F'^2 + F^2) + r^{-2}HH'(2FF'' - 4F'^2) + r^{-4}H^2(F'^2 + 2F'^2)]d\theta$$
$$= \delta \int_0^1 [H'^2 + (1 + 2\langle F'^2\rangle)r^{-2}H'^2 + \langle F''^2 - 4F'^2\rangle r^{-4}H^2]rdr = 0 \quad \ldots\ldots [25]$$

On noting Equations [22] and [23], there results the differential equation[15]

$$r^4H^{IV} + 2r^3H''' - (1 + 2\omega^{-2}\langle f'^2\rangle)(r^2H'' - rH') + \langle \omega^{-4}f''^2 - 4\omega^{-4}f'^2\rangle H = 0 \quad \ldots\ldots [26]$$

which is solved by

$$H_k(r) = ar^{\xi_k + i\eta_k} + br^{\xi_k - i\eta_k} + cr^{2-\xi_k+i\eta_k} + dr^{2-\xi_k-i\eta_k} \qquad (\xi_k > 0) \quad \ldots\ldots [27a]$$

or by

$$H_k(r) = ar^{\xi_{ka}} + br^{\xi_{kb}} + cr^{2-\xi_{ka}} + dr^{2-\xi_{kb}} \qquad (\xi_{ka} > \xi_{kb} > 0) \quad \ldots\ldots [27b]$$

(a, b, c, d, are arbitrary constants.) Here

$$\zeta_k = \xi_k + i\eta_k \quad \ldots\ldots [28]$$

denote the complex roots, with positive real and imaginary parts, ξ_{ka}, ξ_{kb} denote the positive real roots of

$$\zeta^4 - 4\zeta^3 + (4 - 2\omega^{-2}\langle f_k'^2\rangle)\zeta^2 + 4\omega^{-2}\langle f_k'^2\rangle\zeta + \langle \omega^{-4}f_k''^2 - 4\omega^{-4}f_k'^2\rangle = 0 \quad \ldots\ldots [29]$$

Real and imaginary parts of the first three roots are plotted in Figs. 3(a, b) versus ω in full line. If $\xi_k + i\eta_k$ is a complex root, then so are $\xi_k - i\eta_k$, $2 - \xi_k \pm i\eta_k$; if ξ_{ka}, ξ_{kb} are real roots (this may happen only for $\omega > 70°$) then so are $2 - \xi_{ka}$, $2 - \xi_{kb}$. The roots are tabulated, up to $k = 9$, in Table 5.[16]

For treating the problem of the ring sector, $0 < r_i \leqslant r \leqslant 1$ (r_i = inside radius, 1 = outside radius), all four roots enter the analysis (boundary conditions are prescribed on both inner and outer arcs), but for the full sector $0 \leqslant r \leqslant 1$, with which we are concerned, only the two roots with the largest positive real parts are needed. It will be noted that for $\omega > \pi/2$ there may be only one root with $\xi_k > 2$. This indicates that, disregarding very special tractions where the modes of ζ_2 (or the modes of both ζ_2 and ζ_3) are missing from the load, infinite stresses are bound to occur in the corner, $r = 0$, when $\omega > 90°$ (or when $\omega > 135°$). The fact that self-equilibrating boundary tractions may funnel their effect into another portion of the structure and create there an infinite stress, is rather unexpected. However, this conclusion agrees with the results of Williams (5). Fig. 3(a) shows the very close agreement of ξ_2 derived from our approximate equation, Equation [29], and the value derived from Williams' rigorous equation (our $\zeta - 1$ is Williams' λ)[17]

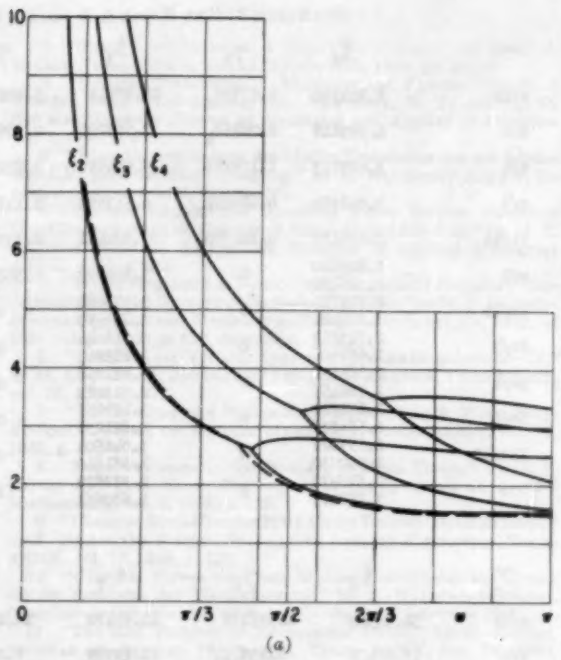

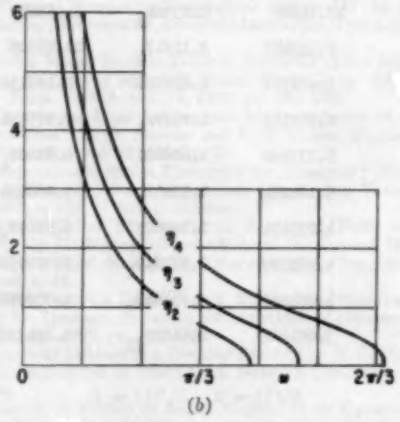

FIG. 3 ROOTS $\xi_k + i\eta_k$ OF EIGENVALUE EQUATION [29] FOR CASE WHERE SELF-EQUILIBRATING TRACTIONS ARE PRESCRIBED ALONG $r = 1$, ZERO TRACTIONS ALONG $\theta = \pm\omega$

(For comparison, the real part of lowest root of Williams' exact Equation [30], as copied from Fig. 1 of his paper, is also shown, in dashes.)

$$\sin [2\omega(\zeta - 1)] = \pm(\zeta - 1)\sin 2\omega \quad \ldots\ldots [30]$$

The similarity of the present Figs. 3(a, b), and Figs. 3(a, b) of (17) also may be pointed out.

Solution [27] may be written (for the full sector) in the case of complex roots, as a linear combination of functions

$$\left.\begin{aligned} H_k(r) &= \eta_k^{-1}r^{\xi_k}\sin(\eta_k \ln r) \\ G_k(r) &= r^{\xi_k}[\cos(\eta_k \ln r) + \eta_k^{-1}(1 - \xi_k)\sin(\eta_k \ln r)] \end{aligned}\right\} \quad \ldots [31]$$

These functions have the property that

$$H_k(0) = H_k'(0) = G_k(0) = G_k'(0) = 0 \quad \ldots\ldots [32a]$$

---

[15] The scalar products $\langle f_k'^2\rangle$ and $\langle f_k''^2\rangle$ are tabulated in Table 3 of reference (11).

[16] All four roots were computed independently with an IBM 650 digital computer which utilizes eight digits. The results were rounded to seven digits in the Table, and where all values of ξ_k (or η_k; or ξ_{ka} and $2 - \xi_{ka}$, ξ_{kb} and $2 - \xi_{kb}$) were not identical the mean value is shown with the averaged digits indicated by lowered print.

[17] Authors are indebted to the Referee for the remark—in addition to his many other helpful suggestions—that reference (19) (not available to the authors) contains rigorous values of $\xi_k + i\eta_k$ also for higher k; the agreement of rigorous and varintional ξ_k is very good for the available k; the agreement of rigorous and variational η_k is very good for $k = 2$, and less good for higher k.

TABLE 5 THE ROOTS $\xi_k + i\gamma_k$, ξ_{ka}, ξ_{kb} OF CHARACTERISTIC EQUATION [29]

ω	ξ_2	γ_2	ξ_3	γ_3	ξ_4	γ_4	ξ_5	γ_5
$\pi/12$	8.941290	4.27707_2	14.97015	5.80279_8	21.08948	7.82146_3	27.51925	10.20119
$\pi/6$	4.993618	2.00157_4	7.993298	2.78980_8	11.04976	3.826841	14.26332	5.03642_3
$\pi/4$	3.689713	1.170957	5.671595	1.7295_{29}	7.705499	2.455117	9.846348	3.28499_4
$\pi/3$	3.048950	0.680091_2	4.513993	1.147758	6.035196	1.73636_5	7.639159	2.385564
$5\pi/12$	2.676179	0.242373_5	3.822411	0.7391177	5.034585	1.27334_4	6.315926	1.82512_1
$\pi/2$	2.815610 2.065490	0	3.364293	0.362971_1	4.368945	0.9306_{594}	5.434721	1.4318_{10}
$7\pi/12$	2.774701 1.798121	0	3.376681 2.703559	0	3.894855	0.64233_{68}	4.806159	1.130786
$2\pi/3$	2.713313 1.657567	0	3.316644 2.28396	0	3.540641	0.346841_3	4.335557	0.8826429
$3\pi/4$	2.654337 1.586455	0	3.221752 2.013214	0	3.545512 2.987533	0	3.970325	0.661546_6
$5\pi/6$	2.601710 1.556722	0	3.129655 1.821235	0	3.514571 2.582772	0	3.678924	0.441169_3
$11\pi/12$	2.555622 1.550930	0	3.046504 1.681610	0	3.435273 2.308670	0	3.441293	0.12692_{44}
π	2.515378 1.558173	0	2.972822 1.580551	0	3.351276 2.101514	0	3.588017 2.900133	0

ω	ξ_6	γ_6	ξ_7	γ_7	ξ_8	γ_8	ξ_9	γ_9
$\pi/12$	34.34360	12.97171	41.59470	16.1510_5	49.28427	19.74507	57.41484	23.7517_1
$\pi/6$	17.67478	6.435_{493}	21.29989	8.03536_6	25.14437	9.8399_{61}	29.20943	11.84901
$\pi/4$	12.11985	4.23384_3	14.53609	5.31201_6	17.09873	6.52363_1	19.8085	7.86943_6
$\pi/3$	9.343407	3.11517_4	11.15505	3.9363_3	13.07667	4.85433_2	15.10874	5.87055_1
$5\pi/12$	7.678387	2.428918	9.127136	3.09958_0	10.66405	3.843651	12.28942	4.66383_4
$\pi/2$	6.569100	1.95792_8	7.775791	2.53165_7	9.056147	3.1620_{61}	10.41033	3.85308_5
$7\pi/12$	5.777402	1.608807	6.81107	2.116922	7.908101	2.66828_6	9.068525	3.26847_4
$2\pi/3$	5.184224	1.33442_9	6.088014	1.79735_5	7.047472	2.29162_7	8.169034	3.0816_{79}
$3\pi/4$	4.723424	1.108023	5.52607	$1.5h056_5$	6.378463	1.992747	7.280406	$2.4756h_2$
$5\pi/6$	4.355320	0.912617_1	5.076938	1.3269_{10}	5.843600	1.74797_8	6.655005	$2.1918h_4$
$11\pi/12$	4.054665	0.735846_6	4.709857	1.143626	5.406306	1.5421_{79}	6.143589	1.95559_6
π	3.804632	0.56622_{71}	4.404335	0.981827_0	5.042200	1.36516_2	5.717669	1.75481_8

$$H_k(1) = 0, \quad H_k'(1) = 1 \qquad [32b]$$

$$G_k(1) = G_k'(1) = 1 \qquad [32c]$$

For the case of real roots, the combinations appropriate to Equations [32] are

$$H_k(r) = \frac{r^{\xi_{ka}} - r^{\xi_{kb}}}{\xi_{ka} - \xi_{kb}}$$

$$G_k(r) = \frac{(\xi_{ka} - 1)r^{\xi_{kb}} - (\xi_{kb} - 1)r^{\xi_{ka}}}{\xi_{ka} - \xi_{kb}} \qquad [33]$$

From Equations [24] and [32c] it is seen that the functions $F_k(\theta)G_k(r)$ do not give rise to shear tractions on $r = 1$. In contrast, the functions $F_k(\theta)H_k(r)$ give rise to both shear and normal distributions along $r = 1$.

The solution of the "arc" problem is carried out in two steps. First, the F_kH_k functions are matched to the difference between the originally prescribed shear stress $\bar{\tau}$ and the shear stress produced at $r = 1$ by Φ_1, by expanding the integral of this difference into orthogonal polynomials

$$-\int_A^\theta (\bar{\tau} - \bar{\tau}_1)d\theta \equiv \bar{\Phi}_{s\tau} = \sum_2^\infty \langle F_k\bar{\Phi}_{s\tau}\rangle F_k$$

$$\equiv \sum_2^\infty C_kF_k(\theta) \qquad [34]$$

($A = 0$ for $\bar{\tau} - \bar{\tau}_1$ even in θ; $A = \omega$ for $\bar{\tau} - \bar{\tau}_1$ odd in θ)
In this fashion one obtains the stress function

$$\Phi_{s\tau} = \Sigma C_kF_k(\theta)H_k(r) \qquad [35]$$

Note that the function $\Phi_{s\tau}$ creates radial tractions, $\sigma_{rs\tau}$, along the arc $r = 1$.

In our next and final step we construct a stress function for the radial traction

$$R(\theta) \equiv \sigma_r - \sigma_{r1} - \sigma_{rs\tau} \qquad [36a]$$

which acts on the arc, by expanding $R(\theta)$ in terms of the non-orthogonal polynomials $F_k'' + F_k$

$$R(\theta) = \Sigma D_k(F_k'' + F_k) \qquad [36b]$$

and writing

$$\Phi_{2\sigma} = \Sigma D_k F_k(\theta) G_k(r) \ldots\ldots\ldots\ldots\ldots [37]$$

Probably the simplest way of determining the coefficients D_k is to construct the auxiliary orthonormal polynomials[12]

$$\left.\begin{aligned} \mathfrak{F}_2(\theta) &= n_2[F_2'' + F_2] \\ \mathfrak{F}_3(\theta) &= n_3[F_3'' + F_3] \\ \mathfrak{F}_4(\theta) &= n_4[F_4'' + F_4 + a_4\mathfrak{F}_2] \\ \mathfrak{F}_5(\theta) &= n_5[F_5'' + F_5 + a_5\mathfrak{F}_3 + b_5\mathfrak{F}_1 + \ldots + c_5\mathfrak{F}_{5-5}] \end{aligned}\right\} . [38a]$$

$$\left.\begin{aligned} a_5 &= -\langle (F_5'' + F_5)\mathfrak{F}_1\rangle, \quad b_5 = -\langle (F_5'' + F_5)\mathfrak{F}_3\rangle, \ldots \\ n_5^{-2} &= \langle F_5''^2 - 2F_5'^2\rangle + 1 - a_5^2 - b_5^2 - \ldots - c_5^2 \end{aligned}\right\} . [38b]$$

in particular

$$\left.\begin{aligned} n_2^{-2} &= 1 + \langle \omega^{-2}\psi_2''^2 - 2\omega^{-2}\psi_2'^2\rangle \\ a_4 &= -n_2\langle \omega^{-2}\psi_4''\psi_2'' - 2\omega^{-2}\psi_4'\psi_2'\rangle \\ n_4^{-2} &= 1 - a_4^2 + \langle \omega^{-2}\psi_4''^2 - 2\omega^{-2}\psi_4'^2\rangle \\ a_6 &= -n_2\langle \omega^{-2}\psi_6''\psi_2'' - 2\omega^{-2}\psi_6'\psi_2'\rangle \\ b_6 &= -n_4[\langle \omega^{-2}\psi_6''\psi_4'' - 2\omega^{-2}\psi_6'\psi_4'\rangle + b_4a_4] \\ n_6^{-2} &= 1 - a_6^2 - b_6^2 + \langle \omega^{-2}\psi_6''^2 - 2\omega^{-2}\psi_6'^2\rangle \end{aligned}\right\} . [38c]$$

where the coefficients are so selected that

$$\langle \mathfrak{F}_k\mathfrak{F}_l\rangle \equiv \int_{-\omega}^{\omega} \mathfrak{F}_k(\theta)\mathfrak{F}_l(\theta)d\theta = \left\{\begin{matrix} 1, k = l \\ 0, k \neq l \end{matrix}\right\} \ldots . [39]$$

Then we expand $R(\theta)$ in terms of $\mathfrak{F}_k(\theta)$

$$R(\theta) = \Sigma \langle \mathfrak{F}_k R\rangle \mathfrak{F}_k(\theta) \equiv \Sigma d_k\mathfrak{F}_k(\theta) \ldots\ldots\ldots [40]$$

and finally rearrange Expression [40] in the form of Formula [36b].[13]

We conclude

$$\Phi_2 = \Phi_{2\tau} + \Phi_{2\sigma} \ldots\ldots\ldots\ldots\ldots [41]$$

is the approximate stress function of the problem along the arc, and the complete solution to the sector problem is obtained in the form

$$\Phi = \Phi_1 + \Phi_2 + \Phi_3 \ldots\ldots\ldots\ldots\ldots [42]$$

Application of the present method to solution of the thermal plane-strain problem (16) of the "sectioned cylinder subject to an r^2 temperature distribution" will be presented in a separate paper (18). The new results do not bear out the original estimates.

[12] We write the general formula for k = even. The expression for k = odd is similar.

[13] The integrals $\langle f_k''f_l''\rangle$ and $\langle f_k'f_l'\rangle$ needed in the evaluation of n_4, a_4, b_4, . . . are tabulated in references (11) and (13).

BIBLIOGRAPHY

1 "Stress Distribution in a Reentrant Corner," by J. H. A. Brahtz, Trans. ASME, vol. 55, APM—55-6, 1933, pp. 31–37.

2 "Integral Transforms in Mathematical Physics," by C. J. Tranter, John Wiley & Sons, Inc., New York, N. Y., 1951, p. 53. See also *Quarterly Journal of Mechanics and Applied Mathematics*, vol. 1, 1948, p. 125.

3 "Über die Anwendung der Mellin-Transformation zur Lösung einer Aufgabe der Plattenbiegung," by S. Woinowsky-Krieger, *Ingenieur-Archiv*, vol. 20, 1952, p. 391.

4 "Surface Singularities Resulting From Various Boundary Conditions in Angular Corners of Plates Under Bending," by M. L. Williams, First U. S. National Congress of Applied Mechanics, ASME, 1951, p. 325.

5 "Stress Singularities Resulting From Various Boundary Conditions in Angular Corners of Plates in Extension," by M. L. Williams, JOURNAL OF APPLIED MECHANICS, Trans. ASME, vol. 74, 1952, p. 526; vol. 75, 1953, p. 590, discussion.

6 "The Complex-Variable Approach to Stress Singularities—II," by M. L. Williams, JOURNAL OF APPLIED MECHANICS, Trans. ASME, vol. 78, 1956, p. 477.

7 "The Bending of a Wedge-Shaped Plate," by S. Woinowsky-Krieger, JOURNAL OF APPLIED MECHANICS, Trans. ASME, vol. 75, 1953, p. 77.

8 "Some Problems in the Bending of Thin Plates," by G. F. Carrier and F. S. Shaw, Proceedings of the Symposia on Applied Mathematics, vol. 3, 1950, p. 125.

9 "Clamped Semi-Circular Plate Under Uniform Bending Load," by S. Woinowsky-Krieger, JOURNAL OF APPLIED MECHANICS, Trans. ASME, vol. 77, 1955, p. 129.

10 "Über die Verwendung von Bipolar Koordinaten zur Lösung einiger Probleme der Plattenbiegung," by S. Woinowsky-Krieger, *Ingenieur-Archiv*, vol. 24, 1956, p. 47. See also reference (20).

11 "The End Problem of Rectangular Strips," by G. Horvay, JOURNAL OF APPLIED MECHANICS, Trans. ASME, vol. 75, 1953, p. 87; p. 576, discussion.

12 "Thermal Stresses in Rectangular Strips—II," by J. S. Born and G. Horvay, JOURNAL OF APPLIED MECHANICS, Trans. ASME, vol. 77, 1955, p. 401.

13 "Some Mixed Boundary-Value Problems of the Semi-Infinite Strip," by G. Horvay and J. S. Born, JOURNAL OF APPLIED MECHANICS, Trans. ASME, vol. 79, 1957, pp. 261–268.

14 "Orthogonal Edge Polynomials in the Solution of Boundary Value Problems," by G. Horvay and F. N. Spiess, *Quarterly of Applied Mathematics*, vol. 12, 1954, p. 54.

15 "Approximate Stress Functions for Triangular Wedges," by I. K. Silverman, JOURNAL OF APPLIED MECHANICS, Trans. ASME, vol. 77, 1955, p. 123; p. 600, discussion.

16 "Stress Relief Obtainable in Sectioned Heat Generating Cylinders," by G. Horvay, Proceedings of the Second Midwestern Conference on Solid Mechanics, Edwards Bros., Inc., Ann Arbor, Mich., 1955, p. 45.

17 "Saint Venant's Principle: A Biharmonic Eigenvalue Problem," by G. Horvay, JOURNAL OF APPLIED MECHANICS, Trans. ASME, vol. 79, 1957, pp. 381–386.

18 "Thermal Stresses in a Circular Sector," by K. L. Hanson and G. Horvay, submitted to Third U. S. National Congress of Applied Mechanics.

19 "Tavola di Radici di Basso Modulo di un'Equazione Interessante la Scienza della Costrusione," by L. Ricci, Pubblicazioni N. 296, Istituto per le Applicazioni del Calcolo, Roma, 1951.

20 See also the earlier work of W. Flügge, "Die strenge Berechnung von Kreisplatten unter Einzellasten," by Julius Springer, Berlin, Germany, 1928, for use of bipolar co-ordinates, and the papers by H. R. Hasse, by H. D. Conway, and M. K. Huang (referred to by Woinowsky-Krieger), and by D. F. Muster and M. A. Sadowsky (JOURNAL OF APPLIED MECHANICS, Trans. ASME, vol. 78, 1956, p. 329) for infinite expansions in solving semicircular plate problems.

Force in the Plane of Two Joined Semi-Infinite Plates

By J. T. FRASIER[1] and LEIF RONGVED[2]

The stress due to a force parallel to the plane of two joined semi-infinite plates is obtained from the three-dimensional state of stress produced by a force operative at a point interior to one of two joined semi-infinite elastic solids. The variation in the traction on the interface of a steel and aluminum plate is shown graphically.

Introduction

THE Papkovitch functions for a force at a point in the interior of one of two semi-infinite elastic solids joined across a plane boundary have been determined by Rongved.[3]

Using a method introduced by Flamant,[4] Rongved's solution is applied here to find the state of stress caused by a force parallel to the plane of two joined semi-infinite plates and which is operative at a point in one of the plates. The solution is given in closed form in terms of arbitrary values of the elastic constants of the two materials. The details of the solution are rather lengthy, so it will only be outlined here and the results presented.

Method of Solution

The solution is in two parts: (*a*) for a force normal and (*b*) for a force parallel to the interface of the plates. Proper superposition of these two solutions will give the state of stress caused by a force with any inclination to the interface.

The first step of the solution is to use the Papkovitch functions to express the stress components σ_{zz}, σ_{xx}, and σ_{xz} for the three-dimensional solution in the general form

$$\sigma = Pf(x, y, z) \quad [1]$$

where P is the concentrated force acting at the point (O, O, c). Next, in the Expressions [1] P is replaced by a uniformly distributed line load Q, acting over the infinitesimal length dy; this gives

$$\sigma = Qf(x, y, z)dy \quad [2]$$

The Equations [2] are then integrated with respect to y between the limits minus and plus infinity. This integration gives the stress components σ_{zz}, σ_{xx}, and σ_{xz} in two joined semi-infinite solids subjected to a uniformly distributed line load of force on a line parallel both to the interface of the solids and the y-axis. These stress components are of the form

$$\sigma = Qg(x, z) \quad [3]$$

and represent a state of plane strain. By performing the standard transformation of elastic constants[5] we obtain the corresponding plane-stress solution, i.e., the state of stress in two joined semi-infinite plates of unit thickness subjected to a force uniformly distributed through the thickness of the plate and operative at the point (O, c), Figs. 1 and 2.

[5] "The Mathematical Theory of Elasticity," by A. E. H. Love, Dover Publications, New York, N. Y., fourth edition, 1944.

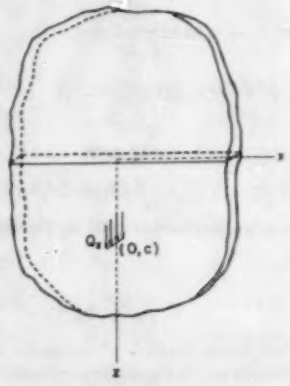

Fig. 1 Force Directed Normal to Interface of Two Joined Semi-Infinite Plates

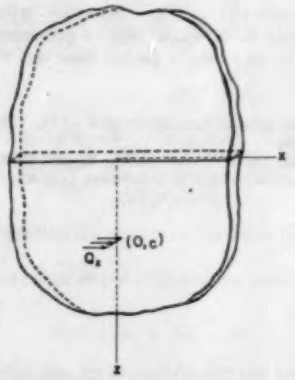

Fig. 2 Force Directed Parallel to Interface of Two Joined Semi-Infinite Plates

[1] Du Pont Fellow in Engineering Mechanics, The Pennsylvania State University, University Park, Pa.

[2] Member of Technical Staff, Bell Telephone Laboratories, Inc., Murray Hill, N. J.; formerly, Assistant Professor of Engineering Mechanics, The Pennsylvania State University, University Park, Pa.

[3] "Force in the Interior of One of Two Joined Semi-Infinite Solids," by L. Rongved, presented at the Second Midwestern Conference on Solid Mechanics, Lafayette, Ind., September 8–9, 1955.

[4] "Sur la Répartition des Pressions dans un Solide Rectangulaire Charge Transversalement," by Flamant, *Comptes Rendus*, Academie des Sciences, Paris, France, vol. 114, 1892, p. 1465.

Contributed by the Applied Mechanics Division and presented at the Fall Meeting, Hartford, Conn., September 23–25, 1957, of The American Society of Mechanical Engineers.

Discussion of this paper should be addressed to the Secretary, ASME, 29 West 39th Street, New York, N. Y., and will be accepted until January 10, 1958, for publication at a later date. Discussion received after the closing date will be returned.

Note: Statements and opinions advanced in papers are to be understood as individual expressions of their authors and not those of the Society. Manuscript received by ASME Applied Mechanics Division, September 23, 1955. Paper No. 57—F-7.

Results

The stress components in the plates due to a load Q_z directed normal to their interface, Fig. 1, are[6]

$$\sigma_{zz} = \{Q_z/4\pi\}\{(1-\nu)(z-c)/r_1^3 - 2(1+\nu)x^2(z-c)/r_1^4 - [(1+\nu)K_2(z+c) + 6(1-\nu)K_1c]/r_2^3 + 2K_1[2(1-\nu)c(z+c)^2 - 2(1+\nu)c^3(z+c) - (3-\nu)x^2(z-c)]/r_2^4 - 16(1+\nu)K_1cx^2z(z+c)/r_2^6\} \ldots [4]$$

$$\sigma_{xx} = \{Q_z/4\pi\}\{-(1-\nu)(z-c)/r_1^3 - 2(1+\nu)(z-c)^3/r_1^4 + [K_2(z+c) - 2(1-\nu)K_1c]/r_2^3 + 2K_1(z+c)[4(2+\nu)c(z+c) - (3-\nu)(z+c)^2 - 6(1+\nu)c^2]/r_2^4 - 16K_1(1+\nu)cx(z+c)^2/r_2^6\} \ldots [5]$$

$$\sigma_{xz} = \{Q_zx/4\pi\}\{-(1-\nu)/r_1^3 - 2(1+\nu)(z-c)^2/r_1^4 + K_2/r_2^3 + 2K_1[2(3+\nu)c(z+c) - (3-\nu)(z+c)^2 - 2(1+\nu)c^2]/r_2^4 - 16K_1(1+\nu)(z+c)^2cz/r_2^6\} \ldots [6]$$

$$\sigma'_{zz} = \{Q_zK_3\}\{(z-c)\mu[(1-\nu')(1+\nu) + (1-\nu)(3-\nu')]/r_1^3 + 2c[(1-\nu)(1+\nu')\mu' - (1-\nu')(1+\nu)\mu]/r_1^3 + 2x^2c(1+\nu)[(1+\nu')\mu' + (3-\nu')\mu]/r_1^4 - 2x^2z(1+\nu')[(1+\nu)\mu + (3-\nu)\mu']/r_1^4\} \ldots [7]$$

$$\sigma'_{xx} = \{Q_zK_3\}\{-(z-c)\mu[(1+\nu)(1-\nu') + (1-\nu)(3-\nu')]/r_1^3 + 2c[(1-\nu)(1+\nu')\mu' - (1-\nu')(1+\nu)\mu]/r_1^3 + 2(z-c)^2c(1+\nu)[(1+\nu')\mu' + (3-\nu')\mu]/r_1^4 - 2(z-c)^2z(1+\nu')[(1+\nu)\mu + (3-\nu)\mu']/r_1^4\} \ldots [8]$$

$$\sigma'_{xz} = \{2K_3Q_zx\}\{-\mu[(2-\nu')(1+\nu) - \nu(3-\nu')]/r_1^3 + (z-c)c(1+\nu)[(1+\nu')\mu' + (3-\nu')\mu]/r_1^4 - (z-c)z(1+\nu')[(1+\nu)\mu + (3-\nu)\mu']/r_1^4\} \ldots [9]$$

where

$$K_1 = (\mu - \mu')(1+\nu)/[(1+\nu)\mu + (3-\nu)\mu']$$

$$K_2 = (1-\nu) - \mu\mu'\{(1-\nu)[(1+\nu')(1+\nu) + (3-\nu)(3-\nu')] + 2(1-\nu')(1+\nu)(3-\nu)\}/[(1+\nu')\mu' + (3-\nu')\mu][(1+\nu)\mu + (3-\nu)\mu']$$

$$K_3 = \mu'/\pi[(1+\nu)\mu + (3-\nu)\mu'][(1+\nu')\mu' + (3-\nu')\mu]$$

$$r_1 = [x^2 + (z-c)^2]^{1/2}$$

$$r_2 = [x^2 + (z+c)^2]^{1/2}$$

μ is the shear modulus, and ν is Poisson's ratio.

The stress components due to a force Q_x directed parallel to the interface of the plates, Fig. 2, are

$$\sigma_{xx} = \{Q_x(1+\nu)/4\pi\}\{-(1-\nu)x/(1+\nu)r_1^3 - 2x^3/r_1^4 + K_4x/r_2^3 + 2K_1x[-[(1+\nu)\mu + (3-\nu)\mu']x^2/(\mu+\mu')(1+\nu) + 2\mu(1-\nu)(z+c)^2/(1+\nu)(\mu+\mu') - 2(3+\nu)c(z+c)/(1+\nu) + 6c^2]/r_2^4 + 16K_1x^3cz/r_2^6\} \ldots [10]$$

$$\sigma_{zz} = \{Q_x(1+\nu)/4\pi\}\{(1-\nu)x/(1+\nu)r_1^3 - 2x(z-c)^2/r_1^4 + K_4x/r_2^3 + 2K_1x[2c^2 + 2(1-\nu)c(z+c)/(1+\nu) - (3-\nu)(z+c)^2/(1+\nu)]/r_2^4 \ldots + \nu)]/r^4 + 16K_1cxz(z+c)^2/r_2^6\} \ldots [11]$$

[6] A prime denotes expressions and elastic constants related to the plate occupying $z \leq 0$.

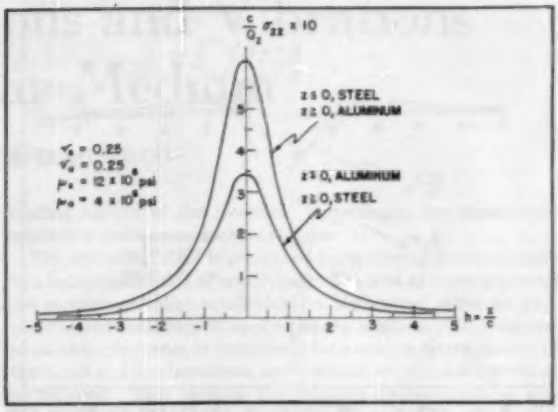
$\frac{c}{Q_z}\sigma_{zz} \times 10$
z ≥ 0, STEEL
z ≤ 0, ALUMINUM
z ≥ 0, ALUMINUM
z ≤ 0, STEEL
$\nu_s = 0.25$
$\nu_a = 0.25$
$\mu_s = 12 \times 10^6$ psi
$\mu_a = 4 \times 10^6$ psi
h = z/c

Fig. 3 Normal Stress on Interface of Plates of Steel and Aluminum for Case of Normal Force

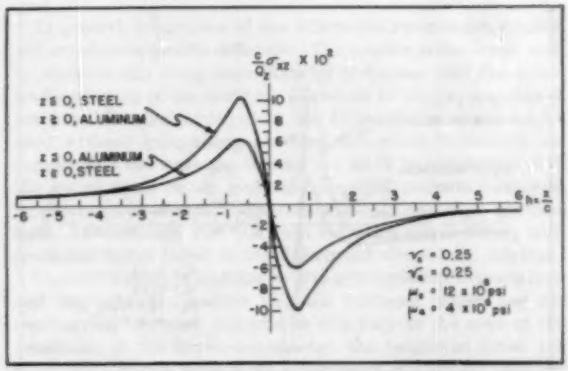
$\frac{c}{Q_z}\sigma_{xz} \times 10^2$
z ≥ 0, STEEL
z ≤ 0, ALUMINUM
z ≥ 0, ALUMINUM
z ≤ 0, STEEL
$\nu_s = 0.25$
$\nu_a = 0.25$
$\mu_s = 12 \times 10^6$ psi
$\mu_a = 4 \times 10^6$ psi
h = z/c

Fig. 4 Shear Stress on Interface of Plates of Steel and Aluminum for Case of Normal Force

$$\sigma_{zz} = \{Q_x(1+\nu)/4\pi\}\{-(1-\nu)(z-c)/(1+\nu)r_1^3 - 2x^2(z-c)/r_1^4 + [K_6(1+\nu)(z+c) - 2K_1(1-\nu)c]/(1+\nu)r_2^3 + 2K_1[2(1-\nu)x^2c/(1+\nu) - (3-\nu)x^2(z+c)/(1+\nu) - 2cz(z+c)]/r_2^4 + 16K_1cx^2z(z+c)/r_2^6\} \ldots [12]$$

$$\sigma'_{xx} = \{Q_x\mu'(1+\nu')\}\{K_7x/r_1^3 - x[x^2 + (\mu-\mu')(1-\nu')(z-c)^2/[(1+\nu')\mu' + (3-\nu')\mu] + K_8c(z-c)]/\pi(\mu+\mu')r_1^4\} \ldots [13]$$

$$\sigma'_{zz} = \{Q_x\mu'x/\pi\}\{\mu[(1-\nu')(1+\nu) + (1-\nu')(3-\nu')]/[(1+\nu)\mu + (3-\nu)\mu'][(1+\nu')\mu' + (3-\nu')\mu]r_1^3 + 4c(z-c)[(1-\nu')(1+\nu)\mu - (1-\nu)(1+\nu')\mu']/[(1+\nu)\mu + (3-\nu)\mu'][(1+\nu')\mu' + (3-\nu')\mu]r_1^4 - 2(1+\nu')(z-c)^2/[(1+\nu')\mu' + (3-\nu')\mu]r_1^4\} \ldots [14]$$

$$\sigma'_{xz} = \{Q_x\mu'/\pi\} < \{-(z-c)\mu[(1+\nu)(1-\nu') + (1-\nu)(3-\nu')] - 2c[(1-\nu')(1+\nu) - \mu'(1-\nu)(1+\nu')]\}/r_1^3 [(1+\nu)\mu + (3-\nu)\mu'][(1+\nu')\mu' + (3-\nu')\mu]$$

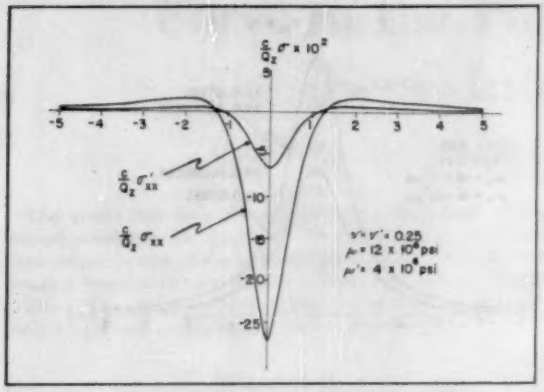

FIG. 5 σ_{zz} AND σ'_{zz} ON INTERFACE OF PLATES OF STEEL AND ALUMINUM FOR CASE OF NORMAL FORCE

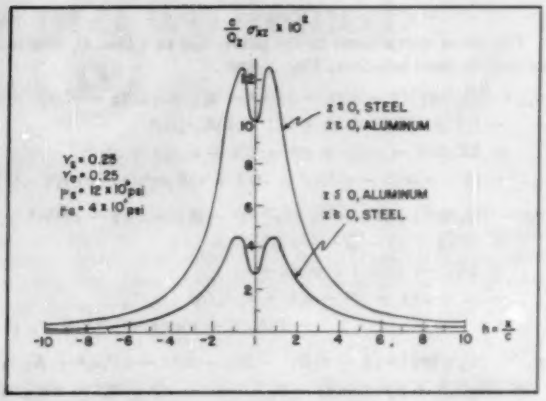
$\frac{c}{Q_z}\sigma_{xz} \times 10^2$
z ≤ 0, STEEL
z ≥ 0, ALUMINUM
z ≤ 0, ALUMINUM
z ≥ 0, STEEL
$\nu_s = 0.25$
$\nu_a = 0.25$
$\mu_s = 12 \times 10^6$ psi
$\mu_a = 4 \times 10^6$ psi
$h = \frac{z}{c}$

FIG. 7 SHEAR STRESS ON INTERFACE OF PLATES OF STEEL AND ALUMINUM FOR CASE OF PARALLEL FORCE

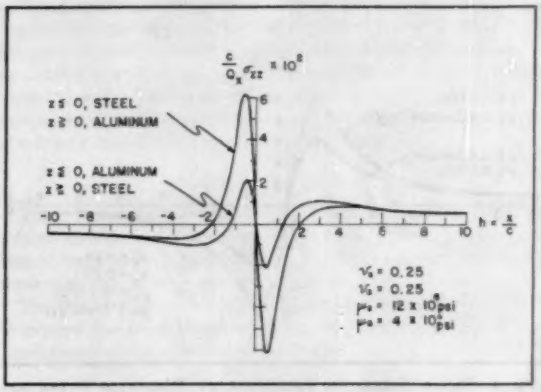
$\frac{c}{Q_x}\sigma_{zz} \times 10^2$
z ≤ 0, STEEL
z ≥ 0, ALUMINUM
z ≤ 0, ALUMINUM
z ≥ 0, STEEL
$h = \frac{z}{c}$
$\nu_s = 0.25$
$\nu_a = 0.25$
$\mu_s = 12 \times 10^6$ psi
$\mu_a = 4 \times 10^6$ psi

FIG. 6 NORMAL STRESS ON INTERFACE OF PLATES OF STEEL AND ALUMINUM FOR CASE OF PARALLEL FORCE

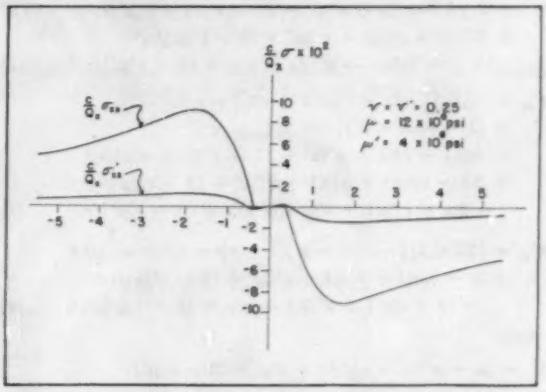

FIG. 8 σ_{zz} AND σ'_{zz} ON INTERFACE OF PLATES OF STEEL AND ALUMINUM FOR CASE OF PARALLEL FORCE

$$+ 4x^2c[\mu(1-\nu')(1+\nu) - \mu'(1-\nu)(1+\nu')]/[(1+\nu)\mu + (3-\nu)\mu'][(1+\nu')\mu' + (3-\nu')\mu]r_1^4 - 2x^2(z-c)(1+\nu')/[(1+\nu')\mu' + (3-\nu')\mu]r_1^4\rangle \ldots [15]$$

where

$$K_4 = \{-3\mu^2(1-\nu)(3-\nu') + \mu^2\mu'[(1+\nu')(1-\nu) + 4(1-\nu')(1-2\nu)] + \mu\mu'^2[(1-\nu)(1+\nu') - 8\nu(1+\nu')/(1+\nu) + 4\nu'(3-\nu)] + \mu'^3(1-\nu)(1+\nu')(3-\nu)/(1+\nu)\}/(\mu+\mu')[(1+\nu)\mu + (3-\nu)\mu'][(1+\nu')\mu' + (3-\nu')\mu]$$

$$K_5 = \{-\mu^2(1-\nu)(3-\nu') + \mu^2\mu'[(1-\nu)(3-\nu') + 4(\nu-\nu')] + \mu\mu'^2[(3-\nu)(1+3\nu-3\nu'-\nu\nu')]/(1+\nu) + \mu'^3(1-\nu)(3-\nu)(1+\nu')/(1+\nu)\}/(\mu+\mu')[(1+\nu)\mu + (3-\nu)\mu'][(1+\nu')\mu' + (3-\nu')\mu]$$

$$K_6 = \{\mu^2(1-\nu)(3-\nu') - 2\mu\mu'(1-\nu')(3-\nu) + \mu'^2(3-\nu)(1-\nu)(1+\nu')/(1+\nu)\}/[(1+\nu)\mu + (3-\nu)\mu'][(1+\nu')\mu' + (3-\nu')\mu]$$

$$K_7 = (1-\nu)(\mu-\mu')[\mu'(3-\nu)(1-\nu') - \mu(3-\nu')(1-\nu)]/2\pi(1+\nu')(\mu+\mu')[(1+\nu)\mu + (3-\nu)\mu'][(1+\nu')\mu' + (3-\nu')\mu] + \{\mu[2\nu'(1-\nu') - (1-\nu)(3-\nu')] - \mu'(1-\nu')[(1+\nu')(1+\nu) + \nu'(1-\nu)]\}/2\pi(1+\nu')(\mu+\mu')[(1+\nu')\mu' + (3-\nu')\mu]$$

$$K_8 = (1-\nu')(\mu-\mu')/[(1+\nu')\mu' + (3-\nu')\mu] + [\mu(1-\nu')(1+\nu) - \mu'(1+3\nu'-3\nu-\nu\nu')]/(1+\nu')[(1+\nu)\mu + (3-\nu)\mu']$$

Figs. 3 through 8 show the distribution of these stresses over the interface ($z = 0$) of plates having elastic constants approximately equal to those of steel and aluminum.

Stress-Strain Relations and Vibrations of a Granular Medium[1]

By J. DUFFY[2] and R. D. MINDLIN[3]

A differential stress-strain relation is derived for a medium composed of a face-centered cubic array of elastic spheres in contact. The stress-strain relation is based on the theory of elastic bodies in contact, and includes the effects of both normal and tangential components of contact forces. A description is given of an experiment performed as a test of the contact theories and the differential stress-strain relation derived from them. The experiment consists of a determination of wave velocities and the accompanying rates of energy dissipation in granular bars composed of face-centered cubic arrays of spheres. Experimental results indicate a close agreement between the theoretical and experimental values of wave velocity. However, as in previous experiments with single contacts, the rate of energy dissipation is found to be proportional to the square of the maximum tangential contact force rather than to the cube, as predicted by the theory for small amplitudes.

Introduction

THE relation between stress and small strain in a granular medium may be derived from a study of the behavior of the individual grains of the medium considered as elastic bodies in contact. In previous studies (1, 2, 3, 4)[4] the relation between the contact force and the displacement of the grains was based on Herts' theory (5). In the present paper both normal and tangential components of contact force are considered. While the classical theory of Herts is retained, the theories of Cattaneo (6), Mindlin (7), and Mindlin and Deresiewicz (8) make possible the inclusion of the tangential components of the forces at the contacts between grains. The stress-strain relation is found for the case of a medium composed of elastic spheres arranged in a face-centered cubic array.

As a result of the nonlinearity in the relation between the normal component of contact force and the displacement, the stress-strain relation is nonlinear. Furthermore, since the relation between the tangential component of contact force and displacement is inelastic, the stress-strain relation depends upon the entire loading history of the medium. Accordingly, the stress-strain relation is given as an incremental one.

The derivation itself is performed by satisfying simultaneously two independent sets of conditions. The first of these expresses the requirement that equilibrium be maintained when an arbitrary incremental load is applied to the medium. This requirement alone, however, is insufficient for a unique determination of the forces and displacements, and a second set of conditions must be imposed. This requires that relative displacements of material points in the medium be compatible. Satisfying these two sets of conditions simultaneously provides a relation giving increments in relative displacements in terms of increments in applied load.

In general, integration of the differential stress-strain relation will entail considerable difficulty. The relation is nonlinear, and, in addition, the integration must be performed over the entire loading history of the medium. However, in the investigation of problems of wave propagation, the differential relation may be used without integration, provided the stress increments accompanying the wave disturbance are small in comparison with the initial stress on the medium. Experiments were performed in which waves of small amplitude were propagated in granular bars. It was found that the wave velocities agreed closely with predicted values based on the differential stress-strain relation.

Contact theory, in addition to giving the relation between load and displacement, predicts that the frictional energy loss accompanying the wave disturbance will vary as the cube of the amplitude of the displacement when the tangential forces are small (8). In this respect the experiments of granular bars did not corroborate the theory, giving a rate of energy dissipation depending on the square of the amplitude. This result is in agreement with previous experiments (9, 10) on single contacts.

Pairs of Spheres

If two identical elastic spheres are in contact under the action of a force N, the Herts theory gives, for the contact radius a and the displacement α

$$a = [3(1 - \nu)NR/8\mu]^{1/3} \quad [1]$$

$$\alpha = 2[3(1 - \nu)N/8\mu R^{1/2}]^{2/3} \quad [2]$$

where R is the radius of a sphere, and ν and μ are, respectively, Poisson's ratio and the shear modulus of the material of the spheres. From these the normal compliance

$$C = d\alpha/dN = (1 - \nu)/2\mu a \quad [3]$$

may be obtained.

The theory was extended by Cattaneo (6) and Mindlin (7) to include a component of force T, tangential to the contact surface. According to this theory, when a monotonically increasing tangential force is added to a contact under a constant normal force, slip occurs at the contact surface, starting at the circumference of the area of contact and progressing radially inward so that the portion on which slip occurs is an annulus of outer radius a and inner radius

$$c = a(1 - T/fN)^{1/3} \quad [4]$$

[1] This investigation was supported by the Office of Naval Research under Contract Nonr-266(09), with Columbia University.

[2] Assistant Professor, Division of Engineering, Brown University, Providence, R. I.; formerly, Research Assistant, Department of Civil Engineering and Engineering Mechanics, Columbia University, New York, N. Y.

[3] Professor of Civil Engineering, Columbia University, New York, N. Y. Mem. ASME.

[4] Numbers in parentheses refer to the Bibliography at the end of the paper.

Presented at the Applied Mechanics Division Summer Conference, Berkeley, Calif., June 13–15, 1957, of The American Society of Mechanical Engineers.

Discussion of this paper should be addressed to the Secretary, ASME, 29 West 39th Street, New York, N. Y., and will be accepted until January 10, 1958, for publication at a later date. Discussion received after the closing date will be returned.

Note: Statements and opinions advanced in papers are to be understood as individual expressions of their authors and not those of the Society. Manuscript received by ASME Applied Mechanics Division, December 3, 1956. Paper No. 57—APM-39.

where f is the coefficient of friction. The relative tangential displacement of the centers of the two spheres is given by

$$\delta = 3fN(2-\nu)[1-(1-T/fN)^{2/3}]/8\mu a \quad [5]$$

yielding

$$S = d\delta/dT = (2-\nu)/4\mu a(1-T/fN)^{1/3} \quad [6]$$

for the tangential compliance. The Expression [5] for the tangential displacement has been confirmed experimentally by Johnson (9).

Mindlin, Mason, Osmer, and Deresiewicz (10) studied the effects produced by reversals of direction of the tangential force. This theory shows that, as a result of slip, the relation between force and displacement changes upon reversals of the direction of the tangential force. If the tangential force oscillates between $\pm T^*(<fN)$, a stable cycle is obtained after the first quarter cycle. The existence of an annulus of slip and Equation [4] for its inner radius were verified experimentally in this investigation. Experiments by Johnson (9) confirmed the relation between load and displacement as well as the existence of an annulus of slip.

Mindlin and Deresiewicz (8) further extended the theory to include the addition of a varying force of constant obliquity across a contact surface under an initial normal force, N_0. The theory provided the load-displacement relations for first loading, first unloading, and for the subsequent stabilized cycle. In the stabilized cycle, if the tangential component of force oscillates between $\pm T^*$, the tangential compliance during loading is given by

$$S_R = \frac{2-\nu}{4\mu a}\left\{\theta + (1-\theta)\left[1-(1+\theta)\frac{L^*+L}{2(1+\theta L)}\right]^{-1/3}\right\} \quad [7]$$

where

$$L = T/fN_0 \qquad L^* = T^*/fN_0$$
$$\theta = f/\beta \qquad \beta = dT/dN \geq f$$

For the unloading part of the stabilized cycle, the compliance S_U is obtained by reversing the signs of θ and L.

For small L^*, the frictional energy loss per cycle, obtained from the area of the load displacement diagram, is given by

$$F = (2-\nu)(T^*)^2(1-\theta^2)/18\mu a_0 fN_0 \quad [8]$$

for the stabilized load cycle, where a_0 is the radius of the contact circle corresponding to the normal force N_0.

Face-Centered Cubic Array of Spheres

As a result of the inelastic behavior at the contacts, the stress-strain relation for a granular medium depends upon load history. Until load history is specified it is appropriate to express the stress-strain relation in terms of differential increments of stress and strain. It is to be noted that the incremental stress-strain relation must involve the compliances which, themselves, depend on the history of the loading.

Consider a medium composed of identical spheres in a face-centered cubic array. Take as an element of the medium the cube shown in Fig. 1. This cube is chosen to contain a sufficient portion of the medium to define the arrangement. Increments of force dP_{ij} act on the faces of the cube, Fig. 2, and are assumed to be distributed among the spheres in proportion to the areas of their sections exposed on the faces of the cube. Incremental stress components are defined by $d\sigma_{ij} = dP_{ij}/8R^2$, where $8R^2$ is the gross area of a face. Each sphere in the medium is in contact with twelve other spheres. By the definition of a face-centered cubic array the disposition of these contacts on the surfaces of the

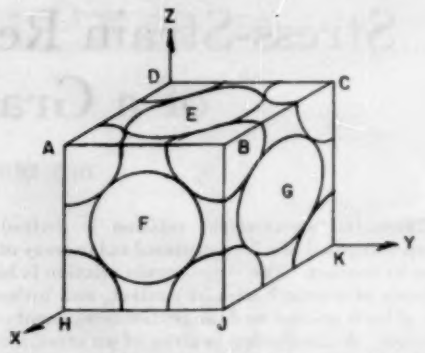

Fig. 1 Element of Volume of a Face-Centered Cubic Array of Spheres

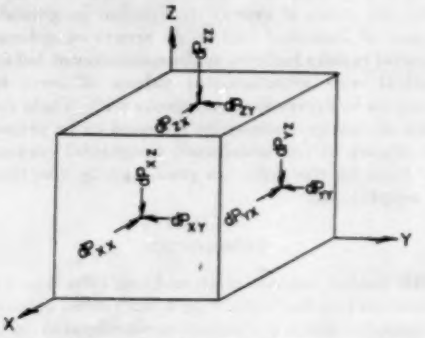

Fig. 2 Incremental Forces Acting on Faces of an Element of Volume

spheres is the same for each sphere in the medium; i.e., the spheres are indistinguishable one from another as far as disposition of contacts with other spheres is concerned. At the contacts between spheres the normal and tangential components of incremental force are designated by dN and dT, respectively. Subscripts i, j, k ($i \neq j \neq k$) are used to identify contacts. Each one of i, j, or k may be any one of x, y, or z. A contact with its normal in the i, j-plane has force increments dN_{ij}, dT_{ij}, and dT_{kk}, in which no significance is attributed to the order in which subscripts are written. It may be seen, Fig. 3, that the contact normals always lie in the co-ordinate planes. Hence, dN_{ij} lies in the i, j-plane, while the tangential components dT_{ij} and dT_{kk}, are chosen to lie in and normal to the i, j-plane, respectively. The contact normal, however, may have either of two possible orientations in a plane and a prime is used to designate forces at a contact having a normal whose components are of unlike sign.

The first step in the derivation of the stress-strain relation for the medium is to find expressions for the increments in the forces at the contacts between the spheres in the cube (i.e., dN_{ij}, dT_{ij}, and dT_{kk}) in terms of the increments in force dP_{ij}, applied to the faces of the cube, Fig. 2. Once this has been done, then, since the contact forces dN_{ij}, dT_{ij}, and dT_{kk} and the relative displacements of the centers of the spheres are related through the compliances, the relative displacements can be obtained in terms of the unknown compliances and the increments of applied force dP_{ij}. One set of relations between the increments of contact forces, dN_{ij}, dT_{ij}, and dT_{kk} and the increments of applied force dP_{ij} is found by requiring that equilibrium be maintained when arbitrary increments in applied force dP_{ij} are added to the faces of the cube. However, equilibrium conditions alone do not pro-

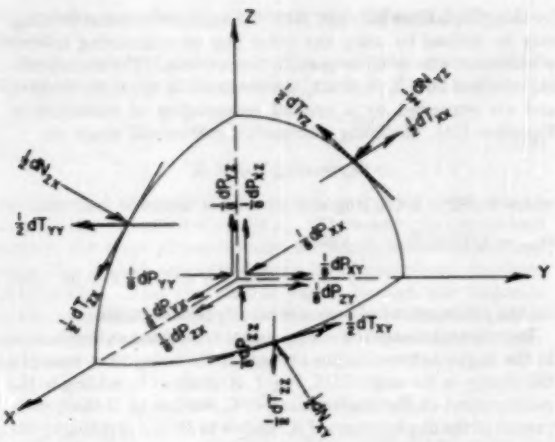

FIG. 3 FORCES ACTING ON AN OCTANT OF A SPHERE
(Octant shown here is located at origin in Fig. 1.)

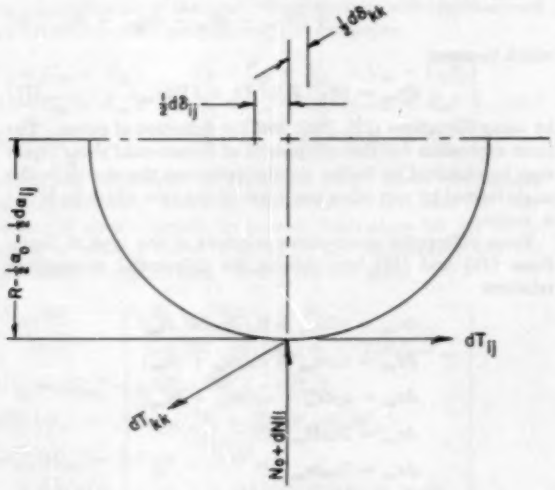

FIG. 4 COMPONENTS OF FORCE AT A CONTACT AND CORRESPONDING COMPONENTS OF DISPLACEMENT OF THE CENTER OF A SPHERE

vide sufficient equations to be able to solve for the increments in contact forces. The additional necessary conditions are provided by requiring that the relative displacements of the centers of spheres be compatible. Together, the equilibrium and the compatibility conditions are sufficient to determine the increments in the contact forces uniquely in terms of the compliances and the relative displacements of centers of spheres.

Consider the representative cube, Fig. 1, in equilibrium under an arbitrary initial stress imposed on the medium. If an arbitrary increment in stress is added to the initial stress, then the forces on the faces of the cube will be increased by corresponding increments dP_{ij}, Fig. 2. It is now desired to find the unknown increments in force at the contacts between the spheres within the cube which result from the addition of the increments in force dP_{ij} on the faces of the cube. Suppose that the stress increment in the medium is taken temporarily as homogeneous. Then, in going from one sphere to another, the contact forces will be equal at contacts having corresponding positions on the surfaces of the spheres. Since each sphere has 12 contacts, the number of unknown contact-force components will be 36. However, for each sphere the contact forces at diametrically opposed points are equal, so that only 18 of the contact forces are independent. The problem is to find these 18 increments in contact forces, dN_{ij}, dT_{ij}, and dT_{kk} for arbitrary increments in the forces dP_{ij}, applied on the faces of the cube. Not only must the cube as a whole remain in equilibrium under the action of the increments in applied forces dP_{ij}, but each sphere and each portion of a sphere, Fig. 3, within the cube also must remain in equilibrium. Since the portions of spheres in the cube are acted upon both by applied forces and by contact forces, the equations of equilibrium provide expressions relating the increments in applied forces to the increments in contact forces. By writing equilibrium equations for various portions of spheres in the cube it may be shown that there are 9 independent equations expressing equilibrium of increments in force. These are given by any three of the following equations

$$\left.\begin{aligned}
4dT_{xx} + 2\sqrt{(2)}(dN_{xx} + dN_{xy} - dT_{xx} + dT_{xy}) &= dP_{xx} + dP_{xy} + dP_{xz} \\
4dT_{xx}' + 2\sqrt{(2)}(dN_{xx}' + dN_{xy} - dT_{xx}' + dT_{xy}) &= dP_{xx} + dP_{xy} - dP_{xz} \\
4dT_{xx} - 2\sqrt{(2)}(dN_{xx}' + dN_{xy}' - dT_{xx}' + dT_{xy}') &= -dP_{xx} + dP_{xy} + dP_{xz} \\
4dT_{xx}' - 2\sqrt{(2)}(dN_{xx} + dN_{xy}' - dT_{xx} + dT_{xy}') &= -dP_{xx} + dP_{xy} - dP_{xz}
\end{aligned}\right\} \quad \ldots [9]$$

and six others obtained by cyclical permutation of subscripts. Moment equilibrium equations are given by three of the type

$$(dT_{yz}' - dT_{yz})R - (dT_{xx}' - dT_{xx} + dT_{yy}' + dT_{yy})\sqrt{(2)}R/2 = 0 \ldots [10]$$

These equations, however, are not independent of Equations [9], so that equilibrium considerations yield only 9 equations to be solved for 18 unknown components of force. The problem is thus statically indeterminate; additional equations must be obtained from conditions of compatibility of relative displacements of centers of spheres.

Components of relative displacements of the centers of spheres are designated by $d\alpha_{ij}$, $d\delta_{ij}$, and $d\delta_{kk}$, to correspond, respectively, to the forces dN_{ij}, dT_{ij}, and dT_{kk}, Fig. 4. Consider the centers of spheres F, B, and G in the element of volume, Fig. 1, noting that spheres F and G are in contact at a point within the cube. In order that the displacements of the centers of these spheres be single valued, the vector distance around the closed path through the centers of the spheres must vanish both before and after the medium is strained. Hence the sum of the relative displacements of the centers of these spheres around the closed path must vanish. An expression of this condition for all possible paths connecting the centers of spheres in the medium is given by any three of the following equations

$$\left.\begin{aligned}
\sqrt{2}(d\delta_{xx}) &= -d\alpha_{yz}' + d\alpha_{xz} + d\delta_{yz}' + d\delta_{xz} \\
\sqrt{2}(d\delta_{xx}) &= +d\alpha_{yz} - d\alpha_{xz}' - d\delta_{yz} - d\delta_{xz}' \\
\sqrt{2}(d\delta_{xx}') &= -d\alpha_{yz} + d\alpha_{xz} + d\delta_{yz} + d\delta_{xz} \\
\sqrt{2}(d\delta_{xx}') &= +d\alpha_{yz}' - d\alpha_{xz}' - d\delta_{yz}' - d\delta_{xz}'
\end{aligned}\right\} \quad \ldots [11]$$

and six others obtained by cyclical permutation of subscripts. Equations [11] may be expressed in terms of force increments by using

$$\left.\begin{aligned}
d\alpha_{ij} &= C_{ij}dN_{ij}, & d\alpha_{ij}' &= C_{ij}'dN_{ij}' \\
d\delta_{ij} &= S_{ij}dT_{ij}, & d\delta_{ij}' &= S_{ij}'dT_{ij}' \\
d\delta_{kk} &= S_{kk}dT_{kk}, & d\delta_{kk}' &= S_{kk}'dT_{kk}'
\end{aligned}\right\} \quad \ldots [12]$$

where subscripts identify the contact (and no summation convention is employed). After substitution of Equations [12] into Equations [11], the latter along with Equations [9] furnish 18 independent equations containing the components of the applied forces dP_{ij}, and the 18 independent components of contact forces dN_{ij}, dT_{ij}, and dT_{kk}, which it is desired to determine. However, these 18 equations are not linear in the components of contact forces since the equations contain the compliances; and the compliances, as may be seen by Equations [3], [6], or [7], are themselves dependent upon the contact forces, either directly or through the radius of the contact circle a. Indeed, even the expressions which are to be used for compliances depend upon load history. Hence, Equations [9], [11], and [12] can be solved for the components of contact forces, dN_{ij}, dT_{ij}, and dT_{kk}, only as functions of both applied forces dP_{ij}, and compliances.

Initial Isotropic Stress

A solution was first obtained for the case of small increments in stress applied to a medium under an initial isotropic stress σ_0. If the loading history up to this initial stress is homothetic then it may be shown from considerations of symmetry that the initial contact forces are all equal and have no tangential components. Using Equations [9] and the definition of stress, we find the initial contact forces to be $N_0 = \sqrt{(2)}(R^2\sigma_0)$. In addition, since the loading history at each contact is the same, the initial compliances do not vary from contact to contact. If, to the medium under the initial stress σ_0, additional arbitrary increments in stress are applied such that the total stress never departs from the initial stress by more than a small increment, approximate values for the compliances may be found by letting $L^* \to 0$ in the expressions for compliances. Thus, using Equations [7], one obtains for the tangential compliance

$$S = S_R = S_U = (2 - \nu)/4\mu a_0 \quad \ldots\ldots [13]$$

and the normal compliance is given by Equation [3] if a is replaced by a_0. For a given initial stress these compliances may be considered as constants; and Equations [9], [11], and [12] furnish a set of simultaneous linear equations in the increments of contact forces. The solution of these equations yields the following expressions

$$\left.\begin{aligned} dN_{zz},\ dN_{zz}' &= \sqrt{(2)}[(k+1)(dP_{zz} + dP_{yy}) \\ &\quad - (k-1)dP_{xx} \pm 2k(k+3)dP_{xy}/(k+1)]/8(k+3) \\ dT_{xy} &= dT_{xy}' = \sqrt{(2)}(dP_{xx} - dP_{yy})/4(k+3) \\ dT_{xz},\ dT_{xz}' &= (dP_{xz} \pm dP_{yz})/4(k+1) \end{aligned}\right\} \quad \ldots [14]$$

where

$$k = S/C = (2 - \nu)/2(1 - \nu)$$

and 12 others obtained by cyclical permutation of subscripts. In these expressions the upper signs refer to unprimed contact forces and lower signs to primed contact forces.

Having determined the contact forces it is now possible to obtain expressions for relative incremental displacements of the centers of spheres in terms of applied incremental forces. For example, the x-component of the relative incremental displacement of the centers of spheres A and D, Fig. 1, is given by (see Fig. 4)

$$d\Delta_{xx} = (d\alpha_{xy} + d\delta_{xy})/\sqrt{2} + (d\alpha_{xy}' + d\delta_{xy}')/\sqrt{2}$$

or

$$d\Delta_{xx} = C[(3k+1)dP_{xx} + (k-1)(dP_{yy} + dP_{zz})]/4(k+3) \quad \ldots\ldots [15]$$

by using Equations [12] and [14]. The same expression for $d\Delta_{xx}$ may be derived by using any other pair of neighboring spheres whose centers lie on a line parallel to the x-axis. The corresponding relations for $d\Delta_{yy}$ and $d\Delta_{zz}$ are obtained by the same method, and are expressed by a cyclical permutation of subscripts in Equation [15]. Defining incremental extensional strain as

$$d\epsilon_{ii} = d\Delta_{ii}/2\sqrt{(2)}R$$

where $2\sqrt{(2)}R$ is the length of an edge of the cube, one obtains

$$d\epsilon_{xx} = \sqrt{(2)}RC[(3k+1)d\sigma_{xx} + (k-1)(d\sigma_{yy} + d\sigma_{zz})]/2(k+3) \quad \ldots [16]$$

for the x-component of incremental extensional strain.

Incremental shear-strain components are defined as the changes in the angles between adjacent faces of the cube. For example, the change in the angle CDA, Fig. 1, is obtained by adding to the x-component of the displacement of C relative to D the y-component of the displacement of A relative to D, and dividing by the length of a side, $2\sqrt{(2)}R$. This sum is

$$d\gamma_{xy} = (d\alpha_{xy} + d\delta_{xy} - d\alpha_{xy}' - d\delta_{xy}')/4R + (d\alpha_{xy} - d\delta_{xy} - d\alpha_{xy}' + d\delta_{xy}')/4R$$

which becomes

$$d\gamma_{xy} = [2\sqrt{(2)}RS/(k+1)]d\sigma_{xy} \quad \ldots\ldots [17]$$

by using Equations [12], [14], and the definition of stress. The same expression for this component of incremental shear strain may be obtained by basing the derivation on the change in the angle formed by any other two edges of the cube which lie in the x, y-plane.

From differential strain-stress relations of the type of Equations [16] and [17] one obtains the differential stress-strain relations

$$\left.\begin{aligned} d\sigma_{xx} &= c_{11}d\epsilon_{xx} + c_{12}(d\epsilon_{yy} + d\epsilon_{zz}) \\ d\sigma_{yy} &= c_{11}d\epsilon_{yy} + c_{12}(d\epsilon_{zz} + d\epsilon_{xx}) \\ d\sigma_{zz} &= c_{11}d\epsilon_{zz} + c_{12}(d\epsilon_{xx} + d\epsilon_{yy}) \\ d\sigma_{xy} &= 2c_{44}d\epsilon_{xy} \\ d\sigma_{xz} &= 2c_{44}d\epsilon_{xz} \\ d\sigma_{yz} &= 2c_{44}d\epsilon_{yz} \end{aligned}\right\} \quad \ldots\ldots [18]$$

where

$$c_{11} = 2c_{44} = \frac{1}{\sqrt{(2)}R}\left(\frac{1}{C} + \frac{1}{S}\right) = \frac{4 - 3\nu}{2 - \nu}\left[\frac{3\mu^2\sigma_0}{2(1-\nu)^2}\right]^{1/3}$$

$$c_{12} = \frac{1}{2\sqrt{(2)}R}\left(\frac{1}{C} - \frac{1}{S}\right) = \frac{\nu}{2(2 - \nu)}\left[\frac{3\mu^2\sigma_0}{2(1-\nu)^2}\right]^{1/3}$$

Initial Isotropic and Uniaxial Stress

When an isotropic stress is applied homothetically to a medium composed of identical spheres in a face-centered cubic array the forces do not vary from one contact to another. Hence, in deriving the stress-strain relation given by Equations [18], it was not necessary to distinguish between different contacts in the medium in the expressions for the compliances. As a result, integration of Equations [18] over finite increments in stress is limited to increments in which the stress remains always isotropic, because for any other stress increment the contact forces and hence the compliances will vary from contact to contact. To obtain a stress-strain relation which may be integrated over other than isotropic increments, the derivation must be performed anew, distinguish-

ing between compliances at contacts with different loading histories.

As an example of such a derivation, consider the case in which the stress, in terms of the co-ordinate axes in Fig. 1, is given by

$$\left.\begin{aligned} \sigma_{xx} = \sigma_{yy} = \sigma_0, \qquad \sigma_{zz} = \sigma_0 + \sigma_a \\ \sigma_{yz} = \sigma_{zx} = \sigma_{xy} = 0 \end{aligned}\right\} \quad \ldots\ldots [19]$$

and for which the entire load history is one which always can be described by variations of σ_0 and σ_a. Then during the entire load history, the three planes through the center of the elementary cube, Fig. 1, which are parallel to the co-ordinate planes are planes of symmetry. Also the vertical planes through the diagonals of the horizontal faces are planes of symmetry. For each pair of contacts lying on opposite sides of planes of symmetry the contact forces must be mirror images of each other. Hence

$$\left.\begin{aligned} N_{xy} = N_{xy}' \qquad N_{yz} = N_{yz}' = N_{zx} = N_{zx}' \\ T_{xy} = T_{xy}' = 0, \qquad T_{yz} = T_{yz}' = -T_{zx} = -T_{zx}' \\ T_{xx} = T_{xx}' = T_{yy} = T_{yy}' = T_{zz} = T_{zz}' = 0 \end{aligned}\right\} \quad .. [20]$$

during application of this load. Since contacts with identical load histories have equal compliances, one can define

$$\left.\begin{aligned} C_1 = C_{xy} = C_{xy}', \qquad C_2 = C_{yz} = C_{yz}' = C_{zx} = C_{zx}' \\ S_1 = S_{xy} = S_{xy}', \qquad S_1 = S_{yz} = S_{yz}' = S_{zx} = S_{zx}' \\ S_1 = S_{xx} = S_{xx}', \qquad S_2 = S_{yy} = S_{yy}' = S_{zz} = S_{zz}' \end{aligned}\right\} \quad .. [21]$$

which may be inserted in Equations [12]. These compliances are still unknown. However, Equations [9], [11], and [12] may be solved simultaneously to provide expressions for the increments of contact forces in terms of the compliances and the increments of applied load. Such a solution gives

$$\left.\begin{aligned} dN_{xy}, dN_{xy}' &= B_1(C_2 + S_2)(dP_{xx} + dP_{yy}) \\ &\quad - B_1(S_2 - C_2)dP_{zz} \pm \sqrt{(2)}B_4S_2dP_{xy} \\ dT_{xy} = dT_{xy}' &= 2B_1C_2S_2(dP_{xx} - dP_{yy}) \\ dT_{xz}, dT_{xz}' &= \sqrt{(2)}B_2C_2(S_2 + S_2)(dP_{xx} \pm dP_{yz}) \\ dN_{yz}, dN_{yz}' &= B_1C_1(dP_{xx} + dP_{yy}) \\ &\quad - B_2S_1S_2\,(dP_{xx} - dP_{yy}) + B_1(C_1 + S_2)dP_{zz} \pm B_2dP_{yz} \\ dT_{yz}, dT_{yz}' &= B_1C_1(dP_{xx} + dP_{yy}) \\ &\quad - B_2C_2S_1(dP_{xx} - dP_{yy}) - B_1(C_1 + C_2)dP_{zz} \\ &\quad \pm B_2(S_1 - S_1)C_2dP_{yz} \\ dT_{xx}, dT_{xx}' &= B_4C_1dP_{xy} \pm \sqrt{(2)}B_2C_2(S_2 + S_1)dP_{xz} \\ dN_{xx}, dN_{xx}' &= B_1C_1(dP_{xx} + dP_{yy}) \\ &\quad + B_2S_1S_2(dP_{xx} - dP_{yy}) + B_1(C_1 + S_2)dP_{zz} \pm B_2dP_{xz} \\ dT_{xz}, dT_{xz}' &= -B_1C_1(dP_{xx} + dP_{yy}) \\ &\quad + B_2C_2S_1(dP_{yy} - dP_{xx}) + B_1(C_1 + C_2)dP_{zz} \\ &\quad \pm B_2(S_1 - S_2)C_2dP_{xz} \\ dT_{yy}, dT_{yy}' &= \pm B_4C_1dP_{xy} + \sqrt{(2)}B_2C_2(S_2 + S_1)dP_{yz} \end{aligned}\right\} \quad .. [22]$$

where the upper signs refer to the unprimed contact forces and lower signs to the primed contact forces, and where

$$B_1 = 1/4\sqrt{(2)}(2C_1 + C_2 + S_2)$$
$$B_2 = 1/2\sqrt{(2)}(2C_2S_2 + 2S_2S_1 + S_2S_2 + S_2S_2 + C_2S_1 + C_2S_2)$$
$$B_3 = 1/4\sqrt{(2)}(2C_2S_2 + S_1C_2 + S_1S_2)$$
$$B_4 = 1/4(C_1 + S_2)$$
$$B_5 = B_2(2S_2S_1 + S_2S_2 + S_2S_1)$$

Proceeding with the solution of the problem by the same method as that used for the initial isotropic stress, one obtains for the differential stress-strain relation

$$\left.\begin{aligned} d\sigma_{xx} &= c_{11}d\epsilon_{xx} + c_{12}d\epsilon_{yy} + c_{13}d\epsilon_{zz} \\ d\sigma_{yy} &= c_{12}d\epsilon_{xx} + c_{11}d\epsilon_{yy} + c_{13}d\epsilon_{zz} \\ d\sigma_{zz} &= c_{13}d\epsilon_{xx} + c_{13}d\epsilon_{yy} + c_{33}d\epsilon_{zz} \\ d\sigma_{yz} &= 2c_{44}d\epsilon_{yz} \\ d\sigma_{zx} &= 2c_{44}d\epsilon_{zx} \\ d\sigma_{xy} &= 2c_{66}d\epsilon_{xy} \end{aligned}\right\} \quad \ldots\ldots [23]$$

where

$$c_{11} = (C_1^{-1} + S_1^{-1} + C_2^{-1} + S_2^{-1})/2\sqrt{(2)}R$$
$$c_{12} = (C_1^{-1} - S_1^{-1})/2\sqrt{(2)}R, \quad c_{33} = (C_2^{-1} + S_2^{-1})/\sqrt{(2)}R$$
$$c_{13} = (C_2^{-1} - S_2^{-1})/2\sqrt{(2)}R, \quad c_{66} = (C_1^{-1} + S_1^{-1})/2\sqrt{(2)}R$$
$$c_{44} = \frac{1}{2\sqrt{(2)}R}\left[\frac{1}{C_2} + \frac{2S_2 + S_1 + S_2}{2S_1S_2 + S_2(S_1 + S_2)}\right]$$

As pointed out before, the compliances in these equations depend upon stress history, and are determined for each particular case in accordance with the results given in reference (8).

To obtain the strain resulting from finite increments in stress it is necessary to integrate Equations [23] over the stress history. However, integration of these equations is limited to increments in stress describable in terms of variations of σ_0 and σ_a. To determine the compliances in Equations [23] the contact forces must be obtained by an integration of Equation [22]. Using the definition of stress, and inserting the values of stress given by Equations [19] into Equations [22], one obtains for the quantities to be integrated for the contact forces

$$\left.\begin{aligned} dN_{xy} &= B_3R^2[(3C_2 + S_2)d\sigma_0 + (C_2 - S_2)d\sigma_a] \\ dN_{yz} &= B_3R^2[(3C_1 + S_2)d\sigma_0 + (C_1 + S_1)d\sigma_a] \\ dT_{yz} &= -B_3R^2[(C_2 - C_1)d\sigma_a + (C_2 + C_1)d\sigma_a] \end{aligned}\right\} \quad .. [24]$$

where

$$B_3 = \sqrt{(2)}/(2C_1 + C_2 + S_2)$$

and, as a result of Equations [20]

$$dN_{xy} = dN_{xy}'$$
$$dN_{yz} = dN_{yz}' = dN_{zx} = dN_{zx}'$$
$$dT_{yz} = dT_{yz}' = -dT_{zx} = -dT_{zx}'$$

and the remaining tangential forces are zero. At each step in the loading history, the expressions for the compliances are the same in Equations [23] and [24]. If, for any particular case, Equations [24] can be integrated, the compliances can be evaluated and, hence, the coefficients in the differential stress-strain relation will be known functions of stress.

For infinitesimal increments in stress Equations [23] may be used without integration to give the relation between stress and strain. The medium must be under an initial stress whose entire history is describable in terms of σ_0 and σ_a, and the additional arbitrary increments in stress must be such that the total stress never departs from the initial stress by more than a small incre-

ment. The compliances are made to depend solely on initial stress by finding the limit as the increments in the contact forces approach zero. The values of the initial contact forces to be used to determine the compliances are obtained by an integration of Equations [24] over the past stress history up to the initial stress. Once this integration has been performed Equations [23] may be used directly for the relation between stress and strain.

Application of Differential Stress-Strain Relations to Wave Propagation in a Granular Bar

The differential stress-strain Relations [18] are applicable, without integration, to a study of the problem of wave propagation as long as the stress increments accompanying the wave disturbance are small in comparison with the initial stress on the medium. Experiments were performed in which compressional waves were propagated in granular bars. These bars were constructed of steel bearing balls arranged in a face-centered cubic array and were subjected to an initial isotropic stress σ_0. As may be seen from Equations [18] the medium is anisotropic, so that the velocity of compressional waves in a bar of the granular medium depends upon the orientation of the bar with respect to the symmetry axes of the medium. The axes of the granular bars constructed were oriented in either of two directions: bar A in the [100] direction, and bar B in the [110] direction. (These orientations were chosen to avoid a coupling with flexural waves.) If the linear dimensions of the cross section of the bar are sufficiently small in comparison with the wave length, the elementary theory of longitudinal vibrations of slender bars may be employed to find the expression for the wave velocity in terms of the material constants. In the present case, we find.

$$\left.\begin{aligned} \rho_M v_A^2 &= c_{11} - \frac{2c_{12}^2}{c_{11}+c_{12}} = \frac{2(8-7\nu)}{(8-5\nu)}\left[\frac{3\mu^2\sigma_0}{2(1-\nu)^2}\right]^{1/3} \\ \rho_M v_B^2 &= \frac{4c_{44}(c_{11}-c_{12})(c_{11}+2c_{12})}{2c_{11}c_{44}+(c_{11}-c_{12})(c_{11}+2c_{12})} \\ &= \frac{2(4-3\nu)(8-7\nu)}{(4-3\nu)^2+(8-7\nu)(2-\nu)}\left[\frac{3\mu^2\sigma_0}{2(1-\nu)^2}\right]^{1/3} \end{aligned}\right\} \quad [25]$$

where ρ_M is the mass density of the granular medium, i.e., the density of the material of the spheres multiplied by $\pi/3\sqrt{2}$, the packing of the spheres. For steel balls the velocities become

$$v_A = 1330\sigma_0^{1/3}\ \text{fps}, \qquad v_B = 1350\sigma_0^{1/3}\ \text{fps} \quad [26]$$

where σ_0 is in pounds per square inch.

It is interesting to compare the velocities in Equations [25] and [26], which are based on the theories of Cattaneo (6), Mindlin (7), and Mindlin and Deresiewicz (8), with the expressions obtained when the effect of the tangential forces acting at the contacts is neglected. If only normal forces act at the contacts the elastic contants of the medium are

$$c_{11} = 2c_{12} = 2c_{44} = 1/\sqrt{2}RC$$

so that

$$\rho_M v_A^2 = \frac{2}{3}\left[\frac{3\mu^2\sigma_0}{2(1-\nu)^2}\right]^{1/3} \qquad \rho_M v_B^2 = \left[\frac{3\mu^2\sigma_0}{2(1-\nu)^2}\right]^{1/3}$$

give the velocities of longitudinal waves for slender granular bars. These velocities are

$$v_A = 800\sigma_0^{1/3}\ \text{fps}, \quad v_B = 980\sigma_0^{1/3}\ \text{fps}$$

for bars made of steel balls.

Description of Experiment

The granular bars were constructed of steel bearing balls arranged in a face-centered cubic array (Table 1). The balls were held in place by an externally applied hydrostatic pressure, Fig. 5. Velocities of longitudinal waves were determined by resonance tests, and the rate of energy dissipation was found from observations of the decay of free vibrations.

Table 1 Description of Granular Bars

Miller indexes for longitudinal axis of bar	Length, in.	Length to width ratio	Number of spheres in bar	Number of contacts in bar
[1, 0, 0]	4.243	7.99	1201	5796
[1, 1, 0]	5.1266	8.12	1869	9228

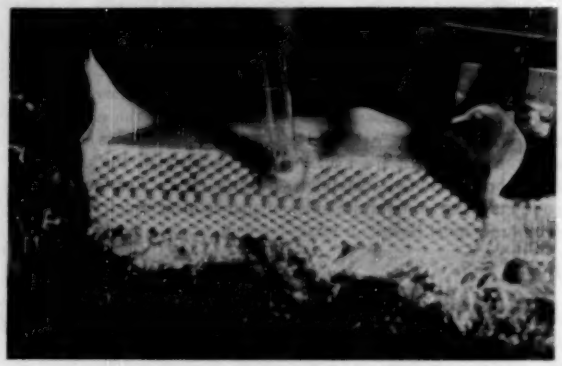

Fig. 5 Experimental Bar Under a Pressure of 1 Atm

The stainless-steel balls (AISI No. 440C) were of $^1/_8$ in. diam and of either of two dimensional tolerances: $\pm 50 \times 10^{-6}$ in. or $\pm 10 \times 10^{-6}$ in. The balls were cleaned in successive baths of carbon tetrachloride, toluol, and acetone, and carefully packed in a face-centered cubic array. During packing the arrangement of the balls was preserved by holding them in a box. The inside of the box contained indentations to prevent rolling of the balls and the box was lined with a thin rubber sheet (0.007 in. thick). After packing was completed, the rubber sheet was wrapped about the array of balls, closed, and sealed. The sealed bag was evacuated, locking the balls in place and permitting the bar to be removed from the box. Evacuation was performed through a glass tube piercing the rubber sheet at the mid-point of the bar, i.e., at a node of the odd harmonics.

During the tests the bar was supported along its entire length by a polished lucite surface lubricated by a thin coat of powdered talc. This type of support avoided bending of the bar, which would have changed the values of the compliances at the contacts between the steel balls.

Wave velocities were found from measurements of resonant frequencies of the bars. The drive was provided by an induction coil and a permanent magnet placed at one end of the bar. At the other end a crystal phonograph pick-up connected to a vacuum tube audio-voltmeter measured the response of the bar. Maximum-voltage output determined the resonant frequency, and the shape of the output was observed on an oscilloscope.

In order to measure the amplitude of displacement of the ends of the bar a short piece of a sewing-needle was inserted in a sphere at each end of the bar and made to protrude through the rubber sheet. The tip of the phonograph needle was placed against the projection. Calibration was performed at various frequencies over a range of amplitudes by comparing output voltage with known amplitudes as measured by means of a microscope.

Energy dissipation was determined by photographic observation of the decay of free vibrations. The exciting voltage was cut off by a synchronizing switch which also initiated

the single sweep of the oscillograph. Observation of the steady motion immediately before cut-off was provided by using a variable time delay in the switch. Amplitude calibration was performed by measuring the voltage output of the phonograph pickup prior to cutoff. The frequency of the vibrations provided the time scale.

Results of Resonance Tests

Figs. 6 and 7 show experimental frequencies together with theoretical values. Results are in close agreement with predicted values, and closer to values based on the theory which includes both normal and tangential contact forces than to values based on the theories which neglect tangential contact forces (1, 2, 3, 4). In addition, as the dimensional tolerance of the balls is improved, the measured velocities tend to approach the theory which includes both the normal and tangential contact forces.

In the case of higher tolerance balls the dependence of wave velocity upon pressure was very nearly as predicted. Variation with the $^1/_4$th power of pressure was followed down to about 10 psi, changing slowly for lower pressures. For the [110] orientation velocities decreased more rapidly with pressure presumably because, in this orientation, the balls on the edge of the bar did not all lie within the same vertical plane, so that the packing was loosened by the weight of the balls themselves.

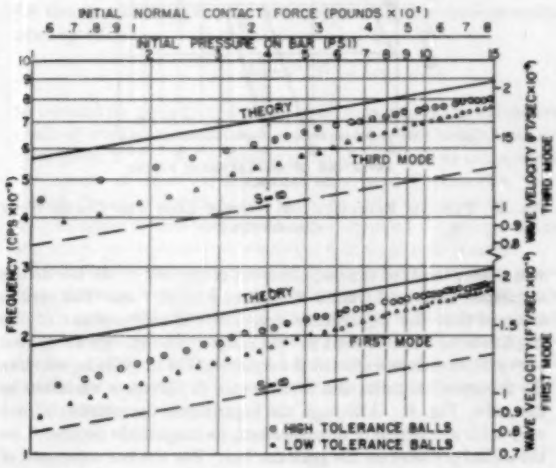

Fig. 6 Resonant Frequency of Bar as a Function of Pressure for [1, 0, 0] Orientation

In a close-packed arrangement of identical spheres under an isotropic stress the normal forces at the contacts would all be equal, as would the relative approaches of the centers of the spheres in contact. However, this is not true in practice, because of dimensional variations in the balls. A comparison of tolerances with relative approach, Table 2, shows that in this experiment there probably were contacts which did not make at all, even in the case of the better tolerance and the highest pressures used. Thus

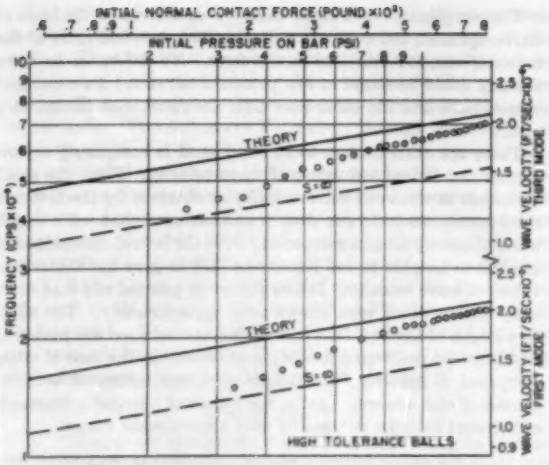

Fig. 7 Resonant Frequency of Bar as a Function of Pressure for [1, 1, 0] Orientation

the stiffness of the medium is diminished and wave velocities are reduced as compared with a bar of identical spheres. Such an effect should be more pronounced for poorer tolerances and at lower pressures. Experimental results are consistent with these conclusions.

Referring to Fig. 6, it may be seen that a change in tolerance affects the levels of the experimental curves. This may be ascribed to the fact that the difference in tolerances between the two samples of balls used is large compared to the relative approaches, so that presumably the number of contacts making is substantially larger in one bar than in the other. In addition, for the poorer tolerance balls, the change in relative approach for a pressure change of 1 atm is small as compared to the dimensional tolerance, so that the number of contacts making is probably not very different at the two pressure extremes. As indicated in Fig. 6, the change in slope with pressure for the poorer tolerance balls was much less than for the higher tolerance balls, for which, presumably, there is an appreciable change in the number of contacts making as the pressure is changed by 1 atm.

Additional improvements in the tolerance probably would produce further increases in wave velocity. However, once the dimensional tolerances become less than the relative approaches it is expected that the changes in the wave velocity would be smaller.

Since the theoretical relation between stress and strain is limited to differential increments, it was necessary in the experiment to limit stress increments to small quantities. In order to determine the effect of the magnitude of the stress increments used, measurements were made of the variation of resonant frequency with amplitude of motion. It was found that the frequency was increased by about 1 per cent when the amplitude of the end of the bar was reduced from 12×10^{-7} to 2×10^{-7} in. The frequency tests were made at the latter amplitude.

Table 2 Behavior of Spheres in Contact in a Face-Centered Cubic Medium Under an Isotropic Stress

		Hertz theory						Dimensional tolerance of balls in experiment, in. × 10^{-6}	
σ_0, psi	N_0, lb	Max normal stress, psi	Max shear stress, psi	Contact radius, in. × 10^{-4}	Relative approach, in. × 10^{-4}	Normal compliance, $\frac{\text{in.}}{\text{lb}} \times 10^{-4}$	Tangential compliance, $\frac{\text{in.}}{\text{lb}} \times 10^{-4}$	Lower	Higher
2.00	0.01105	86300	26750	2.48	1.955	1.178	1.428	±50	±10
5.00	0.0276	117100	36300	3.36	3.60	0.869	1.053	±50	±10
10.00	0.0552	147200	45600	4.23	5.71	0.690	0.837	±50	±10
14.70	0.0812	167000	52000	4.81	7.39	0.607	0.737	±50	±10

The compliances used in the theory were derived on the basis of elastic spheres, and evidence indicates that the yield limit of the material was not exceeded in the tests. No difference in wave velocity could be found at low pressures between bars composed of new balls and the same bars after they had been loaded to 1 atm.

There are other factors to be considered in comparing experimental and theoretical values of wave velocity. First, the small difference in observed wave velocity as obtained by the first and third harmonics (0.75 per cent) is an indication that wave length was sufficiently long in comparison with the lateral dimensions of the bar to be able to use Equations [25] to give the theoretical values of wave velocity. It also should be pointed out that there were factors which were known only approximately. The effective length of the bar, that is, the distance between the planes at which the waves were reflected, is unknown, in the case of a bar composed of spheres. The length used was measured between centers of end spheres. Lastly, the values of the elastic constants of the steel balls are necessarily only approximate values.

Energy Dissipation in a Granular Bar

The logarithmic decrement δ, defined by

$$\delta = \log (A_i/A_{i+1}) \quad [27]$$

was obtained from observation of the decay of free vibrations. In this expression A_i and A_{i+1} are successive amplitudes of the displacement of the end of the bar as determined, in this experiment, from oscillograph records of the decay.

Since the relation between stress and strain is assumed linear, the experimental values of energy loss, per cycle, of the bar may be obtained from

$$W_T = 2\delta W_E \quad [28]$$

whenever $\delta^2 \ll 1$; where W_E is the maximum elastic energy of the bar during a cycle. Under the assumptions of the classical one-dimensional wave theory, the incremental strain energy per unit length of the bar is given by

$$\frac{1}{2} Sd\sigma d\epsilon = \frac{1}{2} S\left[c_{11} - \frac{2c_{12}^2}{c_{11} + c_{12}}\right](d\epsilon)^2$$

where S is the cross-sectional area of the bar, and where $d\sigma$ and $d\epsilon$ are, respectively, the increments in the longitudinal components of stress and strain in the bar. By taking a sinusoidal displacement distribution along the length of the bar one obtains

$$W_E = \frac{S}{l}\left(\frac{A\pi}{2}\right)^2\left[c_{11} - \frac{2c_{12}^2}{c_{11} + c_{12}}\right] \quad [29]$$

where A is the amplitude at the end of the bar and l is the length of the bar.

The theoretical frictional energy loss per cycle for the bar (F_T) was found by a summation of the energy dissipated at the individual contacts as given by Equation [8], and by taking a sinusoidal displacement distribution along the length of the bar. The damping tests were performed on bars oriented in the [100] direction, in which case

$$F_T = 293.9 \times 10^6(0.816 - f^2)A^2/f\sigma_0^{1/3} \quad [30]$$

and, from Equations [28] and [29]

$$W_T = 4.54 \times 10^4\sigma_0^{1/3}\delta A^2 \quad [31]$$

for the size of bar used.

Results of Decay Tests

Values of logarithmic decrement were obtained from oscillographic recordings of the decay of free vibrations. Measurements were made of the displacement of the end of the bar as the amplitude decreased from 5×10^{-7} to 1×10^{-7} in. The results indicate that the logarithmic decrement is independent of the amplitude of displacement in this range. The energy dissipated per cycle, therefore, varies as the square of the amplitude, whereas the theory of Mindlin and Deresiewicz (8) predicts variation as the cube, Fig. 8. Although the logarithmic decrement did not vary with amplitude of displacement, its magnitude depended on the initial pressure on the granular bar. For the bar composed of the better tolerance balls the values of logarithmic decrement ranged from 0.054 at a pressure of 14.7 psi to 0.129 at a pressure of 1.92 psi. For the bar composed of the poorer tolerance balls the logarithmic decrement was about 25 per cent smaller. However, the dependence of the rate of energy loss on the square of amplitude of displacement was obtained for either tolerance of balls and for the entire pressure range of the tests. The significance of these results can be better evaluated when considered in conjunction with the results of the experiments of Mindlin, Mason, Osmer, and Deresiewicz (10), and of Johnson (9) on single contacts.

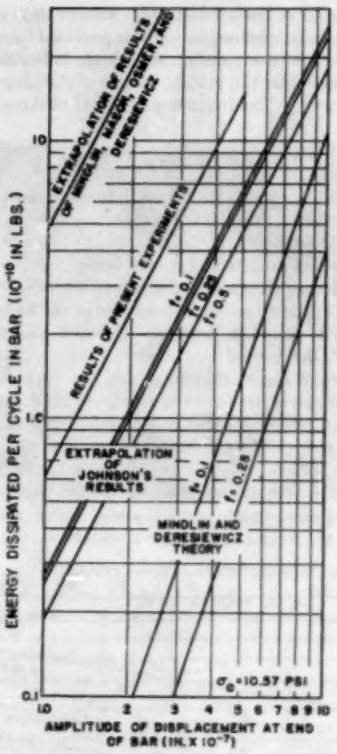

Fig. 8 Typical Variation of Energy Loss per Cycle With Amplitude

In his experiments, Johnson found, in general, close agreement between his results and predictions based on the theories of Mindlin (7) and Mindlin and Deresiewicz (8). This applies, in particular, to the tests which Johnson performed on the relation between the tangential force and the displacement for initial loading, for repeated loading, and for dynamic loading. As regards the damping tests, however, Johnson found that the energy loss was approximately of the magnitude predicted by the theory, but that the variation did not follow the predicted dependence on amplitude of displacement. In particular, he found that at very

small amplitudes the damping loss followed approximately a square law and only approached the law predicted by the theory at large amplitudes. A similar dependence on amplitude of displacement had been obtained previously by Mindlin, Mason, Osmer, and Deresiewicz (10) in their experiments.

All of the measurements of energy dissipation, to date, indicate that the assumed law of Coulomb friction is a reasonably good approximation over the portion of the annulus of slip where the relative displacement of the contiguous surfaces is large, but not in the neighborhood of the inner edge of the annulus where the relative displacement is small. At very small T/fN the latter region predominates and, accordingly, the theory fails to predict the correct law of energy dissipation. Since the dissipation is small, the stiffnesses are not appreciably affected by it and the theory gives good results for load versus displacement and for velocities of propagation even for small displacements of the spheres.

Fig. 8 shows the theoretical and experimental values of the rate of energy loss at the contacts. The curve marked "Extrapolation of Johnson's Results" was obtained in the following way: For small amplitudes of oscillation Johnson shows that his results tend toward a value given by the expression

$$W_D = 0.02(T^*)^3/\mu a \quad \ldots\ldots\ldots\ldots\ldots\ldots [32]$$

for the dissipation per cycle at a contact. If this value is multiplied by a factor of

$$1 - f^2/\beta^2$$

to account for the effect of an oblique force, and if the values are summed over all contacts in the granular bar one obtains the results given in Fig. 8. A similar method was used to extrapolate the results of Mindlin, Mason, Osmer, and Deresiewicz. Although the experiments do not yield the same rate of energy loss, they all agree in that they give a dependence on the square of the amplitude of displacement whenever this amplitude is small.

With respect to dependence of energy dissipation upon pressure, the significance of a comparison of the present tests with theory is somewhat uncertain since results, in this case, varied with dimensional tolerance. The theory predicts that energy dissipation will vary with the $-1/3$ power of initial pressure, while experimental results give a dependence on approximately the $-1/4$ power.

The principal source of error in the present tests affecting measurements of energy dissipation is the degree of cleanness of the balls. Thus improper cleaning of the balls (using only acetone for instance) easily doubled the values obtained for W_T. Another factor affecting energy dissipation was the dimensional tolerance of the balls. This influences W_T mainly through the number of contacts which will or will not be made within the granular bar. It was found that the value of W_T was lower for the poorer tolerance balls indicating that in this case dissipation occurs at fewer contacts. An increase in pressure will increase the number of contacts. However, for the pressure range over which the tests were made, this increase in the number of contacts was probably small. It had been expected that the change in the dimensional tolerance would not affect the variation of W_T with amplitude of displacement. This was borne out experimentally, and thus the results showing a variation of W_T with the square of the amplitude of displacement appear reliable from this standpoint.

BIBLIOGRAPHY

1 "Theorie der akustischen Schwingungsausbreitung in gekörnten Substanzen und Experimentelle Untersuchungen an Kohlepulver," by G. Hara, *Elektrische Nachrichtentechnik*, vol. 12, 1935, pp. 191–200.

2 "Velocity of Elastic Waves in a Granular Substance," by K. Iida, *Bulletin Earthquake Research Institute*, Japan, vol. 17, 1939, pp. 783–808.

3 "On the Theory of Elastic Waves in a Granular Substance," by T. Takahashi and Y. Satô, *Bulletin Earthquake Research Institute*, Japan, vol. 27, 1949, pp. 11–16; and vol. 28, 1950, pp. 37–43.

4 "Elastic Waves Through a Packing of Spheres," by F. Gassmann, *Geophysics*, vol. 16, 1951, pp. 673–685.

5 "Theory of Elasticity," by S. Timoshenko and J. N. Goodier, McGraw-Hill Book Company, Inc., New York, N. Y., 1951, pp. 372–377.

6 "Sul contatto di due corpi elastici," by C. Cattaneo, *Accademia dei Lincei, Rendiconti*, series 6, vol. 27, 1938, pp. 342–348, 434–436, and 474–478.

7 "Compliance of Elastic Bodies in Contact," by R. D. Mindlin, JOURNAL OF APPLIED MECHANICS, Trans. ASME, vol. 71, 1949, p. A-259.

8 "Elastic Spheres in Contact Under Varying Oblique Forces," by R. D. Mindlin and H. Deresiewicz, JOURNAL OF APPLIED MECHANICS, Trans. ASME, vol. 75, 1953 pp. 327–344.

9 "Surface Interaction Between Elastically Loaded Bodies under Tangential Forces," by K. L. Johnson, Proceedings of the Royal Society of London, series A, vol. 230, 1955, pp. 531–548.

10 "Effects of an Oscillating Tangential Force on the Contact Surfaces of Elastic Spheres," by R. D. Mindlin, W. P. Mason, T. F. Osmer, and H. Deresiewicz, Proceedings of the First U. S. National Congress of Applied Mechanics, 1951, pp. 203–208.

The Elastic Coefficients of the Theory of Consolidation

By M. A. BIOT[1] and D. G. WILLIS[2]

The theory of the deformation of a porous elastic solid containing a compressible fluid has been established by Biot. In this paper, methods of measurement are described for the determination of the elastic coefficients of the theory. The physical interpretation of the coefficients in various alternate forms is also discussed. Any combination of measurements which is sufficient to fix the properties of the system may be used to determine the coefficients. For an isotropic system, in which there are four coefficients, the four measurements of shear modulus, jacketed and unjacketed compressibility, and coefficient of fluid content, together with a measurement of porosity appear to be the most convenient. The porosity is not required if the variables and coefficients are expressed in the proper way. The coefficient of fluid content is a measure of the volume of fluid entering the pores of a solid sample during an unjacketed compressibility test. The stress-strain relations may be expressed in terms of the stresses and strains produced during the various measurements, to give four expressions relating the measured coefficients to the original coefficients of the consolidation theory. The same method is easily extended to cases of anisotropy. The theory is directly applicable to linear systems but also may be applied to incremental variations in nonlinear systems provided the stresses are defined properly.

1 Introduction

THE theory of the deformation of a porous elastic solid containing a viscous compressible fluid was established by Biot in several earlier papers (1, 2, 3, 4).[3] In reference (1) the isotropic case is considered, and in reference (2) the theory is generalized to anisotropic materials. General solutions to the elastic equations are established in reference (3). The theory of wave propagation in such systems is examined in reference (4).

Gassman (5, 6) has examined the properties of "open" and "closed" porous elastic systems corresponding to the case of constant pore pressure ($\sigma = 0$) and constant fluid content ($\zeta = 0$), respectively. The elastic properties of a porous solid were considered by Geertsma (7) who described methods for their measurement with jacketed and unjacketed compressibility tests, in the case of a homogeneous and isotropic porous matrix. Hughes and Cooke (8) described measurements of pore volume and porosity in jacketed compression tests, which would apply to a system containing an incompressible fluid completely filling the pores.

In the present paper methods of measurement are described for the determination of the elastic coefficients of references (1, 2, 3, 4). The physical interpretation of the elastic coefficients in various alternate forms is also discussed.

In Section 2 it is shown that the elastic coefficients A, N, Q, and R may be expressed in terms of four directly measurable coefficients μ, κ, δ, γ, and the porosity factor f. It is pointed out that under certain assumptions the coefficient γ does not need to be measured if we know the fluid compressibility c and already have measured δ and f. Other elastic coefficients μ, λ, α, and M are discussed in Section 3. They may be expressed in terms of the measurable coefficients μ, κ, δ, and γ without reference to porosity. Use of the constants μ, λ, α, and M are more convenient in application to consolidation problems, i.e., when the inertia forces are neglected, while A, N, Q, and R have been introduced in connection with wave propagation (4).

In addition to these four measurements it is possible to measure directly the constant α by a fifth and entirely independent measurement. This redundant information results from the fact that it is possible to define five physically different coefficients, two of which must be equal as a result of the assumption that we are dealing with a conservative elastic system. The redundancy thus provides a check on the validity of this assumption.

In Section 4 the case of transverse isotropy is considered using a different method and different measurements, and the case of general anisotropy is discussed in Section 5.

The measurements described are directly applicable to linear systems. They also will apply to incremental variations in nonlinear systems such as those having unconsolidated porous materials, provided the stresses are defined properly. This will be discussed in Section 6.

2 The Isotropic Case

The stress-strain relations for the isotropic case (2) are

$$\left.\begin{aligned} \sigma_{xx} &= 2Ne_{xx} + Ae + Q\epsilon \\ \sigma_{yy} &= 2Ne_{yy} + Ae + Q\epsilon \\ \sigma_{zz} &= 2Ne_{zz} + Ae + Q\epsilon \\ \sigma_{yz} &= Ne_{yz} \\ \sigma_{zx} &= Ne_{zx} \\ \sigma_{xy} &= Ne_{xy} \\ \sigma &= Qe + R\epsilon \end{aligned}\right\} \quad \ldots\ldots\ldots\ldots [1]$$

in which the σ_{ij} are the forces acting on the solid portions of the faces of a unit cube of porous material, and σ is the force acting on the fluid portions.

The average displacement vector of the solid has the components u_x, u_y, u_z, and that of the fluid U_x, U_y, U_z. The solid strain components are then given by

---

[1] Consultant, Shell Development Company, New York, N. Y. Mem. ASME.

[2] Shell Development Company, Exploration and Production Research Division, Houston, Texas. Now Research Scientist at Missile Systems Division, Lockheed Aircraft Company, Palo Alto, Calif.

[3] Numbers in parentheses refer to the Bibliography at the end of the paper.

Presented at the Applied Mechanics Division Summer Conference, Berkeley, Calif., June 13–15, 1957, of The American Society of Mechanical Engineers.

Discussion of this paper should be addressed to the Secretary, ASME, 29 West 39th Street, New York, N. Y., and will be accepted until January 10, 1958, for publication at a later date. Discussion received after the closing date will be returned.

Note: Statements and opinions advanced in papers are to be understood as individual expressions of their authors and not those of the Society. Manuscript received by ASME Applied Mechanics Division, January 22, 1957. Paper No. 57—APM-44.

$$\left.\begin{aligned} e_{xx} &= \frac{\partial u_x}{\partial x}, \quad e_{xy} = \frac{\partial u_y}{\partial y} + \frac{\partial u_x}{\partial x}, \ldots \text{etc.} \\ e &= e_{xx} + e_{yy} + e_{zz} \end{aligned}\right\} \quad \ldots\ldots [2]$$

The fluid dilatation ϵ is given by

$$\epsilon = \frac{\partial U_x}{\partial x} + \frac{\partial U_y}{\partial y} + \frac{\partial U_z}{\partial z} \quad \ldots\ldots [3]$$

It should be pointed out that this expression is not the actual strain in the fluid but simply the divergence of the fluid-displacement field which itself is derived from the average volume flow through the pores.

In Equations [1] attention is called to the fact that the properties of linearity alone would lead to five distinct elastic coefficients. The assumption that there exists a potential energy for the [illegible] reduces to four the number of independent elastic coefficients. This is the reason why the constant Q which appears in the last Equation [1] is the same as in the three first equations. An equivalent way of formulating this property is by stating that the matrix of elastic coefficients is symmetric with respect to the main diagonal. This symmetry property appears throughout when dealing with both isotropic and anisotropic media, and is further illustrated by Equation [30] and in the treatment of anisotropic media in Sections 4 and 5. The symmetry property is the reason for the redundancy in the measurement of the elastic coefficients. As will be pointed out, it is possible to derive the quantity $f(Q + R)/R$ from two independent physical measurements.

Four independent measurements, in addition to the porosity f, are required to fix the four elastic coefficients A, N, Q, and R. Satisfactory combinations of measurements may be made in a variety of different ways, but the most convenient appears to be the combination of measurement of shear modulus, jacketed and unjacketed compressibility of the porous solid, and an unjacketed coefficient of fluid content.

The shear modulus μ of the bulk material is equivalent to N, which is therefore obtained directly.

In the jacketed compressibility test, a specimen of the material is enclosed in a thin impermeable jacket and then subjected to an external fluid pressure p'.

To insure constant internal fluid pressure, the inside of the jacket may be made to communicate with the atmosphere through a tube. The conventional jacketed test is usually performed on a dry specimen, and in that case such precaution is of course not necessary. However, the dry specimen may not exhibit the same properties as the saturated one. As an example of this we may cite the case where the elastic properties result from surface forces of a capillary nature at the interface of the fluid and the solid.

The dilatation of the specimen is measured and a coefficient of jacketed compressibility κ is determined by

$$\kappa = -\frac{e}{p'} \quad \ldots\ldots [4]$$

In this test the entire pressure of the fluid is transmitted to the solid portions of the surfaces of the specimen.

Therefore

$$\sigma_{xx} = \sigma_{yy} = \sigma_{zz} = -p' \quad \ldots\ldots [5]$$

Furthermore, the pore pressure remains essentially constant

$$\sigma = 0 \quad \ldots\ldots [6]$$

In addition the solid strains will be

$$\left.\begin{aligned} \epsilon &= -\kappa p' \\ e_{xx} = e_{yy} &= e_{zz} = -\frac{\kappa p'}{3} \end{aligned}\right\} \quad \ldots\ldots [7]$$

From Equations [1] we obtain the two relations

$$\left.\begin{aligned} -p' &= -\frac{2}{3} N\kappa p' - A\kappa p' + Q\epsilon \\ 0 &= -Q\kappa p' + R\epsilon \end{aligned}\right\} \quad \ldots\ldots [8]$$

Eliminating ϵ and p gives

$$\frac{1}{\kappa} = \frac{2}{3} N + A - \frac{Q^2}{R} \quad \ldots\ldots [9]$$

thus indicating that the quantity $A - (Q^2/R)$ is equivalent to the Lamé coefficient λ of the porous material under conditions of constant pore pressure.

In the unjacketed compressibility test, a sample of the material is immersed in a fluid to which is applied a pressure p'. When the fluid pressure has penetrated the pores completely, the dilatation of the sample is then measured and an unjacketed compressibility coefficient δ is determined by

$$\delta = -\frac{e}{p'} \quad \ldots\ldots [10]$$

In this case the pressure acts both on the solid portion $(1 - f)$ and the fluid portion f of the surfaces of the specimen giv[illegible]

$$\sigma_{xx} = \sigma_{yy} = \sigma_{zz} = -(1 - f)p'$$

$$\sigma = -fp' \quad \ldots\ldots [11]$$

The strains are given by

$$\left.\begin{aligned} e_{xx} = e_{yy} = e_{zz} &= -\frac{\delta p'}{3} \\ e &= -\delta p' \end{aligned}\right\} \quad \ldots\ldots [12]$$

And we obtain from Equations [1] the relation

$$1 - \left(\frac{Q + R}{R}\right) f = \left[\frac{2}{3} N + \left(A - \frac{Q^2}{R}\right)\right] \delta \quad \ldots\ldots [13]$$

giving with Equation [9]

$$\left(\frac{Q + R}{R}\right) f = 1 - \frac{\delta}{\kappa} \quad \ldots\ldots [14]$$

An independent and redundant measurement of this expression is furnished if we consider the quantity $f(e - \epsilon)$, which is denoted by ζ in Section 3, and represents the volume of fluid which enters the pores of a unit volume of bulk material. If, during a jacketed compressibility test the interior of the jacket is connected to the atmosphere by a tube the fluid volume passing through this tube is equal to $f(e - \epsilon)$. Putting $\sigma = 0$ in the last Equation [1] yields

$$\left(\frac{Q + R}{R}\right) f = \frac{f(e - \epsilon)}{\epsilon} \quad \ldots\ldots [15]$$

Since we also have measured the solid strain e, this again yields the value of the quantity

$$\frac{(Q + R)f}{R}$$

Measurements of changes in pore volume and porosity in a

jacketed test have been made by Hughes and Cooke (8), which are equivalent to measurements of $f(e - \epsilon)$.

To fix the properties of the system, one additional measurement is required which must involve the fluid strain. There is apparently no standard test which would provide a satisfactory measurement, and we must therefore define a new elastic coefficient. Again we consider the volume of fluid which enters the pores of a unit volume of porous material, $f(e - \epsilon)$, but in this case with reference to an unjacketed compressibility test. We may define a coefficent γ of fluid content by

$$\gamma = \frac{f(e - \epsilon)}{p'} \quad [16]$$

for an unjacketed compressibility test. This gives for the fluid strain

$$\epsilon = -\frac{\gamma}{f} p' + e \quad [17]$$

or

$$\epsilon = -\frac{\gamma}{f} p' + \delta p' \quad [18]$$

Expressions [17] and [18] substituted into the last of Equations [1] give

$$f = Q\delta + R\delta + R\frac{\gamma}{f} \quad [19]$$

Summarizing the measurements

$$\left.\begin{aligned} N &= \mu \\ \frac{2}{3}N + \left(A - \frac{Q^2}{R}\right) &= \frac{1}{\kappa} \\ \left(\frac{Q+R}{R}\right) f &= \left(1 - \frac{\delta}{\kappa}\right) \\ f &= Q\delta + R\delta + R\frac{\gamma}{f} \end{aligned}\right\} \quad [\ldots 20]$$

These equations are easily solved for N, A, Q, and R to give their values in terms of the measured parameters

$$\left.\begin{aligned} N &= \mu \\ A &= \frac{\frac{\gamma}{\kappa} + f^2 + (1-2f)\left(1 - \frac{\delta}{\kappa}\right)}{\gamma + \delta - \frac{\delta^2}{\kappa}} - \frac{2}{3}\mu \\ Q &= \frac{f\left(1 - f - \frac{\delta}{\kappa}\right)}{\gamma + \delta - \frac{\delta^2}{\kappa}} \\ R &= \frac{f^2}{\gamma + \delta - \frac{\delta^2}{\kappa}} \end{aligned}\right\} \quad [21]$$

The coefficient of fluid content γ may be determined by the following experiment: A unit volume of porous material containing fluid is placed within a closed chamber which has been filled with fluid. Fluid is then injected into the chamber under pressure and the volume of injected fluid is measured. Care must be exercised that the pores of the specimen are completely saturated with the same fluid or mixture of fluids as existed in the original system. In particular for a liquid-saturated solid it is important that no air be trapped in the pores near the surface. The volume of fluid injected per unit pressure will be the sum of the solid compressibility δ, the volume of fluid which has entered the pores γ, and a fixed quantity depending upon the elastic properties of the chamber and the fluid. The porous material is then removed from the chamber and its volume replaced by fluid. The volume of fluid injected per unit pressure is again measured and in this case will be the sum of the same fixed quantity as in the previous measurement, and the fluid compressibility c representing the new unit volume occupied by the fluid. Therefore the difference between the volumes injected with and without the porous material in the chamber will be given by

$$\Delta V = \delta + \gamma - c \quad [22]$$

If the fluid compressibility c is then measured independently, the coefficient of fluid content γ may then be determined. There are of course ways of avoiding this additional measurement of the fluid compressibility, which is not directly relevant, but the procedures involved appear to be more elaborate.

For the special case in which the material of the porous matrix is homogeneous and isotropic and the fluid completely saturates the pores, it is possible to determine the coefficient of fluid content γ directly from the fluid compressibility c. Considering the unjacketed test, the pore space in this special case will undergo the same strain as the solid matrix. Therefore the porosity f of the material will not undergo any strain and, if the fluid completely saturates the pores, the fluid dilatation will be given by

$$\epsilon = -cp' \quad [23]$$

This gives for the coefficient of fluid content

$$\gamma = f(c - \delta) \quad [24]$$

This relation will be strictly valid only for materials such that the pore volume and the bulk volume remain in constant ratio; i.e., the porosity does not vary when the specimen is subjected to fluid pressure in an unjacketed test. This of course will be true if the material of the porous matrix is homogeneous, isotropic, and elastically linear.

However, this is not a necessary condition, and we may visualize cases where the matrix material is heterogeneous but behaves approximately like a homogeneous solid so that it undergoes approximately the same strain as the pores in an unjacketed test. Therefore Relation [24] may provide a satisfactory approximation for γ in many cases. On the other hand, one also could imagine a porous matrix which is statistically isotropic but does not behave in isotropic fashion when considered from the standpoint of the individual pores.

Further remarks concerning the validity of Relation [24] will be made in Section 6 in connection with its application to incremental stresses.

3 Elastic Coefficients with Alternative Variables

As shown in reference (3), it is possible to introduce as alternative variables the total forces acting on the surfaces of a unit cube

$$\left.\begin{aligned} \tau_{xx} &= \sigma_{xx} + \sigma \\ \tau_{yy} &= \sigma_{yy} + \sigma \\ \tau_{zz} &= \sigma_{zz} + \sigma \\ \tau_{yz} &= \sigma_{yz} \\ \tau_{zx} &= \sigma_{zx} \\ \tau_{xy} &= \sigma_{xy} \end{aligned}\right\} \quad [25]$$

the fluid pressure p, and the fluid content, already mentioned

$$\zeta = f(e - \epsilon) \quad [26]$$

We use the Lamé coefficients μ and[4]

$$\lambda = A - \frac{Q^2}{R} \quad [27]$$

and two new coefficients $M = \frac{R}{f^2}$

$$\alpha = \left(\frac{Q + R}{R}\right) f \quad [28]$$

With these variables and coefficients Equations [1] may be written

$$\left.\begin{aligned} \tau_{xx} + \alpha p &= 2\mu e_{xx} + \lambda e \\ \tau_{yy} + \alpha p &= 2\mu e_{yy} + \lambda e \\ \tau_{zz} + \alpha p &= 2\mu e_{zz} + \lambda e \\ \tau_{yz} &= \mu e_{yz} \\ \tau_{zx} &= \mu e_{zx} \\ \tau_{xy} &= \mu e_{xy} \\ \zeta &= \frac{1}{M} p + \alpha e \end{aligned}\right\} \quad [29]$$

An alternate form of these equations is obtained by solving the last equation for p and substituting in the first three. We find

$$\left.\begin{aligned} \tau_{xx} &= 2\mu e_{xx} + (\lambda + \alpha^2 M)e - \alpha M\zeta \\ \tau_{yy} &= 2\mu e_{yy} + (\lambda + \alpha^2 M)e - \alpha M\zeta \\ \tau_{zz} &= 2\mu e_{zz} + (\lambda + \alpha^2 M)e - \alpha M\zeta \\ \tau_{yz} &= \mu e_{yz} \\ \tau_{zx} &= \mu e_{zx} \\ \tau_{xy} &= \mu e_{xy} \\ p &= -\alpha M e + M\zeta \end{aligned}\right\} \quad [30]$$

These equations express the total stress components τ_{ij} and the pore pressure p in terms of strain components e_{ij}, e, and ζ. We note that, because the same coefficient $-\alpha M$ appears in the first three equations and the last, the matrix of coefficients is symmetric. This again results from the existence of an elastic potential energy with p and ζ acting as conjugate variables. The elastic potential per unit volume is expressed as

$$W = \frac{1}{2}(\tau_{xx}e_{xx} + \tau_{yy}e_{yy} + \tau_{zz}e_{zz} + \tau_{yz}e_{yz} + \tau_{zx}e_{zx} + \tau_{xy}e_{xy} + p\zeta) \quad [31][5]$$

Equations [30] are equivalent to

$$\left.\begin{aligned} \tau_{ij} &= \frac{\partial W}{\partial e_{ij}} \\ p &= \frac{\partial W}{\partial \zeta} \end{aligned}\right\} \quad [32]$$

We note also from Equations [30] that $\lambda + \alpha^2 M$ plays the role of a Lamé constant λ for $\zeta = 0$; i.e., for a "closed system."

As before, μ may be measured directly as the modulus of shear.

In the jacketed compressibility test, $p = 0$, giving for the fluid content

$$\zeta = \alpha e \quad [33]$$

Since the fluid pressure remains constant, the significance of α may be seen to be the ratio of change in pore volume to dilatation in a jacketed test. If the interior of the jacket is connected with the atmosphere by a tube we may measure the quantity ζ by the amount of fluid which is flowing through this tube. This will furnish the value of α.

If we designate the external pressure on the jacket by p', we have

$$\left.\begin{aligned} \tau_{xx} = -p', \quad \tau_{xy} = 0, \quad &\text{...etc.} \\ p &= 0 \\ e &= -p'\kappa \end{aligned}\right\} \quad [34]$$

giving with Equations [29] the relation

$$\frac{1}{\kappa} = \frac{2}{3}\mu + \lambda \quad [35]$$

In the unjacketed test

$$\left.\begin{aligned} \tau_{xx} = -p', \quad \tau_{xy} = 0, \quad &\text{...etc} \\ p &= p' \\ e &= -\delta p' \end{aligned}\right\} \quad [36]$$

giving with Equations [29]

$$-(1 - \alpha)p' = \left(\frac{2}{3}\mu + \lambda\right)e \quad [37]$$

Hence

$$\delta = (1 - \alpha)\kappa \quad [38]$$

$$\alpha = \left(1 - \frac{\delta}{\kappa}\right) \quad [39]$$

which provides a further interpretation of the coefficient α which is physically different from that given by Equation [33]. That they yield equal values for α results from the symmetry of the coefficient matrix in Equations [30] and this in turn is a consequence of the assumption that there exists an elastic potential energy for the fluid-solid system.

An alternative interpretation of the coefficient α which does not depend on the existence of a potential energy and is equivalent to Equation [39] is given by the first three of Equations [29]. In this case α represents the proportion of fluid pressure which will produce the same strains as the total stress.

The coefficient M may be determined from the coefficient of fluid content γ for the unjacketed test. In this case

$$\zeta = \gamma p' = \frac{1}{M}p' - \alpha\delta p' \quad [40]$$

giving for M

$$M = \frac{1}{\gamma + \delta - \frac{\delta^2}{\kappa}} \quad [41]$$

Another alternate way of writing Equations [29] is by introducing a stress τ' defined as

$$\left.\begin{aligned} \tau_{xx}' &= \tau_{xx} + p \\ \tau_{yy}' &= \tau_{yy} + p \\ \tau_{zz}' &= \tau_{zz} + p \\ \tau_{yz}' &= \tau_{yz} \\ \tau_{zx}' &= \tau_{zx} \\ \tau_{xy}' &= \tau_{xy} \end{aligned}\right\} \quad [42]$$

[4] μ and λ are designated by S and N in references (2) and (3).

[5] Expression [31] is identical with that introduced in reference (1) in connection with the derivation of the property of symmetry of the coefficients. The notations σ and θ were used instead of p and ζ.

The total stress τ is then represented as a superposition of hydrostatic pressure p, the same as in the fluid pores and a residual component τ' which acts only in the solid matrix. With this definition the first three Equations [29] are replaced by

$$\left.\begin{aligned} \tau_{xx}' - (1-\alpha)p &= 2\mu e_{xx} + \lambda e \\ \tau_{yy}' - (1-\alpha)p &= 2\mu e_{yy} + \lambda e \\ \tau_{zz}' - (1-\alpha)p &= 2\mu e_{zz} + \lambda e \end{aligned}\right\} \quad \ldots\ldots [43]$$

As shown in references (1) and (3) the elastic coefficients μ, λ, α, and M may all be determined without reference to the porosity f. Furthermore if the Darcy equation for volume flow is used, all the equations of consolidation theory may be developed without reference to porosity.

It is interesting to examine the limits of the coefficient α. Consider first the last of Equations [1]

$$\sigma = Qe + R\epsilon \quad \ldots\ldots [44]$$

If a positive fluid force σ is applied to the system at the same time that e is held fixed, a positive fluid strain ϵ must result. Therefore R must be positive. Alternatively, if the fluid force is held constant and a positive solid force is applied, e must be positive. In addition there must be a net increase in the porosity, requiring a negative fluid strain ϵ. Therefore, Q also must be positive. Since both Q and R are positive, it may be seen from the relation

$$\alpha = \left(\frac{Q+R}{R}\right) f \quad \ldots\ldots [28]$$

that α cannot be smaller than f. Alternatively, since the unjacketed compressibility δ cannot be less than zero, it follows from the relation

$$\alpha = \left(1 - \frac{\delta}{\kappa}\right) \quad \ldots\ldots [39]$$

that α cannot be greater than unity.

If the unjacketed compressibility δ is very small compared to the jacketed compressibility κ, we may approximate the value of α by putting $\alpha = 1$. This will be true in some cases for a water-saturated gel or clay (1, 2).[6]

4 Transverse Isotropy

For the case of transverse isotropy the stress-strain relations may be written (2)

$$\left.\begin{aligned} \sigma_{xx} &= Pe_{xx} + Ae_{yy} + Fe_{zz} + Me \\ \sigma_{yy} &= Ae_{xx} + Pe_{yy} + Fe_{zz} + Me \\ \sigma_{zz} &= Fe_{xx} + Fe_{yy} + Ce_{zz} + Qe \\ \sigma_{yz} &= Le_{yz} \\ \sigma_{xz} &= Le_{xz} \\ \sigma_{xy} &= Ne_{xy} \\ \sigma &= Me_{xx} + Me_{yy} + Qe_{zz} + R\epsilon \end{aligned}\right\} \quad \ldots\ldots [45]$$

in which $P = A + 2N$ and there are eight independent elastic coefficients. It will therefore require eight independent measurements to fix the values of the coefficients.

Consider the matrix

$$\begin{bmatrix} P & A & F & M \\ A & P & F & M \\ F & F & C & Q \\ M & M & Q & R \end{bmatrix} \quad \ldots\ldots [46]$$

and let its inverse be represented by

$$\begin{bmatrix} a & d & g & h \\ d & a & g & h \\ g & g & b & m \\ h & h & m & n \end{bmatrix} \quad \ldots\ldots [47]$$

Also let

$$\left.\begin{aligned} \frac{1}{N} &= s \\ \frac{1}{L} &= t \end{aligned}\right\} \quad \ldots\ldots [48]$$

The inverse stress-strain relations will then be

$$\left.\begin{aligned} e_{xx} &= a\sigma_{xx} + d\sigma_{yy} + g\sigma_{zz} + h\sigma \\ e_{yy} &= d\sigma_{xx} + a\sigma_{yy} + g\sigma_{zz} + h\sigma \\ e_{zz} &= g\sigma_{xx} + g\sigma_{yy} + b\sigma_{zz} + m\sigma \\ e_{yz} &= t\sigma_{yz} \\ e_{xz} &= t\sigma_{xz} \\ e_{xy} &= s\sigma_{xy} \\ \epsilon &= h\sigma_{xx} + h\sigma_{yy} + m\sigma_{zz} + n\sigma \end{aligned}\right\} \quad \ldots\ldots [49]$$

in which there are nine coefficients but only eight independent ones because of the original relation ($P = A + 2N$).

For this material under conditions of constant pore pressure, it will be possible to measure two separate Young's moduli by

$$\left.\begin{aligned} \frac{1}{E_1} &= \frac{\partial e_{xx}}{\partial \sigma_{xx}} = \frac{\partial e_{yy}}{\partial \sigma_{yy}} = a \\ \frac{1}{E_2} &= \frac{\partial e_{zz}}{\partial \sigma_{zz}} = b \end{aligned}\right\} \quad \ldots\ldots [50]$$

Three separate Poisson's ratio also exist and may be measured by

$$\left.\begin{aligned} -\nu_1 &= \frac{\left(\frac{\partial e_{yy}}{\partial \sigma_{xx}}\right)}{\left(\frac{\partial e_{xx}}{\partial \sigma_{xx}}\right)} = \frac{d}{a} = E_1 d \\ -\nu_2 &= \frac{\left(\frac{\partial e_{zz}}{\partial \sigma_{zz}}\right)}{\left(\frac{\partial e_{xx}}{\partial \sigma_{zz}}\right)} = \frac{g}{z} = E_2 g \\ -\nu_3 &= \frac{\left(\frac{\partial e_{zz}}{\partial \sigma_{zz}}\right)}{\left(\frac{\partial e_{zz}}{\partial \sigma_{xx}}\right)} = \frac{g}{a} = E_1 g \end{aligned}\right\} \quad \ldots\ldots [51]$$

[6] As pointed out in reference (1) the case where the solid matrix and the fluid are incompressible corresponds to $\alpha = 1$, $M = \infty$.

In reference (1) several other coefficients are used. E, G, and ν have their conventional significance as measured with constant pore pressure. The coefficient α has the same significance as in Equations [29]. The coefficient H is given by $1/(\kappa - \delta)$. The coefficients Q and R of reference (1) should not be confused with Q and R of Equations [1]. In reference (1) Q is equivalent to M and R is given by $1/(\gamma - \delta + \kappa)$.

There are only four independent coefficients between the two moduli and the three ratios. From the last two of Equations [51]

$$\frac{\nu_2}{E_2} = \frac{\nu_3}{E_1} \quad \ldots\ldots [52]$$

The coefficients a, b, d, and g may thereby be determined by a minimum of four measurements.

Two shear moduli also may be measured by

$$\left.\begin{aligned} \frac{1}{\mu_1} &= \left(\frac{\partial e_{xy}}{\partial \sigma_{xy}}\right) = s \\ \frac{1}{\mu_2} &= \left(\frac{\partial e_{xz}}{\partial \sigma_{xz}}\right) = \left(\frac{\partial e_{yz}}{\partial \sigma_{yz}}\right) = t \end{aligned}\right\} \quad \ldots\ldots [53]$$

Because of the original relation in Equations [45] of $P = A + 2N$, the first modulus μ_1 does not represent an independent measurement and could be determined from the other measurements.

In an unjacketed compression test

$$\left.\begin{aligned} \sigma_{xx} = \sigma_{yy} = \sigma_{zz} &= -(1-f)p' \\ \sigma &= -fp' \end{aligned}\right\} \quad \ldots\ldots [54]$$

giving the relations

$$\left.\begin{aligned} e_{xx} &= [(f-1)(a+d+g) - fh]p' = -\delta_1 p' \\ e_{yy} &= [(f-1)(a+d+g) - fh]p' = -\delta_1 p' \\ e_{zz} &= [(f-1)(g+g+b) - fm]p' = -\delta_2 p' \end{aligned}\right\} \quad \ldots [55]$$

in which δ_1 represents the change in the two equal principal axes and δ_2 the change in the third principal axis of the ellipsoid of revolution formed by a unit sphere of material strained under unit pressure in an unjacketed compression test.

This measurement permits the two additional coefficients h and m to be determined.

For a final measurement the coefficient of fluid content γ may be used, giving for the fluid strain

$$\epsilon = [(f-1)(h+h+m) - fn]$$

$$= -\frac{\gamma}{f}p' - (2\delta_1 + \delta_2)p' \quad \ldots\ldots [56]$$

from which the coefficient n may be determined.

These measurements give for the Matrix [47]

$$\begin{bmatrix} \left(\frac{1}{E_1}\right) & \left(\frac{-\nu_1}{E_1}\right) & \left(\frac{-\nu_2}{E_1}\right) & \left[\frac{\delta_1}{f} - \left(\frac{1-f}{f}\right)\left(\frac{1-\nu_1-\nu_2}{E_1}\right)\right] \\ \cdots & \left(\frac{1}{E_1}\right) & \left(\frac{-\nu_2}{E_2}\right) & \left[\frac{\delta_1}{f} - \left(\frac{1-f}{f}\right)\left(\frac{1-\nu_1-\nu_2}{E_1}\right)\right] \\ \cdots & \cdots & \left(\frac{-1}{E_2}\right) & \left[\frac{\delta_2}{f} - \left(\frac{1-f}{f}\right)\left(\frac{1-2\nu_2}{E_2}\right)\right] \\ \cdots & \cdots & \cdots & \left[\frac{\gamma}{f_2} - \left(\frac{1-2f}{f}\right)\left(\frac{2\delta_1+\delta_2}{f}\right) + \left(\frac{1-f}{f}\right)^2\left(\frac{1-2\nu_2}{E_2} + \frac{2(1-\nu_1-\nu_2)}{E_1}\right)\right] \end{bmatrix} \quad \ldots\ldots [57]$$

and the two relations $\quad s = \frac{1}{\mu_1}; \quad t = \frac{1}{\mu_2}$ $\quad \ldots\ldots [58]$

The individual values of the coefficients in the Matrix [46] may be found by the inversion of the Matrix [57].

The ten measured values

$$\left.\begin{aligned} &E_1\ \nu_1\ \mu_1\ \delta_1\ \gamma \\ &E_2\ \nu_2\ \mu_2\ \delta_2 \\ &\nu_3 \end{aligned}\right\} \quad \ldots\ldots [59]$$

have been used. Only eight of these are independent since

$$\frac{\nu_2}{E_2} = \frac{\nu_3}{E_1}$$

and since μ_1 may be determined from the relation $P = A + 2N$.

An alternate form of the coefficients of course could be easily written in terms of the variables p and ζ instead of σ and ϵ. These new coefficients will not involve the porosity f.

5 Complete Anisotropy

The stress-strain relations may be expressed in matrix form by (2)

$$\begin{bmatrix} \sigma_{xx} \\ \sigma_{yy} \\ \sigma_{zz} \\ \sigma_{yz} \\ \sigma_{zx} \\ \sigma_{xy} \\ \sigma \end{bmatrix} = \begin{bmatrix} C_{11}C_{12}C_{13}C_{14}C_{15}C_{16}C_{17} \\ C_{22}C_{23}C_{24}C_{25}C_{26}C_{27} \\ C_{33}C_{34}C_{35}C_{36}C_{37} \\ C_{44}C_{45}C_{46}C_{47} \\ C_{55}C_{56}C_{57} \\ C_{66}C_{67} \\ C_{77} \end{bmatrix} \begin{bmatrix} e_{xx} \\ e_{yy} \\ e_{zz} \\ e_{yz} \\ e_{zx} \\ e_{xy} \\ \epsilon \end{bmatrix} \quad \ldots\ldots [60]$$

in which $C_{ij} = C_{ji}$.

Eliminating ϵ by means of the last equation

$$\left.\begin{aligned} \sigma_{xx} &= \left(C_{11} - \frac{C_{17}C_{17}}{C_{77}}\right)e_{xx} + \left(C_{12} - \frac{C_{17}C_{27}}{C_{77}}\right)e_{yy} + \ldots + \frac{C_{17}}{C_{77}}\sigma \\ \sigma_{yy} &= \left(C_{12} - \frac{C_{17}C_{27}}{C_{77}}\right)e_{xx} + \left(C_{22} - \frac{C_{27}C_{27}}{C_{77}}\right)e_{yy} + \ldots + \frac{C_{27}}{C_{77}}\sigma \\ \sigma_{zz} &= \quad \ldots \quad \ldots \quad \ldots \quad \ldots \quad \ldots \quad \ldots \quad \ldots \\ \sigma_{yz} &= \quad \ldots \quad \ldots \quad \ldots \quad \ldots \quad \ldots \quad \ldots \quad \ldots \\ \sigma_{zx} &= \quad \ldots \quad \ldots \quad \ldots \quad \ldots \quad \ldots \quad \ldots \quad \ldots \\ \sigma_{xy} &= \quad \ldots \quad \ldots \quad \ldots \quad \ldots \quad \ldots \quad \ldots \quad \ldots \end{aligned}\right\} \quad \ldots [61]$$

in which the 21 terms

$$\left(C_{11} - \frac{C_{17}C_{17}}{C_{77}}\right) \ldots\ldots \left(C_{66} - \frac{C_{67}C_{67}}{C_{77}}\right) \quad \ldots\ldots [62]$$

are the classical coefficients of anisotropic elasticity, as would be measured with a constant pore pressure ($\sigma = 0$).

Seven additional measured quantities are then required to fix the properties of the system. Six of these may be obtained from an unjacketed compressibility test. An original unit sphere of the porous material will be deformed into a triaxial ellipsoid. For the general case in which the principal axes of the ellipsoid are not parallel to the co-ordinate axes, the six coefficients of strain as a function of pressure may be measured as

$$\left.\begin{aligned} \delta_{xx} &= -\frac{e_{xx}}{p'} \\ \delta_{yy} &= -\frac{e_{yy}}{p'} \\ \delta_{zz} &= -\frac{e_{zz}}{p'} \\ \delta_{yz} &= -\frac{e_{yz}}{p'} \\ \delta_{zx} &= -\frac{e_{zx}}{p'} \\ \delta_{xy} &= -\frac{e_{xy}}{p'} \end{aligned}\right\} \quad \ldots\ldots\ldots\ldots\ldots\ldots [63]$$

Alternatively it would be possible to measure the mutually perpendicular principal strains of the specimen

$$\left.\begin{aligned} \delta_1 &= -\frac{e_1}{p'} \\ \delta_2 &= -\frac{e_2}{p'} \\ \delta_3 &= -\frac{e_3}{p'} \end{aligned}\right\} \quad \ldots\ldots\ldots\ldots\ldots\ldots [64]$$

and three angles describing their orientation and to express the co-ordinate strains in terms of these.

For the special case in which the principal axes of the ellipsoid are parallel to the co-ordinate axes, the coefficients δ_{xx}, δ_{yy}, and δ_{zz} are given directly by the principal strains and coefficients δ_{yz}, δ_{zx}, and δ_{xy} are zero.

For a final measurement the coefficient of fluid content γ may again be used, permitting the fluid dilatation in the unjacketed compressibility test to be given by

$$\left.\begin{aligned} \epsilon &= -\frac{\gamma}{f}\,p' - (\delta_1 + \delta_2 + \delta_3)p' \\ \text{or} \\ \epsilon &= -\frac{\gamma}{f}\,p' - (\delta_{xx} + \delta_{yy} + \delta_{zz})p' \end{aligned}\right\} \quad \ldots\ldots [65]$$

Therefore the strains in the unjacketed test may be expressed in terms of seven measured coefficients and the fluid pressure. The stresses again will be

$$\left.\begin{aligned} \sigma_{xx} = \sigma_{yy} = \sigma_{zz} &= -(1-f)p' \\ \sigma_{yz} = \sigma_{zx} = \sigma_{xy} &= 0 \\ \sigma &= -fp' \end{aligned}\right\} \quad \ldots\ldots\ldots [66]$$

and by substitution into Equations [60] seven equations relating the original coefficients and the measured coefficients will be obtained. These relations together with the 21 relations between the Expressions [62] and the classical coefficients permit the original coefficients to be determined. Again we may remark that a different set of coefficients not involving explicitly the porosity can be derived easily by introducing the variables p and ζ.

6 Elastic Coefficients for Incremental Deformations of a Prestressed Material

In the foregoing we have assumed the strains to be small and linearly related to the stresses. We will now examine how the relations between stress and strain may be expressed if the porous solid-fluid system is still elastic but nonlinear. In particular we are interested to know if the results of the foregoing sections are directly applicable to the linearized problem when we consider small incremental stresses and strains in the vicinity of a prestressed condition.

We shall restrict ourselves to the case where the prestress is isotropic. We consider an initial state 1 which is unstressed. The state of prestress denoted as 2 results from the application of isotropic stresses in the fluid and the solid. We consider the forces acting on the solid portion of the material per unit area of the bulk material in state 2. This being an isotropic state of stress these forces are represented by the matrix

$$\begin{bmatrix} \sigma' & 0 & 0 \\ 0 & \sigma' & 0 \\ 0 & 0 & \sigma' \end{bmatrix} \quad \ldots\ldots\ldots\ldots\ldots [67]$$

Similarly the forces acting on the fluid portion per unit area of bulk material are represented by

$$\begin{bmatrix} \sigma & 0 & 0 \\ 0 & \sigma & 0 \\ 0 & 0 & \sigma \end{bmatrix} \quad \ldots\ldots\ldots\ldots\ldots [68]$$

The prestressed state 2 is now considered as a new initial state and small incremental deformations e_{ij} are superimposed leading to state 3. The incremental strain tensor is defined in terms of the incremental displacements $\mathfrak{u}$ and $\mathfrak{U}$ of the solid and the fluid measured from state 2 as origin. The incremental strains give rise to a new state of stress obtained by adding incremental components $\Delta\sigma_{ij}$ and $\Delta\sigma$. We represent the solid stress in state 3 by forces acting on the solid portion of the material per unit area in state 2. They are

$$\begin{bmatrix} \sigma' + \Delta\sigma_{xx} & \Delta\sigma_{xy} & \Delta\sigma_{xz} \\ \Delta\sigma_{xy} & \sigma' + \Delta\sigma_{yy} & \Delta\sigma_{yz} \\ \Delta\sigma_{xz} & \Delta\sigma_{yz} & \sigma' + \Delta\sigma_{zz} \end{bmatrix} \quad \ldots [69]$$

The forces acting on the fluid in state 3 per unit area in state 2 are

$$\begin{bmatrix} \sigma + \Delta\sigma & 0 & 0 \\ 0 & \sigma + \Delta\sigma & 0 \\ 0 & 0 & \sigma + \Delta\sigma \end{bmatrix} \quad \ldots\ldots\ldots [70]$$

We now assume that the incremental stresses and strains are small enough so that they are related linearly. The material in state 2 remains isotropic and therefore the incremental stress-strain relations are isotropic. This requires that they be of the form

$$\left.\begin{aligned} \Delta\sigma_{xx} &= 2Ne_{xx} + Ae + Q\epsilon \\ \Delta\sigma_{yy} &= 2Ne_{yy} + Ae + Q\epsilon \\ \Delta\sigma_{zz} &= 2Ne_{zz} + Ae + Q\epsilon \\ \Delta\sigma_{yz} &= Ne_{yz} \\ \Delta\sigma_{zx} &= Ne_{zx} \\ \Delta\sigma_{xy} &= Ne_{xy} \\ \Delta\sigma &= Q'e + R\epsilon \end{aligned}\right\} \quad \ldots\ldots\ldots [71]$$

We see that based on isotropy alone there are five elastic coefficients for incremental stresses and strains. These coefficients

are functions of the initial stresses σ and σ'. In order to simplify the writing we may without loss of generality consider an incremental stress which is also isotropic. We put

$$\left.\begin{aligned} \Delta\sigma_{xx} = \Delta\sigma_{yy} = \Delta\sigma_{zz} = \Delta\sigma' \\ e_{xx} = e_{yy} = e_{zz} = \frac{1}{3}\,e \\ \Delta\sigma_{yz} = \Delta\sigma_{zx} = \Delta\sigma_{xy} = 0 \\ e_{yz} = e_{zx} = e_{xy} = 0 \end{aligned}\right\} \quad \ldots\ldots\ldots [72]$$

Equations [71] become

$$\left.\begin{aligned} \Delta\sigma' = \left(\frac{2}{3}\,N + A\right)e + Qe \\ \Delta\sigma = Q'e + Re \end{aligned}\right\} \quad \ldots\ldots\ldots [73]$$

We assume the existence of an elastic potential energy for incremental deformations in the vicinity of the prestressed state 2. If W denotes this potential energy per unit volume of the material in state 2 we may write

$$dW = (\sigma' + \Delta\sigma')de + (\sigma + \Delta\sigma)de \ldots\ldots\ldots [74]$$

This being an exact differential we have

$$\frac{\partial}{\partial e}(\Delta\sigma') = \frac{\partial}{\partial e}(\Delta\sigma) \ldots\ldots\ldots [75]$$

hence from Equations [73]

$$Q = Q' \ldots\ldots\ldots [76]$$

The matrix of elastic coefficients in Equations [71] is therefore symmetric and there are only four distinct coefficients.

We must bear in mind that the quantities $\Delta\sigma'$ and $\Delta\sigma$ are not the forces acting per unit area of the final deformed state 3 but per unit area of the prestressed state 2. Therefore, they are not represented by actual fluid pressures in a test but are related to them through the incremental deformations. Let us imagine a jacketed test with an initial state of stress such that the fluid pressure inside the jacket is p, while a fluid pressure p' is applied outside. Our purpose here is to point out an important difference between the test with prestress and the test without prestress. In the case of prestress, it is not as simple to evaluate the quantities $\Delta\sigma'$ and $\Delta\sigma$ in terms of the fluid pressure as for the case without prestress. This can be seen as follows. Denoting by f the porosity in the prestressed state 2 we may still write as before

$$\left.\begin{aligned} \sigma' + \sigma = -p' \\ \sigma = -fp \end{aligned}\right\} \quad \ldots\ldots\ldots [77]$$

If we now apply incremental fluid pressures $\Delta p'$ and Δp, these fluid pressures are applied to changing areas. The new area for p' is $(1 + {}^1/_{s\theta})^3$ and for p it is $(f + \Delta f)(1 + {}^1/_{s\theta})^3$. We note by Δf the increment of the porosity factor. Hence

$$\left.\begin{aligned} \sigma' + \sigma + \Delta\sigma' + \Delta\sigma = -(p' + \Delta p')\left(1 + \frac{1}{3}\,e\right)^3 \\ \sigma + \Delta\sigma = -(p + \Delta p)(f + \Delta f)\left(1 + \frac{1}{3}\,e\right)^3 \end{aligned}\right\} \quad \ldots [78]$$

Retaining only incremental terms of the first order, Equations [78] are written

$$\left.\begin{aligned} \Delta\sigma' + \Delta\sigma = -\Delta p - \frac{2}{3}\,p'e \\ \Delta\sigma = -f\Delta p - p\Delta f - \frac{2}{3}\,fpe \end{aligned}\right\} \quad \ldots\ldots [79]$$

We see that $\Delta\sigma'$ and $\Delta\sigma$ are not exactly equal to $(1 - f)\Delta p'$ and $-f\Delta p$. The correction terms, in general, will be small but nevertheless will vanish only if the initial stress is zero.

With these limitations the results of the previous sections may be applied to incremental deformations except for a reservation regarding the validity of Expression [24] for the coefficient of fluid content γ. We have remarked that, for the unstressed initial state, this expression holds if the material of the porous matrix is homogeneous and isotropic. This is a sufficient condition only if $p = p'$, i.e., if the initial pressures on the solid and on the pores are the same. If these initial pressures are not equal, then equal increments of these pressures may produce a change in porosity thereby invalidating Relation [24].

BIBLIOGRAPHY

1 "General Theory of Three-Dimensional Consolidation," by M. A. Biot, *Journal of Applied Physics*, vol. 12, 1941, pp. 155–165.

2 "Theory of Elasticity and Consolidation for a Porous Anisotropic Solid," by M. A. Biot, *Journal of Applied Physics*, vol. 26, 1955, pp. 182–185.

3 "General Solutions of the Equations of Elasticity and Consolidation for a Porous Material," by M. A. Biot, JOURNAL OF APPLIED MECHANICS, Trans. ASME, vol. 78, 1956, pp. 91–96.

4 "Theory of Propagation of Elastic Waves in a Fluid Saturated Porous Solid, Parts I and II," by M. A. Biot, *Journal of the Acoustical Society of America*, vol. 28, no. 2, 1956, pp. 168–191.

5 "Elastic Waves through a Packing of Spheres," by Frits Gassman, *Geophysics*, vol. 16, 1951, pp. 673–685.

6 "Ueber die Elastizität poröser Medien," by Frits Gassman, *Vierteljahrsschrift der Naturforschenden Gesellschaft in Zürich*, vol. 96, 1951, pp. 1–23.

7 "The Effect of Fluid Pressure Decline on Volume Changes of Porous Rocks," by J. Geertsma, paper presented before the American Institute of Mining, Metallurgical, and Petroleum Engineers, Los Angeles, Calif., October, 1956.

8 "The Effect of Pressure on the Reduction of Pore Volume of Consolidated Sandstones," by D. S. Hughes and C. E. Cooke, Jr., *Geophysics*, vol. 18, 1953, pp 298–309.

Calendering of a Viscoelastic Material

By P. R. PASLAY,[1] CAMBRIDGE, MASS.

The solution of the calendering problem for viscous materials is extended to include the first effects of elasticity. A numerical procedure for the solution of the approximate equations is contained in the Appendix.

Nomenclature

The following nomenclature is used in the paper:

- a = parameter in stress-deformation-rate equation
- d_{ij} = deformation-rate tensor
- $f(x)$ = pressure along passage (see Equation [39])
- F = function of x defined by Equation [42]
- G = elastic shear modulus
- J_2 = second invariant of deformation-rate tensor
- p = negative average of three normal stresses
- R = radius of calendering rolls
- S_{ij} = reduced stress tensor = $\sigma_{ij} + \delta_{ij}p$
- $t(x)$ = one half the thickness of passage between rolls at corresponding value of x
- t_0 = minimum value of $t(x)$
- u = velocity component in x-direction in region of calendering flow under consideration
- u_j = jth component of velocity
- u_{max} = maximum value of velocity component u
- u_0 = velocity of roll surface
- v = velocity component in y-direction in region of calendering flow under consideration
- v_{max} = maximum value of velocity component v
- x_j = jth Cartesian co-ordinate
- x_0 = value of x where material leaves surface of rolls
- α = time
- δ_{ij} = Kronecker delta = $\begin{cases} 1 & i = j \\ 0 & i \neq j \end{cases}$
- η = viscosity
- ω_{ij} = rotation rate = $\frac{1}{2}(u_{i,j} - u_{j,i})$
- $\rho = 0(\zeta)$ = should read: "ρ is of the order of magnitude of ζ"
- σ_{ij} = stress tensor
- $\tau = \sigma_{xy}$ = shear stress in plane strain

Introduction

Calendering is the term applied to the process of rolling bulk plastic into sheets. In 1950 R. E. Gaskell (1)[2] obtained a solution for the calendering of a viscous material. Gaskell's solution furnishes suitable predictions so long as the material shows no appreciable elastic effects. The solution given here is an approximate solution for a material that exhibits both elastic and viscous behavior.

Stress-Deformation-Rate Relations

To obtain a solution to this problem a stress-deformation-rate equation must be selected that is easy to manipulate mathematically and that gives suitable physical predictions. The purpose of this section is to motivate the stress-deformation-rate equation used in this work.

Materials commonly calendered may be treated as Newtonian viscous fluids to obtain analytical solutions except when the elastic properties of the material are pronounced. The linear superposition stress-deformation-rate equation of viscoelasticity that most nearly meets the requirements for calendering is the Maxwell material equation. The formulation of the Maxwell material equation will now be outlined.

The equations are derived by assuming the deformation rate to have viscous and elastic parts. The viscous and elastic deformation rates are added linearly. In the case of an isotropic, incompressible material there results

$$d_{ij} = \frac{\check{S}_{ij}}{2G} + \frac{S_{ij}}{2\eta} \quad \ldots\ldots [1]$$

where d_{ij} is the deformation rate tensor, S_{ij} the reduced stress tensor,[3] $\check{S}_{ij}$ the reduced stress-rate tensor, and G, η material constants (G is a shear modulus and η a coefficient of viscosity).

The deformation rate d_{ij} and the reduced stress-rate tensor $\check{S}_{ij}$ appearing in Equation [1] will now be discussed. As usual, in fluid-flow problems, an Eulerian representation is used; that is, x_i represents a fixed point in the field of flow.

Tensor d_{ij} may be expressed as a function of the velocity gradients as[4]

$$d_{ij} = \frac{1}{2}(u_{i,j} + u_{j,i}) \quad \ldots\ldots [2]$$

where u_i is the velocity in the ith direction. Tensor d_{ij} in general is a function of time and position in the field. It is the instantaneous time rate of change of strain.

The stress rate $\check{S}_{ij}$ must be expressed in terms of partial derivatives as follows

$$\check{S}_{ij} = S_{ij,\alpha} + u_k S_{ij,k} - \omega_{ik}S_{kj} + \omega_{kj}S_{ik} \quad \ldots\ldots [3]$$

where α is time and

$$\omega_{ij} = \frac{1}{2}(u_{i,j} - u_{j,i}) \quad \ldots\ldots [4]$$

This result is due to Cauchy and is called Cauchy's flux principle

---

[1] Assistant Professor of Mechanical Engineering, Massachusetts Institute of Technology. Currently with General Electric Company, Schenectady, N. Y. Assoc. Mem. ASME.

[2] Numbers in parentheses refer to the Bibliography at the end of the paper.

Presented at the Applied Mechanics Division Summer Conference, Berkeley, Calif., June 13–15, 1957, of The American Society of Mechanical Engineers.

Discussion of this paper should be addressed to the Secretary, ASME, 29 West 39th Street, New York, N. Y., and will be accepted until January 10, 1958, for publication at a later date. Discussion received after the closing date will be returned.

Note: Statements and opinions advanced in papers are to be understood as individual expressions of their authors and not those of the Society. Manuscript received by ASME Applied Mechanics Division, December 13, 1956. Paper No. 57—APM-1.

[3] The hydrostatic component of the stress is subtracted from the normal stress components. S_{ij} is often referred to as the extra stress tensor or the deviatoric stress tensor.

[4] The notation is that conventionally with Cartesian tensors; that is

$$\sigma_{ii} = \sigma_{xx} + \sigma_{yy} + \sigma_{zz} \quad \text{and} \quad u_{i,j} = \frac{\partial u_i}{\partial x_j}$$

See, for example, reference (8).

by Truesdell [2]. Equation [3] is derived by requiring that a rigid rotation be incapable of changing the state of stress relative to co-ordinates fixed in the body.

As Fromm (3, 4) has pointed out, Equation [1] can lead to physical predictions that are not suitable. He illustrates this by considering two parallel plates sliding over one another with a constant relative velocity. For this case let the plates be parallel to the zz-plane and the velocity in the x-direction. Equation [1] gives, in component form

$$\begin{Bmatrix} 0 & d_{xy} & 0 \\ & 0 & 0 \\ & & 0 \end{Bmatrix} = \begin{Bmatrix} -2\sigma_{xy} & -\sigma_{yy}+\sigma_{xx} & 0 \\ & +2\sigma_{xy} & 0 \\ & & 0 \end{Bmatrix} \frac{d_{xy}}{2G} + \begin{Bmatrix} \frac{2}{3}\sigma_{xx}-\frac{1}{3}\sigma_{yy} & \sigma_{xy} & 0 \\ & \frac{2}{3}\sigma_{yy}-\frac{1}{3}\sigma_{xx} & 0 \\ & & 0 \end{Bmatrix} \frac{1}{2\eta} \quad \ldots [5]$$

The terms in brackets are the six components of the corresponding symmetric tensors; d_{xy} has the same value everywhere in the field of flow for a prescribed σ_{xy}. The three equations resulting from Equation [5] are

$$\frac{\sigma_{xy}}{G} = \frac{2\frac{\eta}{G}d_{xy}}{1+\left[2\frac{\eta}{G}d_{xy}\right]^2} \quad \ldots [6]$$

and

$$-\frac{\sigma_{yy}}{G} = +\frac{\sigma_{zz}}{G} = \frac{\left[2\frac{\eta}{G}d_{xy}\right]^2}{1+\left[2\frac{\eta}{G}d_{xy}\right]^2} \quad \ldots [7]$$

Equation [6] predicts a maximum shear stress σ_{xy} of $\frac{1}{2}G$ when $2d_{xy}$ is G/η and a decreasing σ_{xy} for deformation rates greater than this. This prediction is not reasonable for most materials since the total shear load as a function of the relative velocity of one plate to the other would be similar to Equation [6]. Fromm (3) and Noll (5) have suggested that this mathematical prediction would correspond to unstable flow in the physical case.

To avoid the foregoing difficulty a different type stress-deformation-rate equation may be chosen or Equation [1] may be modified. In order to have a mathematically simple formulation and to introduce greater generality in the material properties treated here the stress-deformation-rate relation of Equation [1] was modified in the following way

$$\left.\begin{aligned} (1+aJ_2)d_{ij} &= \frac{\tilde{S}_{ij}}{2G}+\frac{S_{ij}}{2\eta} \\ J_2 &= \frac{1}{2}d_{ij}d_{ji} \end{aligned}\right\} \quad \ldots [8]$$

where J_2 is a second invariant of the deformation-rate tensor and a is a material constant found by comparison with experimental results.

If the parallel-plate problem just referred to is solved with Equation [8] replacing Equation [1] there results

$$\frac{\sigma_{xy}}{G} = \frac{(1+ad_{xy}^2)\left(2\frac{\eta}{G}d_{xy}\right)}{1+\left(2\frac{\eta}{G}d_{xy}\right)^2} \quad \ldots [9]$$

and

$$-\frac{\sigma_{yy}}{G} = +\frac{\sigma_{zz}}{G} = \frac{(1+ad_{xy}^2)\left(2\frac{\eta}{G}d_{xy}\right)^2}{1+\left(2\frac{\eta}{G}d_{xy}\right)^2} \quad \ldots [10]$$

Fig. 1 shows a plot of σ_{xy} versus d_{xy}, in dimensionless form, from Equation [9] for various values of a. The difficulty of the peak in the shear stress from Equation [1] can now be avoided by a suitable selection of the parameter a. For a given material a may be found by a comparison of the shear load versus velocity relation determined experimentally.

The solution of two other simple problems illustrate that Equation [8] is capable of giving reasonable predictions for other physical situations.

First consider a bar with a constant uniform uniaxial tension applied in the x-direction. In this case Equation [8] yields

$$\frac{\sigma_{xx}}{3\eta} = \left(1+\frac{3a}{4}d_{xx}^2\right)d_{xx} \quad \ldots [11]$$

which is physically acceptable.

The second case is a bar on which is imposed a prescribed uniform uniaxial strain in the x-direction at $\alpha = 0$, α being time. The problem is to find the variation of stress with time. The solution of the problem using Equation [8] is

$$\sigma_{xx} = \sigma_{xx0}e^{-\frac{a\eta}{\eta}} \quad \ldots [12]$$

where σ_{xx0} is the stress at time $\alpha = 0^+$. This result shows that the stress decreases exponentially with time, a prediction which is reasonable.

Equation [8] will now be used to obtain an approximate solution to the calendering problem.

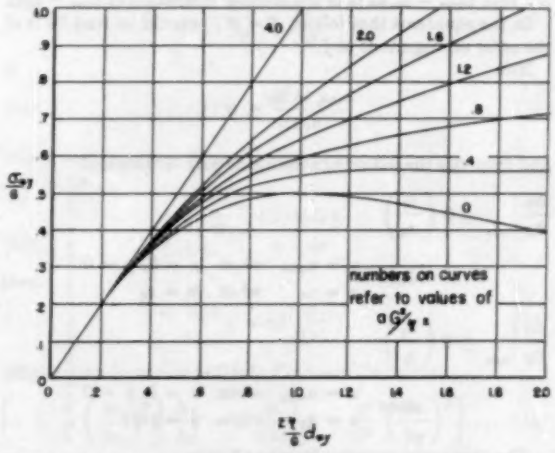

FIG. 1 PLOT OF EQUATION [9] SHOWING VARIATION OF SHEAR STRESS σ_{xy}, WITH SHEAR DEFORMATION RATE d_{xy} FOR VARIOUS VALUES OF THE PARAMETER a

Solution of Calendering Problem

Fig. 2 shows a sketch of the region of interest in the calendering problem.

The following assumptions will be made regarding the steady-state calendering process.

1 The passage-thickness variation $2[t(x_0) - t_0]$ is no greater than the order of magnitude of the minimum passage thickness, $2t_0$. This means that $t(x_0) - t_0/t_0$ is of no higher order of magnitude than 1.0.

2 The passage length $2x_0$ is long compared to the thickness of the passage $2t_0$.

3 The axial length of the rolls is long compared to the passage length $2x_0$. This permits the approximation of plane strain. The plane-strain approximation will be good except at the edges of the sheet.

4 The material adheres to the surface of the rolls so that there is no slipping between material and rolls.

Statement 3 yields

$$\left.\begin{aligned} d_{zz} = d_{yz} = d_{xz} = 0 \\ s_{zz} = 0 \quad \sigma_{xz} = \sigma_{yz} = 0 \\ p = -\sigma_{zz} = -\frac{\sigma_{xx} + \sigma_{yy}}{2} \end{aligned}\right\} \quad \ldots\ldots\ldots [13]$$

Since an incompressible material has been assumed from the outset the velocity profiles at the various sections may be roughly sketched as shown in Fig. 3.

The rough shapes of the velocity profiles and assumption 1 imply that $u_{max} - u_0/u_0$ is of the order of magnitude of $t_{max} - t_0/t_0$.

In the equations that follow, $\rho = 0(\zeta)$ should be read "ρ is of the order of magnitude of ζ."

Now

$$\frac{u_{max} - u_0}{u_0} \leq 0(1) \ldots\ldots\ldots [14]$$

and from this the following statements may be obtained

$$\left.\begin{aligned} \left.\frac{\partial u}{\partial x}\right|_{max} \leq 0\left(\frac{u_0}{x_0}\right) \\ \text{since} \quad \begin{aligned} u &= u_{max} \quad \text{when} \quad x = 0, y = 0 \\ u &= u_0 \quad \text{when} \quad x = x_0 \end{aligned} \end{aligned}\right\} \quad \ldots [15]$$

$$\left.\begin{aligned} \left.\frac{\partial u}{\partial y}\right|_{max} \leq 0\left(\frac{u_0}{t_0}\right) \\ \text{since} \quad \begin{aligned} u &= u_{max} \quad \text{when} \quad x = 0, y = 0 \\ u &= u_0 \quad \text{when} \quad y = t(x) \end{aligned} \end{aligned}\right\} \quad \ldots [16]$$

The continuity equation for plane flow is

$$\frac{\partial u}{\partial x} + \frac{\partial v}{\partial y} = 0 \ldots\ldots\ldots [17]$$

which means that

$$\left.\frac{\partial v}{\partial y}\right|_{max} = 0\left(\frac{\partial u}{\partial x}\right)_{max} \leq 0\left(\frac{u_0}{x_0}\right) \ldots\ldots\ldots [18]$$

Then

$$v_{max} \leq 0\left(\frac{u_0 t_0}{x_0}\right) \ldots\ldots\ldots [19]$$

and

$$\left.\frac{\partial v}{\partial x}\right|_{max} \leq 0\left(\frac{u_0 t_0}{x_0^2}\right) \ldots\ldots\ldots [20]$$

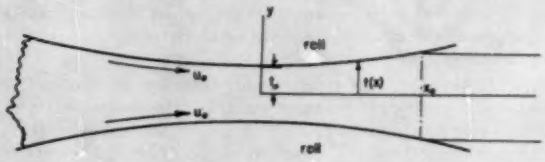

Fig. 2 Schematic Diagram of Region of Interest in Calendering Problem

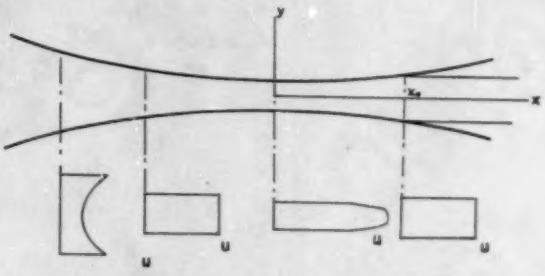

Fig. 3 Diagram Showing Plots of Velocity u Versus Position Across Passage for Several Locations Along Passage

From the foregoing order-of-magnitude study and assumption 2, $t_0/x_0 \ll 1$, some consequences are

$$u_{max} \gg v_{max} \quad \left.\frac{\partial u}{\partial y}\right|_{max} \gg \left.\frac{\partial u}{\partial x}\right|_{max} \ldots\ldots\ldots [21]$$

$$\left.\frac{\partial u}{\partial y}\right|_{max} \gg \left.\frac{\partial v}{\partial y}\right|_{max} \quad \left.\frac{\partial u}{\partial y}\right|_{max} \gg \left.\frac{\partial v}{\partial x}\right|_{max} \ldots\ldots [22]$$

The stresses may be analyzed in a similar way. This solution is intended to be for a material and geometry that exhibit primarily viscous behavior so for an order of magnitude study the following is assumed

$$\tau_{max} = 0\left(\eta \left.\frac{\partial u}{\partial y}\right|_{max}\right) \leq 0\left(\eta \frac{u_0}{t_0}\right) \ldots\ldots\ldots [23]$$

$$\left.\begin{aligned} \left.\frac{\partial \tau}{\partial x}\right|_{max} \leq 0\left(\frac{\eta}{t_0}\frac{u_0}{x_0}\right) \\ \text{since} \quad \begin{aligned} \tau &= 0 \quad \text{when} \quad x = x_0 \\ \tau &= \tau_{max} \quad \text{at} \quad x = 0, y = t_0 \end{aligned} \end{aligned}\right\} \quad \ldots [24]$$

and

$$\left.\begin{aligned} \left.\frac{\partial \tau}{\partial y}\right|_{max} \leq 0\left(\eta \frac{u_0}{t_0^2}\right) \\ \text{since} \quad \begin{aligned} \tau &= 0 \quad \text{when} \quad x = 0, y = 0 \\ \tau &= \tau_{max} \quad \text{when} \quad x = 0, y = t_0 \end{aligned} \end{aligned}\right\} \quad \ldots [25]$$

The remaining reduced stresses to be considered are $\sigma_x + p$ and $\sigma_y + p$ which reduce to a single variable in the following way

$$\sigma_x + p = \sigma_x - \frac{\sigma_x + \sigma_y}{2} = \frac{\sigma_x - \sigma_y}{2} \ldots\ldots [26]$$

$$\sigma_y + p = \sigma_y - \frac{\sigma_x + \sigma_y}{2} = -\frac{\sigma_x - \sigma_y}{2} \ldots\ldots [27]$$

Both of the reduced stresses $\sigma_x + p$ and $\sigma_y + p$ are results of shearing stresses acting on a rotating element for this problem, so it is anticipated that

$$(\sigma_x + p)|_{max} = 0\,(\tau_{max}) \leq 0\left(\frac{\eta u_0}{l_0}\right) \quad [28]$$

$$\left.\frac{\partial(\sigma_x + p)}{\partial x}\right|_{max} = 0\left(\left.\frac{\partial \tau}{\partial x}\right|_{max}\right) \leq 0\left(\frac{\eta}{l_0}\frac{u_0}{x_0}\right) \quad [29]$$

$$\left.\frac{\partial(\sigma_x + p)}{\partial y}\right|_{max} = 0\left(\left.\frac{\partial \tau}{\partial y}\right|_{max}\right) \leq 0\left(\frac{\eta u_0}{l_0^2}\right) \quad [30]$$

The order of magnitude of $\sigma_x + p$ will have to be checked in the solution to see if the foregoing conditions are satisfied.

The equations make suitable simplifications so that an approximate solution is possible. To simplify this analysis it is convenient to consider cases where

$$\sqrt{a}\left.\frac{\partial u}{\partial y}\right|_{max} \leq 0(1) \quad [31]$$

The stress-deformation-rate equations, with Equations [13], [26], and [27] substituted, are now written out for examination.

$$\left\{1 + \frac{a}{2}\left[\left(\frac{\partial u}{\partial x}\right)^2 + \left(\frac{\partial v}{\partial y}\right)^2 + \frac{1}{2}\left(\frac{\partial u}{\partial y} + \frac{\partial v}{\partial x}\right)^2\right]\right\} \begin{Bmatrix} \frac{\partial u}{\partial x} & \frac{1}{2}\left(\frac{\partial u}{\partial y} + \frac{\partial v}{\partial x}\right) & 0 \\ & \frac{\partial v}{\partial y} & 0 \\ & & 0 \end{Bmatrix}$$

$$= \frac{1}{2\eta}\begin{Bmatrix} \sigma_x + p & \tau & 0 \\ & -(\sigma_x + p) & 0 \\ & & 0 \end{Bmatrix} + \frac{u}{2G}\begin{Bmatrix} \frac{\partial(\sigma_x + p)}{\partial x} & \frac{\partial \tau}{\partial x} & 0 \\ & -\frac{\partial(\sigma_x + p)}{\partial x} & 0 \\ & & 0 \end{Bmatrix}$$

$$+ \frac{v}{2G}\begin{Bmatrix} \frac{\partial(\sigma_x + p)}{\partial y} & \frac{\partial \tau}{\partial y} & 0 \\ & -\frac{\partial(\sigma_x + p)}{\partial y} & 0 \\ & & 0 \end{Bmatrix} + \frac{\frac{1}{2}\left(\frac{\partial v}{\partial x} - \frac{\partial u}{\partial y}\right)}{2G}\begin{Bmatrix} +2\tau & -\sigma_x + \sigma_y & 0 \\ & -2\tau & 0 \\ & & 0 \end{Bmatrix} \quad [32]$$

The plan followed is that the maximum order of magnitude of each term of each stress-deformation-rate equation is written out by referring to Equations [15], [16], [18], [19], [20], [23], [24], [25], [28], [29], [30], and [31] and then, keeping the viscous case in mind, only the highest order terms will be retained thus leading to simplified equations. There results:

xx stress-deformation-rate equation

$$\sigma_x + p = \frac{\eta}{G}\frac{\partial u}{\partial y}\tau \quad [33]$$

and therefore, $\sigma_x + p$ is no larger than the order of τ if

$$\left.\frac{\eta}{G}\frac{\partial u}{\partial y}\right|_{max} \leq 0(1) \quad [34]$$

xy stress-strain equation

$$\left[1 + \frac{a}{4}\left(\frac{\partial u}{\partial y}\right)^2\right]\frac{\partial u}{\partial y} = \frac{\tau}{\eta} + \frac{\sigma_x + p}{G}\left(\frac{\partial u}{\partial y}\right) \quad [35]$$

Eliminating $\sigma_x + p$ between Equations [33] and [35] gives

$$\left[1 + \frac{a}{4}\left(\frac{\partial u}{\partial y}\right)^2\right]\frac{\partial u}{\partial y} = \frac{\tau}{\eta}\left[1 + \frac{\eta^2}{G^2}\left(\frac{\partial u}{\partial y}\right)^2\right] \quad [36]$$

The continuity equation, Equation [17], implies that when u has been determined then v may be determined.

The remaining equations are the equilibrium equations. If, for creeping flow, inertial terms are neglected these equations are

$$\frac{\partial p}{\partial x} = \frac{\partial(\sigma_x + p)}{\partial x} + \frac{\partial \tau}{\partial y} \quad [37]$$

$$\frac{\partial p}{\partial y} = -\frac{\partial(\sigma_x + p)}{\partial y} + \frac{\partial \tau}{\partial x} \quad [38]$$

An order-of-magnitude study of these equations shows that the change in pressure p along the section is much greater than the change in pressure across the section so that the dependence on y is neglected and

$$p = f(x) \quad [39]$$

By disregarding higher-order terms in the equilibrium equations we obtain

$$\frac{\partial \tau}{\partial y} = \frac{df(x)}{dx} \quad [40]$$

or

$$\tau = \frac{df(x)}{dx}y \quad [41]$$

since $\tau = 0$ when $y = 0$ for all values of x.

Now let

$$F = \frac{t(x)}{\eta}\frac{df(x)}{dx} \quad [42]$$

then

$$\tau = \eta F\frac{y}{t(x)} \quad [43]$$

Substituting Equation [43] into Equation [36] gives

$$\left[1 + \frac{a}{4}\left(\frac{\partial u}{\partial y}\right)^2\right]\frac{\partial u}{\partial y} = F\frac{y}{t(x)}\left[1 + \frac{\eta^2}{G^2}\left(\frac{\partial u}{\partial y}\right)^2\right] \quad [44]$$

The integrated form of the continuity equation furnishes the last requirement

$$\int_0^{t(x)} u\,dy = \text{const} = u_0 t(x_0) \quad [45]$$

Now the value of x_0 is seen to be arbitrary; that is, this solution does not allow the determination of a value for x_0. The physical reason why x_0 cannot be found with this solution is because the adhesive characteristics between the roll and calendered material have not been considered here. Experimental results of R. E. Gaskell mentioned by M. Finston (6) show that a good approximation to x_0 may be given by the following equation

$$x_0 \simeq \left(\frac{Rt_0}{2}\right)^{1/2} \quad [46]$$

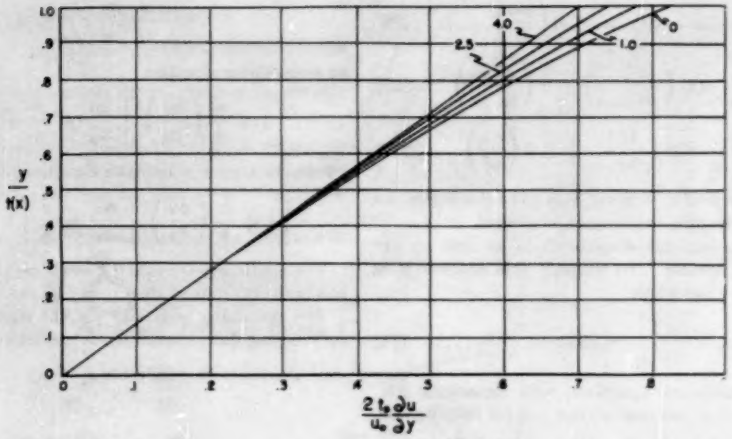

FIG. 4 PLOT OF DIMENSIONLESS VELOCITY GRADIENT $\frac{2t_0}{u_0}\frac{\partial u}{\partial y}$ ACROSS PASSAGE FOR $\frac{2t_0}{u_0}F = 0.7$, $\frac{u_0}{t_0}\frac{\eta}{G} = 1.0$, AND VARIOUS VALUES OF $a\frac{G^2}{\eta^2}$

This equation supplies a value of x_0 so that problems may be worked for comparison purposes.

A numerical procedure may be set up to solve Equations [33], [39], [42], [43], [44], and [45]. A suggested procedure is given in the Appendix. The numerical method in the Appendix was used to solve cases as follows:

$$\text{Radius of rolls} = 14 \text{ in.}$$

$$2t_0 = 0.100 \text{ in.}$$

$$u_0 = 100 \text{ ips}$$

$$\frac{u_0}{t_0}\frac{\eta}{G} = 1.0, \sqrt{0.5}, \sqrt{0.1}$$

$$x_0 = 0.446 \text{ in.}$$

The following values of a were used

$$a = 0, \frac{\eta^2}{G^2}, 2.5\frac{\eta^2}{G^2}, 4\frac{\eta^2}{G^2}$$

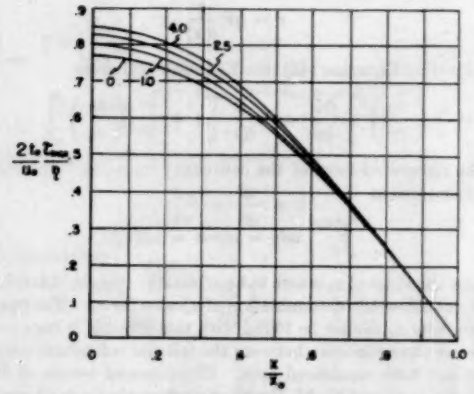

FIG. 5 PLOT OF DIMENSIONLESS MAXIMUM SHEAR STRESS ACROSS PASSAGE, $\frac{2t_0}{u_0}\frac{\tau_{max}}{\eta}$ VERSUS POSITION ALONG PASSAGE $\frac{x}{x_0}$, FOR $\frac{u_0}{t_0}\frac{\eta}{G} = 1.0$ AND VARIOUS VALUES OF $a\frac{G^2}{\eta^2}$

Figs. 4, 5, 6, and 7 illustrate the results of these calculations. Fig. 4 shows the variation in

$$\frac{2t_0}{u_0}\frac{\partial u}{\partial y}$$

across the section for

$$\frac{2t_0}{u_0}F = 0.7, \frac{u_0}{t_0}\frac{\eta}{G} = 1.0$$

and various values of the parameter $a(G^2/\eta^2)$. Fig. 5 shows the values of maximum shear stress in dimensionless form at the corresponding values of x/x_0 along the passage for the selected values of

$$a\left(\frac{G^2}{\eta^2}\right) \text{ and } \frac{u_0}{t_0}\frac{\eta}{G} = 1.0$$

and Fig. 6 shows the pressure variation, in dimensionless form,

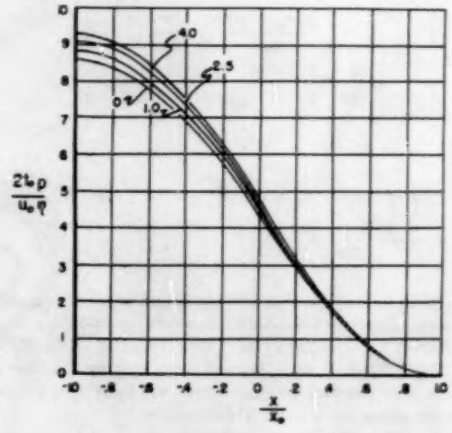

FIG. 6 PLOT OF DIMENSIONLESS PRESSURE $\frac{2t_0}{u_0}\frac{p}{\eta}$ VERSUS POSITION ALONG PASSAGE $\frac{x}{x_0}$, FOR $\frac{u_0}{t_0}\frac{\eta}{G} = 1.0$, AND INDICATED VALUES OF $a\frac{G^2}{\eta^2}$

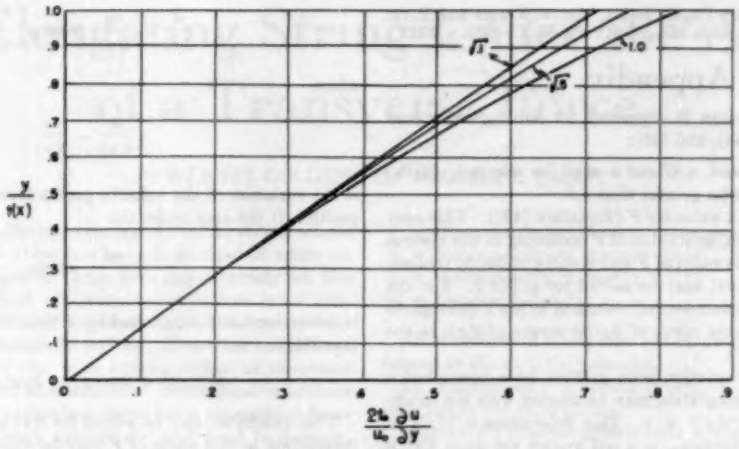

FIG. 7 PLOT OF VELOCITY GRADIENT $\frac{2l_0}{u_0}\frac{\partial u}{\partial y}$ ACROSS PASSAGE FOR $\frac{2l_0}{u_0}F = 0.7$, $a = 0$, AND VARIOUS VALUES OF $\frac{u_0}{l_0}\frac{\eta}{G}$

along the passage. Fig. 7 shows the variation in the velocity gradient across the section for $2l_0F/u_0 = 0.7$, $a = 0$ and various values of $(u_0/l_0)(\eta/G)$. As the speed of rolling is decreased, the solution deviates less from the viscous solution. As G is decreased, the variation from the viscous solution becomes more pronounced.

CONCLUSIONS

The most important result shown here is the variation in $\partial u/\partial y$ from the viscous case at the surface of the material.

The maximum per cent difference between

$$\left.\frac{\partial u}{\partial y}\right|_{\max}$$

for the viscoelastic cases and the viscous cases presented here was from 0 to 14 per cent for equal values of the maximum shearing stress.

The per cent difference depends on the value of the material constant a and the speed of rolling. The percentage difference goes up as the speed is increased and down as a is increased.

The difference in variation of $\partial u/\partial y$ across the section for an elastic-viscous material as compared to a viscous material explains the failure of the viscous solution in making suitable predictions regarding the behavior of a viscoelastic material. The approximate method included here certainly indicates which direction the variables go if a suitable value of a is known.

The results of the numerical solution indicate that the pressure and shear stress drop as G is lowered. This is because the viscosity is held constant and the lowering of G corresponds to a reduction of stiffness of the material. In other words, the material may accommodate a given load by elastic as well as viscous deformation so that the load for a prescribed time-dependent deformation will in general go down as G decreases. Therefore, these results show a slight decrease in total lateral force pushing the rolls apart between $-x_0 < x < x_0$ when G decreases (maximum decrease of 7.5 per cent for these calculations).

$(u_0/l_0)(\eta/G)$ is seen to be an important parameter in this problem. From a physical point of view $(u_0/l_0)(\eta/G)$ interrelates the kinematic and material properties of the problem since u_0/l_0 is the order of magnitude of the maximum shear-deformation rate and η/G is the ratio of two of the material constants.

The reader should note that this approximate solution does not include the determination of the elastic recovery of the material after it has left the rolls.

This solution should be of use to manufacturers who use the calendering process. From the standpoint of the manufacturer, the speed of rolling should be the highest speed compatible with producing a prescribed quality sheet. The material to be calendered is often heated to reduce the power requirements for calendering or to improve the quality of the product. Owing to energy dissipated in the shear flow and the resulting temperature rise of the material, the surface of the sheet may have undesirable characteristics. To make faster speeds of rolling possible the rolls are often cooled to improve the surface of the sheet. When the rolls are cooled the limiting speed of rolling is usually determined by blistering of the material under the surface. Knowledge of how the variables of the problem change when the material has elastic as well as viscous properties may be used as a guide in selecting the speed of rolling, the temperature of the bulk to be rolled, and the amount of cooling of the rolls necessary.

ACKNOWLEDGMENT

The author is grateful to Prof. G. F. Carrier of Harvard University who suggested the problem and who provided advice throughout the investigation. This presentation is a condensed version of the author's doctoral thesis (7).

BIBLIOGRAPHY

1 "The Calendering of Plastic Materials," by R. E. Gaskell, JOURNAL OF APPLIED MECHANICS, Trans. ASME, vol. 72, 1950, p. 334.

2 "The Mechanical Foundations of Elasticity and Fluid Dynamics," by C. Truesdell, *Journal of Rational Mechanics and Analysis*, vol. 1, 1952, p. 125.

3 "Laminare Stromung Newtonscher und Maxwellscher Flussigkeiten," by H. Fromm, *Zeitschrift für angewandte Mathematik und Mechanik*, vol. 25–27, 1947, p. 147.

4 Ibid., vol. 28, 1948, p. 43.

5 "On the Continuity of the Solid and Fluid States," by Walter Noll, *Journal of Rational Mechanics and Analysis*, vol. 4, 1955, p. 3.

6 "Thermal Effects in Calendering Viscous Fluids," by M. Finston, JOURNAL OF APPLIED MECHANICS, Trans. ASME, vol. 73, 1951, p. 12.

7 "The Calendering of Elastic-Viscous Materials," by P. R. Paslay, M.I.T. Mechanical Engineering Doctoral Thesis, 1955.

8 "Theory of Perfectly Plastic Solids," by W. Prager and P. G. Hodge, Jr., John Wiley & Sons, Inc., New York, N. Y., 1951, p. 232.

Appendix

The following procedure is suggested for solving Equations [33], [39], [42], [43], [44], and [45]:

1 The geometry, speed, η/G and a must be selected; $(u_0/l_0)(\eta/G)$ must not be of order greater than 1.0.

2 Arbitrarily select a value for F (Equation [43]). This may be selected, to start with, as a value of F occurring in the viscous solution. Now with this value of F and a value of $\partial u/\partial y$ (chosen arbitrarily) Equation [44] may be solved for $y/[t(x)]$. For the selected value of F calculate several values of $y/[t(x)]$ (enough to give a sufficiently accurate curve of $\partial u/\partial y$ versus $y/[t(x)]$ in the region $0 < y/[t(x)] < 1$).

3 With the $\partial u/\partial y$ variation with $y/[t(x)]$ for a prescribed a and η/G a numerical integration may be started with the condition that $u = u_0$ at $y/[t(x)] = 1$. This determines $u/[t(x)]$ at every point across the section. u is not known yet since $t(x)$ is unknown. Since $\partial u/\partial y$ versus $y/[t(x)]$ is nearly linear (the viscous case is linear), the trapezoidal rule furnishes a sufficiently accurate method of numerical integration.

4 $u/t(x)$ may now be plotted against $y/[t(x)]$. If the area under this curve is obtained (by Simpson's rule or some other appropriate means) then $t(x)$ may be determined from Equation [45]. One method which is convenient and accurate is to plot

$$\frac{u}{t(x)} - \frac{u_0}{t(x)} \quad \text{versus} \quad \frac{y}{t(x)}$$

where

$$\frac{u}{t(x)} - \frac{u_0}{t(x)}$$

is the variation of the velocity profile from the uniform velocity profile. If the area under the

$$\frac{u}{t(x)} - \frac{u_0}{t(x)} \quad \text{versus} \quad \frac{y}{t(x)}$$

is determined and designated by A then from continuity (Equation [45])

$$A[t(x)]^2 + 2u_0 t(x) - 2u_0 t(x_0) = 0$$

This quadratic may be solved for $t(x)$ and the value of x corresponding to this value of F may be determined as well.

5 Steps 1 through 4 are carried out for enough values of F to obtain a sufficiently accurate plot of F versus x. F is the maximum shear stress for the corresponding values of x so that $\tau|_{max}$ versus x is known. $[df(x)]/(dx)$ in Equation [42] may be found as a function of x. A numerical integration may be used to find $f(x)$ for each value of x. The boundary condition to be used is that $f(x) = 0$ when $x = x_0$.

An Elongating String Under the Action of a Transverse Force[1]

By WERNER GOLDSMITH,[2] BERKELEY, CALIF.

The motion of a uniform undamped flexible string whose length increases with time has been investigated when an arbitrary time-dependent force acts transversely at the free end. The method of characteristics has been employed to derive analytical expressions for the transverse displacement in the subsonic regime. Cases are considered when the free end of the wire moves either at constant velocity or at constant acceleration. Numerical solutions are presented in dimensionless form for a sinusoidal forcing function of arbitrary amplitude and fixed frequency. The possibility of the existence of resonances in the string has been examined.

Nomenclature

The following nomenclature is used in the paper:

A = cross-sectional area of wire, sq in.
F = time-dependent transverse force, lb
G = forcing function $= -\frac{1}{T}F(t)$
L = length of string at time t, ft
Q = dimensionless force amplitude, fraction of string tension
T = string tension, lb
a = acceleration of string in the x-direction, ft/sec^2
c = velocity of sound in the string, fps
d = differentiation symbol
f = displacement of string at free end, ft
g = acceleration of gravity, 32.2 ft/sec^2
m = exponent in summation
n = direction of interior normal to path of integration
$q = \frac{1-\beta}{1+\beta}$
s = co-ordinate of path of integration
t = time, sec
u = transverse displacement of string, ft
v = longitudinal velocity of string end in x-direction, fps
w = Green's function satisfying adjoint differential equation
x = co-ordinate along direction of undisturbed string, ft
y = ct
Ω = frequency, rad/sec
β = Mach number of string, $\beta = \frac{v}{c}$
ξ = dimension co-ordinate in space plane
η = time co-ordinate in space plane
ρ = string density, lb-sec^2/in.^{4}
ω = frequency, rad/ft

All subscripts of lower case letters denote differentiation with respect to the variable indicated.

All parentheses ( ) denote functional dependence upon the variables in the parentheses.

A prime (′) denotes differentiation with respect to the argument.

Introduction

Rockets are used in a number of applications involving the unreeling of a long flexible cord or wire from a relatively fixed source. The end of the cord which is attached to the rocket experiences transverse oscillatory displacements in accordance with the more or less regular yawing and pitching motions of the rocket.

It is of interest to discover whether or not the coupled motions of the rocket and the cord are capable of producing resonances which will result in the generation of transverse waves of large amplitude in the cord. The occurrence of large amplitude waves in the cord probably would result in a modification of the trajectory of the rocket in such a way as to deflect it from the desired course. An analysis of this problem is the object of this paper.

The mathematical model for this situation involves a flexible string of increasing length under tensile stress. One end of the string is attached to a drum, while the other is subjected to the action of a known time-dependent forcing function. Gravitational effects are neglected. The solution for the case of a string of constant length excited by a force at one boundary is amply described in the literature.[3,4] The feature of increasing span of the string gives rise to a traveling boundary condition, and problems of this type are most readily attacked by the Riemann-Volterra method of characteristics.[5,6]

Webster[7] presents a solution for a source moving subsonically along a string, but his initial value problem differs radically from the boundary-value problems considered in this paper. It should be emphasized that the solutions developed are applicable only in the subsonic range; in other words, only in the range where the longitudinal velocity of the free end is less than the sound velocity in the string.

---

[1] Work performed for the U. S. Naval Ordnance Test Station, China Lake, Calif.

[2] Associate Professor, Engineering Design, University of California; also, Mechanical Engineer, U. S. Naval Ordnance Test Station, China Lake. Assoc. Mem. ASME.

Presented at the Applied Mechanics Division Summer Conference, Berkeley, Calif., June 13–15, 1957, of The American Society of Mechanical Engineers.

Discussion of this paper should be addressed to the Secretary, ASME, 29 West 39th Street, New York, N. Y., and will be accepted until January 10, 1958, for publication at a later date. Discussion received after the closing date will be returned.

Note: Statements and opinions advanced in papers are to be understood as individual expressions of their authors and not those of the Society. Manuscript received by ASME Applied Mechanics Division, December 18, 1956. Paper No. 57—APM-9.

[3] "Vibration and Sound," by P. M. Morse, McGraw-Hill Book Company, Inc., New York, N. Y., second edition, 1948, pp. 91–97, 133–146.

[4] "Theory of Vibrations," by N. W. McLachlan, Dover Publications, New York, N. Y., 1951, pp. 79–83.

[5] "Methoden der Mathematischen Physik," by R. Courant and D. Hilbert, Julius Springer, Berlin, Germany, second edition, vol. 1, 1931, pp. 321–337.

[6] "Partial Differential Equations in Physics," by A. Sommerfeld, translated by E. G. Straus, Academic Press, New York, N. Y., 1949, pp. 52–54.

[7] "Partial Differential Equations of Mathematical Physics," by A. G. Webster, Dover Publications, New York, N. Y., 1955, pp. 250–253.

Mathematical Development

The assumed physical system is shown in Fig. 1. A flexible string of constant cross-sectional area and density is stretched by a constant tensile force T acting in the direction of increasing length and is further driven transversely by a known force $F(t)$. Solutions will be developed for the case of no damping when the end of the string moves either at constant velocity or at constant acceleration.

The governing differential equation for the transverse displacement of the system u is the ordinary wave equation

$$c^2 u_{xx} = u_{tt} \quad [1]$$

which is a hyperbolic type of equation. The sound velocity in the string c is defined by

$$c^2 = \frac{T}{144\rho A} \quad [2]$$

where T is the tension, A the cross-sectional area, and ρ the mass density for the string. Replacement of $y = ct$ in Equation [1] provides the homogeneous relation

$$u_{xx} = u_{yy} \quad [3]$$

The boundary conditions are

$$u(0, t) = 0 \quad [4]$$

corresponding to zero displacement at the drum, and

$$-Tu_x(L(t), t) = F(t) \quad \text{or } u_x \equiv G(y)|_{x=L} \quad [5]$$

where $$G(y) = -\frac{1}{T} F(ct)$$

which describes the slope at point $L(t)$ as the direction of the resultant of the two forces acting at this station. In addition, the motion of the free end of the wire is prescribed as

$$L(t) = vt \quad [6]$$

in the case of constant velocity, and

$$L(t) = \frac{1}{2} at^2 \quad [7]$$

in the case of constant acceleration.

The technique employed for the solution of the problem utilizes the method of characteristics, which involves a contour integration in the x-y plane. The solution for the displacement at an arbitrary space point $u(\xi, \eta)$ of the general second-order partial differential equation requires the determination of a Green's function w which satisfies the adjoint differential equation and must also fulfill certain requirements along the characteristics $y \pm x = \text{const}$.[5,7] The simple wave equation, however, is self-adjoint, and it can be shown that for this case $w = 1$. Solutions for the desired displacement can then be derived from the integral relation

$$\sum_{\text{contour}} \int \{-u_x \cos(n, x) + u_y \cos(n, y)\} ds = 0 \quad [8]$$

where n denotes the direction of the interior normal and ds describes the path of integration.

String End Travels at Constant Velocity. The first case considered will be that when the end of the string $L(t)$ has a constant velocity

$$L(t) = vt = \beta y \quad [9]$$

where $\beta \equiv v/c$. The plane of integration for this situation is

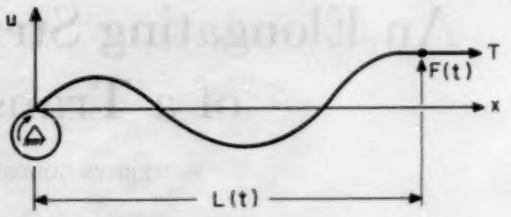

Fig. 1 Diagram of Physical System

represented by Fig. 2. Line OA denotes the location of the end of the string, and is inclined to the y-axis at an angle less than 45 deg in view of the subsonic condition $v < c$, or $\beta < 1$. The arbitrary space point $P(\xi, \eta)$ is connected by characteristics to corresponding points A and B on the boundaries. The equation of line AP is

$$x - \xi = \eta - y \quad [10]$$

while line PB is defined by

$$x - \xi = y - \eta \quad [11]$$

The co-ordinates of point A are obtained by simultaneous solution of Equations [9] and [10], so that

$$x_A = \frac{\beta[\xi + \eta]}{1 + \beta} \qquad y_A = \frac{\xi + \eta}{1 + \beta} \quad [12]$$

The co-ordinates of point B are

$$x_B = 0 \qquad y_B = \eta - \xi \quad [13]$$

The slopes of the characteristics are ± 1. Further

$$\left.\begin{aligned}
&\text{Along } AP\text{: } ds = \sqrt{(2)}dy = -\sqrt{(2)}dx \\
&\qquad \cos(n, x) = -\frac{1}{\sqrt{2}} \quad \cos(n, y) = -\frac{1}{\sqrt{2}} \\
&\text{Along } PB\text{: } ds = -\sqrt{(2)}dx = -\sqrt{(2)}dy \\
&\qquad \cos(n, x) = \frac{1}{\sqrt{2}} \quad \cos(n, y) = -\frac{1}{\sqrt{2}} \\
&\text{Along } BO\text{: } ds = -dy, \quad dx = 0 \\
&\qquad \cos(n, x) = 1 \quad \cos(n, y) = 0 \\
&\text{Along } OA\text{: } ds = \sqrt{1 + \beta^2}\, dy = \frac{\sqrt{1 + \beta^2}}{\beta} dx \\
&\qquad \cos(n, x) = \frac{-1}{\sqrt{1 + \beta^2}} \quad \cos(n, y) = \frac{\beta}{\sqrt{1 + \beta^2}}
\end{aligned}\right\} \quad [14]$$

Substitution of Equations [14] in Equation [8] provides the relation

$$-\int_A^P \{u_x dx + u_y dy\} + \int_P^B \{u_x dx + u_y dy\} + \int_B^0 u_x dy + \int_0^A \{u_x + \beta u_y\} dy = 0 \quad [15]$$

and the displacement $u(\xi, \eta)$ is then obtained by integration of Equation [15] as

$$u(\xi, \eta) = \frac{1}{2}\left\{u\left(\frac{\beta[\xi + \eta]}{1 + \beta}, \frac{\xi + \eta}{1 + \beta}\right) + u(0, \eta - \xi) + \int_{\eta - \xi}^0 u_x(0, y) dy + \int_0^{\frac{\xi + \eta}{1 + \beta}} [u_x + \beta u_y](\beta y, y) dy\right\} \quad [16]$$

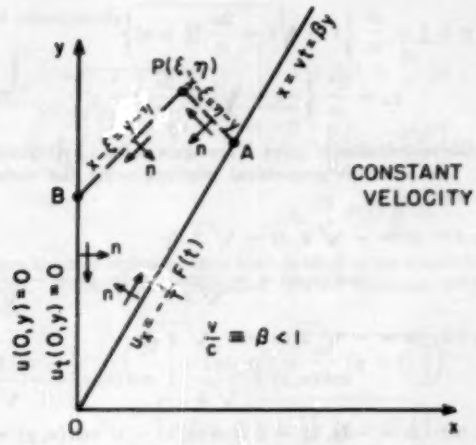

FIG. 2 SPACE PLANE FOR CASE OF CONSTANT VELOCITY

An explicit evaluation of Equation [16] cannot be performed directly since the required boundary values $u_x(0, y)$ and $u_y(\beta y, y)$ are unknown. It will be assumed that the displacement u along $x = \beta y$ is given by $f(y)$. Then, since $dx = \beta dy$

$$du(\beta y, y) = f' = u_x dx + u_y dy = \{\beta u_x + u_y\} dy = \{\beta G(y) + u_y\} dy$$

and

$$u_y = f'(y) - \beta G(y) \quad \ldots\ldots [17]$$

Subetitution of Equation [17] in Equation [16] yields

$$u(\xi, \eta) = \frac{1}{2}\left\{[1+\beta] f\left(\frac{\beta[\xi+\eta]}{1+\beta}, \frac{\xi+\eta}{1+\beta}\right) - \int_0^{\eta-\xi} u_x(0, y)dy + [1-\beta^2]\int_0^{\frac{\xi+\eta}{1+\beta}} G(y)dy\right\} \quad \ldots [18]$$

since $u(A) \equiv f$, and since further $f(0, 0) = u(0, y) = 0$ for compatibility. Now let point P approach the boundary line $y = 0$. This corresponds to $\xi \to 0$ in Equation [18], or

$$u(0, \eta) = 0 = \frac{1}{2}\left\{[1+\beta] f\left(\frac{\beta\eta}{1+\beta}, \frac{\eta}{1+\beta}\right) - \int_0^{\eta} u_x(0, y)dy + [1-\beta^2]\int_0^{\frac{\eta}{1+\beta}} G(y)dy\right\}$$

Then

$$\int_0^{\eta} u_x(0, y)dy = [1+\beta] f\left(\frac{\beta\eta}{1+\beta}, \frac{\eta}{1+\beta}\right) + [1-\beta^2]\int_0^{\frac{\eta}{1+\beta}} G(y)dy$$

and

$$-\int_0^{\eta-\xi} u_x(0, y)dy = -[1+\beta] f\left(\frac{\beta[\eta-\xi]}{1+\beta}, \frac{\eta-\xi}{1+\beta}\right) - [1-\beta^2]\int_0^{\frac{\eta-\xi}{1+\beta}} G(y)dy \quad \ldots\ldots [19]$$

Combination of Equations [18] and [19] then provides the relation

$$u(\xi, \eta) = \frac{1}{2}\left\{[1+\beta]\left[f\left(\frac{\beta[\eta+\xi]}{1+\beta}, \frac{\eta+\xi}{1+\beta}\right) - f\left(\frac{\beta[\eta-\xi]}{1+\beta}, \frac{\eta-\xi}{1+\beta}\right)\right] + [1-\beta^2]\int_{\frac{\eta-\xi}{1+\beta}}^{\frac{\eta+\xi}{1+\beta}} G(y)dy\right\} \quad \ldots [20]$$

If point P now approaches the other boundary $x = \beta y$, or $x \to \beta\eta$, $y \to \eta$, then

$$u(\beta\eta, \eta) = \frac{1}{2}\left\{[1+\beta][f(\beta\eta, \eta) - f(\beta q\eta, q\eta)] + [1-\beta^2]\int_{q\eta}^{\eta} G(y)dy\right\} \quad \ldots\ldots [21]$$

where the constant q is defined as

$$q = \frac{1-\beta}{1+\beta} \quad \ldots\ldots [22]$$

It should be observed that this limiting process can be accomplished only in the subsonic regime. In the supersonic region $\beta \geq 1$, the characteristic BP cannot be extended to intersect line OA, and the procedure described here will be invalid. Denoting $f(\beta\eta, \eta)$ by $f(\eta)$, Equation [21] may be written as

$$f(\eta) + \frac{1}{q} f(q\eta) = [1+\beta]\int_{q\eta}^{\eta} G(y)dy \quad \ldots\ldots [23]$$

Differentiation with respect to η yields

$$f'(\eta) + f'(q\eta) = [1+\beta][G(\eta) - qG(q\eta)] \quad \ldots\ldots [24]$$

Equation [24] will now be used as a recursion formula

$$\left.\begin{aligned} f'(\eta) &= -f'(q\eta) + [1+\beta][G(\eta) - qG(q\eta)] \\ &= f'(q^2\eta) + [1+\beta]G(\eta) - 2G(q\eta) + q[1+\beta]G(q^2\eta) \\ &= -f'(q^3\eta) + [1+\beta]G(\eta) - 2[G(q\eta) - G(q^2\eta)] - q[1+\beta]G(q^3\eta) \\ &= f'(q^4\eta) + [1+\beta]G(\eta) - 2[G(q\eta) - G(q^2\eta) + G(q^3\eta)] + q[1+\beta]G(q^4\eta) \\ &= \ldots\ldots \end{aligned}\right\} \quad \ldots [25]$$

Thus

$$f'(\eta) = [-1]^m f'(q^m\eta) + [1+\beta]G(\eta) + 2\sum_{m=1}^{m-1}[-1]^m G(q^m\eta) + q[1+\beta]G(q^m\eta) \quad \ldots\ldots [26]$$

Now let $m \to \infty$; since $q < 1$, $q^m \to 0$. Furthermore, compatibility requires that G be a continuous function at the origin and that $G(0) = 0$. Thus, since $u_x(0) = 0$

$$f'(0) \equiv u_x dx + u_y dy\big|_{\substack{x=0\\y=0}} = 0$$

and further $G(q^m\eta) \to G(0) \to 0$. Equation [26] may then be written as

$$f'(\eta) = 2\sum_{m=1}^{\infty}[-1]^m G(q^m\eta) + [1+\beta]G(\eta) \quad \ldots\ldots [27]$$

Integration of Equation [27] leads to

$$f(\eta) = 2\sum_{m=1}^{\infty}[-1]^m\int_0^{\eta}G(\eta^m\eta)d\eta + [1+\beta]\int_0^{\eta}G(\eta)d\eta \quad\ldots\ldots[28]$$

and thus

$$f\left(\frac{\eta\pm\xi}{1+\beta}\right) = [1+\beta]\int_0^{\frac{\eta\pm\xi}{1+\beta}}G(\eta)d\eta + 2\sum_{m=1}^{\infty}[-1]^m\int_0^{\frac{\eta\pm\xi}{1+\beta}}G(\eta^m\eta)d\eta \quad\ldots\ldots[29]$$

Finally, replacing ξ by x and η by ct in Equation [20] yields

$$u(x,ct) = \frac{1}{2}\left\{[1+\beta]\left[f\left(\frac{\beta[ct+x]}{1+\beta},\frac{ct+x}{1+\beta}\right) - f\left(\frac{\beta[ct-x]}{1+\beta},\frac{ct-x}{1+\beta}\right)\right] + [1-\beta^2]\int_{\frac{ct-x}{1+\beta}}^{\frac{ct+x}{1+\beta}}G(y)dy\right\}\ldots[30]$$

where the unknown functions f are determined from Relation [29] as

$$f\left(\frac{\beta[ct\pm x]}{1+\beta},\frac{ct\pm x}{1+\beta}\right) = [1+\beta]\int_0^{\frac{ct\pm x}{1+\beta}}G(y)dy + 2\sum_{m=1}^{\infty}[-1]^m\int_0^{\frac{ct\pm x}{1+\beta}}G(\eta^m y)dy \quad\ldots\ldots[31]$$

String End Travels at Constant Acceleration. The motion of the end of the wire is now defined by the relation

$$L(t) = \frac{1}{2}at^2 = \frac{1}{2}\frac{a}{c^2}y^2 \quad\ldots\ldots[32]$$

and the corresponding x-y plane is shown in Fig. 3. Simultaneous solution of Equations [32] and [10] determines the co-ordinates of point A as

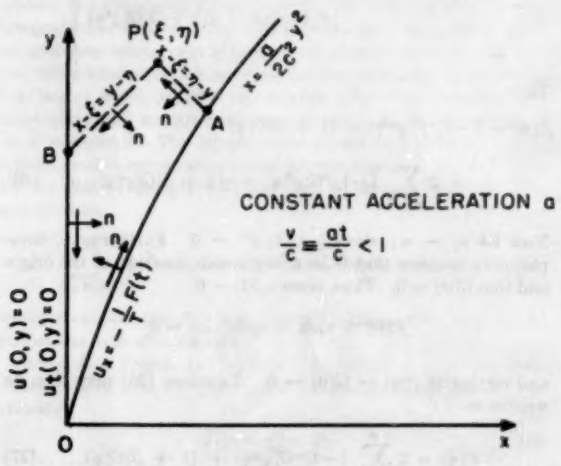

FIG. 3 SPACE PLANE FOR CASE OF CONSTANT ACCELERATION

$$x_A = \eta+\xi+\frac{c^2}{a}\left\{1-\sqrt{1+\frac{2a}{c^2}[\xi+\eta]}\right\}$$

$$y_A = \frac{c^2}{a}\left\{-1+\sqrt{1+\frac{2a}{c^2}[\xi+\eta]}\right\}\quad\ldots\ldots[33]$$

while the co-ordinates of point B are again defined by Equation [13]. The pertinent geometrical relations along the various paths are given by

Along AP: $ds = -\sqrt{2}\,dx = \sqrt{2}\,dy$

$$\cos(n,x) = -\frac{1}{\sqrt{2}}\quad\cos(n,y) = -\frac{1}{\sqrt{2}}$$

Along PB: $ds = -\sqrt{2}\,dx = -\sqrt{2}\,dy$

$$\cos(n,x) = \frac{1}{\sqrt{2}}\quad\cos(n,y) = -\frac{1}{\sqrt{2}}$$

Along BO: $ds = -dy,\ dx = 0\quad\cos(n,x) = 1\quad\cos(n,y) = 0$

Along OA: $ds = \frac{c^2}{ay}\sqrt{\left\{1+\frac{a^2y^2}{c^4}\right\}}\,dx = \sqrt{\left\{1+\frac{a^2y^2}{c^4}\right\}}\,dy$

$$\cos(n,x) = \frac{-1}{\sqrt{\left\{1+\frac{a^2y^2}{c^4}\right\}}}\quad\cos(n,y) = \frac{ay}{c^2\sqrt{\left\{1+\frac{a^2y^2}{c^4}\right\}}}$$

$\ldots\ldots[34]$

Substitution of Equations [34] in the contour integration formula [8] leads to

$$\int_A^P\{-u_x dx - u_y dy\} + \int_P^B\{u_x dx + u_y dy\} + \int_B^0 u_x dx + \int_0^A\left\{u_x + \frac{ay}{c^2}u_y\right\}dy = 0\quad\ldots\ldots[35]$$

The value of u_x along the line $x = (a/2c^2)y^2$ is given by $G(y)$, and the value of u on this boundary will again be denoted by f. The same procedure as employed in the previous section then leads to the relation

$$u(\xi,\eta) = \frac{1}{2}\left\{f\left(\eta+\xi+\frac{c^2}{a}\left[1-\sqrt{1+\frac{2a}{c^2}\{\eta+\xi\}}\right],\ \frac{c^2}{a}\left[-1+\sqrt{1+\frac{2a}{c^2}\{\eta+\xi\}}\right]\right) - \int_0^{\eta-\xi}u_x(0,y)dy + \int_0^{\frac{c^2}{a}\left[-1+\sqrt{1+\frac{2a}{c^2}\{\xi+\eta\}}\right]}\left\{\left[\left[1-\frac{a^2y^2}{c^4}\right]G(y) + \frac{ay}{c^2}f'(y)\right]\right\}dy\right\}\quad\ldots\ldots[36]$$

When $\xi \to 0$, Equation [36] becomes

$$u(0,\eta) = 0 = f\left(\eta+\frac{c^2}{a}\left[1-\sqrt{1+\frac{2a\eta}{c^2}}\right],\ \frac{c^2}{a}\left[-1+\sqrt{1+\frac{2a\eta}{c^2}}\right]\right) - \int_0^{\eta}u_x(0,y)dy + \int_0^{\frac{c^2}{a}\left[-1+\sqrt{1+\frac{2a\eta}{c^2}}\right]}\left\{\left[\left[1-\frac{a^2y^2}{c^4}\right]G(y) + \frac{ay}{c^2}f'(y)\right]\right\}dy$$

and consequently

$$-\int_0^{\eta-\xi} u_x(0,y)dy = -f\left(\frac{c^2}{a}\left[-1+\sqrt{1+\frac{2a}{c^2}\{\eta-\xi\}}\right]\right) - \int_0^{\frac{c^2}{a}\left[-1+\sqrt{1+\frac{2a}{c^2}\{\eta-\xi\}}\right]} \left\{\left[1-\frac{a^2y^2}{c^4}\right]G(y) + \frac{ay}{c^2}f'(y)\right\}dy \quad \ldots\ldots [37]$$

where the x-co-ordinates have been deleted in the functional notation. Substitution of Equation [37] in Equation [36] then yields

$$u(\xi,\eta) = \frac{1}{2}\left\{f\left(\frac{c^2}{a}\left[-1+\sqrt{1+\frac{2a}{c^2}\{\eta+\xi\}}\right]\right) - f\left(\frac{c^2}{a}\left[-1+\sqrt{1+\frac{2a}{c^2}\{\eta-\xi\}}\right]\right) + \int_{\frac{c^2}{a}\left[-1+\sqrt{1+\frac{2a}{c^2}\{\eta-\xi\}}\right]}^{\frac{c^2}{a}\left[-1+\sqrt{1+\frac{2a}{c^2}\{\eta+\xi\}}\right]} \left\{\left[1-\frac{a^2y^2}{c^4}\right]G(y) + \frac{ay}{c^2}f'(y)\right\}dy\right\} \quad \ldots\ldots [38]$$

Now let $P \to A$; this procedure is also valid only in the region where $v = at < c$. Along the curve OA

$$\xi = \frac{a}{2c^2}\eta^2, \quad u = f\left(\frac{c^2}{a}\left[-1+\sqrt{1+\frac{2a\eta}{c^2}+\frac{a^2\eta^2}{c^4}}\right]\right) = f(\eta)$$

and substitution of these terms in Equation [38] results in the integral equation

$$f(\eta) + f\left(\frac{c^2}{a}\left[-1+\sqrt{1+\frac{2a\eta}{c^2}-\frac{a^2\eta^2}{c^4}}\right]\right) = \int_{\frac{c^2}{a}\left[-1+\sqrt{1+\frac{2a\eta}{c^2}-\frac{a^2\eta^2}{c^4}}\right]}^{\eta} \left\{\left[1-\frac{a^2y^2}{c^4}\right]G(y) + \frac{ay}{c^2}f'(y)\right\}dy \quad \ldots\ldots [39]$$

Differentiation and some manipulation then yields the result

$$f'(\eta) = -f'\left(\frac{c^2}{a}\left[-1+\sqrt{1+\frac{2a\eta}{c^2}-\frac{a^2\eta^2}{c^4}}\right]\right) + \left[1-\frac{a\eta}{c^2}\right]G(\eta) - \left[2-\sqrt{1+\frac{2a\eta}{c^2}-\frac{a^2\eta^2}{c^4}}\right] G\left(\frac{c^2}{a}\left[-1+\sqrt{1+\frac{2a\eta}{c^2}-\frac{a^2\eta^2}{c^4}}\right]\right) \quad \ldots\ldots [40]$$

Since

$$\frac{c^2}{a}\left[-1+\sqrt{1+\frac{2a\eta}{c^2}-\frac{a^2\eta^2}{c^4}}\right] < \eta$$

Equation [40] is also amenable to a solution by a recursion formula. In practice, however, it will be found more convenient to use a numerical method of evaluation for $f'(\eta)$, followed by a graphical integration to yield $f(\eta)$. The final solution in the form corresponding to Equation [30] is then given by

$$u(x,ct) = \frac{1}{2}\left\{f\left(\frac{c^2}{a}\left[-1+\sqrt{1+\frac{2a}{c^2}\{ct+x\}}\right]\right) - f\left(\frac{c^2}{a}\left[-1+\sqrt{1+\frac{2a}{c^2}\{ct-x\}}\right]\right) + \int_{\frac{c^2}{a}\left[-1+\sqrt{1+\frac{2a}{c^2}\{ct-x\}}\right]}^{\frac{c^2}{a}\left[-1+\sqrt{1+\frac{2a}{c^2}\{ct+x\}}\right]} \left\{\left[1-\frac{a^2y^2}{c^4}\right]G(y) + \frac{ay}{c^2}f'(y)\right\}dy\right\} \quad \ldots\ldots [41]$$

where the values of

$$f\left(\frac{c^2}{a}\left[-1+\sqrt{1+\frac{2a}{c^2}\{ct+x\}}\right]\right), \quad f\left(\frac{c^2}{a}\left[-1+\sqrt{1+\frac{2a}{c^2}\{ct-x\}}\right]\right), \quad \text{and} \quad \int \frac{ay}{c^2}f'(y)dy$$

are to be obtained from the integral curves of the solution of Equation [40].

Numerical Example

Numerical results have been obtained for the cases of constant velocity and constant acceleration using a sinusoidal forcing function

$$F(t) = -QT\sin\Omega t = -QT\sin\omega ct \quad \text{or} \quad G(y) = Q\sin\omega y \quad [42]$$

where Q represents the force amplitude as a fraction of the tension. For the case of constant velocity, substitution of Equation [42] in Equations [30] and [31] yields, respectively

$$u(x,ct) = \frac{1}{2}\left\{[1+\beta]\left[f\left(\frac{\beta[ct+x]}{1+\beta}, \frac{ct+x}{1+\beta}\right) - f\left(\frac{\beta[ct-x]}{1+\beta}, \frac{ct-x}{1+\beta}\right)\right] + [1-\beta^2]\,Q\int_{\frac{ct-x}{1+\beta}}^{\frac{ct+x}{1+\beta}} \sin\omega y dy\right\} \quad \ldots\ldots [43]$$

$$f\left(\frac{\beta[ct\pm x]}{1+\beta}, \frac{ct\pm x}{1+\beta}\right) = Q\left\{[1+\beta]\int_0^{\frac{ct\pm x}{1+\beta}} \sin\omega y dy + 2\sum_{m=1}^{\infty}[-1]^m\int_0^{\frac{ct\pm x}{1+\beta}} \sin q^m\omega y dy\right\} \quad \ldots\ldots [44]$$

and combination of Equations [43] and [44] leads to the final result

$$\frac{u(x,ct)}{Q} = \frac{2[1+\beta]}{\omega}\left\{\sin\frac{\omega x}{1+\beta}\sin\frac{\omega ct}{1+\beta} + \sum_{m=1}^{\infty}[-1]^m\frac{1}{q^m}\sin\frac{q^m\omega x}{1+\beta}\sin\frac{q^m\omega ct}{1+\beta}\right\} \quad \ldots\ldots [45]$$

Calculations were performed for a value of $T = 200$ lb, $A = 0.001$ sq in., a velocity $v = 1000$ fps, a density $\rho g = 0.279$ lb/in.^{3}, and a frequency of disturbing force of 10 cps, corresponding to a value of $\omega = 0.0453987$ rad/ft. The sound velocity in the string is 1384 fps, and the Mach number for the string $\beta = 0.722543$. Displacements were computed at intervals of $0.1(x/L)$ for four different times of 0.02, 0.1, 0.5, and 1 sec, corresponding to string

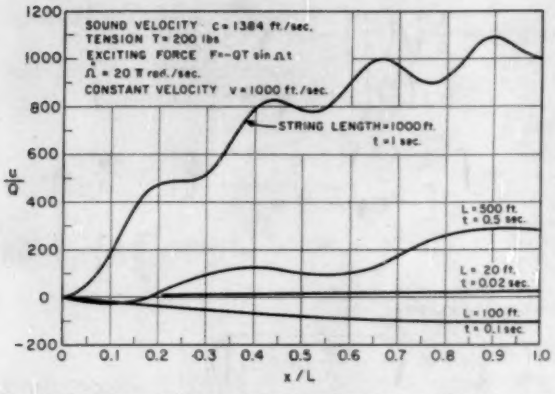

FIG. 4 TRANSVERSE DISPLACEMENT OF STRING AS A FUNCTION OF DIMENSIONLESS LENGTH FOR CASES OF CONSTANT VELOCITY

lengths of 20, 100, 500, and 1000 ft, respectively, as shown in Fig. 4.

It was found that six terms of the expansion

$$\sum_{m=1}^{\infty} [-1]^m \frac{1}{q^m} \sin \frac{q^m \omega x}{1+\beta} \sin \frac{q^m \omega ct}{1+\beta}$$

sufficed to produce convergence of the displacement to less than 0.1 per cent for the longest time considered. Only three terms were required to yield comparable results for the shortest travel time. The definition of the curves was considerably improved with an interpolation process which superposed the sinusoidal variation resulting from the first term of Equation [45] on the less rapidly changing component contributed by the summation. The latter permitted the construction of a reasonably smooth curve with only 10 computed points.

Application of the sinusoidal forcing function, Equation [42], to Equation [41] yields for the case of constant acceleration

$$\frac{u(x,ct)}{Q} = \frac{1}{2}\left\{f\left(\frac{c^2}{a}\left[-1+\sqrt{1+\frac{2a}{c^2}\{ct+x\}}\right]\right) - f\left(\frac{c^2}{a}\left[-1+\sqrt{1+\frac{2a}{c^2}\{ct-x\}}\right]\right) + \int_{\frac{c^2}{a}\left[-1+\sqrt{1+\frac{2a}{c^2}\{ct-x\}}\right]}^{\frac{c^2}{a}\left[-1+\sqrt{1+\frac{2a}{c^2}\{ct+x\}}\right]} \left\{\left[\left[1-\frac{a^2y^2}{c^4}\right]\sin \omega y + \frac{ay}{c^2} f'(y)\right]\right\} dy\right\} \quad [46]$$

which, for purposes of calculation, can be reduced futher to

$$\frac{u(x,ct)}{Q} = \frac{1}{2}\left\{f\left(\frac{c^2}{a}\left[-1+\sqrt{1+\frac{2a}{c^2}\{ct+x\}}\right]\right) - f\left(\frac{c^2}{a}\left[-1+\sqrt{1+\frac{2a}{c^2}\{ct-x\}}\right]\right) - \frac{1}{\omega}\left[\left[\cos\frac{\omega c^2}{a}\left[-1+\sqrt{1+\frac{2a}{c^2}\{ct+x\}}\right] - \cos\frac{\omega c^2}{a}\left[-1+\sqrt{1+\frac{2a}{c^2}\{ct-x\}}\right]\right]\right] - \frac{a^2}{c^4}\left[\left[\frac{2c^2}{\omega^2 a}\left[-1+\sqrt{1+\frac{2a}{c^2}\{ct+x\}}\right]\right.\right.\right.$$

$$\sin\frac{\omega c^2}{a}\left[-1+\sqrt{1+\frac{2a}{c^2}\{ct+x\}}\right] + \left[\left[\frac{c^4}{a^2}\left[-1+\sqrt{1+\frac{2a}{c^2}\{ct+x\}}\right]^2 - \frac{2}{\omega^2}\right]\right]$$

$$\left.\left.\left.\omega\cos\frac{\omega c^2}{a}\left[-1+\sqrt{1+\frac{2a}{c^2}\{ct+x\}}\right]\right]\right] + \frac{a^2}{c^4}\left[\left[\frac{2c^2}{\omega^2 a}\left[-1+\sqrt{1+\frac{2a}{c^2}\{ct-x\}}\right]\right.\right.$$

$$\sin\frac{\omega c^2}{a}\left[-1+\sqrt{1+\frac{2a}{c^2}\{ct-x\}}\right] + \left[\left[\frac{c^4}{a^2}\left[-1+\sqrt{1+\frac{2a}{c^2}\{ct-x\}}\right]^2 - \frac{2}{\omega^2}\right]\right]$$

$$\left.\left.\left.\omega\cos\frac{\omega c^2}{a}\left[-1+\sqrt{1+\frac{2a}{c^2}\{ct-x\}}\right]\right]\right] + \left[-1+\sqrt{1+\frac{2a}{c^2}\{ct+x\}}\right] f\left(\frac{c^2}{a}\left[-1+\sqrt{1+\frac{2a}{c^2}\{ct+x\}}\right]\right) - \left[-1+\sqrt{1+\frac{2a}{c^2}\{ct-x\}}\right] f\left(\frac{c^2}{a}\left[-1+\sqrt{1+\frac{2a}{c^2}\{ct-x\}}\right]\right) - \frac{a}{c^2}\int_{\frac{c^2}{a}\left[-1+\sqrt{1+\frac{2a}{c^2}\{ct-x\}}\right]}^{\frac{c^2}{a}\left[-1+\sqrt{1+\frac{2a}{c^2}\{ct+x\}}\right]} f(\eta)d\eta\right\} \quad [47]$$

by integration by parts. Substitution of Equation [42] in the relation for $f'(\eta)$, Equation [40], results in the expression

$$f'(\eta) = -f'\left(\frac{c^2}{a}\left[-1+\sqrt{1+\frac{2a\eta}{c^2}-\frac{a^2\eta^2}{c^4}}\right]\right) + \left[1-\frac{a\eta}{c^2}\right]\sin\omega\eta - \left[2-\sqrt{1+\frac{2a\eta}{c^2}-\frac{a^2\eta^2}{c^4}}\right] \sin\frac{\omega c^2}{a}\left[-1+\sqrt{1+\frac{2a\eta}{c^2}-\frac{a^2\eta^2}{c^4}}\right] \quad [48]$$

A numerical method of successive approximation was employed for the solution of Equation [48]. Initially, a sequence of value of $f'(\eta)$ was assumed, an approximate curve of $f'(\eta)$ as a function of η was plotted, the values of the term

$$f'\left(\frac{c^2}{a}\left[-1+\sqrt{1+\frac{2a\eta}{c^2}-\frac{a^2\eta^2}{c^4}}\right]\right)$$

were then read from the curve and resubstituted in Equation [48] until convergence was obtained. For sufficiently large values of η, the value of the term

$$f'\left(\frac{c^2}{a}\left[-1+\sqrt{1+\frac{2a\eta}{c^2}-\frac{a^2\eta^2}{c^4}}\right]\right)$$

was located in an interval already computed, and Equation [48] could be evaluated directly. While some question exists concerning the accuracy of the computations of $f'(\eta)$, the subsequent process of integration would tend to smooth out any errors.

Only the integrals of the $f'(\eta)$ versus η-curve are employed in the solution of the problem.

The constants employed in this example involved a sound velocity of 1384 fps and a constant acceleration of 161 ft/sec², or $5g$. A curve of $f'(\eta)$ was computed at intervals of 10 units of η. Fig. 5 shows the calculated curve for a range of η from 0 to 750, while Fig. 6 portrays the corresponding integral curve $f(\eta)$. These curves were obtained by a graphical integration with the aid of a planimeter. The range of these curves encompasses an interval of time of about 0.545 sec, permitting a string elongation to a length of approximately 24 ft.

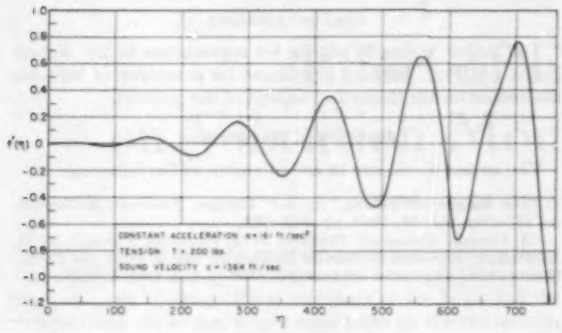

FIG. 5 $f'(\eta)$ AS A FUNCTION OF η

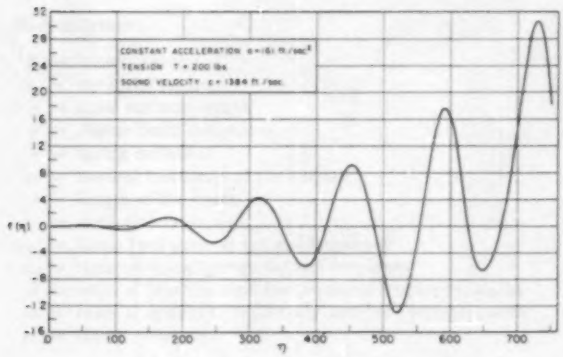

FIG. 6 $f(\eta)$ AS A FUNCTION OF η

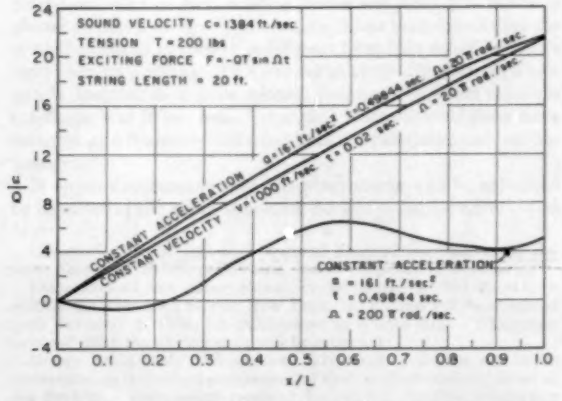

FIG. 7 TRANSVERSE DISPLACEMENT OF STRING AS A FUNCTION OF DIMENSIONLESS LENGTH FOR CASES OF CONSTANT ACCELERATION

The displacements for the constant velocity case were calculated for four selected string lengths covering the region of practical interest. It may be noted from Equation [45] that the transverse motion is described by the superposition of a term involving the product of two sine functions and a sum of alternating products of similar character. This alternating series eventually converges quite rapidly, although the initial terms of this sequence may be diverging. The sign of the quantity $\sin [q^n \omega c t]/[1 + \beta]$ of the dominant term of this series determines the location of the average displacement with respect to the neutral position of the string. Since this term alternates in sign with increasing time, the average displacement also will oscillate about the zero-displacement axis. Although the mean amplitude of motion increases with time, it always will remain bounded.

An interesting feature of this case is the reduction of the frequency of oscillation of both terms in Equation [45] from that of the exciting force by the factor $1/[1 + \beta]$. This phenomenon is the result of a Doppler effect which will halve the response frequency of the string at sonic velocity. When the string is still relatively short, the first term of Equation [45] is overshadowed by the alternating series, and the ripples produced in the string by this component cannot be detected in Fig. 4 or 7. At later times, however, this term causes a significant deviation from the mean displacement of the string, and, near the origin, may even result in a total displacement of opposite phase to that of the average motion.

In the case of constant acceleration, the first four terms of Equation [47] determined the resulting transverse motion within about 1 per cent for a forcing frequency of 100 cps. As may be observed from Fig. 7, the smaller frequency is too slow to portray effectively the oscillatory nature of the phenomenon, which is governed by the quantity

$$\frac{1}{\omega}\left\{\cos\frac{\omega c^2}{a}\left[-1+\sqrt{1+\frac{2a}{c^2}\,[ct+x]}\right]\right.$$
$$\left.-\cos\frac{\omega c^2}{a}\left[-1+\sqrt{1+\frac{2a}{c^2}\,[ct-x]}\right]\right\}$$

However, the existence of this feature is clearly demonstrated when the forcing frequency is increased by a factor of 10. Such a change also severely curtails the maximum amplitude of the displacement.

The shape of the displacement curves for the cases of constant velocity and constant acceleration for the same forcing frequency and string length are quite similar, although the velocity of the free end of the wire and the travel time differ radically for the

DISCUSSION

The displacements for the constant velocity case were calculated for four selected string lengths covering the region of practical interest. It may be noted from Equation [45] that the transverse motion is described by the superposition of a term involving the product of two sine functions and a sum of alternating products of similar character. This alternating series eventually converges quite rapidly, although the initial terms of this sequence may be diverging. The sign of the quantity $\sin [q^n \omega c t]/[1 + \beta]$ of the dominant term of this series determines the location of the average displacement with respect to the neutral position of the string. Since this term alternates in sign with increasing time, the average displacement also will oscillate about the zero-displacement axis. Although the mean amplitude of motion increases with time, it always will remain bounded.

An interesting feature of this case is the reduction of the frequency of oscillation of both terms in Equation [45] from that of the exciting force by the factor $1/[1 + \beta]$. This phenomenon is the result of a Doppler effect which will halve the response frequency of the string at sonic velocity. When the string is still relatively short, the first term of Equation [45] is overshadowed by the alternating series, and the ripples produced in the string by this component cannot be detected in Fig. 4 or 7. At later times, however, this term causes a significant deviation from the mean displacement of the string, and, near the origin, may even result in a total displacement of opposite phase to that of the average motion.

In the case of constant acceleration, the first four terms of Equation [47] determined the resulting transverse motion within about 1 per cent for a forcing frequency of 100 cps. As may be observed from Fig. 7, the smaller frequency is too slow to portray effectively the oscillatory nature of the phenomenon, which is governed by the quantity

$$\frac{1}{\omega}\left\{\cos\frac{\omega c^2}{a}\left[-1+\sqrt{1+\frac{2a}{c^2}\,[ct+x]}\right]\right.$$
$$\left.-\cos\frac{\omega c^2}{a}\left[-1+\sqrt{1+\frac{2a}{c^2}\,[ct-x]}\right]\right\}$$

However, the existence of this feature is clearly demonstrated when the forcing frequency is increased by a factor of 10. Such a change also severely curtails the maximum amplitude of the displacement.

The shape of the displacement curves for the cases of constant velocity and constant acceleration for the same forcing frequency and string length are quite similar, although the velocity of the free end of the wire and the travel time differ radically for the

two conditions. The case of constant acceleration exhibits an amplitude approximately 5 per cent in excess of that shown by the constant-velocity curve. This is a surprisingly small increase inasmuch as the disturbing force with constant acceleration of the string acts over a time interval twenty-five times as long as in the case of constant velocity.

Series expansion of the trigonometric terms in Equation [45] indicates the bounded nature of the motion for constant string end velocity, and consequently no resonance involving infinite displacement is permitted for the undamped string. The same prognosis cannot be stated immediately for the case of constant acceleration since the terms involving the function f will increase with time. However, regardless of the magnitude of the acceleration, there always will exist a time when the end of the string has attained sonic velocity. This condition serves as the upper limit of the applicability of the solution, and thus provides an effective upper bound to the magnitude of the displacement.

The technique described is applicable for any arbitrarily chosen forcing function satisfying the required conditions of a null value and continuity at the time origin. Any function of this type can be expanded in a Fourier sine series and the solutions for each frequency can be superposed.

In the supersonic regime, the space point P in Fig. 2 or 3 will be located on the other side of line OA and must be connected by characteristics to the x-axis. The motion of the string is thus governed not by the boundary condition at the fixed end, but rather by the initial conditions present in the wire. Physically, this signifies that any disturbance generated at the free end of the string will never be transmitted to the distal terminus, and reflections at this point cannot be generated. Consequently, resonances cannot be excited in the string under supersonic conditions. At sonic velocity, disturbances generated in the string are frozen and will not propagate in either direction.

Acknowledgment

The author wishes to express his appreciation to Dr. Robert Fuchs and Prof. Bernard Friedmann for a number of valuable discussions on the theoretical aspects of the problem.

Additional References

The author would like to call attention to the following:

"The Spaghetti Problem," by G. F. Carrier, *American Mathematical Monthly*, vol. 56, 1949, pp. 669–562.

"A Certain Boundary Problem of a Vibrating String," by J. Litwinisan, *Archivum Mechaniki Stosowanej*, vol. 2, 1950, pp. 75–88. (See *Applied Mechanics Reviews* No. 3785, vol. 4, Oct., 1951.)

Design Data and Methods

It is important that the data contained in technical papers be made readily available to design engineers. In order to satisfy these needs of industry, this section of the Journal includes a concise presentation of data and information drawn chiefly from papers previously published by the Applied Mechanics Division of The American Society of Mechanical Engineers.

Effect of Elastic Racks on Vibration Mounting of Equipment

By R. A. DI TARANTO,[1] CAMDEN, N. J.

The over-all fundamental natural frequency of a uniform beam supported at each end by equal springs is determined in terms of the first-mode bending natural frequency of the beam and the natural frequency of the lumped mass beam on the two springs. This is qualitatively applied to the case of electronic equipment on elastic racks supported on vibration mounts.

Nomenclature

T = kinetic energy
V = potential energy
ρ = mass per unit length
y = elastic beam deflection
δ = spring deflection
ω = natural frequency of the system
l = length of the beam
γ = deflection ratio, y/δ
ω_g = beam fundamental natural frequency
ω_0 = rigid body on springs natural frequency
β = ratio of beam to rigid-body natural frequency, ω_g/ω_0
α = ratio of system to rigid-body natural frequency, ω/ω_0
K = spring constant

Introduction

In many practical problems where electronic equipment is placed on racks or such holding device and then this device is placed on shock or vibration mounts, it has been found that the system's natural frequency is different from that calculated for a rigid body on a spring. This has led to much difficulty, as a system is designed to a given natural frequency to avoid resonant condition, and it has been found that resonant conditions have occurred at a frequency different from the calculated natural frequency.

It appears reasonable that this phenomenon can be explained by considering the racks or holding devices as elastic members on the elastic springs. The actual case is rather complicated, being at times a plate or four beams in the form of a box on four mounts. In most cases an order-of-magnitude effect of the elasticity of the rack or mounting device on the natural frequency of the equipment on mounts is required. To this end, the following analysis and results are given.

The analysis considers a simply supported uniform beam with a uniform mass distribution representing the equipment, mounted on two equal springs. The method of solution used is the Rayleigh type solution.

Analysis

General Considerations

The analysis considers the rack and equipment as an effective uniform beam placed on springs (the vibration mounts). The kinetic energy is calculated considering the beam bending in its first mode and the movement of the total motion of the beam due to the spring.

The potential energy is calculated considering the elastic bending energy of the beam and the potential energy stored in the springs. The maximum values of these two energies are equated as per the Rayleigh method.

This results in an expression having three unknowns: the nondimensional natural frequency of the combination ω/ω_0; the nondimensional elastic natural frequency ω_g/ω_0; and the ratio of the beam displacement to the spring displacement γ. A relation between the ratio of displacement γ and the nondimensional natural frequency ω/ω_0 is obtained by use of the dynamic force of the beam onto the spring, yielding a deflection relationship.

This latter relationship yields an equation in the nondimensional natural-frequency ratio ω/ω_0 and the nondimensional natural frequency ω_g/ω_0. This is a cubic equation, which is solved to obtain the desired results.

Equations of Motion

In considering the beam on springs, Fig. 1, the kinetic energy of the uniform mass of the beam and the added uniform mass can be written in terms of the deflection of the spring and the elastic bending of the beam. The springs are considered as moving together in phase and through the same amplitudes. The kinetic energy is

$$T = \frac{1}{2}\int_0^l \rho dx(\dot{y} + \dot{\delta})^2 = \frac{\rho}{2}\int_0^l (\dot{y}^2 + 2\dot{y}\dot{\delta} + \dot{\delta}^2)dx \quad [1]$$

[1] Engineer, Mechanical and Material Engineering Standards, Defense Electronic Products Division, Radio Corporation of America.

Discussion of this paper should be addressed to the Secretary, ASME, 29 West 39th Street, New York, N. Y., and will be accepted until January 10, 1958, for publication at a later date. Discussion received after the closing date will be returned.

NOTE: Statements and opinions advanced in papers are to be understood as individual expressions of their authors and not those of the Society. Manuscript received by ASME Applied Mechanics Division, November 13, 1956.

Fig. 1 Uniformly loaded beam on equal-stiffness mounts

If we assume that the motion is harmonic and the beam is bending in its first mode, then we can assume

$$\left.\begin{aligned} y &= y_0 \sin \frac{\pi x}{l} \cdot \cos \omega t \\ \delta &= \delta_0 \cos \omega t \end{aligned}\right\} \quad [2]$$

Substituting these in Equation [1] yields

$$T = \left[\frac{\rho l}{4} y_0^2 + \frac{2\rho l}{\pi} \delta_0 y_0 + \frac{\rho l}{2} \delta_0^2\right] \omega^2 \sin^2 \omega t \quad [3]$$

or

$$T = \omega^2 \delta_0^2 \left[\frac{M}{4} \gamma^2 + \frac{2M}{\pi} \gamma + \frac{M}{2}\right] \sin^2 \omega t \quad [4]$$

Where $\rho l = M$ = total mass.

The potential energy of the system is composed of the elastic bending energy of the beam plus the energy of the two springs. This may be written as

$$V = \frac{EI}{2} \int_0^l \left(\frac{d^2 y}{dx^2}\right)^2 dx + \frac{1}{2} (2K) \delta^2 \quad [5]$$

Substituting for y and δ and integrating Equation [5], we get

$$V = \frac{EI}{2} y_0^2 \left(\frac{\pi}{l}\right)^4 \frac{l}{2} \cos^2 \omega t + K \delta_0^2 \cos^2 \omega t \quad [6]$$

or

$$V = \delta_0^2 \left[\frac{EI}{4} \frac{\pi^4}{l^3} \gamma^2 + K\right] \cos^2 \omega t \quad [7]$$

For no dissipation of energy, the maximum kinetic energy is equal to the potential energy, or

$$T_{max} = V_{max}$$

Equating [4] and [7], we obtain

$$\omega^2 \delta_0^2 \left[\frac{M}{4} \gamma^2 + \frac{2M}{\pi} \gamma + \frac{M}{2}\right] = \delta_0^2 \left[\frac{EI\pi^4}{4l^3} \gamma^2 + K\right] \quad [8]$$

Solving [8] for ω^2 we obtain

$$\omega^2 = \frac{\frac{\gamma^2}{4}\left(\frac{EI\pi^4}{\rho l^4}\right) + \frac{K}{\rho l}}{\frac{\gamma^2}{4} + \frac{2\gamma}{\pi} + \frac{1}{2}} \quad [9]$$

But the elastic beam natural frequency is

$$\omega_E^2 = \frac{EI\pi^4}{\rho l^4} \quad [10]$$

and the natural frequency of the rigid beam on the springs is

$$\omega_0^2 = \frac{2K}{\rho l} \quad [11]$$

Equation [9] then becomes

$$\omega^2 = \frac{\frac{\omega_E^2}{4} \gamma^2 + \frac{\omega_0^2}{2}}{\frac{\gamma^2}{4} + \frac{2\gamma}{\pi} + \frac{1}{2}} = \pi \left[\frac{\omega_E^2 \gamma^2 + 2\omega_0^2}{\pi\gamma^2 + 8\gamma + 2\pi}\right] \quad [12]$$

or

$$\alpha^2 = \left(\frac{\omega}{\omega_0}\right)^2 = \pi \left[\frac{\beta^2 \gamma^2 + 2}{2\pi + 8\gamma + \pi\gamma^2}\right] \quad [13]$$

where

$$\beta = \frac{\omega_E}{\omega_0} \quad [14]$$

$$\gamma = \frac{y_0}{\delta_0} \quad [15]$$

$$\alpha = \frac{\omega}{\omega_0} \quad [16]$$

In order to obtain a relationship between γ and α we must consider the force of the loaded vibrating beam on the springs and the subsequent deflection of the springs under this load. Considering the force of the beam onto both springs as P, we can write this force as follows

$$P = \int_0^l \rho dx (y + \delta) \omega^2 = \rho \omega^2 \int_0^l \left[y_0 \sin \frac{\pi x}{l} + \delta_0\right] dx \quad [17]$$

Integrating [17] we get

$$P = (\rho l) \omega^2 \left[\frac{2}{\pi} y_0 + \delta_0\right] \quad [18]$$

or using $\rho l = M$

$$P = M\omega^2 \left[\frac{2}{\pi} y_0 + \delta_0\right] \quad [19]$$

now

$$\delta_0 = \frac{P}{2K} \quad [20]$$

whereupon

$$\delta_0 = \frac{M\left[\frac{2}{\pi} \gamma + 1\right] \omega^2 \delta_0}{2K} \quad [21]$$

or solving for γ

$$\gamma = \frac{\pi}{2M\omega^2} [2K - M\omega^2] \quad [22]$$

or

$$\gamma = \frac{\pi}{2}\left[\frac{2K}{M\omega^2} - 1\right] = \frac{\pi}{2}\left[\frac{\omega_0^2}{\omega^2} - 1\right] = \frac{\pi}{2}\left[\frac{1 - \alpha^2}{\alpha^2}\right] \quad [23]$$

where

$$\alpha = \frac{\omega}{\omega_0}$$

Substituting [23] into [13] we obtain

$$\alpha^2 = \pi \left[\frac{\beta^2 \left(\frac{\pi}{2}\right)^2 \left[\frac{1-\alpha^2}{\alpha^2}\right]^2 + 2}{2\pi + 4\pi \left[\frac{1-\alpha^2}{\alpha^2}\right] + \pi \left[\frac{\pi}{2}\right]^2 \left[\frac{1-\alpha^2}{\alpha^2}\right]^2} \right] \quad [24]$$

Let

$$\alpha^2 = \lambda$$

Then

$$\lambda \left[2 + 4 \left(\frac{1-\lambda}{\lambda}\right) + \frac{\pi^2}{4} \left(\frac{1-\lambda}{\lambda}\right)^2 \right] = \beta^2 \left(\frac{\pi}{2}\right)^2 \left(\frac{1-\lambda}{\lambda}\right)^2 + 2 \quad [25]$$

or

$$(1-\lambda)[\lambda^2(8-\pi^2) + \lambda\pi^2(1+\beta^2) - \pi^2\beta^2] = 0 \quad [26]$$

and finally

$$(1-\lambda)[\lambda^2 - 5.3(1+\beta^2)\lambda + 5.3\beta^2] = 0 \quad [27]$$

The solution of this last equation yields the desired results. There will be two roots associated with and varied with each value of β. The roots are

$$\lambda = 1$$

and

$$\lambda = 2.65(1+\beta^2) \pm \{[2.65(1+\beta^2)]^2 - 5.3\beta^2\}^{1/2}$$

With each of these roots is associated a mode shape, which can be evaluated by use of Equation [23]. The roots represent three possible conditions which can be listed as:

Condition A. The value of α is less than 1 for all values of β and approaches 1 as β increases. The relative deflections of the springs are in phase, with the deflection of the spring being less than the elastic deflection of the beam, for $\beta < 1.18$. Beyond this value the deflections are in phase, with the deflection of the spring being greater than the center deflection of the beam.

Condition B. The value of α is greater than 2.3 for all values of β, and for large values of β can be approximated by the relation: $\alpha = 2.3\beta$. The relative deflection of the beam and the springs are 180 deg out of phase, with the deflection of the spring being less than the center deflection of the beam, i.e., $\gamma < -1$.

A third root which is independent of β is $\alpha = 1$.

Condition C. This is the condition where $\alpha = 1$ or the over-all natural frequency ω is equal to the rigid body on spring natural frequency ω_b. The modal relation is $\gamma = 0$, which indicates that the beam vibrates on the springs as a rigid body in this mode.

Results. The results appear in a nondimensional form in terms of the rigid-body natural frequency ω_b and the first-mode elastic bending natural frequency ω_E, and are plotted in Figs. 2 and 4. The analysis indicates that there are three physically possible natural frequencies. One is less than the natural frequency of rigid body on springs ω_b, condition A; another is always greater than this natural frequency, condition B; and the third is equal to ω_b. For large values of the ratio ω_E/ω_b, i.e., where the elastic beam first-mode natural frequency is much greater than the natural frequency of the rigid beam on spring natural frequency, the lower over-all natural frequency ω, condition A, approaches the rigid body on spring natural frequency ω_b. There is a difference between these values of 5 per cent when $\beta = 2.6$. The higher natural frequency, condition B, approaches the relation $\alpha = 2.3\beta$ when the ratio ω_E/ω_b becomes large. The third frequency is equal to that of a rigid beam on springs ω_b. The mode shapes associated with each of these natural frequencies indicate that the elastic

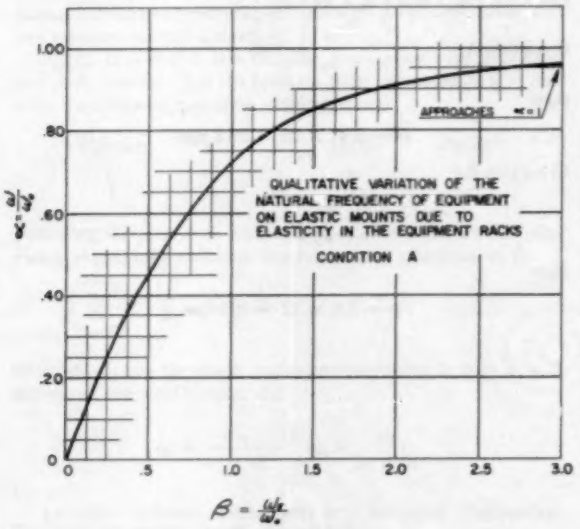

Fig. 2

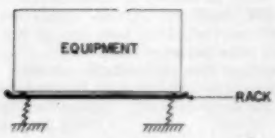

Fig. 3 Elastic rack with equipment on vibration mounts

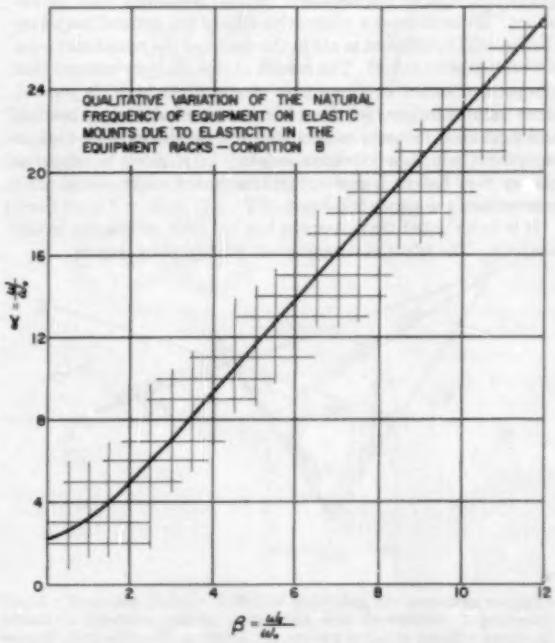

Fig. 4

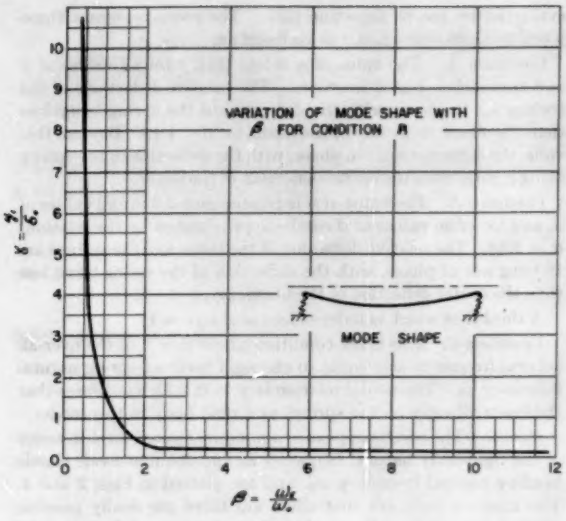

Fig. 5

beam deflection is in phase with the spring deflection for condition A, and the two deflections are 180 deg out of phase for condition B. The two mode relationships are shown in Figs. 5 and 6, respectively. The third mode is independent of the elastic effect of the beam and is exactly the mode of vibration of the rigid beam on springs.

Conclusions. The effect on the natural frequency of elasticity in the structure supporting electronic equipment placed on shock or vibration mounts can be qualitatively analyzed by use of the results obtained herein. Thus, if one knows the bending natural frequency of the structure and the natural frequency of the equipment on the mounts, then by use of the plots shown herein a qualitative idea of the resultant natural frequency may be obtained. In most cases a qualitative idea of the natural-frequency change will be sufficient to aid in the design of the equipment from a vibration standpoint. The results of this analysis indicate that vibration-mounted equipment on elastic racks have, in general, three natural frequencies due to first-mode elastic beam bending and rigid-body motions on springs. The results indicate that an equipment which is vibration-isolated to a given natural frequency may have a higher natural frequency which would yield a secondary resonance condition.

It is to be noted that damping has not been considered in this analysis. The effect of damping will modify these results.

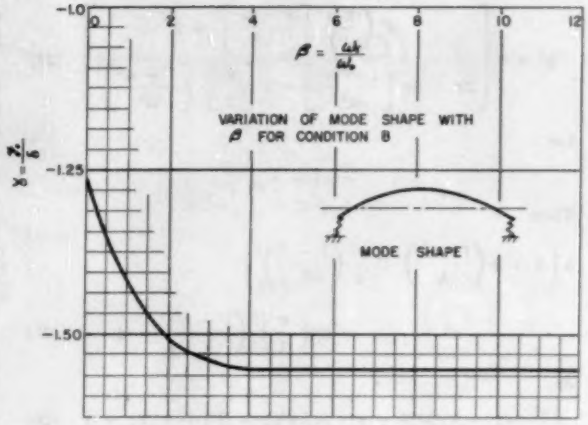

Fig. 6

Example

Consider the equipment and elastic rack on the vibration mounts, as shown in Fig. 3. If the natural frequency of the equipment on the mounts is 22 cps and the natural frequency of the equipment on rack natural frequency is 50 cps, then it is required to find the over-all natural frequency. This means

$$\omega_0 = 22 \text{ cps} \qquad \omega_E = 50 \text{ cps}$$

then

$$\beta = \frac{\omega_E}{\omega_0} = 2.27$$

and from Fig. 2 and Fig. 4 we find

Condition A

$$\frac{\omega}{\omega_0} = 0.93$$

then

$$\omega = 0.93 \times 22 = 20.5 \text{ cps}$$

Condition B

$$\frac{\omega}{\omega_0} = 5.5$$

then

$$\omega = 5.5 \times 22 = 121 \text{ cps}$$

Brief Notes*

On the recommendations of the Executive Committee of the ASME Applied Mechanics Division, it has been decided to initiate a section devoted to brief notes on technical matters in mechanics. These notes must not be longer than 750 words (about 2½ double-spaced typewritten pages, including figures) and will be subject to the usual review procedure prior to publication. After approval such notes will be published as soon as possible, normally in the next issue of the Journal. The notes should be submitted to the Technical Editors of the *Journal of Applied Mechanics*.

Five-Line Construction for a Computing Linkage Satisfying Five Precision Requirements

By F. Freudenstein,[1] New York, N. Y.

The design of a four-bar function generator having five precision points generally involves construction of center-point curves (1)[2] or extended calculations (2, 3). Simpler methods for special cases have been obtained by K. Hain (4, 5, 6) using the principle of point-position-reduction. This principle can be combined with analytical studies (3) and collineation axis considerations (7, 8) to yield a five-line construction for a computing linkage having two precision points, two precision derivatives, and one precision second derivative.

In Fig. 1, A-B-C-D is a four-bar mechanism with A-D fixed and A-B_1 driving. Let the function to be generated be $y = f(x)$ with the following precision requirements

Position	x	y	dy/dx	d^2y/dx^2
1	x_1	y_1	y_1'	y_1''
2	x_2	y_2	y_2'	—

Following the procedure described in reference (3), we can convert $y = f(x)$ into a relation involving crank rotations, ϕ, ψ

$$y = \frac{\psi - \psi_0}{r_\psi} \qquad x = \frac{\phi - \phi_0}{r_\phi}$$

where ϕ_0, ψ_0 are the crank angles corresponding to $x = y = 0$ and r_ϕ, r_ψ, are scale factors; e.g.

$$r_\phi = \frac{\phi_{12}}{x_2 - x_1} \qquad r_\psi = \frac{\psi_{12}}{y_2 - y_1}$$

and ϕ_{12}, ψ_{12} are the values of the crank rotations corresponding to $(x_2 - x_1)$ and $(y_2 - y_1)$, respectively.

Let the values of x_1, x_2, and r_ψ/r_ϕ be prescribed. Then

$$m_1 = d\psi/d\phi \text{ at position } 1 = \frac{r_\psi}{r_\phi}\, y_1' \quad \ldots\ldots [1]$$

$$m_2 = d\psi/d\phi \text{ at position } 2 = \frac{r_\psi}{r_\phi}\, y_2' \quad \ldots\ldots [2]$$

The velocity ratio $d\psi/d\phi$ is equal to OA/OD whence $DO_1 = 1/(1 - m_1)$ measured from D toward O_1.

Hain (4, 5, 6) has shown that constructional simplifications occur when B_1, Fig. 1, coincides with the relative pole of the crank displacements ϕ_{12}, ψ_{12}, whence $\angle B_1AD = \frac{1}{2}\phi_{12}$ and $\angle B_1DA = -\frac{1}{2}\psi_{12}$; further, that the precision derivative, m_2, can be obtained when B_1 lies on circle H-K-D, with diameter $HD = (AD)/(1 - \frac{1}{2}m_1 - \frac{1}{2}m_2)$ measured left from D(H, O_1 separate D, O_2 harmonically).

An approximate value of $\frac{1}{2}\phi_{12}$ can be obtained graphically by varying the position of B_1 on circle H-K-D until

$$\frac{\phi_{12}/2}{\psi_{12}/2} = \frac{r_\phi(x_2 - x_1)}{r_\psi(y_2 - y_1)} \quad \ldots\ldots [3]$$

The exact value of ϕ_{12} in Fig. 1, can then be determined with the aid of the Newtonian iteration procedure applied to the equation

$$1 - m_1 - m_2 = \frac{\sin(\frac{1}{2}\phi_{12} - \psi_{12})}{\sin \frac{1}{2}\phi_{12}} \quad \ldots\ldots [4]$$

The value of ψ_{12} is obtained next from Equation [3]. Furthermore

$$r_\phi = \phi_{12}(x_2 - x_1) \quad \ldots\ldots [5]$$

$$r_\psi = \psi_{12}(y_2 - y_1) \quad \ldots\ldots [6]$$

and from Equation [16], reference (7)

$$\tan \lambda = \frac{1}{r_\phi} \frac{y_1''}{y_1'\left(1 - \frac{r_\psi}{r_\phi} y_1'\right)} \quad \ldots\ldots [7]$$

(Fig. 1)

The linkage is constructed as follows: A-D is drawn with unit length. B_1 is located at the intersection of rays I and II, making angles of $(\frac{1}{2}\phi_{12})$, $(-\frac{1}{2}\psi_{12})$ with A-D, respectively. P lies at the intersection of A-B_1 and O_1-P, where $\angle B_1O_1P = \lambda$, as obtained from Equation [7]. The sense of λ is determined by the

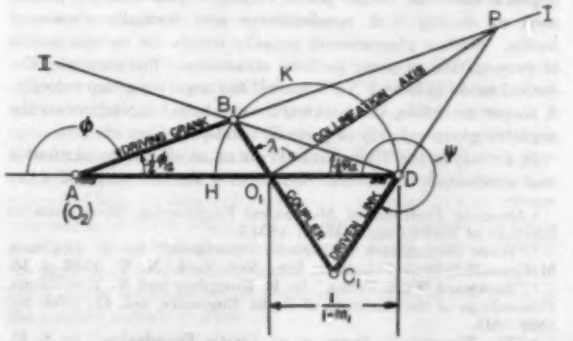

Fig. 1 Four-bar linkage A-B-C-D satisfying five precision requirements (2 precision points, 2 precision first derivatives, 1 precision second derivative—in position 1); arrows indicate positive sense of angles

[1] Associate Professor, Department of Mechanical Engineering, Columbia University. Assoc. Mem. ASME.

[2] Numbers in parentheses refer to the Bibliography at the end of this paper.

* Discussion of papers in Brief Notes should be addressed to the Secretary, ASME, 29 West 39th Street, New York, N. Y., and will be accepted until January 10, 1958, for publication at a later date. Discussion received after the closing date will be returned.

Note: Statements and opinions advanced in papers are to be understood as individual expressions of their authors and not those of the Society. Manuscript received by Applied Mechanics Division, July 2, 1957.

fact that, for a positive value of $d^2\psi/d\phi^2$, O_1 moves toward A during an infinitesimal displacement $d\phi$. If the value of $\tan\lambda$ from Equation [7] is indeterminate, l'Hôpital's rule gives

$$\tan\lambda = \frac{r_\phi y''}{y'''}\left(1 - \frac{r_\psi}{r_\phi}y'\right)$$

With the foregoing method, a large range ϕ_{12} is obtained only when the divided difference $(y_2 - y_1)/(x_2 - x_1)$ differs sufficiently from the average derivative $^1/_2(y_1' + y_2')$. If the value of y_1' is not prescribed, the values of r_ϕ and r_ψ can be chosen arbitrarily, thus leading to a direct determination of ϕ_{12} and ψ_{12} from Equations [5] and [6].

Example. Fig. 1 shows the construction for the function $y = \sin x$, with $x_1 = 0°$, $x_2 = 90°$, r_ϕ is positive and $r_\psi/r_\phi = -1.5$, whence $m_1 = -1.5$, $m_2 = 0$, $\psi_{12}/\phi_{12} = -0.95493$, $DH = 0.57143$, $^1/_2\phi_{12} = 19.661°$, $r_\phi = 25.033°/x$, $r_\psi = -37.550°/y$, $\lambda = 90°$, and from an approximate drawing $DA = 10$, $AB = 5.125$, $BC = 6.050$, $CD = 3.688$, $\phi_0 = 160°20'$, $\psi_0 = -61°54'$, and the maximum error in ψ is 0.67 deg.

Bibliography

1 "Kinematische Getriebesynthese," by R. Beyer, Springer Verlag, Berlin, Germany, 1953, pp. 99–101, 108–109.

2 "Zur Algebraischen Mass-Synthese Ebener Kurbelgetriebe," by K. H. Sieker, *Ingenieur-Archiv*, vol. 24, 1956, part 1, no. 3, pp. 188–215; part 2, no. 4, pp. 233–257.

3 "Approximate Synthesis of Four-Bar Linkages," by F. Freudenstein, TRANS. ASME, vol. 77, 1955, pp. 853–861.

4 "Angewandte Getriebelehre," by K. Hain, H. Schroedel Verlag, Hannover, Germany, 1952, Chapter N, pp. 326–380.

5 "Periodische Winkelgeschwindigkeits- und Drehmomentwandler," by K. Hain, *Zeitschrift des Vereins Deutscher Ingenieure*, vol. 93, 1951, pp. 239–244.

6 "Volle Ausnutzung des Gelenkvierecks als Funktionsgetriebe," by K. Hain, *Regelungstechnik*, vol. 2, no. 2, 1956, pp. 40–45.

7 "On the Maximum and Minimum Velocities and the Accelerations in Four-Link Mechanisms," by F. Freudenstein, TRANS. ASME, vol. 78, 1956, pp. 779–787.

8 "Kinematic Analysis and Synthesis Using Collineation-Axis Equations," by W. J. Carter, TRANS. ASME, vol. 79, 1957, pp. 1305–1312.

Negative Group Velocities in Continuous Structures

BY S. H. CRANDALL,[1] CAMBRIDGE, MASS.

WAVE propagation in which the energy transport is in the opposite direction to the phase velocity seems unusual to one used to dealing with nondispersive and normally dispersive media. Such a phenomenon actually occurs for certain modes of propagation in some periodic structures. For example, the optical mode in Born's NaCl model[2] has negative group velocity. A recent invention, the backward wave tube,[3] capitalizes on the negative group velocity of periodic band-pass-filter circuits.

In a study of the Timoshenko beam on an elastic foundation[4] it was accidentally discovered that over a limited range of wave lengths the fundamental mode had negative group velocity. Since negative group velocities apparently have not been noticed in continuous media before, a more general treatment of the question is given in this note. It is found that negative group velocities do in fact occur in many media. An example is given of a medium whose group velocity is negative for all wave lengths.

[1] Associate Professor of Mechanical Engineering, Massachusetts Institute of Technology. Mem. ASME.

[2] "Wave Propagation in Periodic Structures," by L. Brillouin, McGraw-Hill Book Company, Inc., New York, N. Y., 1946, p. 15.

[3] "Backward Wave Tubes," by R. Kompfner and N. T. Williams, Proceedings of the Institute of Radio Engineers, vol. 41, 1953, pp. 1602–1611.

[4] "The Timoshenko Beam on an Elastic Foundation," by S. H. Crandall, presented at the Third Midwestern Conference on Solid Mechanics, Ann Arbor, Mich., April 2, 1956.

Manuscript received by ASME Applied Mechanics Division, April 24, 1957.

Anomalous Dispersion

A plane wave advancing along the x-axis may be represented by $\psi = Ae^{i(nx-\omega t)}$ where n is the number of wave lengths in 2π units of x, and ω is the circular frequency. The phase velocity v, and the group velocity (the velocity of energy transport) V, are given by

$$v = \frac{\omega}{n} \qquad V = \frac{d\omega}{dn} \quad \ldots\ldots [1]$$

The dispersion of the medium is said to be "normal" or "anomalous" according whether the index of refraction (which is proportional to $1/v$) increases or decreases with increasing ω. Since

$$\frac{d(1/v)}{d\omega} = \frac{\omega\dfrac{dn}{d\omega} - n}{\omega^2} = \frac{n(v-V)}{V\omega^2} \quad \ldots\ldots [2]$$

the dispersion is normal if $0 < V < v$. The usual case of anomalous dispersion occurs when $0 < v < V$. The definition of anomalous dispersion is satisfied, however, if with n and v positive, the group velocity V is negative.

Structure of Medium

We consider a generalized one-dimensional medium with a single displacement co-ordinate, $\psi(x)$. Let the potential energy per unit length and kinetic energy per unit length be

$$\left.\begin{aligned} U &= \frac{1}{2}(k_0\psi^2 + k_1\psi_x^2 + k_2\psi_{xx}^2 + \ldots) \\ T &= \frac{1}{2}(\rho_0\psi_t^2 + \rho_1\psi_{xt}^2 + \rho_2\psi_{xxt}^2 + \ldots) \end{aligned}\right\} \quad \ldots\ldots [3]$$

where the k_i and ρ_i are non-negative constants. By applying Hamilton's principle it is a straightforward matter to obtain the equation of motion

$$k_0\psi - k_1\psi_{xx} + k_2\psi_{xxxx} - \ldots = -\rho_0\psi_{tt} + \rho_1\psi_{xxtt} - \rho_2\psi_{xxxxtt} + \ldots [4]$$

Substituting $\psi = Ae^{i(nx-\omega t)}$ we find

$$\omega^2 = \frac{k_0 + n^2k_1 + n^4k_2 + \ldots}{\rho_0 + n^2\rho_1 + n^4\rho_2 + \ldots} \quad \ldots\ldots [5]$$

and

$$v = \frac{1}{n}\left(\frac{k_0 + n^2k_1 + n^4k_2 + \ldots}{\rho_0 + n^2\rho_1 + n^4\rho_2 + \ldots}\right)^{1/2} \quad \ldots\ldots [6]$$

$$V = n\,\frac{\rho_0k_1 - k_0\rho_1 + 2n^2(\rho_0k_2 - k_0\rho_2) + n^4(3\rho_0k_3 - 3k_0\rho_3 + \rho_1k_2 - k_1\rho_2) + \ldots}{(k_0 + n^2k_1 + n^4k_2 + \ldots)^{1/2}(\rho_0 + n^2\rho_1 + n^4\rho_2 + \ldots)^{1/2}} \quad \ldots\ldots [7]$$

We see that the numerator in Equation [7] is a polynomial in n^2 whose coefficients may be positive or negative depending on the properties of the medium. If all of these coefficients are non-negative the numerator is non-negative and so is V; but if some of the coefficients are negative it is possible that V may be negative over portions of the range $0 < n < \infty$.

Examples

Let $\psi(x)$ be the small transverse displacement of an infinitely long uniform rod or wire of mass per unit length ρ_0. The stiffness coefficients may then be interpreted as follows: k_0 is the modulus of an elastic foundation in which the rod is embedded, k_1 is the longitudinal tension carried in the wire, k_2 is the flexural modulus.

If the only nonzero inertia coefficient is ρ_0, then it is clear from Equation [7] that the group velocity can never be negative.

If rotatory inertia is considered, then ρ_1 is positive, and negative group velocities are possible. For example, consider Rayleigh's model[5] of a beam (in which rotatory inertia is considered but shear flexibility is ignored) upon an elastic foundation. Here

$$\rho_1 = r^2\rho_0,\ k_0 > 0,\ k_1 = 0, \text{ and } k_2 = EI$$

where r is the radius of gyration of the section. Substituting in Equation [7], we find

$$V = \left(\frac{k_0}{\rho_0}\right)^{1/4} \frac{-n + 2\,EI\,n^3/k_0r^2 + EIn^5/k_0}{(1 + EIn^4/k_0)^{1/2}(1 + n^2r^2)^{3/4}} \quad [8]$$

and hence that V is negative in the range

$$0 < n < [(1/r^4 + k_0/EI)^{1/2} - 1/r^2]^{1/2} \quad [9]$$

When $k_0r^4 << EI$ this result is very nearly the same as that obtained[4] for the Timoshenko beam (which includes transverse shear as well as rotatory inertia) since in the long wave lengths involved there is very little transverse shear.

Consider now a taut string with no bending stiffness embedded in an elastic foundation and having appreciable rotatory inertia. Here $\rho_1 = r^2\rho_0$, $k_0 > 0$, $k_1 > 0$ and hence according to Equation [7]

$$V = \left(\frac{k_0}{\rho_0}\right)^{1/4} \frac{n(k_1/k_0 - r^2)}{(1 + n^2k_1/k_0)^{1/2}(1 + n^2r^2)^{1/4}} \quad [10]$$

If $k_1/k_0 < r^2$ then the group velocity is negative for all wave numbers. For this medium the pass band for wave transmission is between the frequencies $(k_0/\rho_0)^{1/4}$ and $(k_1/\rho_1)^{1/2}$.

If a transverse force which varies harmonically at a frequency within the pass band is applied at the origin, the steady-state motion which results consists of a pair of wave trains converging on the origin. The phase velocities are directed inward but the group velocities and hence the energy transports are outward.

Oblique Contact of Nonspherical Elastic Bodies[1]

By H. Deresiewicz,[2] New York, N. Y.

The Hertz theory of contact of elastic solids was extended by Cattaneo (1)[3] to account for the effect of additional forces statically equivalent to a single force acting in the plane of contact and directed parallel to one of the principal axes of the contact ellipse. Confining his attention to a monotonically increasing force T, superposed on the constant normal force N, he found that slip, in the direction of T, takes place between the two bodies, initiating at the outer edge of the contact and progressing inward over an annular area whose inner boundary is homothetic with the ellipse of contact. The remainder of the contact surface displaces uniformly, by an amount δ, with respect to distant points in either body. Having assumed that Coulomb's law of sliding friction holds at each point of the area of slip, and that the resultant tangential component of traction on the contact is in the direction of the applied force, Cattaneo found the resultant tangential traction to be

$$\left.\begin{aligned} \tau &= f\sigma, \quad a_1 \le x \le a,\ b_1 \le y \le b \\ \tau &= f\sigma - f\sigma_1(1 - T/fN), \quad x \le a_1,\ y \le b_1 \end{aligned}\right\} \quad [1]$$

where

$$\sigma = (3N/2\pi ab)\,(1 - x^2/a^2 - y^2/b^2)^{1/2} \quad [2]$$

is the Hertz normal pressure

$$\sigma_1 = (3N/2\pi a_1b_1)\,(1 - x^2/a_1^2 - y^2/b_1^2)^{1/2} \quad [3]$$

and f is the coefficient of Coulomb friction. a and b are the semiaxes of the contact ellipse, whose magnitude is given by the Hertz theory (2); a_1 and b_1 denote the semiaxes of the inner boundary of slip and obey the relations

$$(a_1/a)^2 = (b_1/b)^2 = 1 - T/fN \quad [4]$$

The theory has been extended further by Mindlin, Mason, Osmer, and Deresiewicz (3) to describe the effect, on a system of two spheres in Hertz contact, of a reduction of applied tangential force from its initial amplitude $T^* < fN$ to an arbitrary value $T < T^*$. In the course of unloading, slip again occurs, again over an annular area whose bounding curves are homothetic, but this time in the direction opposite to that of initial slip. When the applied tangential force is reduced to zero, the displacement of the adhered (nonslip) region does not vanish and the corresponding tangential component of traction, though self-equilibrating, is not identically zero. Upon further reduction of the tangential force to $T = -T^*$ the region of counterslip penetrates to the depth of initial slip; the traction and displacement at this stage are identical with those at $T = T^*$ except for a reversal of sign. An increase of the force from $T = -T^*$ causes a repetition of events which occurred in the course of unloading from $T = T^*$, with signs of all quantities reversed. It is found, on returning to $T = T^*$, that the displacement δ is identical with that obtained on initial loading, so that the path in the load-displacement plane forms a closed loop. Subsequent oscillation of the force between the limits $-T^* \le T \le T^*$ causes the same loop to be traversed. The area enclosed in the loop is a measure of the energy dissipated by friction in one cycle of loading.

The purpose of this note is to derive the solution for the contact of a pair of nonspherical bodies subjected to the loading dealt with in (3) for the problem of two spheres. To that end, it is necessary first to evaluate the (constant) displacement of the adhered region for Cattaneo's problem. This is done most conveniently by means of the expressions for the displacement in terms of Cerruti's potential functions. Referred to a set of rectangular axes whose origin is at the center of contact, the z-axis normal to the plane of contact and the x-axis coincident with the principal axis of contact parallel to the direction of the applied force T, the displacement, in the direction of T, of any point on the contact surface is given by[4]

$$u = \frac{1}{2\pi\mu}\frac{\partial^2 F_1}{\partial x^2} + \frac{\lambda}{4\pi\mu(\lambda + \mu)}\frac{\partial^2 F_1}{\partial z^2} \quad [5]$$

[5] "Theory of Sound," by Lord Rayleigh, Dover Publications, New York, N. Y., vol. 1, 1945, p. 293.

[1] This work was supported by the Office of Naval Research.

[2] Associate Professor of Mechanical Engineering, Columbia University. Assoc. Mem. ASME.

[3] Numbers in parentheses refer to the Bibliography at the end of the paper.

Manuscript received by ASME Applied Mechanics Division, April 15, 1957.

[4] Reference (2), p. 242.

where the derivatives are evaluated at $z = 0$. λ and μ are Lamé's constants

$$F_1 = \int\int \tau_{zz}(\xi, \eta)\, \Omega\, d\xi d\eta \quad \ldots\ldots [6]$$

$$\Omega = z \log (z + R) - R \quad \ldots\ldots [7]$$

$$R = [(\xi - x)^2 + (\eta - y)^2 + z^2]^{1/2} \quad \ldots\ldots [8]$$

and

$$\nabla^2 F_1 = 0 \quad \ldots\ldots [9]$$

the integration in Equation [6] being extended over the loaded area of the plane $z = 0$. It is convenient to rewrite Equation [5], using Equation [9], in the form

$$u = \frac{1}{4\pi\mu(\lambda + \mu)} \left[(3\lambda + 4\mu) \frac{\partial^2 F_3}{\partial x^2} + \lambda \left(\frac{\partial^2 F_3}{\partial x^2} - \frac{\partial^2 F_3}{\partial y^2} \right) \right]_{z=0} \quad \ldots\ldots [10]$$

Thus for any point in the adhered region ($x \leq a_1, y \leq b_1$), we find, on inserting Equation [1] in [6] and the result in Equation [10], that the displacement u is constant and given by

$$\delta = \frac{3fN(2 - \nu)}{16\mu a} \left[1 - \left(1 - \frac{T}{fN} \right)^{2/3} \right] \Phi \quad \ldots\ldots [11]$$

where ν is Poisson's ratio and

$$\Phi = \left\{ \begin{array}{l} [4a/\pi b(2 - \nu)]\ [(1 - \nu/k^2)\mathbf{K} + \nu\mathbf{E}/k^2], \ a < b \\ 1, \quad a = b \\ [4/\pi(2 - \nu)][(1 - \nu + \nu/k_1^2)\mathbf{K}_1 - \nu\mathbf{E}_1/k_1^2], \ a > b \end{array} \right\} \quad [12]$$

$\mathbf{K}$ and $\mathbf{E}$ are, respectively, complete elliptic integrals of the first and second kind of argument $k = (1 - a^2/b^2)^{1/2}$; $\mathbf{K}_1$ and $\mathbf{E}_1$ are similar integrals of argument $k_1 = (1 - b^2/a^2)^{1/2}$.

We note that Equation [11], which expresses the relation between the tangential load and the corresponding displacement, is qualitatively the same for spherical and nonspherical bodies as well as for loading parallel to either principal axis of the area of contact. Quantitatively, the difference in the various cases lies in the constant factor Φ which, from Equation [12], is seen to depend only on the parameters of the Herts problem.

The tangential compliance of each body, computed from Equation [11], is

$$S = \frac{d\delta}{dT} = \frac{2 - \nu}{8\mu a} \left(1 - \frac{T}{fN} \right)^{-1/3} \Phi \quad \ldots\ldots [13]$$

Its initial value, obtained from Equation [13] by setting $T = 0$, has been given by Mindlin (4).

The effect on the contact of a reduction of the applied tangential force from $T = T^*$ may now be studied. Following the procedure employed in the case of two spheres in contact (3), we find that the tangential component of traction to be superposed on the traction in Equation [1] is

$$\left. \begin{array}{l} \tau_x = -2f\sigma, \quad a_2 \leq x \leq a, b_2 \leq y \leq b \\ \tau_x = -2f\sigma + 2f\sigma_2[1 - (T^* - T)/2fN], \ x \leq a_2, y \leq b_1 \end{array} \right\} \ldots [14]$$

where

$$\sigma_2 = (3N/2\pi a_2 b_2)\,(1 - x^2/a_2^2 - y^2/b_2^2)^{1/2} \quad \ldots\ldots [15]$$

and a_2, b_2 denote, respectively, the semiaxes of the inner boundary of counterslip, this being an ellipse homothetic with the ellipse of contact; they are related to the semiaxes a, b by means of the expressions

$$\left. \begin{array}{l} (a_2/a)^3 = (b_2/b)^3 = 1 - (T^* - T)/2fN \\ \geqslant (a_1^*/a)^3 = (b_1^*/b)^3 = 1 - T^*/fN \end{array} \right\} \quad \ldots\ldots [16]$$

where a_1^*, b_1^* are the semiaxes of the inner boundary of slip at $T = T^*$. The resultant tangential component of traction at level T during unloading is given by the sum of Equation [1] (with T replaced by T^*) and Equation [14]

$$\left. \begin{array}{l} \tau_x = -f\sigma, \quad a_2 \leq x \leq a, b_2 \leq y \leq b \\ \tau_x = -f\sigma + 2f\sigma_2[1 - (T^* - T)/2fN], \\ \qquad a_1 \leq x \leq a_2, b_1 \leq y \leq b_2 \\ \tau_x = -f\sigma + 2f\sigma_2[1 - (T^* - T)/2fN] \\ \qquad + f\sigma_1^*(1 - T^*/f_1N), \ x \leq a_1, y \leq b \end{array} \right\} \ldots [17]$$

where σ_1^* is given by Equation [3] with a_1 and b_1 replaced by a_1^* and b_1^*, respectively.

The displacement of the adhered region corresponding to the additional traction, Equation [14], is

$$\delta_a = -\frac{3fN(2 - \nu)}{8\mu a} \left[1 - \left(1 - \frac{T^* - T}{2fN} \right)^{2/3} \right] \Phi \quad \ldots [18]$$

so that the resultant displacement during unloading, associated with the traction in Equation [17], is given by the sum of the displacements in Equation [11] (with T replaced by T^*) and Equation [18]

$$\delta_u = \frac{3fN(2 - \nu)}{16\mu a} \left[2 \left(1 - \frac{T^* - T}{2fN} \right)^{2/3} - \left(1 - \frac{T^*}{fN} \right)^{2/3} - 1 \right] \Phi \quad \ldots [19]$$

where Φ is given by Equation [12].

It is seen from Equations [17] and [19] that, qualitatively, the situation during unloading is the same in the case of contact of nonspherical bodies as it is for a pair of spheres. Hence without the need for further calculation, we may, guided by the results in (3), infer the establishment of a closed loop in the load-displacement plane due to the oscillation of the applied force T between the limits $\pm T^* < fN$, accompanied by energy loss due to the presence of friction. The expressions for the displacement, compliances, and energy loss may be obtained from the corresponding expressions in (3) simply by multiplying the latter by the constant Φ. Moreover, owing to the fact that, in the Herts problem, a change in the normal contact force gives rise to an area of contact whose bounding ellipse is homothetic with that of initial contact, the results obtained by Mindlin and Deresiewicz (5) for the contact of two spheres subjected to simultaneously varying normal and tangential forces may be extended immediately to the contact of nonspherical bodies.

Bibliography

1 "Sul contatto di due corpi elastici: distribuzione locale degli sforzi," by C. Cattaneo, *Accademia dei Lincei, Rendiconti*, series 6, vol. 27, 1938, pp. 342–348, 434–436, 474–478.

2 "Treatise on the Mathematical Theory of Elasticity," by A. E. H. Love, Cambridge University Press, fourth edition, 1927, pp. 193–198.

3 "Effects of an Oscillating Tangential Force on the Contact Surfaces of Elastic Spheres," by R. D. Mindlin, W. P. Mason, T. F. Osmer, and H. Deresiewicz, Proceedings of the First U. S. National Congress of Applied Mechanics, Chicago, Ill., 1951, pp. 203–208.

4 "Compliance of Elastic Bodies in Contact," by R. D. Mindlin, JOURNAL OF APPLIED MECHANICS, TRANS. ASME, vol. 71, 1949, pp. 259–268.

5 "Elastic Spheres in Contact Under Varying Oblique Forces," by R. D. Mindlin and H. Deresiewicz, JOURNAL OF APPLIED MECHANICS, TRANS. ASME, vol. 75, 1953, pp. 327–344.

Discussion

The State Principle—Some General Aspects of Relationships Among Properties of Systems[1]

J. H. KEENAN.[2] In order to discuss intelligently the authors' derivation of the phase rule, it is necessary to compare it with the derivation of Gibbs. It will be found, of course, that Gibbs' treatment was simple and direct, but that its starting point was different from that of the authors.

Gibbs' starting point was the assumption that the maximum number of independent properties for a *phase* was $(n + 2)$, where n is the number of "components" of the phase. (The definition of the term component will be discussed later.) The authors' starting point is the assumption that the maximum number of independent properties for a heterogeneous (and simple) system is $(n' + 2)$, where n' is the number of components of the heterogeneous system.

The assumption of Gibbs is more primitive than that of the authors. In fact, the first and second laws enter the Gibbs proof as he proceeds from his assumption concerning the phase to the authors' assumption concerning the system.

Nevertheless, the authors have performed a service in pointing up the simplicity of the derivation of the phase rule when starting from their empirical rule concerning heterogeneous systems. In fact, it is good to be reminded that this simple empirical rule exists.

Gibbs said, "the substances . . . of which we consider the mass composed (components), must of course be such that the values of the differentials dm_1, dm_2, . . . dm_n shall be independent, and shall express every possible variation in the composition of the homogeneous mass considered. . . ." At first glance this would seem to mean the same as what the authors call "independent and determinate set of components" for which the authors' definition is less concise than Gibbs'. The authors' example 2, however, shows that an "independent and determinate set" may not satisfy the Gibbsian definition of "component."

In Example 2, it is shown that a set of species may be "independent and determinate" without satisfying the requirement that variations in the masses of the species shall express every possible variation in the composition of the system. Thus the set is not a set of components in the Gibbsian sense. This example illustrates not so much the need for a definition of a "free simple system" as it does the need for Gibbs' definition of "component."

The classification of components, which by some other authors are called "species," into independent and determinate components seems to be a cumbersome device. An analog of this device could be found in the algebra of the pure substance. We know, for instance, that in the absence of motion, capillarity, and external force fields, the energy of a homogeneous closed system is a function of two independent variables; thus

$$U = U(p, T)$$

On the other hand, we may alter the state to other equilibrium states, not only by increasing or decreasing p or T, but also by increasing or decreasing the volume V. Thus by analogy with the definition of independent component, we may say that p, T, and V constitute a set of independent variables. Also by analogy with the definition of determinate component, we could say that p, T, and V constitute determinate variables. Then we would have to invent a new name for a set like p and T which are usually called independent variables. They are independent because, by analogy with Gibbs' definition of an independent component, dp and dT are independent and together they describe every possible variation in the state of a homogeneous system. The analogy is by no means perfect, but it may serve to point up what the writer considers to be the cumbersomeness of the system of definitions adopted by the authors.

The authors' "free simple system" seems to be what Gibbs referred to as a system of "heterogeneous masses in contact when uninfluenced by gravity, electricity, distortion of the solid masses, or capillary tensions." Gibbs made it clear that the words "in contact" implied that the mass of each phase was variable whether or not the intensive state was fixed.

The choice of terms in the paper is unfortunate in other instances. For example, the authors decide to "call any one of the functional relations among properties . . . an equation of state." Objection can be taken to this decision only on the basis of accepted usage, which is, that an equation of state is a relation between pressure, volume, and temperature.

The authors have made a useful distinction between properties which can be observed and measured without reference to the concepts of state and change of state, their "primary property," and those which cannot. To the writer this distinction seems to lie at the heart of their effort to improve on the exposition of thermodynamics. If this is so, then it might have been better to give a name to the class of properties which is not primary (for example, energy and entropy) such as "deduced property." Their definition of state in terms of primary properties seems a logical one.

The definitions of "macroscopic property," which is fixed when state is fixed, and primary property which may not be, may be suitable to their approach. The writer, however, is one of those who adopts the alternative view suggested by the authors, namely, that all observable characteristics are always properties, but that some have either no effect or negligible effect in some systems. From this point of view, the term macroscopic property which overlaps on the mutually exclusive primary and deduced classifications, can be dropped in favor of the term property which includes both primary and deduced. It seems to the writer that much of the complexity of the authors' discussion of property and state is owing to the difficulty of disentangling the overlapping concepts of primary and macroscopic property.

The proposed formulation of the "state principle" will serve an excellent purpose if it stimulates some clarifying discussion. To the writer, items 1 and 2 of the authors' formulation seem superfluous. Since a value for each property is fixed by a state, and this value may change with change in state, it follows that a group of functional relations must exist among the properties. Moreover, it may be inferred from the authors' definition of state that the number of independent properties for a system of finite complexity is finite, and that some relations may involve fewer independent properties than others.

[1] By S. J. Kline and F. O. Koenig, published in the March, 1957, issue of the JOURNAL OF APPLIED MECHANICS, Trans. ASME, vol. 79, pp. 29–34.

[2] Professor of Mechanical Engineering, Massachusetts Institute of Technology, Cambridge, Mass. Fellow ASME.

This leaves part 3 as the significant and axiomatic part of the state principle. Part 3 says, in effect, that the number of independent properties is not fixed by any principles of thermodynamics but is determined by empirical observation.

The paper may be criticized, in the opinion of the writer, on the following grounds: (1) Its methods are cumbersome. (2) They take too little cognizance of and sometimes add confusion to the good methods of the past. (3) The "state principle" is invested with more dignity than it can well support.

The value of the paper lies in the following: (1) It stimulates a re-examination of the definitions of property and state. (2) It suggests an interesting and probably important distinction between "primary" properties and all other properties. (3) It shows that the phase rule can be derived simply from an empirical observation which is not, however, as primitive as the starting point of Gibbs. (4) It offers a "state principle" which may be helpful in exposition.

J. KESTIN.[3] The writer does not agree that the definition of "state" and "property" presents as many difficulties as the authors seem to imply, and cannot see why defining both concepts simultaneously and by successive stages should be undesirable. The writer does not think that a detailed classification of various properties, as carried out in the paper, is either necessary or desirable. Any new definition must be justified on grounds of utility before it can be accepted universally. The writer agrees that the statement asserting that the maximum number of independent properties for a given system must be known empirically is correct, but doubts whether it merits the elevation to the dignity of a principle of thermodynamics.

The authors' derivation of the phase rule from their assumption regarding the number of independent properties of a heterogeneous system appears to the writer to be entirely equivalent to assuming that the phase rule is an independent principle in thermodynamics. In order to make certain that the phase rule is independent of the first and second laws of thermodynamics, it would be necessary to prove that the phase rule cannot be derived from these two rules in a logical way and without introducing additional assumptions. It has been so long accepted that this is not the case, and the writer agrees with the accepted view, that it appears to be necessary to prove the contrary explicitly before the authors' assertion can be accepted.

The authors should be congratulated for having drawn our attention to the possibility of the existence of some inconsistencies in the usual derivation of the phase rule, and the writer would be interested to see an explicit proof of this fact.

A. K. OPPENHEIM.[4] An elevation of a lemma into a theorem or a rule into a principle is an important step in the evolution of science. Although, in the spirit of the election year, it seemed good fun to vote for the adoption of the state principle as an independent postulate in thermodynamics, this is really not a jovial matter.

In an attempt to arrive at a complete set of foundations for an axiomatic exposition of thermodynamics, the authors point out the important omission of a specific route by which results of empirical observations are fed into the analysis. Most of their statements, it would seem, are quite true and the writer, for one, is personally obliged to them for bringing the matter to the focus of attention. Furthermore, he sympathizes with their attempt to contribute in the true tradition of the great founders, Clausius, Gibbs, Carathéodory, Poincaré . . . , to the background required for an axiomatic set of the principles of thermodynamics, by stating the need of admitting honestly what we know and what we don't know.

However, as pointed out by Myron Tribus (see final discussion), this is not a sufficient argument for an independent postulate. A critical examination of the authors' formulation of the state principle reveals the following:

For a microscopic system in equilibrium, the proposed principle states essentially the existence of (*a*) a group of functional relations, (*b*) between a finite number of independent properties, (*c*) depending on the specification of the system and found by *empirical* observation.

But this is indeed the quintessence, the synthesis of the first and the second law of thermodynamics, which can be considered as stating that internal energy is a state function (I Law) and entropy is a state function (II Law). In other words, since the salient property of a state function is the fact that its differential exists, not only is the number of relations and variables (parameter) finite, but they must be all known to the analyst. It seems obvious that knowledge of variables requires all the know-how concerned with the specification of the system in accordance with empirical observations—how else?

A rigorous proof, starting from the famous formulation of the two laws proposed by Clausius (1),[5] "Die Energie der Welt is constant—Die Entropie der Welt strebt einem maximum zu," was deduced first by Gibbs (2), and subsequently presented in a more axiomatic manner by Carathéodory (3) and Poincaré (4).

In the writer's opinion, the clearest development of the phase rule is obtained from Gibbs' abstract (5), and Butler's (6) elucidation. The arguments are so pertinent to the present discussion, that it seems best simply to cite them here:

"Let ϵ, η, v, t, and p denote respectively the energy, entropy, volume, (absolute) temperature, and pressure of a homogeneous mass, which may be either fluid or solid, provided that it is subject only to hydrostatic pressures; and let m_1, m_2, . . . m_n denote the quantities of its independently variable components, and μ_1, μ_2, . . . μ_n the potentials for these components. It is easily shown that ϵ is a function of η, v, m_1, m_2, . . . m_n, and that the complete value of $d\epsilon$ is given by the equation

$$d\epsilon = td\eta - pdv + \mu_1 dm_1 + \mu_2 dm_2 \ldots + \mu_n dm_n \text{"} \quad (7)$$

It should be noted here that this equation results from a direct application of the first and second laws to a closed system in equilibrium under the absence of gravity, capillarity, electricity, magnetism, and so on; i.e., all externally imposed forces (or work potentials) other than pressure. Continuing:

"In this equation, there are altogether $2n + 5$ variables, viz.

$$m_1, m_2, \ldots m_n$$

$$\mu_1, \mu_2, \ldots \mu_n$$

and

$$\epsilon, t, \eta, p, v$$

"These quantities are not all independent, for the $n + 2$ quantities, t, p, μ_1, μ_2, . . . μ_n can be derived from the original equation by differentiation. Thus the equations

$$\left(\frac{d\epsilon}{d\eta}\right)_{v, m_1, \ldots m_n} = t, \quad \left(\frac{d\epsilon}{dv}\right)_{\eta, m_1, \ldots m_n} = -p$$

$$\left(\frac{d\epsilon}{dm_1}\right)_{\eta, v, m_2, \ldots m_n} = \mu_1, \text{ etc.}$$

give us $n + 2$ independent relations between the $2n + 5$ variables.

[3] Professor of Engineering, Brown University, Providence, R. I. Mem. ASME.

[4] Associate Professor of Mechanical Engineering, University of California, Berkeley, Calif. Mem. ASME.

[5] Numbers in parentheses refer to the Bibliography at the end of this discussion.

The original equation is an additional relation, so that if ϵ is known as a function of $\eta, \nu, m_1, \ldots m_n$, there are altogther $n + 3$ known relations between the $2n + 5$ variables and the remainder $n + 2$ in number, are independent.

"The homogeneous body may thus undergo $n + 2$ independent variations, e.g., the quantities $m_1, \ldots m_n, \eta, \nu$ may be varied independently of each other. But if they are all varied in the same proportion, the result is a change in the *amount* of the body, while its state and composition remain unchanged. A variation of the *state* or *composition* of the body involves a change in at least one of the ratios of these quantities. There are $n + 1$ independent ratios of these $n + 2$ quantities (e.g., the ratios $m_1/\nu, m_2/\nu, \ldots m_n/\nu, \eta/\nu$) so that the number of independent variations of state and composition of a homogeneous body is $n + 1$" (8).

In the words of Gibbs: "In considering the different homogeneous bodies which can be formed out of any set of component substances, it is convenient to have a term which shall refer solely to the composition and thermodynamic state of any such body without regard to its size or form. The word *phase* has been chosen for this purpose" (9).

Hence the last sentence of the previous quote essentially states: "...the number of independent variations *of the phase* of a homogeneous body which contains n independent components is $n + 1$" (8).

Thus the *total* number of variations in r-phases considered separately is $(n + 1)\,r$. But when the r-phases are coexistent, these variations are subject to conditions of equilibrium

$$t' = t'' = t''' = t^r$$
$$p' = p'' = p''' = p^r$$
$$\mu_1' = \mu_1'' = \mu_1''' = \mu_1^r$$
$$\mu_2' = \mu_2'' = \mu_2''' = \mu_2^r$$
$$\vdots \quad \vdots \quad \vdots \quad \vdots$$
$$\mu_n' = \mu_n'' = \mu_n''' = \mu_n^r$$

Counting the number of equal signs, this provides a total of $(r - 1)\,(n + 2)$ conditions. The number of independent phase variations of which the system is capable (i.e., degrees of freedom) is therefore

$$F = (n + 1)\,r - (n + 2)\,(r - 1) = n - r + 2$$

BIBLIOGRAPHY

1 "Über die bewegende Kraften der Warme und die Gesetze welche sich daraus für die Warmelehre selbst ableiten lassen," by R. Clausius, Pogg. Ann., series 3, Book 79, 1850, pp. 368, 500.

2 "On the Equilibrium of Heterogeneous Substances," by J. W. Gibbs, Transactions of the Connecticut Academy III, October, 1875–May, 1876, pp. 108–248, and May, 1877–July, 1878, pp. 343–524; reprinted as Article III in "The Collected Works of J. Willard Gibbs, Ph.D., L.L.D.," Longmans, Green and Company, New York, N. Y., 1931, pp. 55–353, especially pp. 85–89 and 96–100.

3 "Grundlagen der Thermodynamik," by C. Carathéodory, *Mathematik Annalen*, vol. 67, 1909, p. 355.

4 "Thermodynamique," by H. Poincaré, Gauthiers-Villars, Paris, France, 1908.

5 "On the Equilibrium of Heterogeneous Substances," by J. W. Gibbs, *American Journal of Science*, series 3, vol. 41, December, 1878, pp. 441–458, reprinted as Article IV in "The Collected Works of J. W. Gibbs," Longmans, Green and Company, New York, N. Y., 1931, pp. 354–371.

6 "The General Thermodynamical System of Gibbs," by J. A. V. Butler, Chapter D of "A Commentary on the Scientific Writings of J. Willard Gibbs," edited by F. G. Donnan and A. Haas, Yale University Press, New Haven, Conn., 1936.

7 Cited from reference (4), p. 357.

8 Cited from reference (5), pp. 105–106.

9 Cited from reference (4), pp. 358 and 359.

J. S. Thomsen.[6] The authors' presentation of the phase rule is a useful contribution. They have certainly clarified some aspects of the application of this rule and also have given a new derivation, which does not make use of the first and second laws. However, it should not be inferred from this, that the use of the first and second laws is entirely superfluous in the usual classical derivation.[7,8]

The difference between these derivations may be summarized as follows:

	K and K Analysis		Classical Analysis
	Assumptions		
1	Arbitrary system (in general polyphase) has $C + 2$ independent properties.	1	Single phase has $C + 2$ independent properties.
2	Mass of each phase is independently variable at equilibrium (definition of free simple system).	2	First and second laws.
	Results		
1	Phase rule.	1	Mass of each phase is independently variable at equilibrium.
		2	Phase rule.

The foregoing table does not, of course, include the various assumptions (either implicit or explicit), common to both analyses.

Since the first K and K-assumption implies the classical one but not vice versa, it would seem that the classical one makes less use of empirical observation at this point. Furthermore, granted the fact that pressure, temperature, and mass are independent variables in a particular type of system with one constituent, it would seem to follow almost by definition that each new independent constituent will provide one additional one, thus giving a total of $C + 2$ for a single-phase system with C independent constituents. On the other hand, this is not as obvious in a polyphase system; one is tempted to think that the final state of equilibrium might depend on the particular phase to which a given constituent is added.

The second assumptions differ quite radically. The authors naturally emphasize the omission of the first and second laws in their approach. However, a part of their definition of a free simple system is obtained as a result in the classical treatment. (This follows from the fact that phase equilibrium depends only upon chemical potentials, which are intensive quantities.)

It seems impossible to say categorically that one analysis is better or more general than the other. It may be that the classical treatment is preferable in economy of postulates (since the first and second laws are obviously needed for many other purposes), but that the authors' approach is superior pedagogically. In any event, their alternative approach is an interesting one.

It also may be noted that a considerable part of the content of the state principle is implied in the excellent analysis of the first law by Bridgman,[9] although he does not summarize it in the clear and concise form given by the authors.

Myron Tribus.[10] Consider a system represented by a quantity of material enclosed by a surface which is impervious

[6] Assistant Professor of Mechanical Engineering, The Johns Hopkins University, Baltimore, Md.

[7] "Heat and Thermodynamics," by M. Zemansky, McGraw-Hill Book Company, Inc., New York, N. Y., third edition, 1951, Chapter 19.

[8] "Treatise on Thermodynamics," by M. Planck, Dover Publications, New York, N. Y., third edition, 1945, part IV, Chapters 2, 3.

[9] "The Nature of Thermodynamics," by P. W. Bridgman, Harvard University Press, Cambridge, Mass., 1941.

[10] Associate Professor, Engineering Department, University of California, Los Angeles, Calif. Mem. ASME.

to the transfer of matter. Let the bounding surface be such that it transfers heat and deforms without resistance to accommodate changes in volume of the system. Exclude from further consideration effects due to relativity, "electricity, magnetism, gravity, capillarity, motion, and fluid shear." Such a system is the authors, "simple" system. The system has mass, pressure, temperature, volume, energy, and entropy, as well as many other measurable properties. In considering the number of degrees of freedom a system may have, we are concerned with the determination of the number of variables minus the number of independent equations linking these variables. The many derived thermodynamic properties, such as enthalpy or free energy, need not be of concern since the introduction of each such quantity permits the introduction of the corresponding defining equation without therefore altering the degrees of freedom. The phase rule is concerned with equilibrium among coexisting phases and since the equilibrium corresponds to a state of rest, it cannot be affected by transport properties such as viscosity, electrical conductivity, and so on.

As the authors point out, there is an indefinite number of properties, but if one wishes to consider thermodynamic (more properly thermostatic) questions, the relevant properties are the mass, energy, entropy, pressure, temperature, and composition. Given all of these for differing conditions of the system, one may compute every thermodynamic variable and its change in going from one condition to another.

When all of these are known, we may say that a "thermodynamic state" is known, though we can give no assurance about color, taste, viscosity, and so on, being uniquely determined by thermodynamic state without recourse to experiment or some other principle.

If we consider a single-component homogeneous system of unit mass, the pertinent[11] thermodynamic variables are: the specific energy specific entropy, specific volume, temperature, and pressure. The question now arises: "When the mass and composition are fixed, how many of the remaining five variables are independent?" Following Gibbs, we may reduce the number of variables by two through the use of the first and second laws. The system must obey the first law, i.e., $du = dQ - dW$ where dQ and dW are the heat and work effects during a small change along a given path. If we restrict our considerations to conditions of equilibrium and denote specific entropy by s, then $dQ = Tds$, where T represents absolute temperature.

We now make the following trivial observation: A fixed mass enclosed in an impermeable but flexible envelope, in the absence of gravitational, electrical, magnetic, anisotropic, velocity, shear or capillary effects can raise a weight only by moving its boundaries. By well-known reasoning we may show therefore that $dW = Pdv$ where P represents pressure and v represents specific volume. The first and second laws combined with the deduction concerning dW yield the equation $du = Tds - Pdv$. If there exists an equation $u = u(s,v)$ this equation, in Gibbs' words, represents a "fundamental equation," for from it one may derive relations among all five quantities, u, s, v, P, and T. Differentiation with respect to v and s yields $T = (\partial u/\partial s)_v = T(s,v)$ and $-P = (\partial u/\partial v)_s = P(s,v)$. Term s may be eliminated between the last two equations to give a relation among P, v, T. Given only the "fundamental equation" the "equation of state" may be deduced, but not vice versa.

The derivation of the existence of a relation among P, v, T was shown without recourse to a state principle but used only the first and second laws and a trivial observation: "A system enclosed in an envelope and subject to the enumerated restrictions can do work only by expansion." These results are in contrast with statement 3 of the proposed principle.

To the writer it appears that the "state principle" has been derived from the two laws of thermodynamics. If some additional fact is to be elevated to the status of a principle, then assuredly it must be the trivial observation given in the foregoing quotations since the proposed principle can be deduced from the observation, but not vice versa, and therefore the observation is more fundamental.

Statement 1 of the proposed state principle may be viewed as an "existence postulate" for the "fundamental equation"; that is, the statement says, "The function $u(s,v)$ exists," or more simply, "thermodynamics is relevant."

Prompted by a reading of the paper, the writer has reviewed a number of thermodynamics books published in this country and abroad, to see how this question of the equation of state is handled. He agrees with the authors that it is usually poorly done and in many cases not even mentioned.

Authors' Closure

The paper under discussion covers three related topics. These are: (*a*) The general concepts and definitions needed such as state and property; (*b*) the need for and nature of the additional assumption required to complete a system of classical macroscopic thermodynamics beyond the First and Second Law; and (*c*) discussion of the particular assumption of type (*b*) needed for a very special, but very important, class of systems which are governed by the phase rule. This includes careful definition of this class of system and its associated special terminology.

The authors are very pleased that the paper has evoked such a considerable body of comment; the extreme diversity of opinion expressed by the many very able discussers suggests that a re-examination of this fundamental topic was indeed long overdue. In the following the authors will remark on the comments offered, and will then attempt to summarize the status of each of the three topics just listed above.

The authors would like to express their appreciation to Professor Keenan not only for his characteristically thoughtful and constructive comments but also for the several occasions on which he has offered encouragement and comment on earlier versions of the work.

In regard to the comment that Gibbs' starting place is more primitive, the authors agree: This point is discussed in detail in connection with Professor Thomsen's remarks following.

In regard to the relation between the definitions of component, etc., used by Gibbs and those suggested in the paper, the authors cannot agree. The crux of the matter is that the authors' independent plus determinate is not the same as Gibbs' independent plus "express every possible variation." In the authors' view, Gibbs' description, which is quoted by Keenan, is necessary but not sufficient for the following reason. Gibbs' independent plus "express every possible variation" would admit not only proper sets of components but also sets that are independent and indeterminate. Independent and indeterminate sets of components do not obey the phase rule, as is clearly shown by the examples numbered 3 and 5 in Table 1 of the paper.

If the authors read Gibbs correctly, and, admittedly, his writing is such that a unique interpretation is sometimes extremely hard to arrive at, then examples 3 and 5 of Table I do satisfy Gibbs' requirements, but they do not give proper answers in the phase rule. Furthermore, independent and indeterminate sets of components cannot be dismissed as trivial since they necessarily appear in discussions of homogeneous equilibrium.

The analogy offered by Professor Keenan is not in agreement with the authors' understanding of what is stated in the paper. Certainly, the authors would not and do not propose to vary the

[11] Pertinent in the sense that, if these variables are known for a succession of values, the heat effects, work effects, availability, and reversibility associated with a process are determined.

mass of a closed system, which by definition is fixed. Yet such a variation is apparently required in Professor Keenan's analogy; hence the authors fail to see that this analogy proves any "cumbersomeness" in the methods of the present paper.

It is, of course, hard for the authors to view the two systems of definitions with equal objectivity. But it is perhaps worth noting that the authors devised the new set of definitions relating to sets of components primarily because of the long continued and uniform difficulty found in teaching classes to use the phase rule correctly by the classical methods. The new methods have now been used by both authors in the classroom teaching for several years; the results of this experience can be summarized as follows. When the new methods are used, far better results, measured in terms of more correct answers on examinations and problems, are obtained with less expenditure of class time. This is particularly true in undergraduate classes.

Professor Keenan's distinction of "deduced" as opposed to "primary" properties appears to be a useful term; the authors appreciate this addition to the ideas involved.

Professor Keenan's observation that an unnecessary overlap exists between items 1 and 2 of the State Principle and the definition of state is a very pertinent point. The authors agree that it would be both more logical and more economical of statement to include points 1 and 2 in the discussion of state and property. This would not only reduce the overlap of statement but would also make a clear exposition available before the development of either the First or the Second Law. In the authors' opinion, such an exposition should be given explicitly, and it should definitely precede formulation of the First and Second Laws since both those laws involve key properties, energy and entropy, as a central portion of their meaning. The authors had originally intended to give the entire discussion of the State Principle of the paper prior to the First and Second Laws. However, on further consideration, it can be seen that it may be very desirable to present parts 1 and 2 of the formulation of the principle with a discussion of state and property prior to the First Law, but to discuss part 3 after either or both of the First and Second Laws have been introduced. The authors also agree with Professor Keenan that part 3 is the essence of the additional assumption required, beyond the First and Second Laws, to complete a rational discussion of the behavior of systems from a macroscopic point of view.

Professor Kestin apparently agrees with the authors that an additional explicit assumption regarding the maximum number of independent properties of the system under analysis is needed, but questions the terminology used to describe this assumption. The authors believe that what this assumption is called is not of first importance; but that the logic of the subject is. If this is so, the important point is not whether one chooses to call this assumption a fact, an observation, a postulate, a rule, or a principle, but that the assumption be made explicit rather than implicit. The fact that this assumption has not been made sufficiently explicit in the past is evidenced clearly by the discussion of Professor Oppenheim who, despite his obvious ability and knowledge of the subject, believes that such an assumption is not needed at all. Professor Kestin's further question is discussed later.

In respect to the comments of Professor Oppenheim, the authors not only stand firm but repeat here that some additional information or postulate is required in addition to the First and Second Laws. The authors are glad that the contrary point of view has been expressed by Professor Oppenheim, since in the authors' opinion this idea represents a long-standing and very common misconception. However, we cannot in any way agree with the statements given by Professor Oppenheim. If the authors' view is correct, then it is necessary that the proof offered by Dr. Oppenheim contain some circularity; a demonstration that this is indeed the case is given in the next paragraph.

Professor Oppenheim's argument proceeds as follows. First, general statements about "quintessence" and "synthesis" are made. These prove nothing, and numerous similar suggestive arguments can be presented for the other side of the case. The next statement made by Professor Oppenheim is a quotation from Butler as follows: "It is easily shown that E is a function of S, V, m_1, m_2, $\ldots\ldots m_c$, and that the complete value of dE is given by the equation[13]

$$dE = TdS - pdV + \mu_1 dm_1 + \mu_2 dm_2 + \ldots \mu_c dm_c'' \ldots . [7]$$

Professor Oppenheim then continues with a considerable body of discussion purporting to prove that he has derived the number of independent properties from the First and Second Laws alone. However, his final result is already contained *explicitly* in Equation [7]; the proof follows. In functional form, Equation [7] states identically

$$E = E(S, V, m_1, m_2, \ldots\ldots m_c) \ldots\ldots\ldots\ldots [7']$$

The authors submit that this equation contains $C + 2$ independent variables. Furthermore, any mathematical operations on either Equation [7] or Equation [7'] that fail to take proper cognizance of the existence of $C + 2$ independent variables are thereby immediately deprived of either mathematical or physical significance. Since Equation [7] is offered by Butler (and Oppenheim) on no basis other than the words, "It is easily shown that," the proof given is, at best, a mere verification of the content of the initial statement.

Similar remarks apply to all of the formulations known to the authors which purport to derive the phase rule from the First and Second Laws alone. However, it is sometimes far more difficult to pinpoint the circularity involved due to the lengthy discussions and interjections of other material that appear in most of the treatments of this topic. It is not impossible that some future synthesizer may achieve a derivation of the phase rule (or more generally of the number of independent variables for any system) from the First and Second Laws alone. However, the authors are not aware of any such proof at the present time. Consequently, at present the required information must be introduced as some form of postulate or assumption in order to complete a rational scheme of macroscopic thermodynamics on a postulational basis.

The authors also feel that a further comment on the matter of citing Gibbs and his commentators as a sort of "final authority," as has been done by Oppenheim, is badly needed.

In the authors' opinion, the results obtained by J. Willard Gibbs in thermodynamics cannot be praised too highly. His contributions are unquestionably of first rank importance, and are probably at least as great as those of any other single individual. However, it is dangerous to conclude from this that his methods cannot be improved upon, and hence to continue year after year to simply reinterpret Gibbs with no attempt to perfect better methodology. The authors believe it is important, for the sake of the subject, to draw a clear distinction between Gibbs' results, which cannot be overvalued, and his methods, which are often far from the simplest or clearest possible and which are almost always couched in language which needs further "interpretation." Indeed, the mere existence of the very extensive volume of commentary is in itself sufficient proof of this need.

Certainly no one today would recommend the methods of Newton's "Principia" as clear or concise. In many ways the relation of Newton's volume to mechanics is similar to that of

[13] This quotation is exact except that the symbols have been altered from the notation of Gibbs to the more modern usage to aid the reader.

Gibbs' "Collected Works" to thermodynamics. The most important difference, in the authors' opinion, is that Newton's work has been available roughly five times as long, and thus while Newton's results have remained essentially unaltered, the methodology used in obtaining and applying those results has been greatly improved. If this analogy has any validity, then a failure to distinguish between Gibbs' results and Gibbs' methods can only lead to stifling of further progress in the methodology of thermodynamics.

Professor Thomsen's comment on the derivation of the phase rule is extremely germane and very well put. The authors appreciate the added clarification which is brought out by his clear exposition of the matter, and on careful reconsideration agree with Professor Thomsen's clear summary of the relative merits of the two methods as they now stand. A few further comments are in order.

In regard to the logical economy of the two systems, there is a slight additional unstated assumption in the classical argument that is not included in Thomsen's summary (or any other discussion of the matter known to the authors); this is as follows. In order to use Thomsen's item 1 of the classical analysis it is necessary to assume not only that the number of independent properties for a one phase simple system is $C + 2$, but also that this number does not change when more than one phase is brought into equilibrium with other phases except for the restricting conditions of equilibrium derived from the First and Second Laws.

In other words, bringing two or more phases into equilibrium introduces restrictions owing to establishment of heterogeneous equilibrium, but it does not also introduce new independent variables by some form of interaction between the phases. This lack of new variables is not trivial, and indeed such variables do arise in many nonequilibrium situations. This statement should therefore probably be added as an item 3 in Thomsen's list of assumptions for the classical derivation. If one includes this item 3, then an assumption regarding the number of independent variables of the system being discussed (the simple, heterogeneous system) has been made. This is important, since it shows that one does not derive the number of independent variables from a less complicated system by use of the First and Second Laws. Even in the classical method, one assumes something about the total number of independent properties of the type of system under study, and then uses the First and Second Laws to show that, for this particular kind of system, there exists a lesser number of independent variables, those fixing intensive state, which can be used to simplify most analyses. Thus, when closely scrutinized, the classical proof is not in disagreement in any way with the formulation of the State Principle or its implications as given in the paper.

Despite the above remark, Professor Thomsen's point regarding logical economy is still well taken. Even if the item 3 suggested previously is added to Thomsen's list of the assumptions of the classical analysis, it is still true that the classical assumptions are contained in the assumptions used by the authors; but the authors' assumptions cannot be derived from the classical ones without use of the First and Second Laws.

It is worth noting that in treatments where maximum logical economy is considered essential, this can be achieved at the expense of some additional complication in the derivation while still retaining some of the better features of the present method. This can be accomplished as follows: Start with the minimum assumptions of Thomsen's list (plus item 3). Use the classical method to derive the phase rule; in this process the definitions of the free simple system and of independent and determinate sets of components can be employed to aid in clarity and precision.

There is one point in Thomsen's summary of the assumptions and results of the two methods used in deriving the phase rules that is not clear to the authors. Professor Thomsen lists the "free system" definition as a derived result of the classical method. The authors do not understand how this can occur. First of all, the authors have never been able to find any discussion of the need for a free system in Gibbs or in other existing treatments. Furthermore, the example of the BiOCL reaction, given in the paper, shows that for the definition of components used by the authors, the phase rule will not work on nonfree systems. Thus, the free system would seem to be a necessary part of the structure of the definitions rather than a derived result in the authors' formulation. It is possible that Professor Thomsen has some other definition of component in mind which would give the result he suggests, but the authors don't know what this would be.

It is also pertinent at this point to remark that the simple system, that is, the class of systems to which the phase rule applies, is perhaps the commonest and best known class of systems, and it was for this reason that it was discussed. However, in some ways this class of systems is an exceptional one in so far as the State Principle is concerned. This point was illustrated by several examples on more general types of systems in the first draft of the paper. Unfortunately, these examples had to be deleted due to length requirements. It is hoped that someone will provide a careful discussion of the number of independent variables in some of the more important nonsimple systems of engineering in the near future. In the authors' opinion, such a treatment is long overdue.

In regard to the remarks of Professor Tribus, it is apparent that he now agrees with the authors that some additional assumption is needed. In connection with the remark that this assumption is trivial, the authors would like to point out that the triviality arises not from the general assumption discussed in the paper but from the extreme simplicity of the system chosen as an example by Professor Tribus. Examination of more general systems shows that the scope of the assumption required increases approximately in proportion to the complexity of the system considered.

In conclusion, the authors would like to attempt a summary of status on each of the three topics discussed. On the matter of definition of concepts, some of the points raised by the discussers and the authors should be of aid in future treatments. However, the matter is clearly a subjective one, and equally clearly it can still stand further improvements particularly in reference to the definition of state and property. On the need for an additional postulate beyond the First and Second Laws, the authors believe firmly that such a postulate is needed, and this seems to agree with the consensus of the discussers. Parts 1 and 2 of the principle proposed by the authors might better be incorporated into the discussion of State and Property since, as noted by Keenan, there is an overlap, and these matters logically precede the First and Second Laws. The essence of the postulate required is part 3 of the present statements, that is, explicit assumption of the number of independent properties for the system as defined. In regard to the derivation of the phase rule suggested by the authors, it would appear to have certain advantages of clarity and precision of definitions, but it is less adequate than the classical treatment in regard to logical economy, as noted by Thomsen. A method has been suggested in the closure by which the better features of methods of the paper can still be utilized while maintaining maximum logical economy at the expense of some additional complication.

Stresses and Displacements in an Elastic-Plastic Wedge[1]

D. C. Drucker.[2] So few elastic-plastic solutions have been found that the additional one provided by the author is a very substantial contribution. It is worth noting, perhaps, that two of the interesting features of this plane-strain solution can be established directly without finding the solution itself. They are: the lack of dependence on the radial co-ordinate r, and the symmetry of the regions of plastic action, $\varphi_1 = \beta - \varphi_2$, Fig. 1($a$) of this discussion.

The independent variables of the problem are the co-ordinates r, θ, the elastic constants, say E and ν, the yield stress k, the uniform load p, and the wedge angle β. Dimensional analysis then shows that any component of stress σ, and any component of displacement u must be given by the following functional forms or their equivalents

$$\frac{\sigma}{k} = f\left(\frac{p}{k}, \frac{k}{E}, \nu, \beta, \theta\right)$$

$$\frac{u}{r} = F\left(\frac{p}{k}, \frac{k}{E}, \nu, \beta, \theta\right)$$

The co-ordinate r cannot appear in f or F.

The symmetry of the plastic regions may be established for the Mises yield criterion or any of the wide class of symmetric yield or loading functions which are independent of the mean normal stress. With such a criterion, a hydrostatic pressure may simply be superposed on any elastic-plastic solution. The answer to the original problem of Fig. 1(a) is then exactly the same as the sum of the hydrostatic pressure $p/2$ of Fig. 1(b), and the antisymmetric problem of Fig. 1(c), $p/2$ compression applied at $\theta = 0$ and $p/2$ tension at $\theta = \beta$. As hydrostatic compression is assumed to be without influence on the plastic action, the plastic zones are the symmetrically located ones of the antisymmetric case.

[1] By P. M. Naghdi, published in the March, 1957, issue of the Journal of Applied Mechanics, Trans. ASME, vol. 79, pp. 98–104.

[2] Chairman, Division of Engineering, Brown University, Providence, R. I. Mem. ASME.

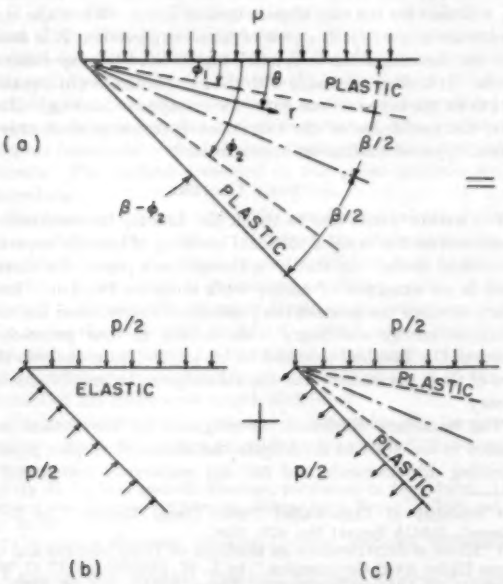

Fig. 1 Symmetry of Plastic Regions, $\varphi_1 = \beta - \varphi_2$, (a) = (b) + (c)

Author's Closure

The author is very appreciative of Professor Drucker's interesting observations on two aspects of the solution.

New Method to Measure Prandtl Number and Thermal Conductivity of Fluids[1]

J. Kestin.[2] Most methods which are used for the measurement of thermodynamic and transport properties may be called static, as they are based on the principle of effecting the smallest possible departure from equilibrium in the fluid to be measured. The authors have demonstrated that a dynamic method involving high velocities of flow is also feasible. The ingenious concept leads to a very simple experimental setup in which the major sources of error can be eliminated. In principle, as the experimental data determine the Prandtl number, Equation [1] of the paper, any one of the three quantities μ, c_p, or k can be evaluated if the other two are sufficiently well known. The authors rightly point out that, from the point of view of existing accuracy, the determination of thermal conductivity k will benefit most from the introduction of the new method, as its direct measurement constitutes a very difficult experimental task. It is to be hoped that the authors will continue to perform measurements with an improved and more elaborate setup, as they clearly intend to do.

Personally the writer always finds it regrettable that limitations of space in contemporary scientific journals make it impossible to quote tables of experimental results. Nevertheless, he would like to ask the authors to indicate some numerical values concerning the following quantities:

1 Temperature fluctuation in the main chamber (as measured by thermocouple f).

2 Maximum and minimum values of the pressure ratio p_s/p_t.

3 Range of exit velocities used.

4 Maximum and minimum temperature difference $t_t - t_s$ used in the measurements.

5 The values of γ chosen for insertion into Equation [6].

It is believed that publication of these numerical values will permit a more accurate appraisal of the potentialities of this excellent new idea.

Authors' Closure

In response to Professor Kestin's questions, we are pleased to submit the following information:

1 The heat capacity of the storage-type heat exchanger was such that the air temperature as indicated by the total temperature thermocouple f was constant within ± 0.1 F for approximately 40 sec after the flow was started. During this period the time fluctuations of the indicated temperature were within 0.05 F.

2 to 4 The choice of the ratio static to total pressure which determines the exit velocity is dictated by the following con-

[1] By E. R. G. Eckert and T. F. Irvine, Jr., published in the March 1957, issue of the Journal of Applied Mechanics, Trans. ASME, vol. 79, pp. 25–28.

[2] Professor of Engineering, Brown University, Providence, R. I. Mem. ASME.

siderations: The larger the velocity the larger is the temperature variation throughout the boundary layer. On the magnitude of the temperature variation depends the error connected with the use of the constant property relation, Equation [3], for the recovery factor. This error can well be calculated from available solutions of the laminar boundary-layer equations for variable property fluids. A decrease of the velocity, on the other hand, decreases the difference between total and recovery temperature and increases the errors connected with the measurement of this value. It is advisable to optimize conditions with respect to these errors for each investigation. In the reported measurements the pressure ratio was adjusted on the basis of these considerations to values between $p_t/p_s = 1.27$ and 1.82. Occasionally, because of air supply limitations, the pressure ratio was lower than optimum. Correspondingly, the exit velocity varied from 661 to 1135 ft/sec, the Mach number from 0.60 to 0.96, and the difference between total and recovery temperature from 5.67 F to 22.4 F. The temperature with which a measured Prandtl number was associated and the temperature at which the property values were introduced were the "reference temperature," familiar in boundary-layer analysis.[3] In these particular data, choosing the extremes of either the total or free-stream static temperature as a reference produced a data shift within the accuracy of the measurements. In Fig. 2, the Prandtl number is plotted over the reference temperature as calculated from Eckert.[3]

5 The heat capacity ratio required for evaluation of Equation [6] was obtained from Keenan and Kaye[4] and introduced at the total temperature.

Buckling of Initially Imperfect Cylindrical Shells Subject to Torsion[1]

T. T. Loo.[2] The author is to be commended for his continuous interest and effort in this problem, which is one of considerable technical importance. Experiments have shown that the buckling strengths of thin-shell structures are usually sensitive to initial imperfections; thus the need for large-deflection theories in such a class of problems is self-evident.

In 1952, the writer, as a student of Prof. L. H. Donnell, established a large-deflection theory for both perfect and imperfect thin cylindrical shells under pure torsion.[3] In developing the theory, some approximations were made to simplify algebraic computations that otherwise would be very tedious. In the expression for radial displacement w, there appear four parameters. Two of these, γ and n, were assumed to take values as given by small-deflection theory. This was done before making the first variation of the total potential energy of the system stationary. The fact that close agreement was obtained in the buckling strengths of this simplified theory with those from Donnell's more accurate method[4] has warranted such a simplification. Even though it may be expected that there will be somewhat less reduction of resistance during the postbuckling stage due to such a simplification, it seems to have little effect on the values of critical loads, which is all we are really interested in.

The author has made a valuable contribution in his discussion of the condition for periodicity of the circumferential displacement v. This condition will lead to a relationship between the parameters, making three rather than four independent parameters actually involved in the total potential-energy expression. Thus the computational difficulties might be lessened to the extent that a more accurate solution could be found readily without the writer's simplification. But the author obviates this saving by introducing a new and unnecessary parameter.

In the energy method of solution of torsion loading, the boundary condition of vanishing radial displacement w at both ends is usually considered to be more important than other conditions required for either clamped or simply supported shells. By introducing a uniform radial displacement, which is in effect a fifth parameter, in his assumed expression for w, Equation [6] and Equation [7], the author complicates the computation and, by violating the major rather than the secondary boundary condition, he has thus treated a problem with even less rigorous boundary conditions. The result of such an introduction, instead of "obtain(ing) the minimum theoretical buckling load," results in values which are much too high in comparison with those of the existing theories.[3,4]

In previous publications,[3,5] attempts were made to express the inherent imperfections of the specimens in terms of their physical dimensions. It is obvious that the imperfections in any specimen are independent of the type of loading; with this in mind the writer has suggested a rational formula[3] which seems to be reasonably satisfactory in the light of its adaptability to both buckling under axial compression and under pure torsion. This formula without any change of parameters accounts for the widely contrasting phenomena which have been observed from tests in these cases. However, in the present paper, a similar formula, but with a different value for the unknown parameter U_0, was used for the case of pure torsion alone. When the same parameter is used for the case of axial compression, it is found that the theoretical curve is much higher than the experimental result. It is always possible with the two parameters in Equation [21] to fit the experimental curve for one type of loading. However, the usefulness of the expression becomes evident only if several types of loading are approximated.

Author's Closure

The author would like to thank Dr. Loo for his constructive comments on the topic of torsional buckling of initially imperfect cylindrical shells. As stated in the author's paper, the current work is an extension of earlier work done by Dr. Loo. In an effort to refine the process, the present author rendered the total potential energy stationary with respect to four parameters, whereas Dr. Loo had assumed in his approximate analysis that two of these parameters had the values given by small-deflection theory.

The boundary conditions investigated by the author were chosen in an effort to investigate the effects of various possible buckling displacements and did not necessarily correspond to

[3] "Engineering Relations for Heat Transfer and Fluid Friction in High-Velocity Laminar and Turbulent Boundary-Layer Flow Over Surfaces With Constant Pressure and Temperature," by E. R. G. Eckert, Trans. ASME, vol. 78, 1956, pp. 1273–1283.

[4] "Gas Tables," by J. Keenan and J. Kaye, John Wiley and Sons, Inc., New York, N. Y., 1949, p. 34.

[1] By W. A. Nash, published in the March, 1957, issue of the Journal of Applied Mechanics, Trans. ASME, vol. 79, pp. 125–130.

[2] Associate Professor of Mechanics, Rensselaer Polytechnic Institute, Troy, N. Y.

[3] "Effects of Large Deflections and Imperfections on the Elastic Buckling of Cylinders under Torsion and Axial Compression," by T. T. Loo, Ph.D. dissertation, Illinois Institute of Technology, 1952; Proceedings of the Second U. S. National Congress for Applied Mechanics, 1954.

[4] "Stability of Thin-Walled Tubes Under Torsion," by L. H. Donnell, NACA Report No. 479, 1934.

[5] "Effect of Imperfections on Buckling of Thin Cylinders and Columns Under Axial Compression," by L. H. Donnell and C. C. Wan, Journal of Applied Mechanics, Trans. ASME, vol. 72, 1950, pp. 73–83.

conditions commonly encountered. This is particularly true with respect to the uniform radial displacement. Even though end conditions would not ordinarily permit such a displacement, it was considered desirable to investigate the effect of such a term. It was shown that inclusion of such a term has only a very slight effect upon the final load-deflection curves. This had previously been established by the author in regard to hydrostatic loading of cylindrical shells.

Vibration Modes of Stators of Induction Motors[1]

P. L. ALGER.[2] This paper is considered to be an important contribution to the art of motor design. Besides meeting the basic requirements of good all-round performance and low cost, designers nowadays are required to make motors both good looking and pleasant sounding. That is, the art of making motors quiet sounding, or "sonance design," is rapidly becoming comparable in importance to the art of "appearance design."

The frequency of the magnetic-force waves imposed on the stator of an induction motor is proportional to the number of rotor slots and the speed. The number of slots is normally larger the greater the diameter of the motor. Thus the force waves imposed on a motor go through the whole range from zero to full frequency each time the motor starts, and the top frequency is higher the larger the motor size. On the other hand, the natural frequency of the stator for a given number of nodes decreases as the size increases. Therefore every motor of larger than about 5 hp size must go through one or more periods of resonant-frequency vibration of the stator each time it starts.

How to design the motor to locate these resonances properly with respect to the motor speed, and how to control them so that they will not be noticeable, presents a difficult problem to the designer that is of growing importance. This paper surely will be helpful to those who have to deal with this problem.

C. J. STUDERUS.[3] While working in the General Electric Medium Induction Motor Department, the writer applied the method described in the paper to a stator of different design than that used by the authors. The principal objective was to have an accurate and yet relatively simple method of determining the resonant frequencies and forced response of the dynamically coupled frame and core of already existing and proposed lines of motors. The method presented in this paper provides such a procedure.

The frame mentioned was of the same general size and dimensions as that of the authors. However, the ribs constituting the coupling between rings was decidedly different both in size and location. Some pertinent dimensions are shown below. A radial rib at $\theta = 0$ contacted the entire length of the inner core, Fig. 1. The radial ribs at $\theta = 60$ deg and $\theta = 300$ deg were only in contact with the core along 1.5 in. of their axial lengths. Along the bottom of the core was a saddle rib covering an arc of 45 deg and contacting the entire axial length of the core.

The general procedure followed to determine the frequencies was to set up the energy expressions for each of the elements

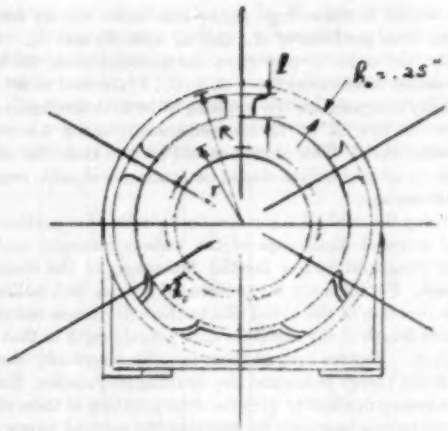

FIG. 1

4 pole—30 hp—1800 rpm—220/440 volts
$R = 7.715$ in., $r = 6.1$ in.
$L_c = 4.5$ in., $L_o = L_i = 11.0$ in.
$h_o = 0.25$ in., $h_i = 1.3$ in., $h_r = 1.125$ in.
$l = 0.9375$

of the motor frame (outer ring, inner ring, radial ribs, and so on), using the energy expressions described by the authors (e.g., Equations [11], [16], [18]). These expressions were then evaluated using second mode ($m = 2$) terms only. A comparison of the magnitudes of the resulting energy terms indicated which of the elements contributed an insignificant amount to the energy stored. This procedure permits the significant vibrational elements of the system to be isolated with a minimum of numerical work. Only the significant elements need then be evaluated when terms from the higher modes are used. The significant elements were the three radial ribs, the inner ring, and the outer ring.

The determinant using terms from all six modes was set up. While this was being checked out, the 4×4 determinant comprised of only the second-mode terms was solved by hand. The resulting values are shown in Table 1, together with the actual second-mode frequencies obtained experimentally, using an experimental arrangement similar to that of the authors.

TABLE 1

	In-tact cosine, cps	In-tact sine, cps	Counter-tact sine, cps	Counter-tact cosine, cps
Computed f_2.....	701	878	8649	8895
Experimental f_2.....	684	860	....	....

The higher value second-mode frequencies could not be excited with the equipment used.

The authors mention that in their case the even and odd modes separated, producing separate determinants from which the even and odd frequencies could be determined. This was due to the symmetry of their idealized frame about both vertical and horizontal axes, since the four tangential ribs were ignored as insignificant energy-storing elements. In the frame used by the writer, the idealized frame was symmetrical about the vertical axis but not about the horizontal axis owing to the location of the radial ribs. Thus for this case the assumed sine and cosine modes of deflection for the rings separated so that the frequencies associated with each mode could be evaluated separately. In

[1] By E. Erdelyi and G. Horvay, published in the March, 1957, issue of the JOURNAL OF APPLIED MECHANICS, Trans. ASME, vol. 79, pp. 39–45.

[2] Consulting Engineer, General Electric Company, Schenectady, N. Y. Fellow ASME.

[3] Aircraft Gas Turbine Division, General Electric Company, Cincinnati, Ohio. Assoc. Mem. ASME.

other words, in the energy expressions there are no terms involving cross products of A_m and a_m with B_m and b_m. Consequently, the order of any given determinant could be halved. If six modes of vibration ($m = 2, 3 \ldots . 7$) are used to set up the frequency determinant, the resulting 24×24 determinant can be reduced to two 12×12 determinants, reducing the required numerical work. This always should be true since the idealized system in all probability should be symmetrical with respect to at least one axis.

In using the method, some familiarity with what portion of the actual physical dimensions of the various elements contribute to the structural and/or inertial dimensions of the elements is essential. For instance, the presence of quarter-inch radius fillets at the junction of the radial ribs to the outer frame reduced the effective length of the ribs from their actual length to that length less $^1/_4$ in. Factors such as these can affect seriously the accuracy of the energy terms and the resulting frequencies. However, the necessary familiarity with the determination of these effective dimensions can be gained by applying the method to one or two stators. Along these same lines might be mentioned the need for carrying out the numerical terms to at least four decimal places, since the method inherently requires the subtraction of large numbers.

The method presented by the authors not only provides a means of determining the many frequencies that can be expected from a given design, but also permits a mathematical means of experimentation. The resulting changes in frequency response that occur by varying the dimensions of the coupling ribs can be predicted readily in advance of any actual construction. The optimum coupling can then be selected to avoid any resonance effects or driving-force responses.

Authors' Closure

The authors appreciate the interesting comments of Messrs. Alger and Studerus. The importance of "sonance design" will undoubtedly stimulate further analytical work in vibration evaluation of complex structures. However, such analytical work can never be completely successful unless it is paralleled by confirming experimental evaluation. It is gratifying to note that Mr. Studerus has undertaken the task of extending the authors' work both in its theoretical and experimental aspects.

Yield Loads of Slabs With Reinforced Cutouts[1]

F. A. Gaydon.[2] The paper maintains the usual high standard of clarity associated with work of author and his associates.

Equation [16b] implies that the value of μ obtained from the bent-beam approach is valid when $\delta/a \geq 2$. It is thought that this is unduly optimistic. In fact, it is to be doubted if the bent-beam approach provides a statically admissible stress field unless δ/a is small, when neglect of the shear in the yield criterion is probably permissible; however, when the reinforcement is wide, $\delta/a \geq {}^1/_2$ say, it is doubted whether neglect of the shear is justifiable. If one considers a stress field in the square reinforcement similar to that depicted in the slab in Fig. 4 of the paper, for the dimensions $^1/_2 \leqslant \delta/a < 2$, and if in Equations [11a], [11b], [11c], μ is made zero, λ_1, λ_2 are replaced by μ_1, μ_2 and accompanying dimensional changes are made, the lower bound μ of the reinforcement is given by

$$\mu = \min (\mu_1, \mu_2)$$

where

$$\mu_1 \, h/H = \frac{(b-a)^2}{2ab} = \frac{\delta^2}{2ab}$$

and

$$\left\{1 - \frac{\mu_2 ha/H}{b-a}\right\}^2 = \frac{4a^2 (\mu_2 \, h/H)^2}{(b-a)^2 - (\mu_2 \, bh/H)^2}$$

Then μ_1 is seen to be less than the value given by Equation [16a] and it follows that μ also is less than this value. If, therefore, the beam approach were applied to the base slab with the corresponding dimensions ($^1/_2 < b \leqslant {}^3/_4$), a lower bound better than λ_{TL} would be obtained. This seems unlikely, and it is suggested that for such dimensions the beam approach is inadmissible.

The foregoing remarks in no way invalidate the comparison in Table 1, since $\delta/a \leqslant {}^1/_2$ for all the specimens contained therein.

The paper demonstrates strikingly that the methods of limit analysis provide valuable information for the designer of reinforced plates.

D. D. Vasarhelyi.[3] It is gratifying indeed to see that the results of a research concluded several years ago can be useful in some new way and in a different type of work. Especially so when the new use made of the results, as in this case, is entirely independent from the original scope of the earlier investigation.

The writer recently compared the same general yielding values with values computed by simply multiplying the net cross section of the specimen with the corresponding coupon yield-strength values. It was found that all actual general yielding values are within 10 per cent from 93 per cent of the computed value. This was done in order to satisfy the writer that it is possible by an elementary means to predict the general yield load of rather complex structural elements similar to our specimens. The rather definite 93 per cent to the writer represents the efficiency of these structures in the sense as this word is used in structural design, and is thought to be just another formulation of the term called "design factor" by the authors. The rather close agreement of this elementary approach with the more fundamental one of the authors is a further proof of the correctness of the underlying assumptions.

Authors' Closure

The authors wish to thank Professors Gaydon and Vasarhelyi for their kind comments. Professor Gaydon is quite right in pointing out that care must be taken in applying the theory to be sure that the assumptions are reasonably well satisfied. This, of course, is generally true of the mathematical solution to any physical problem. In the present example, good judgment must be used in deciding if the hub dimensions are such that beam theory may be used, and if the slab dimensions are such that plane-stress theory may be used.

The authors were most interested to learn that Professor Vasarhelyi's elementary formula yields essentially the same results as their own more nearly exact analysis. It should be pointed out that the range of parameters in the specimens tested was rather limited, and that there is no assurance that the empirical figure of 93 per cent would always be valid. However, the analysis given in the paper provides a means by which any such empirical formula may be checked and hence made available for engineering use.

---

[1] By P. G. Hodge, Jr., and Nicholas Perrone, published in the March, 1957, issue of the Journal of Applied Mechanics, Trans. ASME, vol. 79, pp. 85–92.

[2] Department of Theoretical Mechanics, University of Bristol, Bristol, England.

[3] Associate Professor of Civil Engineering, University of Washington, Seattle, Wash.

Longitudinal Impact of a Semi-Infinite Circular Elastic Bar[1]

C. W. CURTIS.[2] The author has presented a neat and ingenious method for solving an important case of a long standing problem. Although it has been possible for some time to treat rigorously the propagation of an elastic strain pulse in an infinitely long bar, the problem of satisfying time and space-dependent boundary conditions at the end of a semi-infinite bar has presented difficulties in all but trivial cases. Since the solution given by the author satisfies exactly the end conditions, as well as the condition of a lateral free surface, it represents, in the writer's opinion, a significant contribution.

Attention is called to recent strain measurements of Dr. George Fox which can be compared with the theoretical predictions of this paper. The experimental strains were produced in a long bar by reflection of an air shock from one end. For distances greater than about 75 radii from the end of the bar and for times less than the arrival time for the first maximum, the agreement between the leading portion of Fig. 5 of the paper and the experimental strain-time records is remarkably good. Beyond the first maximum, however, Equations [35] and [36] no longer provide an adequate representation of the Pochhammer-Chree frequency equation, and it is necessary to solve the frequency equation numerically. Values so obtained for the frequency and wave number can then be used in an asymptotic expression, derived from Equation [32] of the paper by the saddle-point method, to predict both amplitudes and frequencies of the first-mode oscillations following the first maximum. These predictions agree with experiment up to the time corresponding to the onset of second-mode vibrations. We have not as yet tested quantitatively the consequences of Equation [32] beyond this time, but qualitatively it predicts correctly the onset of second-mode vibrations and an abrupt decrease in amplitude at a time corresponding to the minimum group velocity of the first mode.

This agreement may appear somewhat surprising since the experiments of Dr. Fox were carried out by suddenly applying to the end of the bar a constant, uniform pressure rather than by imposing a constant, uniform velocity as stipulated by the author. It can be shown, however, for large distances of travel that at least the leading portion of the pulse should be the same in the two cases.

As a closing remark, it may be of interest to know that Mr. Robert Folk of our laboratory has quite recently made another advance in the theory. He has found by using appropriate sine and cosine transforms, instead of the Fourier transform employed by the author, that it is possible to solve problems involving more general end conditions. In particular, the end conditions may be given by specifying as any desired functions of radial position r, and time t, either the axial displacement u_z, and the tangential stress σ_{rz}, or the radial displacement u_r, and the normal stress σ_{zz}. The problem considered in this paper is a special case in which the axial displacement at the end is independent of r but increases linearly with positive t and the tangential stress is independent of r and t.

M. K. HUBBERT.[3] In reading this interesting paper, the writer has had difficulty in reconciling the author's theoretical conclusions with mutually confirmatory experimental results, obtained independently by McMillen[4] and by Hughes, Pondrom, and Mims[5] on the transmission of elastic waves along cylindrical bars.

McMillen suspended bars in a vessel of water and produced elastic waves in them by firing steel balls into their exposed upper ends. The wave propagation was observed by means of spark photography of the secondary shock waves in the water produced by propagation of the elastic waves in the bar. His essential

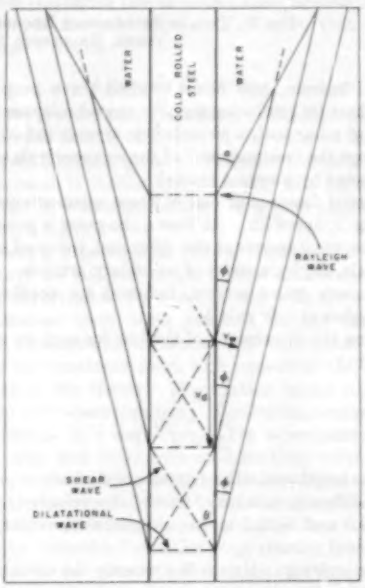

FIG. 1 SHOCK WAVES IN WATER RESULTING FROM AN IMPACT ON UPPER END OF COLD-ROLLED STEEL BAR
(Drawing from an enlargement of spark photograph by McMillen.)

results for cold-rolled steel are shown in Fig. 1 of this discussion, which has been made directly from an enlarged copy of one of his spark photographs. The water waves making the angle ϕ with the axis of the bar are generated by waves traveling along the bar with velocity

$$v_d = v_w/\sin\phi \quad \ldots\ldots [1]$$

From the figure, ϕ is about 14 deg; and v_w at 20 C is 1476 m/sec, giving $v_d \cong 6100$ m/sec. McMillen's mean of several measurements was 5994 ± 34 m/sec, which would give a mean value for ϕ of 14.25 deg. This is in reasonably close agreement with the velocity of the dilatational wave in an infinite medium

$$v_d = \left[\frac{E(1-\sigma)}{\rho(1+\sigma)(1-2\sigma)}\right]^{1/2} \quad \ldots\ldots [2]$$

whose value from handbook data on the elastic constants was found to be 5850 m/sec.

The repetition of the waves making the angle ϕ was ascribed by McMillen to "internal reflections" in the bar. The low-velocity wave, generating the water wave of angle α, had a measured velocity of 2959 m/sec, as compared with the calculated value of 2940 m/sec for Rayleigh surface waves. No transverse waves were observed.

[1] By Richard Skalak, published in the March, 1957, issue of the JOURNAL OF APPLIED MECHANICS, Trans. ASME, vol. 79, pp. 59–64.
[2] Department of Physics, Lehigh University, Bethlehem, Pa.
[3] Shell Development Company, Houston, Texas.

[4] "The Velocity of Dilatation and Rayleigh Waves in Metal Bars," by J. H. McMillen, *Journal of the Acoustical Society of America*, vol. 18, 1946, pp. 190–199.
[5] "Transmission of Elastic Pulses in Metal Rods," by D. S. Hughes, W. L. Pondrom, and R. L. Mims, *Physical Review*, vol. 75, 1949, pp. 1552–1556.

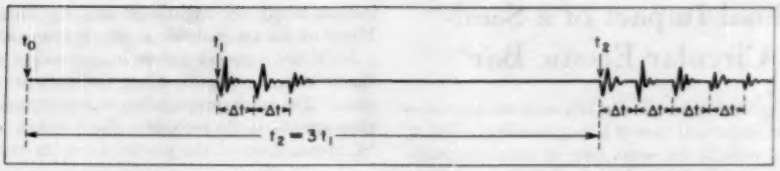

FIG. 2 TYPE OF SEISMOGRAM RECORDED BY HUGHES, PONDROM, AND MIMS AT END OF STEEL CYLINDER, RESULTING FROM MICROSECOND PULSE AT OPPOSITE END

Hughes, Pondrom, and Mims studied wave propagation in cylindrical bars by producing equally spaced microsecond pulses on one end of a bar with a piezoelectric crystal and observing on an oscilloscope the "seismogram" of the wave arrivals at the other end, as detected by a second crystal.

The essential features of one of these seismograms are illustrated in Fig. 2, herewith. At time t_0 the pulse is generated, and at time t_1 the wave arrives at the other end, followed at constant time intervals, Δt, by a series of secondary arrivals. At time t_2 another primary wave arrives, followed by another train of secondary pulses at intervals Δt.

By varying the dimensions of the bar for a given material, it was found that

$$\left.\begin{aligned} t_1 &\propto l \\ t_2 &= 3t_1 \\ \Delta t &\propto d \end{aligned}\right\} \quad \ldots\ldots\ldots\ldots\ldots\ldots [3]$$

where l is the length and d the diameter of the bar.

For two different cold-rolled steels, the velocity t_1/l had the values 5880.0 and 5892.2 m/sec, respectively, corresponding to the dilatational velocity v_d.

The wave arriving at time t_2 is obviously the dilatational wave once reflected.

The time delay Δt, which was proportional to the bar diameter, corresponded to the time of transit across the bar of a wave of shear velocity v_s at the critical angle θ to the bar diameter, where

$$v_s = (\mu/\rho)^{1/2} \ldots\ldots\ldots\ldots\ldots\ldots [4]$$

and

$$\sin\theta = v_s/v_d \ldots\ldots\ldots\ldots\ldots\ldots [5]$$

These several observations combine to give the physical picture shown in Fig. 3, herewith, of the propagation of short-wavelength elastic waves along a circular cylindrical bar. A primary

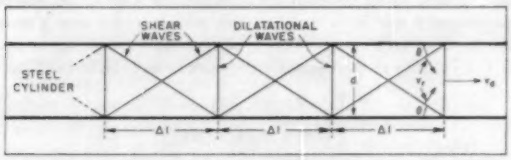

FIG. 3 ELASTIC WAVE TRAIN IN STEEL CYLINDER IMPLIED BY EXPERIMENTS OF MCMILLEN AND OF HUGHES, PONDROM, AND MIMS

plane wave moves through the bar at the dilatational velocity v_d. Its intersection with the boundary sets up elastic disturbances which act as Huygens' sources for shear waves traveling at the velocity v_s. Since these waves are generated along a circle around the bar, moving at the velocity v_d, they produce a conical wave front making an angle θ with the boundary of the cylinder, having the dilatational wave as the forward base of the cone.

At a distance Δl behind the dilatational wave front, given by

$$\Delta l = d/\tan\theta \ldots\ldots\ldots\ldots\ldots\ldots [6]$$

this cone again intersects the surface where it is reflected as a shear wave and also generates another dilatational wave. The arrival of these "nodes" at the end of the bar produces the secondary pulses at time intervals Δt.

The result of all this is that the initial wave front is followed by a stationary wave train of fixed geometrical form, with the entire train traveling at the dilatational velocity v_d. The train increases in length with distance, and since it derives its energy from that of the initial wave, it follows that the front of the train must become continually attenuated as the rearward part is augmented.

Were this train to be propagated through a bar immersed in water, then a spark photograph should reveal conical shock waves in the water originating at each "node," at the intervals Δl along the bar, where the shear waves are reflected. This, in fact, is what happens as is shown by the repeated shock waves at intervals Δl obtained from McMillen's photograph. The angle θ derived from the photograph by means of Equation [6] agrees within experimental error with the value in Equation [5] based upon the ratio of the shear and dilatational velocities.

As Hughes, Pondrom, and Mims have shown, it is possible, by means of this theoretical interpretation, to compute from their seismographic data, all the elastic constants of the material with a higher precision than usually has been possible heretofore.

JULIUS MIKLOWITZ.[6] The author's ingenious solution of a very difficult problem has resulted in an interesting contribution to the theory of wave propagation in an elastic rod. The writer and C. R. Nisewanger[7] recently presented some work, dealing with approximate theories of compressional waves in an elastic rod,[8] that contains supporting information for the author's findings. Fig. 4 of this discussion shows two strain-time records taken from Fig. 1, Part II of the quoted work.[8] The records are representative of highly reproducible tests employing an aerodynamic shock tube and a long 1-inch-diameter duraluminum rod. The test is similar to that employed by Curtis (reference 9 of paper). In it a step pressure is applied to the free end of a "semi-infinite" rod. Specifically, the records shown here are those of a station 20 diameters from the source; (a) representing the radial strain at the surface of the rod, obtained with a cylindrical

[6] Associate Professor of Applied Mechanics, California Institute of Technology, Pasadena, Calif. Mem. ASME.

[7] Research Engineer, U. S. Naval Ordnance Test Station, Pasadena, Calif.

[8] "The Propagation of Compressional Waves in a Dispersive Elastic Rod, Part I: Results From the Theory," by J. Miklowitz, JOURNAL OF APPLIED MECHANICS, Trans. ASME, vol. 79, June, 1957, pp. 231–239; and "Part II: Comparison of Experimental Results and Theory," by J. Miklowitz and C. R. Nisewanger, ibid., June, 1957, pp. 240–244.

condenser microphone, and (*b*) the axial strain at the surface of the rod, obtained with 20 very short strain gages (type C-19) mounted in series, and axially, around the rod circumference.

If one neglects the small-amplitude high-frequency oscillations in the axial-strain record (*b*), the two records shown here in Fig. 4

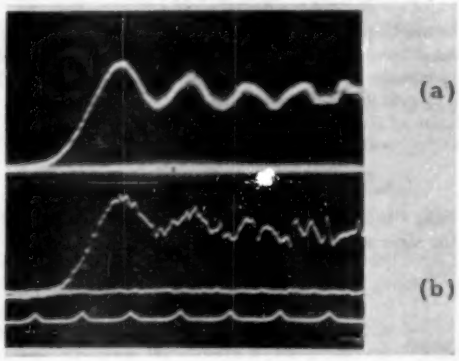

FIG. 4 TIME RECORDS OF (*a*) RADIAL STRAIN AND (*b*) AXIAL STRAIN AT THE SURFACE OF A CIRCULAR ROD FOR A STATION 20 DIAMETERS FROM THE SOURCE (AN END UNIFORM-PRESSURE STEP)

have an almost identical shape for the early times (up to approximately 40 microsec). This was pointed out in the writer's work as support for the Rayleigh approximation. These records are support then, for the author's findings, on the likeness of the radial-strain and axial-strain solutions, which stem from employing Rayleigh's approximation, i.e. Figs. 4 and 5 of the paper. As pointed out in the paper, the works of Davies (reference 2) and Curtis (reference 9) are support for the author's axial-strain solution.

The afore-mentioned early appearing high-frequency oscillations exhibited by the axial-strain record (*b*) can be explained in terms of activity from the higher modes of transmission. Other similar records in the writer's work (see Fig. 1, Part II),[8] representing stations closer to the source, showed that these disturbances were more severe as one would expect. These higher mode disturbances then determine the applicability of the Rayleigh approximation for early times at a station; that is, they determine the limit on how close the station can be to the source for good representation of the strain record by the approximation. As the author points out, the works of Davies (reference 2) and Curtis (reference 9) have indicated the limitations on the use of the approximation, imposed by the short-wave activity of the first and second modes of transmission, for the larger times at a station.

The agreement of the author's solution with Fig. 4 of this discussion, and the results in references (2) and (9) of the paper imply the important fact that, at large enough distances from the source, the solutions are alike for a step-velocity input (author's case) and a step-pressure input (Fig. 4 here and quoted works). This makes the author's work even more valuable when one considers the further difficulty that is added to the analytical problem, when end stress conditions must be specified as in the case of the latter problem.

The writer would agree with the author's comment that for an approximate theory to yield results similar to the author's long-time solution, it would have to preserve the Rayleigh approximation to the first (longitudinal) mode of Pochhammer's frequency equation. In this connection, it was shown in the writer's work,[8] that the Mindlin-Herrmann theory (references 5, 7) does not preserve the Rayleigh approximation, since its upper mode governs the early disturbance, yielding very short waves there.[9] The Sutton theory[10] (reference 8) is even less accurate at the early times. It contains a set of infinite characteristic velocities and associated sizable disturbances. It should be noted that, in both of these theories, the stated defects are not reflected in the excellent agreement both theories have with the basic Pochhammer mode of transmission. Hence to the writer's knowledge, the Love equation (Equation [46] of paper) incorporating Rayleigh's approximation, is the only approximate theory that will agree with the author's results.

AUTHOR'S CLOSURE

The author is grateful to the discussers as the experimental and theoretical results cited greatly add to the value of the original paper. The confirmation given by Professor Curtis is especially interesting because it verifies Equation [32] to a further extent than the range in which the author's long time approximation, Equation [43], is valid.

The interesting experimental results cited by Dr. Hubbert appear to have no relation to the author's theoretical results because the experiments were conducted with very different loading conditions than were assumed in the theory and because the experimental measurements were made at times which would be considered short with respect to the long time approximation of the theory. The loading in the experiments was a pulse of very short duration. The loading assumed in the theory was essentially a step wave. The experiments cited by Professors Curtis and Miklowitz indicate that when the test conditions approximate the conditions assumed in the theory, the theoretical and experimental results are in good agreement.

Professor Miklowitz's remarks on the early disturbances predicted by the Mindlin-Herrmann and Sutton approximate theories appear to be correct. The statements in the original paper should accordingly be amended to the effect that these approximate theories contain contributions in their long time approximations which are of the form given by Equation [43] due to the fact that the basic Pochhammer mode is essentially preserved in the approximate theories, but that there may be, in addition, unrealistic contributions present as pointed out by Professor Miklowitz.

Synthesis of Four-Bar Mechanisms by the Method of Components[1]

N. ROSENAUER.[2] The paper is an attempt to replace the elegance of vectorial methods by ordinary Cartesian representation. The statement of the author in the summary that his method permits the synthesis for prescribed conditions concerning angular velocities, accelerations, and length of links makes the wrong impression that the vectorial method would not permit the solution of such problems, but this is not so. The same problems may be solved by vectorial methods as well, and here is the solution:

Instead of six equations used by the author, the vectorial method requires only three, which are derived in the writer's publication (footnote 5 of the paper)

---

[9] The same mode, however, gives physically realistic results for later times.

[10] This theory was also derived earlier by Bishop, "Longitudinal Waves in Beams," *Aeronautical Quarterly*, vol. 3, February, 1952, pp. 280–293.

[1] By J. Hirschhorn, published in the March, 1957, issue of the JOURNAL OF APPLIED MECHANICS, Trans. ASME, vol. 79, pp. 22–24.

[2] New South Wales University of Technology, Sydney, Australia.

$$\bar{q} = \omega_q\omega_r(\omega_q - \omega_r) + (\omega_q\alpha_r - \omega_r\alpha_q)i \quad [1]$$

$$\bar{r} = \omega_s\omega_s(\omega_q - \omega_s) + (\omega_s\alpha_s - \omega_s\alpha_q)i \quad [2]$$

$$\bar{s} = \omega_s\omega_r(\omega_q - \omega_r) + (\omega_s\alpha_r - \omega_r\alpha_q)i \quad [3]$$

and an additional condition representing the closed polygon of Fig. 1(*a*) of the author's paper

$$\bar{p} = \bar{q} + \bar{r} - \bar{s}$$

Solution of Example 1. Given $\omega_q = 10$ rad/sec, $\alpha_q = 0$, $s_x = 4$ in., $s_y = 4.625$ in., $\omega_s = 5$ rad/sec, $\alpha_s = 10$ rad/sec^2. It should be noted that for the determination of the mechanism it is not necessary to give the value of p, but it is sufficient to assume p horizontal; i.e., $p_y = 0$. Find q, r, ω_r, α_r, and p.

Introducing the scale factor k between the elements of angular motion and the lengths of the links, and taking the real axis in the X-direction and the imaginary axis in the Y-direction, we have

$$ks_y = \omega_q\alpha_r - \omega_r\alpha_q = \omega_q\alpha_r$$

since $\alpha_q = 0$, and

$$ks_x = \omega_q\omega_r(\omega_q - \omega_r)$$

from which

$$\frac{\omega_q\omega_r(\omega_q - \omega_r)}{\omega_q\alpha_r} = \frac{ks_x}{ks_y}$$

$$\frac{\omega_r(10 - \omega_r)}{\alpha_r} = \frac{4}{4.625}$$

$$\omega_r(10 - \omega_r) = 0.865\alpha_r \quad [4]$$

If the fixed link should be horizontal

$$p_y = q_y + r_y - s_y = 0$$

or

$$\omega_s\alpha_r - \omega_r\alpha_s + \omega_q\alpha_s - \omega_s\alpha_q - \omega_q\alpha_r + \omega_r\alpha_q = 0$$

$$5\alpha_r - 10\omega_r + 100 - 10\alpha_r = 0$$

$$\alpha_r = 20 - 2\omega_r \quad [5]$$

Substituting this in Equation [4] we obtain a much simpler quadric equation than in the author's solution derived from Equation [11]

$$\omega_r^2 - 11.73\,\omega_r + 17.3 = 0$$

This equation has two roots; $\omega_r = 10$ rad/sec and $\omega_r = 1.73$ rad/sec. The first root gives $s_x = 0$, and does not satisfy the condition $s_x = 4$ in. The second root establishes the following solution

$$\alpha_r = 20 - 3.46 = 16.54 \text{ rad/sec}^2$$

The scale factor k may be found either from

$$k = \frac{\omega_q\alpha_r}{s_y} \quad \text{or} \quad k = \frac{\omega_q\omega_r(\omega_q - \omega_r)}{s_x}$$

and its value is $k = 35.77$.

Now the links are easily calculated

$$\left.\begin{aligned} q_x &= \frac{\omega_s\omega_r(\omega_s - \omega_r)}{k} = 0.79 \text{ in.} \\ q_y &= \frac{\omega_s\alpha_r - \omega_r\alpha_s}{k} = 1.828 \text{ in.} \end{aligned}\right\} \quad q = 1.992 \text{ in.}$$

$$\left.\begin{aligned} r_x &= \frac{\omega_q\omega_s(\omega_q - \omega_s)}{k} = 7.0 \text{ in.} \\ r_y &= \frac{\omega_q\alpha_s - \omega_s\alpha_q}{k} = 2.8 \text{ in.} \end{aligned}\right\} \quad r = 7.54 \text{ in}$$

$$p = q_x + r_x - s_x = 3.79 \text{ in.}$$

and the mechanism is shown in Fig. 1.

Small differences with the author's results are probably due to the inaccuracies in the establishment of the final form of Equation [11] with its six-figure coefficients.

Solution of Example 2. Given $p = 5$ in., $q = 2$ in., $\omega_q = 10$ rad/sec, $\alpha_q = 0$

$$s_y/s_x = 4/3, \quad \omega_s = 5 \text{ rad/sec}, \quad \alpha_s = 0$$

Find links r and s.

In the same way

$$ks_x = \omega_q\omega_r(\omega_q - \omega_r)$$

$$ks_y = \omega_q\alpha_r - \omega_r\alpha_q$$

from which

$$\frac{\omega_q\omega_r(\omega_q - \omega_r)}{\omega_q\alpha_r - \omega_r\alpha_q} = \frac{3}{4}$$

or

$$\alpha_r = \frac{4}{3}\omega_r(10 - \omega_r) \quad [6]$$

Further

$$p_x = q_x + r_x - s_x$$

$$p_y = q_y + r_y - s_y$$

which gives

$$kp_x = 250 - 5\omega_r(15 - \omega_r) \quad [7]$$

$$kp_y = -5\alpha_r i$$

and

$$k^2p^2 = 25[\omega_r(15 - \omega_r) - 50]^2 + 25\alpha_r^2 \quad [8]$$

similarly from Equation [1]

$$k^2q^2 = 25\omega_r^2(5 - \omega_r)^2 + 25\alpha_r^2 \quad [9]$$

Dividing Equation [8] by [9] and substituting α_r from Equation [6] we obtain an equation of the fourth degree for ω_r

$$\omega_r^2[25(5 - \omega_r)^2 + 37.3(10 - \omega_r)^2] - 4[\omega_r(15 - \omega_r) - 50]^2 = 0 \quad [10]$$

One root of this equation is $\omega_r = 1.18$ rad/sec.

Further, from Equation [6], $\alpha_r = 13.87$ rad/sec^2.

The scale factor is found from Equation [9] and its value $k = 36.45$. The lengths of the required links are now

$$\left.\begin{aligned} r_x &= \frac{\omega_q\omega_s(\omega_q - \omega_s)}{k} = 6.86 \text{ in.} \\ r_y &= \frac{\omega_q\alpha_s - \omega_s\alpha_q}{k} = 0 \end{aligned}\right\} \quad r = 6.86 \text{ in.}$$

$$\left.\begin{aligned} s_x &= \frac{\omega_q\omega_r(\omega_q - \omega_r)}{k} = 2.85 \text{ in.} \\ s_y &= \frac{\omega_q\alpha_r - \omega_r\alpha_q}{k} = 3.80 \text{ in.} \end{aligned}\right\} \quad s = 4.75 \text{ in.}$$

To check the solution, components of links q and p are calculated and their lengths determined:

$$\left.\begin{aligned} q_x &= \frac{5\omega_r(5-\omega_r)}{k} = 0.618 \text{ in.} \\ q_y &= \frac{5\alpha_r}{k} = 1.902 \text{ in.} \end{aligned}\right\} \quad q = 2 \text{ in.}$$

$$\left.\begin{aligned} p_x &= \frac{250 - 5\omega_r(15-\omega_r)}{k} = 4.62 \text{ in.} \\ p_y &= \frac{-5\alpha_r}{k} = -1.902 \text{ in.} \end{aligned}\right\} \quad p = 5 \text{ in.}$$

This mechanism shown in Fig. 2, however, differs from the two obtained by the author, but completely satisfies the prescribed conditions.

The solution of example 3 follows straightforward from Equations [1], [2], [3], and was given in the writer's reference (footnote 5 of the paper).

Comparing the two methods of solution, the reader has now the opportunity to decide for himself which treatment is simpler—the component method or the vectorial method developed by the writer.

However, the more solutions forthcoming for the same problem, the more popularity will be gained toward the ideas of synthesis and, therefore, this paper should be considered as a valuable contribution to the synthesis of mechanisms.

Author's Closure

Although, as far as I know, my paper was the first published attempt at solving problems of synthesis of mechanisms involving lengths of links, I did not intend my summary to imply that such problems could not be solved by vectorial methods.

I also have no intention of replacing the "elegance" of vectorial methods by "ordinary" Cartesian representation, but merely wish to put forward an alternative method which, in my experience, would prove more palatable to the engineering student or practicing engineer than one involving complex algebra.

So far as the two specific examples are concerned, Dr. Rosenauer, using the vectorial representation of links in complex form, completely misses the correct solution in each case.

Regarding example 1, Dr. Rosenauer asserts that the length of the fixed link p is not necessary for the determination of the mechanism, provided this link is assumed horizontal. He then proceeds with his calculations and arrives at some results which, being based on a different premise, naturally differ from mine. These differences Dr. Rosenauer attributes to my (probably) faulty arithmetic.

If Dr. Rosenauer's statement regarding the redundancy of the length of p were correct, there would exist only one mechanism which would satisfy the remaining prescribed conditions. That this is not so, and that there exists a different mechanism for every given length p should be obvious to anyone taking the trouble of reading my paper with care.

As a matter of interest, if p were changed from the originally prescribed value of 3.375 in. to 5 in., the following mechanism would be obtained: $q_x = 0.90$ in., $q_y = 1.95$ in.; $r_x = 8.10$ in., $r_y = 2.67$ in.; $s_x = 4$ in., $s_y = 4.625$ in. (This mechanism is not an enlarged version of the original mechanism, as link s has the same length in both cases.)

That Dr. Rosenauer was at all capable of obtaining a definite result without prescribing the length of p was due to the additional restriction of the—in this case—unwarranted assumption of a "scale factor," i.e., a magnifying factor having the same value for all links (and link projections) of the mechanism.

Regarding example 2, Dr. Rosenauer's assertion that his solution completely satisfies the prescribed conditions is incorrect.

I prescribed an angle $\phi_s = 53°8'$ ($\tan \phi_s = {}^4/_3$) between the fixed link p (which, in my method, is always coincident with the x-axis) and the driven link s, while in Dr. Rosenauer's solution the angle of 53°8′ is the angle between an x-axis, which has no *predetermined* positional relationship with the fixed link, and link s, and thus is completely irrelevant as regards the mechanism. As it happens, in Dr. Rosenauer's solution the angle between p and s is approximately 76°.

A Simple Procedure for Improved Accuracy in the Resistor-Network Solution of Laplace's and Poisson's Equation[1]

S. C. Redshaw.[2] The procedure described by the author does not appear to differ in any way from the well-known network described some years ago by Persico.[3] It is of interest to note that if a network with diagonal resistances is used to solve Poisson's equation, the leading error term depends on the type of function involved whether or not a worth-while reduction in the truncation error results.[4] The transformation from

$$\nabla^2 w = f(x,y)$$

to

$$\nabla^2 W = 0$$

where we define

$$u = W + w$$

does not avoid this difficulty.

It has been accepted, without dispute, that the use of diagonal resistances improves the accuracy of the network for the solution of Laplace's equation, and the extra resistors are easily installed for small networks with coarse mesh separations. However, a coarse net, even with diagonal resistances, is usually only of use for demonstration purposes and for problems which do not involve curved or awkwardly shaped boundaries. It is the writer's belief that it is better to adopt a simpler constructional technique,[5] either using a very fine mesh separation or a graded net,[6] thus avoiding time-consuming corrections at boundary points which do not coincide with mesh nodes.

Victor Paschkis.[7] The author's suggestion of diagonal resistors is very interesting and promising. The following re-

[1] By H. G. Landau, published in the March, 1957, issue of the Journal of Applied Mechanics, Trans. ASME, vol. 79, pp. 93–97.

[2] Professor of Civil Engineering, The University of Birmingham, Birmingham, England.

[3] "A New Resistor Network for the Integration of Laplace's Equation," by E. Persico, *Nuovo Cimento*, vol. 9, 1952, pp. 74–89.

[4] "Resistance-Network Analogues," by G. Liebmann, Journées Internationales du Calcul Analogique, Bruxelles, 1955, pp. 346–369.

[5] "A Resistance Network of Novel Construction for Solving Certain Problems in Elasticity," by S. C. Redshaw, Journées Internationales du Calcul Analogique, Bruxelles, 1955, pp. 406–409.

[6] "An Electrical Resistance Analogue With a Graded Mesh," by P. J. Palmer and S. C. Redshaw, *Journal of Scientific Instruments*, July, 1957.

[7] Technical Director, Heat and Mass Flow Analyzer Laboratory, Columbia University, New York, N. Y. Mem. ASME.

marks are made from the viewpoint of practical application of this method to a network study.

Consider separately the case of a pure resistor network and one in which capacitances or inductances are used in addition to resistances. Adding diagonal resistors always means doubling the number of resistances in a network. Consider now first a pure resistor network requiring a certain degree of accuracy for the result. The question must then be examined if a larger number of nodes without diagonal resistors or a smaller number of nodes with diagonal resistors requires less equipment. Since introduction of diagonal resistors doubles the necessary number of resistors as compared with a straight network, the use of diagonal resistors will be justified if they result for a certain magnitude of error in a reduction to at least one half of the required number of nodes.

However, the term magnitude of error still needs clarification. In the example given by the author one can give a certain figure as the "solution of the problem." But consider the case where a potential distribution in a body is to be determined by means of a network; although the potential at the individual nodes will be determined more accurately if diagonal resistors are used, the reduction of the number of nodes made possible by the use of diagonal resistors will make the drawing of isopotential lines more difficult. And this may reduce the usefulness of the diagonal resistors for such cases.

In the case of networks comprising other elements than resistors, conditions are somewhat different in two respects:

(*a*) The number of such other elements is reduced if the number of nodes can be reduced by introduction of diagonal resistors. This is often important even if the total magnitude of such additional equipment is not reduced; it may be easier to introduce 10 capacitances of 20 microfarads each than 20 capacitances of 10 microfarads each.

(*b*) Introduction of capacitances and/or inductances is considered mainly in connection with transient problems. Then the need often arises to change resistances and/or capacitances during a computation. Such change becomes quite difficult if at each node four instead of two resistances have to be changed. In such cases the use of the diagonal resistors may be much harder to justify than in the case of pure resistance networks.

These remarks are made purely from the viewpoint of practical experimentation with analogs and do not detract from the great significance of recognition of the relationships as explained by the author.

Author's Closure

I wish to thank Prof. Redshaw for calling attention to Persico's prior publication of the diagonal resistor network for Laplace's equation, which had been missed by myself and several other people with whom the subject was discussed. However, Persico did not mention the use of this network for Poisson's equation.

Prof. Redshaw's comments indicate that some of the points made in the paper on the use of diagonal resistors for Poisson's equation were not completely clear. It is certainly true that if a diagonal resistor network is used to solve Poisson's equation, the leading error term depends on the type of function involved. The nature of this dependence is given precisely by equation [20] of the paper, so there need never be any ambiguity. Also when the transformation

$$u = W + w$$

is used, w is a known function so that its value can be determined with zero error. The error in u is then simply the error in W resulting from the diagonal resistor network solution for W. Since W satisfies Laplsce's equation this error is of order h^4.

On page 94 of the paper it was stated that the diagonal resistors do not eliminate errors due to curved or irregular boundaries. Depending on the particular problem and on the accuracy needed, a graded net may be the most efficient procedure. In this case, also, diagonal resistors could be used in the interior of the region to give increased accuracy.

As to Prof. Paschkis' first point, if diagonal resistors are introduced and the number of nodes cut in half compared with the usual network, so as to require the same total number of resistors, then the accuracy of the solution will always be increased. This results from the fact that the error becomes of higher order in h.

In drawing isopotential curves, a simple procedure is to first interpolate numerically between nodal values to obtain the values at other points. Equation [8] of the paper could be used first to obtain interpolated values at the center point of each square of the net, and then Equation [6] to obtain values at the mid-points of the horizontal and vertical lines connecting nodes. This could be repeated if even more closely spaced values are desired. It is easy to see that if the solution is obtained on a coarse-mesh diagonal resistor network and intermediate values obtained by interpolation in this way, the resulting values will be more accurate than those from the usual network with a fine mesh.

Theoretical Criterion for Fracture of Metals Under Combined Alternating Stresses[1]

E. Orowan.[2] In the derivation of the fracture criterion no use has been made of the circumstance that the material, according to the title of the paper, is supposed to be under alternating stresses; the argument is based on the assumption of a steady stress throughout. It may be asked, therefore, why a criterion obtained on the assumption of a steady state of stress should be expected to apply to fatigue fracture.

Down to Equation [6], the consideration refers to a single crystal subjected to a special type of uniaxial tension (the projection of the direction of tension upon the active slip plane is assumed to be parallel to the slip direction). After Equation [6], for no obvious reason, the conclusions are assumed to apply to polycrystalline metals under states of combined stress. Could the author give some justification for this?

Equations [6] and [11] are stated to represent envelopes of Mohr stress circles. But the normal stress $\sigma_{\varphi_m} + \pi/2$ and the shear stress τ_{φ_m} which occur in these equations are not variable stresses in planes of variable orientation; they are material constants. $\sigma_{\varphi_m} + \pi/2$ is the tensile stress in the plane normal to the slip direction, and τ_{φ_m} the shear stress in the slip plane resolved in the slip direction, in the single crystal of the most unfavorable orientation with respect to a uniaxial tension, at the moment when the theoretical fracture stress is reached in it at an obstacle to slip. Thus Equations [6] and [11] cannot represent Mohr envelopes for the reason that they do not contain the necessary variables σ and τ. Yet the author's fracture criterion seems to rest on the assumption that these equations contain the variables σ and τ, and are envelopes of certain Mohr circles.

Author's Closure

The author is very grateful to Professor Orowan for raising three points which should have been included in the paper.

[1] By Takeo Yokobori, published in the March, 1957, issue of the Journal of Applied Mechanics, Trans. ASME, vol. 79, pp. 77–80.

[2] Massachusetts Institute of Technology, Cambridge, Mass.

The first question concerns the mechanism of fatigue. Although experimental studies have done much to clarify the micromechanism of fatigue damage in its early stages, mechanism of fatigue seems to be not yet well understood. Many dislocation models for fatigue fracture have been introduced, such as piling-up mechanism, taking into account the notch effect by the obstacle itself[3] proposed in this article; mechanism due to vacancies formation,[4,5] or mechanism by polygonization.[6] All of them seem to be able to explain the same phenomenon of fatigue fracture. The problem is to obtain a unique mechanism from among them or one not yet proposed, by comprehensive understanding of the characteristic experimental evidences.

The object of this article is to find a clue to get a unique dislocation model of fatigue fracture by checking the agreement with experimental data of the conclusion derived on a basis of dislocations piling-up mechanism, taking into account the notch effect by the obstacle itself. The present article concerns only the "stress condition for fatigue fracture; that is, failure at relatively later stage among the whole fatigue process consisting of several different stages." As for the difference from the case of static (unidirectional) stress or a steady state of stress, it is assumed that under alternating stresses some dislocations are also in cyclic motion, and they are pushed and piled up cyclically against certain obstacles, such as inclusions during forward and backward movements.

If the theory proposed is valid, the value of q_1 obtained by fitting the present theory to the data should be considerably large as shown in Table 1. On the other hand, in static (ductile) fracture, q_1 at the moment of initiation of fracture may be supposed to be not so large. In that, the theory may be regarded as not suitable for fracture at a steady state of stress, but for fatigue fracture. The reason is not yet theoretically explained why q_1 should be so large in fatigue fracture. In our experience, the specimen which was subjected to cyclic stress by rotating uniform bending tester until just before rupture of the whole cross section, and in which fatigue crack propagated to a considerable part of the cross section, will survive longer or even permanently, when the machines are stopped; that is, the same "constant" and not "alternating" stress is applied as the previously applied stress amplitude. Besides, in the static test the specimen shows as high strength as that of the specimen which has not been subjected to cyclic stressing. This fact may be related to the problem mentioned above, but also seems to have not yet been explained in any theory of fatigue.

The tentative explanation for these problems may be as follows: The binding force on the interface between the referred obstacle and matrix gradually decreases, or submicroscopic crack initiates on the interface during cyclic stress. Even in the case of static test of the specimen after being subjected to the severe cyclic stress until the initiation of large crack and just before rupture, the stress concentration by the piling-up dislocations will initiate the operation of other Frank-Read sources in the adjacent region successively until many more dislocations pile up against grain boundary so that ductile fracture occurs and the strength does not decrease. At any rate, the fact seems to be a most fundamental problem in fatigue.

To the second question, justification may be given as follows. In this article the condition is required that the "maximum" value of the left-hand side of Equation [6] is equal to the theoretical fracture stress (the right-hand side of Equation [6]). Since the shear stress component in the slip direction on the active slip plane is maximum when the projection of the direction of tension on the active slip plane is parallel to the slip direction, then the type of uniaxial tension assumed in the paper is not special, but has generality. In polycrystalline metals it is assumed that they consist of randomly oriented single crystals; that the referred obstacles or inclusions are also randomly oriented in them; and that the fracture stresses of polycrystalline metals are equal to the stress for initiating the crack in one of aggregates, i.e., a single crystal among them. Therefore, in polycrystalline metals, Equations [2] to [11] can be obtained by assuming φ as the angle between the slip direction of a single crystal and the applied tension axis, or as the angle between the certain sectional plane of the specimen and the applied tension axis, Fig. 1.

To the last question, the envelopes were determined graphically by Mohr stress circles obtained from experimental data[7] under combined stresses. Hence, as envelopes, the author really used

$$q_1\sigma_{\varphi+\pi/2} + c_0q_2^2\tau_\varphi^2 = \alpha E \quad \ldots\ldots\ldots\ldots [6']$$

or

$$q_1\sigma_{\varphi+\pi/2} + \bar{n}q_1\tau_\varphi = \alpha E \quad \ldots\ldots\ldots\ldots [11']$$

In the original paper, as envelopes Equations [6'] and [11'] should have been added, substituting $\sigma_{\varphi+\pi/2}$ and τ_φ for $\sigma_{\varphi_m+\pi/2}$ and τ_{φ_m}, respectively, in Equations [6] and [11], instead of writing the same formula for fracture condition. The author regrets they were omitted when making the article as brief and concise as possible, although they were included in the orginal manuscript. Nevertheless, the conclusions are not affected at all, since envelopes were actually graphically determined, as mentioned above.

[3] "The Theory of Fatigue Fracture of Metals," by Takeo Yokobori, *Journal of Physical Society of Japan*, vol. 10, 1955, p. 368.

[4] "Über den Mechanismus der Zerstörung bei der zyklischen Belastung von Metallen," von I. A. Oding, Colloquium on Fatigue, IUTAM, 1956, p. 178.

[5] "Theories of Fracture in Metals," by N. F. Mott, Deformation and Flow of Solids, IUTAM, 1956, p. 53.

[6] "Dislocations and Mechanical Properties," by E. Orowan, Dislocations in Metals, AIME, 1954, pp. 191–192.

[7] "The Strength of Metal Under Combined Alternating Bending and Torsion (in Japanese)," by T. Nishihara and M. Kawamoto, Transactions of the Japan Society of Mechanical Engineers, vol. 6, 1940, p. 8; vol. 7, 1941, p. 85.

Dependence of Frequency Spectrum of a Circular Disk on Poisson's Ratio[1]

H. Deresiewicz[2] and R. D. Mindlin.[3] We understand that the author has at hand the results of measurements of frequencies of flexural vibration of thick disks. It would be interesting to see the data displayed along with the results computed according to the classical theory of thin plates and those computed from the solution of the equations which include the effects of rotatory inertia and shear deformation.

Also, we should like to call attention to the fact that the functions $xJ_0(x)/J_1(x)$ and $xI_0(x)/I_1(x)$, which appear in the paper and in many other problems set in cylindrical co-ordinates, are special cases of functions which have been studied recently by M. Onoe.[4]

[1] By R. L. Sharma, published in the March, 1957, issue of the Journal of Applied Mechanics, Trans. ASME, vol. 79, pp. 53–54.

[2] Associate Professor of Mechanical Engineering, Pupin Laboratory, Columbia University, New York, N. Y. Assoc. Mem. ASME

[3] Professor of Civil Engineering, Columbia University, New York N. Y. Mem. ASME.

[4] "Formulae and Tables of the Modified Quotients of Cylinder Functions," by M. Onoe, The Institute of Industrial Science, University of Tokyo, vol. 4, 1955, Report No. 32.

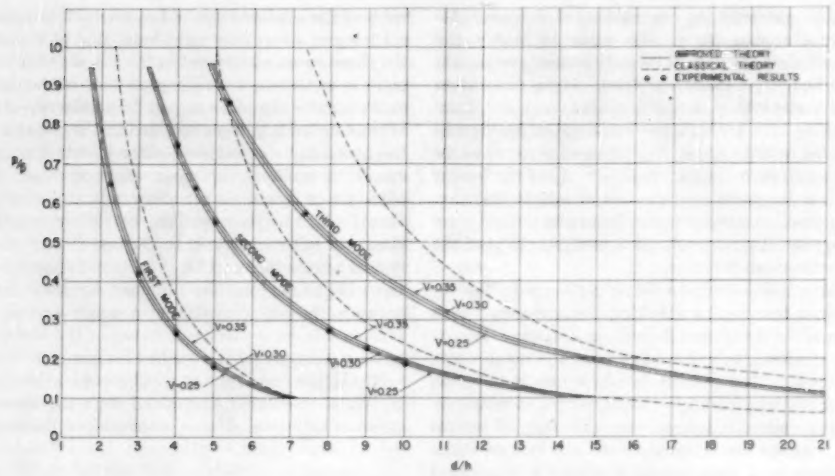

Fig. 1 Comparison between experimental results, computed results due to improved theory of finite disks, and computed results due to theory of thin disks. (d/h) = ratio of diameter to thickness; p/p = ratio of resonant frequency to frequency of pure thickness shear vibration of an infinite plate of thickness h.)

Author's Closure

In the course of the past five years, a great many measured data regarding actual resonant frequencies of thick circular disks vibrating in the axially symmetric flexural modes have been obtained. However, these data concern only the range of p/p and d/h ratios which are of interest from the design considerations of mechanical filters. We have in Fig. 1 the measured data displayed along with the results computed according to the classical theory of thin plates and those computed from the solutions of equations which include the effects of rotatory inertia and shear deformation, for three significant values of Poisson's ratios.

A quick chock will show a great deal of agreement between experiment and improved theory. A closer examination, however, will show that the measured points fall closer to the case $\nu = 0.3$, for p/p values ranging from 0.4 to 0.6. A slight but rather well-defined discrepancy at other regions could be due either to variations in elastic constants of Ni Span C[3] or some other unaccountable causes or both.

The author is thankful to Dr. H. Deresiewicz and Dr. R. D. Mindlin for calling his attention to a very interesting paper by M. Onoe.

Head Loss in Flow Through a Cyclone Dust Separator or Vortex Chamber[1]

Fred Landis.[2] The authors are to be complimented on a simple analysis of the head loss through a vortex chamber which leads to satisfactory predictions under many practical flow conditions.

The analysis is based on frictionless, irrotational flow, and the paper briefly mentions the deviations that should occur if a real fluid is being considered. However, there are several aspects in the flow of the real fluid which may affect the results materially, and which have not been discussed by the authors.

The paper indicates that the solid-body vortex core has a diameter corresponding to 60 per cent of the exhaust-pipe diameter. Experiments in vortex (Hilsch) tubes indicate that the size of the solid core is a very sensitive function of the geometry and, hence, the core size may vary somewhat with the vortex chamber and exhaust-pipe geometry. This may account for some of the deviations between experimental data and analysis.

A more marked contribution may be expected from the effects of secondary vorticity. Since the axial component of the flow is downward in the chamber and upward in the center section, this turning of the flow combined with the rotational behavior caused by the side-wall friction effects must induce secondary circulation. This circulation will impose additional head losses because of the kinetic energy associated with the additional superposed swirling motion. However, it is quite possible that the reduction in head loss anticipated for the flow of a real fluid with wall friction approximately balances the increase caused by secondary circulation.

A study of the flow behavior of a real fluid in a vortex chamber which includes the effects of wall shear, solid-body rotation, and secondary circulation would be a welcome extension of the present paper.

J. Le Conte Smith, Jr.[3] There are several assumptions in the potential-flow analysis as presented, which may be examined profitably. The first is the assumption that the average angular momentum over the inlet is equal to the angular momentum in the vortex. This will be true only when the inlet is one continuous logarithmic spiral, and the incoming fluid has uniform angular momentum. In the normal separator, a stream of straight flowing fluid is brought directly into the separator. The angular momentum then might be increased or decreased dependent upon the nature of the asymmetry of the transformation from linear to vortex flow.

[3] Commercial name of a constant modulus alloy consisting of nickel (42 per cent), chromium (5.2 per cent), titanium (2.3 per cent), iron (48.2 per cent), and impurities (1.3 per cent).

[1] By H. E. Weber and J. H. Keenan, published in the March, 1957, issue of the Journal of Applied Mechanics, Trans. ASME, vol. 79, pp. 16–21.

[2] Associate Professor of Mechanical Engineering, New York University, New York, N. Y. Assoc. Mem. ASME.

[3] Massachusetts Institute of Technology, Cambridge, Mass.

Indeed, it seems possible to conclude that, for the separator with the outer inlet wall tangent to a circular chamber, the interaction of the vortex with the straight incoming flow will cause a contraction and hence an increase in velocity. This contraction was demonstrated by plotting the streamlines of a potential-flow two-dimensional inlet with the aid of an electrical analog field plotter. For the one case considered, the average angular momentum of the vortex was 1.6 times the average angular momentum of the parallel flow. It has been reported[4] that the angular momentum in the vortex, under some circumstances, may be 1.4 times the average inlet angular momentum. This may explain partially why some experimental values of head loss were found greater than the theoretical value.

In this paper, the general plan of the exit separation was taken to be the same as for the flow without swirl, and the free streamline was adjusted to account for the swirl. It seems that a better approximation under some conditions might be obtained by assuming that the flow also separates down the center so that the outflow is a hollow cylinder. Indeed this center separation would be quite obvious if the fluid were liquid discharging into air. In fact, the separation would penetrate to the bottom of the chamber. If the fluid were air discharging into air, the center separation would be the center core which rotates with constant angular velocity because of friction. The center separation also eliminates the unrealistic singularity in v and p at zero radius.

Authors' Closure

The authors wish to thank Professor Landis and Mr. Smith for their discussion of the paper.

Professor Landis has shown that the entire problem of real fluid flow in a vortex chamber is extremely complicated. Evaluation of separate portions of the problem may be the most fruitful.

Mr. Smith has a very valid point regarding the increase of angular momentum possible in the asymmetric flow entering the cyclone. The other effect of flow separation in the center of the vortex actually appears as an inflow of gas at the center with a large axial outflow near the exhaust pipe walls. The latter phenomenon is especially noticeable as the diameter of the exhaust pipe is increased, and would also lead to an increased head loss. In Fig. 4 of the paper the head loss does increase over the theoretical as the exhaust-pipe diameter increases.

Corrections for the Oscillating-Disk Viscometer[1]

F. G. Keyes.[2] The desire to measure the viscosity of fluids has led to the employment of essentially two principal devices based on the measurement of the volume flow in a known interval of time under a measured constant pressure difference through a tube held at constant temperature, and the damping at constant temperature and pressure of a suspended oscillation geometric form in the fluid relative to the oscillatory properties of the identical system in a vacuum. The necessary observations can be carried out with greatest ease of control and compactness of equipment in the case of the oscillating-disk viscometer. However, the development of the relevant theory required to deduce the viscosity exactly for the latter type of viscometer, as the authors indicate in the present and earlier publications, has a long and somewhat painful history. The authors show in detail in the present paper how the theory may be advanced to yield accurate viscosity values to better than 1 part in 500.

The growth of the theory of the effects in evidence when fluids are in motion, or bodies are moving at velocity in fluids, has emphasized the practical importance of accurate values for the viscosity of fluids. The viscosity is a function of both pressure and temperature, and the oscillating-disk viscometer is markedly convenient for investigating the pressure effect.

It is a fortunate circumstance that the authors combine the competence and insight required for the advance of the theory with skill in the arts of experimentation. Their work goes far to raise the oscillating-disk viscometer to the class of instruments providing absolute values. There remains at this time, however, the task of verifying by independent means the pressure dependence of the viscosity of nitrogen which, for calibration, depends solely on the excellently consistent results of Michels and Gibson reported 25 years ago.

Authors' Closure

We owe thanks to Professor F. G. Keyes for his amplifying remarks on the substance of the paper. Although it is true that it is necessary to verify by independent means the pressure effect on the viscosity of nitrogen, it should be realized that the close agreement obtained for several gases provides such an indirect proof. It is possible to take the view that the instrument had been calibrated by another gas, in which case the pressure effect on the viscosity of nitrogen would have been derived from it.

Effect of Stress on Creep at High Temperatures[1]

C. D. Starr.[2] The authors are to be congratulated for continuing this fundamental research program to elucidate the basic mechanism for creep. The previous papers by the authors on the relation between temperature and time have demonstrated the applicability of their functional relationship to calculate and correlate the creep strain for the same applied stress.

The effect of stress on the creep behavior is more difficult to evaluate. For example, the structure parameter S' in Equation [5] must continually change in order to yield the shape of the creep curve obtained experimentally. Thus, in order to study the effect of stress on the creep rate, the authors point out that the comparison must be made under conditions where the structure is identical. Accordingly, their correlation in Figs. 2 and 3 was made by evaluating the initial creep-rate data shown in Figs. 1 and 10. Under these conditions identical structures are evaluated; namely, the structure of the annealed alloy. Presumably, under other conditions, different structures would be obtained and simple correlations of the σ^n type would be invalid.

The writer would like to point out, however, that the data in Fig. 1 correlate equally well when the strain-time data for the linear portion (major portion) of the curves are used. In fact, as close as he can ascertain, the same exponent n that the authors evaluated from the initial creep rate is obtained. Since some

[4] "Study on the Cyclones," by Iinoya, Memoirs of the Faculty of Engineering, Nagoya University, vol. 5, 1953, p. 153.

[1] By J. Kestin and H. E. Wang, published in the June, 1957, issue of the Journal of Applied Mechanics, Trans. ASME, vol. 79, pp. 197–206.

[2] Professor Emeritus—Lecturer, Massachusetts Institute of Technology, Cambridge, Mass. Mem. ASME.

[1] By H. Laks, C. D. Wiseman, O. D. Sherby, and J. E. Dorn, published in the June, 1957, issue of the Journal of Applied Mechanics, Trans. ASME, vol. 79, pp. 207–213.

[2] Chief Research Metallurgist, Wilbur B. Driver Company, Newark, N. J.

structural changes have occurred as evidenced by the change in the shape of the creep curves, this might imply that in the case of high-temperature creep at fairly low stresses, the structure is essentially independent of past history.

Now it has been observed in many commercial alloys that the creep curves obtained at a series of stresses at constant temperature form a homologous series. For example, Tapsell, Forrest, and Tremain[3] tested 0.26 per cent C steel at 400 C, used a stress from 8 to 19 tons/sq in., and found excellent correlation with an equation of the form

$$\epsilon = A\sigma^n \quad [1]$$

where ϵ is the creep strain, σ the applied stress, and A and n are constants.

Again, numerous data, too numerous to be fortuitous, have shown that the effect of stress on the so-called secondary creep rate can be given by the expression

$$\dot{\epsilon}_s = A\sigma^n$$

where $\dot{\epsilon}_s$ is the secondary creep rate.

Since this relationship applies to pure metals and alloys as well as to commercial materials, it appears somewhat general. In view of this, would the authors care to comment on the reasons that might give such correlation? Does it imply that in many commercial alloys the changes in structure even at high stresses and low temperatures are fairly insensitive to past history?

Authors' Closure

The authors wish to express their appreciation to Dr. Dean Starr for his contributions to their paper and for the opportunity he has given them to discuss the stress laws for high-temperature creep in greater detail.

Inasmuch as the stresses that were used in this investigation were quite small, no initial plastic strains were obtained upon applying the stress. Consequently, the initial structure and the initial creep rate that were recorded pertain to the annealed structure. It is true, as shown in Fig. 1 of the paper, that the creep rates for the low stresses did not change appreciably during the course of creep. These observations reveal that only minor insignificant changes in structure accompanied the course of creep in these tests. Consequently, about the same stress law should be obtained over the entire range of conditions that were investigated, as pointed out by Dr. Starr. However, as documented in References (5), (7), and (8) in the paper, this is not generally true. For creep under higher stresses, major structural changes occur as evidenced by the transition from higher primary creep rates to slower secondary creep rates for a given stress. Dorn and Shepard ("What We Need to Know About Creep," ASTM Special Technical Publication No. 165, 1954, pp. 3–30) have clearly shown that, in general, the structural changes attending high temperature creep depend on the stress. The secondary creep rate measured for each stress depends not only on the stress but also on the previous strain history at that stress. Under these conditions it is totally inappropriate to ascribe the changes in the secondary creep rates to the stresses alone. But the structures obtained at the secondary creep rates are functions of the applied stress. And for this reason there is a systematic change in the secondary creep rate with stress as determined by the systematic change in structure with stress as well as that due to the instantaneous stress per se. This effect of precreep history becomes very important in problems where the creep stress is continually changing during the course of creep.

[3] "Creep Due to Fluctuating Stresses at Elevated Temperatures," by H. J. Tapsell, P. G. Forrest, and G. R. Tremain, *Engineering*, vol. 170, August 25, 1950, pp. 189–191.

A Theory of Adhesive Scarf Joints[1]

A. G. H. Dietz.[2] The analysis of stresses in adhesive joints is inherently complex and uncertain because of the interactions of adhesive and adherend coupled with geometry of the joint. Because of the increasing use of adhesives in critical load-bearing structures the problem is becoming a pressing one. The author has performed a valuable service in carrying out the present analysis. His simplifications and approximations are evidently permissible on the basis of the satisfactory correspondence between his predicted values and those obtained by test. It is true that the geometry of the joint analyzed makes the analysis highly insensitive to relatively large variations in the moduli of the adhesives. This points up the desirability of designing engineering joints so that the large variations commonly found in the mechanical constants of adhesives have relatively little effect on their behavior when under stress.

Author's Closure

The author wishes to thank Professor Dietz for his interest in the paper under discussion. No further comment would seem to be required at this point.

Theoretical Analysis of Viscous Flow in Narrowly Spaced Radial Diffuser[1]

W. G. Cornell.[2] The author is to be congratulated on an interesting paper. The analysis assumes flow symmetrical about the channel center line. Asymmetrical flow may occur under certain conditions. A related case is the two-dimensional radial flow between two divergent plane walls, studied by Hamel,[3] solving exactly the Navier-Stokes' equations of fluid motion, for the more general case of laminar flow between logarithmic-spiral walls. A single solution is found for low values of the total amount of fluid flowing. Above a certain critical value of flow, separation occurs and three possible solutions are found: a symmetrical solution with backflow at both walls, and two asymmetrical solutions with backflow at one of the walls. Although the two configurations are not the same, Hamel's results suggest the possibility of flow asymmetry in the separated case of the present configuration.

Artur Mager.[4] This paper analyzing the viscous flow in a narrow radial diffuser represents an important addition to the already large boundary-layer literature. The value of it lies not in the particular example here considered, but in the interesting technique for computation of cases where the boundary-layer flow, as such, determines the appropriate pressure gradient, which in turn affects the boundary-layer development.

As we have seen, the technique, suggested by the author, consists of solving directly the momentum integral equations, not in the usual manner, for the pertinent boundary-layer quantities,

[1] By J. L. Lubkin, published in the June, 1957, issue of the Journal of Applied Mechanics, Trans. ASME, vol. 79, pp. 255–260.

[2] Professor, Civil Engineering Department, Massachusetts Institute of Technology, Cambridge, Mass. Mem. ASME.

[1] By H. W. Woolard, published in the March, 1957, issue of the Journal of Applied Mechanics, Trans. ASME, vol. 79, pp. 9–15.

[2] Engineering Consultant—Aerodynamics, Systems Analysis Section, General Electric Company, Cincinnati, Ohio. Mem. ASME.

[3] "Spiralfoermige Bewegungen zaeher Fluessigkeiten," by G. Hamel, *Jahresbericht der Deutschen Mathematiker-Vereinigung*, vol. 25, 1916.

[4] Research Scientist, Marquardt Aircraft Company, Van Nuys, Calif.

but for the "external" velocity, which is not known in this case. It is clear that such a solution is possible, only because in a diffuser with a known mass flow and an assumed velocity profile, a unique relation exists between the boundary-layer thickness, the width of the passage, and the "external" velocity.

The idea is therefore basically sound; however, the writer feels that the actual procedure, while showing a considerable insight into the problem, is somewhat involved and wonders whether rather drastic simplifications in the method could not be made. For instance, it is noted that the necessity for discerning between the inlet and filled regions occurs only due to the (rather shaky) assumption that in the inlet region the form of the velocity profile remains unchanged. If the velocity profiles were allowed to vary right from the start (as it probably actually happens), then the same procedure would be applicable in the whole diffuser. Consequently, only one differential equation would have to be solved, eliminating automatically any need for matching. Such a procedure would not necessarily have to do away with the integral method of solution, one could probably adapt the Thwaites approach, which ties directly, through a well grounded semi-empirical relation, the three important boundary-layer quantities; namely, the shear at the wall, the form factor H, and the pressure gradient.

As another alternative to this procedure, one probably could have devised also an honest perturbation system, with the zeroth-order terms being given by, say, the hydraulic method, and the higher-order terms accounting for the corresponding boundary-layer flow and its displacement effect on the actual area change.

In addition to these rather general comments on the method of approach, the writer also notes that it would be highly desirable to incorporate the possible asymmetry of the boundary-layer growth in the future solutions of this problem. With the present trend toward high-speed flight, the intake diffusers will surely become very narrowly spaced, and the method should be of great interest there. The boundary-layer growth in such diffusers is usually quite different on each of the walls.

In closing, the author is to be congratulated on the important work which he has done already in connection with this problem, and it is hoped that he will continue it along the lines here suggested.

THEODOR RANOV.[5] The author's analytical attack on the radial-diffuser problem is probably one of the first serious attempts to apply the methods of modern boundary-layer theory to what is essentially a hydraulic-type problem. As such, his research and its results merit special attention because they are an excellent sample of a deliberate disregard of whatever artificial boundaries may have existed between aerodynamics and any of the other sister branches of fluid mechanics. Or, to put it differently, this paper is added evidence of the constant progress toward using the unifying treatment of fluid dynamics in all the branches of mechanics concerned with fluid flow. Perhaps equally important from the special viewpoint of the fluid dynamicist is the fact that the author's analysis falls into the sparsely populated class of solutions of the Navier-Stokes equations which consider simultaneously both viscous and inertia forces. The mathematical difficulties which arise from this challenging undertaking are evident from the paper, but, fortunately, are not discouraging since the problem is solved once and for all in dimensionless form, subject, of course, to the limitations and necessary approximations that were made. Even so, the amount of computational labor is formidable.

The flow described here as taking place in a narrowly spaced radial diffuser has many existing and numerous potential applications to a variety of flow-control problems. In particular, when considering the configuration designated in the paper as "double-disk valve element," it has become apparent as a result of the research by Mohn, Woolard, and Paivanas, that a great deal of additional work is required before some of the unexpectedly complex features of the problem can be given satisfactory explanations. As early as 1951, the University of Buffalo School of Engineering continued Mohn's work by initiating a research program which eventually led to the author's and Paivanas' master's theses. Both these projects are being actively continued, partly under the sponsorship of the Graduate School of Arts and Sciences of the University of Buffalo. A paper which will present the results of Mr. Paivanas' experimental study of the flow of air in a radial diffuser is in preparation.

The comparison of the author's theoretical results with Mohn's experiments must be viewed in the light of the considerable difference between the assumed geometrical configuration and the actual entrance region to the double-disk valve element. It is, therefore, not surprising that the agreement is apparently not overwhelmingly good. If the fact is taken into account that the change in direction of the fluid velocity at the sharp entrance corner violently contracts the flow, and modifies and distorts the flow pattern throughout the entire disk space, the approximate theory offered here by the author appears to be a satisfactory description of the flow over a sizable portion of the radial distance. The fact that it does not attempt to describe the flow in the entrance region to the disk-valve element is perhaps the chief shortcoming of the theory. It is, of course, obvious that the limitations imposed by the severe boundary conditions at the entrance to the disk space make it virtually impossible to consider anything but a separated, discontinuous flow, with a quasi-free boundary immediately downstream of the entrance corner. Whether or not an analytical solution of such a flow case is possible, remains to be seen. However, it is already clear that it involves cavitation in the case of liquids, and shock-wave problems in the case of gases. It is hoped that the current strong interest in this old, but fascinating flow case, will result in further equally significant contributions to our understanding of an important phenomenon.

AUTHOR'S CLOSURE

The author would like to thank Mr. Cornell and Drs. Mager and Ranov for their interesting comments and suggestions.

In reply to Mr. Cornell's comment, if one assumes $u = cf(y)/r$, and $v = w = 0$, a solution for laminar-viscous radial-diffuser flow, analogous to Hamel's solution for two-dimensional diffuser flow, can be formulated. The author tried this method of approach and found solutions in terms of elliptic integrals. These solutions are, however, for widely spaced radial diffusers, i.e., diffusers in which the "external" velocity is uninfluenced by the boundary-layer development, rather than for the narrowly spaced ones treated in the author's paper. The required numerical evaluations have not been completed, but it is apparent that three types of separated flow are possible: a symmetrical flow with reverse flow at both walls, and two asymmetrical flows with reverse flow at both walls.

This is an interesting aspect of the radial diffuser problem which the author hopes to investigate further at a later date.

As Dr. Mager suggests, the Thwaites method can be adapted to the present problem. However, the universality of the Thwaites $l(m)$ and $H(m)$ functions for the positive pressure gradient experienced in the narrowly spaced radial diffuser appears questionable, especially near separation. The linearization process further aggravates the uncertainty of this method of approach, since in essence it requires that the shape parameter H be represented as a linear function of m—an obviously poor approxima-

[5] Professor of Engineering, University of Buffalo, Buffalo, N. Y. Mem. ASME.

tion near separation. The author has not carried out the details of the Thwaites approach and prefers to defer critical discussion until this is done. He also hopes to take a fresh look at the problem in the near future, at which time the perturbation approach and the asymmetric boundary-layer growth suggested by Dr. Mager will be investigated.

It is gratifying to know that the University of Buffalo is continuing its investigations of the many interesting and complex features of the flow in a "double-disk valve element."

Admittedly, the author dealt only with one simplified aspect (relatively speaking) of the more complicated general flow problem. This is, however, the natural step-by-step process of progressing to an understanding of the more complex flow phenomena. It would be very satisfying if the University of Buffalo, as a part of its pioneering efforts in the field, could conduct tests simulating the author's idealized model.

The author would like to correct some errors which appeared in his paper. It should be noted that Equations [13], [14], [17], [18], and [19] are different in the preprint (ASME Paper no. 56—A-18) and in the version published in the JOURNAL OF APPLIED MECHANICS for March, 1957. Except for the case of a constant gap h, the foregoing equations are in error in the JOURNAL, whereas they are correct in the preprint if the nondimensional boundary-layer thickness is defined therein as $\delta^* = 2\delta/h_i$.

The correct forms of the subject equations, for $\delta^* = 2\delta/h_i$, are given below:

$$[2K_0^2(\vartheta - 1)\Lambda^2 U^*\delta^{*2} - K_0(\vartheta - 1)k\Lambda\delta^* + K_0^2\Lambda^2 h^* U^*\delta^*]dU^*/d\Lambda + [K_0^2(\vartheta - 1)\Lambda]U^{*2}\delta^{*2} + [K_0^2\Lambda^2 h^{*\prime} + K_0^2 h^*\Lambda - K_0(\vartheta - 1)\Lambda^2 h^{*\prime}]U^{*2}\delta^* - [K_0(\vartheta - 1)k]U^*\delta^* + 4a_L K_0^2(r_i/h_i)(\nu/U_i h_i)\Lambda^2 = 0 \quad [13]$$

$$\delta^* = (k/\Lambda U^* - h^*)/K_0 \quad [14]$$

$$g_1(\zeta) = \{(1 + \Gamma)\zeta^2 + [2(1 + \Gamma) - (1 + 2\Gamma)k]\zeta + [(1 + \Gamma) - (1 + 2\Gamma)k]\}h^* + \Gamma k^2 \quad [17]$$

$$g_2(\zeta) = 2(\zeta + 1)h^{*2} + 2(\zeta + 1)^2 h^* h^*_\zeta - k(\zeta + 1)h^*_\zeta - kh^* + (\zeta + 1)^2 K_2 \quad [18]$$

$$g_3(\zeta) = -(\zeta + 1)h^{*2} - (\zeta + 1)^2 h^* h^*_\zeta + k(\zeta + 1)h^*_\zeta + kh^* - (\zeta + 1)^2 K_2 \quad [19]$$

The numerical examples in the paper are not influenced by these errors.

It should be noted also that K_0 is more clearly defined as $K_0 = (\vartheta_2 - 1)_L$.

Book Reviews

Analysis of Structures

THE ANALYSIS OF STRUCTURES. By N. J. Hoff. John Wiley & Sons, Inc., New York, N. Y., 1956. Cloth, 9¼ × 6¼ in., x and 493 pp., illus. $9.50

REVIEWED BY P. S. SYMONDS[1]

THIS book on the theory of structures treats the subject mainly from the point of view of the principle of virtual displacements and the theorems of minimum potential energy and minimum complementary energy. It is on a high level as far as structural concepts are concerned, being derived from lecture courses offered to first-year graduate students; mathematically, the level is much lower. Examples are chosen in roughly equal proportion from fields of civil and aeronautical structures.

The book consists of four parts, of which the first is devoted to an exposition of the principle of virtual work and a number of applications (e.g., a redundant space frame, continuous beams). This part includes several topics treated by more conventional methods; e.g., the moment-distribution and slope-deflection procedures for continuous beams and frames. The second part presents the theorem of minimum potential energy. Variational methods are then used to derive the equilibrium equations of beam columns and sandwich-type beams. The approximation techniques of Rayleigh-Ritz and Galerkin are illustrated. Part 3 of the book is concerned with problems of structural stability. The critical load is first discussed as one at which adjacent equilibrium configurations exist, and the differential equations of columns are derived by the minimum potential energy theorem. Illustrations of the Rayleigh-Timoshenko method are given, notably to buckling of thin-walled open-section columns. There is a discussion of the calculation of buckling loads of continuous frames by use of the convergence properties of the moment distribution procedure. Brief discussions of inelastic buckling and of residual stresses are given. The fourth part presents the theory of minimum complementary energy. Applications to problems of statically indeterminate structures include a discussion of stresses in a reinforced monocoque fuselage. There is also a brief but competent introduction to plastic limit-load analysis of beams and frames, mainly from the point of view of failure mechanisms. This would perhaps be improved by the addition of explicit statements of the upper and lower-bound theorems.

This reviewer was delighted with the philosophy and general plan of the book; he agrees with the author that the principle of virtual displacements is probably the most important tool available to the structural analyst. Various features of the book can be criticized. The treatment of mathematical details seems very uneven. The writer feels that the whole treatment of differentials and variations could be considerably clarified and simplified. He feels also that the full power of the principle of virtual displacements could have been displayed still more emphatically. On the one hand, more striking simple examples could have been given of the use of the principle to solve practical problems (for example, to obtain influence lines). Most of the problems discussed in terms of one or the other of the minimum energy theorems could have been treated to advantage directly in terms of the principle of virtual displacements. On the other hand, the power of the principle of virtual displacements as a tool in theoretical developments might have been further displayed by using the principle to prove Maxwell's reciprocal theorem, or the minimal theorems of limit analysis.

These comments aside, which merely represent one reader's personal preference, there is no doubt that the author deserves congratulations and thanks for a difficult and important job that has been extremely well done.

[1] Professor of Engineering, Brown University, Providence, R. I. Mem. ASME.

Thermodynamics and Statistical Mechanics

THERMODYNAMICS AND STATISTICAL MECHANICS. By A. H. Wilson. Cambridge University Press, Cambridge, England, 1957. Cloth, 10 × 7 in., xvi and 496 pp., illus. $9.50.

REVIEWED BY J. KESTIN[2]

THE great diversity of technical problems which come up for solution in modern industry has put a new emphasis on a thorough understanding of the foundations of the physical sciences on the part of contemporary engineers. The mental processes whereby solutions are sought and achieved become increasingly subtle, and what passed for "high-brow" and "long-haired" yesterday is taken in one's stride today. For this reason the gulf between theoretical physics and "down-to-earth," "practical" engineering is being filled. Even fifteen years ago a book of the scope of A. H. Wilson's "Thermodynamics and Statistical Mechanics" would have passed unnoticed by the professional engineering journals, but at the present time engineers cannot afford to ignore it.

The book contains a clear exposition of the subject matter mentioned in the title and is intended, in the words of the author, "mainly for theoretical physicists." The first four chapters deal with classical thermodynamics. They introduce the concept of temperature and the first two laws in a rigorous manner, backed by an interesting discussion of the most important alternative axiomatic formulations together with an exposition of their essential unity. The change in the internal energy of a system is defined as the amount of mechanical work required to make the body pass from its initial to its final state when the body is thermally insulated. Heat is defined as the sum of the change in internal energy and mechanical work done in any general process. The First Law then simply asserts that the internal energy of a system is a function of its state.

The Second Law is formulated by asserting the existence of two functions of state, the absolute thermodynamic temperature and entropy (Carnot's theorem). Its exposition is supported by a discussion of linear differential forms and Carathéodory's formulation.

A good deal of attention is devoted to the study of the thermodynamic functions ("potentials") and the reviewer notes with regret that the author still uses the now largely obsolete terminology. For example, enthalpy is referred to as the heat function, and the Helmholtz and Gibbs functions, respectively, are

[2] Professor of Engineering, Brown University, Providence, R. I.

given the rather clumsy names of "free energy at constant volume" and "free energy at constant pressure." A very useful and complete discussion of fundamental thermodynamic equations is given.

The main concepts of statistical mechanics are introduced in Chapter 5 using, as the author states, the language of quantum rather than of classical mechanics even when quantum effects are negligible. This leads to a great economy in exposition but presupposes a knowledge of quantum mechanics on the part of the reader, at least to the extent of being familiar with the eigenvalues of energy. Chapter 6 is devoted to the usual applications: To the study of the specific heats of gases, crystalline solids, Fermi-Dirac and Einstein-Bose statistics, and radiation. Chapter 7 takes up the study of the Third Law in Nernst's formulation. Chapter 8 deals with gas imperfections and ends with a discussion of the general theory of the equation of state from a statistical point of view.

The remaining chapters cover the following topics: the heterogeneous equilibrium of a single substance (Chapter 9); electric and magnetic phenomena (Chapter 10); gas mixtures and chemical reactions (Chapter 11); solutions (Chapter 12); solutions of electrolytes and electrochemical systems (Chapter 13); and the thermodynamic problems of rubber and superlattices in alloys as well as exact solutions of the one-dimensional order-disorder problem form the subject of the last chapter (Chapter 14).

The theory of "irreversible thermodynamics" is left out of account completely.

The book is provided with an adequate subject index and an authors' index.

The reviewer cannot help but admire the beautiful aesthetic form given to the book by the printers. The choice of format, type, and paper, even the dust cover, are exquisite and result in a book which it is a joy to read and a pleasure to own.

Gas Dynamics

GAS DYNAMICS. By Klaus Oswatitsch, translated from the German into English by G. Kuerti. Academic Press, Inc., New York, N. Y., 1956. Cloth, 9 × 6 in., xv and 610 pp., illus. $12.

REVIEWED BY ASCHER H. SHAPIRO[3]

THIS is an English translation of the German volume "Gasdynamik" published by Springer (Vienna) in 1952, and reviewed previously in this Journal (vol. 21, June 1954, p. 209). In the latter may be found set out, in considerable detail, the topics and subject matter of the book.

The English version is essentially the same as the original, except that the references have been brought up to date, and certain improvements in presentation have been effected. Dr. Oswatitsch gives credit for these to the translator, Prof. Kuerti.

The general spirit of the book is best conveyed by a passage from the author's preface:

"In this book the emphasis is on a clear and intuitively meaningful presentation of the physical and technical problems of gas dynamics, supplemented by the consideration of some of the fundamental experimental results. Although mathematical questions of absorbing interest do arise, mathematics serves here only as a means of formulation and of communication. Physical reasoning, physical results, and examples are introduced as soon as the topic permits it. Nevertheless, this book is not an engineering handbook, and the aeronautical engineer will rarely find the special problem that interests him worked out here. He will have to solve it himself or look for the solution among the references given, but he will find it helpful that the fundamental equations and the important formulas have been given in many different forms and are accompanied by tables and diagrams."

The distinctive contribution of Dr. Oswatitsch which will make this book of enduring value is the concise yet general manner in which he has synthesized the many aspects of gas dynamics—steady and unsteady one-dimensional flows; general theorems; exemplary exact solutions; subsonic, transonic, supersonic, and hypersonic flows; three-dimensional effects, steady and unsteady; viscous flows; and experimental techniques.

Conciseness combined with depth requires a considerable reliance on mathematical description. The meaty character of the resulting presentation makes for slow but nonetheless clear and interesting reading, at least for those who are reasonably fluent in mathematics. While not generally suitable as an introductory text, it will be one of the most useful treatises on the subject for the researcher and the advanced student.

There is no trace in the translation of the book ever having been written in anything but English, and Prof. Kuerti is to be commended for having taken the trouble to give us more than a literal translation.

Finally, the reviewer feels that thanks and congratulations are in order to the Academic Press for making accessible to the English-reading audience this admirable book.

Structural Analysis

THE PLASTIC METHODS OF STRUCTURAL ANALYSIS. By B. G. Neal. John Wiley & Sons, Inc., New York, N. Y., 1956. Cloth, 8¼ × 5¾ in., xi and 353 pp., illus. $7.50.

REVIEWED BY BRUCE G. JOHNSTON[4]

FROM his background of research at Cambridge and at Brown University the author has prepared (on a level suited for textbook use) the best work of its kind that has appeared to date. Printed in Great Britain, the book has been carefully prepared and is pleasing in typography.

Although much of the book is of direct interest to the design engineer who is interested in this rapidly developing field, the author does not make the mistake of putting the word "design" in the title. This is a book on analysis, with, however, adequate recognition of both the potentialities and limitations that are involved in applying analysis to design.

The first three chapters take up basic hypotheses, theorems, and simple illustrative examples of calculation of the collapse load of a continuous beam or frame. The static, kinematic, and uniqueness theorems are stated and applied in ample illustrative examples in the main body of the book. The formal proof of these theorems is included in Appendix C.

Chapter 4 discusses general methods for plastic design. More than average attention is paid to the subject of "Plastic Moment Distribution."

In Chapter 5 on "Estimates of Deflections" there is a review of experimental work covering both the stress-strain diagram of steel and actual tests of steel beams and frames, all correlated with various methods for estimating deflections at various levels up to collapse loads.

Chapter 6 provides a brief review of some of the factors that modify the development of the full plastic moment, including variations in yield stress, normal force, and shear. The practical design significance of these effects is discussed.

Chapter 7 is on the subject of "Minimum Weight Design," but the author cautions that "to assert that minimum weight is the only important criterion in design is to disregard the various

[3] Professor of Mechanical Engineering, Massachusetts Institute of Technology, Cambridge, Mass.

[4] Professor of Structural Engineering, University of Michigan, Ann Arbor, Mich.

other economic features which must always be considered." This is typical of the author's recognition of the practical limitations that are inherent in the design problem.

Chapter 8 on "Variable Repeated Loading" discusses not only incremental collapse and shakedown but the associated problem of fatigue under cyclic plastic loading. Relation both to experiment and design is discussed, and the author comes to an important practical conclusion where, on page 323, he states: "The conclusion can therefore be drawn that unless a design is governed by fatigue, recommended plastic design procedure, in which a specified load factor is provided against plastic collapse, will generally result in a structure which is far less likely to fail by incremental collapse for alternating plasticity than by plastic collapse under a single overload."

One of the noteworthy aspects of this book is the very complete review of both experimental and theoretical developments, starting with the initial work in Hungary by Kazinczy, more than 40 years ago, and culminating in the more recent and more complete series of investigations that have been carried out at Cambridge University in Great Britain and at Brown and Lehigh Universities in this country. There are an average of 25 references per chapter. These references, taken together with the commentary provided in the text, provide the research worker in this rapidly developing field one of the best bibliographic reviews that has currently been made available. The broad and impartial balance with which the author has selected his references is especially laudable since this field of development has been one in which similar books have sometimes tended to give the reader a distorted and limited background as to prior work in the field.

Each chapter is terminated by a number of appropriate examples for which answers are given at the end of the book.

Appendix B of the book provides the reader with tables of plastic moduli of British standard beams. The reader in this country will wish that a similar table of plastic moduli of American standard beam and wide flange shapes were included but he may take comfort in the fact that these will, in the very near future, be made available by the American Institute of Steel Construction.

Developments in plastic analysis and design are rapid, and one may expect important additions and changes when and if a second edition of the author's book or other books in the same field are published. For example, the very recent work of Ketter, which greatly simplifies the design of multispan gable frames, undoubtedly would have been mentioned in the present work had it been available in time.

Turbulent Shear Flow

THE STRUCTURE OF TURBULENT SHEAR FLOW. By A. A. Townsend. Cambridge Monographs on Mechanics and Applied Mathematics, Cambridge University Press, New York, N. Y., 1956. Cloth, 8½ × 5½ in., xii and 315 pp., illus. $7.50.

REVIEWED BY STANLEY CORRSIN[8]

THIS is a detailed monograph on the difficult problem of turbulent shear flow. Its central goal is to unify the rather diverse experimental information now available on turbulent shear flows by providing a connecting backbone of physical interpretation. Although not a well-organized deductive theory in the classical scientific sense, it is surprisingly successful in accounting for many of the important properties of a variety of shear flows. That Dr. Townsend regards his theory as preliminary, is indicated by the words in the preface stating that he intends to "provide targets for criticism instead of ammunition."

[8] Professor and Chairman, Mechanical Engineering Department, The Johns Hopkins University, Baltimore, Md.

The general organization of the book is indicated by its principal section headings: 1. Introduction; 2. The equations of motion in shear flow; 3. Flows without appreciable variation of mean velocity; 4. Uniform distortion of homogeneous turbulence; 5. Free turbulence: unrestricted shear flow; 6. Free Turbulence: Motion of the Large Eddies; 7. The Turbulent Wake; 8. Turbulent Jets; 9. Turbulent Flow in Pipes and Channels; 10. Boundary-layer flow without pressure gradient; 11. Boundary-layer flow in a pressure gradient; 12. Shear flow between rotating cylinders.

The first four sections present general background material. The fifth and sixth sections are preliminary to the seventh and eighth, and the final sections necessarily stand a little apart, although Dr. Townsend succeeds in presenting them with some logical connection to the free shear flows.

This is not intended to be a textbook, so the introductory material is confined largely to facts and conjectures which will be basic to the theoretical interpretation in the later parts of the book. In other words, there are a number of miscellaneous facts about turbulent shear flow which are omitted, presumably as not germane to the connected theoretical account in the present stage of its development.

In addition to Dr. Townsend's admirable attempt at a coherent theory of turbulent shear flows, the principal new contributions made by this book are the following: (*a*) The introduction of a mathematical form for an "eddy" which is spatially more limited than a Fourier component. (*b*) The introduction of a characteristic decay length, L_s, which turns out empirically to be of the same order as the integral scales, but which can be determined experimentally with less effort. (*c*) Some previously unpublished measurements on turbulence in a wake with no mean velocity gradient, hence no production of turbulent kinetic energy from the mean flow kinetic energy. (*d*) The introduction and use of an effective Reynolds number based upon "eddy viscosity" instead of actual viscosity (such a Reynolds number has been discussed informally by turbulence workers in the past, but this appears to be the first time it has actually been used in a published work); (*e*) The first logical analysis giving an estimate of the secondary flow that arises because of edge effects in turbulent shear zones that are almost two-dimensional.

The adverse comments that I have to make are primarily for the benefit of readers with little background in turbulence. They do not reduce the value of the monograph to active workers in the field.

In a number of places Dr. Townsend presents interesting conjectures (most of them probably correct) without labeling them clearly as conjectures, and without listing the underlying conditions or assumptions. Phrases such as "it can be shown" are not always supported with references or with hints as to the approach.

The presentation of explicit references both in the text and in the bibliography is uneven. For example, there seems to be no mention of A. N. Kolmogoroff, whose idea of "local isotropy" is basic. The Prandtl boundary-layer approximation is applied with no mention of Prandtl. No specific paper of Reynolds is referenced.

Some of these difficulties were apparently recognized by the author, since some warning is given in the preface, along with the mention of an understandable difference of opinion on specific matters of terminology.

This remarkable research monograph, though perhaps not a primer, is a necessity for any scientist or engineer who takes up the serious study of turbulence. It has certainly achieved Dr. Townsend's goal as stated in his preface, and should be the most authoritative book on turbulent shear flow for quite some time to come.

Dynamics of Machinery

DYNAMICS OF MACHINERY. By James B. Hartman. McGraw-Hill Book Company, Inc., New York, N. Y., 1956. Cloth, 9¼ × 6¼ in., xvi and 283 pp., illus. $7.50.

REVIEWED BY E. H. LEE[6]

THIS book is intended for advanced undergraduate and graduate students in mechanical engineering. It is designed to follow the usual first courses in mechanics and calculus, and to provide a transition to graduate courses in dynamics. The first 90 pages consist of a review and discussion of basic dynamic theory with solution of engineering problems. There follows a chapter of 37 pages on mechanical vibrations which is mostly for systems with one degree of freedom, but deals with two degrees of freedom, and also presents the Holzer method for certain systems with many degrees of freedom. There follows a chapter of 43 pages on balancing of machinery which in addition to the theory discusses modern automatic machines. A chapter of 42 pages on engine dynamics deals with the theory of reciprocating engines and torsional vibration analysis. The final chapters of 48 pages comprise mechanical transients with an introduction to the Laplace transform method, and the dynamics of automatic control systems, which discusses servomechanisms making use of the previous chapter. An appendix presents a group of problems which might arise in engineering analysis; and a bibliography broken down into topics, answers to selected problems, and an index complete the book.

The reviewer feels that the strongest aspect of the book is the discussion of current engineering problems. The discussion of basic theory appears to be cramped and in several instances definitely misleading. For example: "A system in which the force is a function of displacement only is obviously a conservative system." This is clearly incorrect and, in fact, the author develops the correct requirements for a system to be conservative shortly after this statement. In this section the reviewer found the emphasis on the influence of forces as regards the stress they induce in contrast to merely their effect on equilibrium or motion, with the associated freedom to modify their points of action, to be stimulating. It seems to the reviewer that if the author intends the student to get experience in using the Laplace transform method, he could, with profit, have introduced it before the next to the last chapter, and applied this type of analysis to the mechanical vibrations discussed earlier.

The reviewer feels that this book provides a valuable discussion of applications of dynamics in mechanical engineering and an introduction to automatic control analysis, but that it should be used in conjunction with a more thorough book on the basic theory.

Elasticity

ELASTICITY, FRACTURE, AND FLOW With Engineering and Geological Applications. By J. C. Jaeger. Methuen and Company, Ltd., London, England (John Wiley and Sons, Inc., New York, N. Y.), 1956. Cloth, 7½ × 5 in., viii and 152 pp., illus. $2.50.

REVIEWED BY WILLIAM R. OSGOOD[7]

THIS little book is admirably suited for self-study by nonspecialists in the theory of elasticity and the mechanical theories of flow and fracture. Only a knowledge of the strength of materials and no mathematics beyond the differential and integral calculus are required to read the book. Adequate general references to standard works are given. The only adverse criticism of the book worth mentioning is that relatively few specific references are given at points where they might be helpful; that is, when the author states that "it can be shown that" or "it is known that," he frequently does not refer the reader to a source which "shows" or from which it is "known."

The book consists of three chapters. The first chapter, Stress and Strain, begins with the conventional discussion of the stress at a point, first in two dimensions and then in three, followed by Mohr's representation of stress in three dimensions. The remainder of the chapter is devoted to the consideration of the strain at a point. A clear exposition of finite homogeneous strain in two dimensions and then in three is followed by Mohr's representation of finite homogeneous strain without rotation. The chapter concludes with the conventional discussion of infinitesimal strain in two and then in three dimensions.

The second chapter is entitled Behaviour of Actual Materials. It is concerned with various theories that have been formulated mathematically to reflect the behavior of actual materials, taking up first the stress-strain relations and the strain energy for a perfectly elastic, isotropic solid. There follow sections on anisotropic substances, natural strain, and the equations of viscosity. Several criteria of flow and of fracture are then discussed, the following at length: maximum shear-stress theory, including the internal-friction theory ($\delta_0 = |\tau| + \mu\sigma$); Mohr's theory of fracture; maximum distortional strain-energy theory. The chapter closes with an excellent section on substances with composite properties, involving time-dependent terms in the stress-strain relations.

The title of the last chapter is Equations of Motion and Equilibrium. The subject is introduced by the solution of a few simple problems illustrating the behavior of an elastic solid, an incompressible viscous fluid, a perfectly plastic material, and a Bingham substance. The elastic equations of motion are then derived by the conventional method in engineering presentations, and the special cases of plane strain and plane stress are considered, followed by the solution of some special, illustrative problems in elasticity. There come then two sections on wave propagation and elastic waves, good in so far as they cover the subject, but perhaps too brief for uninitiated readers. The chapter ends with a discussion of the equations of motion of a viscous fluid and the solution of illustrative problems in viscosity and plastic flow in two dimensions.

Gas Dynamics

ELEMENTS OF GASDYNAMICS. By H. W. Liepmann and A. Roshko. John Wiley & Sons, Inc., New York, N. Y., 1957. Cloth, 9 × 6 in., xv and 439 pp., illus. $11.

REVIEWED BY P. GERMAIN[8]

THIS new book, which now appears in the GALCIT series edited by Th. von Karman and Clark B. Millikan, was first planned as a new edition, with revisions and extensions, of the well-known "Introduction to Aerodynamics of a Compressible Fluid" by Liepmann and Puckett. In the preface to the book the authors explain very clearly the reasons for abandoning the original project and for completely rewriting the book. They have decided to devote the present book to the fundamental theories of gas dynamics and to follow it up with another book dealing with the applications of gas dynamics to the field of modern aeronautical engineering. We shall review the main topics in this book in the order in which they appear in the table of contents.

[6] Professor and Chairman, Division of Applied Mathematics, Brown University, Providence, R. I. Mem. ASME.

[7] Head, Department of Mechanics, Rensselaer Polytechnic Institute, Troy, N. Y.

[8] Professor, Institut de Mathématiques, Lille, France.

The first chapter contains an extensive treatment of concepts from thermodynamics which are required in the study of gas dynamics. Evidently, this emphasis on creating a sound basis in thermodynamics as a starting point for their book shows that the authors are very conscious of the importance of the concepts of thermodynamics in modern gas dynamics. Many topics treated here, such as the law of mass action, the mechanics of dissociation and condensation, are not usually given in treatises such as this; but it is clear that they will become very important in aeronautical applications in the near future. The authors seem to have chosen to take the reader as far as possible without the use of general equations and elaborate mathematical techniques. Chapter 2 is devoted to the study of one-dimensional steady flow. Chapter 3 to the study of one-dimensional wave motion (propagation of shock waves, isentropic waves of finite amplitude, acoustic waves) with applications to the shock tube. Chapter 4 gives a similar treatment of two-dimensional steady flow (shock waves, Prandtl-Meyer flow, applications to thin airfoil theory). This is followed by a study of the flow in ducts and wind tunnels and a very important chapter (Chapter 6) on the methods of measurement.

The general equations of frictionless flow appear first in Chapter 7. Chapters 8 and 9 give the most important applications to the classical small-perturbation theory (supersonic thin airfoil theory, planar flows, bodies of revolution and slender body theory). In these chapters the reader will, of course, not find all the known results on the subject, but the reviewer supposes that this material has probably been postponed for treatment in the second volume. Chapter 10 emphasizes the similarity rules (Prandtl-Glauert rule, von Karman's rule for transonic flow, Hayes-Tsien rule for hypersonic flow). Chapter 11 is devoted to the study of transonic flow, and Chapter 12 gives the main aspects of the method of characteristics and stresses some important applications. The book ends with two important chapters: The first one considers the effects of viscosity and thermal conductivity (boundary layers, shock waves, shock wave-boundary layer interaction); and the last chapter explains the principal concepts in the kinetic theory of gases which are useful for the understanding of the basic concepts in the book. This makes a good introduction to superaerodynamics.

As indicated in the title, the book does not pretend to be a complete treatise on fluid dynamics. Some classical topics such as, for example, hodograph methods receive only scanty attention. The authors have preferred to be selective in their choice of subject matter, and the reviewer fully agrees with the soundness of their point of view. This is a very attractive book, and the reviewer is certain that it will meet with the success it deserves because it gives a sound theoretical and physical background for work in modern gas dynamics and high-speed aeronautics.

Lubrication

THEORY AND PRACTICE OF LUBRICATION FOR ENGINEERS. By D. D. Fuller. John Wiley & Sons, Inc., New York, N. Y., 1956. $10.50.

REVIEWED BY JOHN BOYD[9]

PROFESSOR Fuller's book on the "Theory and Practice of Lubrication for Engineers" is probably the best single text on the subject currently available in this country. It is authoritative and well illustrated and contains an extensive list of bibliographical references. Clarity of expression and many illustrative examples reveal the author's long association with the teaching profession.

The first two chapters deal with viscous phenomena including viscosity measurements, the effect of temperature and pressure, and flow and power-loss considerations, and so on.

Chapters 3 and 4 deal with hydrostatic lubrication as does the greater portion of Chapter 9 which concerns air-lubricated bearings. The subject is well handled and is largely based on Professor Fuller's previous publications in the field. Engineers may feel that the subject, important as it is, may be somewhat overemphasized since in the majority of cases found in industry, other types or principles of lubrication are generally employed.

Chapters 5 and 6 cover the hydrodynamic lubrication of simple sliders and journal bearings. In treating bearings of finite (having various length to width ratios) proportions, the author uses leakage factors for both simple sliders and journal bearings. This is probably done for pedagogical reasons since, until recently, no accurate solutions were available for finite journal bearings, and the use of leakage factors makes it possible to handle both types of bearings in the same manner. Solutions for finite sliders have, however, been available and are much more convenient to use than the method of leakage factors.

Chapter 7 takes up friction and power loss in journal bearings, heat balance in self-contained bearings, and oil flow with various grooving arrangements. Engineers will probably feel that the addition of charts or tables for calculating film-temperature rise would be helpful for problems of bearing analysis.

Chapter 8 discusses typical industrial bearings including those lubricated by oil rings, wicks, pads, and waste.

Various examples of air-lubricated bearings operating on hydrodynamic and on hydrostatic principles are given in Chapter 9. Compressibility effects are briefly discussed.

Chapter 10 describes various current concepts of the dry friction and discusses the effect of surface conditions, speed, and temperature.

Chapter 11 on boundary friction discusses oiliness, molecular effects in polar lubricants, additives, etc., and describes a number of typical testing machines for evaluating boundary lubricants.

The final chapter is devoted to bearing materials. The requirements of a good bearing material are discussed and the properties of some of the more common bearing alloys and alloy combinations described. Other materials such as porous metals, hard alloys, glass, plastics, rubber, etc., are briefly considered.

Aerodynamics

AERODYNAMIC COMPONENTS OF AIRCRAFT AT HIGH SPEEDS. High Speed Aerodynamics and Jet Propulsion—Vol. VII. Edited by A. F. Donovan and H. R. Lawrence. Princeton University Press, Princeton, N. J., 1957. Cloth, 6½ × 9½ in., xiv and 845 pp., illus. $17.50.

REVIEWED BY JOSEPH H. CLARKE[10]

THE high level of activity and rapid progress of the postwar years have created a diluvial period in the aeronautical sciences. The Princeton series of twelve volumes dealing with high-speed aerodynamics and jet propulsion was conceived to effect an organization and consolidation of the essential elements of the large literature which has recently appeared in these fields. Volume VII, the latest to be published, is the second of the three sequential volumes which are collectively intended to present a complete theoretical and experimental coverage of external aerodynamics. Together with the first part of Volume VIII, the present Volume VII is designed to offer that body of aerodynamic knowledge of greatest use in the design of high-speed aircraft. It deals with wings in both steady and unsteady motion, bodies, interference effects, propellers, diffusers, and nozzles. Although organically a part of the subject of the present volume, the treat-

[9] Manager, Bearing and Lubrication Section, Westinghouse Research Laboratories, Pittsburgh, Pa.

[10] Associate Professor, Division of Engineering, Brown University, Providence, R. I.

ment of performance, stability, control, and aeroelastic effects is deferred to the first part of the subsequent volume because of space limitations.

The volume opens with a long section on the aerodynamics of wings at high speeds by R. T. Jones and Doris Cohen of the NACA. Chapter 1 begins with the analytical formulation of the action of the wing, containing some interesting observations. The incompressible theory of the two-dimensional thin airfoil is then presented, together with some useful related tables. Chapter 2 deals with three-dimensional subsonic linearized lifting surface theory and includes the reversibility, reciprocal, and combined flow relations. Chapter 3 deals with the aerodynamics of the thin wing at supersonic speeds and is notable for its treatment of the plane-waves method of Jones and a very useful tabulation of conical flow functions. An excellent bibliography accompanies the section.

Though necessarily compressed, this is an incisive and authoritative exposition of linear wing theory. Appearing throughout in judicious balance are the elements of physical discussion, theoretical principles, mathematical development, interpretation, accounting for nonlinear effects, and comparison with experiments. Although required to cover some ground already trod in Volume VI, the authors have successfully endeavored to fortify and complement the prior treatment.

The very brief section on the aerodynamics of bodies at high speeds is contributed by C. E. Brown of the NACA. It treats slender bodies of general cross section, including bodies with shoulders and open noses. Comparisons with experiment are presented, together with an engineering critique of the significance of the results in the light of viscous crossflow and nonlinear effects. Also included are brief treatments of base and skin friction drag. No consideration is given to bodies of optimum shape, to second-order theory and other nonlinear methods, or to any of the numerous hypersonic approximations. Few references are provided.

The next section, by C. Ferrari of Politecnico di Torino, is a long one dealing with interference between aircraft components. The interference between wing and horizontal stabilizer at subsonic speeds is considered in the first chapter. The coverage includes some information on vortex sheet roll-up and the effect of the wake of a flapped or stalled wing. The next chapter on wing-body interference at subsonic speeds is divided between the Multhopp procedure and the Ward theory. Following a treatment of subsonic propeller-wing-tail interference, the interference of wing on tail at supersonic speeds is considered with use of lifting surface and lifting line theory. The final chapter on wing-body interference at supersonic speeds includes a valuable discussion of quick estimates.

Although the style is sometimes quaint in translation, the section is clearly written, well organized, and not especially compressed. This is essentially a collection of material which is, in the main, well established by now but which is otherwise scattered throughout the literature; the formidable task of outlining these laborious calculations appears successfully met. In harmony with the objective of the volume, the emphasis is on methods appropriate to practical design and on the reliability of the computed results therefor. The section should therefore be especially welcomed by practicing aerodynamicists. No consideration is given to important recent developments in the design of low drag wing-body arrangements through establishment of favorable interference. Presumably, the declassification of much of this research fell too close to the publication deadline.

The brief section on propellers for high-speed flight is contributed by C. B. Smith, of Pratt and Whitney. The high-speed propeller is conventionally envisioned as a system of high-aspect-ratio rotating airfoils except that the blade sections now operate at supersonic speeds, the concept of limiting tip speed being, of course, discarded. The section is concerned with propeller efficiencies, optimum pitch distribution, and the other effects of geometry. One reference to the topic is provided.

The section on diffusers and nozzles is written by J. C. Evvard of the NACA. The first chapter deals with problems of fluid mechanical diffusion with emphasis on the aircraft inlet. Following an interesting treatment of boundary-layer separation is a discussion of the various devices to overcome the basic supersonic starting problem. Also included is a discussion of buzz phenomena, diffuser drag, and engine matching. The second brief chapter treats exit-nozzle thrust, the ejector, and exit-jet phenomena. Appropriate to the topic and the fact that underlying analytical methods are presented elsewhere in the series, emphasis is placed on establishing a clear physical understanding of the phenomena, the nature of the various losses present, and means for their minimization.

I. E. Garrick of NACA and M.I.T. has prepared the section on nonsteady wing characteristics. Following some introductory material on the solutions to the linearized boundary-value problems considered, there is treated the two-dimensional airfoil in unsteady incompressible flow, in subsonic oscillating flow, in unsteady supersonic flow, and in linearized unsteady sonic flow. Some of the methods for treating the three-dimensional subsonic and supersonic problems are then sketched. Abounding in citations of the extensive accompanying references and bibliography, the article is a recondite theoretical treatment of an abstruse subject which provides the basis for the consideration of aeroelastic problems and of dynamic response in flight.

The final section by C. W. Frick of the NACA treats the experimental aerodynamics of wings at transonic and supersonic speeds. Considering in succession lift, drag, pitching moments, and the wake, the article provides systematic comparisons between the results of theory and experiment. It suggests where the theory can be used with confidence and where it fails or requires qualification. For instance, in the latter category, it is shown that semiempirical adjustments of the theoretical results can, on occasion, render them accurate. The article includes some imaginative and creative examples in which the governing parameters of phenomena are deduced from theoretical results in limiting cases. Unfortunately, the writing is unclear in a few places and one or two figures do not seem to illustrate what they are represented to illustrate. This useful section provides the basis for intelligent application of the results of small-disturbance wing theory.

The present volume, like the preceding one of the series, is composed not of tightly integrated chapters but rather of a number of monographs which are loosely integrated into the whole by an occasional remark or cross reference. Each author develops his topic in a way which appears suitable to him. Whereas the articles are, in general, of high caliber, they differ in level, orientation, and degree of compression. Aspects of the slender-body theory, for example, appear in six different sections of Volumes VI and VII. Although a certain amount of overlapping is unavoidable and not without its advantages, one wonders whether a single complete and expansive coverage of this topic would not have been both more valuable and more economical. The Princeton series invites comparison with the series on Aerodynamic Theory edited by W. F. Durand a score of years prior. It has been remarked that these books comprised a better integrated, more definitive effort. But it is perhaps also true that the newer series, precisely because it contains articles which, though repetitious at times, are self-contained, tends to be more accessible for specific purposes and therefore more readily put to use.

The preceding remarks notwithstanding, the essential facts are

that this volume, like its predecessor, is a major effort by outstanding members of their respective fields, substantially fulfills an ambitious objective, and therefore constitutes a valuable addition to the literature which belongs in the library of everyone who is concerned with compressible flow.

Torsional Vibration

PRACTICAL SOLUTIONS OF TORSIONAL VIBRATION PROBLEMS—With Examples from Marine, Electrical, Aeronautical, and Automobile Engineering Practice. By W. Ker Wilson. Volume One—Frequency Calculations. Third Edition, Revised. John Wiley & Sons, Inc., New York, N. Y., 1956. Cloth $8^1/_2 \times 5^1/_2$ in., xxxii and 704. $16.

REVIEWED BY CYRUS H. KANO[11]

ALL engineers working in the field of vibration appreciated the value of the two volumes on "Practical Solutions of Torsional Vibration Problems," by this well-known authority. The appearance of a revised edition of Volume 1, with the implication of a coming revision of Volume 2, is therefore opportune.

Because vibration engineers are well acquainted with the previous volumes, this review is confined to a few general comments on this revised third edition.

The natural frequency in torsion can be determined for proposed and/or existing systems by several analytical methods if empirical ones are not feasible. Volume 1 of the latest edition of Ker Wilson's well-known work not only covers the familiar tabular methods by means of detailed examples, but also clearly describes the concepts of "effective inertia" and the related "dynamic stiffness."

The wide range of torsional vibration problems, in which methods employing these concepts offer advantages, are discussed. Simplified analysis, maintenance of physical significance, and separation of a complex assembly into several simpler subassemblies are some of the advantages cited.

Many readers will find the newly added introduction very interesting and instructive. Here, the author presents in a readable style a historical development of the solutions to torsional vibration problems, well documented with important references.

Engineers and mathematicians will welcome the many tables, especially those in the chapters on equivalent masses and shafts and the clearly and strategically placed definitions of symbols. Others, searching for examples of solutions to a particular problem, will be aided by the organized presentation of both subject matter and the extensive bibliography.

Fatigue in Aircraft Structures

FATIGUE IN AIRCRAFT STRUCTURES. Proceedings of the International Conference held at Columbia University, January 30, 31, and February 1, 1956. Edited by Alfred M. Freudenthal. Academic Press, Inc., New York, N. Y., 1956. Cloth, 9 × 6 in., xiii and 456 pp., illus. $12.

REVIEWED BY W. N. FINDLEY[12]

THIS book contains 19 invited papers presented at an international conference on fatigue in aircraft structures sponsored by the Air Research and Development Command, USAF, and Columbia University. All papers are printed in English and include discussion in edited form. The volume is divided into three parts: Physical Theories of Fatigue; Prediction of Fatigue Life and Fatigue Strength; and Prevention of Fatigue Failure. Taken together, these papers cover the field of fatigue rather thoroughly from basic metallurgical observations and theories of the origin of fatigue to practical aspects of design practice to minimize fatigue failure in aircraft structures.

A number of significant contributions are to be found in each section—especially in the section on physical theories of fatigue.

Perhaps one of the most spectacular new observations reported concerning the nature of fatigue was that a thin ribbon of metal was observed to be extruded during fatigue from a region of heavy localized deformation. These extrusions were approximately 0.1μ thick and were observed in lightly cold-rolled aluminum, copper, and age-hardening aluminum alloys.

The authors contributing to the volume were the following: *Part I—Physical Theories of Fatigue:* W. A. Wood (Australia), P. J. E. Forsyth (England), N. Thompson (England), R. F. Hanstock (England), M. Hempel (Germany). *Part II—Prediction of Fatigue Life and Fatigue Strength:* C. E. Phillips (England), W. Weibull (Sweden), A. M. Freudenthal (U.S.A.), R. A. Heller (U.S.A.), E. Gassner (Germany), P. D. Brooks (U.S.A.), H. T. Jensen (U.S.A.). *Part III—Prevention of Fatigue Failure:* B. Lundberg (Sweden), S. Eggwertz (Sweden), R. J. Atkinson (England), P. Kuhn (U.S.A.), J. Cornillon (France), F. Turner (Sweden), H. Giddings (England), R. L. Schleicher (U.S.A.), W. W. Johnstone (Australia), and A. O. Payne (Australia).

Considering that most of the papers were 20 to 50 pages in length, it is unfortunate that so few of them included summaries and lists of the conclusions reached. However, an excellent subject index provides partial compensation. The book is well edited and printed.

Nuclear Energy

PROGRESS IN NUCLEAR ENERGY. SERIES II—REACTORS. Edited by R. A. Charpie, D. J. Hughes, D. J. Littler, and M. Trocheris. McGraw-Hill Book Company, Inc., New York, N. Y., 1956. Cloth, $9^1/_4 \times 6^1/_4$ in., x and 492 pp., illus. $14.

REVIEW BY SALOMON LEVY[13]

THIS volume is an important and useful compilation of selected 1955 Geneva Papers about the basic subject of nuclear reactors. It covers not only research and power reactors, but also it includes descriptions of reactors developed in Canada, United States, France, Sweden, Norway, Great Britain, and Russia. However, as many other compilations of this type, it suffers from great imbalance in the material presented.

Contributors have put different emphasis on different subjects and the treatments run from detailed descriptions to very hasty reviews. Also, grouping of research reactors by countries rather than types, and lack of construction costs make it difficult to compare their design and usefulness. Further, in many instances the material is descriptive, and important technical information which justifies the final selected design is not discussed. Yet, in spite of such shortcomings, the data collected are of sufficient usefulness to insure that this volume will become an important reference book in nuclear reactor work.

A considerable wealth of material is assembled and it includes:

A description, in Chapter 1, of Canadian research reactors by Hurst and Ward, with special emphasis on the NRX design characteristics and operating experience.

A review in Chapter 2 by Weinberg and Huffman of the U.S. research reactors, and in particular of the MTR, CP-5, and water boiler type.

[11] Senior Project Engineer, Lessells and Associates, Inc., Boston, Mass.

[12] Professor of Engineering, Brown University, Providence, Rhode Island.

[13] Specialist, Nuclear Technology, Advance Engineering Subsection, General Electric Company, Atomic Power Equipment Department, San Jose, Calif.

A coverage by Blokhintsev and Feinberg in Chapter 3 of the U.S.S.R. uranium-graphite pile, heavy and light-water research reactors and of their first industrial power station.

A report in Chapter 4 by Gueron, et al., about the European research facilities and some of their applications.

A review in Chapter 5 by Fenning of the eight British critical and test reactors.

A description in Chapters 6–11 of the more important power reactors. The pressurized-water reactor is first discussed in detail by Simpson, Shaw, Mandil, and Palladino. Next comes the boiling-water reactor covered by Dietrich, Lichtenberger, and Zinn, who review the operating experience from Borax III; then the aqueous homogeneous two-region breeder reactor described by Briggs and Swartout; the gas-cooled graphite-moderated reactor only touched upon by Hinton; the sodium-graphite nuclear plants described by Starr, including the SRE and larger plants of that type; and finally, fast reactors, in general, discussed by Zinn with particular attention to important design problems.

The book ends with a worthwhile catalog of all the world reactors built or planned by April, 1956.

Thermodynamics

THERMODYNAMICS AND STATISTICAL MECHANICS. By Arnold Sommerfeld. Edited by F. Bopp and J. Meixner. Translated by J. Kestin. Academic Press, Inc., New York, N. Y., 1956. Cloth, 6 × 9 in., xviii and 401 pp. $7.

REVIEWED BY JAMES A. FAY[14]

THIS volume is the fifth of the series, "Lectures on Theoretical Physics," by A. Sommerfeld. It covers a brief development of thermodynamics, statistical mechanics, and kinetic theory of gases. Written in the style of a textbook, including problems and solutions, it is intended primarily for physics students. A wide variety of applications in all these fields is considered in as concise a manner as possible.

Chapters 1 and 2 are devoted to the laws of thermodynamics and their applications. Chapter 1 covers the first and second laws, including thermodynamic equilibrium and a brief discussion of the third law of thermodynamics. The treatment of the first two laws is perhaps the least effective part of this volume, lacking somewhat in clarity and rigor. The discussion of the thermodynamic potentials and the Maxwell relations is exceedingly well done. The applications considered in Chapter 2 include a discussion of dilute solutions, phase equilibrium, electrochemical potentials, ferro and paramagnetism, and black-body radiation. In considering the latter, the author applies enlightening dimensional arguments. The treatment throughout is quite complete and concise.

Chapters 3 and 5 are devoted to the elementary and exact kinetic theory of gases, respectively. The former chapter, in addition to the usual development of the Maxwellian velocity distribution and the mean free path, also contains interesting discussions of Brownian motion and paramagnetic substances. The latter chapter begins with the derivation of the Maxwell-Boltzmann equation, and develops a solution for the case of rigid-sphere molecules by means of the moment method. It concludes with a derivation and discussion of electrical conductivity in solids.

Chapter 4 develops statistical mechanics using the combinatorial method. The author considers many applications, among which are the specific heats of gases and solids and degenerate gases (including the electron gas in metals). Quantum statistics are nicely introduced and explained simply in the several applications. In particular, the treatment of black-body radiation following Debye's original suggestion, and a particularly clear account of fluctuation theory should be mentioned as indicative of the interesting insight which is brought to bear by the author.

The general purpose of this book, which is to cover these related subjects in as concise a manner as possible while still including the more interesting applications to physical phenomena, precludes a thorough and leisurely treatment which might be possible in any of the three principal subjects considered. A considerable saving in space results from a well-correlated treatment of these related subjects with a resulting gain for the reader who becomes more aware of the mutual relationship among the three fields. It is not likely that this volume would be adequate as an introduction to any of the subjects, but is more suitable for those who have some knowledge of this material.

This volume is distinguished from the many in its field by virtue of the concise and, in many cases, original treatment of the material by the author, which perhaps stems from his experience as a lecturer. In addition, there are careful references to the original literature as well as amusing anecdotes, such as the reason for J. C. Maxwell's use of the pen name dp/dT. There are many points of interest, especially to teachers in these fields.

This volume was completed and published with the aid of the editors, F. Bopp and J. Meixner, following Sommerfeld's death. The translation by J. Kestin, of Brown University, is uniformly good throughout, and there is an adequate index included. There are also 8 pages of problems and 37 pages of "Hints for the solution of problems."

Fluid Dynamics

MOMENTUM TRANSFER IN FLUIDS. By Wm. H. Corcoran, J. B. Opfell, and B. H. Sage. Academic Press, Inc., New York, N. Y., 1956. xi + 394 pp. $9.

REVIEWED BY LLOYD TREFETHEN[15]

THE authors' purpose was "to present a small portion of this field [fluid dynamics] of special interest to chemical engineers." They aimed at providing "sufficient background . . . to give the reader a reasonable understanding of the nature of local fluid motions which are of primary importance in thermal and material transport." The resulting book is an extensive review of such laminar and turbulent shear flows and boundary layers, interspersed with detailed derivations of the basic equations (usually in several co-ordinate systems) and of illustrative solutions.

The coverage is indicated by the chapter titles: "Introduction to momentum transfer"; "Some simple properties of turbulent flow"; "Some macroscopic characteristics of turbulent flow"; "Velocity distribution and friction factors for turbulent flow"; "General equations of fluid motion"; "Some properties of turbulence"; "Boundary layer"; and by the appendixes: "A derivation of Bernoulli's equation"; "An introduction to tensors and the statistical theory of turbulence"; "Constants and conversion factors, dimensions"; and "Analysis of potential flow across a cylinder."

This book achieves its purpose. It would provide the student who has already completed an introductory course in fluid dynamics with the special background information needed for the study of thermal and material transport. The presentation of much recent work makes it useful also as a reference source.

The book would be more useful to chemical engineers if there had been incorporated in it some of the ideas and data on the diffusion of heat and material as well as momentum. (For ex-

[14] Associate Professor of Mechanical Engineering, Massachusetts Institute of Technology, Cambridge, Mass.

[15] Assistant Professor, Division of Engineering and Applied Physics, Harvard University, Cambridge, Mass.

ample, the Reynolds heat-momentum analogy is not mentioned, although mixing lengths and eddy viscosity are discussed at length.) Also, adoption of vector or tensor notation would have reduced the complexity of nomenclature and derivations. Although considerable space has been devoted to several elementary concepts, the reviewer has the impression that these instances reflect problems of student understanding which the authors have encountered.

Civil Engineering

AMERICAN CIVIL ENGINEERING PRACTICE, Volume III. Edited by Robert W. Abbett. John Wiley and Sons, Inc., New York, N. Y., 1957. Cloth, 8 1/2 × 5 3/4 in., xiii and 1279 pp., illus. $25.

REVIEWED BY D. C. DRUCKER[16]

ALTHOUGH written for the practicing civil engineer, there is much of value for those interested primarily in applied mechanics. Section 22 on theory of structures, and Section 34 on earthquakes and earthquake-resistant design are especially relevant.

Engineering Materials Science

THE SCIENCE OF ENGINEERING MATERIALS. Edited by J. E. Goldman. John Wiley & Sons, Inc., New York, N. Y., 1957. Cloth, 6 1/4 × 9 1/4 in., xv and 528 pp., illus. $12.

REVIEWED BY J. GURLAND[17]

THIS series of 18 lectures was presented at the 1954 Carnegie Conference on the Impact of Solid State Science on Engineering Education. It is an outgrowth of the concern of the American Society for Engineering Education and of the National Science Foundation with the integration of solid-state science into the engineering curriculum. As one of the first books of this type offered to engineering students, it is approached with great expectation.

The subject of solid-state physics is introduced by two chapters on solid-state theory by Harvey Brooks, and a chapter on atomic theory by J. Bardeen, W. Bitler, and J. E. Goldman. The remainder of the book deals with the applications of theory to specific problems related to metals and alloys, surfaces, magnetic properties, semiconductors, and nonmetallic materials such as cement, polymers, and glass. Most of the contributors are well known, having played a leading part in the developments that they describe. For instance, the section on metals and alloys has papers by R. Smoluchowski, H. Jones, H. W. Paxton, E. R. Parker, and T. A. Read.

The authors are able to marshal an impressive array of theories dealing with many of the physical properties of materials. Considerable space is given to the two outstanding practical achievements of solid-state science: semiconductors and magnetic materials. The subject treatment, in general, is clear and concise. The editor has made a valiant effort to unify the collection of separate papers, although there still remain a number of duplications and undefined concepts. The book should be of great value to persons engaged in research in mechanics, metallurgy, and physics, who desire a summary of the present status of solid-state science, and of its potential contribution to their own fields.

However, as a textbook it is less satisfactory by not being adapted to the needs of undergraduate students. The gap between the theories of solid-state physics and the behavior of engineering materials has not yet been bridged, except at a very few points, and it requires a great deal of documentation to establish a link between theory and practice, which is not provided here. The scope of the articles is somewhere in between that of a textbook on solid-state physics and that of the periodic review papers which appear in "Progress in Metal Physics." The book does not attain the advantages of either one, namely, the logical development and rigorous derivation of the principal equations or the treatment of advanced topics. Also, because it is a collection of separate papers, the contents of the various sections are, of necessity, disconnected and often presented at very different levels.

In spite of its shortcomings as a textbook, it is recommended as a superior reference work for both undergraduate and graduate engineering students and their teachers.

Failure of Machine Parts

FAILURE OF MACHINE PARTS. Edited by Rune Evaldson and Charles Lipson. University of Michigan, Ann Arbor, Mich., 1955. Paper bound 8 1/2 × 11, 156 pp., illus. $10.

REVIEWED BY R. A. BAREISS[18]

THIS book is a collection of a series of twelve lectures presented at a summer course of the same title given by the University of Michigan, in 1955. Eight of the lecturers were practicing engineers from industry and two were members of the faculty of the College of Engineering.

The book suffers, in general, from a lack of uniformity in the depth and range of treatment of material. Several of the chapters are merely lecture notes devoid of explanatory material usually found in a technical text.

Two of the lectures are worthy of special note. Lecture 9, "Treatment of Metallurgy and Fabrication," by O. J. Horger, presents a considerable number of *S-N* diagrams covering a wide range of materials and material treatments.

Lecture 11, "Use of Appearance of Failed Part," by C. Lipson, is particularly instructive in the manner of analyzing the failure surface in order to determine the conditions under which failure occurred.

This book contains several valuable additions to the subject of failure of machine parts. However, those looking for a complete and comprehensive text on the subject will need to rely on other standard texts in the field.

High Speed Flight

HIGH SPEED FLIGHT. By E. Ower and J. Nayler. Philosophical Library, Inc., New York, N. Y., 1957. Cloth, 6 1/4 × 9 1/4 in., 227 pp., illus. $10.

REVIEWED BY J. R. MOSZYNSKI[19]

THE authors have undertaken what is probably the first attempt to present the rapid developments in aviation which have taken place in the past two decades and the many problems associated with them, in a manner understandable to a comparative layman, and yet comprehensive enough to make it of interest to those familiar with various aspects of aeronautics.

The book gives equal prominence to advances made in this country and the United Kingdom, and contains a considerable amount of information hitherto not available to the general

[16] Professor and Chairman, Division of Engineering, Brown University, Providence, R. I.

[17] Assistant Professor of Engineering, Brown University, Providence, R. I.

[18] Senior Project Engineer, Lessells and Associates, Inc., Boston, Mass.

[19] Research Associate, Division of Engineering, Brown University, Providence, R. I.

public, partly because of its classified nature and partly because it has appeared only in highly technical publications.

The first chapter gives a concise history of aviation from the point of view of speed from the Wright Brothers to modern supersonic research aircraft, and outlines briefly the problems which were encountered and overcome on the way.

Chapters 2 and 3 give a very clear explanation of the fundamentals of flight and phenomena associated with transonic and supersonic speeds.

Subsequent chapters describe the requirements posed by high-speed flight on the propulsive plant, materials, and aircraft structures both from the point of view of existing applications and limitations, and the needs for future developments. Questions of comfort of pilot and possible passengers are discussed fully as well as the former's limitations at very high speeds.

The chapter devoted to experimental research deals with several types of wind tunnels both subsonic and supersonic and the methods of measurement normally employed, together with flow-visualization methods, and includes some striking photographs of shock formations. Hypersonic wind tunnels, shock tubes, and full-scale flight tests are also described.

The last chapters are devoted to flight aids such as radar, landing aids, boundary-layer control, etc., and to guided missiles, respectively. The latter chapter outlines some very recent developments including a brief description of the artificial-earth-satellite project.

The vast amount of material contained in the book is presented in a concise and competent manner with a large number of excellent illustrations.

Shell Theory

ELEMENTARE SCHALENSTATIK. By Alf Pflüger. Zweite erweiterte Auflage der Einführung in die Schalenstatik. Springer-Verlag, Berlin, Göttingen, Heidelberg, 1957. Cloth, 9$^{1}/_{8}$ × 6$^{1}/_{8}$ in., vii and 112 pp., illus. DM 19.50.

REVIEWED BY S. R. BODNER[20]

THE double purpose of this book, as stated by the author, is to serve as a textbook for students in an introductory course on shell theory and as a reference guide for practical engineers engaged in shell structure construction. In the reviewer's opinion, the author has done well toward achieving his purpose in the one-hundred-odd pages the book contains. (This book is a second, enlarged edition of *Einführung in die Schalenstatik* by the author, published in 1948.)

The two main features of the book are: (*a*) a clear presentation of the basic assumptions and approximations and derivation of the equations of shell theory, and (*b*) a large number of illustrative problems of practical interest.

Whereas the book would be useful to the beginning student in shell theory, it does not contain sufficient material for a full course on the topic. Most of the material in the book dates to pre-1940. Especially missing and technically important are the subjects of shell buckling, nonlinear bending of shells, the theory of shallow shells, and asymmetric bending of shells. To have included these and other topics, however, would probably have deviated from the title and modest aim of the book.

The contents of the book are: 1 Introduction; 2 Membrane Theory of Shells of Revolution; 3 Bending Theory of Axially Symmetrically Loaded Shells of Revolution; 4 Membrane Theory of Cylindrical Shells; 5 General Membrane Theory of Shells; 6 Properties of Stress States; 7 Appendix. The Appendix is a very useful catalog of membrane-theory solutions for a large variety of shells and loadings.

[20] Assistant Professor of Engineering, Brown University, Providence, R. I.

Metal Failure

DEFECTS AND FAILURES OF METALS. By E. P. Polushkin. Elsevier Publishing Co., Publisher; D. Van Nostrand Co., Inc., Distributor in U.S.A. and Canada. Cleaves-Hume Press Ltd., London, Distributor in British Commonwealth except Canada. Cloth 9 × 6$^{1}/_{8}$ in., xvi and 399. $12.50.

REVIEWED BY P. E. KYLE[21]

OVER the years it has been difficult to get engineers and metallurgists to publicize defects in their products and alloys. All have been of the opinion, however, that a study of defects can be most informative provided all circumstances surrounding the defect and the failure caused by it, are available.

The author has done an excellent job in uncovering the many examples he uses, and this is commendable particularly when one considers the difficulty in obtaining such data. The most valuable feature of this work to be emphasized is that it has been possible to analyze each major defect and failure group in a standardized form composed of six items: (*a*) Definition and characteristics, (*b*) origin, causes, (*c*) means of discovery, (*d*) occurrence, (*e*) detrimental effects, and (*f*) prevention.

The major defects and failures covered are: segregation, porosity, piping, impurities, decarburization, scaling, residual stresses, fatigue, flakes, heat-treatment failures, embrittlement, cracks, shape and surface defects, wear, and corrosion. There are 295 figures which adequately cover the illustration of the subjects discussed.

Because of the wide coverage of this work, it should be a part of all research and development libraries. Those involved in the production and processing of metals could obtain many suggestions from it in the solution of their manufacturing problems. It is an excellent reference for engineering students and students in the physical sciences.

A unique feature of each chapter is a complete bibliography accompanied by a guide list to this literature broken down according to the major subject headings involved.

[21] Vice-President, Lessells and Associates, Inc., Boston, Mass.

Information for Authors

• Manuscripts should be submitted in final form to the Technical Editors. Each manuscript must be accompanied by a statement that it has not been published elsewhere and has it been submitted for publication elsewhere. A paper which would occupy more than five pages of the Journal may be returned to the author for abridgment.

• The author should state his business connection, the title of his position, and his mailing address. A short abstract (50 to 100 words) should be included on the first page immediately preceding the introductory paragraph of the paper.

• Three copies of the manuscript are required. One of these must be a carefully prepared printer's copy, typed in double spacing, on one side of the page only, with wide margins, on 8½ by 11-in. opaque white paper. Mimeographed manuscripts, if prepared with exceptional care, can be accepted provided they are completely edited.

• All mathematical expressions should be written by hand in ink or set out by typewriter in a way which would define each symbol unambiguously. Care should be taken to distinguish between capital and lower-case letters, between (0) and the letter (O), between the numeral (1) and the letter (l), etc. A list of symbols carefully marked, if it has not been included in the body of the paper, should accompany the manuscript on a separate page.

• Before preparing a manuscript the author should study printed articles in the Journal, with special attention to the form and style of mathematical expressions, tables, footnotes, references, and abstract. Care should be taken to arrange all tables and mathematical expressions in such a way that they will fit into a single column when set in type. Equations that might extend beyond the width of one column (fractions that should not be broken or long expressions enclosed in parentheses) should be rephrased to go on two or more lines within column width. Fractional powers are preferred to root signs and should always be used in more elaborate formulas.

• A normal paper should not exceed five pages in the Journal. It is about 6000 words or twenty to twenty-five double-spaced typewritten pages inclusive of drawings. A Brief Note should not exceed 750 words or about one column in the Journal inclusive of drawings.

• Originals and two copies of figures must accompany the manuscript. Line drawings should not be larger than 8½ × 11 inches, and should be planned for reduction to column width. Lettering should be large enough to be clearly legible when the illustration is reduced. The originals of line drawings must be in India ink on white or pale blue tracing paper or tracing cloth. Photographs of equipment or test specimens must be glossy prints and should be used sparingly. Captions for figures should be typed double-spaced and included as the last page of the manuscript. The figure number and author's name should be written in the margin or on the back of each illustration.

• Titles of papers should be brief. If an adequate description of the subject requires a title which, along with the authors' names, would occupy more than one line on the cover of the Journal, a separate shorter title should be submitted.

• Authors can obtain copies of the ASME Manual MS-4, "An ASME Paper," from the Technical Editors and are urged to do so before drafting their papers in final form.

• Papers published in the Journal of Applied Mechanics must be presented at a Meeting, either in person or by title. Scheduling of papers is in the hands of the Secretary of the Applied Mechanics Division. Authors should indicate their preference in this respect to the Technical Editors when submitting a paper.

• An author is entitled to 25 preprints free of charge (in the case of two authors, 15 each; three or more authors, 10 each). Larger quantities of preprints or reprints can be ordered from Editorial Department, The American Society of Mechanical Engineers, 29 West 39th Street, New York 18, N. Y. Quotations will be sent on request.

D. C. Drucker and J. Kestin, *Technical Editors*

Please address all communications to: Technical Editors
Journal of Applied Mechanics, ASME
Division of Engineering
Brown University
Providence 12, R. I.

Third U. S. National Congress of Applied Mechanics

at Brown University, Providence, Rhode Island
June 11–14, 1958

Complete papers must be submitted to Professor R. M. Haythornthwaite, Chairman of the Editorial Committee, Brown University, before January 1, 1958.

No paper, including text, equations, tables, and figures, should exceed the equivalent of 5000 words. Manuscripts should be submitted in *duplicate*, but it is not required that the first page of each manuscript containing only the title of the paper, the name and affiliation of the author, and an abstract of not more than 100 words be submitted in *triplicate*, because it is planned to publish abstracts of accepted papers in the June, 1958, issue of the *Journal of Applied Mechanics*.

One copy should be in original typewriting (for best clear mimeographing) on only one side of white paper, and be double spaced with margins at least one inch wide. Figures should be submitted in one copy on India ink drawings on separate sheets of drawing paper or cloth. The width of the lines of these drawings and the lettering should allow for the necessary reduction. Photographs should be glossy prints and not larger than 8 by 10 inches.

References should be grouped together in a bibliography at the end of the manuscript, listing title, author, publication or publications, volume, year, and page numbers, in that order. Text references to the bibliography should be made by numbers in brackets, references to equations by numbers in parentheses.

Authors are advised to retain carbon copies of their manuscripts as the original manuscripts will not be returned with the proofs.

Inquiries regarding the Congress should be addressed to the Secretary of the Congress, Brown University, Box D, Providence 12, R. I.

Industrial groups, governmental agencies, and colleges and universities are requested to provide financial support for the Congress.

All industrial groups contributing $500 or more, and all universities or colleges contributing $150 or more, will be listed in the program of the Congress and in the printed Proceedings.